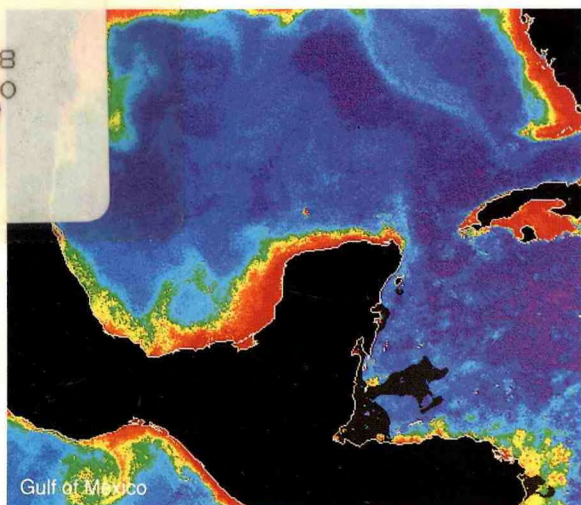
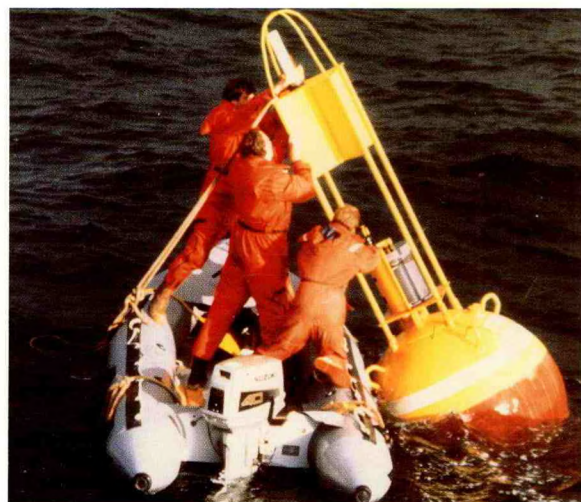


GC  
2  
.C58  
1990  
V.  
C 2



*The  
Coastal Ocean Prediction Systems  
Program:*

*Understanding and Managing  
Our Coastal Ocean*



Volume II: Overview and Invited Papers  
*May 1990*



# COASTAL OCEAN PREDICTION SYSTEMS

Report of a Planning Workshop  
Held  
31 October to 2 November 1989  
at the  
University of New Orleans

---

## VOLUME II: OVERVIEW AND INVITED PAPERS

---

### Co-Sponsoring Agencies

National Oceanic and Atmospheric Administration  
Minerals Management Service  
Environmental Protection Agency  
National Aeronautics and Space Administration  
Department of Energy  
United States Coast Guard  
United States Geological Survey  
National Science Foundation  
Office of Naval Research

### Co-Sponsoring Institution

Ocean Studies Board

### Participating Agency

Corps of Engineers

### Participating Institution

Marine Board

### Convenor

Prof. Christopher N. K. Mooers  
Institute for the Study of Earth,  
Oceans, and Space  
University of New Hampshire

### Managing Institution

Joint Oceanographic Institutions, Inc.

15 May 1990



61C  
2  
.C58  
1990  
V.2  
C.2

## VOLUME II: OVERVIEW AND INVITED PAPERS

### TABLE OF CONTENTS

#### I. NATIONAL RESEARCH COUNCIL REPORT ON "OPPORTUNITIES TO IMPROVE MARINE FORECASTING"

*Summary of Report* 1  
Kenneth W. Ruggles

#### II. AGENCY MISSIONS, PROGRAMS, AND NEEDS

*Agency Missions, Programs, and Needs (Overview)* 3  
William C. Boicourt

#### III. OPERATIONAL AND APPLICATIONS MODELS

*Operational and Applications Models (Overview)* 13  
Christopher N.K. Mooers

*Circulation Modeling Needs of Damage Assessments  
Under CERCLA Legislation* 17  
Mark Reed

#### IV. RESEARCH MODELS

*Research Models (Overview)* 25  
John S. Allen

*Coastal Ocean Circulation Models* 28  
Malcolm L. Spaulding, J. Craig Swanson

*A Limited-Area Coastal Ocean Circulation Model* 35  
Robert L. Haney

*Predicting Coastal Ocean Circulation With the University  
of Miami Finite Element Models* 45  
John D. Wang

*Coastal Ocean Circulation Model* 53  
Dong-Ping Wang

*Semi-Spectral Primitive Equation Regional Ocean Circulation Model* 61  
Dale B. Haidvogel

*The Princeton/Dynalysis Ocean Model* 77  
George L. Mellor, H. James Herring, and Richard C. Patchen

*Coastal Constraints on Quasigeostrophic Flow* 114  
Allan R. Robinson

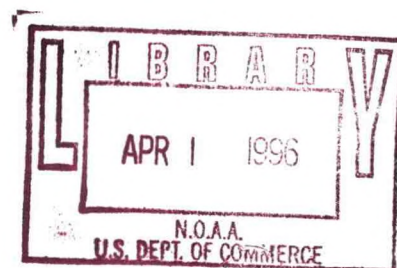




## TABLE OF CONTENTS (Continued)

### V. OPERATIONAL OBSERVING AND DATA SYSTEMS

<i>Operational Real-Time Observing and Data Systems (Overview)</i>	121
Henry R. Frey	
<i>Data Archiving for the Coastal Ocean (Overview)</i>	127
H. James Herring	
<i>A Note on the Availability of Historical Coastal Oceanographic Data</i>	134
Sidney I. Levitus, Ron E. Moffat	
<i>Evaluation of Surface Wind Fields Over the Coastal Ocean off the Western U.S.</i>	146
P. Ted Strub, Corinne James	
<i>National Data Buoy Center Real-Time Environmental Data</i>	166
Glenn D. Hamilton	
<i>U.S. Army Corps of Engineers Field Wave Gaging Program: A Conspectus</i>	177
David D. McGehee	
<i>The Role of the Modernized National Weather Service In the Development of a COPS</i>	181
Stephen T. Rich	

### VI. RESEARCH OBSERVING AND DATA SYSTEMS

<i>Research Observing and Data Systems (Overview)</i>	187
Wendell S. Brown	
<i>A View (from an Ocean's Eastern Boundary) on Research Monitoring (Long Time-Series) Systems and Interannual Variability</i>	229
Robert L. Smith	
<i>Coupling Remote Measures of Ocean Chlorophyll with Observations and Models of Coastal Circulation</i>	235
James A. Yoder	
<i>Radar Mapping of Ocean Surface Currents: Description and Uses in Coastal Oceanography</i>	239
Phillip A. McGillivray	
<i>A National Buoy Network for Continuous, Real-Time Monitoring of Physical, Chemical and Biological Processes in U.S. Coastal Waters</i>	246
Paul G. Falkowski, Charles N. Flagg, Creighton D. Wirick, and Zbigniew S. Kolber	



## TABLE OF CONTENTS (Continued)

### VII. OCEANIC AND ATMOSPHERIC DATA ASSIMILATION

- Oceanic and Atmospheric Data Assimilation (Overview)* 257  
Dale B. Haidvogel

### VIII. SEVERAL CRITICAL COASTAL PHYSICAL PROCESSES

- Submarine Canyons and Their Importance to Models  
of Coastal Circulation* 274  
Barbara M. Hickey
- The Surface Boundary Layer and Sea Surface Fronts* 286  
Dong-Ping Wang
- On the Importance of the Cross-Shelf Structure of the  
Wind Stress to Shelf Flow* 290  
Allan J. Clarke
- Tidal Modeling* 294  
Daniel R. Lynch
- Nearshore Processes* 305  
Robert A. Holman
- Strategems for Coastal Seas* 312  
David A. Brooks
- Coastal Ocean Prediction: Possibilities and Limitations* 315  
Gabriel T. Csanady

### IX. MASTER REFERENCES 320

### X. GLOSSARY OF ACRONYMS 345



## **A SUMMARY OF THE REPORT, "OPPORTUNITIES TO IMPROVE MARINE FORECASTING"**

**Kenneth W. Ruggles  
Systems West  
Carmel, CA 93922**

This presentation summarizes the results of the National Research Council Report, "Opportunities to Improve Marine Forecasting" (1989). While care has been taken to assure that the report is accurately summarized, one should refer to the original document for a full exposition of the findings.

The report was the result of an assessment of the needs and expected benefits associated with improving forecasts of ocean conditions. The study leading to the report was performed by a committee consisting of members from the scientific and technical fields supporting marine forecasting and from the user communities with synoptic-scale phenomena in the atmosphere and mesoscale phenomena in the oceans. It did not address seasonal variability or other long-term phenomena. The inquiry was limited to physical processes; it did not address biological phenomena.

The coastal region emerged as an important area of focus for applying and improving marine forecasting technology. This importance derives from the fact that the majority of our national population is concentrated along the coast-lines, and from the point of view that the overwhelming majority of the nation's marine activities are performed within 200 miles of the U.S. coastline. The safety and economic success of those who work at sea, and of those who are involved with the husbanding of the quality of the marine resources along our coasts, depend upon an effective marine forecasting capability along our national coasts.

There were seven major findings from the study. While not all of them directly or specifically addressed coastal ocean prediction issues, all of them apply to some degree to the coastal problem. The issues of scale and variability in the coastal zone create a demand for observational capability, forecast technology, and a support infrastructure which is not now present. The fundamental findings of the committee were:

1. Management must be improved. The Committee felt that improvements in marine forecasting would be difficult or impossible without clearer national policies, and unless someone would assume the responsibility for implementing them.
2. Hurricane forecasting is adequate and should not be degraded. The thrust of this finding was twofold. First, the quality of the service is consistent with the state of the science; however, the practice of hurricane forecasting is highly dependent upon accurate positioning and meteorological measurements in a storm. The cost of adequate service is adequate reconnaissance.



3. More synoptic data are needed. The basis for good forecasting is good observations. This includes improved reporting systems, improved report collection infrastructure, and the use of ocean sensing satellites to improve oceanic coverage.
4. Improvements are needed in spatial and temporal resolution, and in forecast horizon. This requirement was of particular importance in the nearshore area (0 to 50 miles), where natural coastal variability results in highly variable local conditions under the same general synoptic conditions.
5. Improved dissemination systems and linkage to Navy marine facsimile broadcasts are needed. For forecasts to become more site specific and have higher resolution, the dissemination systems must improve. Should the Navy cancel their support of marine facsimile broadcasts, then there must be another service in its stead.
6. The need for new systems for forecasting internal ocean weather exists. The technology of describing the internal mesoscale variability of the ocean has progressed to the point where nowcasting of ocean processes is becoming practicable, with significant and sustainable benefits to a variety of commercial, military, and recreational oceanic activities.
7. Better knowledge is needed of "bomb" storms and "rogue" waves. The episodic wave and explosive cyclogenesis are phenomena of great concern to the shipping community.

The conclusions and recommendations of the Committee are fully supported by additional facts contained in its report.

## AGENCY MISSIONS, PROGRAMS, AND NEEDS

William C. Boicourt  
Horn Point Environmental Laboratory  
University of Maryland  
P.O. Box 775, Horn Point Road  
Cambridge, MD 21613

Coastal and estuarine waters have resisted attempts to extract general scientific principles of their circulation. Their shallow depths mean that they are prone to rapid change by wind forcing and strong control by topography. The resultant complexity and variability has not only hampered scientific description, but also increased the burden of federal and state agencies charged with research and management of these waters. Government agencies have the additional problems of disparity (and sometimes apparent conflict) of their missions and limitations or overlaps in their purviews. Given the uncertainty of the science and organizational constraints in the management realm, an inability to establish more cooperative programs in the coastal ocean is entirely understandable.

If a partnership program such as the Coastal Ocean Prediction System (COPS) were proposed in the dark ages (10 years ago), the likely reception in both the research and management communities would be rapid dismissal of the idea. In the intervening years, however, the environment has changed significantly. Not only has the pressure to manage man's effects on the coastal waters increased to almost crisis stage, but also the scientific tools required for this task have advanced to the point where real-time observation and modeling can be considered in practical terms. In spite of the disparity in agency missions, there appears a sufficient overlap in research and management needs to warrant a combined approach to the problem. Moreover, given the size of the task, cooperative programs will be necessary, even if substantial increases in management budgets are forthcoming. With increased environmental stress on coastal waters and an increasing capability of science to provide the needed descriptions and even predictions, now seems the opportune time to engage in such a combined attack.

The missions of the agencies responsible for research and management in the coastal ocean span a great range, from basic research to regulation. In the development phases of a COPS, the agency needs are remarkably homogeneous. A significant amount of basic research would be necessary for the design and construction of such a system. Once the system is in place, the cooperative advantages of the program would still be manifold. For instance, while the prediction system supported the targeted missions of the individual agencies, the associated observational resources would continue to supply basic research data. In this sense, the observing system would be analogous to the National Weather Service network of observation stations.



Conceptually, a program designed to provide real-time predictions on the motions and water quality of the coastal ocean would be of obvious benefit to the broad range of agency missions. The specific design, however, would have to be tailored and optimized to maximize the benefit to as many agencies as possible. To provide an overview of what the design criteria might be, a brief survey of agency missions has been conducted. The intent in this survey is to provide a statement of mission, an overview of present and near-future activities in the coastal ocean, and a short assessment of their needs that may be addressed by COPS.

### **National Science Foundation**

The primary mission of the National Science Foundation (NSF) is to fund basic research. The decision for this funding depends ultimately on the community of peers who review proposals for the Foundation. Traditionally, this community does not deem NSF as an appropriate agency for funding research on the applied end of the basic-applied spectrum.

The Ocean Sciences Research Section funds coastal research totaling \$21.1M per year, or approximately one-third of the Core Program. A total of \$10M supports coastal research facilities, primarily research vessels. Polar Programs spends approximately \$1M each on Arctic and Antarctic coastal research. In the nearshore and estuaries, Biotic Systems and Resources funds long-term cooperative research programs. Under the Long-Term Ecosystem Research (LTER) and Land-Margin Ecosystem Research (LMER) programs, \$2M is spent in the coastal ocean.

At present, \$5.2M per year is dedicated to coastal physical oceanographic research (35 grants). In the Informal Guide to prospective proposers to the Foundation, Coastal Ocean Dynamics is listed as an area of emphasis for present and future research. A prospective initiative called Coastal Physical Oceanography (CoPO) has been reconstituted as a coastal interdisciplinary research initiative called Coastal Ocean Processes (CoOP). Upcoming workshops are dedicated to reviewing the state of knowledge and planning future work.

The National Science Foundation would clearly benefit from COPS because such a program would expand funding in basic research in the coastal ocean, especially during the development phase. COPS would also provide a vehicle for application of NSF's basic research results.

### **Office of Naval Research**

The Office of Naval Research (ONR) funds basic research in areas of interest to the Navy. As a result, basic research is apt to be more targeted toward specific programmatic interests. ONR is therefore less heavily committed to research in climate and large-scale circulation than is NSF. These research issues are recognized as important, but ONR elects to emphasize research on temporal and spatial scales that are deemed more relevant to the Navy.

Within the Office of Naval Research, the programs of interest in the coastal ocean are organized under the Ocean Sciences Directorate. The sub-programs which fund the research are: Coastal Science, Geology and Geophysics, Arctic, Marine Meteorology, Acoustics, and Ocean Technology. ONR has two primary funding modes--the core program and Accelerated Research Initiatives (ARI's). ARI's are 5-year programs of increased funding to emphasize identified scientific areas of heightened interest. ONR anticipates level funding over the near future with new starts occurring after the closeouts of active programs. The core funding will remain stable for both programs and scientists. ONR also anticipates that the present 50-50 split of core and ARI funding will change in favor of a higher percentage of core. ONR presently funds coastal research at a level of \$5M annually, with \$2.9M coming from the Coastal Sciences program. Geology and Geophysics contributes \$1.3M in the coastal ocean and the remaining programs amount to \$1.1M.

ONR has broad interests in the coastal ocean, some of which are unique among the funding agencies. At present, the major ONR coastal programs are:

- Nearshore Processes
- Sediment Dynamics on the Shelf
- Arctic Shelves
- Shallow Water Acoustics
- Coastal Meteorology
- Shelf Dynamics
- Biophysical Modeling

Coastal Accelerated Research Initiatives are:

- Strait Dynamics
- Coastal Transitions
- Sediment Transport on the Shelf and Slope (STRESS)

The process-oriented studies will continue to produce new understanding which can be applied to COPS model development and evaluation. COPS models could also be used in planning and synthesizing ONR coastal studies.

#### Department of Energy

The marine research program supported by the Office of Energy Research, Ecological Research Division, is aimed at providing scientific information on major environmental issues facing expansion of energy development and development of energy technologies. Research associated with these activities is concentrated along the coastal margins. The primary focus of the Coastal Ocean Margins program is the formation, transport, and ultimate fate of particles, whether naturally occurring, or produced by energy-related activities. This focus has been a theme in coastal research sponsored by the Department of Energy (DOE), even in the earlier days of the Atomic Energy Commission.



At present, the DOE research is organized primarily into three regional programs. On the Northeast shelf, the Shelf Edge Exchange Program (SEEP) is funded at the annual level of \$2.7M. The longer-term South Atlantic Bight (SAB) study is funded annually at \$1.4M. The relative newcomer to the program is the California Basin Study (CaBS), where \$1.6M is spent annually. These programs are designed from the outset as interdisciplinary approaches to the problem.

For the future, DOE has proposed the Continental Ocean Margins Flux Study (COMFS) to address the role of the coastal ocean in the transport and fate of water-borne materials. Of specific interest are: 1) sources and sinks within the continental margins, 2) fluxes between margins and the oceanic interior, and 3) global cycle transformations. For this reason, this program would fill an important gap in the Joint Global Ocean Flux Study sponsored by NSF. The substantial expertise of DOE programs in coastal ocean exchange processes could be applied to COPS model formulation and evaluation. In turn, COPS models could be used to help synthesize DOE program observations. Also, DOE has developed observing systems which could be considered for adoption by COPS.

#### **Department of the Interior, Minerals Management Service**

The Minerals Management Service (MMS)'s mission is to make Outer Continental Shelf (OCS) energy resources available to meet the Nation's energy needs. To perform this mission, the MMS leases federal offshore acreage. Before leasing can occur, the MMS must gather information and prepare an Environmental Impact Statement (EIS). MMS studies the physical oceanography of the coastal ocean to support the need to make an informed decision and to support the analysis for the environmental documents. In addition, operational safety is also a consideration when contemplating development of the OCS.

The development of the EIS document takes place in four regional centers, the Pacific, Atlantic, Gulf of Mexico, and Alaska. The physical oceanography programs are sponsored through the Branch of Environmental Studies in Herndon, Virginia and administered at the regional level through regional Environmental Studies representatives. The information is used in oil spill transport modeling at the Branch of Environmental Modeling in Herndon, Virginia. Observations for coastal physical oceanography are used by staff preparing the EIS documents at the regional level.

The MMS sponsors many programs in each of the four regions to address the information needs. In general, they have sponsored the development of circulation models off California, the Atlantic, Alaska, and in the Gulf of Mexico. In addition, there are large observational programs conducted in these regions. Some examples of ongoing and recently completed programs are listed below:

- Ocean Circulation of Atlantic Coast Modeling Study
- Frontal Eddy Dynamics Study
- Circulation of S. California Bight Modeling Study
- Northern California Coastal Circulation Study



While many basic modeling research programs and observational projects have been sponsored by MMS, through the environmental studies program, continued research is still needed. At the Galveston Workshop in 1986, regional oceanographers gathered to begin the planning process for the coincident Louisiana/Texas observational field program and Gulf of Mexico modeling program. In addition, the MMS has been conducting a series of Lagrangian studies to develop a Lagrangian database and a means of assessing the accuracy and precision of trajectory simulations. The MMS foresees a continuing need to develop and implement state-of-the-art circulation and oil spill transport modeling while continuing and increasing the database of observations in support of understanding the circulation and supporting the modeling and risk assessment in specific regional areas. The MMS programs have developed databases and models which can be of use to COPS, and, conversely, the improved databases and models in prospect from COPS could aid MMS.

#### Department of the Interior, United States Geological Survey

The primary mission of the United States Geological Survey (USGS) is earth sciences research. The USGS has many programs in the coastal ocean, ranging from physical oceanography, to sediment transport and coastal geology. The main focus of these programs is sediment transport, the flow structure in the benthic boundary layer, and shore erosion. Other programs of importance to the coastal ocean are streamflow monitoring and research, and the measurement and prediction of bottom stress. The product of both of these programs is of crucial value to the development of a Coastal Ocean Prediction System. For this reason, the USGS sees itself primarily as a resource for the development of such a system, rather than an end-user. For example, USGS expertise in bottom stress could be applied to improving COPS models. However, the improved data bases and circulation models offered by COPS could be applied to sediment transport models by USGS to mutual advantage.

#### National Aeronautics and Space Administration

The primary focus of the Oceanic Processes Program of the National Aeronautics and Space Administration (NASA) is on global ocean measurements in support of deciphering the ocean's role in climate. The present focus of efforts for this purpose are: 1) the measurement of ocean circulation with altimetry, 2) the measurement of air-sea fluxes of momentum with scatterometry, and 3) the measurement of heat and moisture fluxes with microwave and infrared radiometry. These activities are therefore focused primarily on the open ocean. At present, the resolution of the physical sensors on satellites are in general inadequate for the coastal ocean. The obvious exceptions are the Advanced Very High Resolution Radiometer (AVHRR) thermal measurements and the Coastal Zone Color Scanner (CZCS)/Compact Wide-Field Scanner (Sea-WiFS). For the coastal ocean, the best present remote sensing capability comes from airborne instruments, such as the Airborne Optical Light Detection and Ranging (LIDAR) (AOL) for measurement of chlorophyll, the NU-labelled scatterometers (NUSCAT) and C-labelled scatterometers (C-SCAT) for measuring winds, the Radar Ocean Wave Spectrometer (ROWS) for measuring wave spectra, and the



Electronically Scanning Thinned Array Radiometer (ESTAR) capable of measuring surface salinity to approximately 0.5 psu. While NASA has the capability to develop shore-based radar systems for sensing currents and waves, the National Oceanic and Atmospheric Administration (NOAA) Wave Propagation Laboratory in Boulder has ongoing programs in this area.

The proposed Earth Observing System is a candidate for a new start in FY 1991. This program would feature a suite of new instruments which would add significantly to the ocean measurement capability.

Though satellite remote sensing systems may not be well-focused on the coastal ocean, they will be vital for determining the seaward open boundary conditions for COPS.

### U.S. Army Corps of Engineers

The U.S. Army Corps of Engineers (USACE or Corps) mission in the coastal ocean is in the following areas:

- Flood Damage Prevention
- Navigation
- Environmental Regulation
- Emergency Operations

Hurricane storm-surge prediction and damage minimization is the main concern of the first effort. USACE has primary responsibility in the development and maintenance of ports and coastal channels. The Corps also has responsibility in the wetland permit process and the construction of permanent coastal structures. Emergency operations refers to activities in support of disaster relief. The primary interest is in shallow coastal waters (less than 20 m deep), bays and estuaries. Deeper waters may be of interest as an area to dispose of dredged materials. Extensive observational programs are carried out to support construction and verification of numerical models. Forecast models have proved useful for scheduling operations, especially emergency operations. Hindcast models are used to develop synthetic climatology where data are not available or to simulate critical events. A major use of models is in Corps project evaluations. Here, very high resolution in time and space is employed to evaluate the effects of flow and waves on structures. Models in current use include:

- Tsunamis
- Storm Surge
- Wind-Wave Generation
- Wind-Wave Propagation
- Wind Stress
- Circulation and Water Level
- Water-Quality
- Sediment Transport

The primary interest in tsunami and storm-surge modeling is the concern for the effects of coastal inundation. Directional-spectra wave models and wave-propagation models are of interest for both their effects on structures and their effects on coastal sediment transport.

A program, Surface Wave Dynamics Experiment (SWADE), is planned for the fall of 1990. The objective of the program will be to improve the understanding of wind wave evolution under rapidly changing winds. The experiment is planned for the edge of the continental shelf between the Chesapeake and Delaware Bays. Instrumentation will include wave and wind sensors, aircraft overflights and joint efforts with NASA and ONR in the modeling component.

Since the Corps is a leader in computational fluid dynamics as applied to the coastal ocean, it has a great deal of expertise to offer COPS. In return, COPS could provide the Corps opportunities to evaluate its models in the context of expanded data sets and alternative models.

#### **U.S. Environmental Protection Agency**

The Environmental Protection Agency (EPA)'s primary responsibility in the coastal ocean is regulatory, mandated by the Clean Water Act and the Ocean Dumping Act (Marine Protected Resource Sanctuary Act). Within this purview, there are three ongoing programs:

- Coastal Prediction
- National Estuaries Program
- Gulf of Mexico Program

The coastal prediction program's goal is to predict the effect of pollutants on the coastal ocean and thereby increase the efficiency and effectiveness of the EPA's regulatory efforts. The National Estuaries Program has developed a baseline assessment of the water quality of important United States estuaries. A new major effort along this line is the Estuarine Mapping (EMAP) program, whereby the assessment methodology is being both developed and applied. EPA is also potentially interested in model simulations of the coastal ocean's response to possible climate change scenarios, including changes in terrigenous inputs, which would benefit from a COPS program. COPS could also assist EPA in designing effective and efficient monitoring networks, and COPS could benefit from access to EPA's databases.

#### **U.S. Coast Guard**

The U.S. Coast Guard (USCG)'s responsibilities in the coastal ocean are broad and varied:

- Search and Rescue
- Oil-Spill Response



Oil-Spill Cleanup  
Marine Safety  
Marine Defense Zone  
Law Enforcement

Each activity has specific needs for accurate marine environmental data. The Coast Guard has a variety of programs to support these needs. The Coastal Weather Program maintains a flow of synoptic weather reports from shore stations to the National Weather Service Forecast centers. Observations from trained observers and measuring systems aboard Coast Guard cutters and ice breakers contribute reports to the Fleet Numerical Oceanography Center. The Navy/Coast Guard Cooperative Bathythermograph (XBT) Program obtains synoptic expandable bathythermograph (XBT) profiles four-times daily from law-enforcement cutters and ice breakers. The Coast Guard also supports the National Data Buoy Center by providing logistical support, servicing and retrieval of moored buoys. In addition the Coast Guard has a program of satellite-tracked surface drifters to improve the surface-current data base. These drifters are primarily deployed in data-sparse areas to support iceberg drift predictions in the Northwest Atlantic.

The proposed Coastal Ocean Prediction System would be in concert with the identified need within the Coast Guard for better real-time circulation and watermass information to support its many missions. The Coast Guard has suggested that the Office of the Federal Coordinator for Meteorological Services might serve as a useful model for interagency coordination in this regard.

### **National Oceanic and Atmospheric Administration**

The National Oceanic and Atmospheric Administration and its predecessors have a long history of measurement in the coastal ocean, extending well back into the 19th century. NOAA's mission in physical oceanography in the coastal ocean, common to NOAA's many programs, is to provide decision-makers with four types of information: data and research results; predictions of long-term and large-scale earth system responses; forecasts and warnings of short-term episodic events; and advice and comments on utilization of earth system resources.

Several NOAA offices have programs in the coastal ocean. For example, the Coastal Ocean Program Office, part of the NOAA Chief Scientist's Office, administers the budget process, recommends resource allocations, assists with program development, and reviews and coordinates input from line offices. Four research labs (Atlantic Oceanographic and Meteorological Laboratory (AOML), Great Lakes Environmental Research Laboratory (GLERL), Pacific Marine Environmental Laboratory (PMEL), Geophysical Fluid Dynamics Laboratory (GFDL)) perform modeling and observational research programs in the coastal ocean. At least two of the NOAA Joint Institutes (Cooperative Institute for Research in Environmental Science (CIRES) (w/ Univ. of Colorado) and Joint Institute of Marine and Atmospheric Research (JIMAR) (w/ Univ. of Hawaii)) perform cooperative government and university science in the coastal ocean.



The National Ocean Service (NOS) is the major Line Office in NOAA dealing in oceanography and marine environmental areas. It is the responsibility of NOS to coordinate and conduct observations of physical, chemical and biological variables and monitor marine environmental changes in the ocean and U. S. coastal waters. As one of its important mission functions, NOS provides the Nation with marine environmental information and services, especially for the civil sector. Many offices in NOS are currently carrying out coastal field observations, pollution monitoring, sea level networking, marine data analysis, and modeling activities in some estuaries and harbors. The Hazardous Materials Program (HAZMAT) office in Seattle, WA has developed an applications model for on-scene prediction of oil spill trajectories. The Estuarine and Ocean Physics Branch is developing the real-time capability for observing and modeling of water levels and currents in some estuaries and harbors. The Office of Ocean Services plans to enhance the global and coastal observational networks, and to initiate a marine environmental data assimilation and modeling system program. A NOAA Ocean Communication Network (NOCN) has been established to address the data flow and information exchange needs among the ocean scientific user community and the NOAA scientific laboratories and ocean service centers. A micro Vax-based Interactive Marine Analysis and Forecast System (IMAFS) has been developed to meet the needs for an inexpensive digital graphic workstation for display and manipulation of atmospheric and oceanic data, as well as model output. These efforts will contribute significantly to the advancement of the coastal ocean operational predictive capability. In addition, NOAA has established the Ocean Product Center (OPC) in Washington, D.C. and the Center for Ocean Analysis and Prediction (COAP) in Monterey, California to support and conduct activities that pertain to coastal ocean operational observations and modeling.

The National Marine Fisheries Service (NMFS) is active in coastal physical oceanography because of the strong impact physical ocean variability has on fisheries. The National Environmental Satellite Data and Information Service (NESDIS) maintains major data archives at the National Oceanography Data Center (NODC). The National Weather Service (NWS) operates the National Data Buoy Center (NDBC) and has a strong involvement in marine forecasting in the coastal ocean.

The Coastal Ocean Program consists of the following sub-programs under these sub-headings:

Prediction of Coastal Ocean Degradation and Pollution:

National Status and Trends  
Habitat Alteration and Pollution  
Nutrient-Enhanced Coastal Productivity

Living Marine Resources:

Stock Assessments  
National Sea Grant Program  
Fisheries Oceanography Coordinated Investigation  
Interactive Marine Analysis and Forecast System



Protection of Life and Property in Coastal Areas:

Warning and Forecast Systems

Pre-Disaster Planning

Changes in Coastline

Advanced Marine Observation Technology

Data Synthesis and Information Transfer

Importantly, the Coastal Ocean Program has activities which will use models, real-time observing systems, databases and the infrastructure and resources inherent to NOAA.

Overall, the operational mission and thrust of NOAA in the coastal ocean provide the most direct and immediate need for COPS. In turn, COPS offers NOAA some of the needed linkage to other agencies' programs, academic and private sector expertise, and a fully national capability and approach. Also, NOAA's research arms have had successful experience in relating academic research to mission-oriented applications and operations, as is central to COPS.

## OPERATIONAL AND APPLICATIONS MODELS

Christopher N. K. Mooers  
Ocean Process Analysis Laboratory  
Institute for the Study of Earth, Oceans and Space  
University of New Hampshire  
Durham, NH 03824-3525

### Introduction

Today, a few agencies have operational and applications models for the coastal ocean:

National Oceanic and Atmospheric Administration (NOAA);  
United States Coast Guard (USCG);  
Minerals Management Service (MMS);  
United States Army Corps of Engineers (COE); and  
Environmental Protection Agency (EPA).

In the future, it is likely that these agencies will acquire additional, improved, and broader models, and other agencies may acquire models for operations and applications, as well as for research. Here, the objective is to characterize the agencies' interests and activities in operational and applications modeling, and to summarize their present status.

### National Oceanic and Atmospheric Administration

NOAA is responsible for providing operational oceanic predictions to the civil sector in general, and for the coastal ocean in particular. In these matters, NOAA collaborates closely with the U.S. Navy (USN). At present, NOAA has two national centers engaged in data product development and dissemination: the Ocean Product Center (OPC) at the National Meteorological Center (NMC) of the National Weather Service (NWS) and the Center for Ocean Analysis and Prediction (COAP) at the Fleet Numerical Oceanography Center (FNOC) of the Naval Oceanography Command. Both NMC and FNOC are major operational centers equipped with supercomputers, global telecommunication networks for the reception of real-time data and dissemination of operational data products, data archives, and suites of operational models, which are primarily meteorological in nature. No oceanic General Circulation Models (GCMs) are being run operationally at either NMC or FNOC at present, though current R&D efforts are aimed in that direction. However, there are ocean thermal structure analyses available on a regular basis (i.e., on standard space-time grids) for the upper 400m of the ocean. These products are basically created by melding sparse, near-real-time data with climatological databases. In some cases, a one-dimensional mixed layer model is used to make prognostications, -- sometimes with the aid of schemes for geostrophic and Ekman heat advection. FNOC also provides analyses and forecasts of wind waves and ice coverage and thickness in selected areas. However, there are no products available with adequate resolution for the coastal ocean.



In addition, the National Ocean Service (NOS) has an operational modeling capability which is deployed in support of actual pollution events; e.g., oil spills. It consists of a diagnostic circulation model, which uses climatological mass fields to calculate geostrophic flows and operational winds to calculate Ekman flow and wind drift. It is used to provide nowcast/forecast support to the USCG on-scene commander for such events. NOS has used this capability on numerous occasions, and in many coastal ocean regions; it has reportedly been successful in many instances.

NOS also has applications models for tidal heights and currents in several bodies of water, including Delaware Bay, New York Harbor, and Long Island Sound. Some have been demonstrated in an operational mode, but then set aside as being ahead of their time. Others may be under development. In some cases, the models deal with density stratification and turbulent boundary layers, and, thus, they are able to treat estuarine circulation and wind response, too.

### Minerals Management Service

MMS is concerned with developing Environmental Impact Statements (EISs) associated with proposed oil and gas exploration and production activities on the outer continental shelf. For these purposes, probabilistic information on the advective and diffusive characteristics of numerous regional regimes is required, as well as for specific sites when they are determined in the latter stages of these activities. This information is used in estimating the risk of oil spills from specified locations impacting specific shoreline domains. The method of analysis is termed Oil Spill Risk Assessment (OSRA), (Amstutz and Samuels, 1984). Some of the necessary information is acquired through observations; other portions are obtained through statistical or dynamical models. Hence, MMS operates primarily in the simulation mode, though it could work beneficially in the data-assimilative hindcast mode. It has begun to work with real-time observing systems for the overall quality control of its regional studies program.

The time scales of concern are hours to days or weeks; thus, it is essential to resolve mesoscale phenomena; e.g., offshore eddies impinging on the shelfbreak, coastal fronts and jets, and the coastal boundary layer.

The MMS has developed regional models for the

- Middle Atlantic Bight (Dynamics),
- South Atlantic Bight (Dynamics),
- California Coast (Dynamics),
- Santa Barbara Channel (Dynamics),
- Gulf of Maine/Georges Bank (Applied Science Associates (ASA)),
- Gulf of Mexico (Jaycor),
- Gulf of Alaska/Bering Sea/Beaufort-Chukchi Seas (Rand), and
- Gulf of Alaska/Bering Sea/Chukchi Seas (ASA)



using the Dynalysis of Princeton GCM, which is now being applied to the Southern California Bight. A decade ago, MMS developed a model for the Gulf of Maine/ Georges Bank region using the ASA GCM. They are also developing a model for the Gulf of Alaska/Bering Sea region using the Greenhorne and O'Mara GCM. In most of these regions, MMS has sponsored an observational program to greatly increase the relevant database, but these programs have not generally been coordinated with the modeling projects, which has complicated model development and evaluation. However, MMS is moving to coordinate such activities in the future, and possibly in its upcoming coastal ocean studies in the Gulf of Mexico.

#### **U. S. Coast Guard**

USCG has responsibilities for search-and-rescue which dictate that it be able to at least nowcast if not forecast currents for limited space and time domains. Hence, USCG is very involved in using Management Information Systems (MIS) to synthesize a variety of data types from a variety of sources. At the present time, it does not use dynamical-numerical models.

A special subset of this activity concerns oil spills, where USCG is responsible for supervising clean-up activities. For oil spill events, NOAA provides operational forecasts of oil spill trajectories to USCG.

By the nature of its mission, the USCG is interested in deployable observing systems which can greatly enhance the ordinarily-available density of observations.

#### **U. S. Army Corps of Engineers**

COE maintains a major facility, the Coastal Engineering Research Center (CERC) at the Waterways Experiment Station (WES) in Vicksburg, MS, for observational and modeling activities in the coastal ocean. They possess a supercomputer center, now a CRAY YMP, and a significant numerical modeling group. They develop and apply datasets and models to problems in wave hindcasting, beach erosion, sediment transport, estuarine circulation and water quality, and related topics. Their applications are to environmental engineering designs for ship channels, flood control, waste disposal, and related earthworks. As COE's activities extend onto the continental shelf and beyond, they inevitably encounter, and become involved in, a broader set of coastal ocean circulation issues. In the future, they could develop an operational use for wind, wave, and current forecasts to guide, for example, their dredging operations.

#### **Environmental Protection Agency**

EPA, with the assistance of the COE, has developed a circulation and water quality model for the Chesapeake Bay. Presumably, the purpose of this model is to



guide environmental management decisions. It seems reasonable to anticipate many more such estuarine model developments as EPA addresses its environmental management responsibilities.

## Summary

The present operational and applications modeling capability can be summarized by placing it in the following categories: data products and trajectory models.

Some thermal structure data products are produced and used in real-time by NOAA (USN). Some current products are available, too. USCG has some MIS capability to support its real-time operations. A broader set of data products is provided by NOAA in delayed-time. However, GCM's are not used, and there is a general lack of resolution in the products for the purposes of operating effectively in the coastal ocean.

Trajectory models, which may use a circulation model as well as climatological currents and synoptic or climatological winds, are used in real-time by USCG, NOAA, and the Navy for search-and-rescue operations and by NOAA and USCG for oil spill events. In delayed-time, MMS and NOAA use these models for reconstruction of past oil spill events. MMS also uses these models for their major task of oil spill risk assessment.

These models, or their later generation versions, could conceivably be used for marine ecosystem analyses or as research tools for process studies, if they were to be evaluated as of sufficient quality.

Noteworthy is that both NOAA and MMS utilize nearly identical large-regional domains, viz., Atlantic Coast, Gulf Coast, Pacific Coast, and Alaska Coast. They also find it necessary to organize their endeavors by smaller-regional subdomains in order to achieve sufficient resolution and focus.

# CIRCULATION MODELING NEEDS OF DAMAGE ASSESSMENTS\* UNDER CERCLA LEGISLATION

Mark Reed  
Applied Science Associates, Inc.  
70 Dean Knauss Drive  
Narragansett, Rhode Island 02882

## Introduction

The Comprehensive Environmental Response, Compensation, and Liability Act of 1980 (CERCLA), allows for compensation by a polluter for costs associated with spill response and damages to natural resources. In the event of a discharge of oil or release of a hazardous substance, the polluter can be required to compensate public and private parties for the cost of responding to and cleaning up the discharge or release. In addition, the affected state or the federal government, in its role as trustee, can assert a claim for compensation for injury to, destruction or loss of natural resources, and for the reasonable cost of conducting a natural resource damage assessment.

The potential applicability of CERCLA is broad in terms of (1) the substances included, (2) the natural resources covered, (3) the potential natural resource damages to be assessed, and (4) the geographic area encompassed by the law. The substances to be considered under CERCLA include any hazardous substance as defined in Section 101(14) of the Act, including those described in relevant sections of the Clean Water Act, the Solid Waste Disposal Act, the Clean Air Act and the Toxic Substances Control Act. Hence, literally hundreds of substances potentially fall within the purview of CERCLA.

CERCLA defines natural resources as "...land, fish, wildlife, biota, air, water, ground water, drinking water supplies, and *other such resources* [emphasis added] belonging to, or otherwise controlled by the United States (including the resources of the fishery conservation zone established by the Fishery Conservation and Management Act of 1976), any state or local government, or any foreign government" (Section 101(16)). Clearly, the listing of natural resources covered by the law is large. Discharge-related injury to virtually any natural resource under the jurisdiction of a federal or state trustee could fall under CERCLA.

The potential injuries to natural resources encompassed by CERCLA also are extensive. Direct and indirect injuries, short- and long-term effects, and the ability of the ecosystem or resource to recover all are to be considered in assessing natural resource damages.

---

\*Editorial note: Although this manuscript does not discuss circulation modeling needs quantitatively, it does so qualitatively and illustrates an area of application which needs more formal development.



Finally, all natural resources under the jurisdiction of the federal government, its territories or possessions, and the states fall within the law, including the natural resources of all navigable waters, waters of the contiguous zone and ocean waters where the natural resources are under the management of the United States. The entire geographic area to which CERCLA applies is potentially over twice the size of the land mass of the fifty United States and involves a wide variety of different climates and environments.

CERCLA allows for both simple (type A) and complex (type B) damage assessment methodologies. The type A category of natural resource damage assessments is intended to apply to incidents for which the benefits of a detailed, site-specific, type B assessment of natural resource damages are judged not to be cost-effective.

Type B natural resource damage assessments, on the other hand, apply to site-specific incidents involving complex situations or extensive discharge of oil or releases of hazardous substances into the environment. In contrast with the type A damage assessment approach, the type B approach could involve surveys and field studies over an extended period, and could be quite costly.

Pollutant transport modeling is an essential component of all damage assessments under CERCLA. Type B assessments in marine and freshwater environments generally include the application of site-specific, two- or three-dimensional hydrodynamic models to supply the current data to the transport model. Type A assessments, as discussed below, have been much more modest in their input requirements. Future improvements in the type A models, however, will expand the need for site-specific current fields.

### Overview of the First Type A Model for the Marine Environment

The first type A model system (Fig. 1) is composed of three major components: physical fates, biological effects, and economic damages submodels (Reed et al., 1989). (This model will be superseded within the next year or so by a more advanced version, described later.) The user enters a chemical identification number and the amount spilled. The model obtains a set of chemical parameters from the chemical database (Feng et al., 1989), which presently consists of more than 460 substances, including crude oils and petroleum products. These parameters, which are required to run the physical fates model, include density, solubility, molecular weight, adsorbed/dissolved partition coefficient, viscosity, degradation rates in water and sediments, and vapor pressure. Based on these parameters, the submodel determines how much of the spilled substance evaporates into the atmosphere, spreads as a surface slick, is dissolved in the water and settles to the bottom.

The physical fates submodel (Reed, 1989) simulates the transport of the pollutant on the water surface (as a slick), in the upper and lower water column, and in the sediments. A surface slick spreads and is transported by wind and currents, with continuous evaporation into the atmosphere, and entrainment and dissolution into the water column. If the slick meets a shoreline, it is assumed to collect there.



A spilled substance entrained or dissolved into the water column is dispersed by horizontal and vertical mixing and is transported by currents. A portion of the dissolved substance may be adsorbed onto suspended particulate matter. These particles will sink to the bottom at a certain rate such that dissolved substances eventually will reach the sediments. A heavy substance will sink directly to the bottom. The material which reaches the seafloor is mixed into the sediments using a simple mixing model. The submodel also includes evaporation from the dissolved state into the atmosphere.

The water column is divided into two layers, upper and lower, so that different densities may be specified in each to simulate stratified conditions. The user must specify values for mean and tidal current velocities, and average wind speed.

The physical fates submodel calculates concentrations in space and time in each of the upper water column, lower water column, and sediments. The area covered by a surface slick (if applicable) also is calculated. This information is passed to the biological submodel, which then calculates the biological effects of those concentrations.

The biological effects submodel (French and French, 1989) receives data from three sources: the physical fates submodel, the toxicological section of the chemical database, and a biological database. The biological effects submodel calculates both short-term and long-term biomass losses, passing these data to the economic damages submodel. Short-term biological losses can fall into two categories: death of adult organisms and lost productivity. Long-term losses treated by the model include lost recruitment due to larvae and juveniles killed, and lost growth of adults killed.

To determine biological losses, the biological submodel utilizes estimates of the abundances of fish, shellfish, birds and mammals, and the productivity of plant and animal communities at the base of the food chain in the environment of the spill. Since specific data are not available for every possible spill location in the U.S., biological data were compiled and averaged by habitat and geographical area. For each of the geographical provinces along the coastline (for example, north of Cape Cod, Cape Cod to Cape Hatteras, Cape Hatteras to Cape Canaveral), habitats are defined by estuarine versus marine, intertidal versus subtidal, and bottom or dominant vegetation type.

Death of fish and shellfish adults, juveniles and larvae is based on exposure of these organisms to the spilled substance and acute toxicity data (as LC50, concentration lethal to 50% of the organisms exposed for 96 hours) contained in the chemical data base. Mortality is a function of concentration, temperature and time of exposure. Exposure time by entrainment into the toxic plume and by active swimming into and out of the affected area is determined by using a random diffusion model and typical swimming speeds of each age and species category.

The biological submodel calculates the biomass of each species killed. Mortality is highest at the center of a spill, where concentration is highest,



decreasing outward until a threshold concentration is reached, below which mortality is zero. The submodel calculates mortality not only over area, but over time, until the concentration of the spilled chemical has everywhere fallen below the threshold concentration. Organisms which are killed in a spill, but which have no direct economic value, are accounted for in a productivity, or food web, section of the biological effects submodel. Plant EC50 values (pollutant concentration which reduces growth rate by 50%) are passed from the chemical database, enabling calculation of lost primary (phytoplankton or other plant) production. This loss is passed partially through zooplankton, partially through the benthos, and is ultimately expressed as a loss of economically valuable species (by biomass) due to loss of potential food. Direct losses of zooplankton are also calculated and passed through the food web to calculate resulting upper trophic level losses.

Long-term losses include lost recruitment of larvae and juveniles into the adult population, and lost future growth of adults. More complex changes, such as alterations of food chains, and chronic effects, such as loss of reproductive potential, are not considered. Such changes require more data to model than are currently available and, in the model, are assumed not to result from small spills.

The economics submodel (Grigalunas et al., 1989) calculates *in situ* use values for commercial and recreational fisheries, for hunting and for non-consumptive uses such as viewing. Fish and shellfish catch losses are allocated between commercial and recreational uses, using estimates of the relative weight of commercial and recreational landings by species and by region. Ex-vessel fish prices (prices at the dock), averaged over three years, are used to evaluate damages. Catch data and prices for commercial fisheries are from National Marine Fisheries Service sources, and prices for recreational sports fishing are adapted from the literature.

Damages resulting from injury to lower trophic, non-commercial organisms are based on the ultimate loss in the *in situ* use value of predator species (commercial and recreational fisheries, waterfowl and shorebirds, and marine mammals) which occurs when an incident affects the productivity of the food web. The submodel quantifies the biological injuries which arise over time as a result of the incident. Economic damages are measured using the concepts and data applicable to commercial and recreational fisheries, to waterfowl and shorebirds, and to marine mammals.

Injury to waterfowl and shorebirds results in losses of consumptive (hunting) and non-consumptive (e.g., viewing, photographing) *in situ* use values. The quantification of biological injury to waterfowl and shorebirds is an output of the biological effects submodel. Damages resulting from losses of consumptive use are measured using available estimates of the marginal value of an additional waterfowl (duck or goose) harvest. Damages arising from losses in non-consumptive use for non-game species are measured by employing an estimate of the marginal change in visitor days associated with a change in bird population for a wildlife refuge. The resulting estimates of lost visitor days then are evaluated based on a unit day value published by the Water Resources Council.



Damages caused by injury to public beaches are measured by the lost *in situ* use value, and depend upon the season, the type of public beach affected and the extent and duration of the injury. The user specifies the location and season of the incident, the type of beach affected (national or other public beach), and the amount and substance spilled. For oil spills, the physical fates submodel determines the extent of beach impaired and the time to removal by natural processes. If cleanup operations are carried out, the user must specify the time of cleanup and the quantity removed. For spills of other substances, the user must specify the length of beach affected and the time to recovery either through natural processes or cleanup.

### The Type A Model for the Great Lakes

The present version of the type A model now under development for the Great Lakes incorporates a geographic information system and a two-dimensional, vertically averaged hydrodynamic model for time-dependent wind-driven flows (Fig. 2). Thus the Great Lakes model is much more site-specific and realistic than its predecessor for the marine environment. The next update of the marine model will probably include many of the improvements being built into the Great Lakes model, including wind time series and two-dimensional current fields.

### Circulation Input Needs for Type A and Type B Methodologies

The development of type A and B methodologies requires that they be based on "best available" information, consistent with the level of effort being expended on the damage assessment. It is clear that both types of assessments could be greatly improved if there existed a reliable, readily accessible database of surface winds and currents for U.S. coastal and inland waters.

If these data were easily available in a uniform format, the type A models could be streamlined to take advantage of them. The increased quality of damage assessments based on these new data would permit broader application of the simpler type A assessments, and a potentially significant reduction in costs as compared with type B assessments.

Ideally, the surface wind and current data would be in the form of synoptic time series, akin to numerical fields produced by the National Weather Service, or the Fleet Numerical Oceanography Center for winds. One avenue to create this database would be to establish a national center to run and update the models, archive the data, and serve user requests. The costs of such an undertaking are non-trivial. An alternate approach would be to establish a center which would hindcast surface winds and currents for user-specified domains on an "as-needed" basis. This approach would certainly be more cost-effective, and could in fact be self-supporting, since the costs would be carried ultimately by the polluter, as part of the overall cost of the damage assessment.



## Summary

The number of natural resource damage assessments being performed probably will increase sharply in the next few years, as more state and federal trustees of natural resources come to understand and apply the CERCLA regulations for damage assessment. These trustees are in general ill-prepared to plan and oversee complex damage assessments. They will therefore continue to turn first to the type A models. This simpler methodology will become the avenue of choice to the extent that the type A assessments are credible, in the sense that they produce results comparable with more complex type B assessments.

Significant improvement in these assessments could be realized if there were a reliable source of wind and current time series data for input to the assessment models. Whether production of this data is an ongoing enterprise, or is performed on an as-needed basis, will depend on the number of other users. The people performing natural resource damage assessments under CERCLA, at least, represent a present and increasing community of potential users. The CERCLA damage assessment methodologies are mandated to be updated every two years; thus, future incarnations of the type A models will be tailored to new databases or sources as they become available.

---

Editorial note: The application of models to the CERCLA problem of compensation for natural resource damage is still in its infancy. The model Reed describes is one example of a comprehensive effort, but by no means the only one. One problem is that the error propagation in such an exercise has not been addressed. The model described has many assumptions built into it--from the ocean physics to the "lost visitor-days". This "comprehensiveness" leads to its use by lawyers as a black box: "Answer all the questions and you get a dollar value out of the system." The ocean model alone has sufficient errors and uncertainties built into it that an error analysis should be part of such a system.

## MODEL SYSTEM OVERVIEW

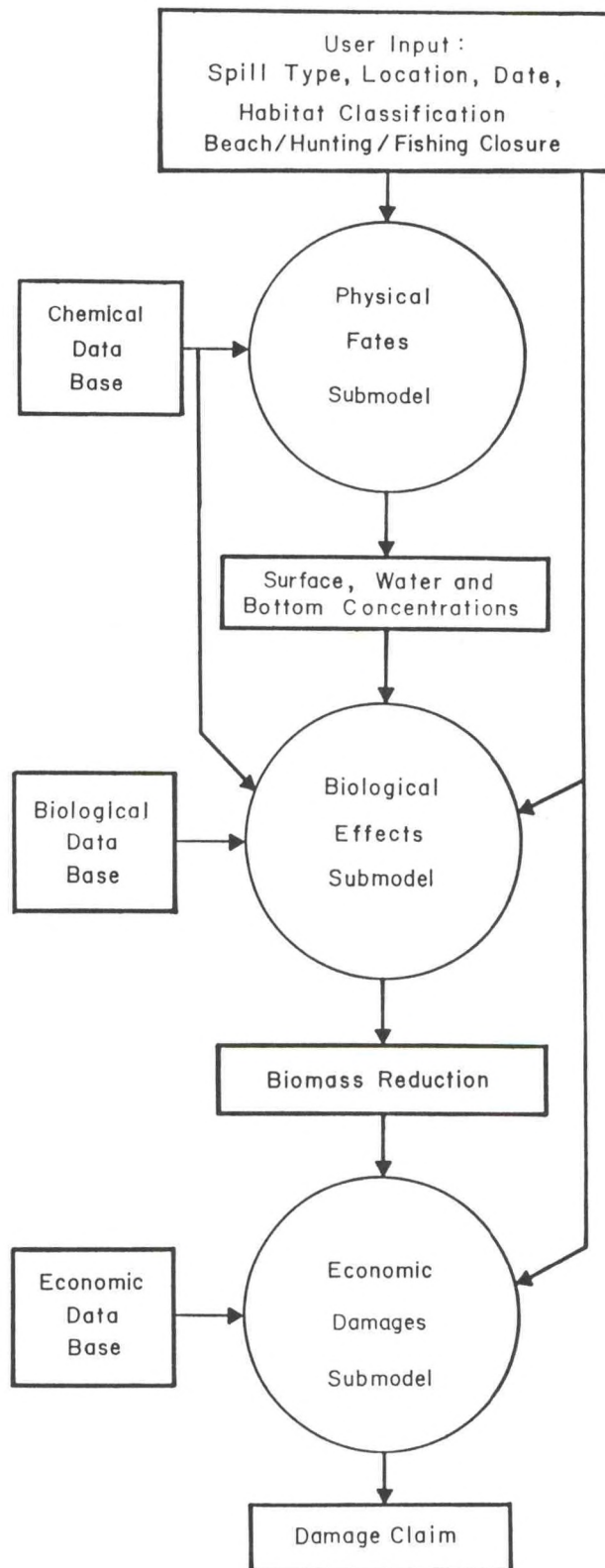


Figure 1. Overview of the Natural Resource Damage Assessment Model for Coastal and Marine Environments (NRDAM/CME). (Source: Reed et al., 1989, p. 87.)



# MODEL SYSTEM OVERVIEW

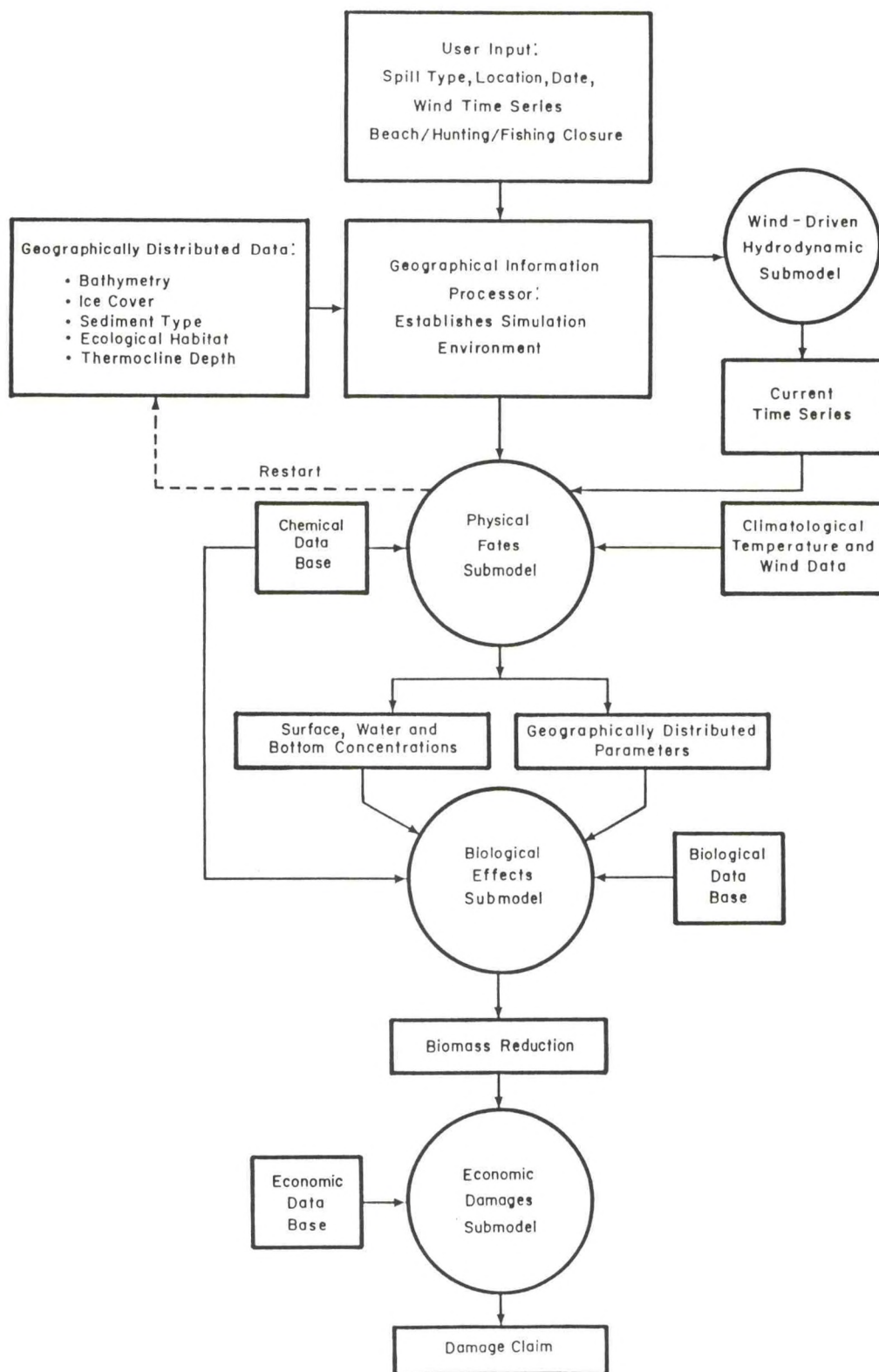


Figure 2. Preliminary overview of the Natural Resource Damage Assessment Model for Great Lakes Environments (NRDAM/GLE).

## RESEARCH MODELS

John S. Allen  
College of Oceanography  
Oregon State University  
Corvallis, OR 97331

### Introduction

A properly verified coastal circulation model would be of obvious value for oceanographic studies of the continental margin. Coastal circulation models may take different forms, depending on the objectives for their use and the type of region to be studied. By 'coastal circulation model,' we generally mean a limited-area continuously stratified numerical model covering a geographical region that extends 100-to-400 km or more alongshore and extending offshore from the coast to a point beyond the outer edge of the continental slope. Such a model would resolve time scales of days to months, horizontal space scales of 5 km or less, and vertical scales of 10 m or less. Forced by appropriate atmospheric variables or buoyancy sources and solved with proper boundary conditions, these circulation models would presumably represent the important dynamical processes over the continental shelf and slope with sufficient accuracy to provide scientifically valuable information on the space- and time-dependent velocity, temperature, and salinity fields.

At the present, this type of verified modeling capability generally does not exist. The development of limited-area coastal circulation models presents a formidable task because of the extremely large range of important energetic space and time scales and the crucial role played by complex turbulent dissipative processes. Work on these models is in the initial stages. In fact, precise definitions of the terms used above, such as 'appropriate' forcing functions, 'proper boundary conditions,' 'important dynamical processes,' and 'sufficient accuracy' are not known at present and will have to be established by future research that will involve thorough model testing, evaluation, and verification by comparison with carefully designed oceanographic field measurements. On the other hand, considerable progress has been made recently on the initial development of coastal circulation models. This progress in model development, coupled with a continuing increase in the capabilities of computers and an expansion of the general knowledge of continental shelf physical oceanographic processes, indicates that substantial gains in coastal circulation modeling capability should be achievable in the near future.

It is the purpose of this paper, and those that follow, to present a summary of the current status of coastal circulation modeling efforts in oceanographic research. Since investigators who are working with coastal circulation models have provided separate papers discussing their individual models and applications of those models, a comprehensive survey is not attempted. Rather, a few studies are noted that are believed to be especially significant and that seem to represent well the present state of the science. These are only briefly discussed here, since more information is included in the respective investigators' papers.



## Highlights of Coastal Ocean Models

The semi-spectral, primitive-equation, regional ocean circulation model described below by D. B. Haidvogel represents a continuously stratified fluid and uses orthogonal curvilinear horizontal coordinates and a vertical sigma coordinate. This model has been applied in two cases of special note. The first, an application by Wilkin and Chapman (1990) on scattering of coastal-trapped waves (CTWs) by irregularities in coastline and topography, involves idealized process studies and a simulation relevant to the east coast of Australia. The simulation of freely propagating CTWs incident on abrupt topographic variations representative of those off Australia showed CTW scattering with results similar to those inferred from observations by Griffin and Middleton (1986). The significance of the Wilkin and Chapman (1990) study is related to the fact that observations have shown that a large component of the energetic fluctuations in alongshore currents over the shelf can be comprised of forced or free CTWs. Even though the dynamics of these waves appear to be linear and relatively simple, it may be expected that the magnitudes of model-produced currents associated with the CTWs will depend sensitively on the proper representation of the bottom topography, stratification, bottom friction effects, and wind-stress forcing. The model must estimate these energetic linear CTW current fluctuations correctly (in magnitude and phase) almost as a necessary condition for the accurate representation of the more complex, nonlinear processes associated with fronts, boundary layers, eddies, and jets. The work by Wilkin and Chapman (1990) establishes the capability of the Haidvogel model to represent important features of these waves and demonstrates the use of the model for their study.

The second application of the Haidvogel model involves process studies of baroclinically unstable coastal currents typical of those observed in the Ocean Prediction Through Observation, Modeling, and Analysis (OPTOMA) program and the Coastal Transition Zone (CTZ) experiment off northern California. The flow processes in this case are strongly nonlinear and exhibit the time-dependent generation of offshore-directed filaments seen in the observations. The model results allow a detailed study of the dynamics associated with the generation and maintenance of the filaments and a determination of the contribution of the filaments to the offshore transport of mass, momentum and energy. The significance of this work lies in the fact that complex, time-dependent, nonlinear current fields, including eddies, jets, and filaments, with time and space scales very close to those observed, are resolved and studied in a region with bottom topography and coastline variations representative of those of the California continental shelf and slope.

The Princeton/Dynalysis ocean model described by Mellor, Herring and Patchen (this volume) likewise represents a continuously stratified fluid governed by the primitive equations and uses orthogonal curvilinear horizontal coordinates and a vertical sigma coordinate. In addition, the model contains an imbedded, second moment, turbulent closure sub-model to provide vertical mixing coefficients. This model has been applied in a Minerals Management Service (MMS)-sponsored study of the Santa Barbara Channel in coordination with a large, one-year field experiment. The model was forced by observed winds and data-derived heat fluxes. Initial



conditions were formulated from fields obtained from hydrographic surveys, and boundary conditions were calculated from current meter measurements. The model-produced fields showed both points of agreement and points of disagreement with the corresponding measured values. It seems clear that additional study of the effect of model parameters (grid resolution, magnitude of horizontal diffusivity, etc.) and of the methods for boundary condition specification on the model-generated fields would be of considerable value, given the availability of the excellent data set and present model results. This study, nevertheless, is a pioneering effort in coastal ocean modeling as it involves the employment of a full three-dimensional, continuously stratified, primitive-equation model with all forcing functions, boundary conditions, and initial conditions provided by ocean or atmospheric observations. The magnitude of the scientific problems associated with such a task should not be underestimated. Substantial additional research work will clearly be required to develop accurate, verified modeling capability for this type of application. It is noteworthy that this ground-breaking coastal research program, involving the *a priori* integration of modeling and field measurements, was planned and carried out with MMS support.

The coastal ocean circulation model described below by Dong-Ping Wang has been applied by Chen and Wang (1989) in a two-dimensional (across-shelf and vertical) mode to the region of the Coastal Ocean Dynamics Experiment (CODE). The model has been forced with winds observed during CODE-2 in summer 1982, and the model-produced current and temperature fluctuations have been compared with CODE measurements. Reasonably good agreement was obtained for the fluctuations in alongshore currents and temperature, and for the across-shelf currents near the surface. Although the current and temperature fields in the CODE region are strongly wind-driven so that some modeling success should be expected here, this study is worthy of note because it is one of the first to be applied in this manner and to actually document just how well a model can do in these circumstances.

## Summary

In summary, a verified coastal circulation modeling capability does not exist at the present. Considerable progress is being made, however, in model development and in applications. Strong contributions to the improvement of modeling capabilities have been provided as a result of model use by investigators other than the model developers. The Wilken and Chapman (1990) work with the Haidvogel model provides a clear example of the benefits of such an arrangement. The availability of coastal models for general use by the physical oceanographic research community should play a critical role in the future development of accurate, verified, circulation models. The Haidvogel model already has a sizeable group of community users, and the Princeton/Dynalysis model is likewise being applied by other investigators. In general, it appears that now is an ideal time for the achievement of major advances in modeling capabilities for coastal physical oceanography.



## COASTAL OCEAN CIRCULATION MODELING AT APPLIED SCIENCE ASSOCIATES, INC.

Malcolm L. Spaulding  
J. Craig Swanson  
Applied Science Associates, Inc.  
70 Dean Knauss Drive  
Narragansett, Rhode Island 02882

Applied Science Associates, Inc. (ASA) has developed, tested, and applied a series of coastal ocean circulation models over the past decade in support of addressing environmental problems in the coastal oceans. Three distinct numerical approaches are embodied in the three-dimensional, time-dependent, finite-difference circulation models described below. These models are:

1. Explicit Legendre Polynomial Model;
2. Semi-implicit Level Model; and
3. Boundary Fitted Semi-implicit Level Model

Although some of the development effort has been interrelated among the models, each will be presented separately below. Included is a short description of the model itself and then descriptions of its applications to various geographical areas and specific problems.

### Explicit Legendre Polynomial Model

The initial development and application of the explicit Legendre polynomial model has been reported by Gordon (1982) and Gordon and Spaulding (1987). The model consists of a nonlinear, finite-difference representation of the basic conservation equations for mass, momentum, salt, and temperature. The variation through depth of the dependent variables, other than the surface elevation, is expressed in terms of a basic set of Legendre polynomials using the Galerkin method. This allows for a continuous representation through the vertical which is not available from layered or leveled models. The model is developed so as to allow continuous density stratification, the inclusion of horizontal diffusion of momentum and mass, and for temporally and spatially varying vertical eddy viscosity. A split mode formulation is developed in which the free surface elevation is treated separately from the internal, three-dimensional flow variables, thus allowing for a significant savings in computational time. The model was tested for a number of cases for which there are known analytical solutions.

The model was also applied to Narragansett Bay. Comparisons were made between modeled and observed values of the  $M_2$  and  $M_4$  tidal constituents for sea surface elevation. The flow resulting from non-local forcing was estimated by using a periodic variation of sea level at the mouth of the Bay with an amplitude of 40 cm



and period of 2 days. Maximum currents of 8 cm/s were induced, indicating that these motions may be significant when compared with the direct action of wind stress. An investigation was also made of the Bay's response to constant, uniform wind forcing. The non-linear interaction between tidally and wind-induced motions were found to significantly affect the steady-state response, with the tidal motions causing an effective increase in bottom stress. Volume transport calculations indicated a significant exchange between the main passages in the estuary. The magnitude of this exchange was seen to depend on the choice of vertical eddy viscosity.

A comparison was made between modeled results and current meter observations of approximately 30 days duration at two locations in the West Passage of Narragansett Bay and a 51-day current meter record taken in the entrance to the Providence River. In these records relatively large fluctuations, which are almost exclusively wind induced, exist at sub-tidal frequencies. The model was found to be capable of reproducing these wind-induced sub-tidal fluctuations with reasonable accuracy.

A two-dimensional, vertically averaged form of the model was also applied to predict the wind-forced circulation in the Bering and Chukchi Seas (Spaulding et al., 1987). A simulation of the steady state flow induced by a  $10^{-6}$  sea surface slope between the North Pacific and Arctic oceans gave a northward transport of 1.97 Sv ( $\text{Sv} = 10^6 \text{ m}^3\text{s}^{-1}$ ) with 67% and 33% of the flow passing through the Anadyr and Shpanberg Straits, respectively. The transport and velocities in the straits scaled linearly with the imposed slope. A wind field derived from the Fleet Numerical Oceanography Center (FNOC) model and validated with available observations was used as input to perform simulations for February 1982. Comparison of model predictions to current and sea elevation observations in the Shpanberg and Bering Straits and Chukchi Sea (from Aagaard et al., 1985) were generally in good agreement ( $R = 0.78$ ). A sensitivity study investigating the influence of open boundary-condition specification, model grid size, bottom-friction coefficient and wind-forcing representation showed that the wind was the most important parameter. The model, however, normally underpredicted the wind-driven response. Model-predicted transports correlated at 0.75 or higher with mean current speed and wind speed were in reasonable agreement with the data. The transport/wind-speed correlation was approximately a factor of two higher than earlier estimates, but varied substantially depending on the simulation period. Simulations showed that the latitudinal and longitudinal momentum balances are essentially geostrophic, and that the area between St. Lawrence Island to Cape Lisburne responds essentially as a unit to wind forcing at periods of 2.5 days and longer.

The two-dimensional vertically averaged version of the model in spherical coordinates with  $0.2R$  latitude,  $0.35R$  longitude resolution was also employed to predict the  $M_2$  and  $K_1$  tidal elevations and currents in the northwestern Gulf of Alaska (Isaji and Spaulding, 1987). Boundary conditions for the model were derived from Schwiderski's global ocean tidal model and observations. Model predictions for the amplitude and phase of the sea elevations were generally within 5 cm and  $2R$  of the observations for the  $M_2$  constituent and 7 cm and  $5R$  for the  $K_1$ . The  $M_2$  standing wave pattern in Shelikof Strait and the tidal resonance in Cook Inlet observed in earlier studies were confirmed by the numerical simulations.



A three-dimensional version of model has been used to study the interaction between the tide and wind-driven flows in the Georges Bank/Gulf of Maine region (Isaji et al., 1982). To determine the appropriate specification of key model parameters, a series of sensitivity studies were performed investigating grid size and open boundary condition approximations. Based on these simulations a grid spacing of 25 km was selected as a compromise between dynamic considerations and computational constraints. Investigation of clamped, gradient, and mixed open boundaries suggested that the clamped offshore, gradient cross-shelf boundary conditions were a reasonable approximation for wind-driven shelf flows.

A series of simulations driven by a spatially uniform and stationary  $1 \text{ dyne/cm}^2$  wind stress from eight points of the compass showed a bimodal response, with transport scaling roughly with the alongshelf component of stress. The effective spin-up times were approximately 4 to 6 hours for friction-dominated regions and 8 to 10 days for model domain adjustment. This latter time was sufficiently long, in comparison to mesoscale atmospheric events (4 to 10 days), that the wind-driven currents reached steady state only in shallow areas.

After the model bottom-friction coefficient had been determined by calibration with the  $M_2$  tide, studies of the interaction between the tide and wind-induced currents revealed that incorporation of tidal forcing reduced the wind-driven component of the flow field compared to a similar simulation with only wind forcing. The relative changes increased as the wind-driven flow velocities decreased as a direct consequence of changes in the effective bottom stress.

The model was then used to hindcast the circulation for a 37-day period starting on 10 January 1978. A statistically hindcast, spatially and temporally varying wind stress and atmospheric pressure field and an  $M_2$  tide were used to force the model. Qualitative comparison of predictions with limited data suggests the model correctly predicts the magnitude and patterns of the flow fields.

The model has also been used to study qualitatively the annual cycle of the residual flows induced by the tide, density, atmospheric and alongshore pressure gradient forces in the Gulf of Maine/Georges Bank region (Isaji et al., 1984). An annual, three-dimensional circulation climatology was produced at a resolution of 25 km in space and seasonal in time. The results demonstrated that the Georges Bank gyre, which is weakly closed on the southwest side, was the result of forcing from all origins except the alongshore pressure gradient. Seasonal changes in the wind and density fields were pivotal in producing the observed spring and summer strengthening of the gyre. The flow of shelf water into the Gulf of Maine through the bottom of the Northeast Channel was clearly demonstrated to be a compensatory response to offshore and alongshore wind-driven surface flows. The observed mean flow to the southwest on the outer shelf could be explained by the presence of an alongshore pressure gradient of  $0.5 \times 10^{-7}$ .

The model was also employed to study the tidally induced residual flow in the Gulf of Maine/Georges Bank study region using a 6.25 km square grid (Isaji and Spaulding, 1984). Tidal elevations in terms of the  $M_2$  phase and amplitude along the



open boundaries were specified using Schwiderski's deep ocean tidal model. The model predicted strong clockwise circulation gyres around Georges Bank and Nantucket Shoals with a weak gyre around Browns Bank. Strong inflow to the Gulf of Maine was predicted near the southwestern tip of Nova Scotia. These results were in good agreement with recent model predictions of Greenberg.

The Legendre model has also been applied to predict the dynamics of a selected region of the Norwegian Coastal Current (58-62RN) (Spaulding and Isaji, 1984). In this application, the model, using a 9.25km grid resolution, was employed to study the development and propagation of eddies and whirls along a front. Initialized with a sinuous wave density field to represent meanders in the front, the model predicted the development of backward-breaking eddies and whirls typical of those observed in satellite imagery. Model-predicted northward frontal propagation at 7-10 km/day, typical coastal current speeds of 30-50 cm/sec, and maximum eddy velocities of 70-120 cm/sec were in good agreement with available data.

The results of this investigation suggested that the hydrodynamic model used can provide the basis, if properly integrated with in-situ and remotely sensed observations, of a forecasting system for the Norwegian Coastal Current.

An application of the model to the Cumberland Basin in the Bay of Fundy was reported by DeMargerie and De Wolfe (1987). In addition to having to address the extraordinarily large tidal energy, the hydrodynamic model also had to deliver an accurate representation of the bottom current profile and provide for the incorporation of tidal flats.

To resolve the tidal flats, the model domain varied with the stage of the tide, although the model equations remained unchanged. As the tide floods and ebbs, each grid cell becomes either wet or dry, depending on water depth. This is a fairly common technique used in two-dimensional surge modeling, which was extended here to a three-dimensional application.

The first phase of the project was to reproduce tidal hydrodynamics in Cumberland Basin. Tidal heights were specified at the mouth of the basin, and the simulation results were compared to currents observed inside the basin. Future work includes incorporating sediment transport dynamics into the model system.

The model has been modified to consider wave-current interaction in the bottom boundary layer (Spaulding and Isaji, 1985, 1987). This study was intended to provide an improved method to predict near-bottom velocity profiles for submarine pipeline stability design on the continental shelf. The model system is comprised of submodels for storm winds, waves, bottom boundary layer and shelf circulation dynamics. The focus of this integrated approach was to correctly account for the influence of wind-generated gravity waves in altering the bottom stress levels and, in turn, the mean steady current fields. The basic conceptual approach to describe these processes was the well known wave-current interaction theory developed by Grant and Madsen, to include the effects of moveable bed dynamics and stratification.



The model has been applied to predict the flow and surface elevation fields for tropical storm Delia (Gulf of Mexico) and compared to available field observations. Sensitivity studies to two- and three-dimensional representations of the vertical eddy viscosity, constant bottom friction coefficient, and wave current interaction have been performed. Results of these simulations in terms of the velocity and surface elevation fields, local force balances, and velocity structure were described.

A large, application-oriented study using the model has recently been completed (Spaulding et al., 1985-1988). The objectives of the project were to supply the Minerals Management Service, through the National Oceanic and Atmospheric Administration Outer Continental Shelf Environmental Assessment Program (NOAA/OCSEAP), with hypothetical stochastic oil spill trajectories from specified launch points in Alaskan coastal seas; to compute dynamic mass balances for oil spills, with spatial resolution of both surface and subsurface hydrocarbon concentrations; to provide medium and high resolution hydrodynamic model output in support of other studies; and to thoroughly document the development and applications of all models.

To accomplish the project objectives, ASA used an integrated, tested and documented coastal sea model system. The hydrodynamic model formed the core of the model system, and with the weather/storm, sea ice, and surface wave models, supplied the environment within which the oil spill trajectory and fates models operate.

The model system was applied to selected planning areas in Alaskan coastal seas (Bering, Chukchi, and Gulf of Alaska waters) to predict oil spill trajectory and fates. The model system has been applied for oil and gas lease sales in Navarin, Shumagin, and St. Georges Basin, and the Gulf of Alaska.

The model was also recently exercised for five test cases to evaluate its performance in an international competition directed by the Metocean Model Program (MOMOP) Committee (Mendelsohn et al., 1989). The test cases included simulations of (1) adjustment under gravity of an initially unbalanced horizontal density gradient, (2) upwelling/downwelling for a stratified fluid with wind forcing, (3) stratified flow over a growing seamount, (4) oscillatory wind-forced flow in a channel with a shelf, slope, and deep basin bathymetry using cyclic boundary conditions, and (5) case (4) simulated with the author's own boundary condition.

The model predictions were in reasonable agreement with available analytic, quasi-analytic, or numerical simulations for these or similar problems. The Legendre polynomial set is not particularly well suited for the present simulations, however, because of the sharp density discontinuities in the selected test cases.

### **Semi-Implicit Level Model**

A three-dimensional, nonlinear, finite-difference numerical model system has been developed for coastal circulation and water quality applications (Swanson,



1986). The model system is composed of a hydrodynamic model component and a pollutant transport model component. The hydrodynamic model solves the conservation of momentum, water mass, salt, and heat on a space-staggered grid system. The solution technique employs a split mode semi-implicit algorithm for both the exterior, vertically averaged flow and the interior vertical structure. This technique eases the time step restrictions typical of explicit algorithms, yet it is more efficient than fully implicit algorithms. The model has been tested against analytic solutions for a standing wave in a closed basin, tidal and wind flow in a basin with variable depth, wind flow in a closed basin, and density forcing in a channel. Simulations show good agreement with the analytic solutions.

A companion pollutant transport model has also been developed. The model system, in a vertically averaged mode, was applied to upper Narragansett Bay to predict levels of fecal coliform under various pollutant loadings. The required hydrodynamic data were model-generated from the M<sub>2</sub> and M<sub>4</sub> tides plus mean river flows emptying into the area. Comparison of model tidal response with observations was good.

The model has also been applied to Halifax Harbor (ASA Consulting, 1986) to estimate water quality impacts from distributed pollutant loadings.

The three-dimensional form of the model, using five levels to represent the vertical structure, has been applied to the Gulf of Maine including adjacent shelf areas from Halifax, Nova Scotia, to Montauk, Long Island (Swanson, in preparation). The model solves the conservation of mass, momentum, heat and salt equations on a 12.5km-square finite difference grid. Forcing to the model included the M<sub>2</sub> tide, a mean oceanic induced alongshore pressure gradient of  $1.3 \times 10^{-7}$ , a winter wind stress of 0.125 Pa heading 30° south of east, and a density distribution developed from averaging winter observations obtained from NODC. Each forcing was applied separately to discern the individual circulation response. The superposition of the responses to individual forcings was then compared to the case of driving the model with all forcings simultaneously.

### **Boundary Fitted Semi-Implicit Level Model**

A major evolution of the semi-implicit approach was to include boundary fitted coordinates (Swanson and Spaulding, 1985; Spaulding and Swanson, 1985; Swanson, 1986; Swanson et al., in press). The basic idea of the approach was to use a set of coupled, quasi-linear, elliptic transformation equations to map the physical domain to a corresponding transformed plane such that all boundaries were coincident with coordinate lines and the transformed mesh was rectangular. The governing equations were solved on a space-staggered grid system by a semi-implicit finite-difference approach. The depth-transformed vertical coordinate was represented by a series of discrete levels and a split mode formulation was employed to reduce computational time. Comparisons of the circulation model predictions for tidally forced flows in a wedge section, with both flat and quadratic bottom topography, were in excellent agreement with corresponding analytic solutions. Simulation of steady state



wind-induced setup in a closed basin, formed using elliptic cylindrical coordinates, and density-induced flow in a rectangular channel, were also in good agreement with the corresponding analytic solutions.

The model has been applied to the Norwegian continental shelf (Mathisen et al., 1987). Boundary fitted coordinates with point attraction were employed to decrease the grid spacing at Haltenbanken and along the shelf edge. The two-dimensional version of the model was used to simulate the semi-diurnal  $M_2$  constituent, showing good agreement with observed amplitudes and phases and with results from other numerical models.

The two-dimensional version of the model was applied to simulating both tidal and storm surge elevation and currents on the Norwegian continental shelf (Mathisen et al., in press). The simulation was carried out for both a coarse and a fine grid. The simulated sea elevation and currents compared favorably with observations and model results from the operational model at the Norwegian Meteorological Institute.

The model has also been applied in a two-dimensional, vertically averaged mode to predict the tidal circulation in Mt. Hope Bay, a small estuary located on the eastern side of Narragansett Bay (Spaulding et al., 1989). Model-predicted current and sea surface elevation were in good agreement with available observations for a bottom drag coefficient of 0.0036. Sensitivity studies showed that sea surface elevation was insensitive to bottom friction, although the predicted velocities decrease as friction increases. The sea surface elevation was approximately three hours out of phase with the currents, in agreement with standing wave theory and observations.

## Summary

ASA has approached the problem of three-dimensional time-dependent coastal ocean circulation modeling from various numerical approaches, each with its unique set of attributes. The Explicit Legendre Polynomial Model offers a continuous vertical representation of the dependent three-dimensional variables, the Semi-Implicit Level Model is not constrained by the surface gravity wave restriction on time step, and the Boundary Fitted Semi-Implicit Level Model incorporates state-of-the-art coordinate transformations to better resolve coastal circulation. All the models have shown their utility in providing accurate hydrodynamic variable fields for various applications.

# A LIMITED-AREA COASTAL OCEAN CIRCULATION MODEL

Robert L. Haney  
Department of Meteorology  
Naval Postgraduate School  
Monterey, CA 93943

## Abstract

A multi-level primitive equation ocean model has been developed to study synoptic scale variability in eastern boundary current regimes with particular application to the California Current region. Process-oriented model simulations, as well as data assimilation, hindcast and forecast studies, are being carried out using the model and data collected in the Coastal Transition Zone (CTZ) program.

## Introduction

For over five years now, the Naval Postgraduate School (NPS) has had a strong ocean research program in the California Current (CC). This research started with the Ocean Prediction Through Observation, Modeling, and Analysis (OPTOMA) Program (Rienecker et al., 1985; Rienecker et al., 1987; Rienecker and Mooers, 1989) and it is continuing with studies in the Coastal Transition Zone (CTZ) program by S. Ramp and T. Stanton and in the World Ocean Circulation Experiment (WOCE) by C. Collins. The present limited area coastal ocean model is being developed to carry out numerical ocean prediction studies as part of these programs. The scientific focus of the studies is on the effects of wind and abrupt coastal topography on synoptic and mesoscale phenomena in eastern boundary current regions.

## Model Description

The basic numerical model, a descendant of Haney's (1985) ocean general circulation model, is a multi-level, hydrostatic, nonlinear primitive equation model. It has a rigid lid and incorporates variable bottom topography using a terrain-following vertical coordinate system (sigma-coordinates). The numerical scheme, which is based on the Arakawa B-grid, maintains accuracy as well as energy and vorticity conservation principles, and it properly represents the interaction between the barotropic and baroclinic modes that occurs with variable bottom topography, i.e., the well-known Joint Effect of Barclinity and Bottom Relief (JEBAR) effect (Huthnance, 1984; Csanady, 1985). In addition, it uses the most accurate possible form of the hydrostatic equation in sigma coordinates to minimize truncation error in computing the horizontal pressure gradient force (Arakawa and Suarez, 1983; Haney, submitted for publication, 1990).

The model domain covers an eastern boundary ocean region up to, but not including, a continental shelf. The eastern boundary is a straight coastal wall,



while the northern, southern and western boundaries are "open." The open boundaries are treated using a modified version of the radiation condition of Ross and Orlanski (1982) and a mild sponge as recommended by Lorenzetti and Wang (1986). The streamfunction for the depth-averaged flow is specified at all open boundaries, while the divergence, vorticity and temperature are specified at inflow boundaries and are predicted by upstream advection at outflow boundaries. The vertical and horizontal grid spacing is adjustable, but on the NPS computer the model is run with 12 levels in the vertical and 8 km by 10 km horizontal resolution.

The physical model is quite simple at the present time. Salinity is included only through the use of a simple T-S relation for the California Current. Vertical turbulent mixing of heat and momentum is parameterized by means of a dynamic adjustment based on a critical Richardson number. There is also a small amount of vertical mixing by means of eddy viscosity and conductivity. Horizontal eddy diffusion of heat and momentum is accomplished by means of biharmonic diffusion which damps features with a space scale of four grid-intervals or less, while leaving the larger scales essentially unchanged. The model is run either with no forcing or with prescribed wind-stress forcing and thermal damping at the surface. Bottom friction is also included in a simple way (geostrophic drag law).

## Model Applications

Although the coastal model is still in a state of development, a number of interesting scientific results have already been obtained using preliminary versions of the model while it was being developed. The following studies were carried out using a version of the model with a flat bottom and no barotropic mode. Concerning process-oriented model simulations, Batteen et al. (1989) studied the development of coastal jets and eddies in response to forcing by steady, upwelling favorable alongshore winds. Starting from a state of rest and horizontally uniform stratification typical of the California Current region in summer, the model was forced by two different profiles of alongshore wind stress (Fig. 1). The stress was steady and upwelling-favorable in both experiments, but in one of the experiments it was constant over the entire domain, while in the other experiment the magnitude varied along the coast (strongest in the central coast) as is typical of observed climatological conditions in summer. As described in Batteen et al. (1989), an alongshore coastal jet and poleward undercurrent developed and became baroclinically unstable, resulting in the establishment of meanders and eddies in the flow (Figs. 2 and 3). Although the meanders and eddies after 90 days of simulation are much weaker than observed in the California Current, and they do not have the kind of extended offshore structure typically seen in coastal ocean filaments, the results indicate that baroclinic instability of the alongshore flow driven by steady climatological winds could be a contributing factor in generating the observed variability. Comparing Figure 2 with Figure 3, it is clear that a representative variation along the coast of the mean alongshore wind stress modifies the model results only slightly. These results, which are obtained from a beta-plane model, are not changed appreciably if the experiments are rerun on an f-plane (Batteen et al., 1989).



Another set of process-oriented model simulations were carried out using composites of coastal jets observed in the CTZ program (CTZ Group, 1988) by Kosro and Huyer (in preparation). Figure 4 shows a vertical cross section of three different coastal jets. The first one (A) is a composite of six crossings of four different coastal jets observed by Kosro and Huyer in the California Current during the summer of 1987. The resulting composite jet has no tilt in the vertical (equivalent barotropic), and it is symmetric in the cross-stream direction. The second jet (B) is a composite of four crossings of a single jet observed in the CC on June 20-27, 1988. It is also equivalent barotropic, but it is highly asymmetric in the horizontal. The positive vorticity on the left (inshore) side of the jet ( $\sim 0.5$  f at the surface) is about 5 times larger than the negative vorticity on the right side of the jet. The third jet (C) is the same as A except that a representative poleward undercurrent is added next to the coast. The resulting composite tilts toward warmer water with depth, and it is somewhat asymmetric. The positive vorticity on the inshore side of this jet ( $\sim 0.2$  f at the surface) is about twice as large as the negative vorticity on the right side. Each jet in Figure 4, with a field of random (white noise) disturbances having root mean square (RMS) velocities of order  $3\text{--}5\text{ cm s}^{-1}$  superposed on them, was used as an initial condition for a model integration. The initial temperature field consisted of a mean vertical stratification and a baroclinic structure in thermal wind balance with the given jet. The near surface temperature fields from the three experiments after 40 days of integration are shown in Figure 5. The first two composite jets, the equivalent barotropic jets with no vertical tilt, were both stable to the random disturbances, which simply damped with time. On the other hand, the composite jet having a vertical tilt became unstable to the disturbances. A meander developed, intensified, and advected warm water shoreward ahead of itself, finally forming a closed cold ring (Fig. 5c). These experiments, being preliminary and having no depth-averaged flow (barotropic mode), have not been analyzed in detail, but it is fairly certain that the eddy growth is due to baroclinic instability of the tilted jet structure. However, the disturbances that grow on the unstable jet and undercurrent resemble classic baroclinic wave structures and do not show the kind of extended offshore filaments or jet meanders seen in observations. These preliminary results, along with the results of Batteen et al. (1989) described above, suggest that baroclinic (or mixed baroclinic/barotropic) instability by itself is not sufficient to generate intense eddies and filaments that have long extensions in the offshore directions as in observations. Additional physical processes such as variable bottom topography and/or fluctuating winds may therefore be essential to the development of observed eddies, and these are being addressed in model studies at the present time.

The model is also being used to carry out model hindcast, or data-assimilation, studies. The CTZ field data, which consist of repeated grids of hydrographic stations taken in the California Current during the summer of 1988, are being used to initialize and verify the model hindcasts. Several different numerical experiments are being made to test the importance of various physical processes (such as variable coastal topography, a non-zero barotropic mode, nonlinearity, the offshore boundary conditions, the onshore boundary conditions, surface forcing, etc.) in determining the evolution of the eddy field observed in the California Current. A preliminary numerical hindcast of this type, using hydrographic data from the OPTOMA program



(Rienecker et al., 1987) in an earlier version of the coastal model, was carried out by an NPS master's thesis student (Johnson, 1988), and some of the results of that study are shown in Figure 6. The main oceanic feature in the initial conditions on June 23, 1984 (top left frame) was a ridge of high dynamic heights offshore and north of Pt. Arena and a trough of low dynamic heights to the south of Pt. Arena with a geostrophic jet directed offshore in between the ridge and the trough. During the subsequent 13 days (left column) the jet widened somewhat and re-oriented itself into a more northeast-southwest direction as the trough in the eastern half of the domain moved northeastward. The P. E. model (middle column) seems to over predict this development, while the quasisgeostrophic (QG) model of Rienecker et al. (last column) seems to underpredict it. The CTZ data that is being utilized in the present hindcast experiments were taken on a uniform grid in the California Current off Pt. Arena with such numerical model experiments in mind. The limited-area coastal model and CTZ data sets will be used to explore the role of bottom topography, variable wind stress and thermal forcing at the surface, and specific forms of nonlinearity in the formation and evolution of observed variability in the California coastal oceans.

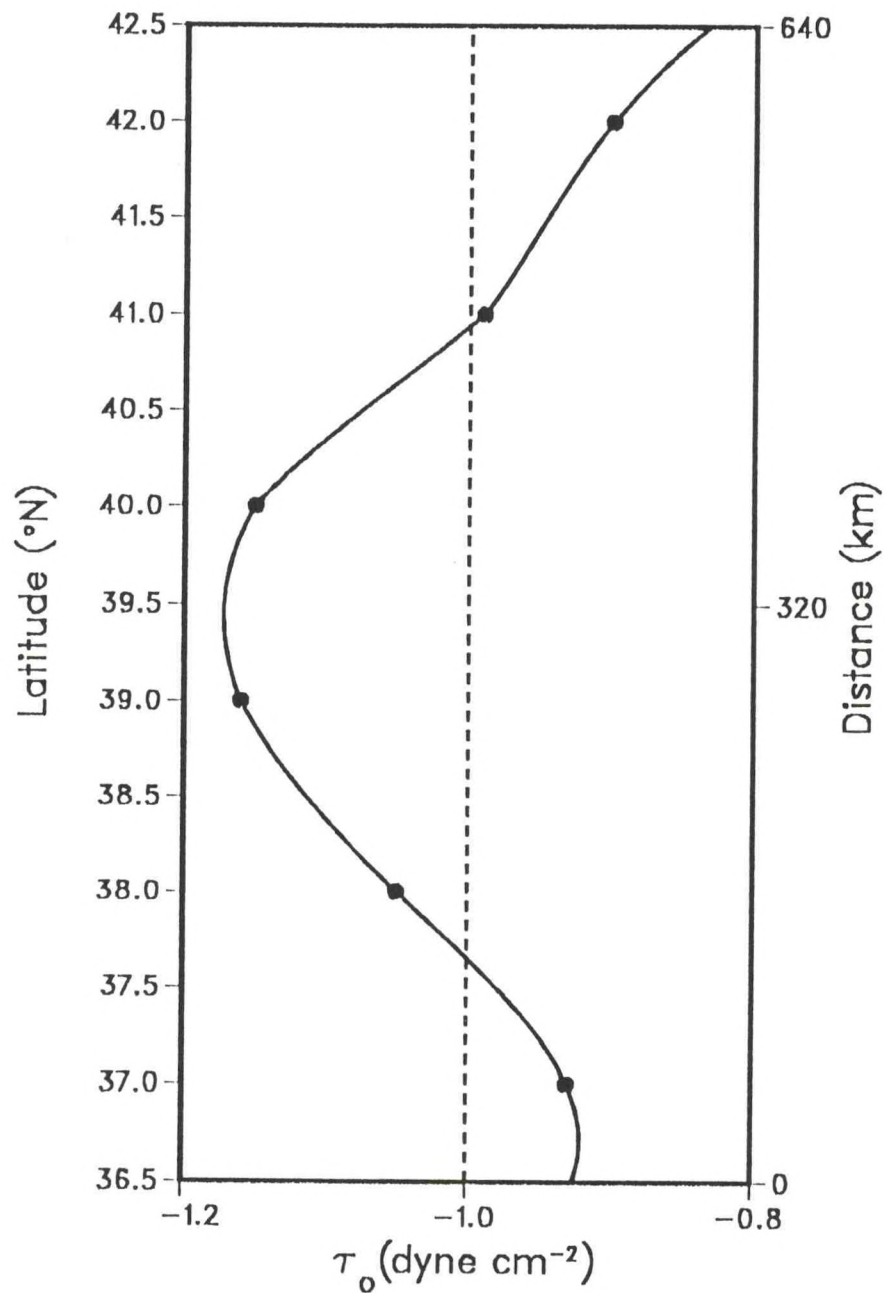


Figure 1. Wind stress a function of latitude (alongshore distance). The uniform stress (dashed line) was used in Experiment 1, while the variable stress (solid line) with larger values in the center of the domain was used in Experiment 2.



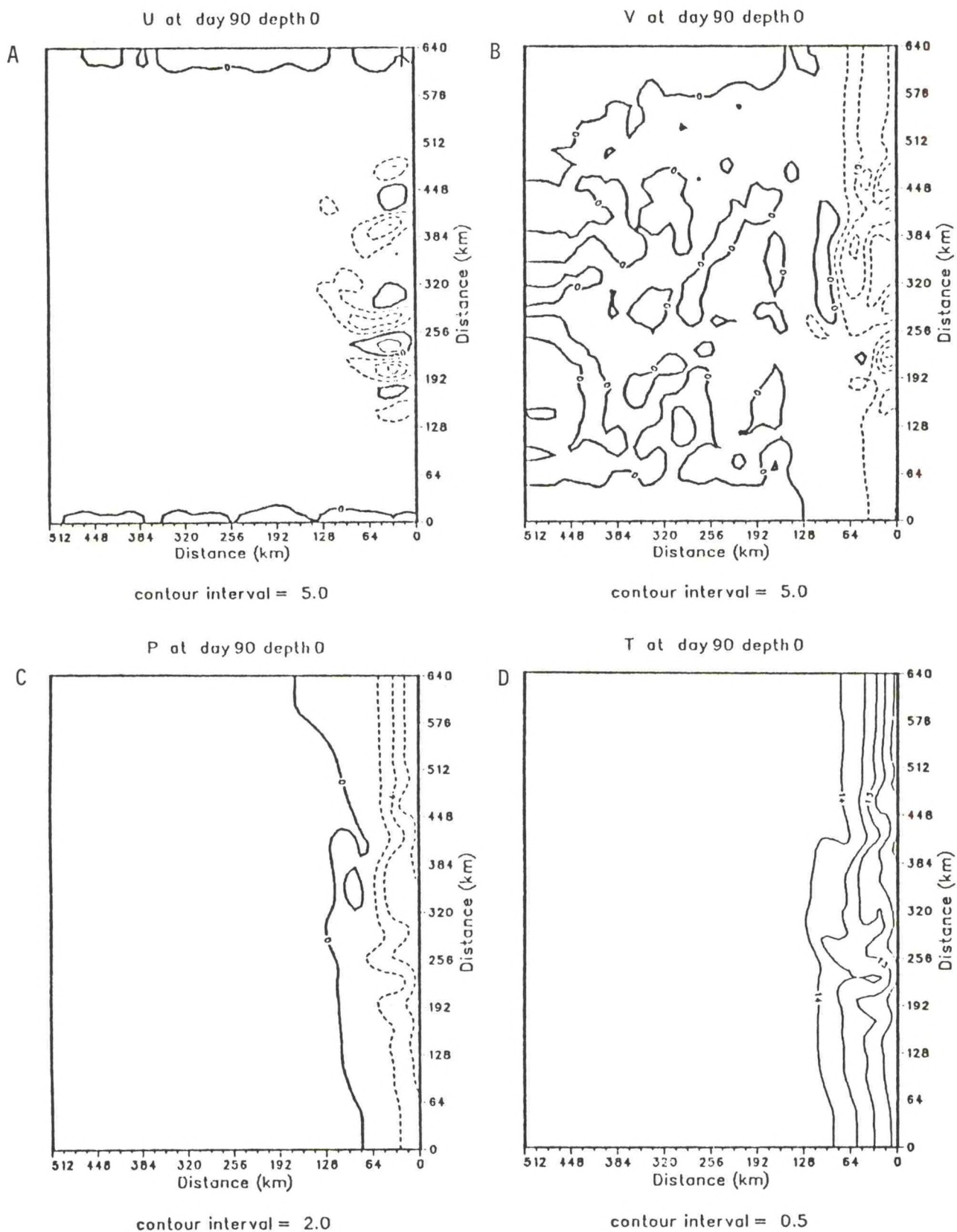


Figure 2. Surface isopleths for Experiment 1 at day 90 of (A) zonal ( $u$ ) velocity ( $\text{cm s}^{-1}$ ), (B) meridional ( $v$ ) velocity ( $\text{cm s}^{-1}$ ), (C) dynamic height (cm) relative to 2400 m, and (D) temperature ( $^{\circ}\text{C}$  for (D)). Dashed lines denote offshore velocities in (A), equatorward velocities in (B) and negative values in (C).

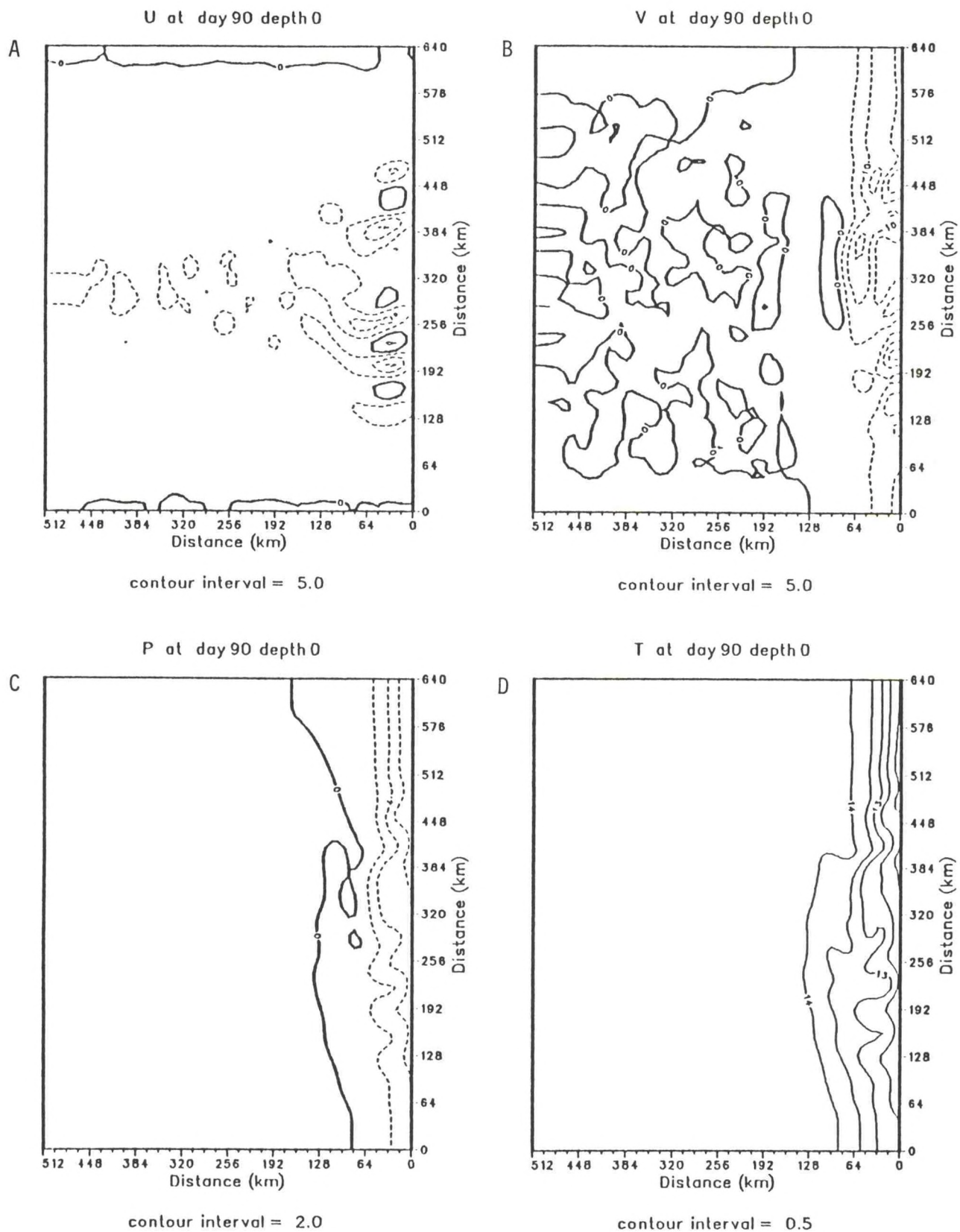


Figure 3. Surface isopleths for Experiment 2 at day 90 of (A) zonal ( $u$ ) velocity ( $\text{cm s}^{-1}$ ), (B) meridional ( $v$ ) velocity ( $\text{cm s}^{-1}$ ), (C) dynamic height (cm) relative to 2400 m and (D) temperature ( $^{\circ}\text{C}$  for (D)). Dashed lines denote offshore velocities in (A), equatorward velocities in (B) and negative values in (C).



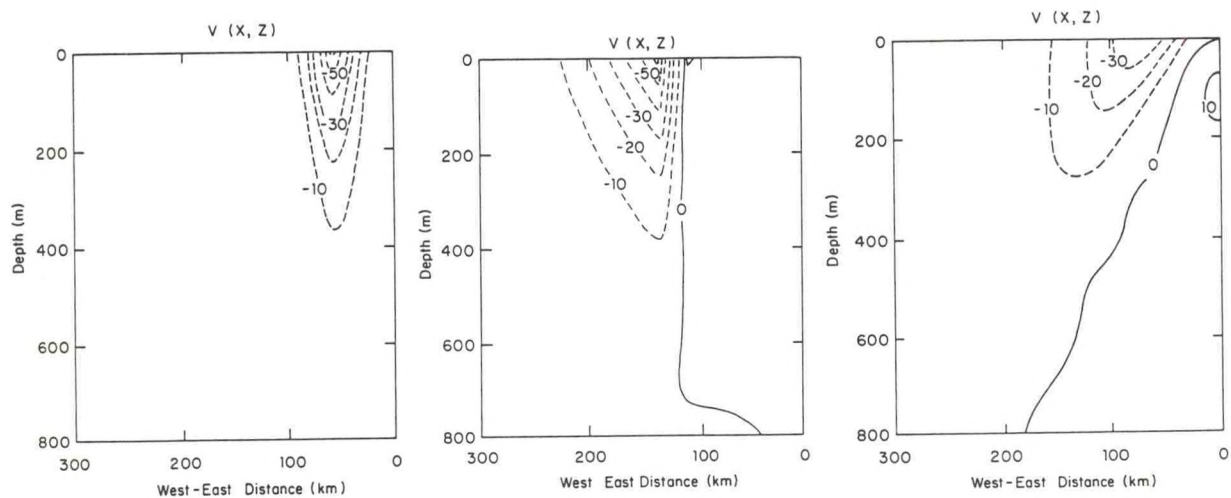


Figure 4. Cross sectional view of three alongshore coastal jets. The symmetric jet (left frame) is a composite made from six crossings of four different coastal jets observed in the California Current during the summer of 1987 by Kosro and Huyer (in preparation). The southward flowing jet is 75 km wide at the surface, has a maximum current of  $0.6 \text{ m s}^{-1}$  at the surface, a vertical scale of 300 m, and no tilt with depth. The maximum relative vorticity on each side of the jet is almost 20% of  $f$  (Coriolis parameter). The asymmetric jet (center frame) is a composite made from four crossings of a single jet (at different downstream locations) by Kosro and Huyer on June 20-27, 1988. It is similar to the symmetric composite from 1987 except for the strong horizontal asymmetry that greatly increases the positive vorticity on the left side of the jet to  $0.5 f$ . The jet in the right frame was obtained by adding a poleward undercurrent on the inshore side of the symmetric, composite jet in A.

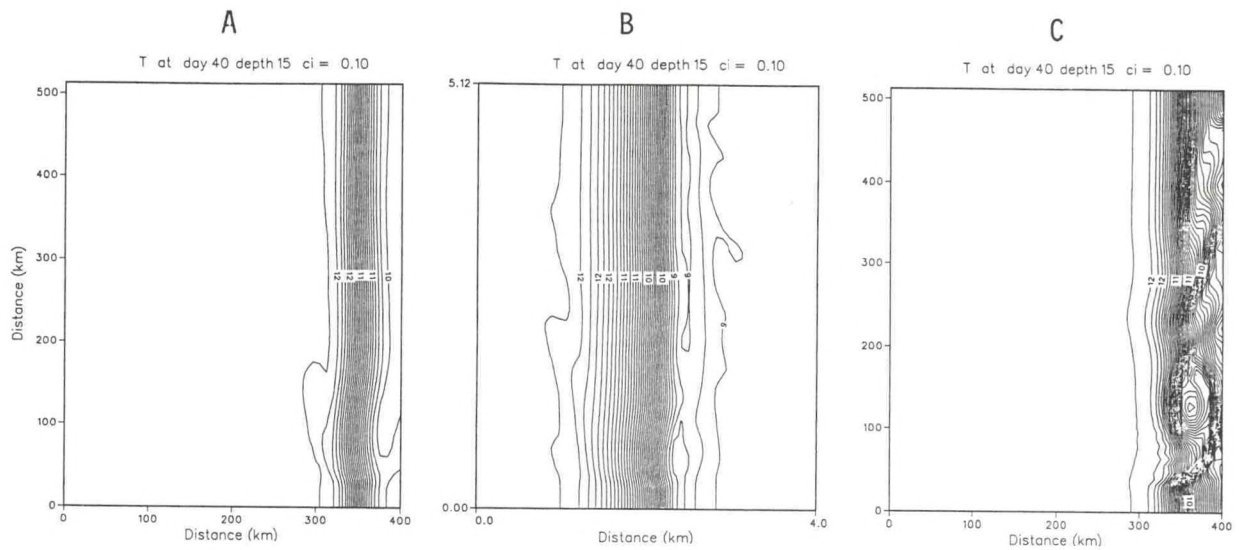


Figure 5. Horizontal maps of the model near surface temperature field after 40 days of integration starting with the three composite jets shown in Figure 4. Maps A, B and C are from the experiments that were initialized with the jets in A, B and C, respectively, in Figure 4.



## OBSERVED

## PREDICTED

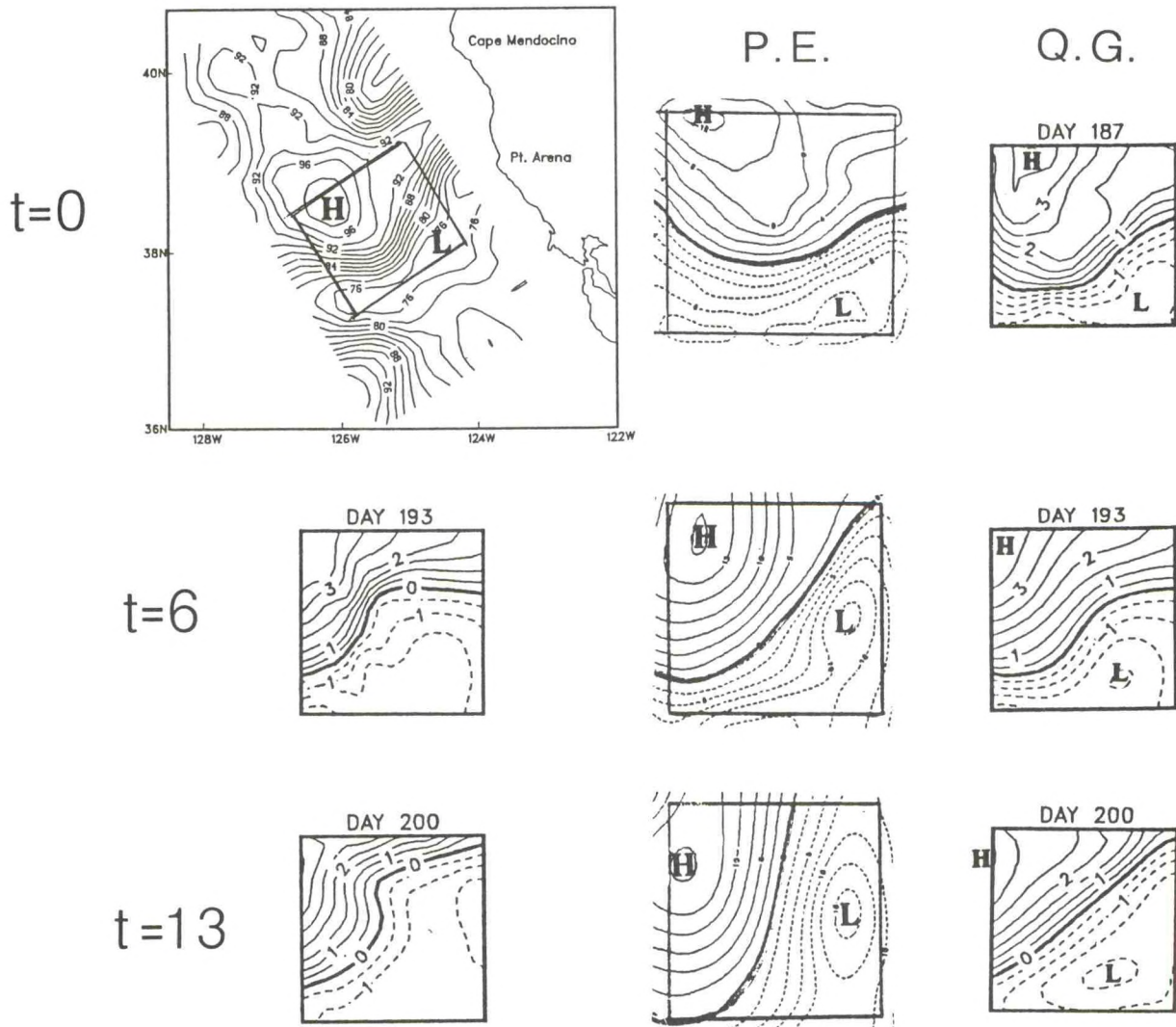


Figure 6. Results of a numerical hindcast experiment in the California Current (Johnson, 1988). The first column shows observed fields and the second two columns show model-predicted fields. The top row is analyzed data representing June 23, 1984 (Julian day 187) which is the initial day ( $t=0$ ) of the predictions. The second row is 6 days later (Julian day 193), and the bottom row is 13 days later (Julian day 200). The observed field at  $t=0$  shows the surface dynamic height in the California Current along with a box that defines the verification region shown in the other frames. The observed fields at  $t=6$  and  $t=13$ , as well as the QG fields in the third column, are geostrophic streamfunctions at 50 m. The PE fields are the pressure at 10 m depth ( $t=0$  frame) and at 50 m depth ( $t=6$  and  $t=13$  frames). The PE model results are from Johnson (1988), while the observed fields and QG predictions are from Rienecker et al. (1989).

# PREDICTING COASTAL OCEAN CIRCULATION WITH THE UNIVERSITY OF MIAMI FINITE ELEMENT MODELS

John D. Wang  
Division of Applied Marine Physics  
Rosenstiel School of Marine and Atmospheric Science  
University of Miami  
4600 Rickenbacker Causeway  
Miami, Florida 33149

## Introduction

The mathematical formulation describing the hydrodynamics of oceans involves a number of conservation partial differential equations of motion and mixing. One way of obtaining solutions is through numerical models. The models described here employ the finite element method (FEM) for spatial discretization. The finite element method, which allows a flexible grid layout, is ideally suited for studying the nearshore and other regions with highly complex geometry and bathymetry. As a result of process-oriented studies of tidal flow, wind-driven flow, and effects of ocean currents, major components of a modeling system have been developed and tested as described below.

## Description of Models

The available models all incorporate the assumption of hydrostatic pressure distribution and thus are primarily intended for nearly horizontal flows. The equations of motion in vertically integrated forms are used in one-layer, two-layer, and multi-layer models, called CAFE-1, CAFE-2, and CAFE-3D, respectively, for "Circulation Analysis with Finite Elements".

CAFE-1 is a barotropic model based on the following equations (Wang, 1978):

$$\frac{\partial \eta}{\partial t} + \frac{\partial q_x}{\partial x} + \frac{\partial q_y}{\partial y} = q \quad (1)$$

$$\begin{aligned} \frac{\partial q_x}{\partial t} + \frac{\partial u q_x}{\partial x} + \frac{\partial v q_x}{\partial y} = & f q_y - g(h+\eta) \frac{\partial \eta}{\partial x} + \frac{\tau_x^s}{\rho} \\ & - C_f \frac{\sqrt{q_x^2 + q_y^2} q_x}{(h+\eta)^2} + \frac{\partial F_{xx}}{\partial x} + \frac{\partial F_{yx}}{\partial y} \end{aligned} \quad (2)$$



$$\begin{aligned} \frac{\partial q_y}{\partial t} + \frac{\partial u q_y}{\partial x} + \frac{\partial v q_y}{\partial y} = & -f q_x - g(h+\eta) \frac{\partial \eta}{\partial y} + \frac{\tau_y^s}{\rho} \\ & - C_F \frac{\sqrt{q_x^2 + q_y^2} q_y}{(h+\eta)^2} + \frac{\partial F_{xy}}{\partial x} + \frac{\partial F_{yy}}{\partial y} \end{aligned} \quad (3)$$

in which  $h$  = depth referred to datum ( $z = 0$ );  $\eta$  = the surface displacement;  $q_x$  and  $q_y$  = the discharges per unit width in the  $x$  and  $y$  directions, respectively;  $u$ ,  $v$  = the depth-averaged velocities;  $q$  represents a volume source;  $f$  is the Coriolis parameter;  $\tau^s$  is the wind shear;  $\rho$  is density; and  $F_{xx}$ ,  $F_{yy}$ , and  $F_{xy}$  are internal stress terms. The usual quadratic law is used to express bottom friction in terms of the flow variables. The model is almost completely input driven and thus requires no changes to program code for adaptation to a variety of applications. It has been applied to a number of circulation problems involving tides and wind (Wang, 1978; Wang et al., 1984; Kourafalou et al., 1984; Wang et al., 1988).

CAFE-2 was designed for strongly stratified conditions with a distinct pycnocline and relatively small mixing between layers. It models the barotropic and first baroclinic modes. The model has been applied to the summer wind-driven circulation in the South Atlantic Bight (Lorenzetti et al., 1988). Ongoing work adapts this model to winter storm conditions and examines the alongshelf and cross-shelf transports and their shears.

CAFE-3D is largely a research tool for studying 3-dimensional flows. For efficiency, it employs the customary splitting of internal and external modes, the latter being solved using CAFE-1, and the former described by

$$w_k - w_{k-1} + \frac{\partial}{\partial x} q_{xk} + \frac{\partial}{\partial y} q_{yk} = 0 \quad (4)$$

$$\begin{aligned} \frac{\partial q_{xk}}{\partial t} + \frac{\partial}{\partial x} (u_k q_{xk}) + \frac{\partial}{\partial y} (v_k q_{xk}) \\ = f q_{yk} - g H_k \frac{\partial \eta}{\partial x} + \frac{\partial}{\partial x} F_{xxk} + \frac{\partial}{\partial y} F_{xy} + \frac{1}{\rho} \{ \tau_{xk} - \tau_{xk-1} \} \end{aligned} \quad (5)$$

$$\begin{aligned} \frac{\partial q_{yk}}{\partial t} + \frac{\partial}{\partial x} (u_k q_{yk}) + \frac{\partial}{\partial y} (v_k q_{yk}) \\ = -f q_{xk} - g H_k \frac{\partial \eta}{\partial y} + \frac{\partial}{\partial x} F_{xyk} + \frac{\partial}{\partial y} F_{yyk} + \frac{1}{\rho} \{ \tau_{yk} - \tau_{yk-1} \} \end{aligned} \quad (6)$$

where  $w_k$  and  $\tau_k$  are the vertical velocity and shear stress, respectively, at the top of layer  $k$ ;  $u_k$  and  $v_k$  are layer-average velocities;  $H_k$  is layer thickness; and  $F_{xxk}$ ,  $F_{xyk}$ , and  $F_{yyk}$  are internal stresses due to turbulence and layer integration.

Turbulence and sub-gridscale effects are parameterized using an eddy viscosity tensor with principal axes along and perpendicular to the local current. No explicit turbulence closure is incorporated to determine the eddy viscosities. Application is limited to a study of hypothetical (unverified) hurricane and Gulf Stream interactions (Wang, 1987).

None of the circulation models has been dynamically coupled with a transport model for density, although such a model has also been developed. Two approaches have been followed. For dispersion-dominated processes, the dispersion analysis (DISPER) model (Christodoulou and Connor, 1980) is a straightforward Galerkin formulation, while a fractional step method, Finite Element Characteristic Advection and Diffusion (FECAD) model, is used for advection-dominated situations (Wang et al., 1988). In FECAD, the method of characteristics is used to solve the time evolution of advective terms, a fourth order Runge-Kutta scheme is used for the characteristic tracing, followed by a quadratic interpolation of parameters. One particular advantage of the characteristic advection approach is apparent when dealing with multiple components including the nonlinear momentum advection terms, since the characteristic is the same in every case and only has to be calculated once.

The models described above use proven numerical methods and have been formulated with careful attention to the physics. No extraneous boundary conditions are required because of the numerical method chosen. These models could serve well in a number of process-oriented studies of, e.g., the relative benefits of high-resolution advection versus sub-gridscale closure, seaward boundary forcing (ocean current) of shelf circulation, and topographic effects. They can also provide a basis for comparison with variable-grid finite difference methods. With further development, it is likely that a system satisfying the goals of COPS could evolve.

A two-layer version of CAFE-3D has been recently applied to winter storm-driven circulation in the South Atlantic Bight (Figs. 1 and 2). Comparison with observed subtidal currents in the Charleston area showed that the model explained 70 to 90% of the inner- and mid-shelf alongshelf current variance over a period of 16 days. At outer shelf stations, only 30 to 40% of the variance in alongshelf current could be attributed to wind. In the cross-shelf direction, there was poor agreement between model and observations. Considering the difficulties of determining cross-isobath flow when the flow is almost along isobaths, and the effects of the Gulf Stream, this should not be very surprising. Nevertheless, the model indicated that the bathymetry associated with capes could cause characteristic patterns of cross-shelf flows. The calculated cross-shore transport at the shelf break (75 m) is shown as a contour plot of vertically integrated transport magnitude versus alongshelf position and time (Fig. 3). The sign of the cross-shore transport changes several times when passing Cape Romain or Cape Fear from south to north. To investigate whether these were actually topographically controlled features, the bathymetry was straightened (Fig. 4). The calculated cross-shore transport for this configuration (Fig. 5) lacks the flow reversals around capes. Thus the model suggests that there may be a relationship between the Cape Romain and Cape Fear topographies and cross-shore transport due to wind.



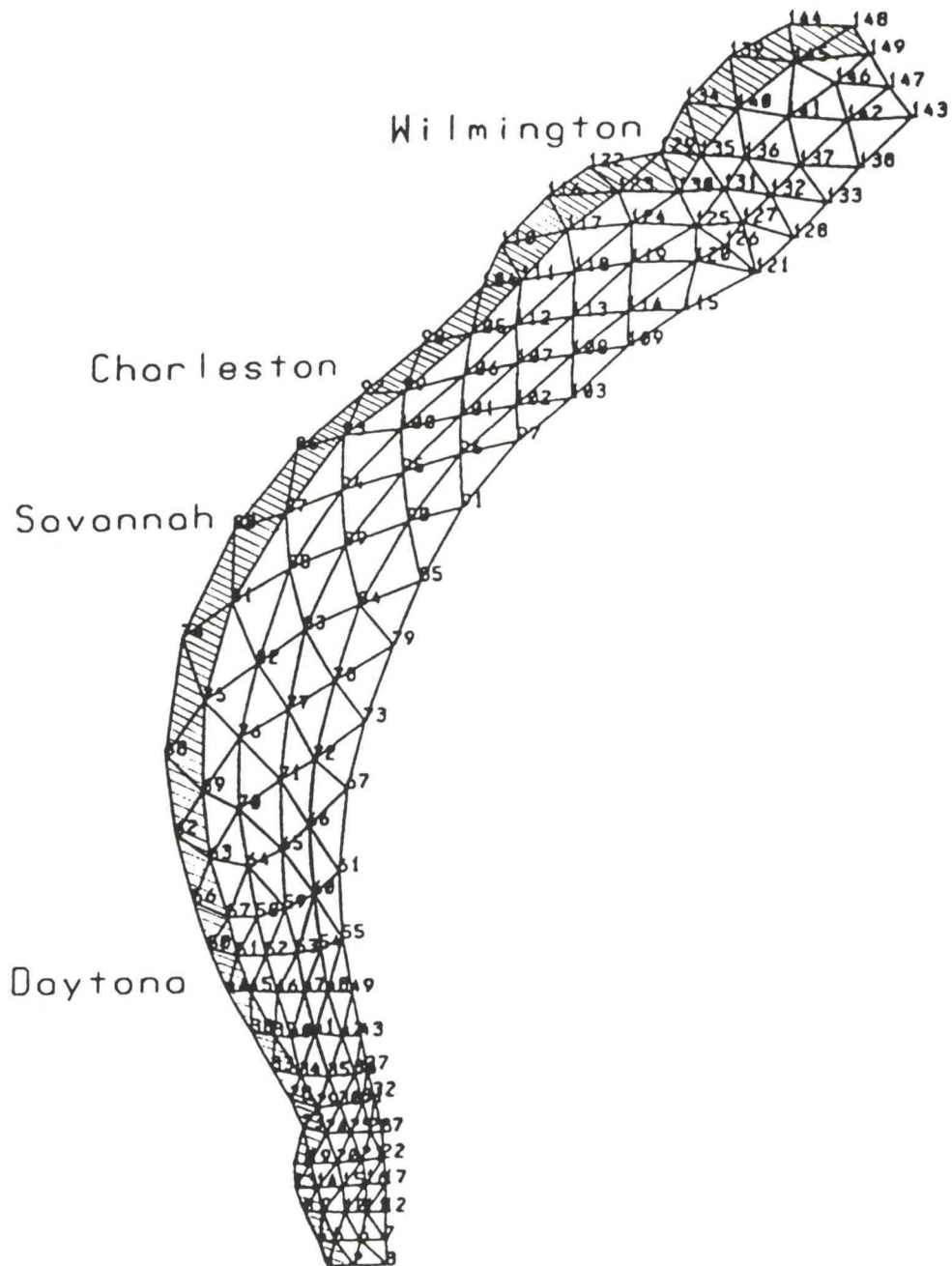


Figure 1. Model grid. The shadow part is the area used only for the upper layer.

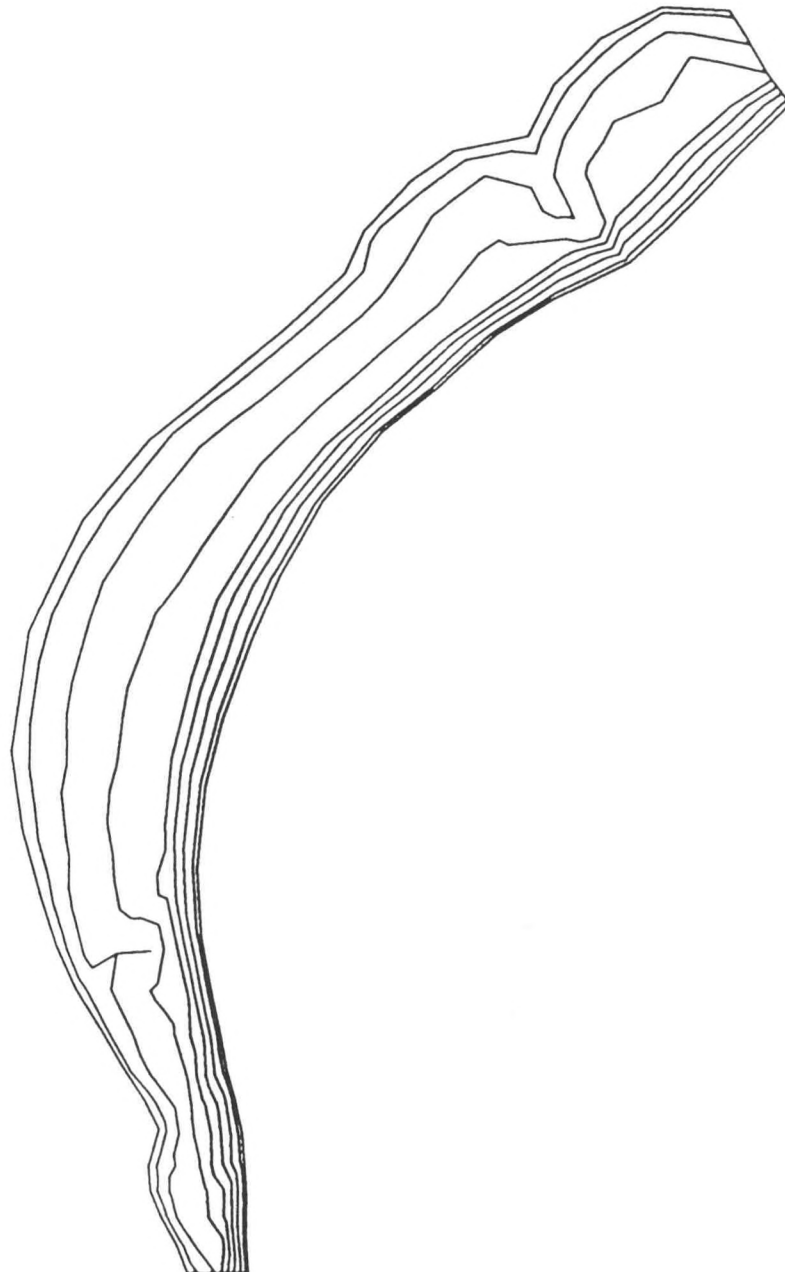


Figure 2. Model topography. The contour interval is 10 m.



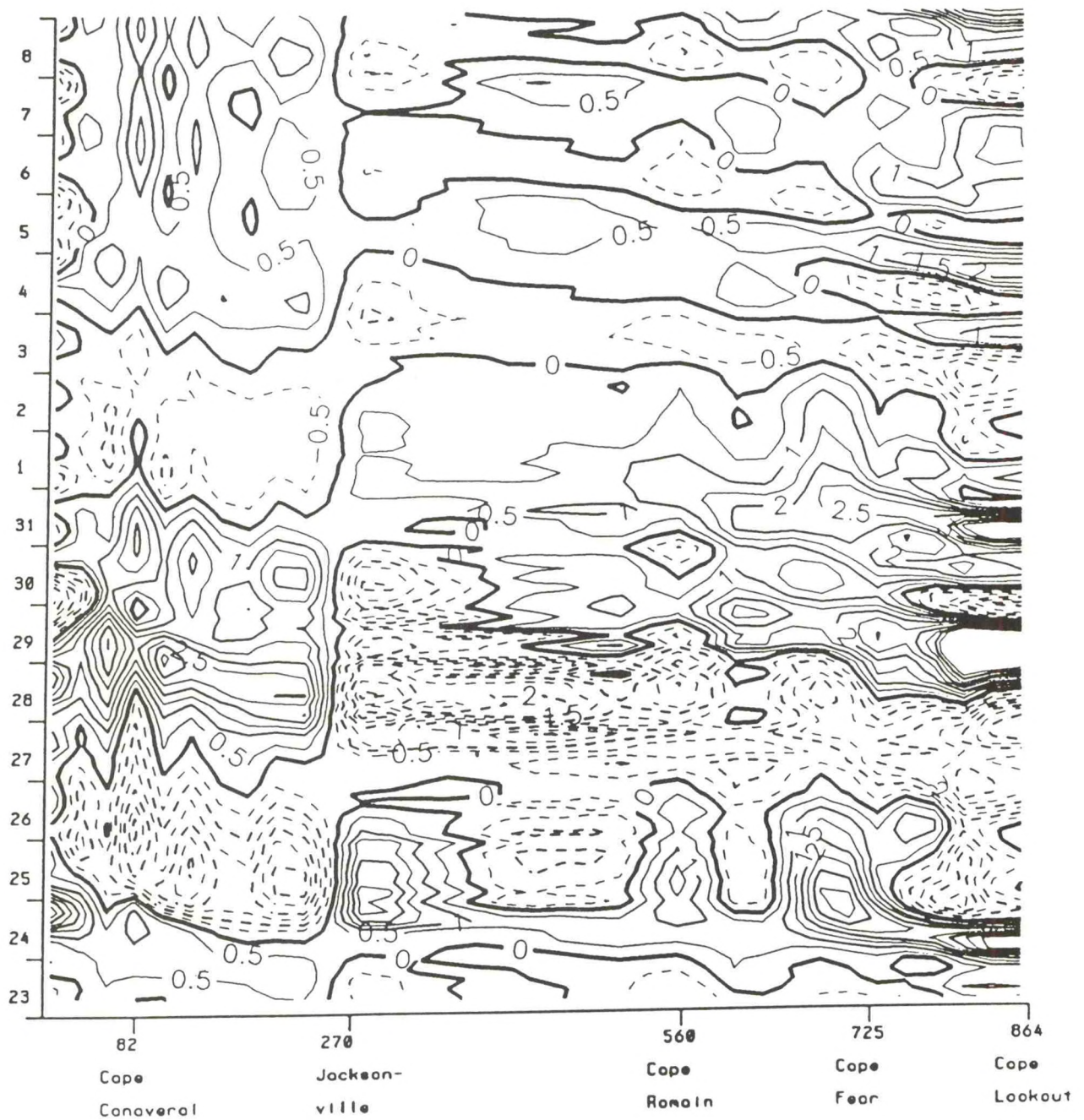


Figure 3. Cross-shore transport for Jan. 23 to Feb. 8. A thick line indicates zero transport, and positive (eastward) and negative (westward) transports are contoured using full and dashed lines, respectively. The interval of the contour is 0.5 m<sup>2</sup>/s.

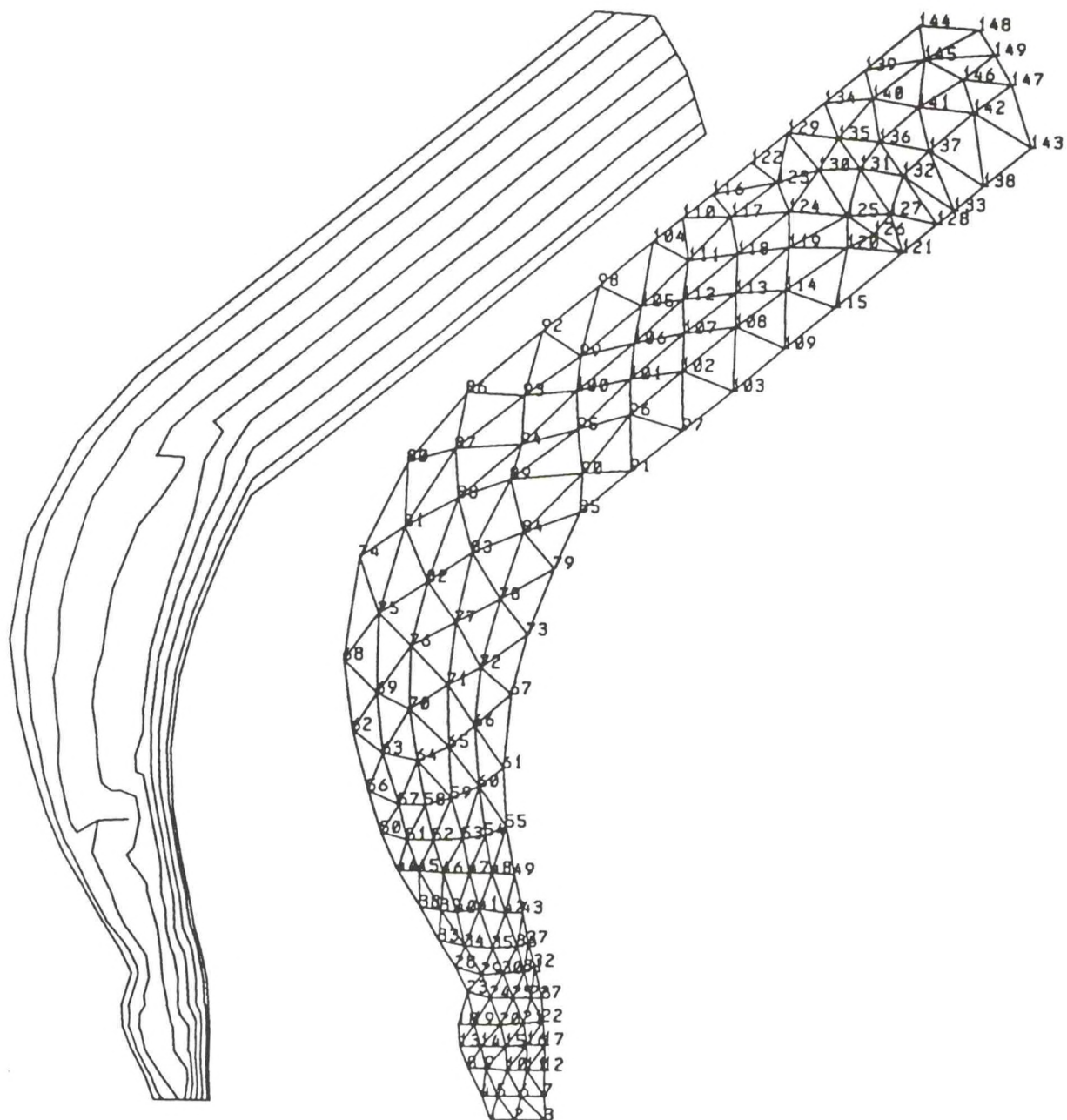


Figure 4. Topography and grid for constant slope bottom.



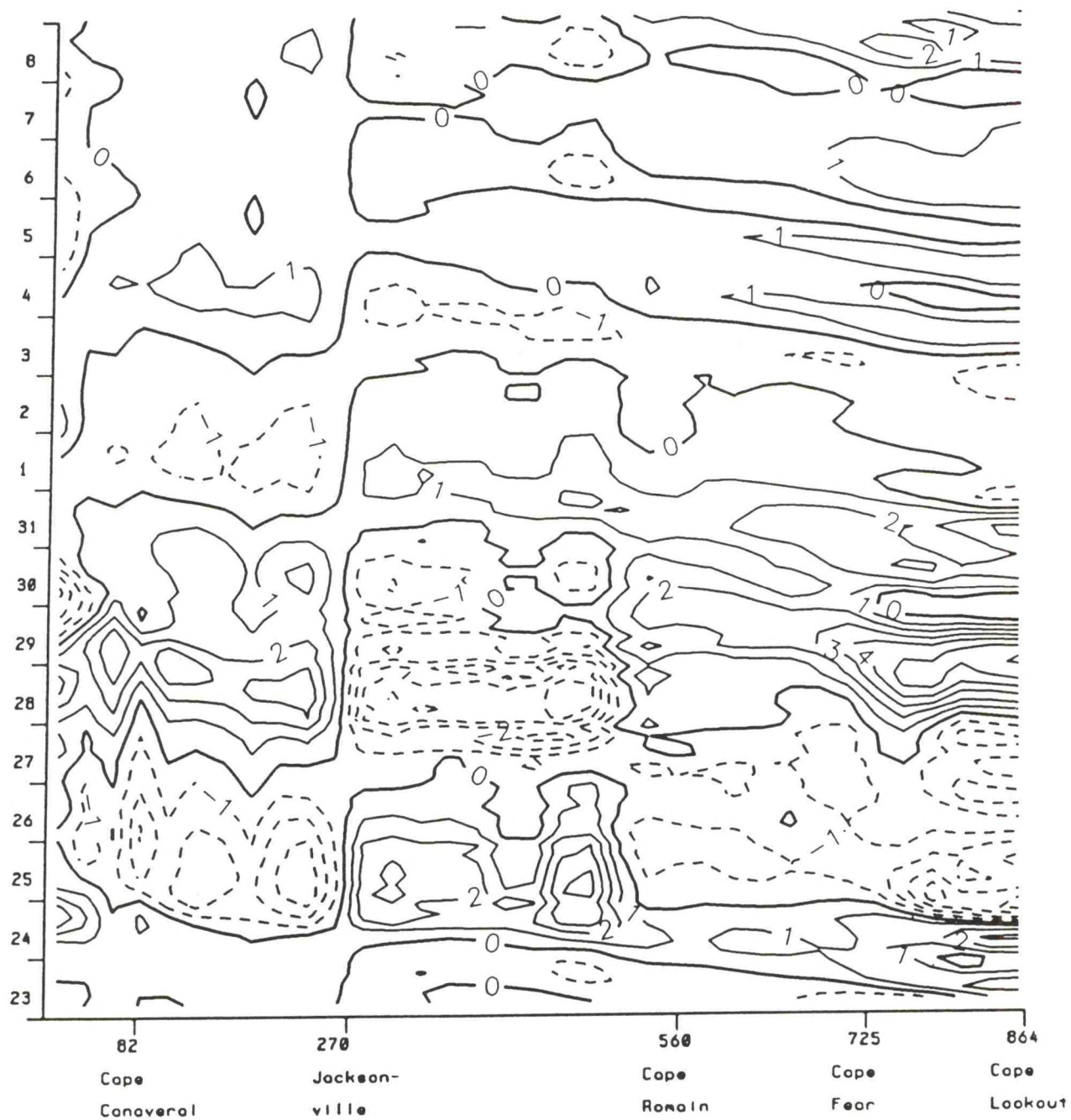


Figure 5. Cross-shore transport from constant slope bottom grid.

## A COASTAL OCEAN CIRCULATION MODEL

Dong-Ping Wang  
Marine Science Research Center  
State University of New York  
Stony Brook, NY 11794

Our coastal general circulation model (GCM) is a time-dependent, free-surface, three-dimensional, primitive-equation model. It is a fixed C-grid, finite-difference model with variable vertical resolution. The model uses a variation of the flux-corrected transport scheme in advective terms to preserve fronts against artificial (numerical) diffusion. The open-boundary condition is based on the Orlanski radiation condition; however, if wind forcing is present at the open boundary, the solution is split into local and nonlocal parts, with the radiation condition applied only to the nonlocal part. The GCM is solved through a two-mode integration in which the external mode (free surface and transport) is updated with a short time step and the internal mode (vertical velocity shears, temperature, and salinity) is updated with a long time step. The vertical eddy coefficients can be either specified from a Richardson-number dependent function (e.g., Munk-Anderson formula) or derived from an embedded one-dimensional mixed-layer model. The mixed-layer model is from Chen et al. (1988), and is based on the Mellor-Yamada level-2 turbulence closure. In the mixed-layer model, the surface boundary condition includes wind forcing and heat flux (long- and short-wave radiation), and the bottom boundary condition includes the logarithmic tidal boundary layer. The thermodynamics are complete, and the density is computed from the equation of state for seawater. The code is vectorized, and is currently running on the IBM 3090-600E of the Cornell National Supercomputer Facility (CNSF). We plan to convert the code into parallel processing to utilize the CNSF six-processor facility.

Most of our earlier model applications are theoretical studies. We investigated the response of island coastal waters to a finite-bandwidth wind forcing (Wang, 1982), the formation of a shelf/slope front (Wang, 1984), the mutual intrusion of a gravity current (Wang, 1985), and the outflow of a strait (Wang, 1987). Our more recent efforts, however, have been toward simulation of the real world (in cases where a comprehensive data set is available). For the purposes of a Coastal Ocean Prediction System (COPS), we will only discuss our recent applications.

### CODE Simulation

The Coastal Ocean Dynamics Experiment (CODE)-2 experiment off northern California in summer of 1982 is by far the most comprehensive coastal study program. Our model simulation started with the two-dimensional case (Chen and Wang, 1990). The simulation was run for the entire CODE-2 period of 103 days, driven by the observed atmospheric forcing. Agreement between observed and predicted mean properties is quite reasonable (Table 1). (Note that there is a constant 26cm/s difference in mean alongshore current.) Prediction of transient fluctuations also is



quite reasonable (Figs. 1 and 2 and Table 2). For comparison, the prevailing coastal-trapped wave model has similar predictive skill in alongshore velocity, but no predictive skill in cross-shore velocity and temperature.

The two-dimensional simulation is promising; however, the model obviously under-predicted the warming episodes. The wind relaxation is being investigated with the three-dimensional model (Chen and Wang, (in preparation)). We use an idealized wind condition and also include a mean poleward alongshore slope.

Figure 3 shows temperature and cross-shore and alongshore velocity along C-line. The southward wind is uniform during the first four days (the spin-up phase) and the coastal water response shows an upwelling front, offshore Ekman flow, and southward jet (Fig. 3a). The wind is shut off on Day 4 in a narrow coastal band ( $<10$  km) south of (including) C-line, and afterward the nearshore water is significantly warmed and the nearshore current also turns poleward (Figs. 3b-3c). The southward wind is shut off everywhere on Day 8, and soon, current is poleward over the whole shelf (Fig. 3d). This simulated wind relaxation scenario is consistent with the limited current meter and satellite observations.

### Internal Tide and Buoyant Outflow

The Gibraltar Strait Experiment in 1985-1986 is a major field study of a tidal strait. Our three-dimensional model study (Wang, 1989) simulated the mean gravitational circulation and the tidal motion under idealized forcing. The GCM is initialized through a lock-exchange adjustment and is driven by barotropic tidal transport at open boundaries. Figure 4 compares predicted and observed density (salinity) oscillation at the sill during spring tide. The model simulation faithfully predicts the 200 m interface excursion, the gradual rise of the interface during ebb, and the sudden plunge of the interface after high water. Excitation of the internal surge, a sharp drop of the interface over 100 m in about 1 hour, is easily handled by the GCM. Indeed, the model simulation reproduces the internal hydraulic process of transition (jump) from subcritical flow to supercritical flow.

The strait flow study may not be directly applicable to the COPS objectives. On the other hand, our expertise in simulating energetic motions in a sea strait virtually assures successful model application to any buoyant outflow problems relating to estuarine circulation and estuary-shelf exchange (Wang, 1988). Another useful application of our strait flow study is to simulate internal tides over the continental slope and shelf. The generation of a nonlinear internal tide over a steep slope is analogous to the generation of an internal surge over the sill. Our model may prove to be a powerful tool to probe the "mysterious" nonlinear internal tides over the slope. To date, no GCM has ever been used in an internal tide study.

In summary, we are making major progress towards genuine real-world simulation of the coastal ocean. Our two-dimensional CODE simulation is the first realistic simulation of coastal upwelling. The model results are very encouraging, which will make a data-assimilation experiment a worthy effort. Data assimilation utilizes both

observed and predicted fields in a certain optimal manner to achieve a better prediction, and in the absence of a better model, data assimilation is the most practical approach towards ocean prediction. Certainly, a three-dimensional real-world simulation (with data assimilation) is an ultimate goal. The Gibraltar Strait, with its constricted geometry and comprehensive data base, probably will be most suitable for an early endeavor. It will be valuable to extend our model study to a real-world simulation using the observed barotropic transport as forcing (at the open boundary). On the other hand, a three-dimensional real-word simulation of CODE may not be feasible because of the incomplete forcing data; the crucial coastal wind information is lacking, nor is there much open-boundary (upstream) data.

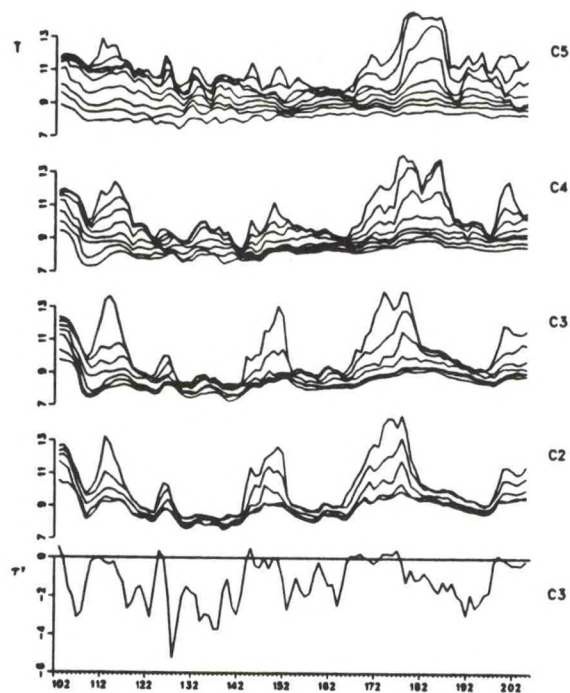


Table 1. Mean values of observed and model-predicted cross-shelf velocity (u), alongshore velocity (v), and temperature (T) at 10 m depth. Subscript m (o) means model-predicted (observed).

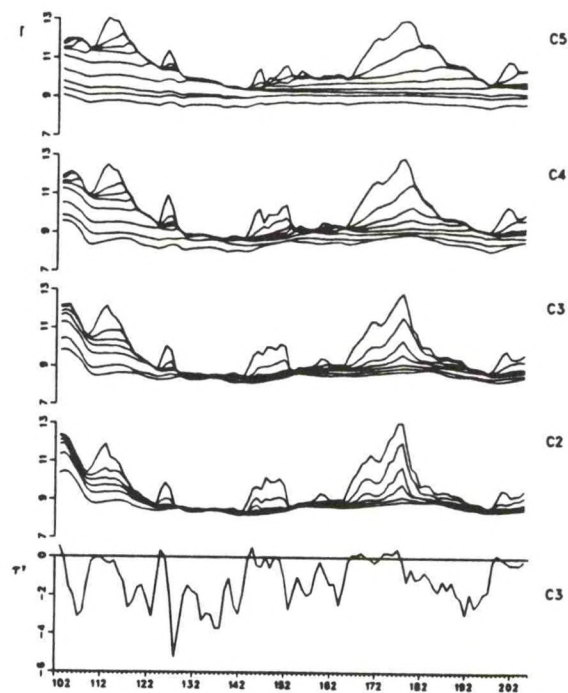
Station	$u_m$	$u_o$	$v_m$	$v_o$	$T_m$	$T_o$
C2	-1.8	-1.5	-17.6	3.4	9.6	9.9
C3	-5.8	-4.7	-29.6	-4.8	9.7	9.8
C4	-7.6	-8.5	-27.7	-21.4	10.4	10.3

Table 2. Correlations ( $\gamma$ ) between observed and model-predicted cross-shelf velocity (u), alongshore velocity (v), and temperature (T) at 10 m depth.

Station	$\gamma_{uu}$	$\gamma_{vv}$	$\gamma_{TT}$
C2	0.72	0.77	0.91
C3	0.82	0.79	0.88
C4	0.75	0.74	0.81



Year Day



Year Day

Figure 1. Observed (left panel) and predicted (right panel) temperature time series at several mooring locations.



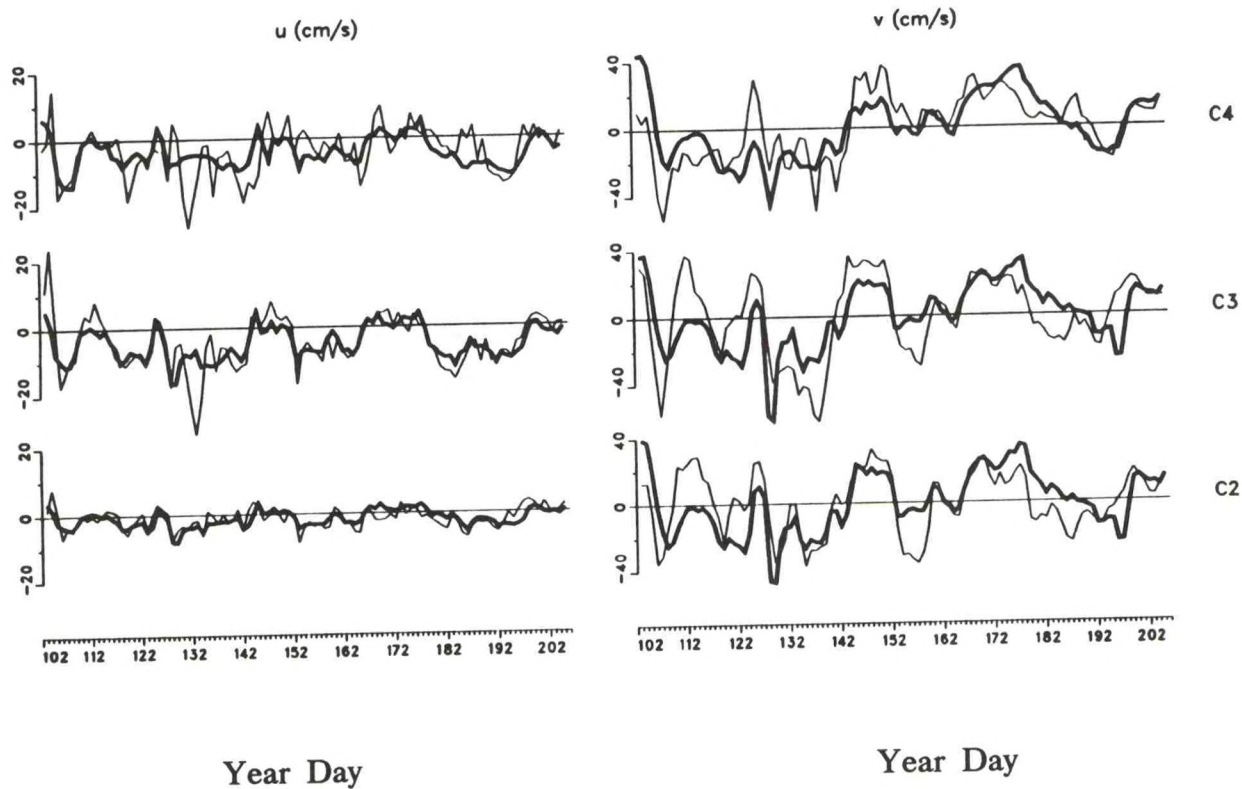


Figure 2. Comparison between observed (light line) and predicted (dark line) cross-shore (left panel) and alongshore (right panel) velocities at several mooring locations. (Note: a constant 30 cm/s poleward mean flow is added to predicted alongshore velocity.)

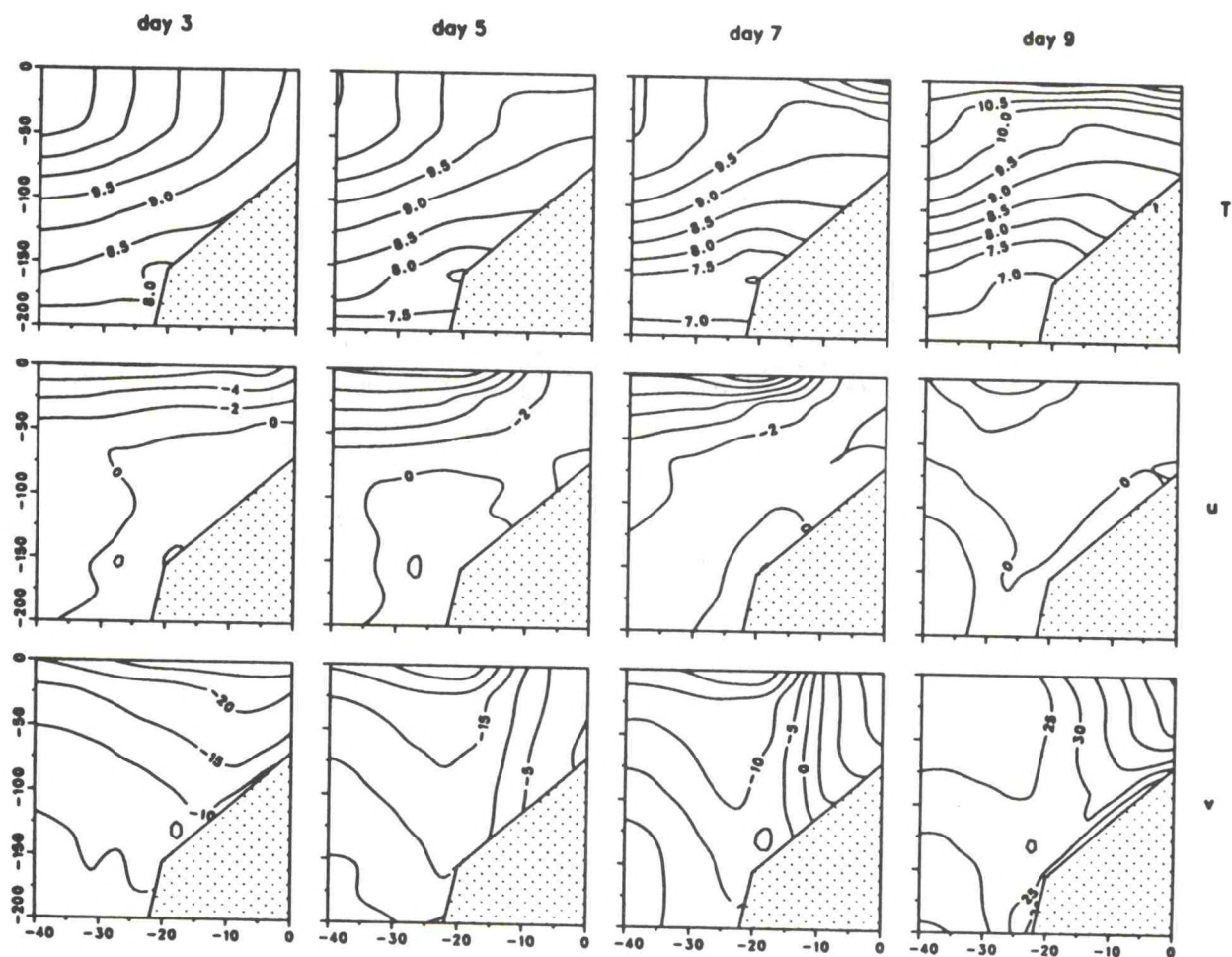


Figure 3. Cross-sections of temperature (T), cross-shore velocity (u) and alongshore velocity (v) along the C-line, from a three-dimensional simulation: (a) day 3; (b) day 5; (c) day 7; (d) day 9.



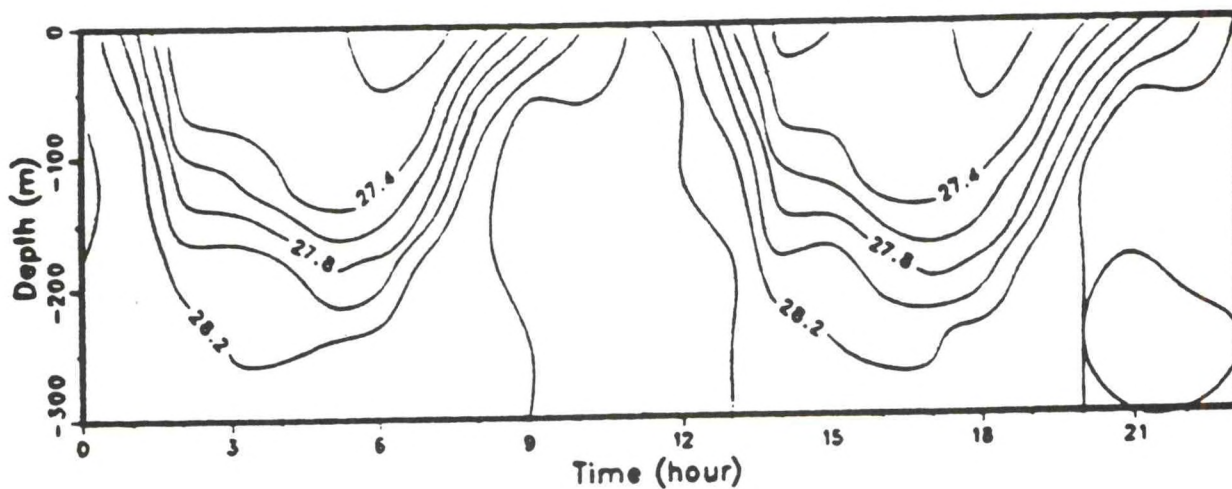
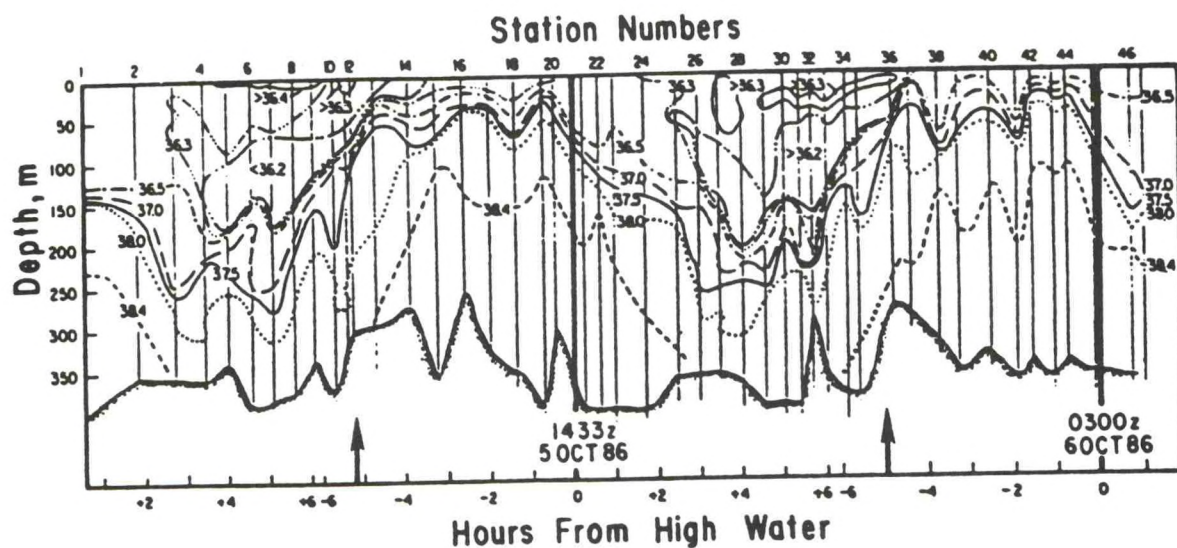


Figure 4. Observed salinity (upper panel) and predicted density (lower panel) over a tidal cycle at the Camarinal Sill. (Note that the time axes of the two panels are somewhat different in scale.)

# SEMI-SPECTRAL PRIMITIVE EQUATION REGIONAL OCEAN CIRCULATION MODEL

Dale B. Haidvogel  
Chesapeake Bay Institute  
The Johns Hopkins University  
Baltimore, MD 21211

The following summarizes in brief detail the present status and ongoing application of a semi-spectral primitive equation regional ocean circulation model (SPEM) which has been under development by the author (and many interested colleagues) for several years. A more complete description of the model, and the variety of test problems on which its performance has been assessed, is available (Haidvogel et al., 1990). An extensive user's manual has also been compiled (Hedstrom, 1989).

As is traditional in diabatic, regional and large-scale ocean modeling (see, for example, Cox, 1985), the equations of motion for the model are the hydrostatic primitive equations. Independent prognostic equations for temperature and salinity--or temperature and a passive tracer--are now incorporated. Alternatives for lateral subgridscale smoothing include Laplacian and biharmonic mixing, and/or Shapiro filtering. In the vertical, mixing is parameterized by depth-dependent viscous and diffusive coefficients. Explicit surface mixed-layer response is accounted for via a Price-Weller-Pinkel-type mixed-layer model (Price et al., 1986); this option is in place, and presently being tested (see below).

The SPEM is bounded at top by a rigid lid (thus filtering out surface gravity waves), and at the bottom by variable bathymetry. With respect to the lateral boundaries, several options are explicitly offered. For example, either periodic channel or closed wall geometries may be selected, and are suitable for a wide range of process-oriented studies. An additional option is for "open" lateral edges, in which the model provides an easy interface for users to provide their favorite open boundary conditions. This latter version is therefore, in principle, suitable for "realistic" regional ocean modeling problems.

Prior to numerical solution, the continuous equations of motion are modified by two coordinate transformations. The first is a sigma (bathymetry-following) coordinate system, a common choice in global and regional atmospheric models. The second is a horizontal orthogonal curvilinear coordinate system capable of handling irregular lateral boundaries (e.g., a coastline) and/or providing a spatially-variable density of coordinate surfaces (i.e., variable resolution). A software package has been developed for the generation of the required two-dimensional orthogonal grid in either a Cartesian or spherical geometry (Hedstrom, 1989).

The numerical solution techniques, at present, are simple in the lateral coordinates and time: second-order-accurate space-differencing (the Arakawa C-grid) and time-differencing (leapfrog-trapezoidal). [In a related project, funded by the



National Science Foundation (NSF), several investigators (Evans, Haidvogel, Boyd and Marshall) are exploring improvements to the temporal and horizontal approximation methods by the addition of three-dimensional boundary-fitting spectral elements and the third-order Adams-Bashforth-Crank-Nicolson (ABCN) scheme (Hussaini and Zang, 1987)]. In the sigma coordinate, a rapidly convergent representation is used in which the vertical dependence of the field variables is expressed as an expansion in continuous vertical structure functions. Though many choices of the functions are possible, the default option in the model is the use of Chebyshev polynomials. Haidvogel et al. (1990) give several dramatic examples of the power of the Chebyshev approximation technique. Although advantageous in many applications by virtue of the rapid convergence typically obtained with them, Chebyshev polynomials are not necessarily optimal in all circumstances since their turning points are distributed so as to favor equally the top (surface) and bottom boundaries. For problems in which the expected vertical structure of the solutions is, for example, surface-confined, as is the case with an active surface mixed layer, it has been shown that the introduction of a mapping of the Chebyshev polynomial turning points onto a more surface-intensified set of grid points provides substantial improvement in accuracy and convergence properties (see below). A preprocessor for the SPEM has been written to automatically compute the transformation matrices associated with any user-selected set of vertical collocation levels (subject only to the requirement that they lead to a well-behaved transformation). As a result of this software, the user has flexible control over the placement of vertical resolution, while retaining the desirable convergence properties of the spectral expansion.

Model performance has been assessed in relation to several suites of simple test problems (Haidvogel et al., 1990). These include: barotropic shelf waves and baroclinic Kelvin waves (for which analytic solutions are available); baroclinic coastal-trapped waves (for which the eigenstructures can be numerically determined (Wilkin, 1987)); scattering of continental shelf waves at a discontinuity in shelf width (analytic solution from Wilkin and Chapman (1987)); mean flow generation by topographic stress in a wind-driven coastal ocean (comparison to the results of Haidvogel and Brink (1986)); and simulation of the wind-driven, mid-latitude ocean circulation (comparison to the results of McWilliams et al. (1990)). The model, vectorized for the Cray-XMP, has been shown to be of comparable computational efficiency to the Bryan/Semtner/Cox primitive equation model for comparable numbers of grid points.

The following are brief descriptions of several of the ongoing applications of the model.

#### **Scattering of Coastal-Trapped Waves by Irregularities in Coastline and Topography** **John Wilkin and Dave Chapman, both Woods Hole Oceanographic Institution (WHOI)**

In this study (Wilkin and Chapman, 1990), we have used a numerical model which accommodates arbitrary density stratification, bathymetry, and coastline, to examine how freely-propagating coastal-trapped waves (CTWs) are scattered by large variations in coastline and topography occurring over alongshelf distances comparable to the



shelf width in a realistically stratified coastal ocean. The strength of the scattering, as measured by the proportion of the incident energy flux scattered into modes other than that of the incident wave, was found to be proportional to a topographic warp factor which estimates the extent to which the topography departs from shelf-similarity. The scattering induced by non-shelf-similar topographic variations is amplified by density stratification. A comparison of the effects of widening and narrowing topographies showed that the amplitudes of the freely-propagating transmitted modes generated by "reciprocal" narrowing and widening topographies are quite similar. Within the scattering region itself, the strengths of the scattered-wave-induced currents exhibit substantial variation over short spatial scales. On both widening and narrowing shelves, there is generally a marked intensification of the flow within the scattering region, and significant differences in the directions of the currents at points separated by a few tens of kilometers indicate the occurrence of rapid variations in phase. On narrowing shelves, the influence of the scattering can extend upstream into the region of uniform topography even when backscattered free waves are not possible. An example of these effects is shown in Figures 1 and 2.

A simulation of CTW scattering was performed at a site on the East Coast of Australia where observations made by Griffin and Middleton (1986) suggest the presence of scattered freely-propagating CTWs (Fig. 3). The simulation supports Griffin and Middleton's (1986) conjecture that the waves they observed were the signature of remotely-forced free CTWs scattered by the abrupt topographic variations of their study region. This supports the notion that realistic shelf geometries can scatter significant levels of CTW energy, and that the scattered waves can have an appreciable signal in current-meter observations made on the continental shelf. Griffin and Middleton's (1986) observation of what is actually a very high mode (mode 6) free wave with a low phase speed ( $0.4 \text{ m s}^{-1}$ ) demonstrates that along irregular coastlines it may be necessary to account for CTW scattering processes if oceanic observations are to be interpreted correctly. The success of the model simulation in reproducing features of Griffin and Middleton's (1986) observations suggests that simulations of free CTW scattering may be useful for predicting features of scattering processes on other continental shelves of interest, and may prove to be a useful tool for improving the design of field experiments, and the interpretation of their results.

#### **Regional Modeling of the Coastal Transition Zone**

**Dale Haidvogel, Chesapeake Bay Institute (CBI) and Kate Hedstrom, Institute for Naval Oceanography (INO)**

The specific objectives of this work are: (a) to develop a dynamically realistic model of the Coastal Transition Zone (CTZ); (b) to explore the ability of local/internal dynamical mechanisms to generate offshore-directed jets and filaments; (c) to characterize the resulting filaments, including their dominant space/time scales, their relationship to coastal and bathymetric geometry, and their contribution to the coastal balances of heat and mass; and (d) to compare the model results where possible with the CTZ field measurements. An extensive sequence of sensitivity



studies has been undertaken to investigate the properties of the SPEM in environmental regimes featuring strongly sheared, baroclinic currents which abut steep continental shelf/slope topography. Much sensitivity has been discovered, showing a complicated dependence on topographic steepness, mean flow structure and strength, resolution in space and time, and the parameterization and strength of both horizontal and vertical sub-grid-scale smoothing. Nonetheless, with careful attention to these choices, we have been able to achieve reasonably representative CTZ simulations (cf., Figs. 4 to 6) featuring all of the following dynamical elements: irregular coastline, (moderately) steep bathymetry, realistic stratification, and strongly sheared mean currents.

We are presently analyzing these simulations, paying particular attention to the scientific issues noted above, i.e., a detailed statistical and dynamical characterization of the filaments, and their contribution to mass, momentum and energy balances in the CTZ region. Preliminary analysis of experiments such as the one summarized in Figs. 4-6 shows, for instance, that generation of the offshore-directed filaments is intimately related to sharp coastline and bathymetric features. For example, removal of all coastline variations suppresses filament generation. Another robust feature of the idealized numerical experiments is the "subduction" of coastal water in the outgoing filaments. Substantial vertical motion of water parcels is invariably observed; density, in contrast, is nearly conserved following water parcels (Fig. 6). Comparisons with the CTZ observational dataset are being explored (see, e.g., below); however, such comparisons are complicated by our use of periodic boundary conditions, a choice made so as to avoid the substantial additional complexity of dealing with open boundaries.

The CTZ numerical model and/or the simulated CTZ dataset are being provided to other interested CTZ investigators for related studies. In particular, we have been working with Dr. Eileen Hofmann to produce the first fully three-dimensional, time-dependent coupled physical/biological model based on the primitive equations. The biological component of this coupled model predicts the space/time evolution of four biological constituents (nutrient nitrogen, phytoplankton, zooplankton and detritus) in response to the combined effects of advective, diffusive and biological processes. The biological model has recently been reformulated by Dr. Hofmann to be numerically compatible with the SPEM, and preliminary coupled experiments are scheduled for the early part of the coming year.

**Investigation of the Processes Contributing to the Zooplankton Community Structure Observed During the 1988 CTZ Field Experiment: A Modeling Study**  
Kate Hedstrom (INO), Dale Haidvogel (CBI), Eileen Hofmann, Old Dominion University (ODU), and David Mackas, Institute of Ocean Sciences (IOS)

During the 1988 Coastal Transition Zone (CTZ) field experiment, the zooplankton populations observed following a Lagrangian drifter underwent rapid changes in community composition in the along-filament direction and were characterized by a species composition that was similar to that observed in the waters to the northwest of the filament. The observed changes in community composition occurred on time



scales shorter than those associated with biological processes, implying that the circulation is a major factor in this evolution. In particular, processes such as across-filament exchange are hypothesized to play an important role. To test this hypothesis, numerous-particle tracking experiments were performed using simulated velocity distributions obtained for the CTZ region with a regional primitive equation model. The circulation model provides time-dependent descriptions of the movement of water parcels and their associated properties (such as temperature). The simulated drifter tracks give estimates of residence times and the vertical and horizontal displacement of particles released in and around the simulated filaments. These results allow quantification of the physical processes that contribute to the observed zooplankton distributions.

#### Initial Experiments With a Coupled Primitive Equation/Upper Mixed Layer Model Hsiao-ming Hsu (WHOI)

A one-dimensional version of the semi-spectral primitive equation numerical model has been created (i) to test the sensitivity of the surface mixed-layer model to changes in vertical resolution, and (ii) to evaluate the benefit of using "mapped" Chebyshev polynomials as the vertical expansion functions. The surface layer model being used is that of Price, Weller and Pinkel (1986). Figure 7 shows the sensitivity of the response of the coupled model to vertical resolution. All the plots have water depth (150 m) on the vertical axis and the duration of the simulation (5 days) on the horizontal axis, and show contours of the vertical/temporal structure of  $\sigma_t$ . The initial condition is neutral (i.e.,  $\sigma_t = 0$ ). A constant wind stress at the surface of 0.7 dyne/cm/cm is applied, along with a thermal flux representative of the mid-latitude diurnal heating/cooling cycle. The upper left corner of Figure 7 shows the time evolution with 24 unevenly distributed (unmapped) Chebyshev collocation points. The mixed-layer and the transition layer are simulated reasonably well. The upper right corner is the same simulation, but using 128 Chebyshev collocation points. The mixed layer is a little deeper, and the transition layer is a little sharper than in the previous case. The lower plot shows the result of the same simulation except using only 24 arbitrarily spaced grid points. Half of the 24 points are evenly distributed in the upper 30 meters of the water column, and the other half throughout the rest of the water column. The result is extremely accurate compared with the case using 128 regular Chebyshev collocation points. The 24 mapped points are assigned manually, then they are mapped to the regular Chebyshev collocation points to take advantage of the high accuracy of using pseudo-spectral approximation.

A two-dimensional version of the coupled model is being used to investigate the formation of a coastal upwelling front. Figure 8 shows some representative results. The component figures are vertical cross-sections of  $\sigma_t$  from a two-dimensional simulation of an upwelling front at the end of second, third, fourth and fifth days of simulation. The water depth is 150 m, and the channel is 100 km long. The initial thermocline is located at a depth of 25 m. The wind-stress has a strength of 2 dyne/cm/cm with a diurnal variation of 1 dyne/cm/cm. The day-time heating as a maximum of 865 watts/m/m and a constant cooling is -60 watts/m/m during the night.



The vertical eddy diffusivity is  $0.1 \text{ cm}^2/\text{sec}$ , and the horizontal eddy diffusivity is  $50 \text{ m}^2/\text{sec}$ . The initial thermocline surfaces during the first two days of the simulation. Because of the accumulated surface heating, a portion of the upwelling front has been pushed back to a subsurface location. This demonstrates the essential roles of surface wind stress and thermal fluxes in the variability of coastal upwelling.

### Pressure Gradient Errors Associated With Steep Topography in a Stratified $\sigma$ -Coordinate Model

Aike Beckmann (CBI) and Dale Haidvogel (CBI)

Various formulations of the pressure gradient terms in the  $\sigma$ -coordinate ocean model of Haidvogel et al. (1990) have been examined for their error properties in the presence of steep topography and realistic stratification. In the limit of smooth, almost flat topography or weak stratification the model may be run successfully for periods of weeks to months without showing obvious signs of unrealistic currents; however, in the case of steep topography (slopes  $\gg 0.01$ ), the simulations become contaminated significantly early on. These systematic errors can be shown to originate (in part) from the finite difference approximation of the continuous pressure gradient terms. (This is not the only source of trouble, we have also found sensitivity to the way we smooth the density field and to the formulation of the advective terms.)

There are several ways of implementing the pressure gradient. SPEM uses the following (historically standard) form:

$$h \nabla \phi|_z = h \nabla \phi|_\sigma + (1 - \sigma) h \left( \frac{\phi}{h} \right)_\sigma \nabla h.$$

In this formulation the correction term due to the  $\sigma$ -coordinates is written as a term proportional to  $\rho$ , which means that  $\rho$  is first averaged and then integrated as opposed to first integrating  $\rho$  and then averaging  $\phi$ . This guarantees that at least linear stratification can be represented correctly.

As shown by Haney (1990), the initial error from these pressure gradient terms can be enormous. The error depends on the local depth, slope and the amplitude of the pressure field. For increased horizontal resolution, the error patterns are the same, but with reduced amplitude. Typically, the error decreases quadratically with increased resolution. However, since the errors may be very large, increasing the resolution within affordable limits does not help in all cases.

We have tested other algorithms for computing the pressure gradient (a modified formulation that guarantees the correct Joint Effect of Barclinity and Bottom Relief (JEBAR); another spectral approach based on z-polynomials; and on hybrid formulation of a z-coordinate system in the upper water column gradually changing into a  $\sigma$ -coordinate system towards the bottom); however, for topographic gradients which are typical for continental slopes and isolated seamounts ( $h_x \geq 0.05$ ), all these formulations are ill-behaved.



A simple example of the kinds of trouble we can encounter with a version of the model is as follows: Using a  $34 \times 33 \times 7$  version of SPEM, we have performed a series of simple runs with a well-resolved gaussian seamount in an initially resting fluid. The initial perturbation stratification was chosen to be the difference between two exponentials with slightly different vertical scales. All the tested cases showed the evolution of artificial vortices (with a maximum local transport of up to several Sverdrups) and/or high vertical mode patterns within a few days. The behavior of the pressure gradient can be improved by subtracting the mean density profile, but in a steep topography/strong stratification situation, or in problems with significant (basin-scale) lateral extent, such measures are also ineffective in significantly reducing error levels.

With continuous representation of the vertical fields by a set of orthogonal polynomials (e.g., Chebyshev polynomials), however, it is possible to compute the pressure gradient directly in the  $z$ -coordinate system. Strictly speaking, this  $z$ -based pressure gradient term is calculable only between the surface and a depth dependent on the minimum of adjacent water columns, thus, excluding a triangular region at the bottom where some kind of extrapolation has to be applied. Using a Taylor-series of  $\phi$  to evaluate the pressure in a  $z$ -coordinate system, we can extrapolate "into the bottom". These corrections to the pressure gradient can be applied in the SPEM, and lead to a reduction of the initial pressure gradient error of about two orders of magnitude. A parameter survey of model resolution, stratification and topographic steepness is currently under investigation.

Lastly, we know of no  $\sigma$ -coordinate, primitive equation model that does not share these problems. For instance, Haney (1990) studies in detail the effects of vertical discretization on the pressure gradient error in a layered model. Also, some of the seamount calculations mentioned below have been duplicated with a  $\sigma$ -coordinate version of the Geophysical Fluid Dynamics Laboratory (GFDL) model, with substantially similar results.

### Formation of Taylor Caps Over a Tall, Isolated Seamount in a Stratified Ocean David Chapman (WHOI) and Dale Haidvogel (CBI)

The flow of a rotating, stratified ocean past an isolated seamount is investigated using a three-dimensional, continuously stratified, primitive-equation numerical model. In particular, we examine the conditions under which closed circulation patterns (i.e., Taylor caps) form in response to a steady, uniform incident flow impinging upon a Gaussian-shaped seamount. For weak incident flows (i.e., small Rossby number;  $Ro = U/fL \ll 1$ , with  $U$  the incident velocity,  $f$  the Coriolis parameter and  $L$  the horizontal length scale of the seamount) and a short seamount (i.e., small fractional seamount height;  $Dh = h/H \ll 1$ , with  $h$  the height of the seamount and  $H$  the total ocean depth), the results are in close agreement with quasi-geostrophic (QG) models. That is, Taylor caps (almost Taylor columns in this case) form when  $Ro/Dh < 0.32$ . As  $Dh$  increases above about 0.3, the occurrence of Taylor caps is limited to substantially lower  $Ro$  than predicted by QG theory. The addition of vertical stratification has two primary effects. First, it tends to



inhibit vertical motions, thus allowing Taylor caps to form at somewhat larger Rossby numbers. Second, the Taylor caps become bottom-trapped with a vertical scale of  $fL/N$  where  $N$  is the buoyancy frequency. For tall seamounts ( $Dh < 0.5$ ), the vertical velocity field can be quite strong and the Taylor caps distorted. Three-dimensional tracking of water parcels shows that, in this limit, the idea of the caps being regions of relatively stagnant flow becomes questionable.

## **Numerical Studies of the Formation and Maintenance of a Shelfbreak Front**

**David Chapman (WHOI)**

Shelfbreak fronts are persistent and stable features which have been observed along a number of continental shelves. However, the dynamics of the shelfbreak front are relatively unknown. For example, the processes which form and maintain the front are uncertain, as are the reasons for its location at the shelf break. The effectiveness of the front as a barrier to cross-shelf exchange and its response to external forcing are also unknown. The long-term goals of this project are therefore to carry out a sequence of idealized numerical experiments designed to provide insight into these issues by starting with relatively simple situations and adding various complexities in an orderly fashion. Simulations will be carried out using the semi-spectral, primitive equation model (SPEM) of Haidvogel et al. (1990). Three sets of experiments are proposed. The first set will primarily address the "tracer" vs. "density" front issue, as well as the question of frontal location. The second set will examine the effects of surface wind stress on the frontal structure and position. The third set will examine the interaction of an offshore eddy with the shelfbreak front. Preliminary simulations using the SPEM have been conducted in the barotropic (constant density) limit, and show good agreement with the simple, depth-integrated model of the shelfbreak front explored by Chapman (1986). Additionally, however, the SPEM results extend those of the simple model by providing a three-dimensional (3-D) description of the circulation. Analysis of the simulated 3-D circulation patterns in the neighborhood of the fronts is underway. Associated technical issues are being addressed, including: incorporation of temperature ( $T$ ) and salinity ( $S$ ) as separate thermodynamic variables (now complete); rotation of the lateral mixing tensor to accommodate smoothing along constant  $z$  or  $\sigma$  surfaces; and development of open boundary conditions suitable for future simulations in the stratified limit.

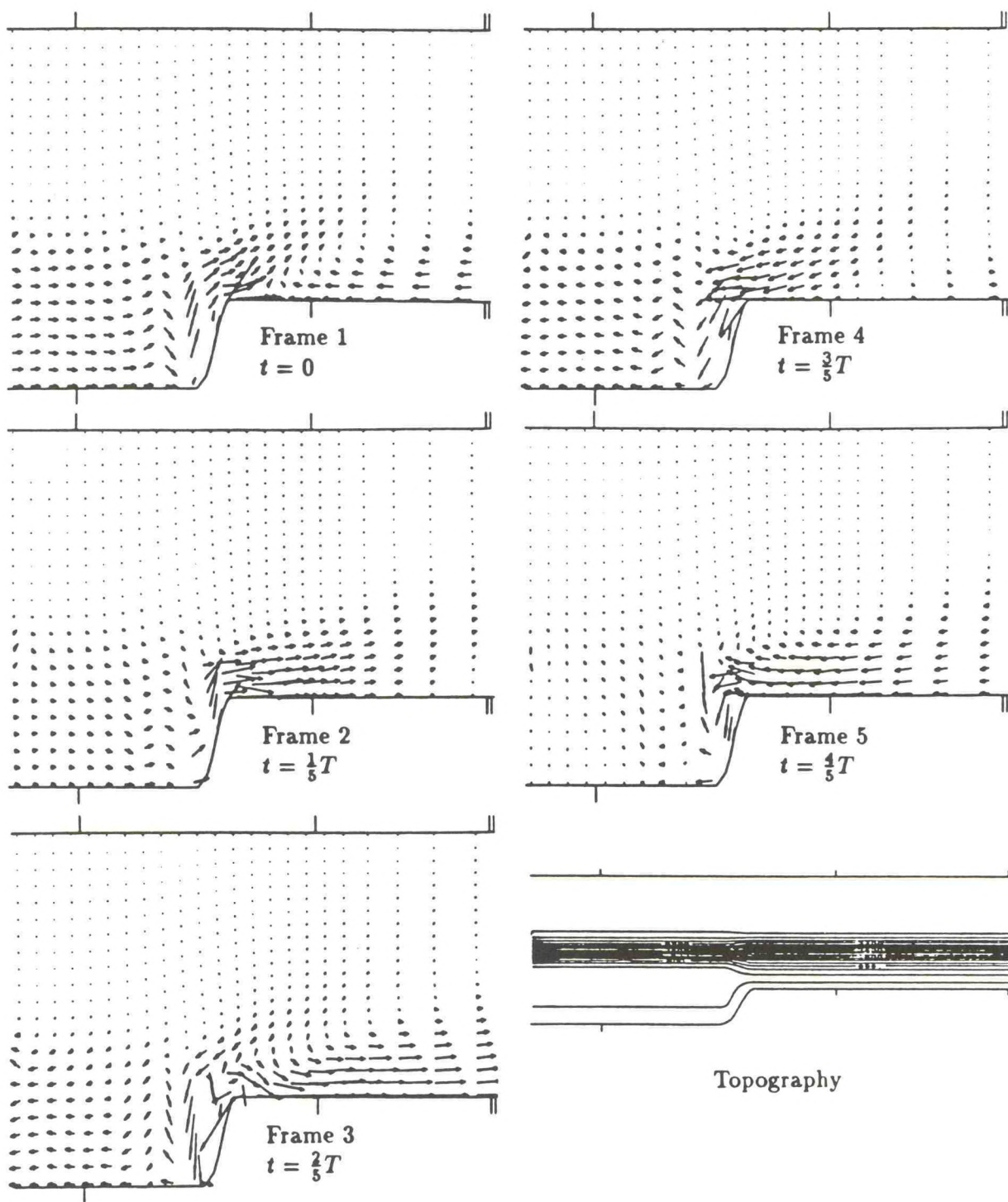


Figure 1. A sequence of plots of surface velocity vectors at different times ( $t$ ) during a single wave period ( $T$ ). The mode 1 incident CTW approaches from the left.  $N^2 = 5.4 \times 10^{-6} \text{ s}^{-2}$ . The across-shelf scale is stretched by a factor of three over the alongshelf scale. Topography is shown with uniform horizontal scales.



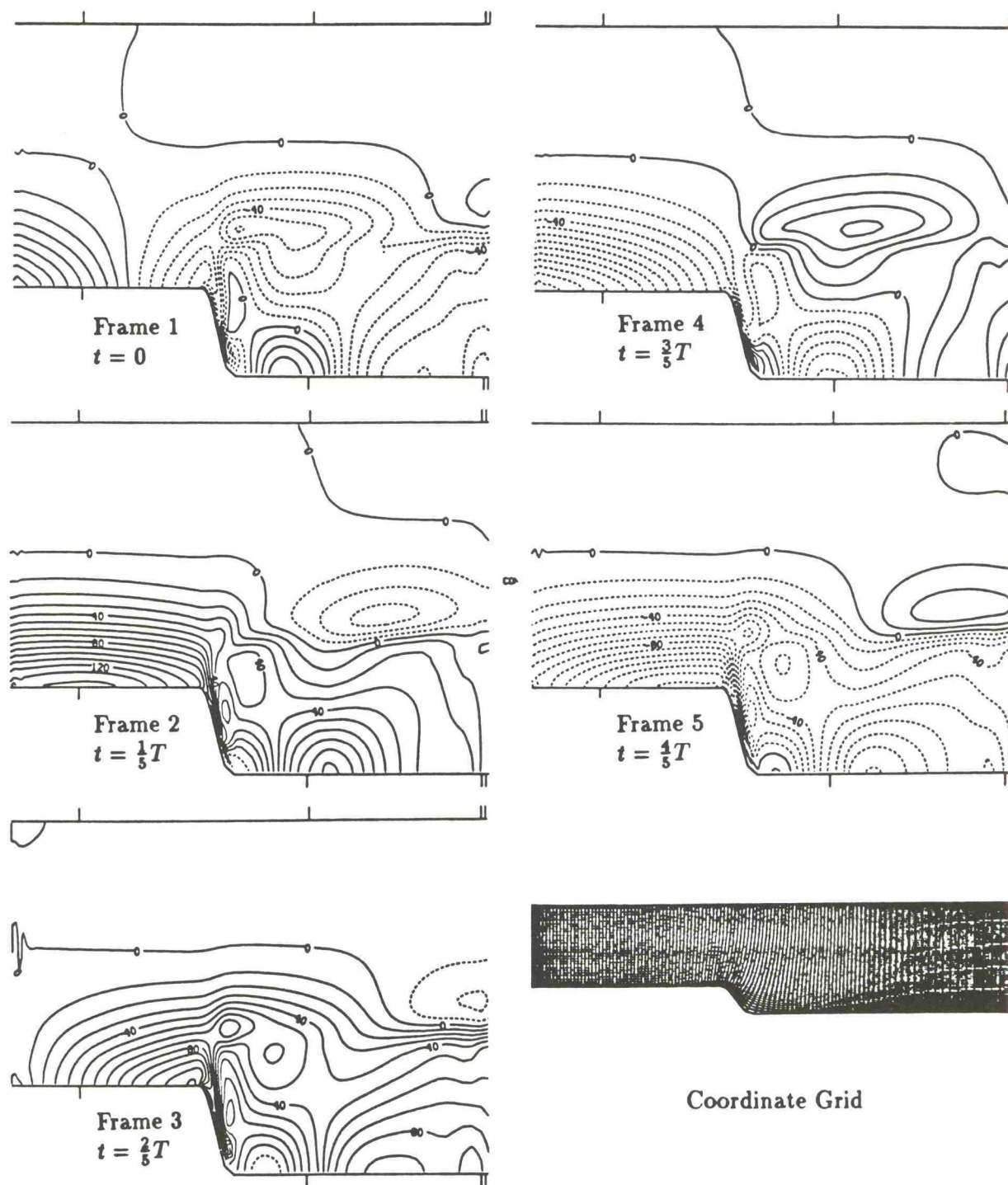


Figure 2. A sequence of plots of surface alongshelf velocity at different times during a single wave period. Incident wave is mode 1.  $N^2 = 5.4 \times 10^{-6} \text{ s}^{-2}$ . The orthogonal curvilinear coordinate grid is shown. The topography is the "reverse" of that shown in Figure 1.

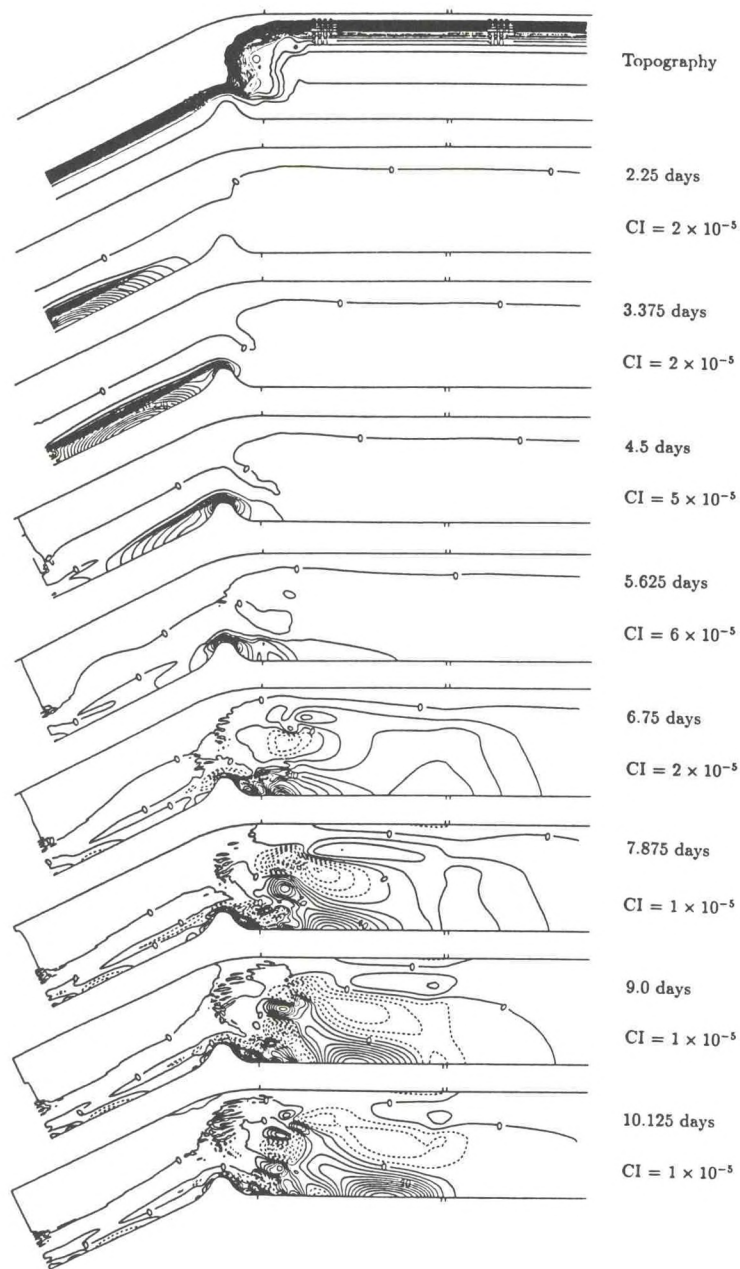


Figure 3. Surface alongshelf velocity at different times during the Griffin & Middleton (1986) simulation. The coastline is at the bottom of each frame. The peninsula represents Fraser Island, on the east coast of Australia. A mode 1 incident CTW pulse approaches from the left and is scattered into several CTW pulses of differing mode number. CI denotes contour interval (arbitrary units).



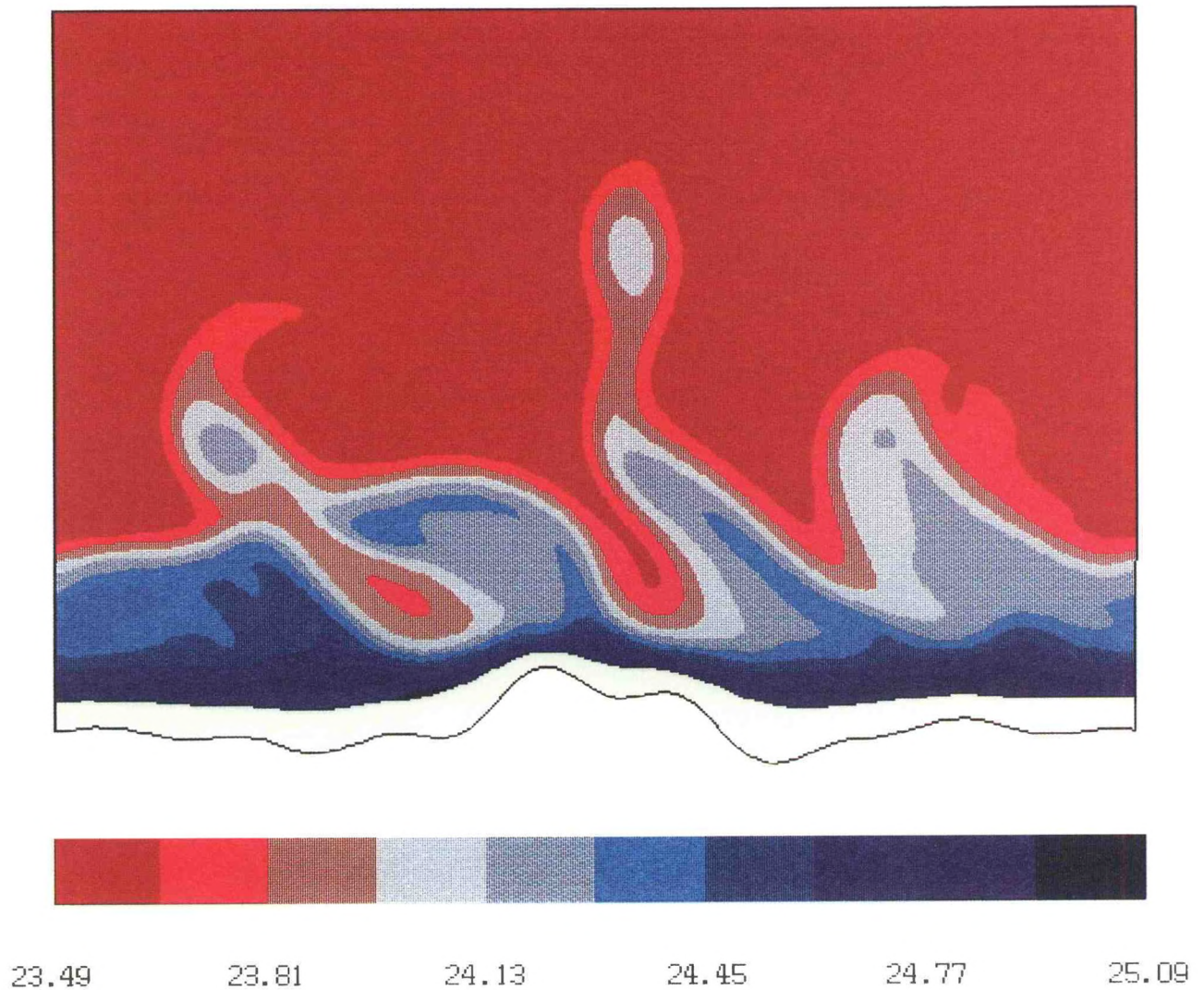


Figure 4. Color-enhanced contour plot of the instantaneous density field at a depth of 100 m showing the initial evolution of an offshore-directed filament. The filament later breaks, forming a detached cold-core eddy. The computational domain is 1000 km by (approximately) 700 km in dimension. Spatial resolution is 130 by 81 points in the horizontal, with a 7-polynomial expansion in the vertical. The horizontal orthogonal grid has a minimum horizontal grid spacing of about 3 km, occurring in the region of maximum coastline curvature.

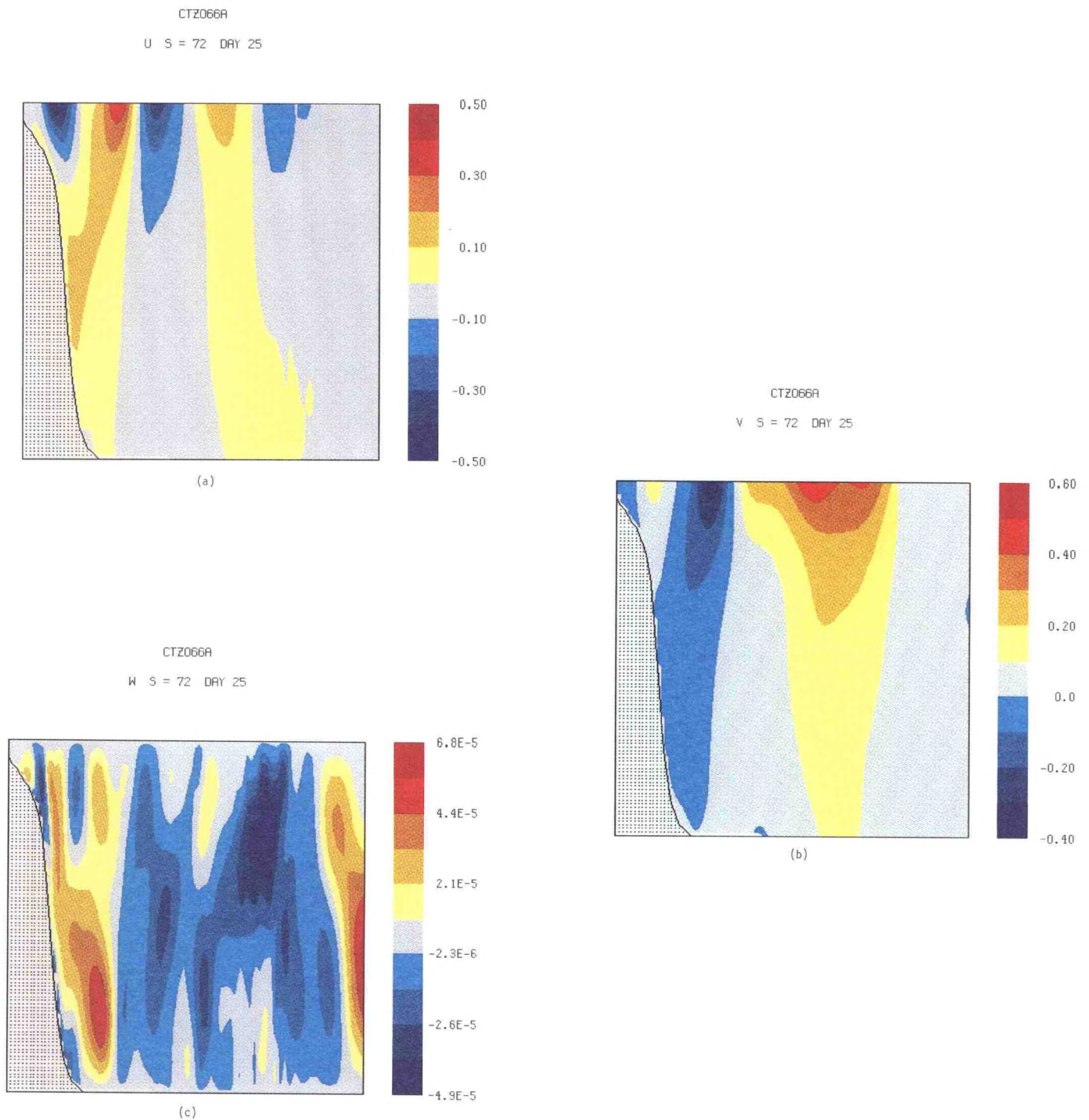


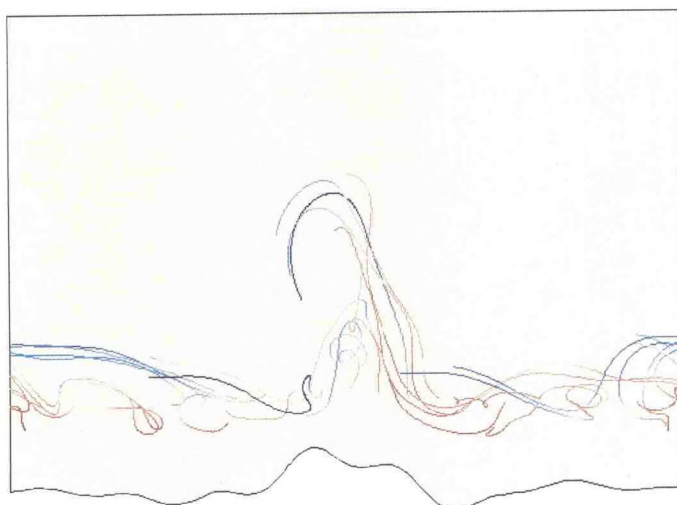
Figure 5. Vertical sections taken perpendicular to the coastline through the emerging filament seen in Figure 4. The depth range covered is zero to 1000 m. Component figures include: (a)  $u$ , alongshore velocity; (b)  $v$ , cross-shore velocity; and (c)  $w$ , vertical velocity. Note in particular the strong, mid-depth downwelling signal associated with the front edge of the emerging filament.



MIN DELTA Z = 7.1  
MAX DELTA Z = 58.9

CTZ066F WITH FL0ATS  
DAYS 60.0 - 100.0

MINIMUM Z = -141.7  
MAXIMUM Z = -62.9

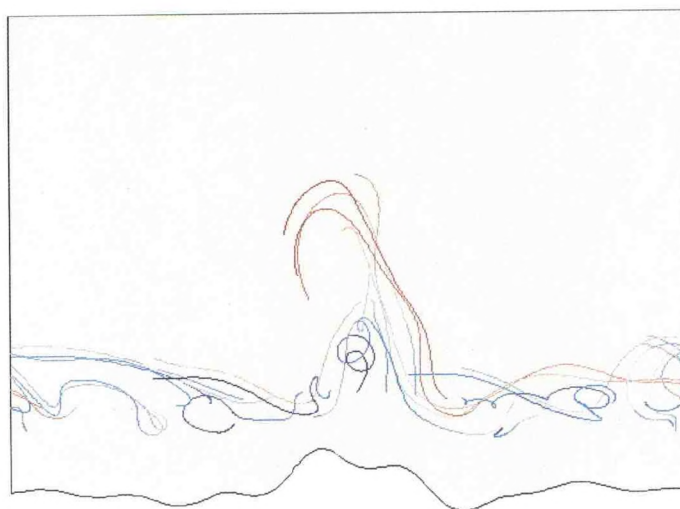


(a)

MIN DELTA RH0 = 0.04  
MAX DELTA RH0 = 0.34

CTZ066F WITH FL0ATS  
DAYS 60.0 - 100.0

MINIMUM RH0 = 23.70  
MAXIMUM RH0 = 24.52



(b)

Figure 6. Evolution of three-dimensional water parcel trajectories in the circulation shown in Figures 4 and 5. Parcels are "released" at a depth of 100 m and subsequently followed for 40 days. Component figures are color-coded to indicate: (a) vertical position of water parcels, (b) value of density following water parcels.

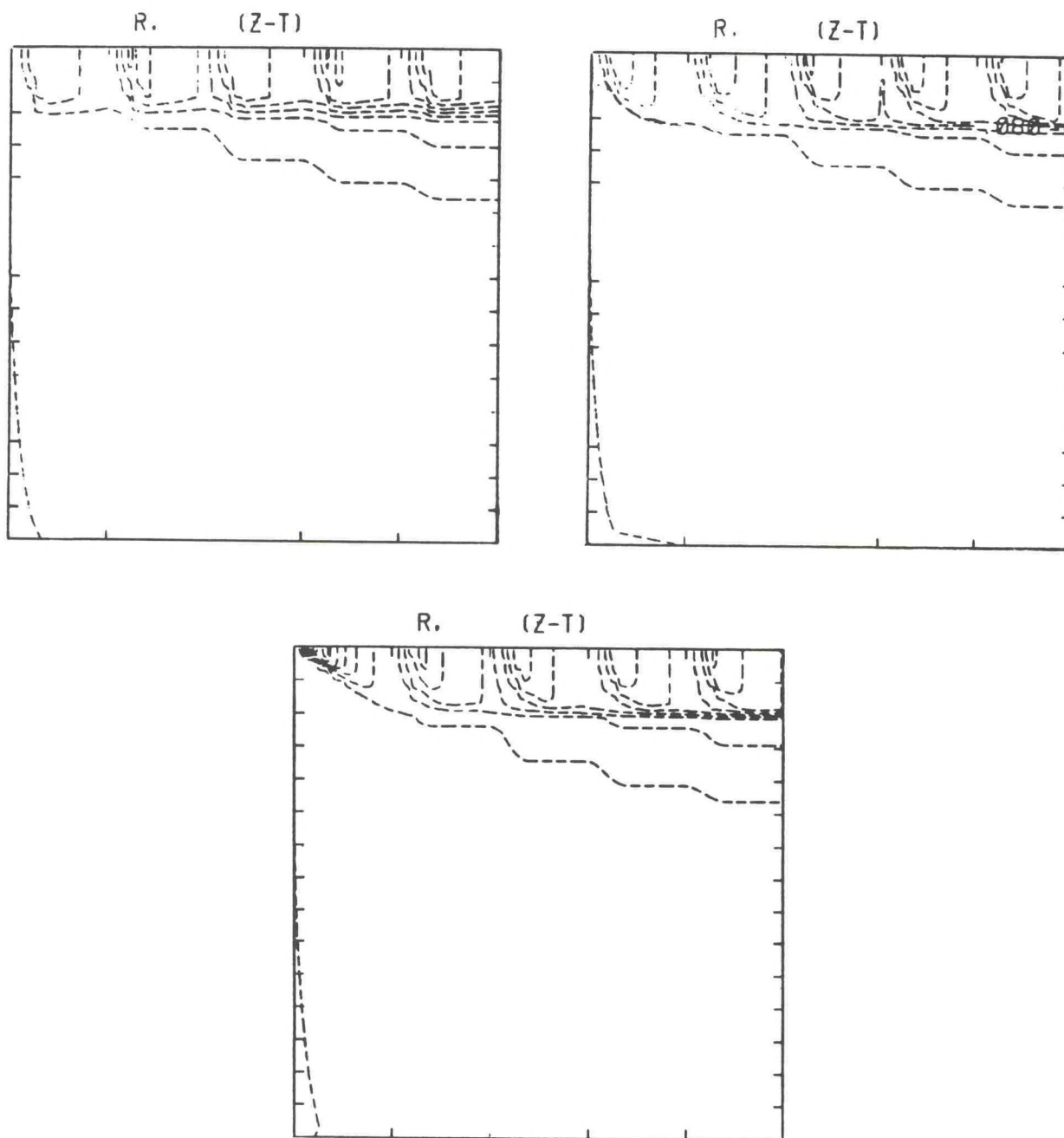


Figure 7. Sensitivity of a one-dimensional coupled ocean/mixed layer model to vertical resolution. See text for a description of the experiment.



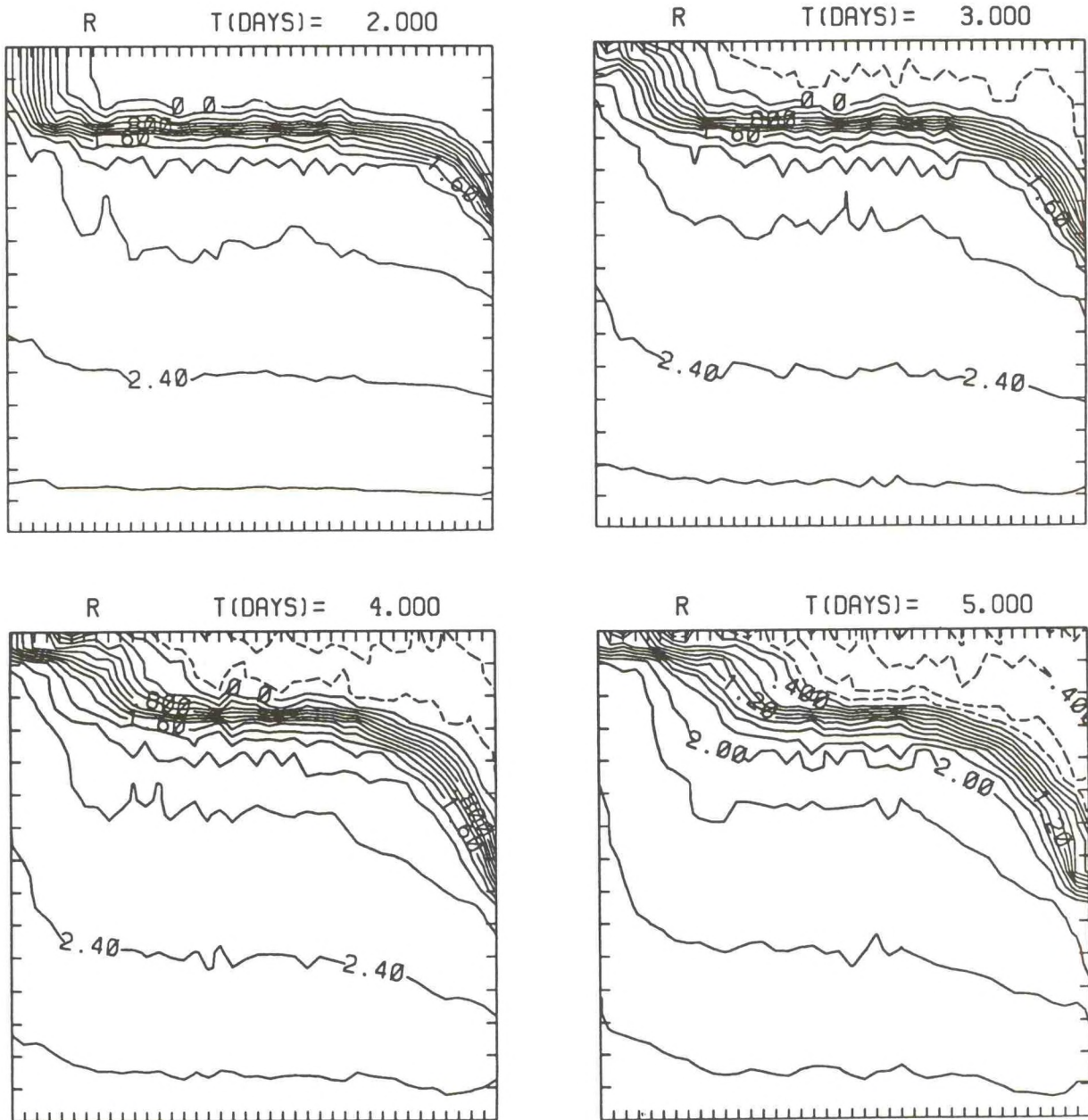


Figure 8. Two-dimensional simulation of the formation of a coastal upwelling front. See text for a description of the experiment.

# THE PRINCETON/DYNALYSIS OCEAN MODEL

George L. Mellor  
James Forrestal Campus  
P.O. Box 308, Princeton University  
Princeton, NJ 08542

and

H. James Herring and Richard C. Patchen  
Dynalysis of Princeton  
219 Wall Street  
Princeton, NJ 08540-1512

## Introduction

The history of the Princeton/Dynalysis General Circulation Model begins with the development of analytical turbulence closure models of small-scale turbulence at Princeton University (Mellor, 1973; Mellor and Yamada, 1974, 1977) such that vertical mixing or the inhibition of vertical mixing of momentum, temperature and salinity (or any other ocean property) can be predicted with considerable confidence. Simple versions of these turbulence models have been adopted by a number of other investigators [Mellor and Durbin, 1975; Weatherly and Martin, 1978; Klein, 1980; Simpson and Dickey, 1981a, 1981b are examples]. Similar versions of the turbulence models were incorporated into the large weather and climate general circulation models at the National Oceanic and Atmospheric Administration (NOAA)'s Geophysical Fluid Dynamics Laboratory, resulting in improved predictive skill (Miyakoda and Sirutis, 1977).

At the same time, the first version of the circulation model was developed by Blumberg and Mellor (1979, 1980) including a turbulent closure model and a time-split, external mode to accommodate tidal and wind-forced free surface variability. Subsequently, refinement has continued at Princeton University and at Dynalysis to expand model capabilities, improve skill and reduce costs. Radiation boundary conditions have been developed to improve treatment of open boundaries (Blumberg and Kantha, 1982; Kantha, 1985). The introduction of a heat flux coefficient in the surface boundary condition has resulted in more realistic thermal layer behavior (Blumberg and Mellor, 1985; Blumberg et al., 1984). Refinements in the formulation of the diffusivity terms have increased accuracy in regions of rapidly changing topography (Blumberg and Mellor, 1985). Finally, the model has been completely recast in orthogonal curvilinear coordinates (Blumberg and Herring, 1984), greatly increasing model efficiency in treating irregularly shaped boundaries and in meeting requirements for high resolution in specific local regions.

The prognostic variables are the three components of velocity, temperature, salinity, turbulence kinetic energy and turbulence macroscale. The momentum equations are nonlinear and incorporate a variable Coriolis parameter. Prognostic



equations governing the thermodynamic quantities, temperature and salinity account for water mass variations brought about by highly time-dependent coastal upwelling processes. The processes responsible for eddy production, movement and eventual dissipation are also included in the model physics. Free surface elevation is also calculated prognostically so that tides and storm surge events can also be simulated. Other computed variables include the density, vertical eddy viscosity and vertical eddy diffusivity. The model incorporates a sigma coordinate system such that the number of grid points in the vertical is independent of depth. The spacing in this transformed coordinate system is also variable so that the dynamically important surface and bottom Ekman layers across the entire sloping shelf are adequately resolved. Realistic coastline and bottom topography are thus easily accommodated. Computational procedures have been formulated to cope gracefully with the large baroclinic and topographic variability found in, among other locations, the Gulf of Mexico and over the California continental shelf.

The model responds to surface wind stress, heat flux, and salinity flux, and to the specification of tidal forcing, fresh water discharge and other lateral boundary conditions. Finally, the computer code has been carefully designed to be economical on modern array-processing computers such as the Cray-1S or Cyber 205, but it also can be run on mini-computers.

The prognostic three-dimensional circulation model and its various submodels have been applied for various investigative purposes to numerous geographic regions. These include the Gulf of Mexico, U.S. eastern continental shelf, California continental shelf, Santa Barbara Channel, Indian Ocean, South China Sea, Arctic and Bering Seas, New York Harbor and Delaware Bay.

### New York Harbor

An application of the General Circulation Model to investigate the tidal flow characteristics of the Hudson-Raritan Estuary, an area which is often termed New York Harbor (Browne and Dingle, 1983), has been formulated by Oey et al. (1985). A realistic computational domain with a 500m by 500m grid employed in the calculations, was Bathymetry (Fig. 1). The calculation covers the period from July through September of 1980 and includes actual water level and wind forcing as well as time-dependent river and sewage discharges.

The model predicts the distribution of the tidal elevation and tidal current with a high degree of accuracy. The National Ocean Service (NOS) Tide Tables provide information on the average range of the tide and on differences in the times of occurrence of high and low water at many points throughout the Harbor region. Values of the average tidal range observed at various locations within the Harbor are composed against computed values obtained when the model is subjected to the average tidal range at the ocean boundary (Fig. 2). The correct clustering of plotted points about an ideal 45-degree line, which would represent an exact simulation, demonstrates the model accuracy. Similarly good correlations are found between predicted and observed time differences for the occurrence of high and low water.



Comparisons of predicted and observed tidal currents show similarly good agreement. The National Ocean Service during the 1980s conducted a comprehensive current measurement program in New York Harbor (Browne and Dingle, 1983). Collected observations have been reduced to consistent tidal conditions and are presented in graphical and tabular form in the eighth edition of the NOS Tidal Current Charts of New York Harbor. At a majority of the NOS current observational stations, currents were measured at three depths: nearsurface, mid-depth and nearbottom. From the graphical and tabulated data available in the Tidal Current Charts it has been possible to find depth-averaged values of currents at 13 stages of an average tidal cycle. These depth-averaged current vectors derived from observations are compared (Figs. 3 and 4) in a side-by-side manner with the predicted vectors at the time of maximum ebb and maximum flood currents at the Narrows. In each figure the current vectors are shown at each grid pint for the model output and at each current meter station for the NOS data. The agreement in current direction and in relative magnitudes is good. Detailed comparisons at particular points of the predicted and observed variation of currents over a complete tidal cycle also reveal excellent agreement in magnitude and phase.

Results from the numerical simulation were also used to analyze salt fluxes at various sections in the estuary. It was found that salt fluxes and volume transports vary considerably over subtidal time scales of days to weeks and that an averaging period of at least 50 days is required to define a statistically stationary estimate.

Salinity measurements along the Sandy Hook-Rockaway transect were made during August 20th and 27th, 1980. The model predicts well the details of the observed salinity distribution (Fig. 5). Throughout the tidal cycle the observations show that unstably stratified water columns are created by advection of waters of different densities which subsequently mix. The observations also show that the water becomes vertically homogeneous during a spring tidal cycle. These complex three-dimensional flow structures and mixing events are predicted remarkably well by the model. There is also good agreement with the observed time-averaged circulation in Raritan Bay.

### Delaware Bay

The General Circulation Model has also been applied to a region which includes the Delaware River, Delaware Bay and the adjacent continental shelf (Fig. 6) (Galperin and Mellor, 1990a, b). The grid resolution in the Bay is 1 km square, and 4 km by 5 km on the shelf. Although the rivers are shown as one grid box wide, the lateral grid metric represents the actual river width.

The model calculation was for the entire year of 1984, which included a period of drought during the late summer and early fall. In an effort to simulate the actual conditions as closely as possible, the model was forced by: a) tidal elevations at the shelfbreak containing 37 astronomical constituents and corrected by measured elevations at the mouth of the Bay, b) surface wind stress and surface heat flux including the diurnal cycle calculated from the meteorological information at



the airport of Atlantic City, c) climatological boundary conditions for temperature and salinity at all three open shelf boundaries, d) seasonal temperature and zero salinity at Town Point and Trenton, and e) fresh water runoff from 16 major rivers and tributaries.

Extensive comparisons were performed between tidal simulations and the tidal data available from the National Ocean Service. The tidal phase is accurately reproduced throughout the estuary, and the amplitude, while predicted well in the Bay, is somewhat attenuated further up the River (Fig. 7). This damping is most probably due to the excessive horizontal mixing imposed, and the agreement could be improved by reducing the mixing coefficient. Comparisons were also made with current meter measurements available for this time period (Fig. 6). Again the phase of the tidal currents and synoptic events are reproduced well at mooring 33 in the upper Bay (Fig. 8).

The effect of winds on the subtidal component in estuarine systems is extremely important. The frictional adjustment time scale for much of the Mid-Atlantic Bight is on the order of 10 hours. Therefore, an important characteristic of the estuary is its response to wind forcing on comparable time scales. Based on the horizontal distribution of currents and salinity, respectively, averaged for a period of approximately two tidal cycles for four separate days during July 1984 (Figs. 9 and 10), the magnitude and direction of the mean wind was considerably different on each of these days but did not vary appreciably over the averaging period.

In the first example day shown in the topmost pair on each figure, the wind is moderate southwesterly, which causes the fresher surface water to flow towards the New Jersey shore. More saline shelf water enters the Bay close to the Delaware shore where the Bay is deeper. It is driven to the right where it mixes with the fresh water coming from the River and is finally advected back to the mouth. Compensating bottom currents flow in the opposite direction from the New Jersey side to the mouth of the Bay. During such a wind event, the two-layer estuarine circulation pattern diminishes.

The second event is produced by a strong wind from the south. In this case (Figs. 9 and 10), the wind opposes the fresh water flowing down the estuary, creating multiple gyres up the center of the Bay and driving the fresh surface water towards the New Jersey shore. The strong wind stress causes mixing which affects the entire water column and generates strong bottom currents. Again the two-layer circulation pattern does not develop. As is evident from the salinity contours (Fig. 10), saline shelf water is forced by the winds deep inside the Bay along the left bank, creating a strong salinity front parallel to the shore and large cross-estuary gradient. The front and the gradient persist throughout the water column and are clearly visible in the map of the near-bottom isohalines (Fig. 10).

A moderate wind blowing from the north enhances the surface currents, which in turn increases the compensating upstream bottom currents and establishes the vigorous classical two-layer estuarine circulation regime (Fig. 9). Although the surface cross-estuary gradients are smaller, freshwater pushed by the wind reaches much



farther into the lower Bay and increases the longitudinal salinity gradient near the mouth of the estuary (Fig. 10). At the same time, strong upstream bottom currents cause significant salinity intrusion, particularly in the deep channels, resulting in increased vertical stratification.

The final example represents the null case of negligible wind stress (Figs. 9 and 10). Surface currents flow towards the Delaware shore, and compensating bottom currents flow towards the New Jersey shore so that two-layer circulation is well developed. Surface salinity is higher near the Delaware bank and has approximately the same structure as in the previous cases. Bottom halines exhibit salinity intrusion, particularly along the deep channels. Due to the weaker wind the salinity intrusion is less vigorous than in the preceding case. Overall (Fig. 9), without an overriding driving force, the surface currents are a complex product of the history of the wind, topographical features and transient hydrographic signatures.

### Middle Atlantic Bight

A barotropic model of the Middle and North Atlantic Bights will be described to a) illustrate the application of an orthogonal curvilinear grid to modeling a coastal domain, b) provide an example of inclusion of tidal forcing in the model, and c) illustrate a realistic simulation of storm driven currents and sea levels in the coastal ocean. A large quantity of oceanographic and meteorological data in the domain were processed and examined to determine the period for which storm simulation could be conducted and a thorough skill assessment carried out. The period from January 1 to March 15, 1980 was chosen for simulation. To represent faithfully in the model the characteristics of coastal-trapped waves propagating along the shelf, a fine cross-shore resolution is necessary, especially near the coast, all along the shelf. An orthogonal curvilinear grid provides the most cost-effective means of satisfying this requirement. The grid (31 x 98) chosen for the storm simulation studies (Fig. 11), has a high cross-shore resolution nearshore (~2.5 km), and expands in size (~20 km) in deeper waters where high resolution is not essential, to conserve computer time requirements.

The surface forcing for the model simulation was derived from National Weather Service surface pressure fields. These fields were reanalyzed to incorporate ship and buoy pressure data not already included in the analysis, and used, through a marine boundary-layer model, to derive the surface wind fields. The resulting wind stress and atmospheric pressure fields were used to drive the model.

To incorporate the dissipational effect of tidal stirring, the major tidal constituent in the region, the  $M_2$  semidiurnal tide, was included in the model simulation. Tides were simulated by prescribing sea level variations at the open boundaries of the model domain due to  $M_2$  tides, with amplitudes and phases determined from the global tidal model of Schwiderski (1980). From the model run with only tidal forcing, a comparison was made between model-produced tidal ellipses and the observed ones (Fig. 12), the latter obtained from the atlas by Moody et al. (1984), at various locations in the domain (Fig. 13). The agreement is quite



adequate for incorporating the impact of tidal-stirring on bottom dissipation into the storm simulations, and surprisingly good, since no effort was made to fine tune the results, contrary to the conventional practice in tidal models.

The storm simulation was run with tidal forcing at the open boundaries, six-hourly wind stress and atmospheric pressure forcing at the sea surface, and sea level forcing as determined from Halifax sea level data at the northern cross-shore boundary, with radiation conditions imposed at the southern boundary. A sample is shown (Fig. 14) of the model-generated vertically-averaged (barotropic) currents from the 75-day storm simulation run in the center of the domain, where verification data are available. Proprietary considerations preclude the display of comparisons between the model and observed currents, but the agreement is quite good. This study and the Santa Barbara Channel study are among the select few, where a one-to-one comparison between predictions of a General Circulation Model and observations has been feasible, and attempted.

### Entire Atlantic Coast Continental Shelf

A three-dimensional ocean circulation model is being applied to the U.S. Atlantic continental shelf to obtain a detailed description of the temporal and spatial structure of the water levels, currents, temperature and salinity. An important feature in this region is the Gulf Stream, which meanders and sheds eddies north and south of the Stream. Therefore, a long-term, stable, fully three-dimensional, prognostic computation is needed.

An important aspect of the modeling activity is the use of observations, and data analysis and modeling products to specify environmental conditions. Bathymetry for the region (Fig. 15) is derived from the NOAA Synthetic Bathymetric Profiling System (SYNBAPS) world ocean bathymetric database which covers the world oceans on a 5' x 5' grid (approximately 8 km for the latitudes of this region). Hydrographic data and surface marine observations have been obtained from the NOAA National Oceanographic Data Center and the U.S. Navy Fleet Numerical Oceanography Center. Other sources of hydrographic data are other government agencies and process-oriented research programs. As well as using meteorological buoys and National Weather Service (NWS) land based stations for describing the atmospheric conditions, data from the NWS Limited Fine Mesh (LFM) model are used. LFM data are the output from the NWS operational three-dimensional atmospheric circulation model that is reinitialized every 12 hours with observations. This data set has the advantage of providing a complete set of atmospheric boundary layer data every 6 hours. These observations and data analysis products are used to specify model boundary conditions and to determine the skill of the model.

Velocities computed by the model at 2 m below the surface after 80 days of simulation are illustrated (Figs. 16 and 17). The signature of the Gulf Stream is evident as the jet through the Florida Straits begins to meander and turn eastward. Three mesoscale eddies are seen, one at approximately 30°N and 78°W. Two others can be seen at approximately 35°N and 70°W.



## Santa Barbara Channel

The Santa Barbara Channel modeling study is an excellent example of an intimate interaction between numerical modeling and observational programs in a coastal ocean. It is a unique study, funded by the Minerals Management Service, where the observational program, in addition to being a stand-alone program, was designed explicitly to be able to provide the input data necessary to drive a General Circulation Model of the region and assess the skill of the model run for a whole year in the prognostic mode.

The observational program consisted of two phases, the Pilot Phase conducted during April-May 1983, and the Main Phase during the year 1984. Current meters were deployed on moorings both on the boundaries of the Channel (to provide velocity and hydrographic boundary conditions for the model) and in the interior (to provide velocity and hydrographic data for comparison with model output) (Fig. 18). A total of approximately 30 Aanderaa current meters and two Vector Averaging Current Meters (VACMs) were deployed, the former below 30 m depth and the latter near the surface, for roughly two months during the Pilot Phase and for two six-month periods in 1984 during the Main Phase (Fig. 19). In addition, a total of six high-resolution hydrographic surveys of the Channel were conducted, four of them during the Main Phase, to provide information on the water mass characteristics of the region, and to provide initialization data for the model at the start of the run and verification data at the end of the run. To provide an understanding of the local wind effects on the circulation in the Channel and to provide surface forcing data for the model, two meteorological buoys were deployed in the Channel as well as four anemometers on oil platforms in the region (Fig. 20). Two shore-tracked drifter buoy studies were also conducted during the Main Phase (Fig. 19).

The extensive observational data base thus generated was used to derive "synoptic" forcing for two model runs of roughly 150 day duration each, corresponding to two six-month deployments of the Main Phase. Six-hour averages of currents, temperature and salinity along the boundaries provided lateral boundary conditions, and six-hour averages of wind stresses and daily-averaged heat fluxes derived from meteorological data provided surface forcing. Mass fields from hydrographic surveys at the beginning of the model runs provided initial temperature and salinity fields.

The General Circulation Model for the Santa Barbara Channel was configured on a 37 x 15 grid with a resolution of about 3.5 km. The number of levels was 15, and a non-curvilinear Cartesian coordinate system was employed. As a sample of the prognostic run, daily averaged currents at 2m and 100m depths are shown about a week apart (Fig. 21). The Channel appears to exhibit major variability at 7-10 day time scales. This variability can be seen in the nearsurface velocity (Fig. 21), and to a lesser extent in the deeper regions. Local wind forcing and its variability are essentially confined to the nearsurface layers, and the subsurface circulation appears to be driven principally by the lateral boundary conditions. Based on sample comparisons between observed and model-predicted time series of currents, temperature and salinity at two locations in the interior of the Channel (see Fig. 18 for locations), the agreement between the model and observations appears to be good



(Figs. 22 and 23). Although the model tends to somewhat underpredict the current magnitudes, the variability, the phase and the scales are reasonably well represented.

This modeling study provides a graphic example of close and successful interaction between observations and modeling in the quest to understand the behavior of the coastal oceans, and perhaps serves as a model for such combined studies in the future.

### California Continental Shelf

The Dynalysis General Circulation Model cast in an orthogonal curvilinear coordinate system was applied to the California continental shelf. In this way, a high-resolution grid can be prescribed in nearshore waters where it is essential, whereas the grid can be coarse in regions beyond the shelf where resolution requirements are not critical. Thus, for example, inner shelf processes such as shelf wave propagation can be better simulated. An example of the application of the curvilinear model to the barotropic simulation of the storm currents in the Middle Atlantic Bight has already been described. Now an application of the full three-dimensional General Circulation Model to the California continental shelf will be described.

The computational grid encompassing the California shelf (Fig. 24) is 30 x 40. There are 21 levels in the vertical. The cross-shore resolution is 4 km close to the coast decreasing to 25 km offshore, while the alongshore resolution varies from 16 km to 50 km. The model was run in both diagnostic and prognostic modes, the former to deduce seasonal mean circulation, and the latter a year-long run simulating circulation during 1981. The diagnostic runs used climatological means of density fields and wind stress as input, whereas in the prognostic mode, six-hourly wind fields derived from the National Weather Service Limited Fine Mesh results provided the primary synoptic variability. River runoff was also incorporated. Based on climatological winter and spring subsurface currents at 200m depth (Figs. 25 and 26), the poleward undercurrent penetrated as far as Monterey Bay during winter. The surface currents are generally southward everywhere except perhaps close to the coast of the central and southern California shelves.

For sample results from the prognostic run for year 1981 (Figs. 27 and 28), the low subsurface salinity near the mouth of San Francisco Bay is due to estuarine outflow there. The surface currents change dramatically with the wind stress, being stronger on the 28th than the 30th of March. The primary variability in the nearsurface currents is wind-induced.

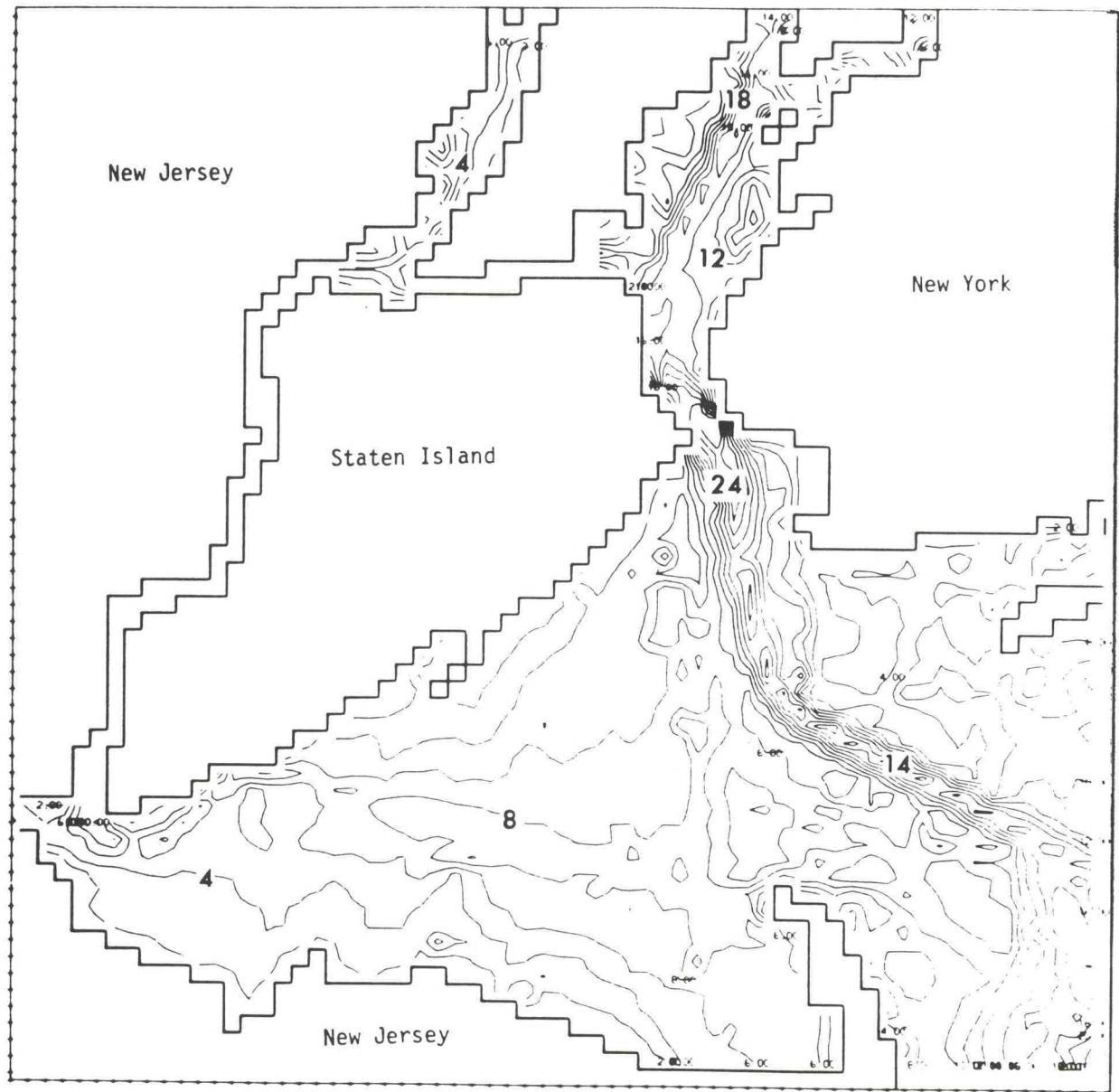


Figure 1. The computational domain of the New York Harbor model. Bottom topography contours in meters (Oey et al., 1982).



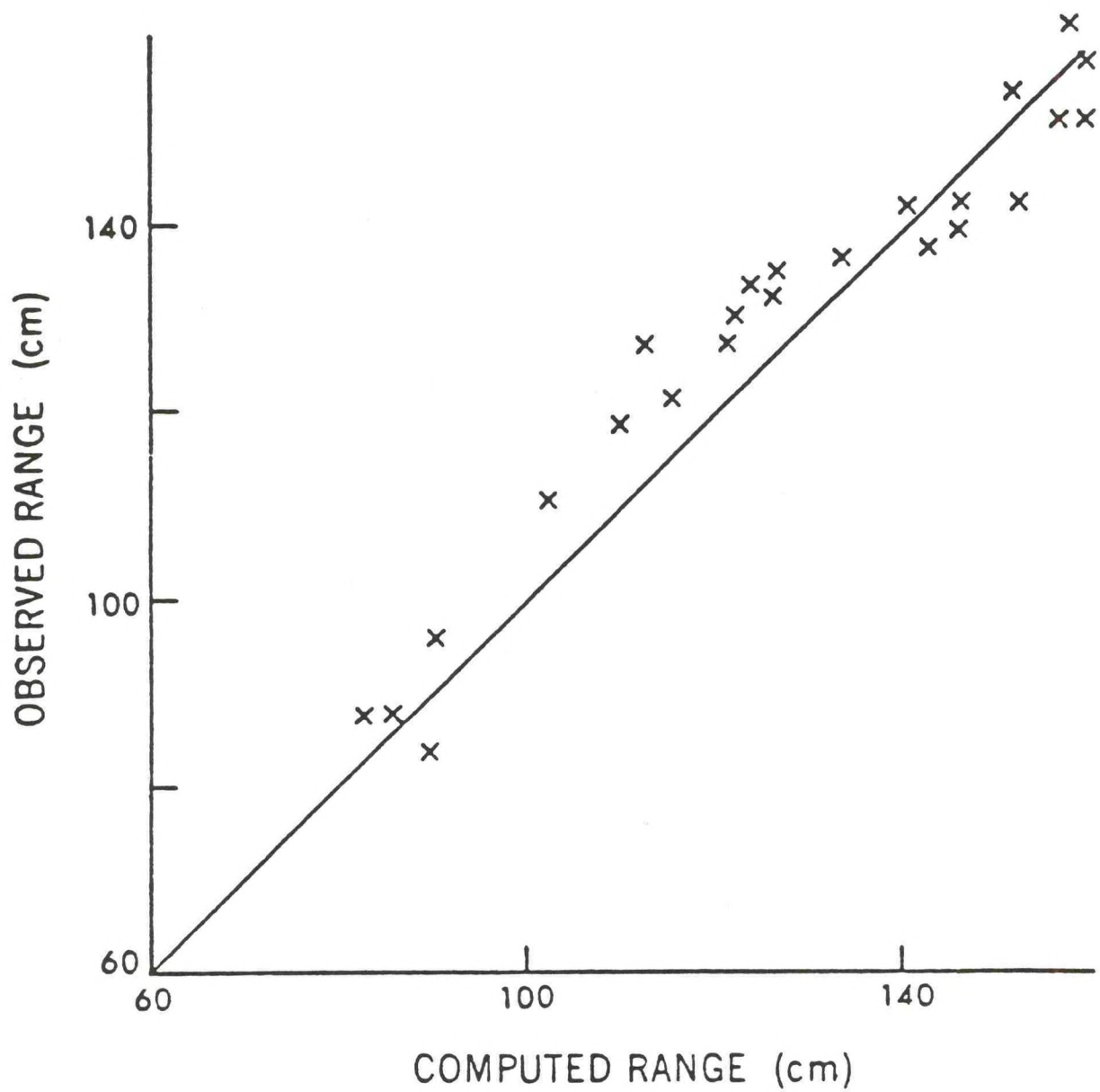


Figure 2. Comparison of observed and computed tidal ranges in New York Harbor (Oey et al., 1982).

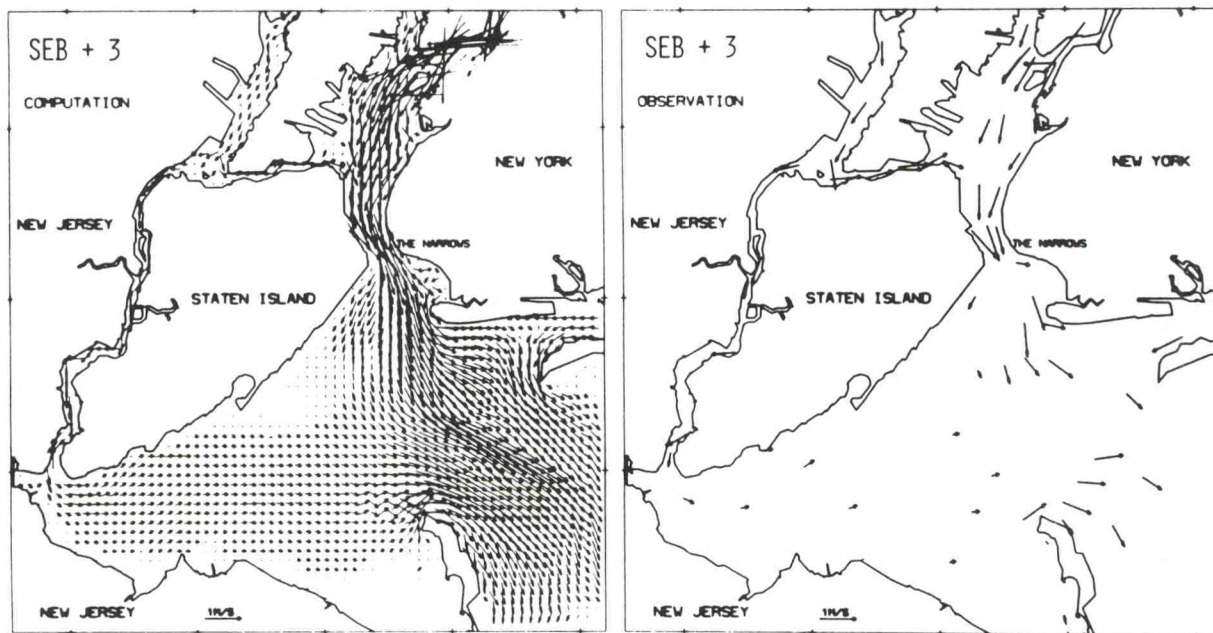


Figure 3. Computed and observed vertically averaged currents at the time of maximum ebb current at the Narrows (Oey et al., 1982).



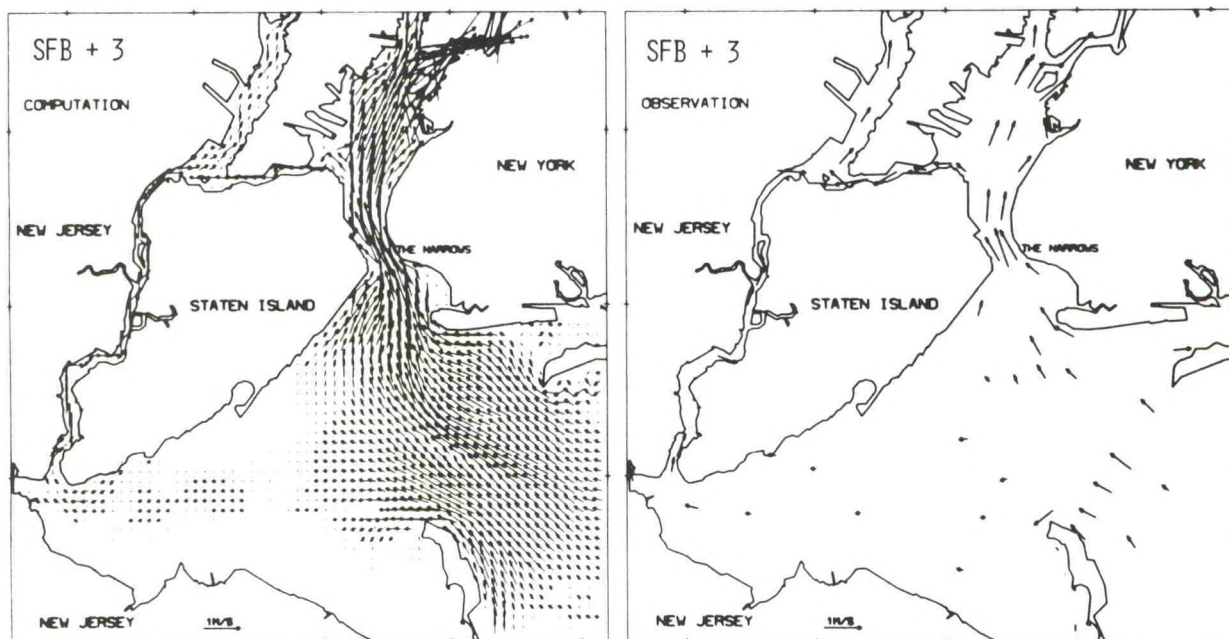


Figure 4. Computed and observed vertically averaged currents at the time of maximum flood currents at the Narrows (Oey et al., 1982).

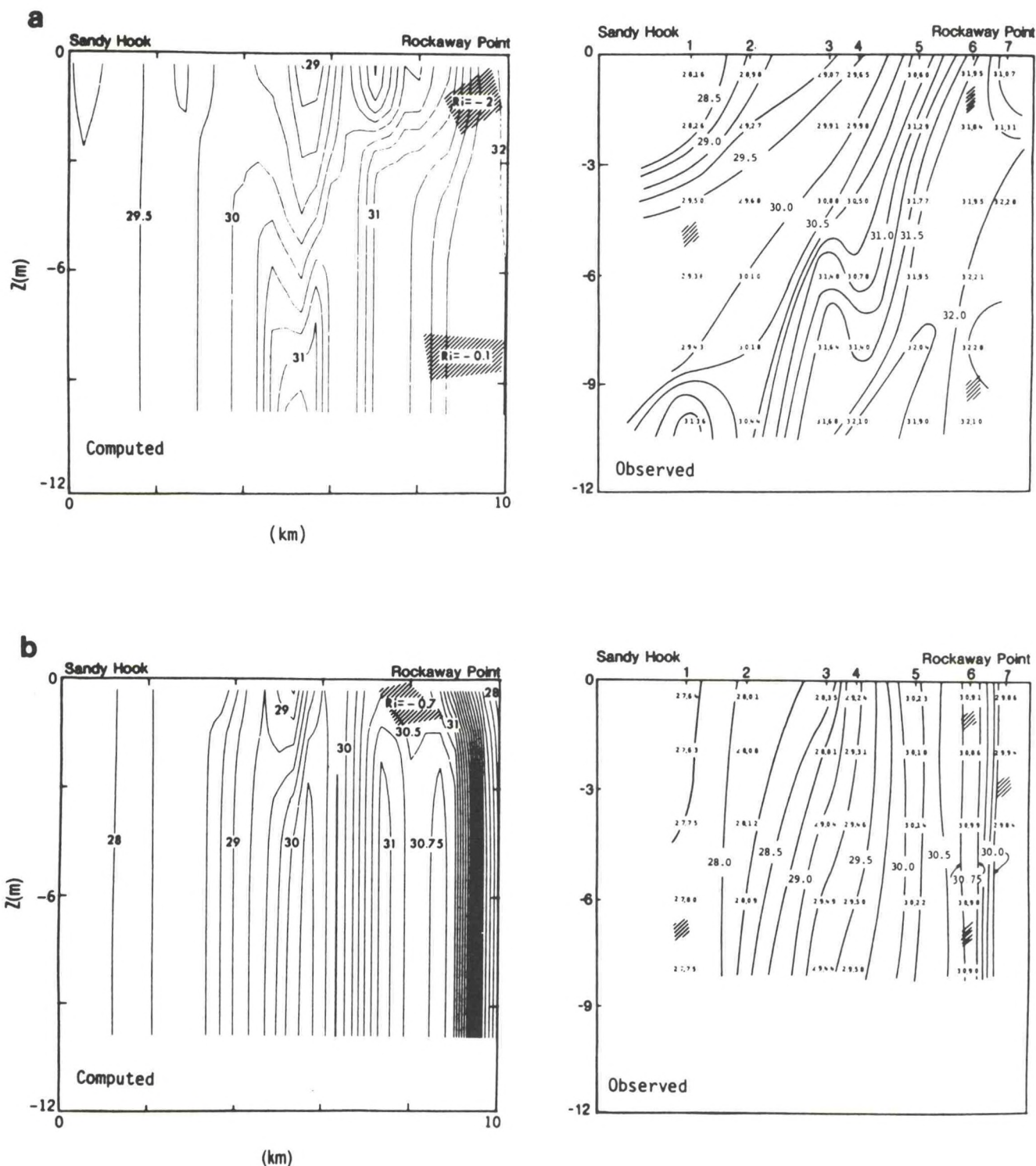


Figure 5. Comparison of computed (left panel) and observed salinity (ppt) distributions across the Sandy Hook-Rockaway Point transect. The hatched areas are where the water columns are unstably stratified. The computed gradient Richardson numbers  $Ri$  are also shown. (a) 1500 GMT 20 August; (b) 2100 GMT 27 August; (c) 2000 GMT 20 August; (d) 1500 GMT 27 August. (a) and (b) correspond approximately to pre-flood slack and (c) and (d) to pre-ebb slack. The small numbers on the observed plots are salinity values in ppt at meter locations (Oey et al., 1985).



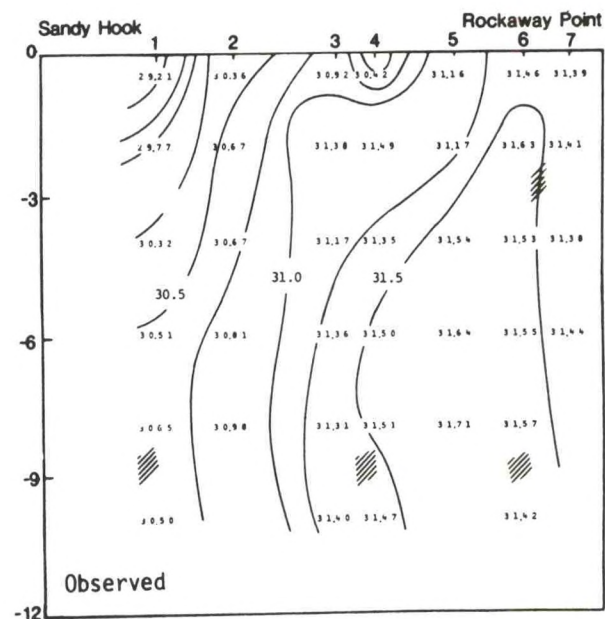
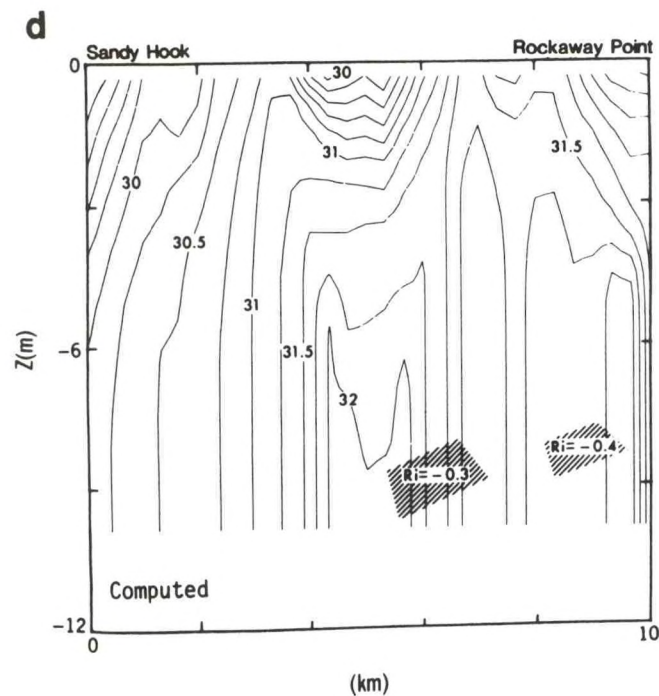
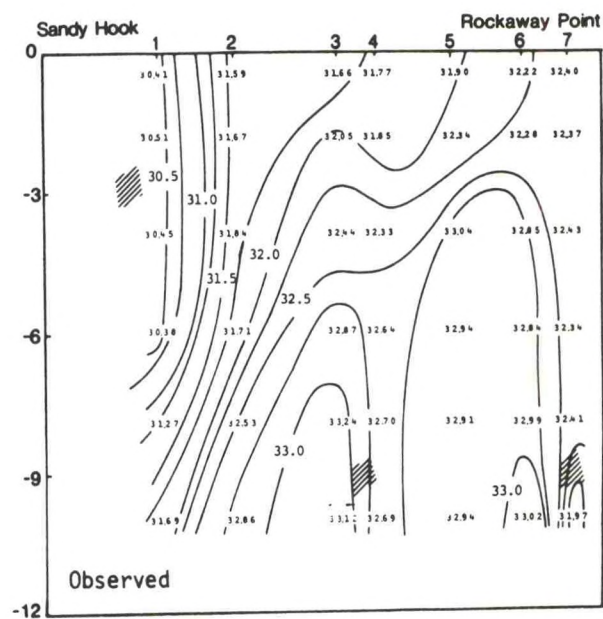
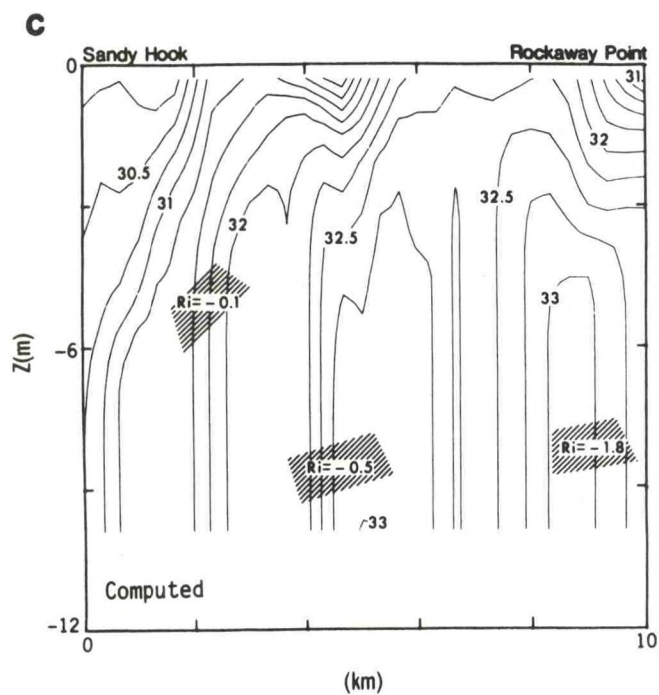


Figure 5. Continued.

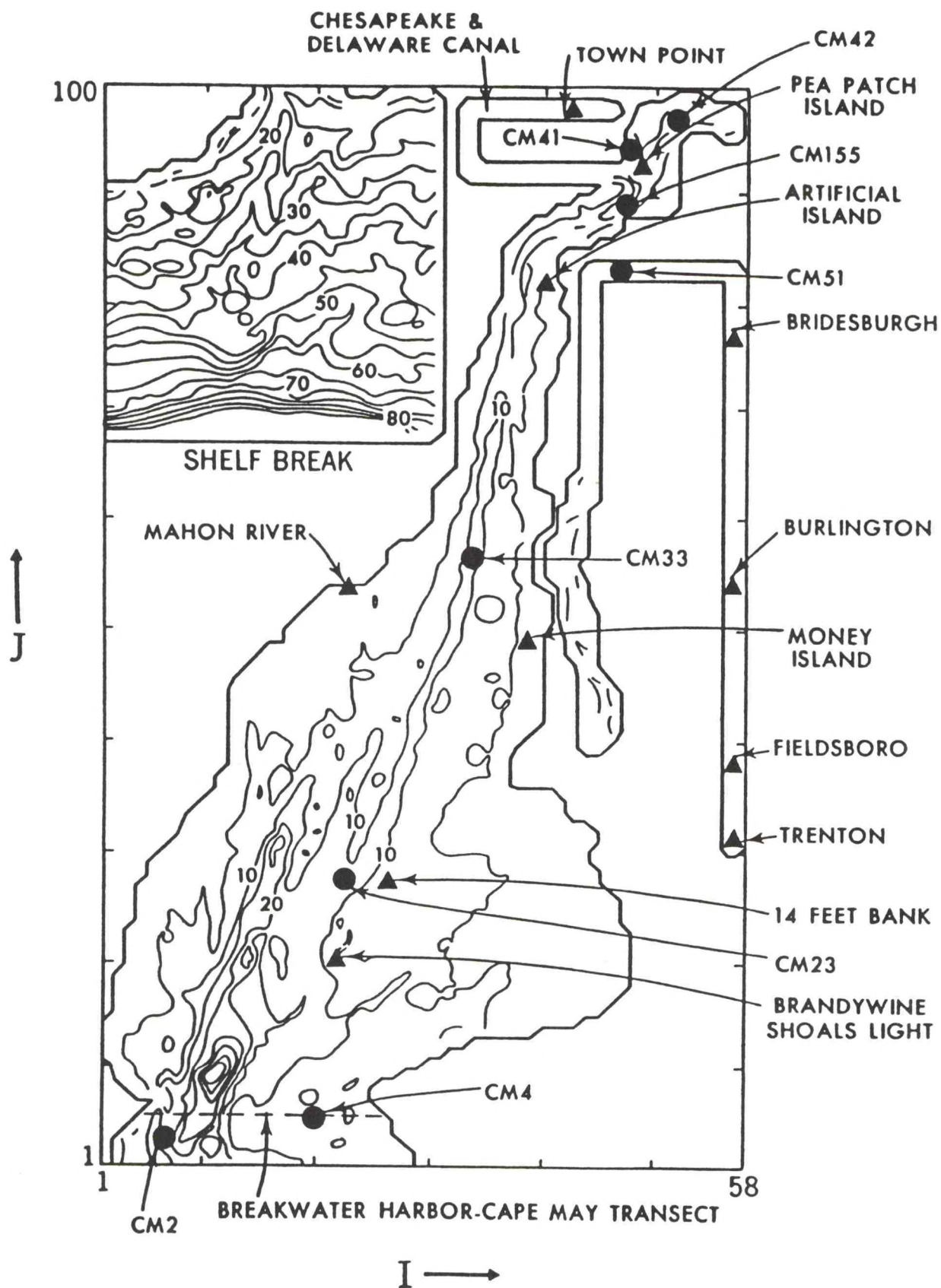


Figure 6. Representation of the Delaware Bay, River and adjacent continental shelf in the computational domain. Depths are in meters. Where rivers are two-dimensional, they are shown with constant width; however, the calculations make use of the local river width as discussed in the text (Galperin and Mellor, 1990a).



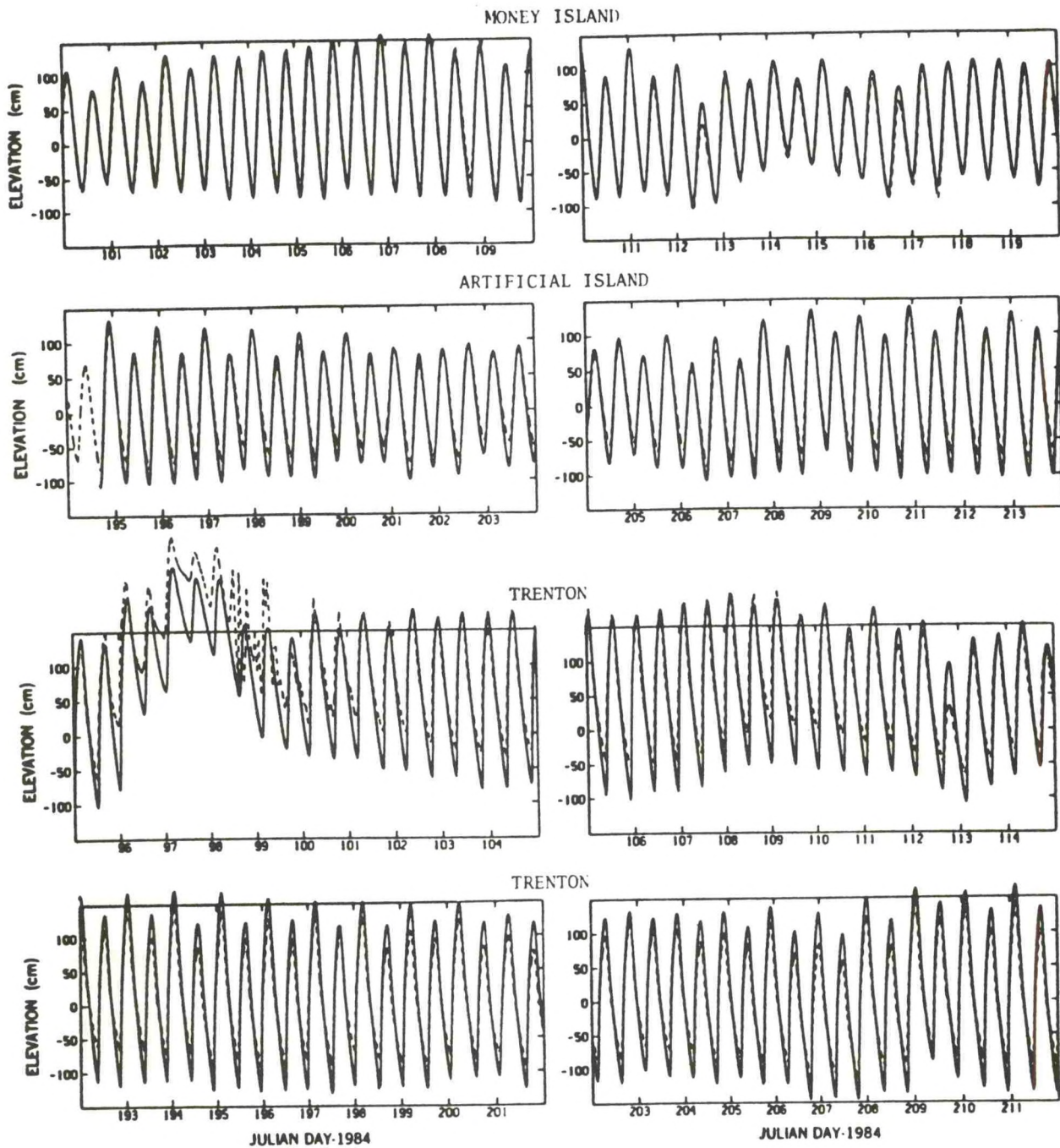


Figure 7. Comparisons of the three-dimensional model generated elevations (dashed curves) with data (solid curves) for different periods of time. Tide gage stations are located in Figure 6 (Galperin and Mellor, 1990a).

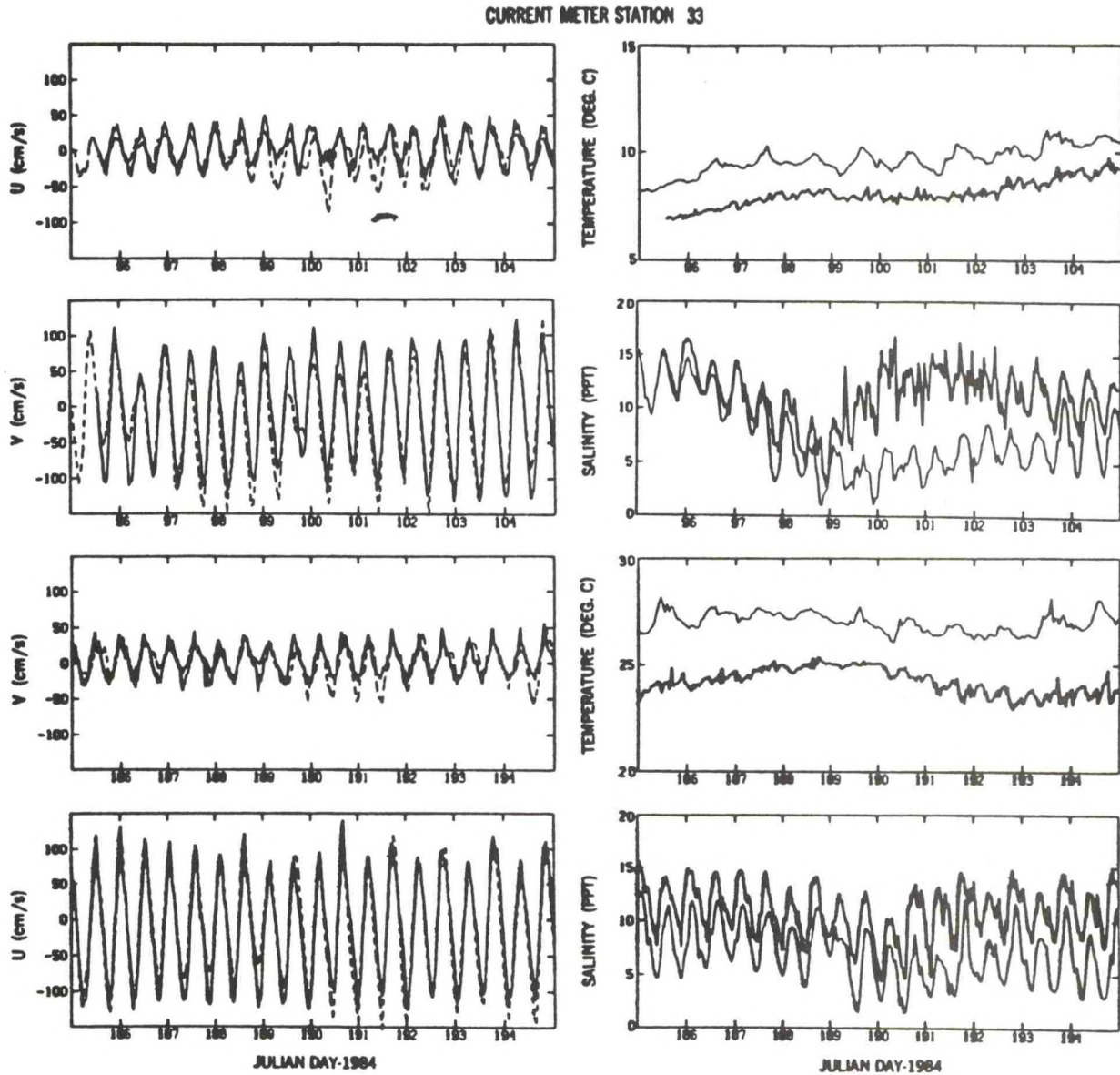


Figure 8. Comparison of model generated currents, temperature and salinity distributions (dashed lines) with data (solid lines) for CM33 at depths 3.7 m (Galperin and Mellor, 1990b).



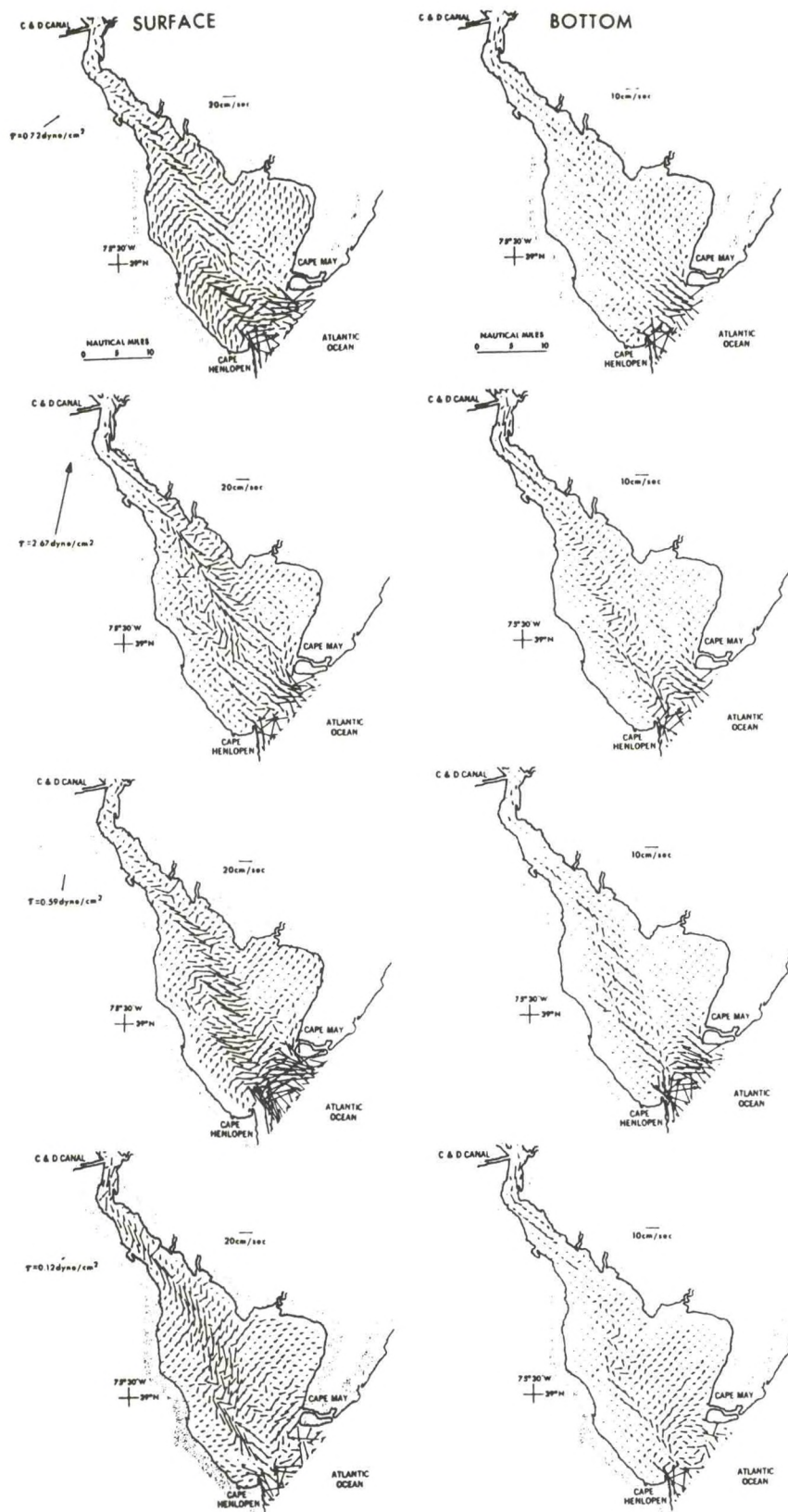


Figure 9. 25-hour, average surface (left column) and near-bottom (right column) currents in Delaware Bay for Julian Days 185, 188, 204, and 210. Corresponding 25-hour average wind stresses are also shown (Galperin and Mellor, 1990b).

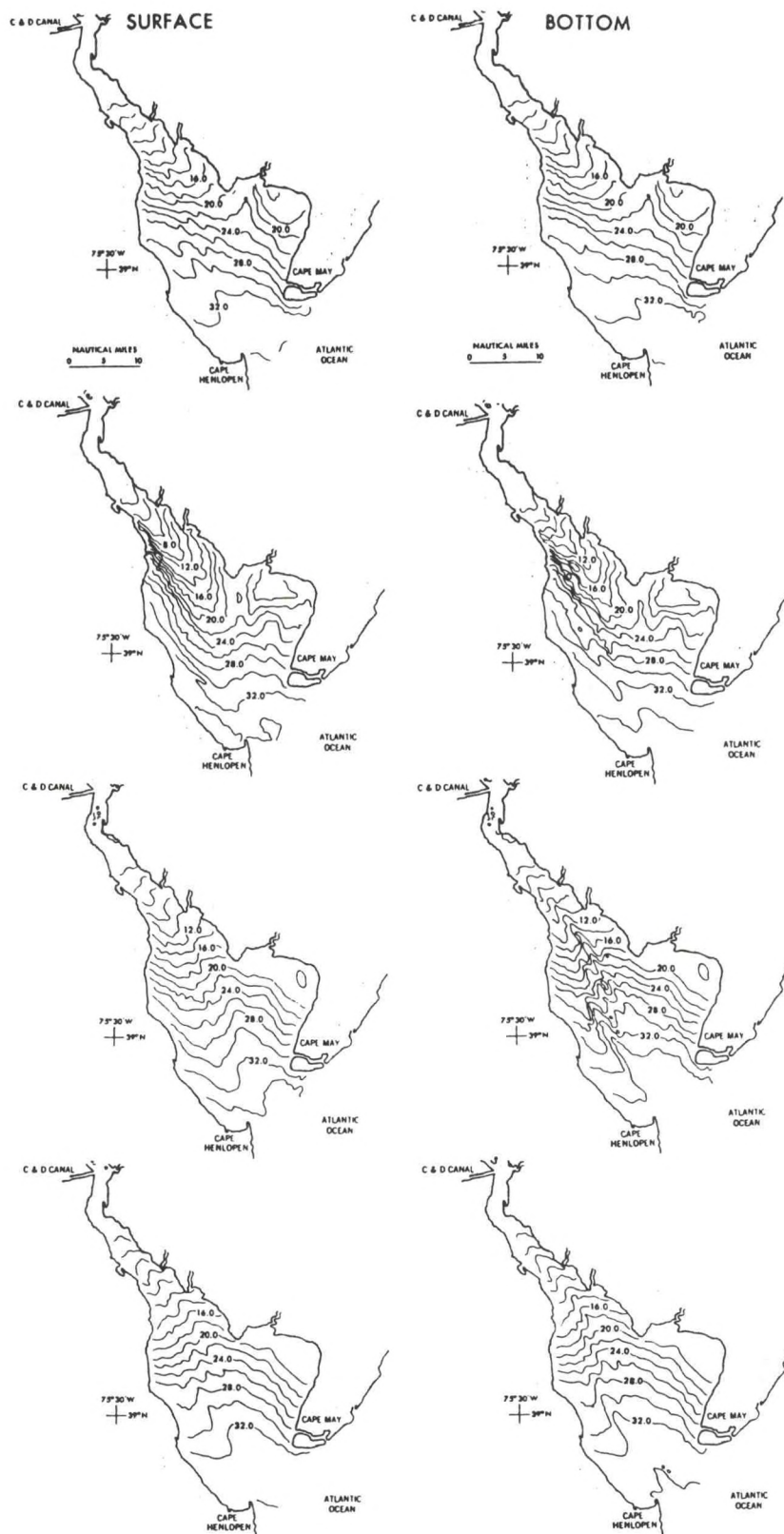


Figure 10. 25-hour, average surface (left column) and near-bottom (right column) salinity distributions in Delaware Bay for Julian Days 185, 188, 204, and 210. Contour interval is 2.0 ppt (Galperin and Mellor, 1990b).



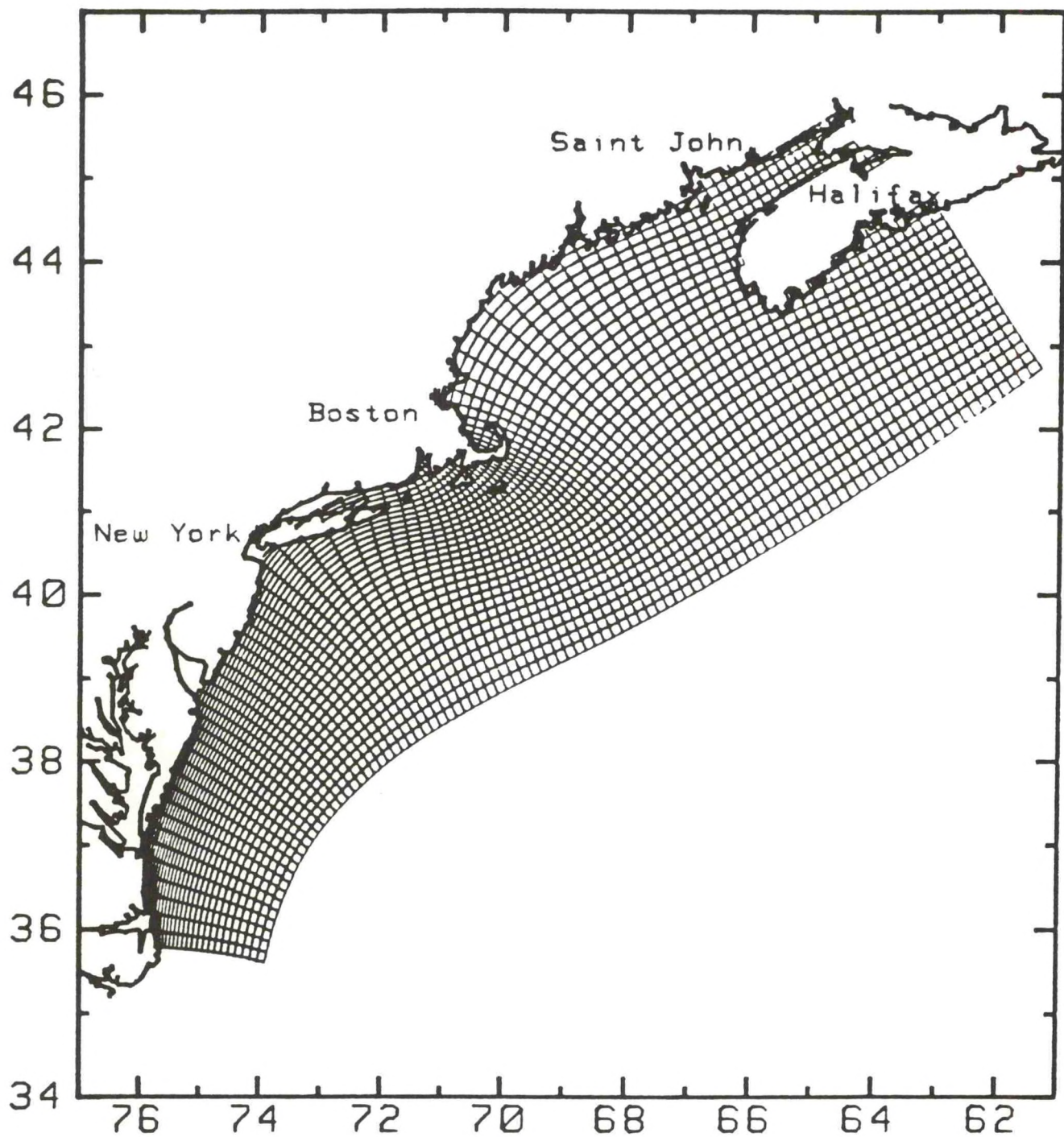


Figure 11. Orthogonal curvilinear coordinate system employed in the numerical simulations of the Middle and North Atlantic Bights (Kantha et al., 1985).

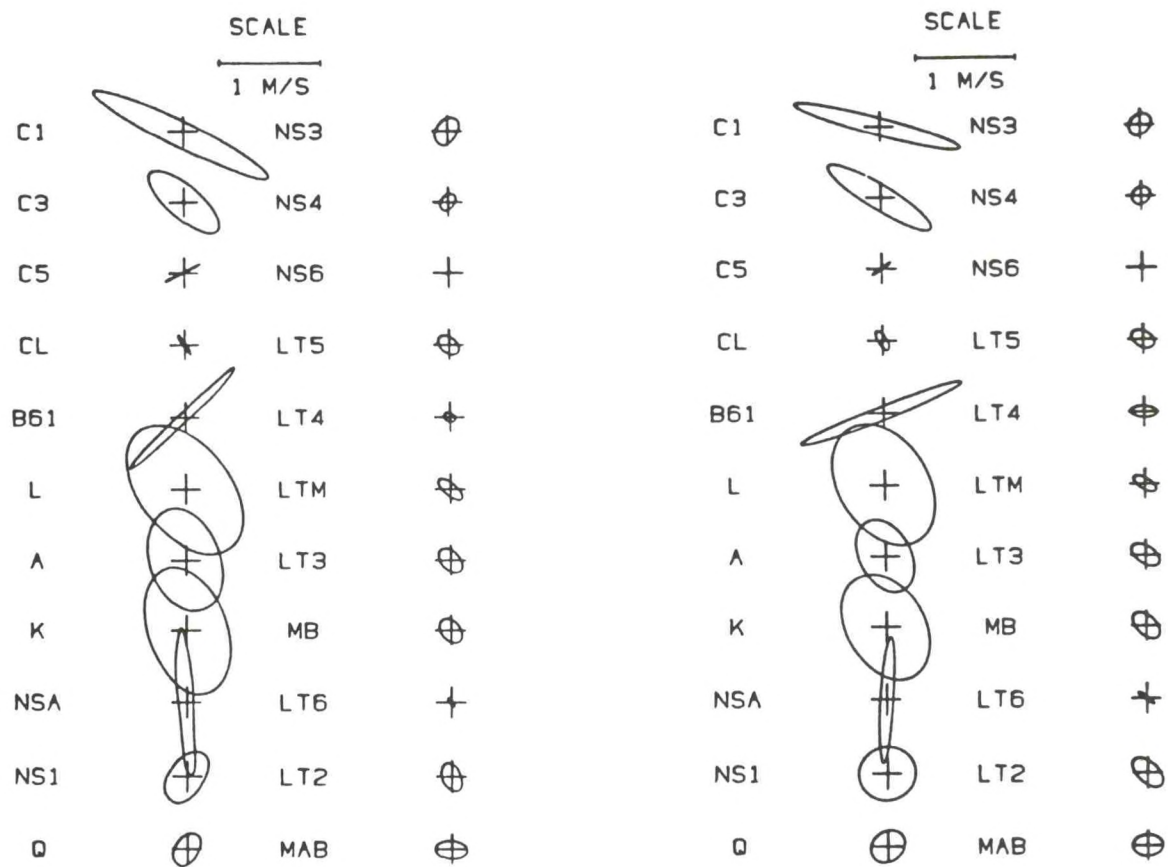


Figure 12. Predicted (left) and observed (right) (Moody et al., 1984) tidal current ellipses at selected locations shown in Figure 4.3 (Kantha et al., 1985).



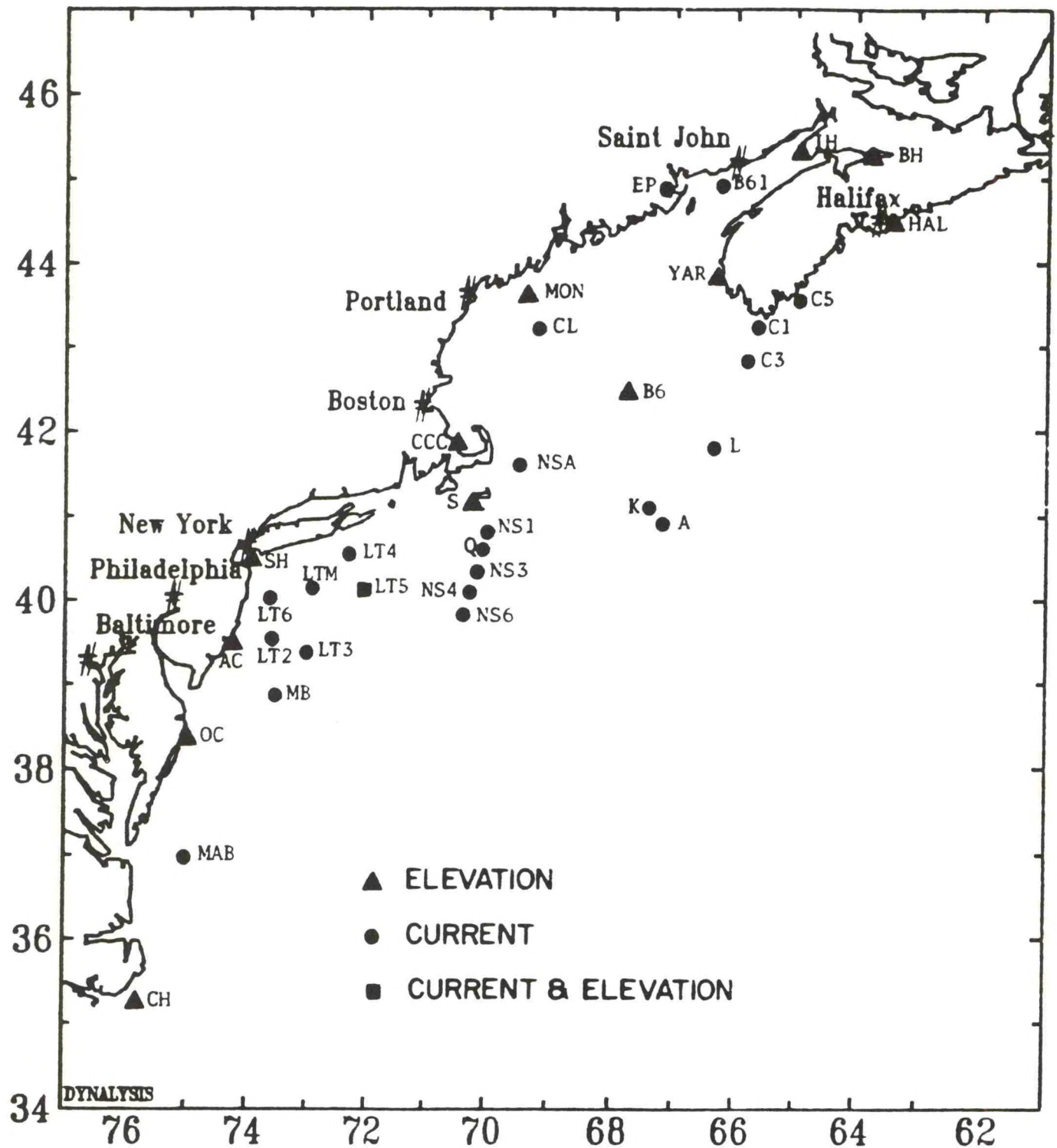


Figure 13. Map of the Mid-Atlantic Bight model domain showing the locations of selected spots at which 12-minute time histories are archived (Kantha et al., 1985).

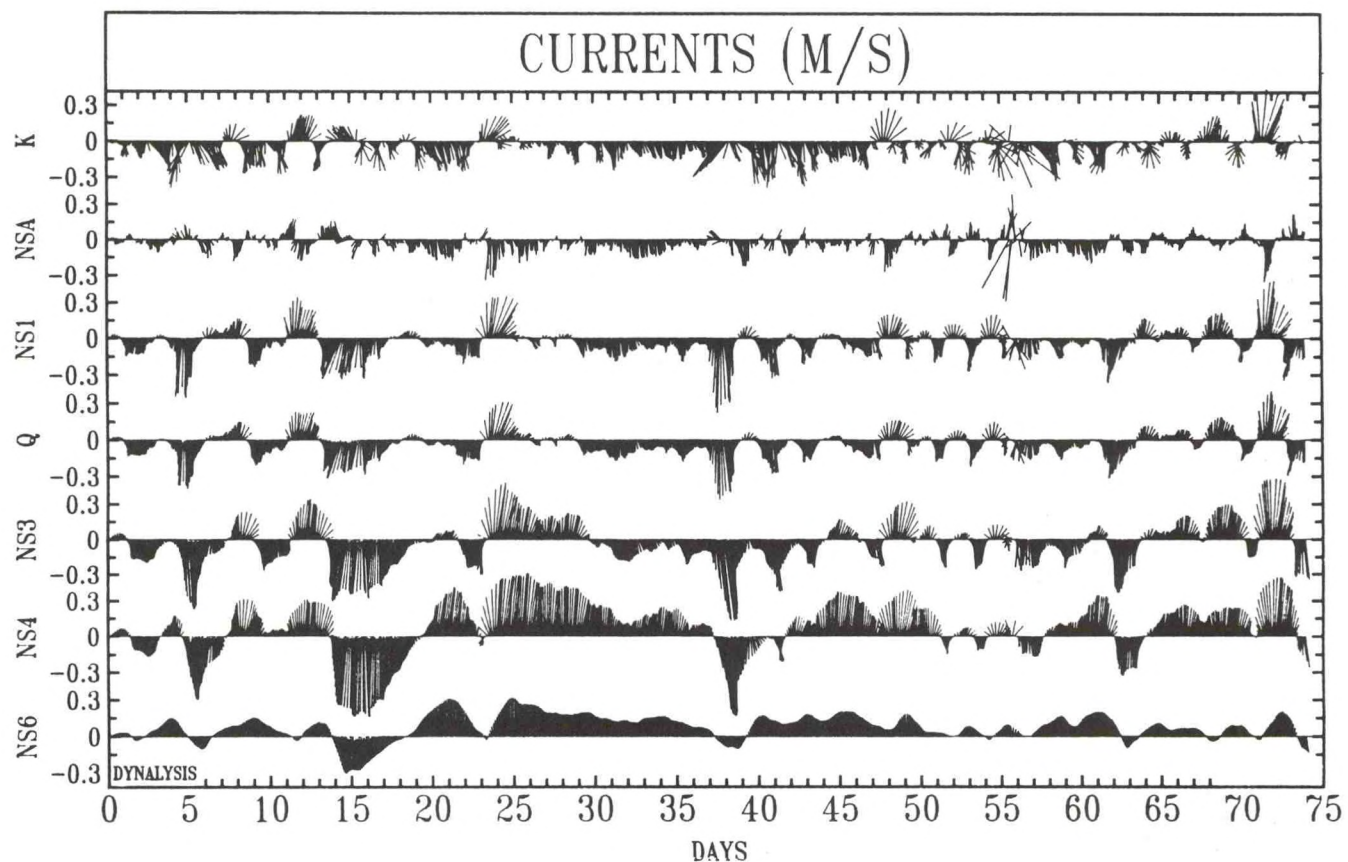


Figure 14. Stick diagrams showing time histories of calculated currents during the storm simulation at selected points (see Figure 2.27, Kantha et al., 1985).



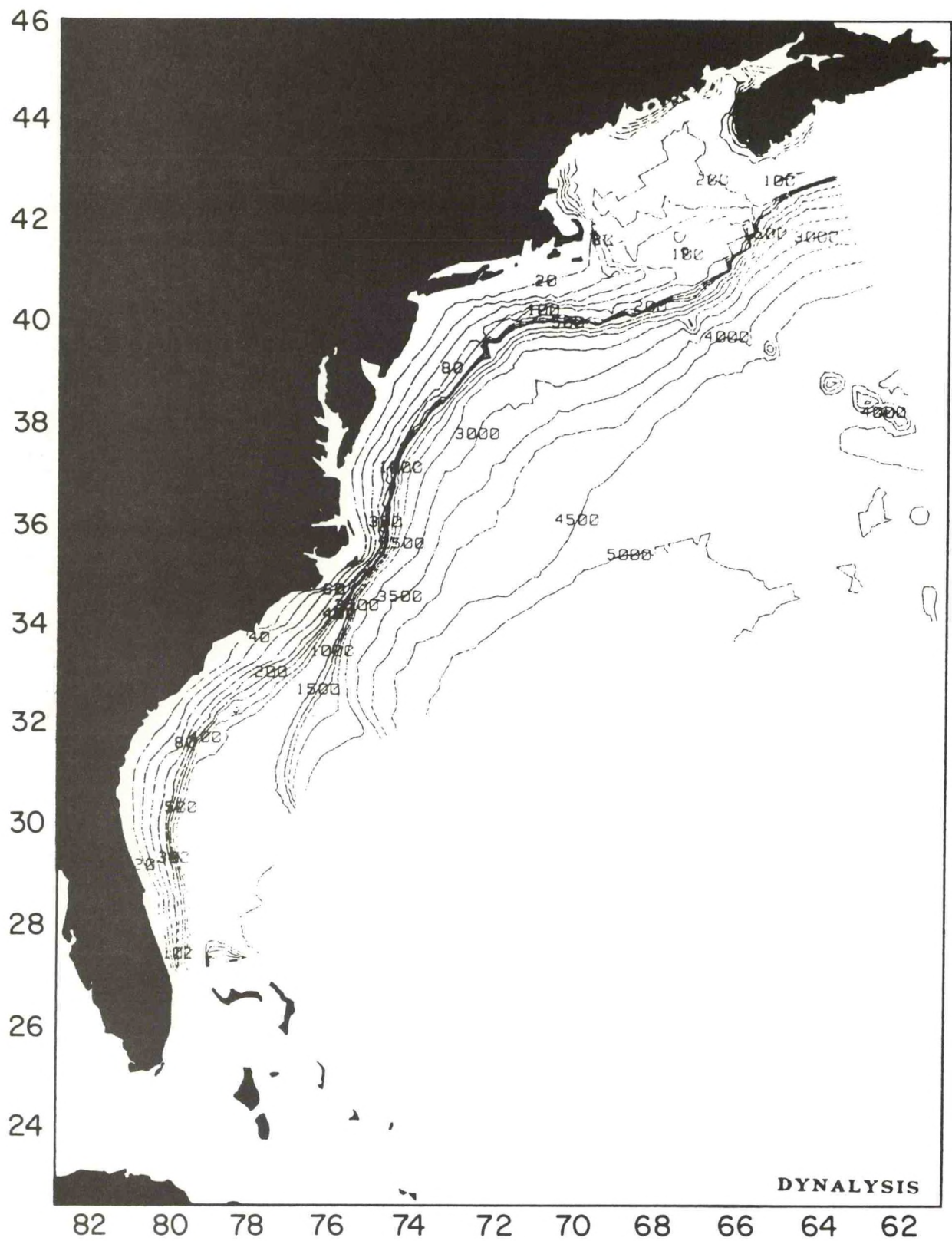


Figure 15. Ocean depth measurement along the Atlantic coastline of North America.

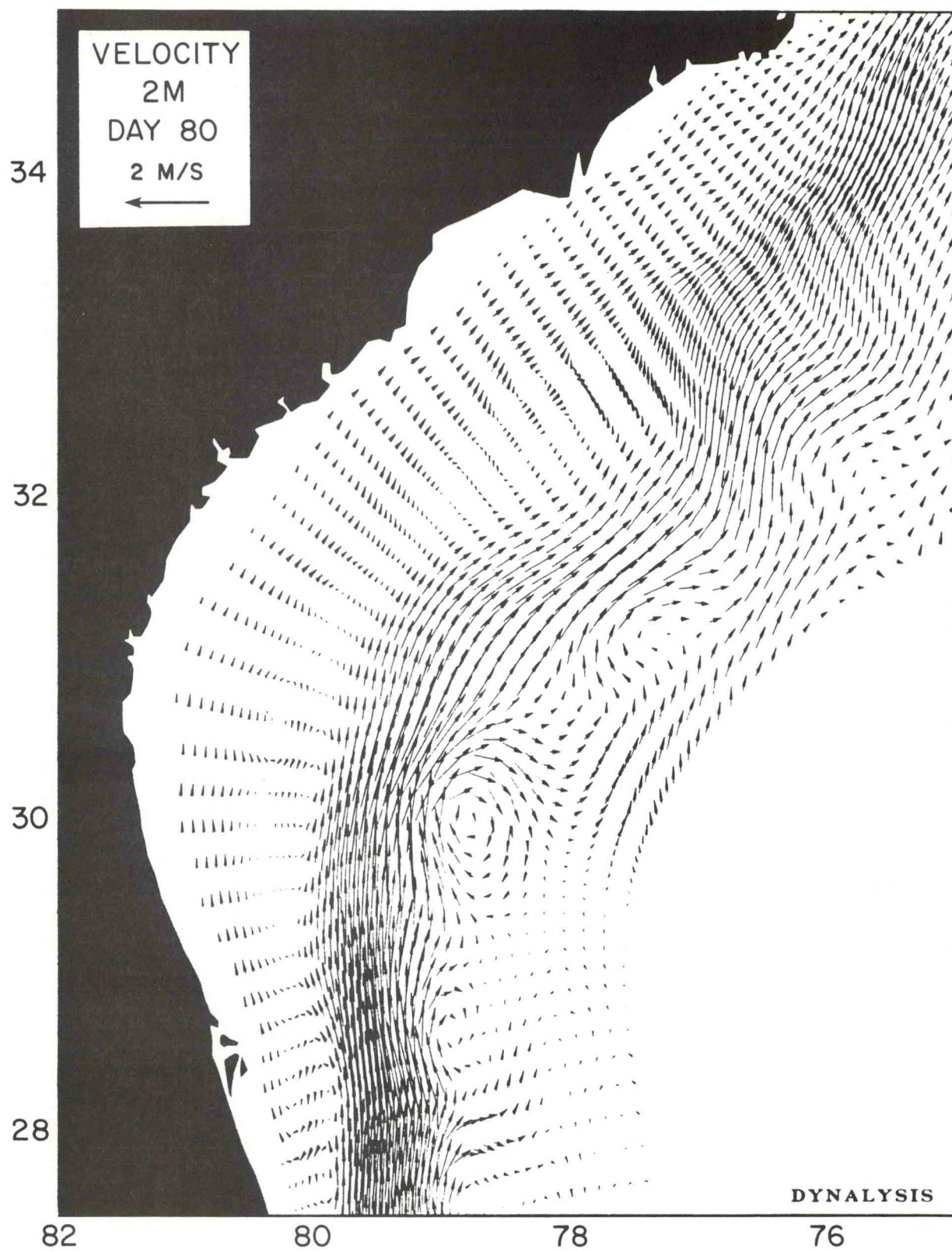


Figure 16. Velocities two meters below the surface after 80 days.



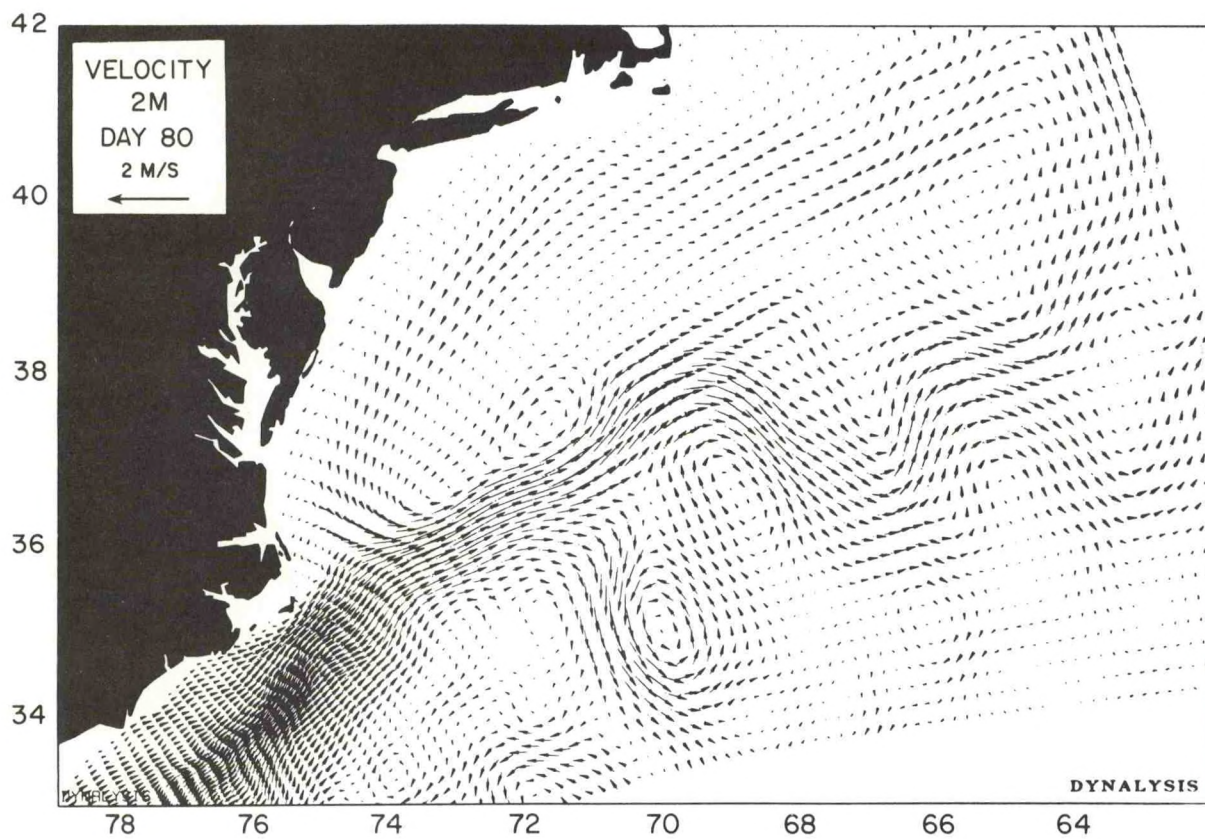


Figure 17. Velocities two meters below the surface after 80 days.

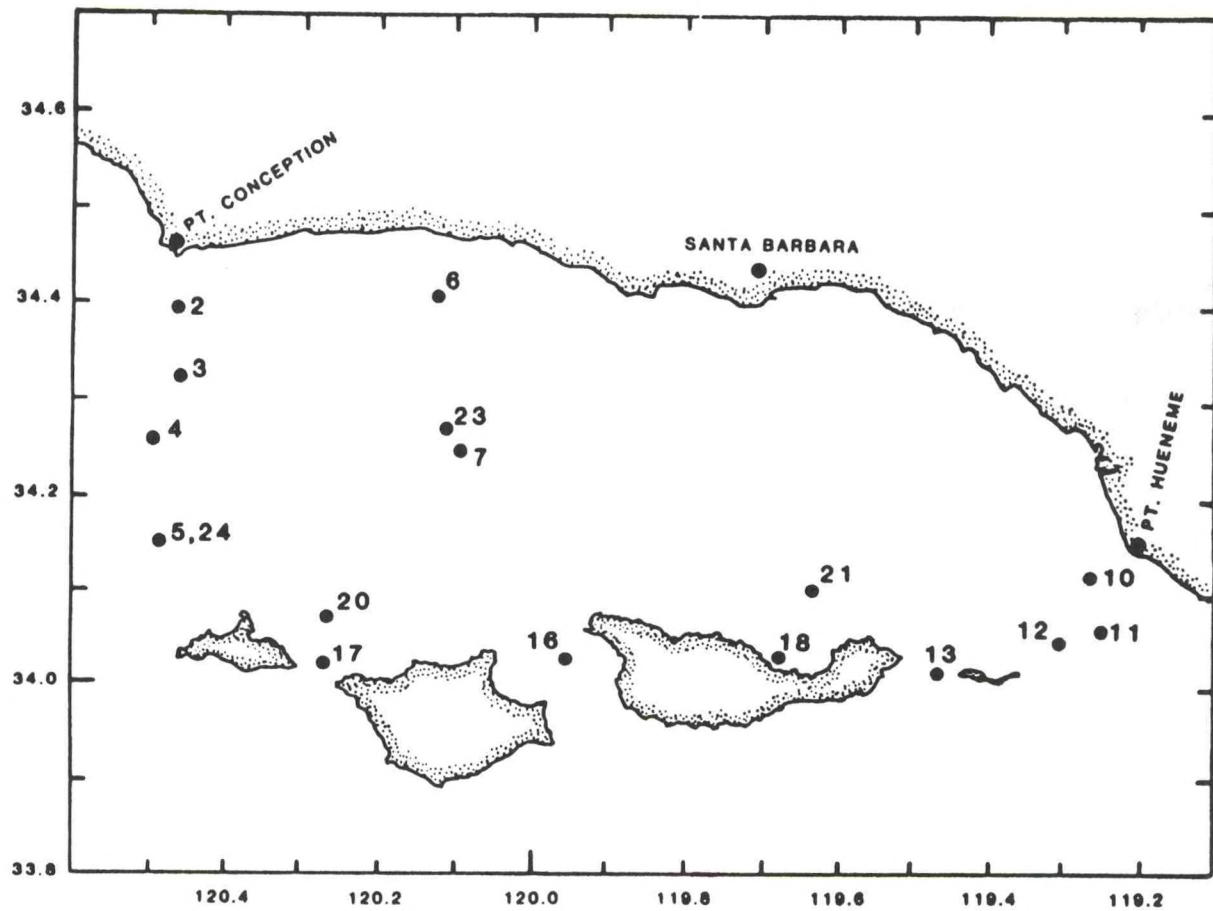


Figure 18. Current meter mooring locations during the Santa Barbara Channel Main Program.



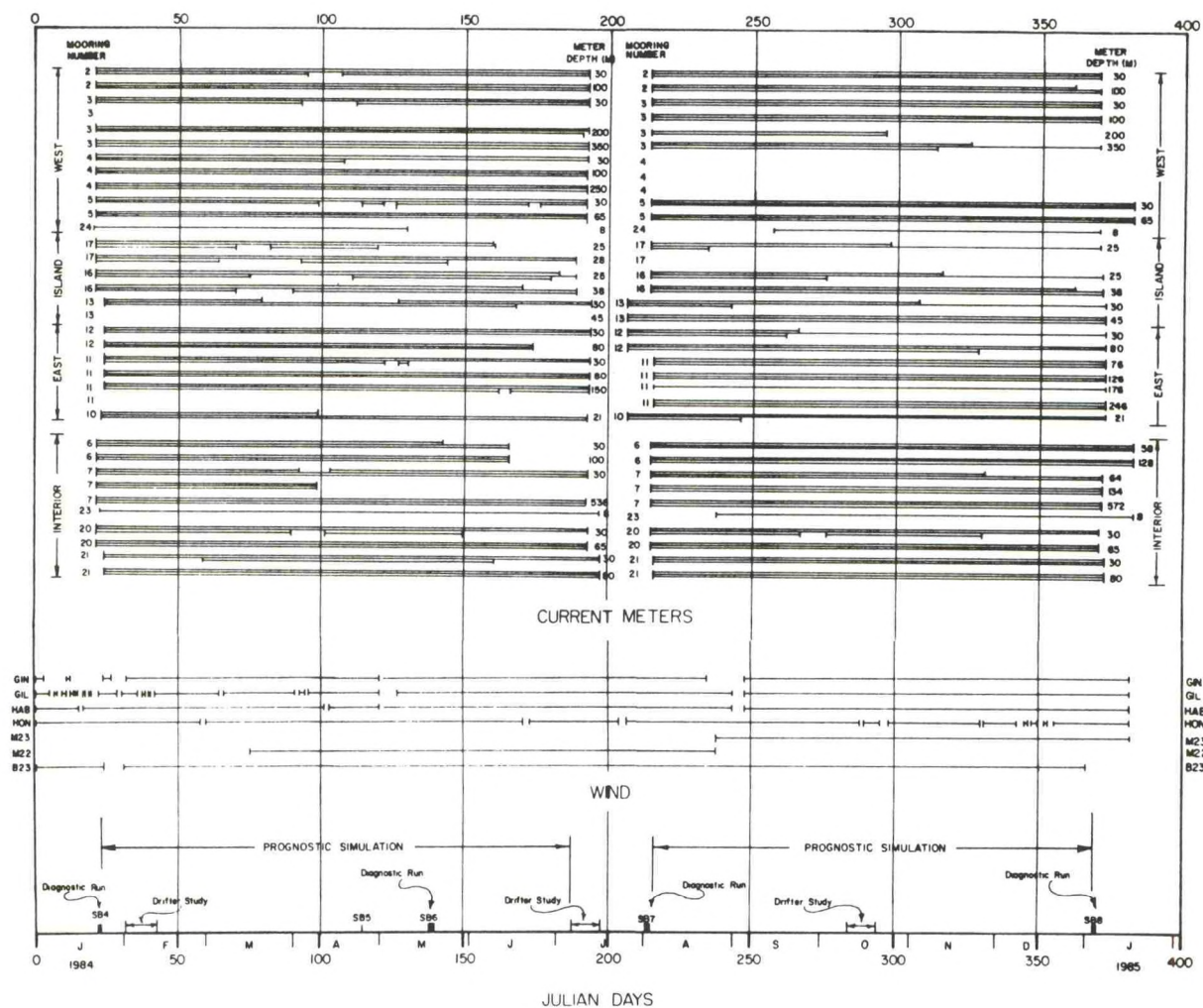


Figure 19. Data return during the Santa Barbara Channel Main Program.

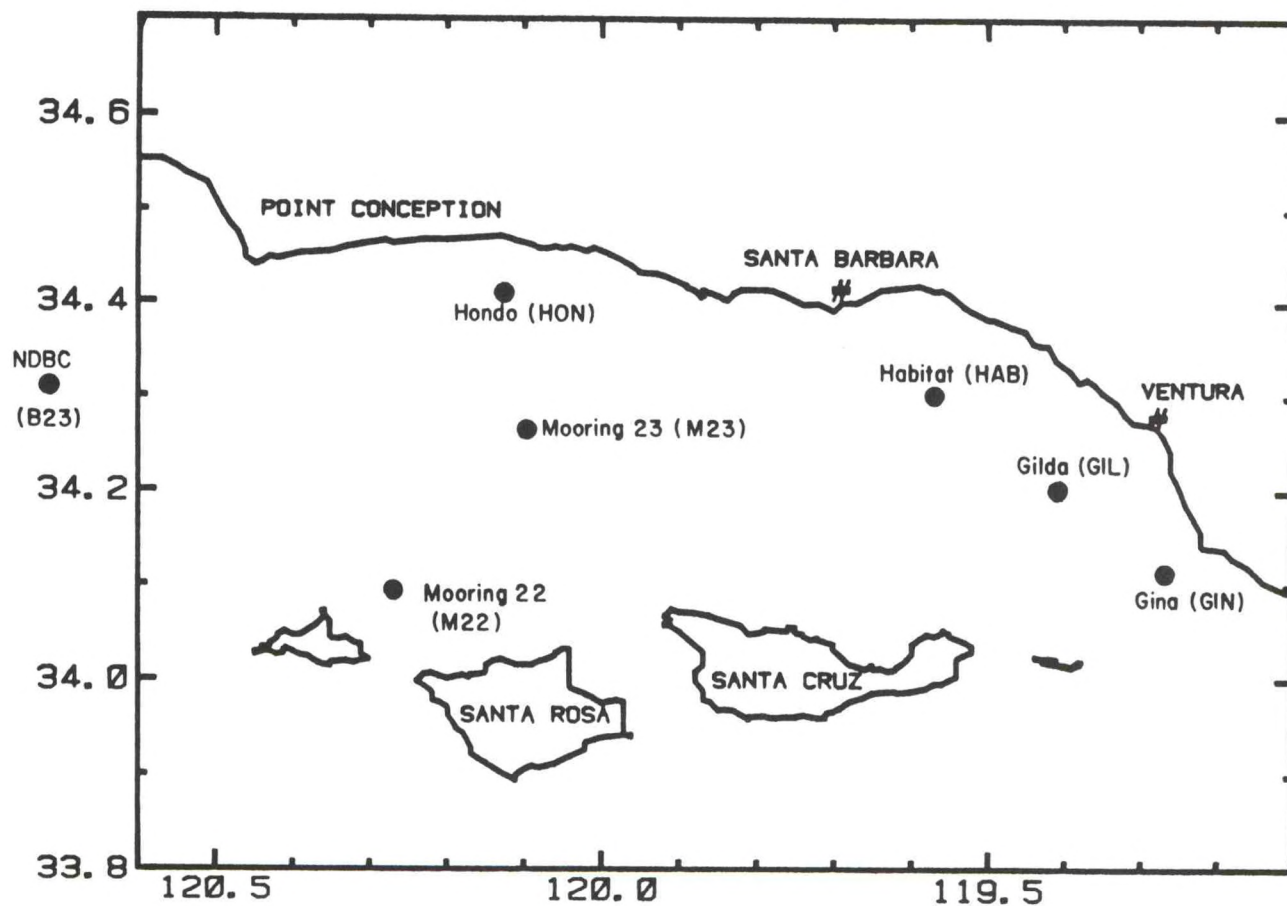


Figure 20. Locations of meteorological stations from which wind data is available during Main Program.



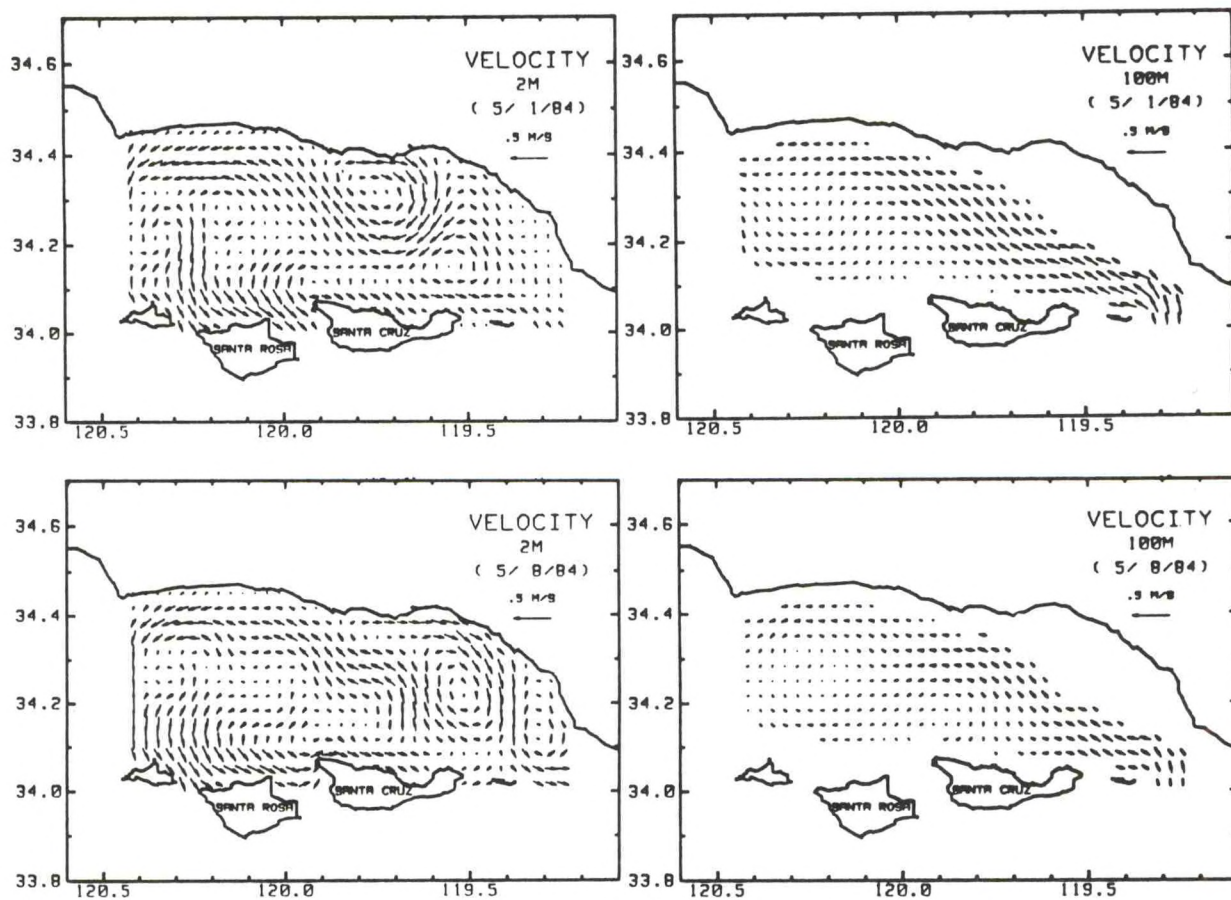


Figure 21. Daily averages of velocity at the surface and 100 m on May 1 and May 8.

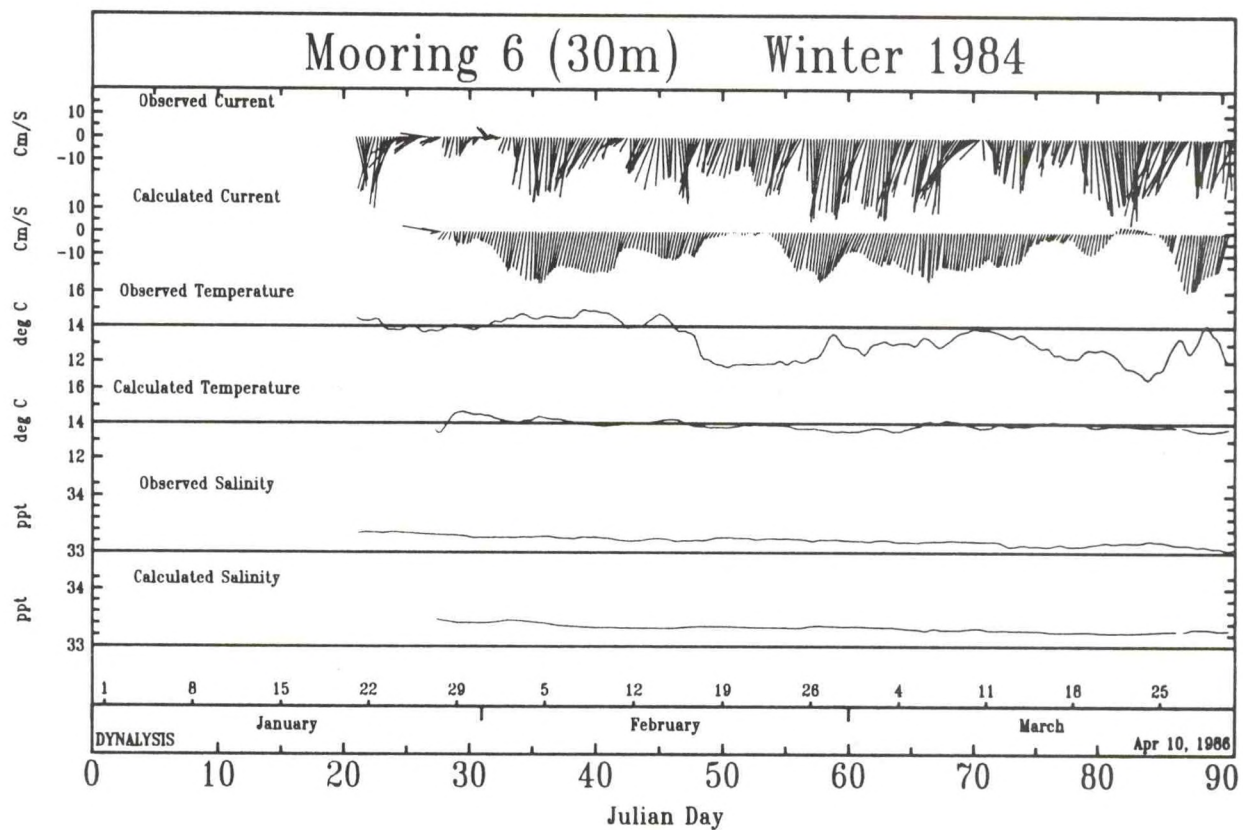


Figure 22. A comparison of observed and calculated data corresponding to the top current meter on Mooring 6 during the winter season.



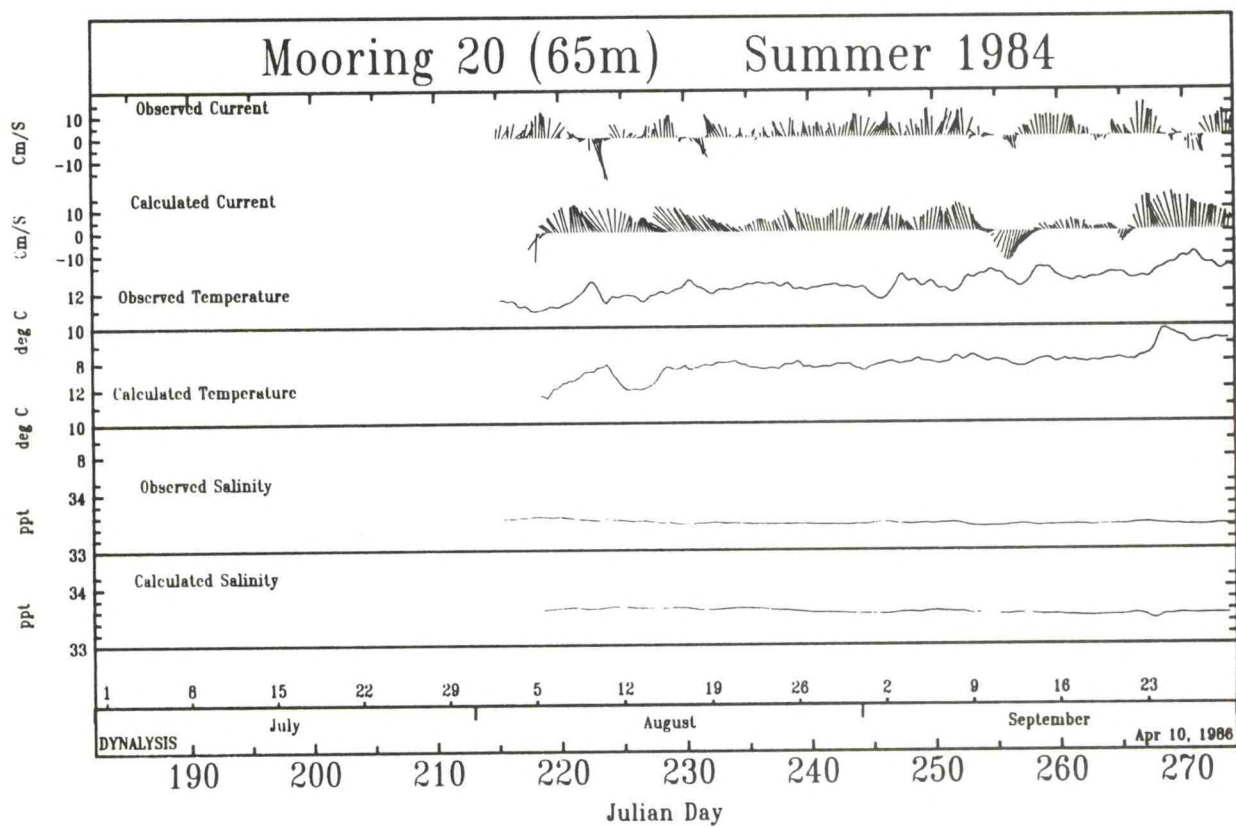


Figure 23. Comparison between observed and calculated data corresponding to the bottom current meter on Mooring 20 during the summer months.

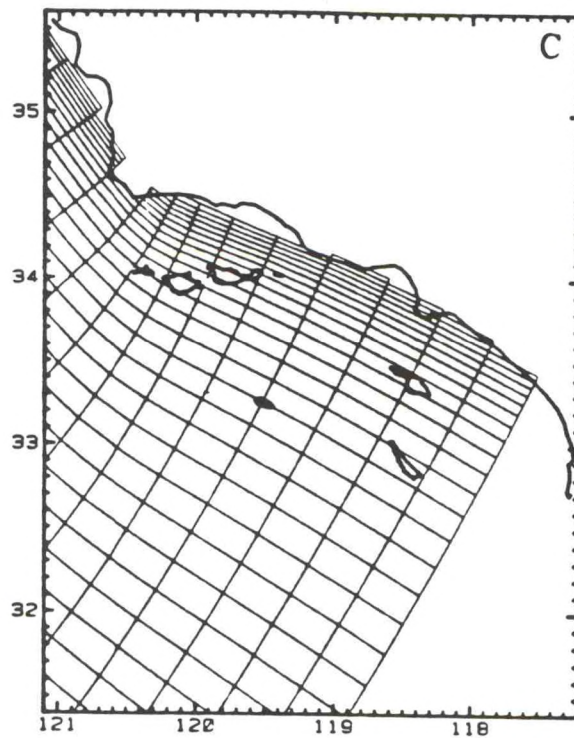
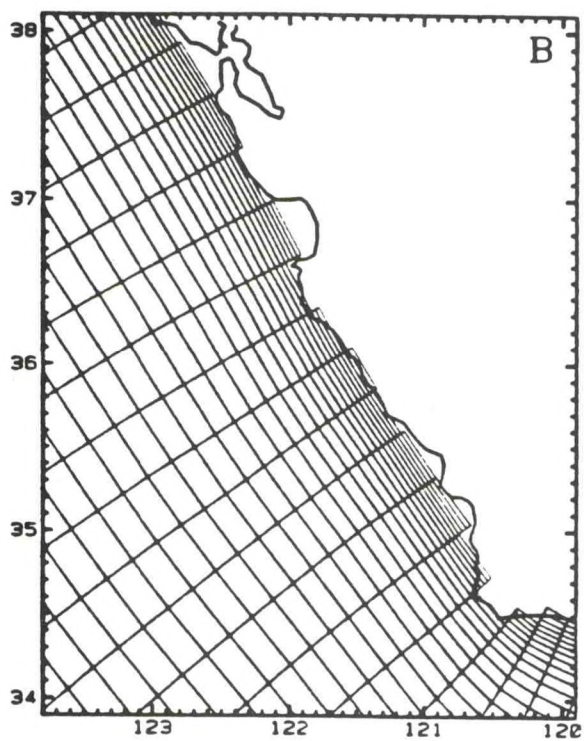
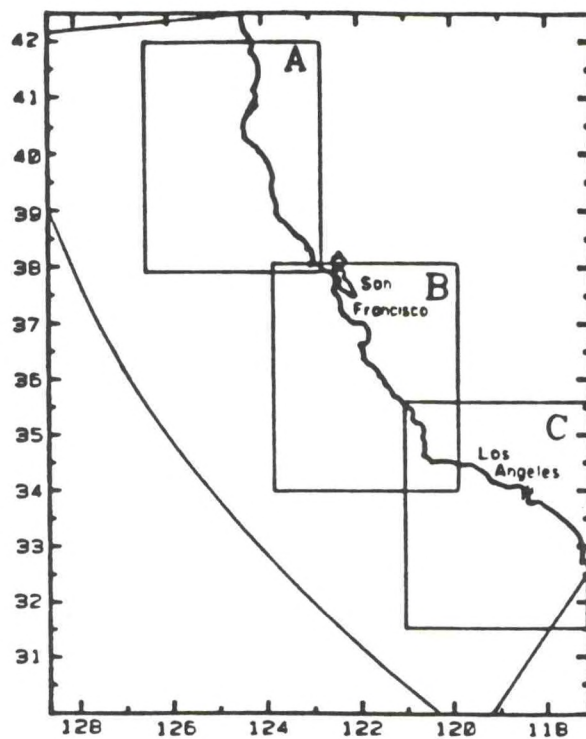
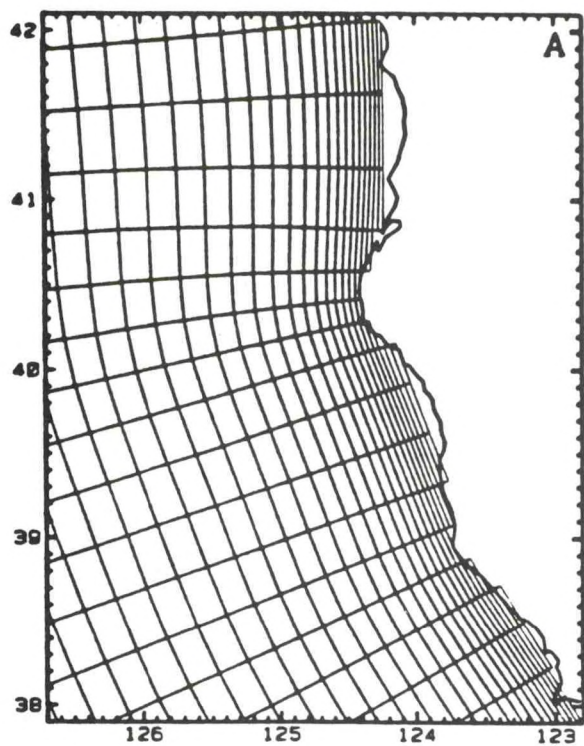


Figure 24. Illustration of the three subdomains used to plot magnified views of the nearshore region and the portion of curvilinear grid included in each.



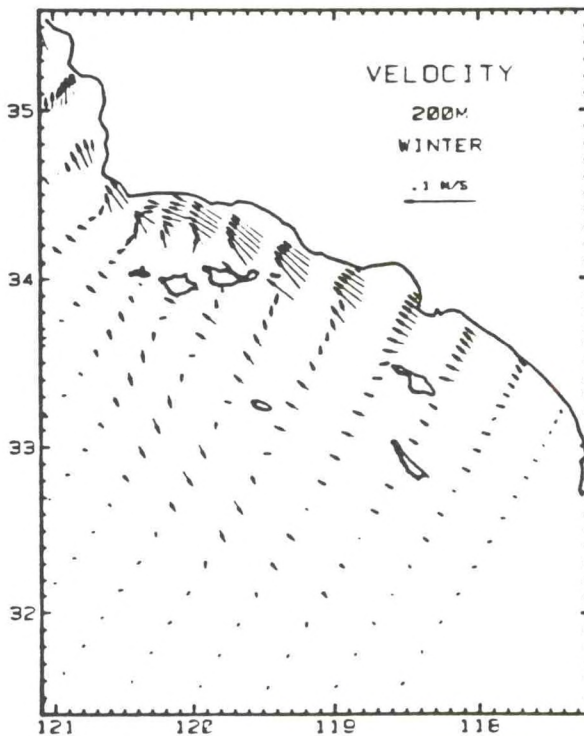
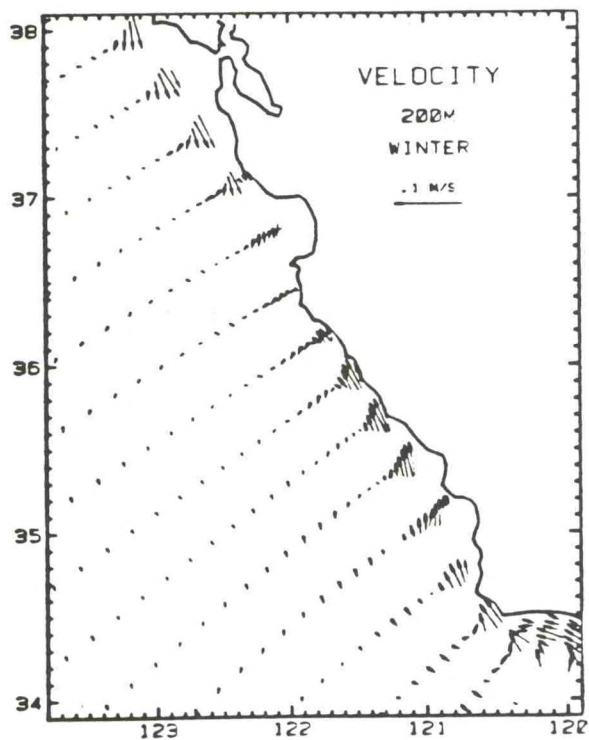
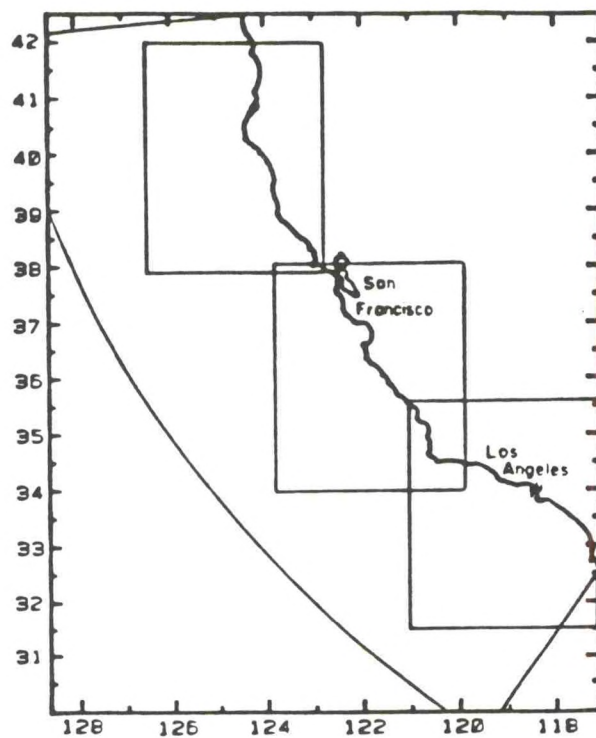
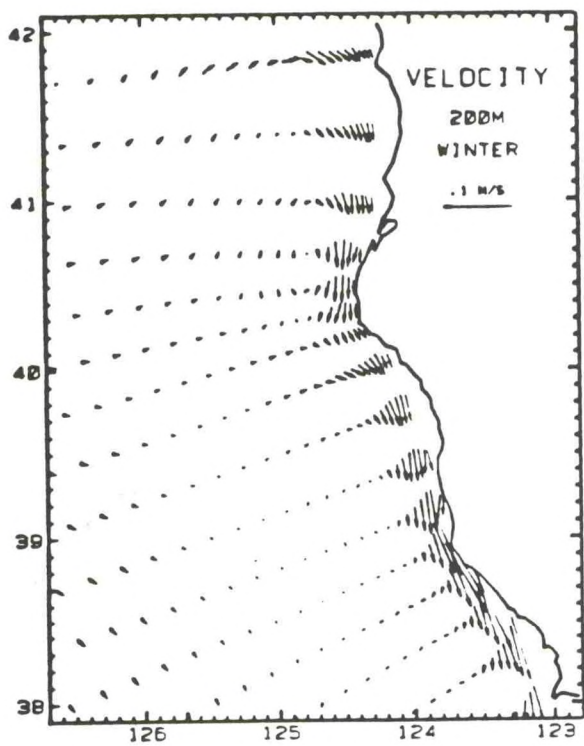


Figure 25. Seasonal mean currents at 200 m depth during winter from the diagnostic General Circulation Model (Blumberg et al., 1984).

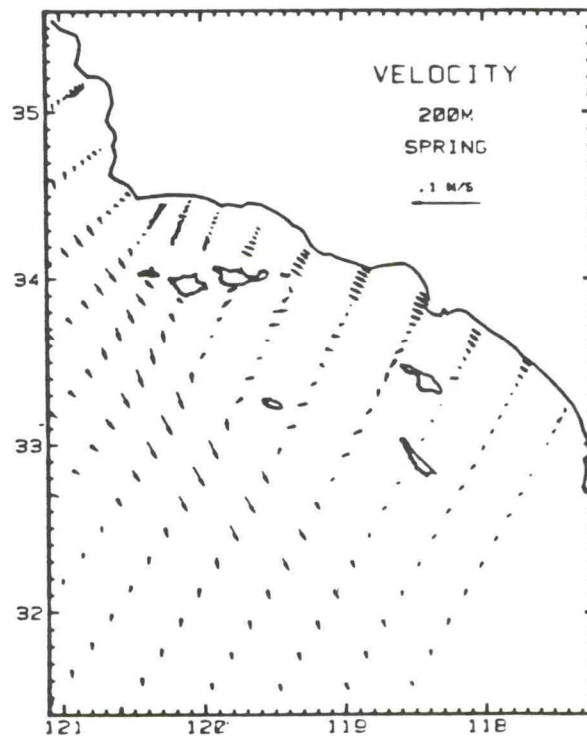
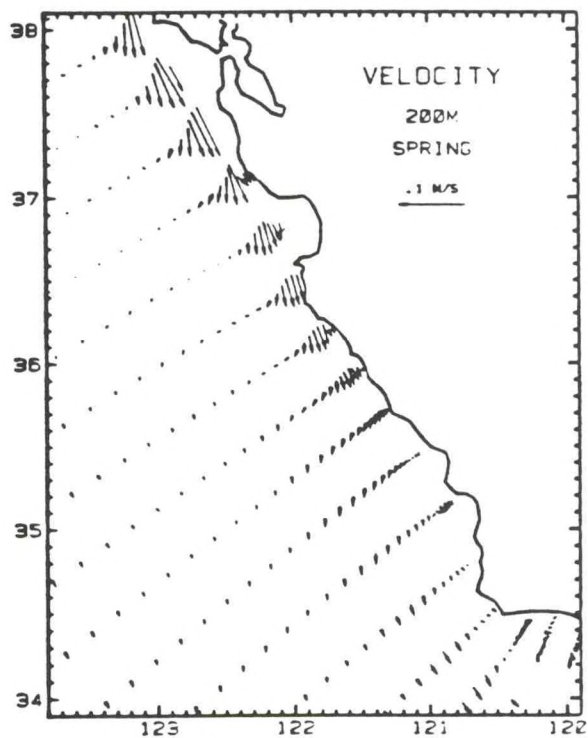
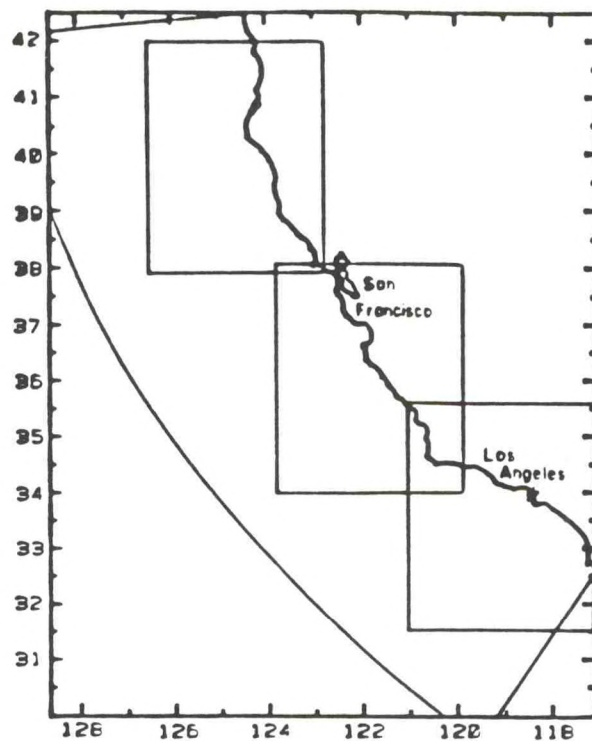
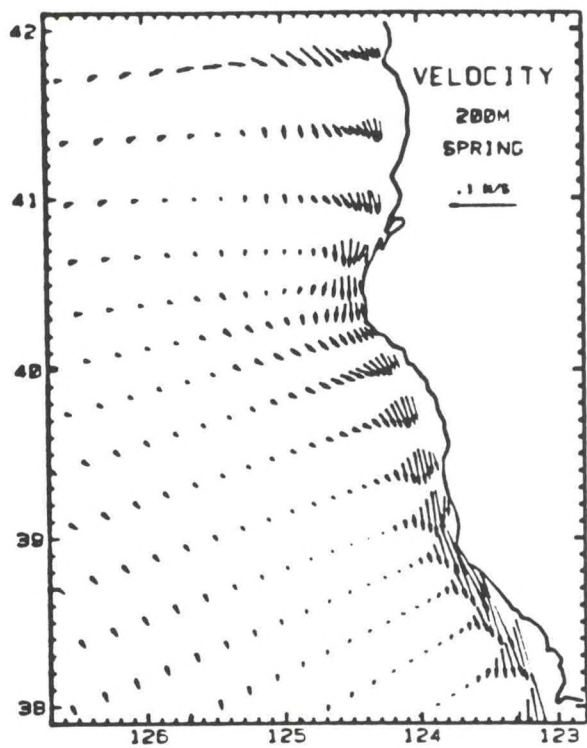


Figure 26. Seasonal mean currents at 200 m depth during spring from the diagnostic General Circulation Model (Blumberg et al., 1984).



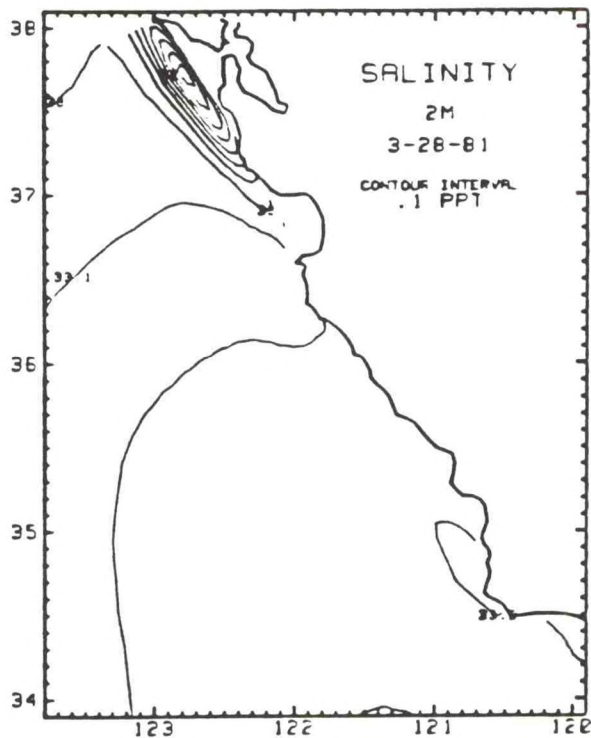
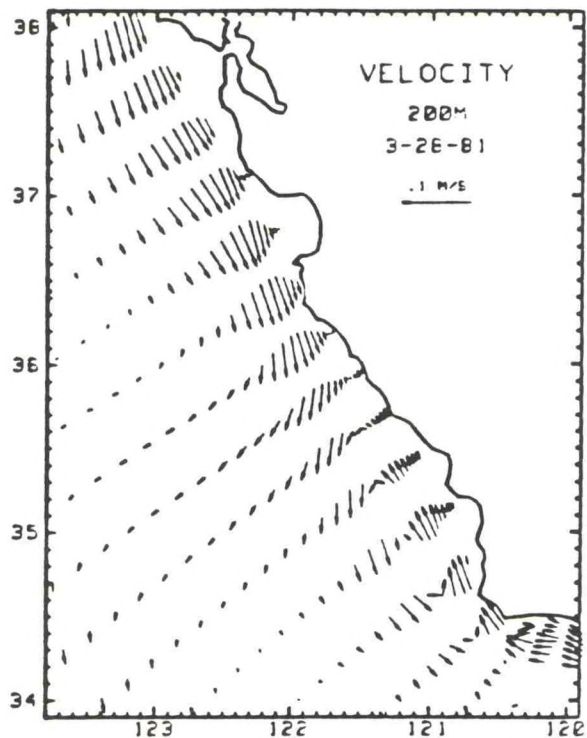
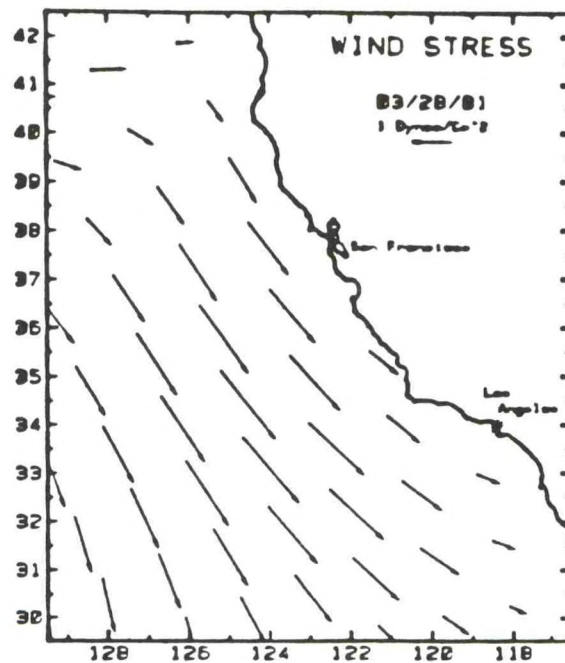
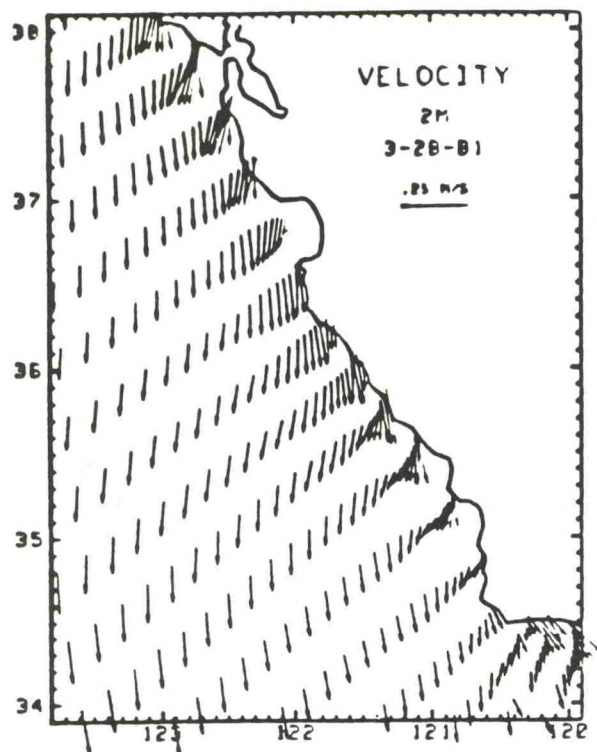


Figure 27. Currents, winds, and salinity at 2 m depth and currents at 200 m depth along the central California coast on 03/02/81 (Blumberg et al., 1984).

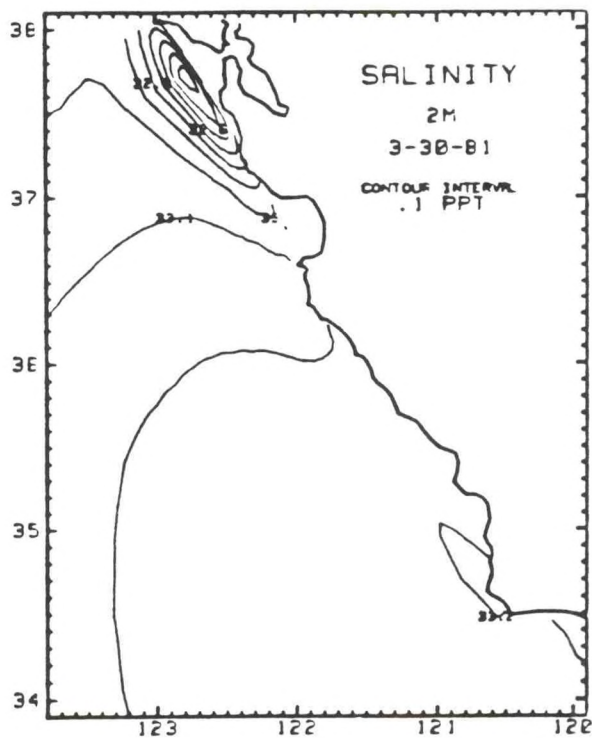
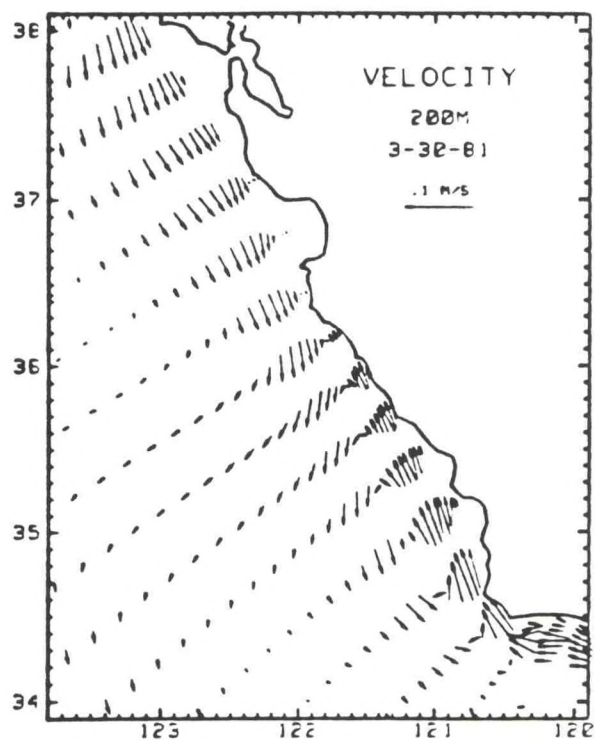
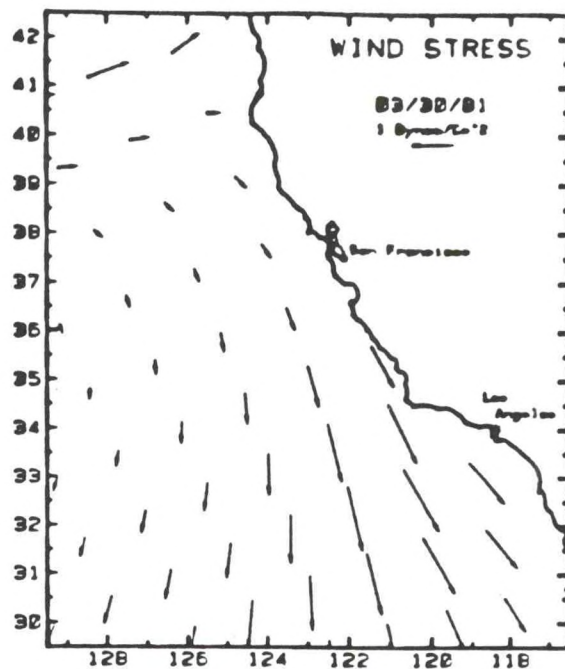
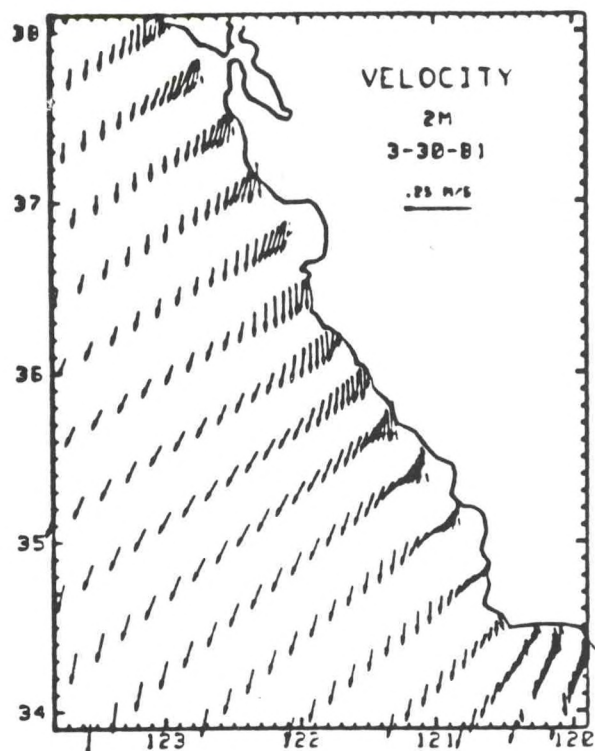


Figure 28. Currents, winds, and salinity at 2 m depth and currents at 200 m depth along the central California coast on 03/30/81 (Blumberg et al., 1984).



# COASTAL CONSTRAINTS ON QUASIGEOSTROPHIC FLOW

Allan R. Robinson  
Division of Applied Sciences  
Harvard University  
Cambridge, MA 02138

Problems of interaction and exchange between the coastal ocean and the deep open ocean are of scientific and practical importance in their own right. Furthermore, such problems enter the parameterization of the deep ocean as a boundary condition for the coastal ocean modelling, and vice versa as the parameterization of the coastal ocean for the deep ocean modeler. Thus, both aspects of the interaction and exchange problem now need to be studied simultaneously from the coastal ocean outward and from the deep ocean inward. The coastal modeler may be interested in the region from the shore to the shelfbreak but choose to model a few hundred kilometers beyond the slope. What aspects of the deep flow must be correct and how can they be achieved? The deep ocean modeler may or may not be interested in the details of the near coastal flow. The degree of interest (phenomenology, time and space scales) influences whether or not it is necessary to refine, in the coastal region, the physical model utilized for the deep ocean flow.

This note reviews two issues associated with the assimilation of real data into the coastal version (Milliff, 1989) of the Harvard quasigeostrophic model (Robinson and Walstad, 1987a). The first issue deals with objective analysis in the presence of arbitrary coasts, and presents a method of imposing no normal flow into an arbitrarily shaped coastline. This is a kinematic constraint on the geostrophic flow required by quasigeostrophic dynamics. The second issue deals with the method of real data initialization of the dynamical model in the presence of arbitrary coasts and the sensitivity to the pretreatment of the data. Each issue is presented by quoting from manuscripts which are available for readers who are interested in further details, context and related issues.

**Coastal Objective Analysis.** Quoted from Robinson *et al.* (1990), and illustrated in Plate 1.

. . . The results presented consist of maps of dynamic height for the upper thermocline (30/450 db) . . . The maps were constructed via objective analysis (Carter and Robinson, 1987) with correlation parameters the same as those chosen at a workshop in Modena, Italy in 1988 (Pinardi, 1988). An important consideration here concerns inhomogeneity related to the coastlines which introduce anisotropy into the analysis and constrain kinematically the geostrophic flow. A new method of dealing with these issues is introduced and utilized. For a strip of coast, coastal data is used to identify a coastal vertical density profile. The coastal profile is then added at intervals along the coast to the observed data set for the objective analysis. This serves both to provide the required along-coastal correlation and to impose the constraint of no normal flow into the coast . . .



The features and the structure of the flow as indicated by the simple isotropic objective analysis map of Figure 4a are correct over the major part of the basin. Aspects of the near coastal flow, however, require a refined treatment associated with the anisotropy and kinematics of the coastal region. An example is the apparent coastal inflow and outflow along the northern Levantine boundary. The sampling scheme was designed to resolve the general circulation, and was generally not altered in the vicinity of the coastal and shelf regions. Thus, we do not attempt to map coastal and shelf phenomena. The general circulation flow is consistently constrained to have no normal flow component into the coast, which is achieved geostrophically by imposing a horizontally uniform density profile along the coast. For the most part, the basin is rimmed by a narrow shelf and steep slope, and the coastal kinematic constraint is imposed on the shelf-break chosen as the 600m isobath.

In practice, the constraint is imposed by adding, to the data set to be mapped, a number of boundary profiles located along the shelf-break less than a decorrelation length apart. Although we continue to map with an isotropic correlation model, the boundary data set imposes upon the maps the required coastal anisotropy with high alongshore correlation. Segments of the coastline are characterized by a boundary profile inferred from near coastal data. The segments are selected subjectively, bounded by major straits or by gaps in near coastal data. For the case of Physical Oceanography of the Eastern Mediterranean, August-September 1987 (POEM AS 87), six boundary profiles were used for the following regions: the northwest and northeast Ionian coasts, Crete, the northern Levantine coast, Cyprus, and the southern Levantine coast together with the south part of the eastern Levantine coast (Fig. 3a).

To determine the boundary profiles, the near coastal data are examined subjectively, and a representative CTD is chosen for the boundary CTD. On each of the station position maps of Figure 3, all near coastal data used for this purpose is indicated, and the CTD selected for the boundary profile is identified . . . . Consideration in each case is given to the distance of a station from the shelf-break, the proximity of data points, data quality, etc. Tests indicate that the procedure is robust and not sensitive to the particular profile selected . . . .

The flow field of the coastal objective analysis (Fig. 7a) compared to the isotropic objective analysis (Fig. 4a) shows the same general circulation features unmodified over most of the basin but with continuous coastal currents and no flow into the coast . . . .

**Dynamical Model Initialization.** Quoted from Milliff and Robinson, (1990) based for the most part on Chapter 4 of Milliff (1989), and illustrated in Plate 2.

. . . . The Rhodes Gyre is a persistent cyclonic feature of the general circulation of the Eastern Mediterranean Sea. The gyre is  $O(300 \text{ km}^2)$  in scale, and centered at about  $36^\circ \text{ N}$ ,  $28.5^\circ \text{ E}$ --south of Turkey and east of the island of



Rhodes. The region has long been suspected to be a site of Levantine Intermediate Water formation, associated in some unknown dynamical way with the variability and stability properties of the Rhodes Gyre flow field, which until now have also remained largely unknown. In this study we seek to characterize the structure and dynamics of the flow system in the region of the Rhodes basin, including the mesoscale variability. The study is based on a new multi-scale dataset, and made possible by an extension of the quasigeostrophic (QG) dynamical interpolation methodology to permit the treatment of coastal domains . . .

. . . The scientific method to be followed in this study derives from the open ocean mesoscale modelling methodology that has been developed and applied to various regions of the world ocean (for a summary, see Robinson and Walstad, 1987a). Briefly, the methodological steps are as follows. A synoptic survey of an ocean region is used to derive an initial condition field for a region of interest. Open boundary conditions for the region can be held constant, forecast, or interpolated between the initial realization and a later sampling of the boundary. An open ocean QG model is integrated ahead in time as a simulation or a so-called 'forecast experiment,' to a second full field realization that is used to verify the model result if such is available. A QG consistent energy and vorticity analysis package can then be applied to a time series of the model fields to diagnose and quantify dynamical processes . . .

The component tools of a coastal QG methodology include an extension of coastal QG theory elucidated in Pinardi and Milliff (1989), and a new coastal QG numerical implementation described by Milliff (1990) . . . The pointwise coastal constraint consistent with the QG approximation requires that the streamfunction be a (time and depth dependent) constant along the coastal boundary (Pinardi and Milliff, 1989) . . .

For the Rhodes Gyre region data, the QG coastline was imposed along the 500m isobath throughout the domain. Figures 4a and b depict the objectively analyzed dynamic topography at 30 m, and the corresponding error maps for the Rhodes Gyre region. Figure 4a results from the implementation of the conventional objective analysis procedure. Figure 4b derives from the objective analysis procedure applied to the same data plus 44 boundary profiles, inserted to provide a coastal geostrophic constraint (note the differences in the error maps). The boundary profiles were inserted along the 500m isobath, at every other boundary grid location on a 7.5km-square grid discretization of the Rhodes Gyre domain.

The sub-basin scale features of the general circulation in the Rhodes Gyre region appear in Figure 4b from the new coastal objective analysis procedure. The relative sizes and strengths of the Rhodes Gyre and Anaximander Anticyclone are consistent with the general circulation picture. The Rhodes Gyre appears as a multi-centered closed cyclone of ~300km scale, with the strongest cyclonic circulation located over the Rhodes Basin. The Anaximander Anticyclone is O(100 km) in scale. The magnitudes of the circulations in the Rhodes Gyre and Anaximander Anticyclone are similar. The Asia Minor Current is coherent from



inflow on the eastern open boundary, south of the Anaximander Anticyclone, north of the Rhodes Gyre, to its outflow at the western open boundary near the top of Crete. Note that these sub-basin scale features are associated with each other, the border flows of the closed circulations forming part of the basin-wide throughflow of the Asia Minor Current.

In contrast, in the field derived from the conventional objective analysis (Figure 4a), the QG coastal boundary condition is clearly violated. There are several instances of flow normal to the discretized boundary. However, there is evidence of a (weak) cyclonic circulation over the Rhodes Basin, which extends to the Eastern Mediterranean Ridge . . . The dominant circulation feature in Figure 4b is a large anticyclonic circulation centered in the region of the Anaximander Seamounts, but covering an area much larger than the seamount chain (including a portion of the Turkish mainland). Most importantly, there is no basin-wide coherent flow along the coast to represent the Asia Minor Current.

Numerical Experiments. In this section we describe the design of numerical experiments to test the sensitivity of the Rhodes Gyre dynamical adjustment and QG model simulations, given physically reasonable variations in initial conditions . . . The two initial condition variations, with and without boundary profiles inserted in the objective analysis step, have just been described . . . After initialization, at the first timestep of a numerical integration, the coastal QG model will impose the geostrophic constraint on the velocity field at the coastal boundary, independent of the initial condition. In a semi-open domain case, such as the Rhodes Gyre domain, the coastal boundary streamfunction value is a function of the nearby open boundary streamfunction specification. At each level we write:

$$\Psi(\partial C) = h[\Psi(\partial O^*, t)]$$

where  $\partial C$  denotes the QG coastal boundary,  $\partial O^*$  is the open boundary region immediately adjacent to the coastal boundary, and  $h$  is a user-specified function that relates the nearshore variability to the QG coastal streamfunction value as described in Milliff (1989). In the Rhodes Gyre case, the coastal streamfunction value is set equal to the nearshore streamfunction on the open eastern boundary, at the inflow of the Asia Minor Current . . .

Dynamical Adjustment. Snapshots of the pycnocline for day 10 are given in Figures 7a,b. Recall from Figure 4 that the initial pycnocline circulations in the Rhodes Gyre and Anaximander Anticyclone are comparable in the coastally constrained case, and that the Anaximander Anticyclone circulation is twice that of the Rhodes Gyre in the conventionally derived initial fields. This distinction is preserved through 10d, as seen by comparing Figures 7a and b. In the conventional initial condition case, the open boundary condition on the southwestern open boundary is near enough to the coast to differ from the constrained case. This leads to some difference in the external shape of the gyre, which is of course maintained. The pycnocline Anaximander Anticyclone is more asymmetric toward the south at 80 m at 10d in the conventional initial



condition case. The Asia Minor Current has invaded the Karpathos Straits, forming a deep meander downstream over the Cretan-Rhodes Ridge . . .

Summary. The methodology of these first simulations of the mesoscale variability in the Rhodes Gyre region support the following conclusions:

- A semi-open domain version of the Harvard QG model has been run successfully for a real data application in a region with complicated coastline and bathymetry.
- A new procedure was developed whereby a coastal streamfunction profile is synthesized from data and inserted into an objective analysis to impose a coastal geostrophic constraint. The coastally constrained analyzed fields can serve as initial conditions for QG model dynamical interpolation calculations.
- QG model dynamical interpolation results can be sensitive to the specification of the coastal geostrophic constraint in the initialization.
- The specification of the coastal constraint in the initial conditions for Rhodes Gyre region dynamical interpolations yielded results that were preferred to the results from initial conditions that did not contain the constraint . . .

Figure 3a

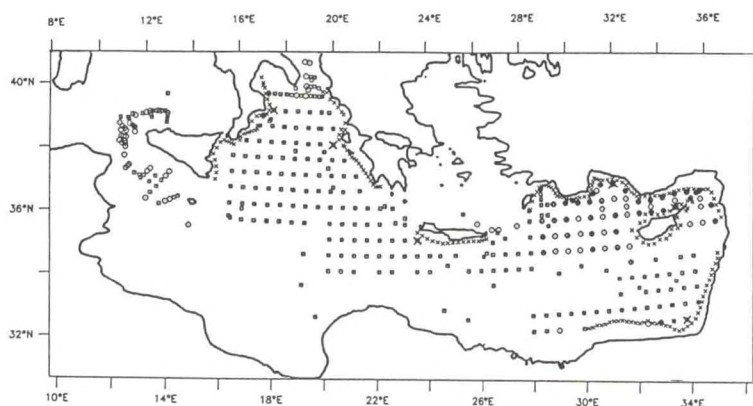


Figure 4a

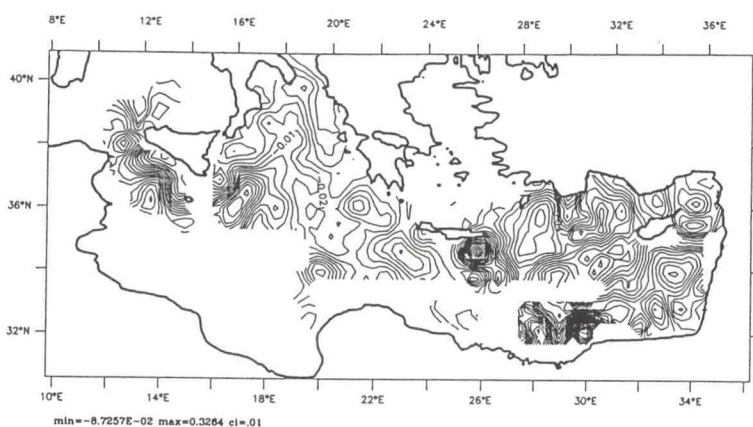
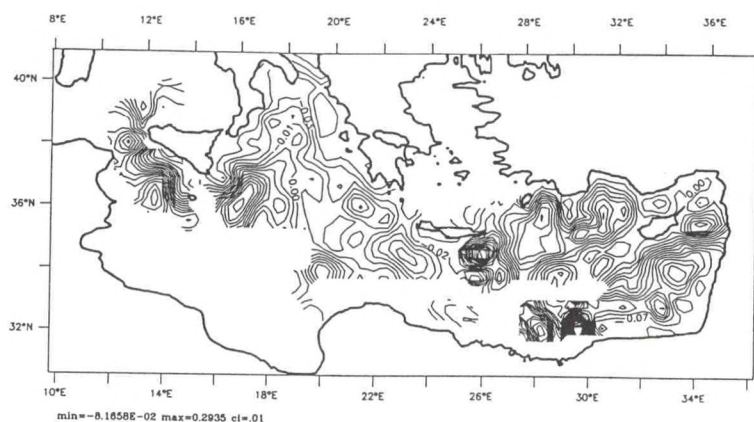


Figure 7a



## Plate 1

### Plate 1.

Figure 3. a) Station locations for POEM AS 87 indicated by O (deeper than 450 m and shallower than 800 m) and □ (deeper than 800 m), near coastal profiles used in the selection of the boundary profile ● or ■, the selected profile for the coastal constraint ● or ■, and the positions of inserted boundary profiles X.

Figure 4. a) Dynamic height anomaly (dm) for 30/450 (db) for AS 87 with no coastal boundary profiles.

Figure 7. a) Dynamic height anomaly (dm) for 30/450 (db) for AS 87 with coastal constraint.



Figure 4

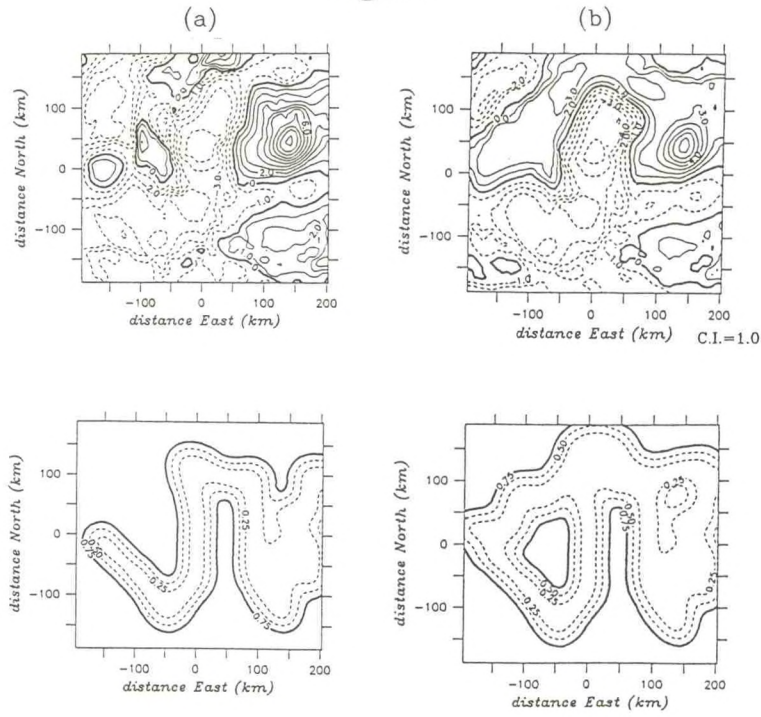


Figure 7

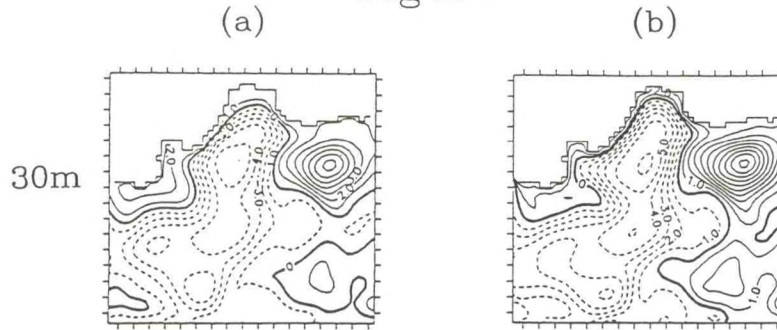


Plate 2.

Plate 2

Figure 4. a), b) Objective analysis comparisons and expected error maps at 30 m for the Rhodes Gyre region mesoscale data, with and without inserted boundary profiles. The objective analysis procedure creates regularly gridded fields from dynamic height anomaly information derived from the hydrographic observations. The expected error map indicates the increase in uncertainty in the analyzed field with distance from an observation point. The error maps reflect the cruise track and the position of the inserted coastal boundary profiles: (a) without inserted coastal boundary profiles, the conventional case; and (b) with inserted coastal boundary profiles, the coastally constrained case.

Figure 7. a), b) Run matrix comparisons at 10d for initial condition and topography parameterization variations in the QG model simulation runs. Streamfunction fields at 30 m for: (a) the central run (coastally constrained initial condition, full topography parameterization); and (b) the conventional initial condition over full topography.

# OPERATIONAL REAL-TIME OBSERVING AND DATA SYSTEMS

Henry R. Frey  
NOAA/National Ocean Service  
6010 Executive Building  
Rockville, MD 20852

## Introduction

There is a growing national need for operational, real-time, physical oceanographic observing and data systems, and a growing technological capability to satisfy that need. This state of affairs, together with the present advanced state of numerical modeling and supercomputers, makes it possible to provide the nation with the higher level of information needed to meet the ever-challenging requirements of users and managers of our coastal ocean.

The boundaries of the coastal ocean are considered in this review paper to be from the tidal mark of rivers that flow into the nation's estuaries to the outer edge of the Exclusive Economic Zone (EEZ). The author believes that this definition of the coastal ocean should be adopted universally.

The operational, real-time oceanographic data required include water level, gravity waves, sea swell, storm surge, tsunamis, sea surface currents, currents in the water column, sea surface temperature, and water column temperature and conductivity. The relevant meteorological data required include wind profiles, surface air temperature, dew point, surface wind stress, and atmospheric pressure at the sea surface.

'Operational', in the context of this review, means simply that data are intended to be applied to decision making for practical purposes--e.g., safe and cost-effective navigation, response to oil and hazardous material spills, and evacuation of coastal areas and offshore structures prior to storms. Real-time data that are sometimes obtained in oceanographic research projects to ensure maximum data return are not considered here to be operational.

'Real-time', in the context of this review, means that data are available for applications with a minimum lag time between sensing over averaging intervals and dissemination. Intermediate steps include processing, quality control, and transmission. The lag time varies for different parameters, of the order of from several minutes to half a day, depending in part on the type of transmission, i.e., hardwire, telephone link, ground wave or sky wave radio telemetry, or satellite telemetry. Lag time may also be affected by the extent of quality assurance imposed on the data prior to dissemination.

This review is based on information received prior to the October/November 1989 Coastal Ocean Prediction System(s) (COPS) workshop from experts who were solicited by the workshop organizers. It is a best effort to summarize the state



of unclassified, operational, real-time observing and data systems and, as such, omits some systems. The author and the convener recognize this limitation. The information summarized in this review paper was provided by Steven Rich, National Oceanic and Atmospheric Administration (NOAA)/National Weather Service (NWS); Glenn Hamilton, NOAA/NWS/National Data Buoy Center (NDBC); Jamie Hawkins, NOAA/National Environmental Satellite, Data and Information Service (NESDIS); Jack Fancher, Bill Woodward, and Rich Barazotto, NOAA/National Ocean Service (NOS); and David McGehee, U.S. Army Corps of Engineers/Coastal Environmental Research Center (CERC).

### **New Generation Water Level Measurement System**

NOS is presently replacing the traditional National Water Level Observation Network (NWLON) with the New Generation Water Level Measuring System (NGWLMS). The old float/stilling well/punched paper tape tide gages are being replaced with new Data Collection Platforms (DCPs). The NWLON consists of about 200 permanent stations along the coast of every coastal state, including those states with Great Lakes coastline, and in the Trust Territory of the Pacific islands. Most of the station locations are in estuaries and bays where the tides are affected by basin configurations, with only about 22 stations along the open coast. In addition, there are from 100 to 150 temporary stations each year. The NGWLMS consists of DCPs, a Data Processing and Analysis Subsystem (DPAS), and a Data Communication System (DCS).

Each DCP has an acoustic sensor that measures water level fluctuations, a backup pressure gage, water temperature sensor, a telephone link, and a Geostationary Operational Environmental Satellite (GOES) uplink. It is also able to measure several optional variables including wind velocity, barometric pressure, current velocity, and water density. Satellite transmission occurs every three hours via GOES to NESDIS, and then to NOS headquarters in Rockville, Maryland. At stations where telephone service is available, the DCP can be interrogated by phone. Servicing personnel can also access the DCP using laptop computers. An alternative transmission mode is VHF radio.

The Data Processing and Analysis Subsystem (DPAS) is a relational software-based database management system. The DPAS receives, verifies, performs quality control checks on, analyzes, and stores the data. Access to the DPAS is through the Data Communication System (DCS) or via the Public Switched Telephone Network (PSTN) and modems connected to the DCS.

Data from the NGWLMS can be obtained by mail in the traditional manner, by Public Switched Telephone Network (PSTN) and modem connection to the DCS (with a three-hour delay), and, for those who demonstrate a critical need that is acknowledged in a specific formal written agreement with NOS, in near-real-time through telephone link to certain DCPs.



## Physical Oceanographic Real-Time Systems

NOS will install the nation's first fully integrated physical oceanographic real-time system (PORTS) in Tampa Bay during FY 1990 and FY 1991. PORTS will include real-time current, water level, and meteorological data at multiple locations. NOS and others have implemented real-time water level systems before, but the Tampa Bay PORTS is the first to include currents, water level, meteorological data, and a fully integrated data delivery system. Requirements for real-time currents were established for three locations where currents are particularly complex and are either exceedingly difficult to predict or are unpredictable. Real-time water level will be provided at the three major ports in Tampa Bay; wind-induced set up or set down of water level affects both the safety and economy of vessel operations. A centralized data acquisition system (DAS), at the U.S. Coast Guard Base, St. Petersburg, will feed the quality assured data to the information dissemination system (IDS), which users will access with PC-compatible microcomputers. Radio communications will be used by dispatchers to relay information to ships' pilots from a presentation display. IDS data will be available as voice messages, text messages, graphics, and data files. When the Tampa Bay PORTS is fully operational, ongoing maintenance and operation will be carried out by the State of Florida.

The Tampa Bay PORTS is the first in a national network of PORTS. The House Committee on Merchant Marine and Fisheries introduced FY 1991 mark-up NOAA funding for the second PORTS in Galveston Bay and the Houston Ship Channel. Through the concept of federal-state partnerships, it is believed that other estuaries will emulate the Tampa Bay PORTS, particularly when statistics on economic benefits are compiled and reported. The future network that is envisioned will provide operational, real-time data along the inner edge of the EEZ and, eventually, a long-term data set for enhanced understanding of estuary-shelf interaction.

## Shipboard Environmental Data Acquisition System

The Volunteer Observing Ships (VOS) Program is a partnership of NOAA, the Navy, universities, and the maritime industry. The maritime industry provides the platforms and personnel; the government provides equipment, logistics support, and training. All of NOAA's main line components are involved, with universities contributing to the NOAA/Office of Oceanic and Atmospheric Research (OAR). Other federal agencies include the U.S. Navy, U.S. Coast Guard, Environmental Protection Agency, and U.S. Geological Survey. The U.S. VOS Program includes about 1,650 ships, 85 percent of which are coordinated by NWS. The worldwide VOS Program includes about 7,000 ships from 47 countries.

NWS has Port Meteorological Officers in major U.S. ports to recruit and interact with its 1,400 participating ships, install and calibrate instruments, and train ships' officers to observe and record data. The Navy has about 90 ships with support personnel stationed at Guam, Japan, the Philippines, and



Spain. The NOS element has about 120 ships equipped with Shipboard Environmental (data) Acquisition Systems (SEAS). SEAS automatically checks and formats data, and transmits the data via GOES to NESDIS; the data are then passed from NESDIS to NWS. All U.S. VOS Program data are transmitted to the National Meteorological Center, Fleet Numerical Oceanography Center, National Climatic Center, and National Oceanographic Data Center. Training and retraining of rotating ships' personnel are important to success. Participating ships are required to monitor their systems and correct any transmitter problems within 24 hours.

### Moored and Fixed Data Acquisition Systems

NDBC operates and maintains a network of about 100 moored and fixed data acquisition systems from coastal areas to the deep ocean. About 20 moored buoys are more than 150 km offshore, where COPS-related interest would be mostly in the influence of ocean dynamics on coastal ocean dynamics, particularly to detect storms and provide input for weather prediction. Another 35 buoys are deployed in the coastal ocean and the Great Lakes. Typical measurements include average and gust wind speed, wind direction, air and surface water temperature, barometric pressure, significant wave height, wave period, and nondirectional wave spectra. Some buoys are also equipped to measure solar radiation, relative humidity, and directional waves. All buoys have redundant wind and barometric pressure sensors.

NDBC's Coastal-Marine Automated Network (C-MAN) includes six of the aforementioned moored buoys, in addition to fixed stations on offshore platforms, lighthouses, beach areas, and fishing piers. All C-MAN stations have redundant wind sensors. The C-MAN stations measure average and gust wind speed, wind direction, barometric pressure and air temperature. Certain stations measure some of the same parameters measured by the offshore buoys.

Both buoy and C-MAN data are transmitted to NESDIS via GOES (both East and West GOES) uplink and downlink. The data are processed by the NWS Telecommunications Gateway, where gross error checks are done and the data are encoded into World Meteorological Organization message formats. NDBC performs further quality control, and forwards validated data on a monthly basis to the National Climatic Data Center (NCDC) and the National Oceanographic Data Center (NODC). The spectral wave data are available only from NODC.

U.S. Army Corps of Engineers (COE)/CERC manages a network of about 35 nearshore wave gages around the U.S. coastline, including Alaska and Hawaii. The network is comprised of (1) nondirectional, bottom-mounted, pressure-type wave gages, (2) directional arrays of bottom-mounted pressure sensors, and (3) directional gages using pressure sensors and electromagnetic current meters in combination. The network obtains data in real-time, but it is not an operational system in that the data are not available online. Data from this network are used to develop wave climate statistics and hindcasts. Monthly and annual data



reports are produced, and a central data archive using compact disc-read only memory (CD-ROM) is under development. For further detail, see McGehee (this volume).

## Satellite Data

NOAA's advanced Tiros-N polar orbiting satellites have meteorological observations as their first, but not exclusive, objective. Management of this program is in NOAA's National Environmental Satellite and Data Information Service. Of particular interest in the COPS context is the multichannel advanced very high resolution radiometer (AVHRR) which detects radiation in the visible, near-infrared, and thermal infrared portions of the spectrum at optical ground resolutions of 1 km and 4 km.

Multispectral image analysis allows precise estimates of cloud cover and other atmospheric variables, as well as hydrological and ocean variables, to be made. Sea surface temperature (SST) analyses are derived from the AVHRR data. Global imagery data are processed on board the satellite to 4km resolution and stored on tape recorders. The 1km high resolution imagery data are recorded on selected portions (no more than one-tenth) of the orbit. These recorded data are read out at the Command and Data Acquisition (CDA) stations at Wallops Island, Virginia and Gilmore Creek, Alaska. Automatic picture transmissions of visible and IR imagery are broadcast continuously worldwide.

Products include 100km global SST analysis, 50km regional SST analysis, 14km regional SST analysis, and monthly mean SST analysis. Hand drawn products include SST thermal analysis of the Great Lakes, Bering Sea, Gulf of Alaska, West Coast, Gulf of Mexico, Northwest Atlantic, as well as water mass analysis of the Gulf Stream, Western Atlantic, and Gulf of Mexico that depicts thermal fronts and eddies. Comparisons between SST computed with AVHRR data and drifting buoy SST measurements indicate rms. errors in the range 0.4 to 0.8 Centigrade degrees.

## Weather Systems

NWS, working jointly with other federal agencies, is implementing three major programs that will improve the measurement and reporting of weather systems, including in the coastal ocean. These programs are (1) Automatic Surface Observing System (ASOS), (2) Next Generation Weather Radar (NEXRAD), and (3) Advanced Weather Interactive Processing System (AWIPS).

ASOS can provide nearly continuous information on barometric pressure, temperature, wind speed and direction, cloud coverage and heights, and precipitation types and amounts. Implementation of ASOS begins in CY 1990 and is expected to be complete in CY 1995, at which time about 1,000 systems will be in place. Three-fourths of these are to be acquired by the Federal Aviation Administration (FAA). NWS plans to acquire about 250 systems, and the U.S. Navy



plans to acquire about 85 systems. While most of these systems will be in the nation's interior, the number and location of near-coastal systems will provide more than adequate coverage for application to coastal ocean predictions. ASOS will be networked, and the data will be available to external users.

NEXRAD has the potential to be a tremendous advancement in meteorological data for improved coastal ocean predictions. The first system was installed in Kansas during FY 1990; completion of the NEXRAD installation is planned for FY 1994. NEXRAD uses Doppler radar plus conventional reflectivity measurement for continuous scanning of the atmosphere, calculations of severe weather speed and direction, precipitation measurements, and (in the nation's interior) early detection of tornadic precursors. It will be acquired through a Joint Systems Program Office sponsored by the Departments of Commerce, Transportation/FAA, and Department of Defense (DOD). The plan is for NWS to operate 121 systems, and FAA and DOD to operate 39 systems. NEXRAD data will be available to external users. Of particular interest to operational coastal ocean predictions is that NEXRAD will provide remotely sensed vertical profiles of winds over the coastal ocean.

AWIPS will collect and integrate high-resolution data from observing systems, centrally collected data, and centrally prepared National Meteorological Center (NMC) analyses and guidance products. It will provide capabilities for rapid analysis, display, data access and manipulation, decision assistance, and warning and forecast product preparation and dissemination. AWIPS will provide communication support for the distribution of centrally collected data, centrally prepared analyses and guidance products, and satellite imagery and soundings. Observations and data will include NEXRAD, upper air soundings, GOES, hydrology, ASOS, and local networks. Information products and services will support the media and the general public, cooperating agencies, and the private sector. AWIPS is in development, and deployment is scheduled to begin in FY 1992 and be completed in FY 1995.

## Outlook

The convergence of three major components required for an effective COPS appears to be happening. First, justification for such a resource-intensive program needs to be established based on demonstrated user needs; this is happening piecemeal, but it is incomplete. Funding of the order needed for COPS will require clear and convincing justification. Second, predictive models must move from research and development to online operational groups, and the computer resources must be available. The present consensus is that real-time operational models are within reach. Third, adequate data must be available to calibrate, drive, and validate the predictive models. The present availability of real-time operational data, together with existing systems that can be upgraded to the real-time measurement mode and the new systems planned to come on line in the next 10 years or so, promise to answer the need for real-time COPS data.



# DATA ARCHIVING FOR THE COASTAL OCEAN

H. James Herring  
Dynalysis of Princeton  
219 Wall Street  
Princeton, NJ 08540-1512

During the past few years, data in the field of geophysical fluid dynamics have become available at an ever accelerating rate, and the demands placed on that data have similarly increased. This attention has resulted in significant advances in data archives and archiving techniques. These improvements are described in documents from various organizations (World Meteorological Organization (WMO), 1986; Institute for Naval Oceanography (INO), 1987; and National Oceanic and Atmospheric Administration (NOAA), 1989). What follows is, from the perspective of application to coastal ocean prediction, a digest of this material, the communications of the invited authors, and personal experience.

To date the predominant emphases have been on archived data bases that are global in scale. Although plans and specifications for global applications are thought-provoking, not all are directly applicable in coastal research. Spatial scales on the shelf are much smaller than ocean scales but, perhaps more importantly, vary widely as a function of location, decreasing rapidly close to shore. Temporal scales are also much shorter as a result of coastal influences such as the land-sea breeze, tides and coastal-trapped waves. Therefore the archiving scales appropriate for the deep ocean are much too large for coastal purposes. On the positive side, higher resolution is frequently possible on the shelf and nearshore since the data density is much larger as a consequence of relative accessibility, greater interest and more ship traffic. The objective of this discussion is to offer a brief catalog of desirable features for data archives that are oriented towards research in coastal oceanography.

As a starting point, it is valuable to review the role of the large archived data set in a coastal ocean prediction system, since by definition the prediction relates to future conditions, whereas the archived data is at best a record of recent history. Actually, archived data are essential for a coastal ocean prediction system for the following reasons:

- Existing conditions, i.e., scales of variability, will aid in choosing model scales and domain.
- Historic data are necessary for model forcing and skill assessment.
- Archived data provide comprehensive initial conditions for forecasts.
- Climatological data are needed to augment real-time boundary conditions.



Observational data will always be the grist for the modeling mill, but regrettably it is likely that there will never be enough to fulfill the needs of the modeler.

Since the development time for the Coastal Ocean Prediction System (COPS) has been designated as of the order of a decade, it is relevant to estimate the computer storage capability that will be available for archiving at that time. Product development being an uneven process, there is often a large lag between announcement of new technology and common usage. The capacity of a single mass storage unit that has been readily available to a research scientist has been graphed as a function of time over the second half of this century (Fig. 1). Extrapolating the trend of an order of magnitude increase every decade, the storage unit available at the turn of the millennium would hold about 10 gigabytes. Using an efficient format, this single storage unit could easily hold all of the oceanographic data presently archived, excluding satellite imagery.

The challenge is to design an archiving system and operating procedure which will make optimum use of this storage capability, and the associated increases in computing power, to provide the quantitative information necessary to support a research effort such as COPS. This question may be addressed by considering the series of tasks that cover all aspects of the data management process from sensor to user. These tasks, which determine all data characteristics including accuracy, reliability, latency, quantity, provenance, quality, resolution, relevance and accessibility, are discussed in the following sections.

### Collection and Acquisition

One of the lessons learned from recent observational studies is the overriding importance of transmitting data immediately to the principal investigators for review and assessment. This innovation, made possible in part by the development of satellite transponders, has changed the pattern of observational work, since it is no longer necessary to wait months to discover equipment loss or malfunction. Perhaps more important in the long run, however, is that the results are now available in near real-time. The conclusions are:

- Reduce human errors through automated data collection in digital format.
- Transmit results frequently to central recording station.
- Monitor data continually for errors, noise or holidays.
- Incorporate results in data base immediately upon receipt.

Ultimately, there should be no distinction between archived and real-time data, since the data acquisition and processing will be completely automated. In that perfect world, real-time data will simply be the most recent addition to the archive.

## Processing and Quality Control

The objectives of this task are to eliminate as many errors from the data as possible and to prevent new errors from entering the data stream due to the human element. Once a clear standard has been set, the identification of erroneous data can be accomplished most reliably using the existing data archive for comparison. The elements of this task are:

- Use only calibrated instruments with known uncertainty.
- Establish well defined and recognized criteria for data quality.
- Verify data representativeness in the climatological context.
- Evaluate data veracity through spatial and temporal consistency.

Evidently, the quality control procedure should insure that the veracity and representativeness comparisons are performed automatically in the data processing step, and that only when the data fall outside the acceptable range are they flagged for human intervention.

## Reduction and Analysis

A certain degree of standardization is highly desirable for the efficient and convenient use of data archives. Data that have been reduced and analyzed using the same techniques are more directly comparable. Since coastal scales vary with location, a consensus grid should be designed and used consistently to archive the data. These goals can be achieved as follows:

- Develop and disseminate standard reduction and analysis software.
- Establish a standard grid appropriate for each class of data.
- Prepare analysis of each data type on its standard grid.
- Distill data to produce standard products of scientific interest.

In addition to the gridded data, a well recognized set of common data properties is very useful in comprehending and taking the measure of a large data set. To the extent that these properties are universal, it would be most efficient to have them available to the user without the necessity of recalculating them.

## Fulfillment and Enhancement

Again, the data archives may be employed to extract more information from a new data set than it has at face value. By using relationships such as temperature-salinity diagrams and empirical orthogonal functions, it is possible to deduce missing or additional information. The specific steps are:

- Fill data holidays using dynamically consistent techniques.
- Estimate coherent properties from similarity considerations.



- Infer spatially or temporally correlated functions from subsamples.
- Calculate physically related properties from governing equations.

In addition to direct application of the archived data in the form of correlations, the suite of data in the archive can also be used as input to an analytic or numerical model to calculate additional dependent variables. In fact, very large archives of these derivative or computational data sets have been maintained for some time and have proven extremely useful as auxiliary data sets for model boundary conditions and further analysis.

### **Cataloging and Archiving**

For a user to access the archives efficiently, a catalog of data specifications must be provided. The catalog might contain several levels of specificity, beginning with basics such as location and extent in time and space and including more details such as statistical properties. The provenance would also be included in the catalog entries. The catalog would be structured to facilitate relational data searches. To a certain extent, the information in the catalog itself would represent data, since the aggregate of all catalog entries would summarize the characteristics of the data archive. The salient points in this task are:

- Maintain documentary files to facilitate retrieval based on criteria.
- Include pedigree of processing and enhancement for reference.
- Provide flexible header-controlled archive format for future growth.
- Compress data in a format usable on both mainframes and work stations.

The data itself would be archived in a packed format to conserve storage without loss of accuracy. Experience has shown that the choice of packed format should be independent of computer hardware and software and designed to accommodate new data types gracefully in a backward-compatible manner.

### **Distribution and Display**

Designation of a single user port for all ocean-related data would aid in the standardization of data format and products. A single source would also eliminate the curse of duplicate data as a result of accessing multiple data sources. The physical location where each archive is stored is actually irrelevant so long as a single entity oversees and controls the user port. Optimum user access can be provided as follows:

- Offer access to all data through one port regardless of repository.

- Display temporal and spatial relationships between data locations.
- Develop graphical interfaces for browsing through data fields.
- Synthesize multiple data sets with simultaneous graphical display.

Graphics should play an important role in the selection and comprehension of the archived data. The process would begin with interrogation of the catalog, resulting in a display of the locations of complementary data sets. Next, the data of interest could be displayed in a convenient serial manner to facilitate identification of salient features. Finally, complementary data sets could be displayed simultaneously in time or space, in order to better visualize their interrelationship.

### Maintenance and Updating

Since the catalog of each data set contains a pedigree, users can judge for themselves which data they will use. Therefore, all data can be available to users immediately upon receipt at the archiving center. Then, as quality control, reduction and analysis proceed, the pedigree of the data set is revised to reflect the upgraded condition. Archive users who examine the data from other perspectives may also identify anomalies and inconsistencies that slipped through the original processing specifications, and which are worthy of note in the pedigree. The task of providing continuing service includes the following items:

- Provide immediate access by user public to newly archived data.
- Encourage and facilitate data quality assessment by users.
- Maintain archive as a compendium plus updates to the compendium.
- Make compendium available on storage medium with updates by wire.

Even over high-speed lines, the transmission time for a large data set is not negligible. Therefore, the optimum utilization of resources is achieved if the user possesses the background compendium of the archive recorded on some mass storage device, and augments his holdings periodically with a relatively small quantity of updates over the communication net.

In addition to the specific data management tasks considered above, there is a larger issue which, although it is not exclusively related to archiving, does have a bearing on data storage. The issue involves the balance of data in the present oceanographic data base. Although an eclectic data base is often useful in understanding existing conditions for descriptive purposes, circulation models require specific quantitative information to provide mathematically complete boundary conditions. At present and at least for the near future, there is a significant imbalance between the data available and that required to operate the present generation of circulation models. The data archives contain vast and rapidly increasing quantities of excellent satellite imagery which, at present, are not being



fully utilized in numerical modeling. It is imperative that the modeling community develop methods of using this data to mitigate the paucity of other essential data.

## **Conclusions And Recommendations**

Archived data represent an essential resource in the development and operation of a coastal ocean model. Also important is that the results from coastal ocean simulations be archived for future reference and analysis. In the preparation of the archives, the primary objectives are to:

- Assure high standards of data accuracy, quality and representativeness.
- Reduce duplication of effort in software development and data analysis.
- Maximize the efficiency of data base storage and processing.
- Facilitate dissemination and utilization of archived ocean data.

The steps described under each of the data management tasks are designed to insure that both observational and computational archives meet these objectives.

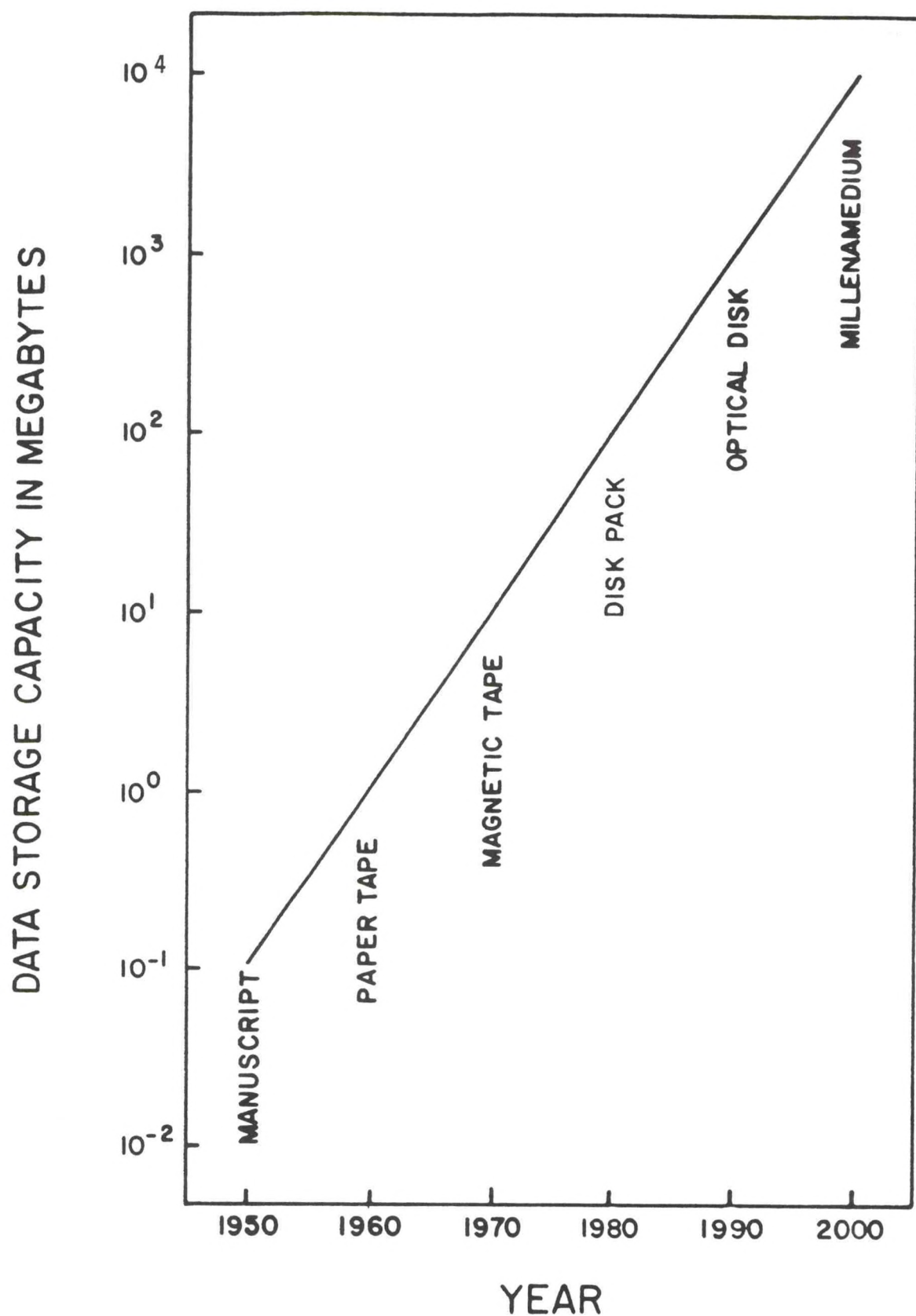


Figure 1. Schematic of the capacity of a single mass storage unit commonly available to a research scientist during the second half of the twentieth century.



# **A NOTE ON THE AVAILABILITY OF HISTORICAL COASTAL OCEANOGRAPHIC DATA**

**Sydney I. Levitus  
National Oceanographic Data Center, NOAA  
Washington, DC 20235**

**Ron E. Moffat  
World Data Center-A for Oceanography  
Washington, DC 20235**

## **Introduction**

For the purpose of studying the coastal oceans of the world, scientists need to have digital access to as much of the historical oceanographic data base as possible. Figures 1-9 show the distributions of physical oceanographic digital data for U.S. coastal regions available from the National Oceanographic Data Center, Washington, D.C. as of April, 1990. Distributions are shown for the Nansen Cast file, the conductivity-temperature-depth (CTD)/salinity-temperature-depth (STD) file, and the expendable bathythermography file (XBT). A box indicates the location of each data profile. The counts of profiles by region are as follows:

## **CTD/STD**

Atlantic  
Gulf  
Pacific

## **Nansen Cast**

Atlantic  
Gulf  
Pacific

## **XBT**

Atlantic  
Gulf  
Pacific

It is emphasized that substantial amounts of coastal data, particularly estuarine data, have not been archived. (N.B. NODC also holds a significant number of current meter and related data sets from the coastal ocean. These, together with the hydrographic data described here, present an excellent opportunity for the development of higher order data bases.) The past practice of "searching" for needed data (in manuscript form), either at data centers or various research institutions, and then digitizing these data is inefficient. By the time data are ready in digital

form, a project requiring these data for planning may be already underway, or even over. (N.B. In other words, real-time observing systems would add to the timeliness and completeness of the data archives.) At present we are aware that substantial amounts of coastal and near coastal data exist in manuscript form for foreign countries.

The World Data Center-A for Oceanography (WDC-A) is collocated with the National Oceanographic Data Center (NODC) in Washington, D.C. The mission of WDC-A is to exchange oceanographic data between countries. These data are increasingly transmitted in digital form, but over the past thirty years significant amounts of data were exchanged in manuscript form. The following is a brief (not exhaustive) list, based on the largest holdings in the manuscript archive, of some data archived at WDC-A:

1) Japanese Fisheries Publications Hydrographic Data

Period of observation:	1963-1984
Approximate number of profiles:	250,000
Location:	Mainly coastal regions off Japan

2) Japanese Digital Bathythermograph Data

Period of observation:	1963-1984
Approximate number of profiles:	250,000
Location:	Mainly coastal regions off Japan

3) Korean Hydrographic Data

Period of observation:	1956-1984
Approximate number of profiles:	34,000
Location:	Mainly coastal regions off Korea

4) East German Hydrographic Data

Period of observation:	1956-1974
Approximate number of profiles:	2,000
Location:	Coastal upwelling region off northwest Africa

5) Swedish Coastal Time Series Data

Period of observation:	1950-present
Approximate number of profiles:	10,000
Location:	Swedish Coastal Waters

6) Data From Other Countries (e.g., Columbia, Venezuela, and others)

Location:	Caribbean Sea and Gulf of Mexico
-----------	----------------------------------



## **Status of Digitization Efforts**

A pilot project is beginning at the NODC, Washington, D.C. to determine the feasibility of using optical scanning technology to digitize data in manuscript form. If this technology is suitable, in the sense that low error rates and relatively fast digitization is possible, then as funds become available these data will be digitized. Support from the research community is vital for the success of this effort.

## **Recommendation**

By whatever means, all historical data, whether in manuscript form or digital form, should be digitally archived at the National Oceanographic Data Center, Washington, D.C. Sources that supplied data in manuscript form should be contacted to see if these data are available in digital form, and if so, they should be obtained.

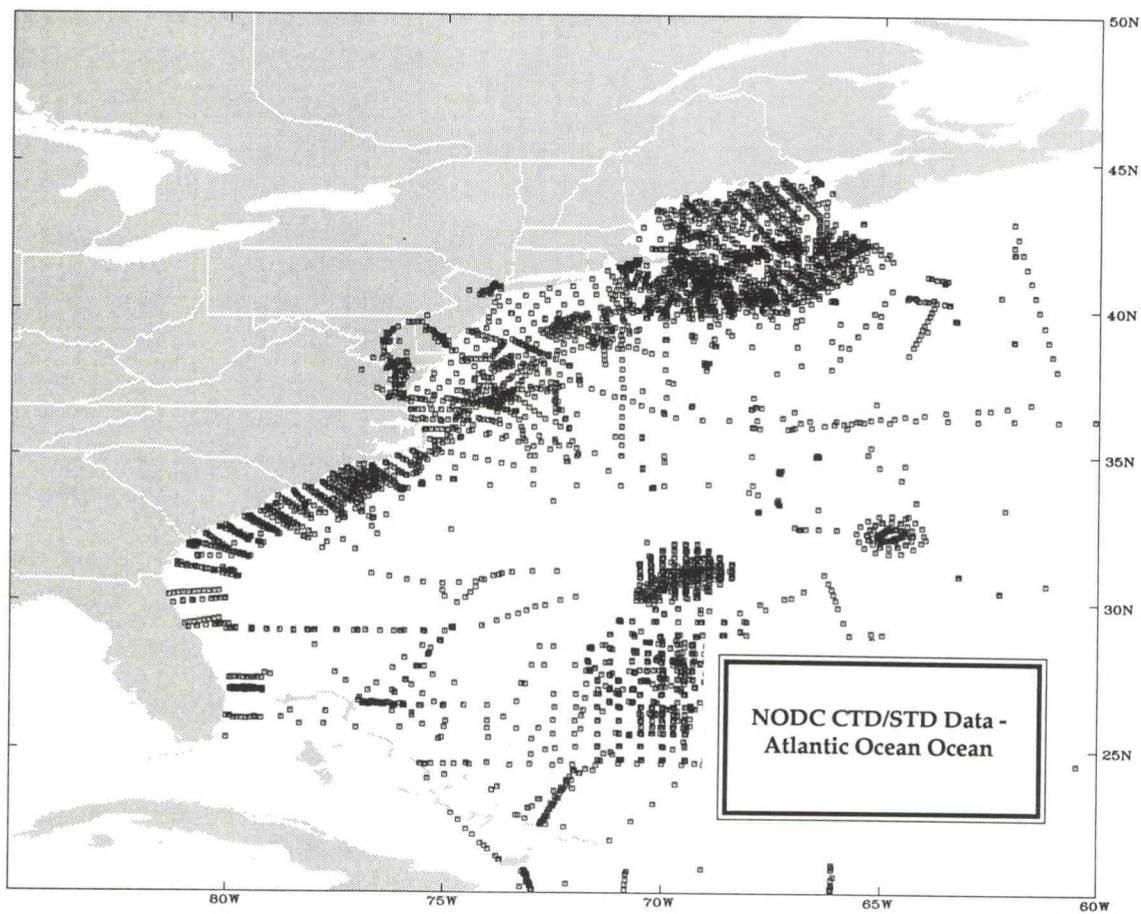


Figure 1.



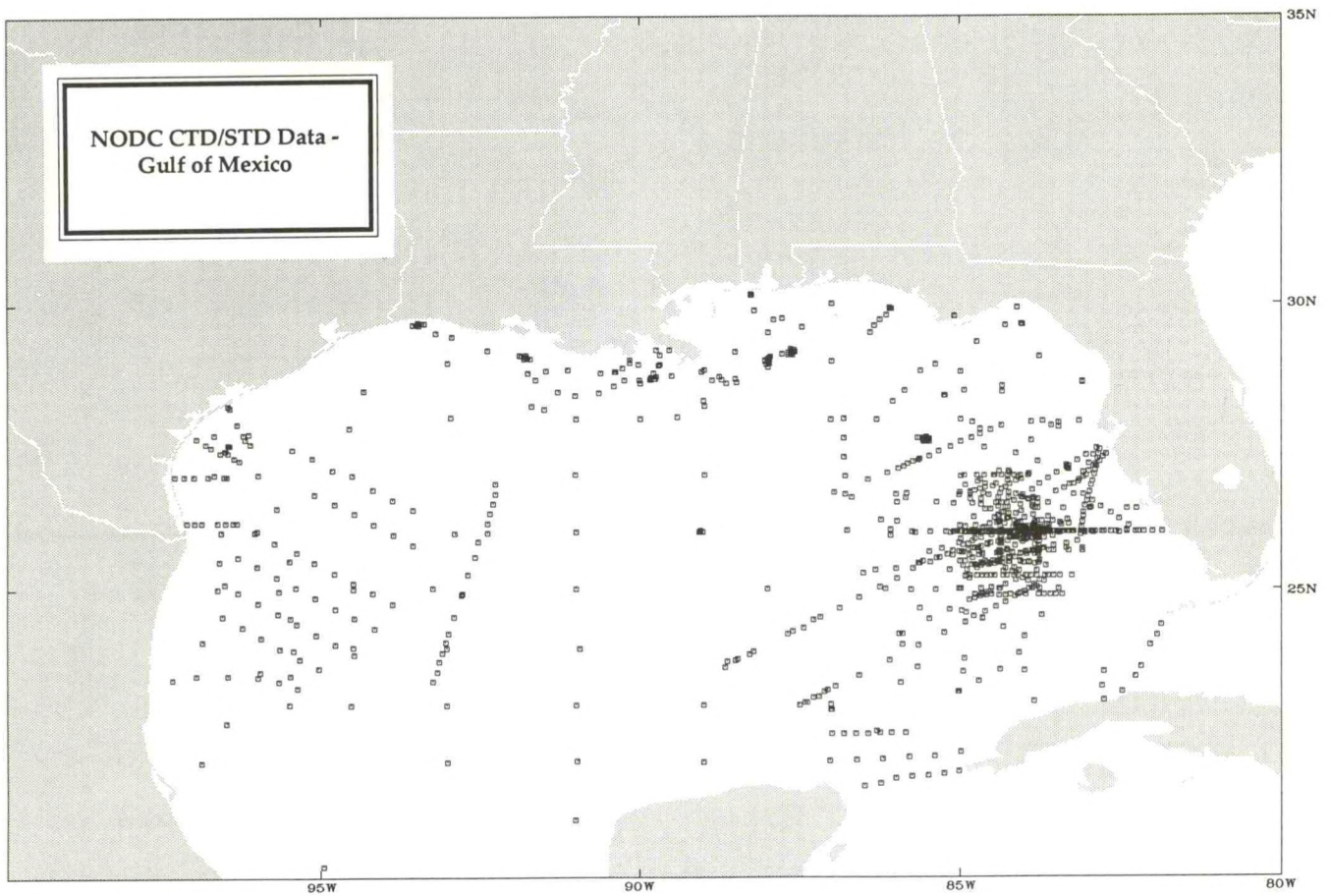


Figure 2.

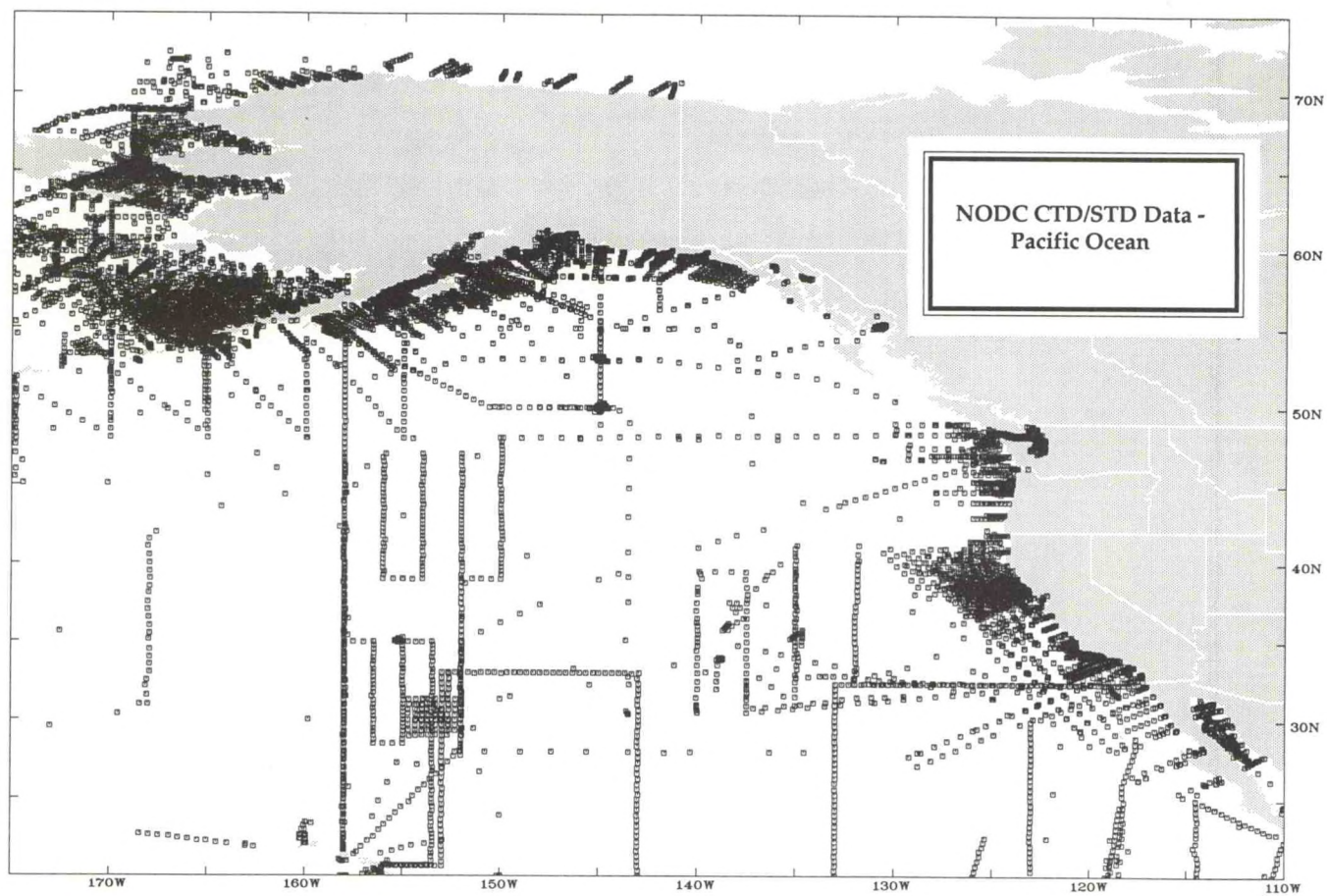


Figure 3.



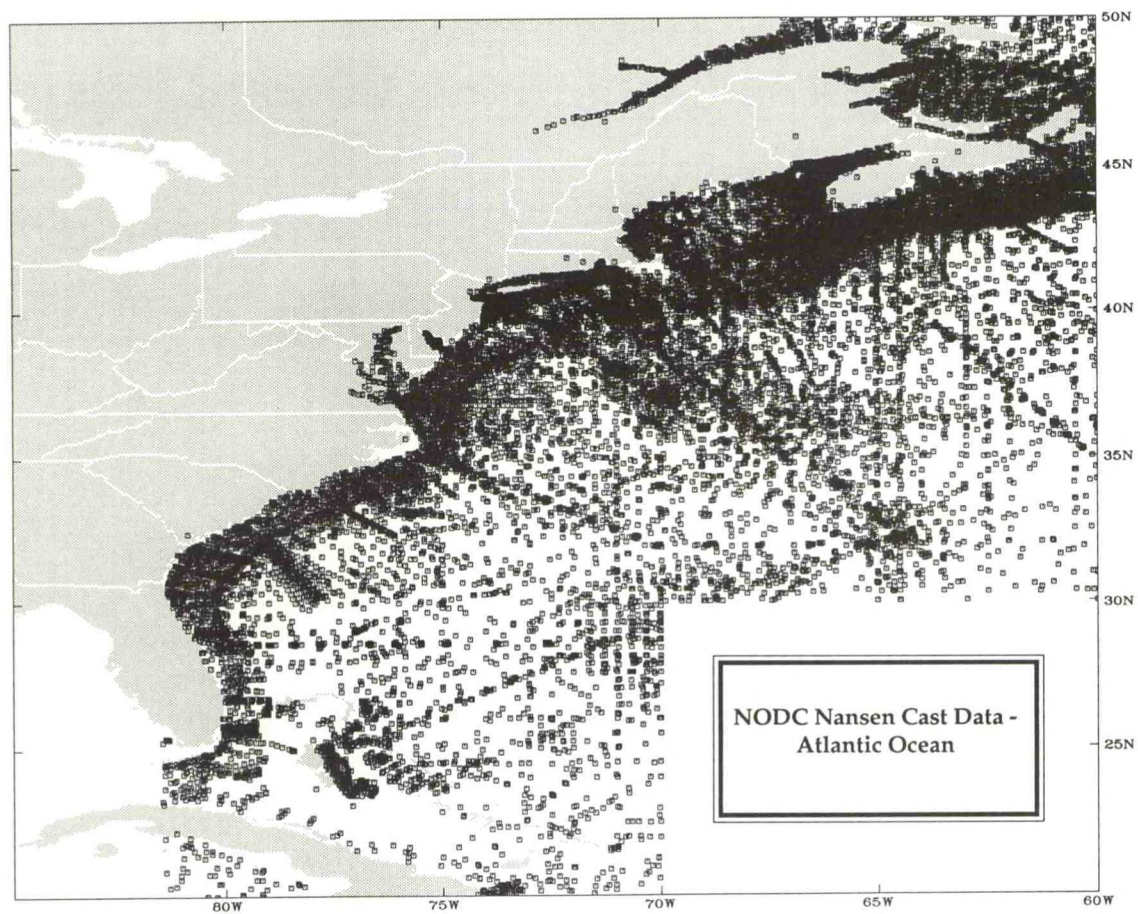


Figure 4.

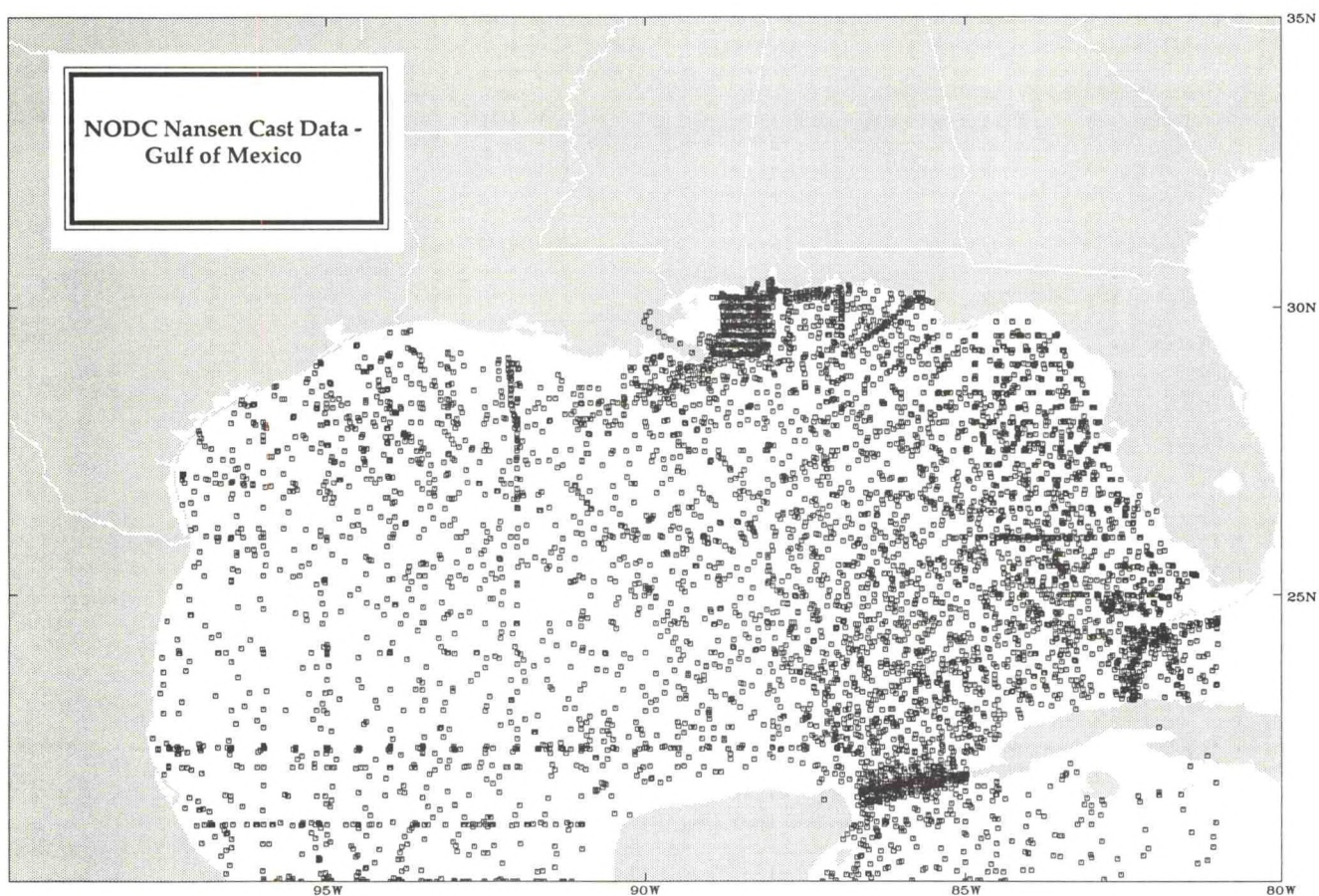


Figure 5.



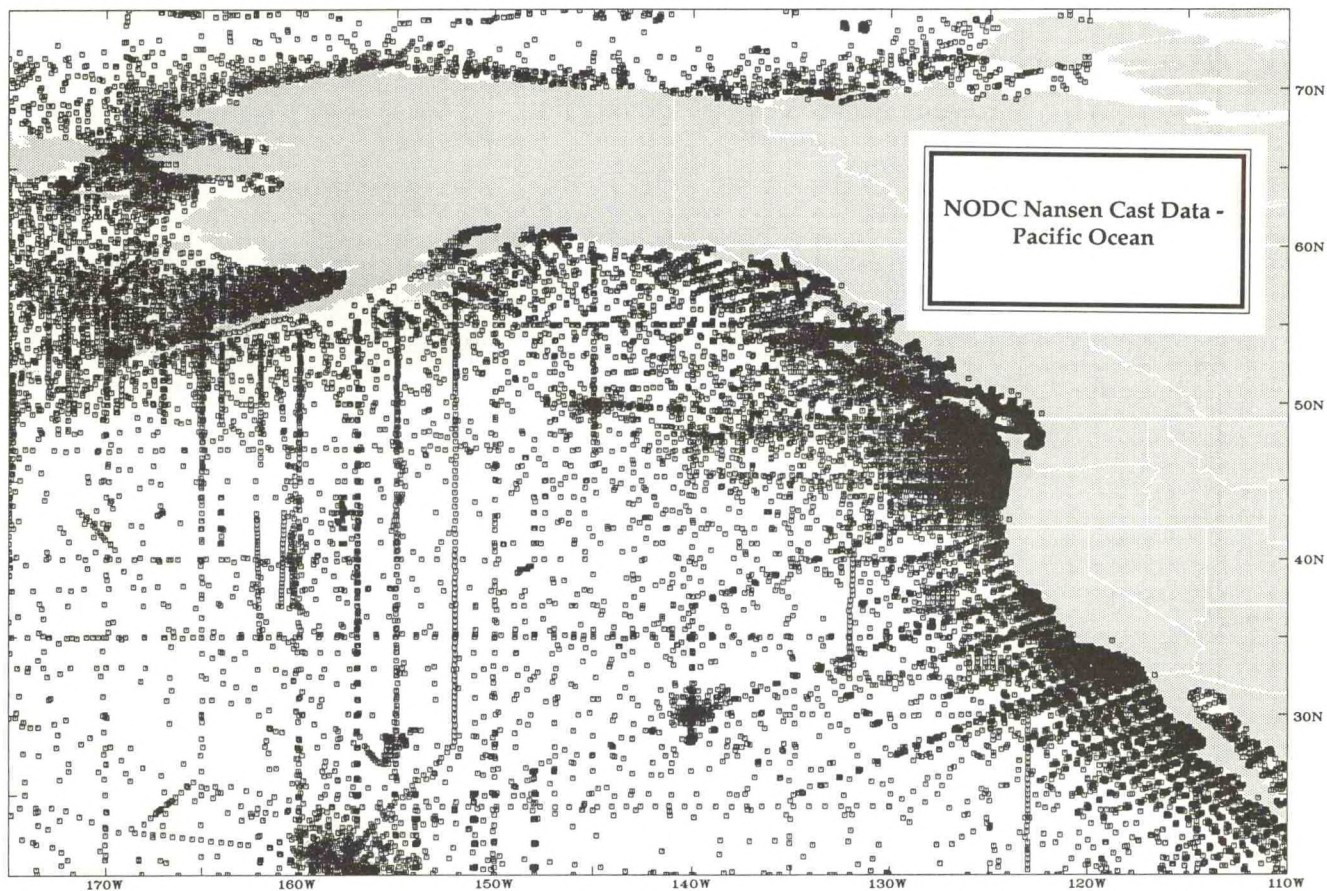


Figure 6.

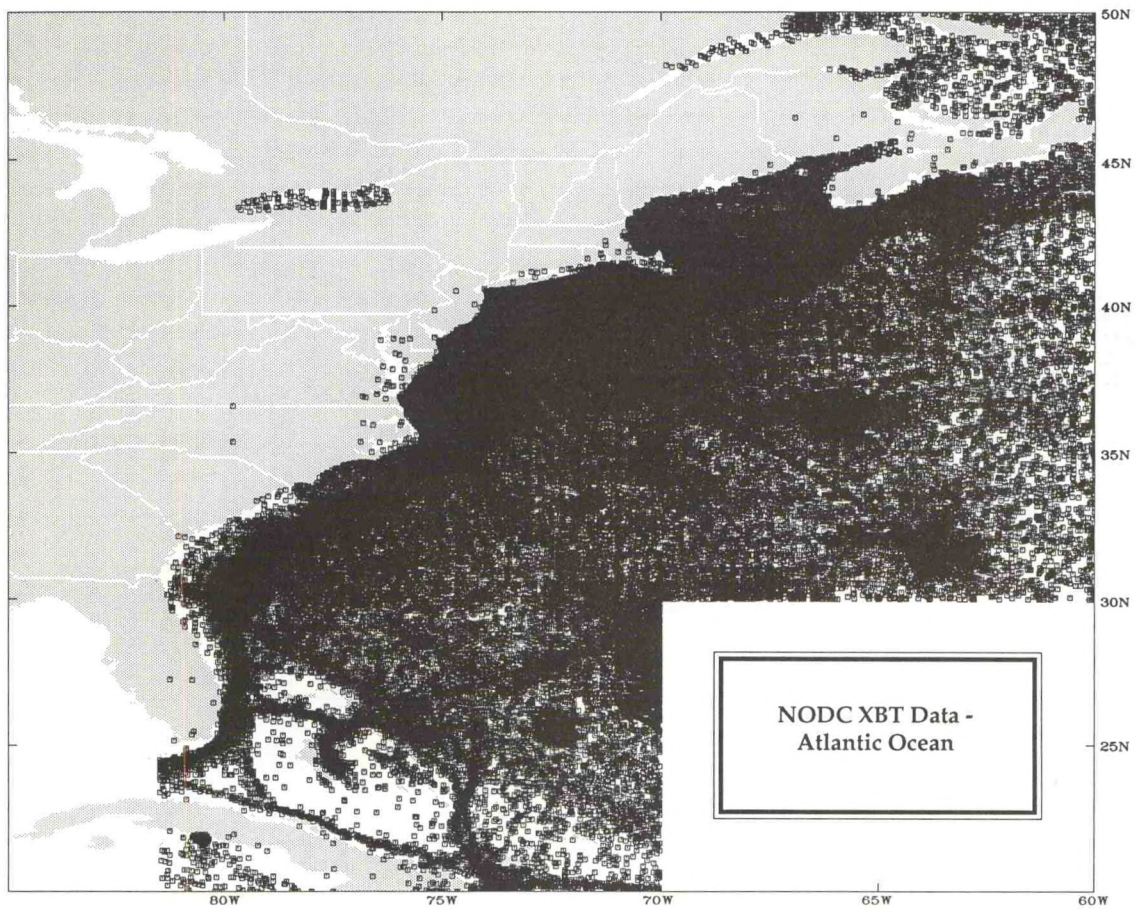


Figure 7.



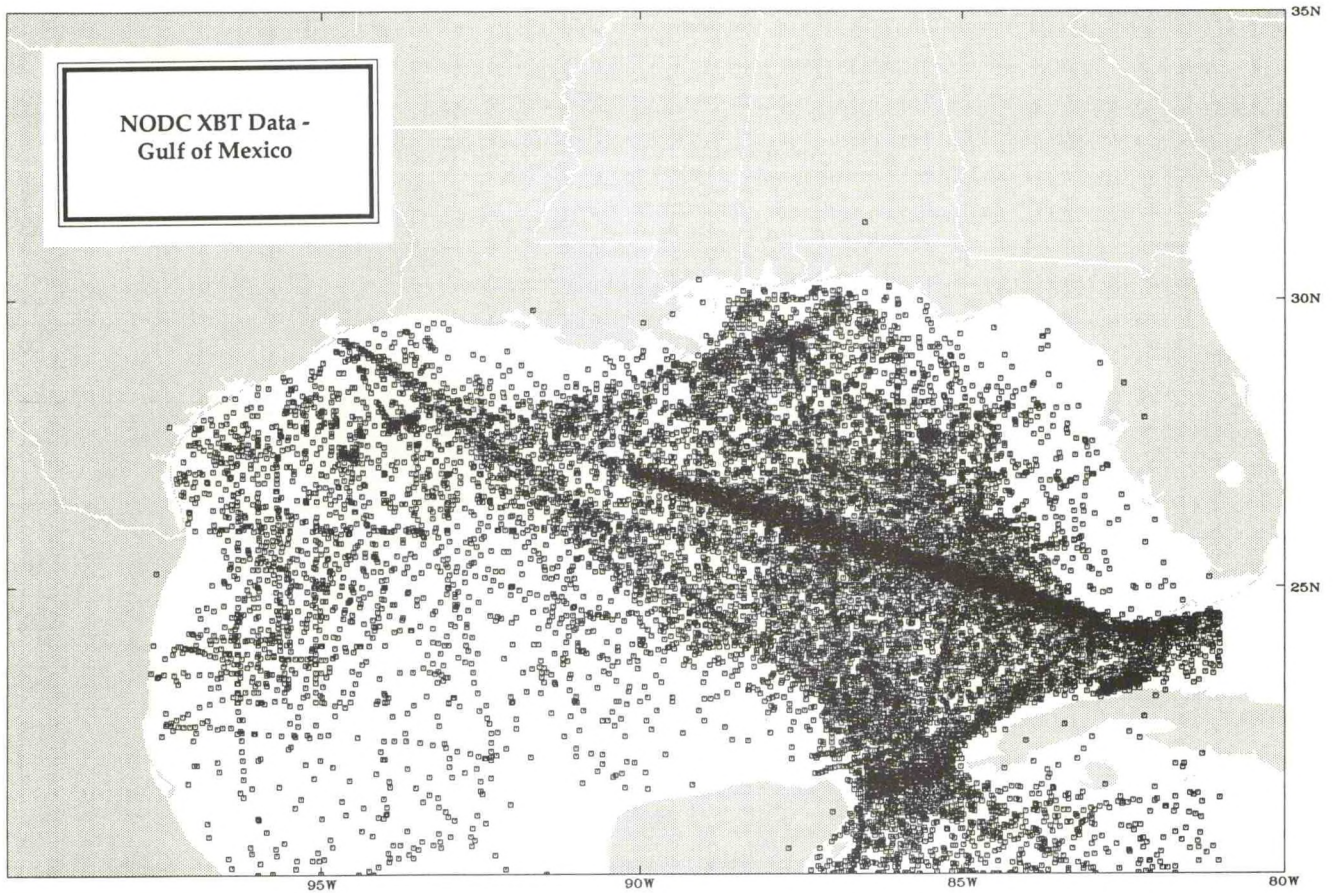


Figure 8.



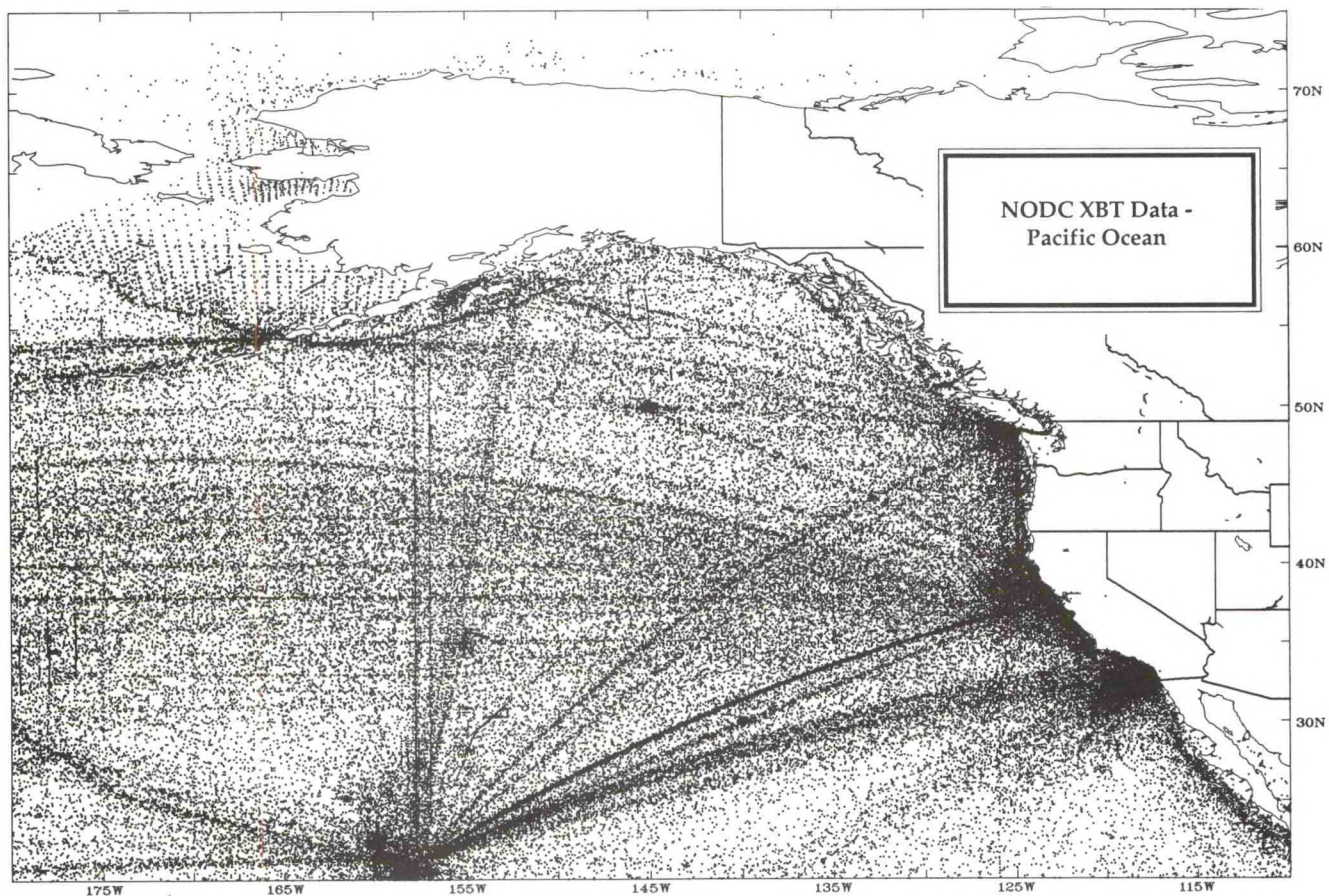


Figure 9.



# EVALUATION OF SURFACE WIND FIELDS OVER THE COASTAL OCEAN OFF THE WESTERN U.S.

P. Ted Strub and Corinne James  
College of Oceanography  
Oregon State University  
Corvallis, OR 97331-5503

## Introduction

This paper presents an evaluation of several of the operational gridded wind fields over the coastal ocean off western North America. These fields provide nearly continuous records of the spatially varying wind for comparison to historical oceanic data. They also provide the surface forcing needed to drive numerical models. For either use, it is important to understand the level of error expected in the fields and in the horizontal gradients of the winds used to calculate fields of wind stress curl.

## Sources of Wind Data

Winds measured at buoys located over the continental shelf and at coastal land stations are available from the National Data Buoy Center (NDBC). Winds reported every six hours by merchant vessels eventually become available as part of the Comprehensive Ocean-Atmosphere Data Set (COADS) at the National Center for Atmospheric Research (NCAR). For periods of a month and greater, the COADS data may be used by themselves to form gridded fields with spatial resolution of  $1^{\circ}$ - $2^{\circ}$ . Such fields have been used to examine the spatial nature of wind stress and wind stress curl (Nelson, 1977; Rienecker and Ehret, 1988) and to drive models of the coastal ocean (Pares-Sierra and O'Brien, 1989). For time scales of less than a month (event time scales), the NDBC buoy winds can be used to calculate wind stress on a linear alongshore grid for comparison to other data or to drive models (Halliwell and Allen, 1987; Denbo and Allen, 1987; Chapman, 1987; Brink, et al., 1987). No useful estimate of the curl can be made from the present arrangement of buoy locations off the west coast of the U.S.

Gridded fields of wind are produced by the Navy's Fleet Numerical Oceanography Center (FNOC) every six hours using measured winds and atmospheric pressure from buoys and merchant vessels (Mendenhall et al., 1977). Grid spacing is approximately 380 km. These winds include a correction for the effect of the atmospheric boundary layer (ABL) using a frictional decrease and rotation factor that depends on the stability of the ABL (Mihok and Kaitala, 1976). The same measured winds and pressures are used by the National Meteorological Center (NMC) to initialize atmospheric forecast models every twelve hours. Although the fields used to initialize the models are not corrected for the influence of the ABL, the forecast models include surface momentum and heat fluxes which retard and rotate the surface layer winds so that the six-hour forecasts compare better to the buoy measurements.



Two forecast models are considered here--the Limited-Area Fine Mesh (LFM) model, with grid spacing of approximately 190 km, and the Nested Grid Model (NGM), which is run on a grid with twice the resolution of the LFM (approximately 95 km) but only archived on the LFM grid. The lowest level of the LFM model is 50 mb thick, and no further modification of the winds is done before archiving. Thus, the LFM winds represent a wind several hundred meters above the surface. The lowest level of the NGM model is 35 mb thick, and a postprocessing step is used to create a "10m" wind product, assuming a neutral surface layer (D. Deaven, J. Hoke, pers. comm.). Winds were screened to eliminate large erroneous values found in some FNOC fields and filtered (half amplitude at 40 hours) to eliminate unrealistic diurnal cycles.

### Comparison of FNOC and LFM Fields

The root mean square (RMS) difference between the FNOC and LFM fields (after interpolating the FNOC fields to the LFM grid) (Fig. 1), calculated from the filtered records over the years 1979-1985, are in the range  $3.5$  to  $4.5 \text{ m s}^{-1}$  over much of the coastal ocean. If the data are further stratified by season, values in the winter reach  $5.5 \text{ m s}^{-1}$  off the northwest coast. Although these values do not indicate whether one or the other of the fields is better, they do show the large degree of uncertainty in the gridded wind fields. If fields of wind stress are calculated from the winds, the equivalent RMS differences are approximately  $0.04$  to  $0.06 \text{ N m}^{-2}$  ( $0.4$  to  $0.6 \text{ dyne cm}^{-2}$ ).

These RMS differences can be caused by differences in either the vector magnitudes or direction. We have quantified these by forming the mean of the absolute magnitude of the instantaneous differences in the speeds (Fig. 1b), and the mean of the absolute magnitude of the difference in directions (Fig. 1c), at each gridpoint. Speeds typically differ by  $2.0$ - $2.4 \text{ m s}^{-1}$  and directions differ by  $40^\circ$ - $70^\circ$ . These differences in direction account for an RMS difference  $2.9$ - $3.8 \text{ m s}^{-1}$ , contributing more to the total RMS difference of  $3.5$ - $4.5 \text{ m s}^{-1}$  than is contributed by differences in magnitude.

These RMS differences represent the magnitude of differences between individual 12-hourly fields, such as might be used for event-scale studies. The average differences calculated over longer periods are smaller in magnitude. The average magnitude of the vector difference between the two fields (Fig. 1d), over the entire seven-year period and the average difference in direction (Fig. 1e), differ systematically by  $1$ - $2 \text{ m s}^{-1}$  in speed (the LFM speeds are greater) and by  $10^\circ$ - $30^\circ$  in direction (the LFM winds are systematically to the left of the FNOC winds). Thus, the difference is consistent with the fact that the LFM winds pertain to greater altitude in the model, with insufficient modification from the boundary layer. Still, the two fields are more similar over the monthly and longer periods typically used in climatological studies.



## Comparison of FNOC and LFM to Buoys

Winds from NDBC buoys from the 1980-83 period are available for comparison to the FNOC and LFM fields. Winds are also available from buoys deployed in the Coastal Ocean Dynamics Experiment (CODE) experiment in the summers of 1981 and 1982. The comparison to NDBC winds is not an independent check on the gridded fields, since those measured winds were incorporated into the analyzed or modeled fields by the Navy and NMC. The CODE buoys were not incorporated into the operational products.

Mean winds from the buoys in summer (Fig. 2a) and winter (Fig. 2b) are examined. (The CODE buoys are those without winter means.) The mean winds show the strong steering effect of the coastline on the winds from the buoys over the continental shelf, in comparison to those farther offshore. Ellipses depicting the standard deviations along the principal major and minor axes (Figs. 3a and 3b) for these buoy winds again show the effect of the coastline in decreasing the cross-shelf component of wind variations, especially in summer. Similar principal axis ellipses for the FNOC and LFM winds (Figs. 3c-3f) show the somewhat better ability of the LFM winds to represent the alongshore orientation of the wind fluctuations, although neither field reproduces the extremely elongated ellipses in the CODE region. The LFM winds usually, but not always, produce ellipses closer in direction to those of the buoys.

One measure of the agreement between the buoy winds and the operational products is the magnitude of the correlation coefficient between the wind components (Table 1). The 99% significance level is about 0.45. The square of the correlation coefficient indicates the fraction of variance common to the two records. Another measure of the accuracy of the operational products is the RMS difference between them and the buoy winds (Table 2). The general results of the correlation calculations are: correlations are higher for the north-south component (v) than the east-west component (u), especially over the shelf; correlations are higher for the offshore buoys than for those over the shelf, except for the northernmost buoy in winter; correlations for the buoys over the shelf are higher in winter than in summer; and correlations with the buoys are slightly higher for the FNOC fields than for the LFM fields. The results of the RMS difference calculation are: RMS differences are greater in the north-south direction, except over the shelf in winter; RMS differences are greater in winter ( $4-6 \text{ m s}^{-1}$ ) than in summer ( $2-5 \text{ m s}^{-1}$ ); in summer, differences are greater over the shelf ( $4-5 \text{ m s}^{-1}$ ) than offshore ( $2-3.5 \text{ m s}^{-1}$ ); in winter, differences are greater offshore ( $5-6.4 \text{ m s}^{-1}$ ) than over the shelf ( $4-5 \text{ m s}^{-1}$ ); and RMS differences are smaller for FNOC winds than for LFM winds. The decrease in correlations closer to the coast compared to those far offshore may indicate a general failure of the operational products to accurately represent the frictional influence of the atmospheric boundary layer. The slightly higher correlations and lower RMS differences of the FNOC winds may reflect the fact that they are analyzed fields formed from measured winds and pressures at the time of the final field, rather than a six-hour forecast from the measurements. Thus, the FNOC winds may be more tightly constrained by the measurements, whereas the LFM fields are more influenced by the dynamics incorporated into the forecast model.



It is common, when correlating winds from individual points, to first rotate and decompose them along their respective principal axes, rather than using the strictly north-south and east-west components. Implicit in this process is the assumption that measured or modeled directions might be wrong but the variations along the major axes are still closely related. Correlations between the buoy winds and FNOC winds after each wind has been rotated along its major axis were examined. In summer, the rotation has the effect of increasing the correlations along the major axis and decreasing them along the minor axis. In winter, the rotation generally increases the correlation of both components. Based on a similar comparison of rotated buoy and LFM winds the only major improvement was at several CODE buoys which previously had insignificant correlations in summer. The degradation of the correlation in the minor axis component is not as great, but there is more often a decrease than an increase in the correlation along the major axis.

One of the advantages of the operational fields is their ability to calculate the curl of the wind stress on short time scales. Over monthly time scales, the wind stress curl calculated from COADS data is generally positive in a 100-to-300 km band adjacent to the coast in summer (Nelson, 1977; Rienecker and Ehret, 1988). This is primarily a result of a maximum in the southward winds that occurs at the offshore edge of this band. The cross-shelf array of four buoys deployed during spring and summer of 1981 and 1982 in the CODE experiment (denoted C2, C3, C4 and C5 from nearshore to offshore) provides an opportunity to look at this component of the curl, although over a smaller domain than we would like. The differences in the major axis components of the wind stresses were formed for each of the possible pairs of the four buoys, for both spring and summer. The correlations between the measured across-shelf gradients and those calculated from the operational products (Table 3) range from very low to surprisingly high. For the spring and summer records, of the pair of buoys with the greatest separation (C2 and C5, approximately 25 km) correlations are 0.88 and 0.77 for the FNOC wind stress and 0.83 and 0.80 for the LFM wind stress. This result suggests that something like 60% of the variance in the relative temporal pattern of this component of the wind stress curl may be reasonably represented by these kinds of fields, even over small spatial and temporal scales. A close examination shows events that are missed in the operational fields as might be expected. Of more significance is the difference in scale between the buoy and operational products. Differences in measured wind stress over 25 km are of the order of  $0.2 \text{ N m}^{-3}$ , while differences computed from the gridded fields are an order of magnitude smaller.

A similar calculation was made for the wind stress series calculated from the entire array of buoys, first rotating them along their principal axes, forming the difference between the major and minor components of all buoys, repeating the calculation for the operational fields and correlating the operational differences with the buoy differences. Since most of the buoys are located in an alongshore array and the principal axis is oriented alongshore, differences in the major components represent alongshore differences in the alongshore wind, and differences in the minor components represent the alongshore differences in the cross-shelf wind. Correlations in these records, as a function of station separation, for the FNOC and LFM fields (Figs. 4a and 4b respectively) indicate that the FNOC winds yield slightly



higher correlations for differences of the alongshore component than do the LFM winds. In both cases, correlations decrease for separation distances below 600 to 900 km in the alongshore component, indicating that features with scales less than this are not well represented in the operational fields.

### Comparison of LFM, NGM, Buoy and Ship Winds

Winds from the NGM model are available starting September 1986. This model has the potential improvements over the LFM model of better vertical resolution and postprocessing to account for vertical fluxes in the ABL and of increased horizontal resolution in its computational grid. Winds from NDBC buoys and several coastal land stations are available from 1987 and 1988. In addition, high quality winds from the research vessel (R/V) WECOMA are available for nearly the entire month of July 1988, from locations approximately 200 km offshore from NDBC buoy 13. The ship and buoy winds can be combined to examine the cross-shelf variation in the wind fields, with scales of 200 km. Unfortunately, FNOC winds are not available to us for this period. Thus, we can only address the question of whether the NGM fields represent an improvement on the LFM fields.

Principal axis ellipses (Fig. 5) again show the strong effect of the coastline in steering the wind and decreasing the component perpendicular to the coast. This is better represented by the LFM than by the NGM model, which is surprising, since the NGM model has greater horizontal and vertical resolution and is thought to have a more "realistic" boundary layer. The one suggestion offered by the NMC modelers to explain this is that the topography in the LFM model might be slightly steeper than that in the NGM model, providing the additional steering (J. Hoke, pers. comm.).

From the buoy and model components of the wind (Table 1) correlations for the LFM in 1987-1988 are similar to those found in 1980-1983, with higher values found in some cases in 1987-1988, especially in the cross-shelf direction, and correlations between the NGM and buoy alongshore winds are slightly higher than those of the LFM, with mixed results for the cross-shelf component. (Only the shelf stations and offshore stations common to both the 1980-1983 and the 1987-1988 data sets are used to form the means.) Based on the RMS difference in winds between buoys and models in 1987-1988 (Table 2) the two models produce similar totals of  $3.4\text{--}4.6\text{ m s}^{-1}$  over the shelf. At the two offshore locations, the NGM model produces much lower RMS differences of  $1.7\text{--}2.6\text{ s}^{-1}$ , in comparison to the LFM's  $2.9\text{--}5.2\text{ s}^{-1}$ . The NGM winds also produce lower RMS differences at the coastal land stations,  $3.6\text{--}3.7\text{ s}^{-1}$  in comparison to values of  $4.3\text{--}4.9\text{ s}^{-1}$  produced by the LFM. This comparison suggests that the NGM winds do represent an improvement over the LFM fields.

During summer 1988, winds from buoys and a ship cruise allow us to examine the degree to which the LFM and NGM fields represent short-term events in the coastal wind. Between July 17 and 18, winds over the shelf relaxed and became northward at  $2\text{--}4\text{ m s}^{-1}$ , as measured by NDBC buoy 13 at  $38.2^\circ\text{N}$ . Winds measured approximately 200 km farther offshore by the R/V WECOMA remained southward during the initial relaxation. Satellite imagery shows a wedge of clouds progressing up the coast,



similar to those described by Dorman (1985, 1987), associated with the northward propagation of Kelvin or gravity waves in the marine boundary layer, bounded on the right by the coastal mountains. Vectors from the ship at approximately  $125^{\circ}\text{W}$  and the buoy at approximately  $123^{\circ}\text{W}$  were superimposed on the NGM wind fields from 6 and 18 Greenwich Mean Time (GMT) on July 17 and 18 (Fig. 6). The ship and buoy show the nearshore reversal of winds while offshore winds remain southward. The NGM winds show a nearshore weakening of the winds, capturing the nature of the change in the cross-shelf gradient in the alongshore winds, but do not show a reversal.

The ability of the LFM and NGM fields to reproduce the ship and buoy winds is explored by comparing the north-south wind component (Fig. 7a) at NDBC buoy 13 (solid line) to LFM (triangles) and NGM (asterisks) winds interpolated to the buoy location for 15 June to 15 August. The wind reversal on 17 July in the buoy wind is only represented by the model winds as a weak decrease in southward speed, not as a reversal. Correlations of model to buoy winds for this entire period are 0.65 for LFM and 0.74 for NGM. An analogous comparison is made for the north-south component of the ship wind and model winds interpolated to the ship's position (Fig. 7b). Both measured winds and model wind fields represent the continued southward winds during the initial nearshore wind relaxation. Analysis during the latter part of the wind relaxation is not possible, since the ship was in port between 22-27 July. Correlations for the entire period shown are 0.79 for LFM and 0.83 for NGM winds.

A direct comparison of the measured and model cross-shelf difference in the north-south winds is made (Figs. 8a and 8b). During the wind relaxation, the cross-shelf difference of the measured winds increases (as would the curl of the stress). The models underestimate this increase. Correlations between measured and modeled wind differences are 0.68 for LFM and 0.66 for NGM winds. The greater correlations of the model winds with the offshore ship winds than with the buoy winds over the shelf raises another possibility for calculation of the major component of the wind stress curl over the 200 km next to the coast. Since we have an alongshore array of NDBC buoys but do not have a similar offshore array of buoys, perhaps the model winds can substitute for the offshore array. To test this, differences between the north-south component of the model winds interpolated to the ship location and the same component from buoy 13 are compared to the real difference between ship and buoy (Figs. 8c and 8d). Model-buoy differences are more like the ship-buoy differences than the model-model differences. Correlations are 0.81 for LFM and 0.86 for NGM. Thus, given the present buoy distribution, the most realistic picture of the alongshore difference in wind stress curl over the 200 km next to the coast and over event time scales might be formed from a combination of buoy winds over the shelf and model winds farther offshore.

Over longer time scales, another approach can be taken to the question of how well the operational wind fields alone represent the horizontal structure of the wind stress curl. A recent model of the California Current concludes that the long term circulation is in approximate Sverdrup balance (Pares-Sierra and O'Brien, 1989). If this is so, then streamlines calculated from the curl of the operational fields should resemble the known large scale structure of the California Current. The mean



summer curl field from the LFM winds in 1987-1988 (Fig 9a) was used to calculate the streamlines resulting from the Sverdrup balance (Fig. 9b). An important feature of the LFM-derived curl field is the fact that the region of positive curl adjacent to the coast does not extend north of approximately  $44^{\circ}\text{N}$ , a feature found also in the fields of curl calculated from the 1979-1985 FNOC and LFM data. We believe this feature to be erroneous, since it is in contrast to the band of positive curl extending along the entire West Coast in summer found by Nelson (1977) and Rienecker and Ehret (1988). The resulting streamlines show southward integrated transport far offshore and northward transport in the 500 km next to shore, south of  $44^{\circ}\text{N}$ . This northward transport is qualitatively similar to that shown by Pares-Sierra and O'Brien (1989), but greatly expanded in the east-west direction. North of  $44^{\circ}\text{N}$  it lacks the northward flow associated with the presumed poleward undercurrent. Based on the mean summer curl field calculated from the NGM winds during the same 1987-1988 period (Fig. 9c) the band of positive curl now extends along the entire West Coast, in agreement with the climatological studies based on ship-of-opportunity data, which is another indication that the NGM winds represent an improvement over the LFM winds. The streamline field (Fig. 9d) is still far broader than expected for the California Current, but shows a narrower and more intense poleward flow next to the coast which extends off Oregon and Washington, although weakly.

## Summary and Conclusions

Comparisons of operational wind fields to each other and to winds from buoys off the west coast of North America lead to the following conclusions:

- 1) RMS differences between FNOC and LFM are between  $3.5$  to  $5.5 \text{ m s}^{-1}$  on a seasonal basis. This result represents the magnitude of the vector differences that can be expected between individual fields and is caused somewhat more by differences in direction than differences in magnitude. The corresponding differences in wind stress are  $0.04$ - $0.06 \text{ N m}^{-2}$ . Differences between longer term averages of the fields (a month and longer) have lower magnitudes, in the range of  $1$ - $3 \text{ m s}^{-1}$ . Thus, these fields are more suitable for climatological studies than for analysis or modeling of events. LFM winds are systematically greater in magnitude and oriented to the left of FNOC winds, consistent with an underestimate of the turning and retardation due to the surface boundary layer.
- 2) Correlations between these fields and buoys shows slightly better agreement for FNOC and NGM winds than for LFM, although no comparison between NGM and FNOC can be made with the data in hand. There is significantly better agreement 200-500 km from the coast than over the shelf at approximately 10 km from the coast or at coastal land stations, especially in the cross-shelf component of the wind. RMS differences between buoys and 1980-1983 LFM and FNOC winds are approximately  $3$ - $6 \text{ m s}^{-1}$  and  $2$ - $5 \text{ m s}^{-1}$ , respectively, with lower values offshore and in summer. RMS differences between the buoys and the 1987-1988 LFM and NGM winds are

approximately  $3\text{-}6 \text{ m s}^{-1}$  and  $2\text{-}5 \text{ m s}^{-1}$ , respectively, again with lower values offshore and in the summer.

- 3) Spatial differences in the alongshore winds over alongshore scales of 600-900 km and more are well represented by the LFM and FNOC, slightly better by the FNOC. Spatial differences in the cross-shelf wind are not as well represented. The increased resolution of the LFM grid does not seem to increase the degree to which it represents small scale features.
- 4) From the few measurements of cross-shelf gradient in the alongshore wind stress, it appears that the operational fields represent the temporal variation of the gradient on scales of 25-200 km moderately well, but underestimate the magnitude by a factor of 10 at 25 km separation and a factor of 4 at 200 km separation. Fields of summer wind stress curl calculated from the FNOC and LFM winds produce a band of positive curl next to the coast south of 44 N in agreement with climatological fields derived from ship data, but this band is broader and weaker than the climatological fields. The lack of a band of positive curl off Oregon and Washington is thought to be an error. Use of the NGM data in the curl calculation produces a band of positive curl that extends along the entire coast and is more concentrated toward the coast, in better agreement with the climatological fields, although still too broad. This suggests that the increase in resolution and improved boundary layer flux parameterizations have resulted in more realistic winds in the NGM fields. Continued improvements in the resolution and surface flux estimates in future models is recommended.
- 5) A suggestion for improved estimates of the wind stress curl field with presently available data is to combine winds measured by buoys over the shelf with those modeled farther offshore, since the model winds are in better agreement there.



Table 1

Mean correlations between buoy and operational winds. Pairs correspond to u, v (E-W, N-S) components.

	LFM 1980-1983		FNOG 1980-1983	
	Summer (u,v)	Winter (u,v)	Summer (u,v)	Winter (u,v)
Shelf (6 locations)	0.12, 0.67	0.72, 0.83	0.46, 0.73	0.63, 0.89
Offshore (2 locations)	0.77, 0.91	0.84, 0.84	0.89, 0.95	0.86, 0.83
CODE (6 locations)	0.44, 0.61		0.43, 0.68	

	LFM 1987-1988		NGM 1987-1988	
	Summer (u,v)	Winter (u,v)	Summer (u,v)	Winter (u,v)
Shelf (6 locations)	0.50, 0.66	0.68, 0.91	0.22, 0.79	0.44, 0.91
Offshore (2 locations)	0.86, 0.94	0.94, 0.92	0.86, 0.97	0.94, 0.96
Coastal Land (4 locations)	0.29, 0.75	0.66, 0.85	0.33, 0.63	0.74, 0.85

Table 2

RMS difference between buoy and operation winds ( $\text{ms}^{-1}$ ). Triplets correspond to u, v components and total.

	LFM 1980-1983		FNOC 1980-1983	
	Summer (u,v, total)	Winter (u,v, total)	Summer (u,v, total)	Winter (u,v, total)
Shelf (6 locations)	2.7, 2.7, 3.8	3.8, 3.4, 5.1	2.4, 2.8, 3.7	3.3, 2.6, 4.2
Offshore (2 locations)	2.2, 2.7, 3.5	3.7, 5.2, 6.4	1.4, 1.7, 2.2	3.0, 4.1, 5.0
CODE (5 locations)	3.3, 3.5, 4.9		2.7, 3.4, 4.4	
	LFM 1987-1988		NGM 1987-1988	
	Summer (u,v, total)	Winter (u,v, total)	Summer (u,v, total)	Winter (u,v, total)
Shelf (6 locations)	2.2, 2.8, 3.6	3.5, 3.0, 4.6	2.4, 2.3, 3.4	3.8, 2.1, 4.4
Offshore (2 locations)	1.9, 2.3, 2.9	2.9, 4.3, 5.2	1.3, 1.1, 1.7	1.9, 1.7, 2.6
Coastal Land (4 locations)	2.6, 3.4, 4.3	2.9, 3.9, 4.9	2.1, 2.9, 3.6	2.5, 2.7, 3.7



**Table 3**

Correlation between offshore gradients of alongshore wind stress.

Buoy and FNOG						
	Spring			Summer		
	C2	C3	C4	C2	C3	C4
C3	0.94			0.70		
C4	0.25	0.12		0.17	0.69	
C5	0.88	0.50	0.95	0.77	0.54	0.89

Buoy and LFM						
	Spring			Summer		
	C2	C3	C4	C2	C3	C4
C3	0.91			0.74		
C4	0.25	0.15		0.07	0.15	
C5	0.83	0.45	0.90	0.80	0.03	0.91

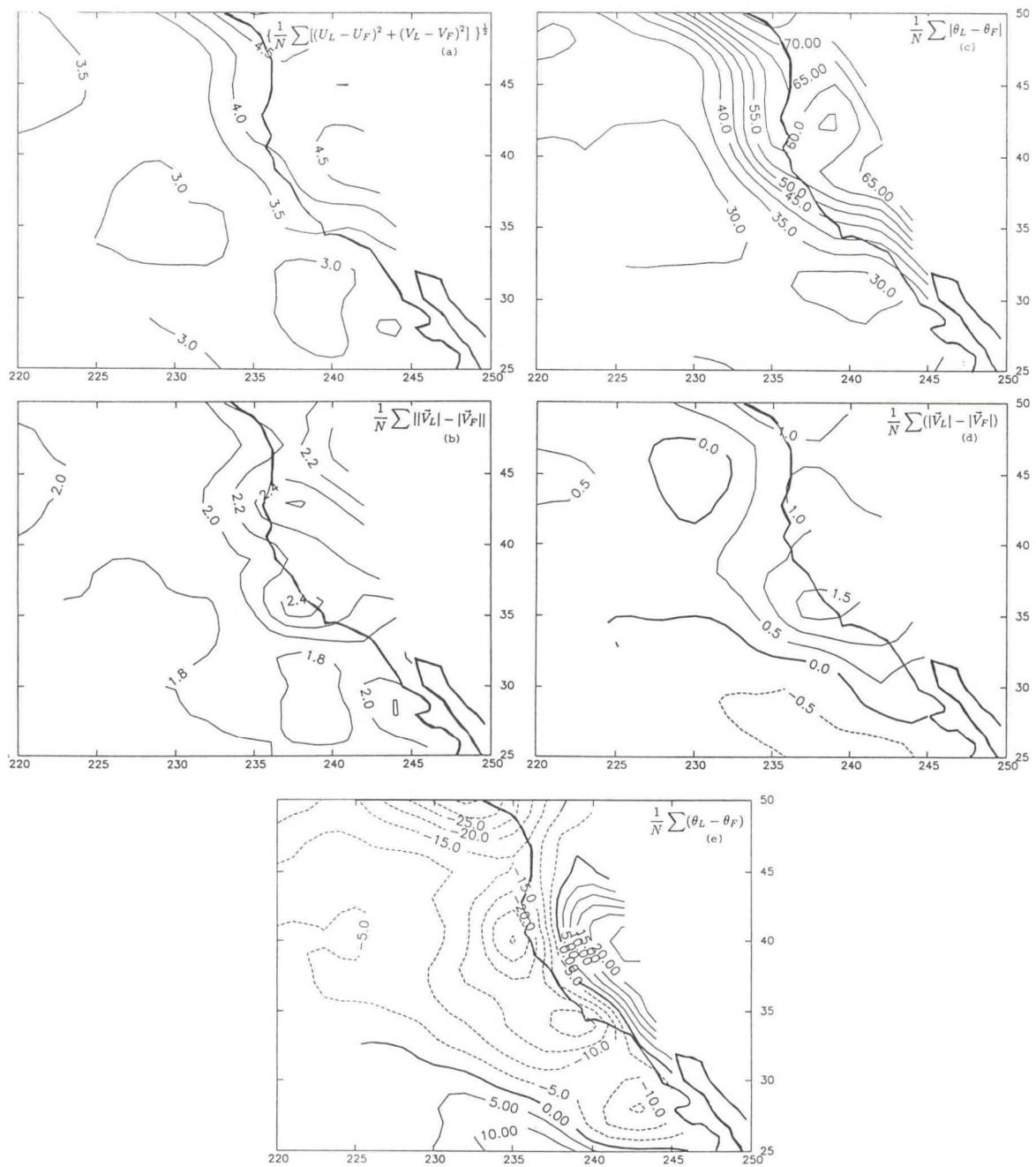


Figure 1. Difference between LFM and FNOC wind fields over the years 1979-1985. Units of wind speed are ( $\text{m s}^{-1}$ ) and wind direction are ( $^{\circ}$ ): a) RMS difference, b) mean of the difference of the absolute magnitudes of the wind speeds, c) mean of the difference of the absolute magnitude of the directions, d) long-term mean difference of the wind speeds, e) long-term mean difference of the directions.



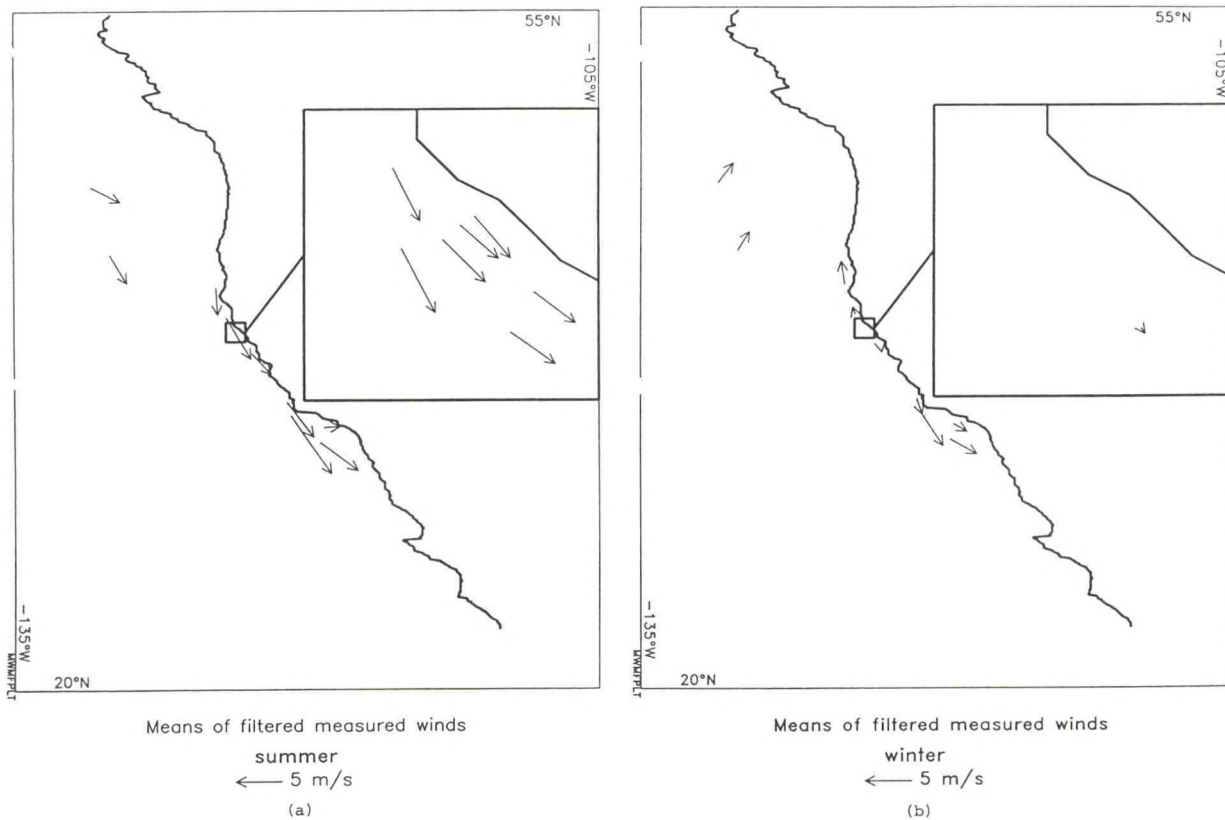


Figure 2. Vector mean winds from buoys in 1980-1983: a) summer, including NDBC and CODE buoys; b) winter, NDBC buoys only.

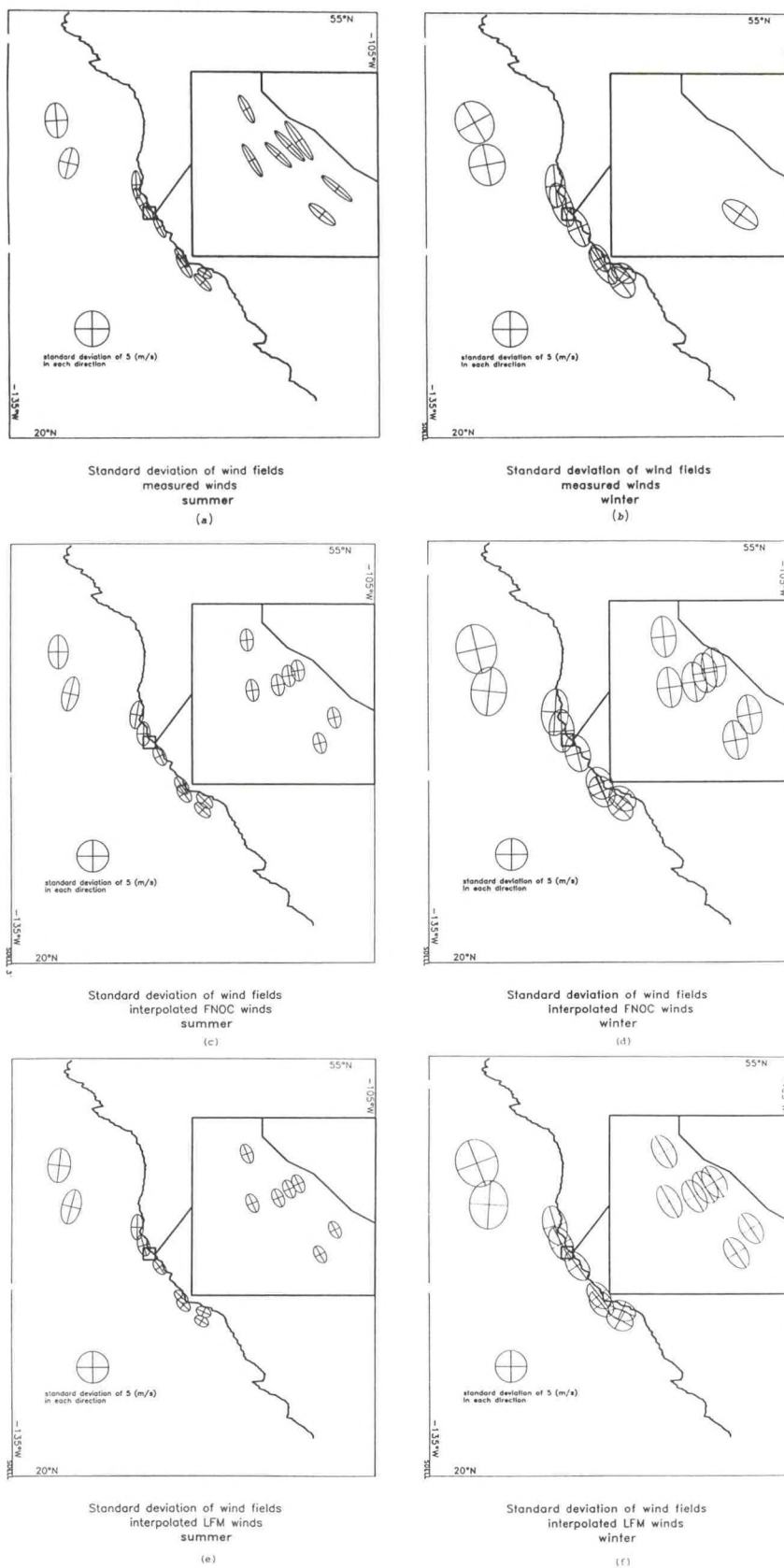
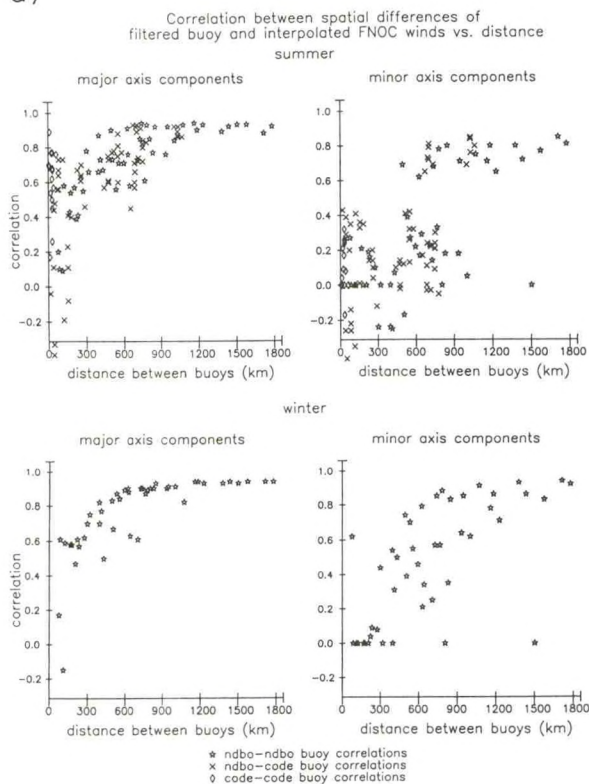


Figure 3. Principal axis ellipses of measured and operational winds 1980-1983: a)-b) measured winds in summer and winter; c)-d) FNOC winds in summer and winter; e)-f) LFM winds in summer and winter.



a)



b)

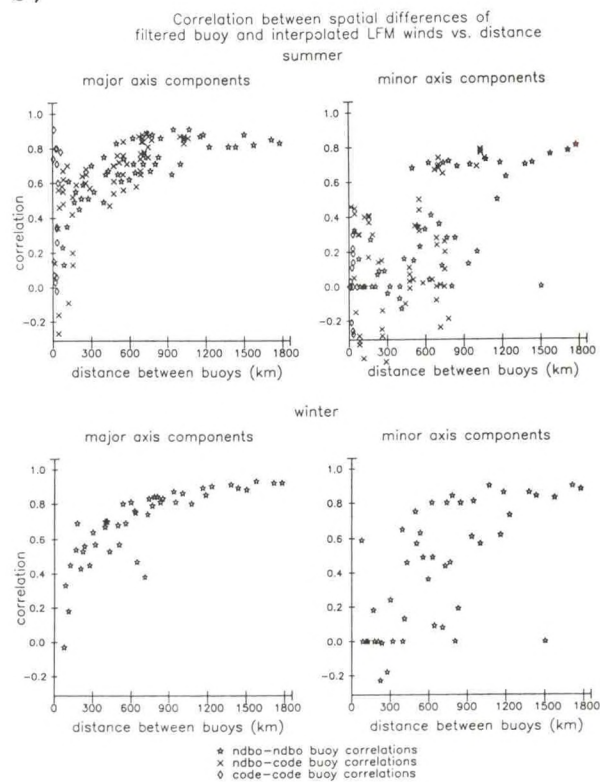


Figure 4. Correlations between spatial differences of buoy and operational winds as a function of spatial separation, after rotation about their principal axes: a) buoy and FNOC; b) buoy and LFM.

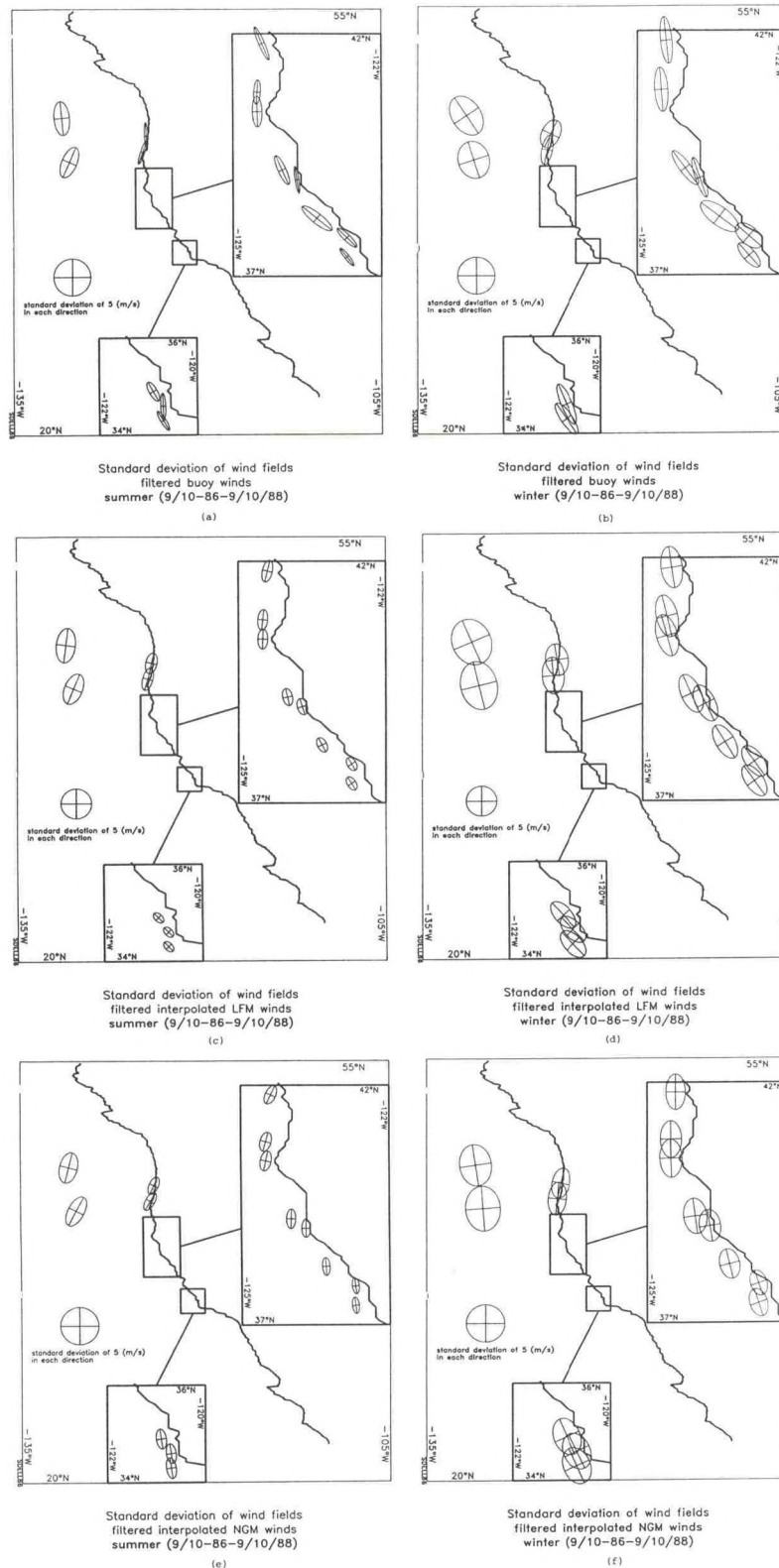


Figure 5. Principal axis ellipses of measured and operational winds, 1987-1988: a)-b) measured winds in summer and winter; c)-d) LFM winds in summer and winter; e)-f) NGM winds in summer and winter. (Model winds have been interpolated to the buoy locations as in Fig. 3.)



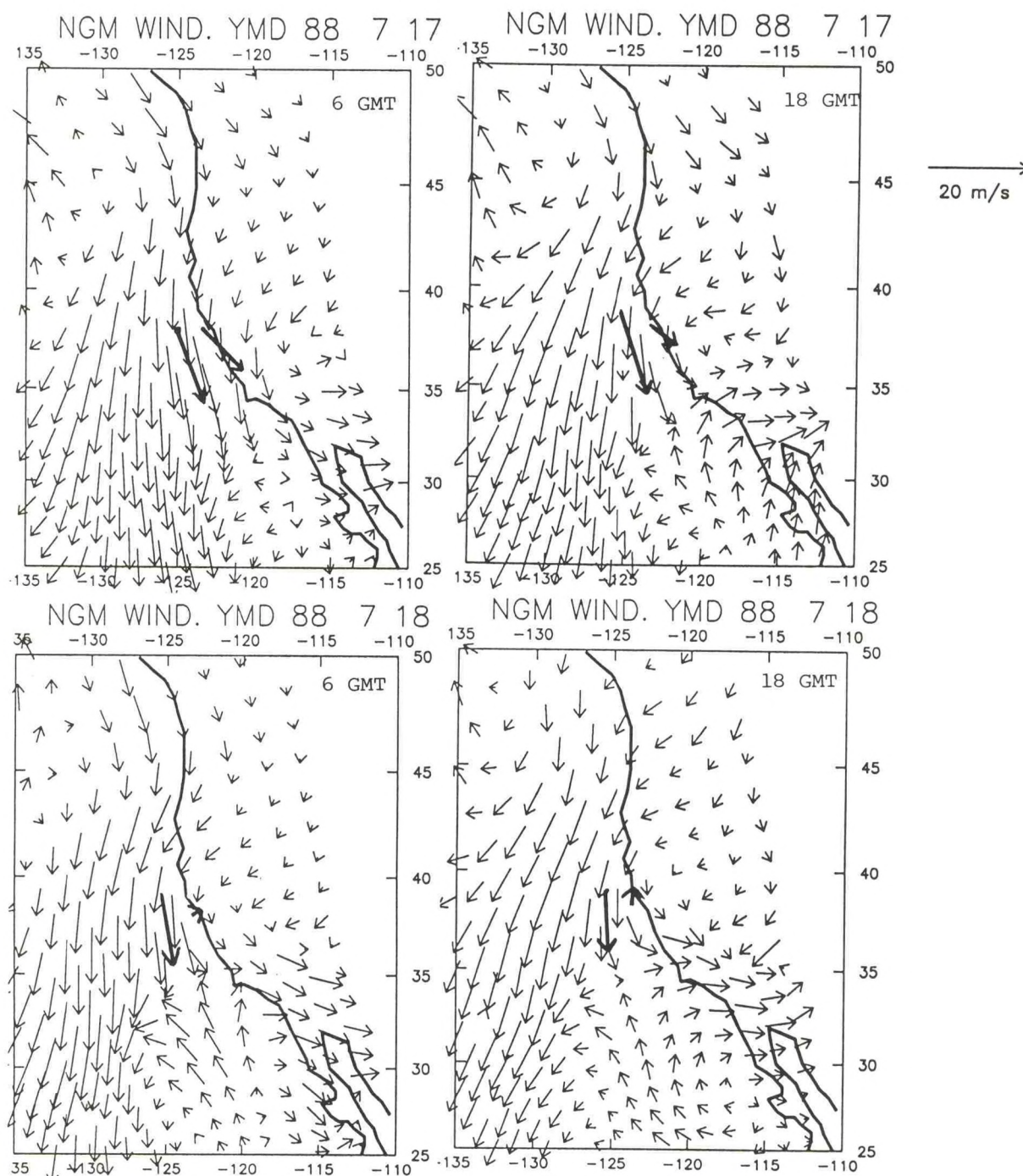


Figure 6. Wind vectors from the R/V WECOMA (heavy vector farthest from shore), NDBC buoy 13 (heavy vector nearest to shore), and the NGM wind field (lighter vectors) for 6 and 18 GMT on 17-18 July, 1989.

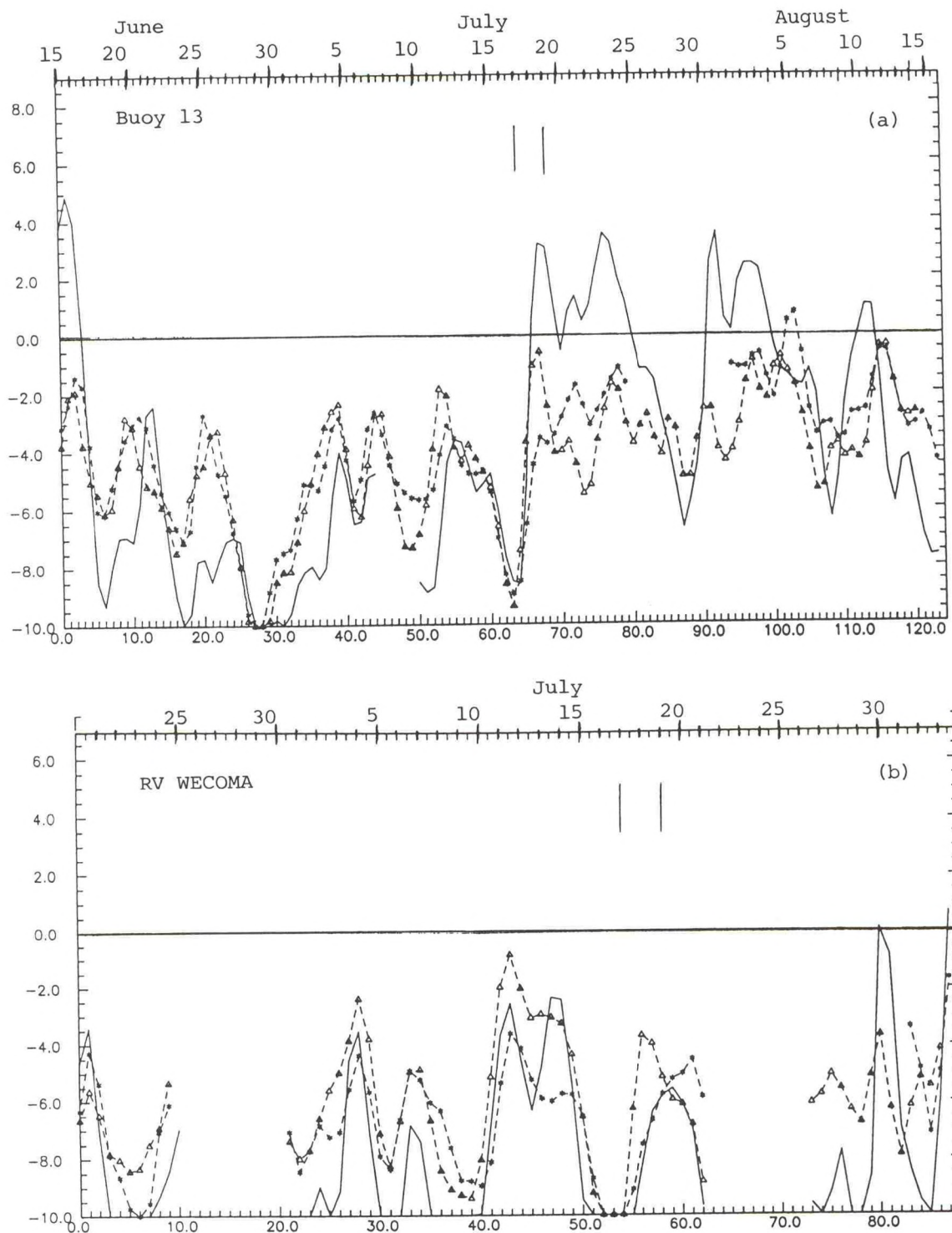


Figure 7. N-S component of the wind from buoy or ship measurements (solid line) compared to LFM (triangles) and NGM (asterisks). Units are ( $\text{m s}^{-1}$ ): a) NDBC buoy 13 for the period 15 June 1989-15 August 1989; b) R/V WECOMA for the period 21 June 1989-3 August 1989. Note the change in periods as seen in the x coordinate. Vertical lines indicate the period 17-19 July 1988, corresponding to the fields shown in Fig. 6.



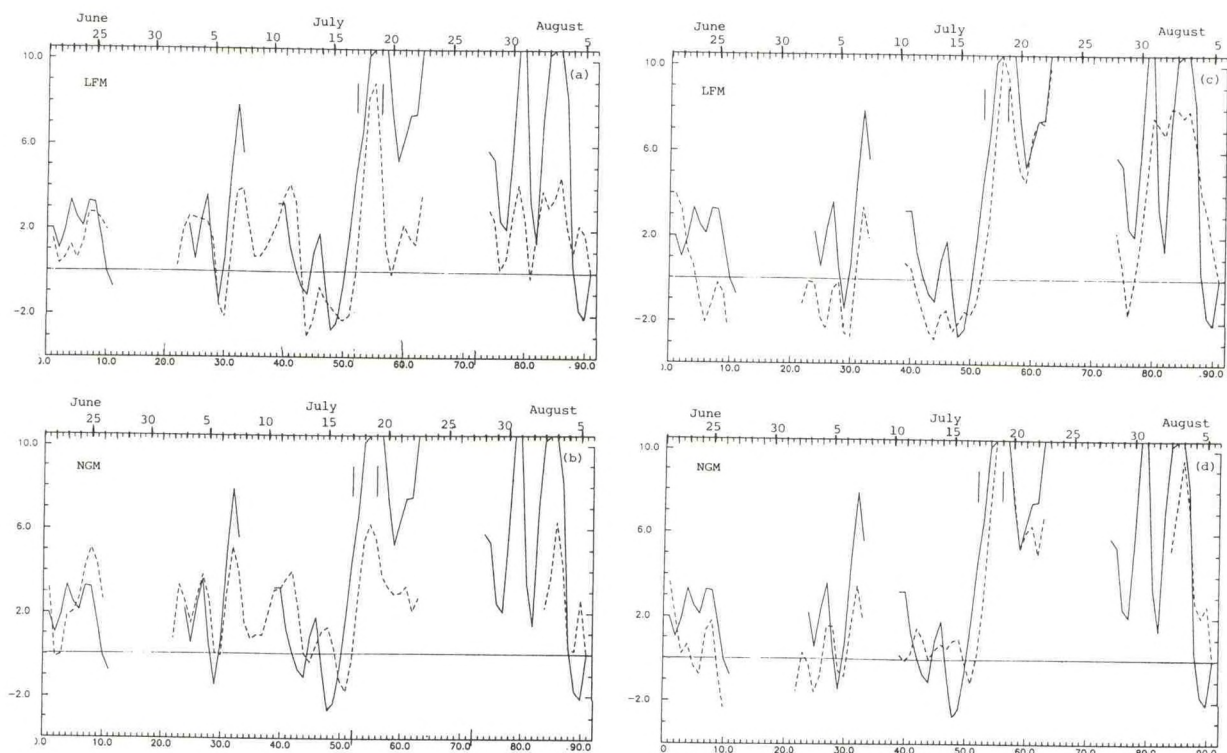
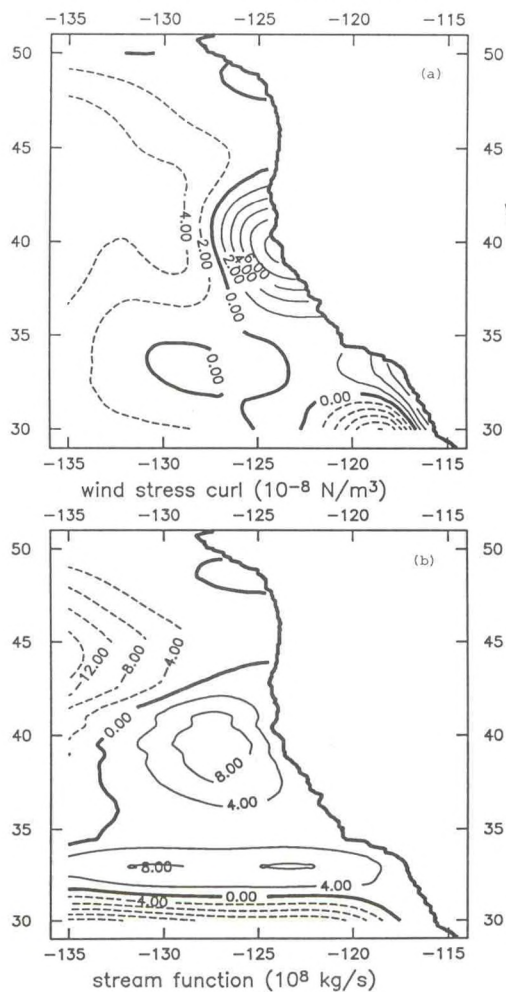


Figure 8. Cross-shelf differences in N-S component of the wind at locations of the ship and buoy 13 for the period from 21 June 1988 to 5 August 1988. Units are ( $\text{m s}^{-1}$ ): a) buoy 13--ship (solid) and LFM fields, interpolated to the same locations (dashed); b) buoy 13--ship (solid) and NGM fields, interpolated to the same locations (dashed); c) buoy 13 -- ship (solid) and buoy 13--LFM fields, interpolated to the ship location (dashed); d) buoy 13--ship (solid) and buoy--NGM fields, interpolated to the same location (dashed).

Wind stress curl and streamlines from LFM winds  
from the summers of 87 & 88



Wind stress curl and streamlines from NGM winds  
from the summers of 87 & 88

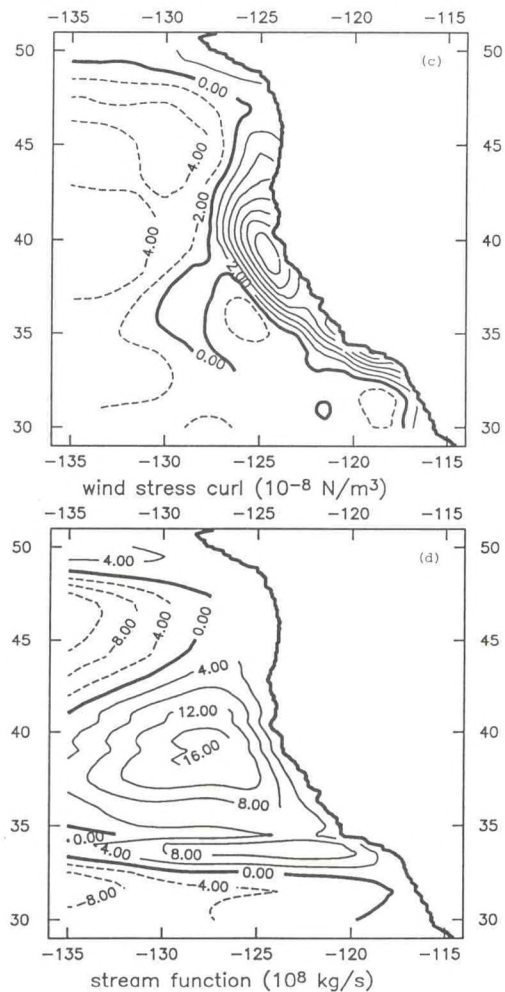


Figure 9. Mean wind stress curl for summer 1987 and 1988 and the streamline calculated from the Sverdrup relation: a) LFM wind stress curl; b) streamlines derived from the LFM curl; c) NGM wind stress curl; d) streamlines derived from the NGM curl. Units are noted on the figure.



# NATIONAL DATA BUOY CENTER REAL-TIME ENVIRONMENTAL DATA

Glenn D. Hamilton  
National Data Buoy Center  
Stennis Space Center, MS 39529

## Introduction

The National Data Buoy Center (NDBC), a part of the National Weather Service (NWS), operates and maintains approximately 100 moored and fixed automated data-acquisition systems in the deep ocean and coastal areas to provide real-time environmental observations from data-sparse areas. In 1988, these NDBC stations delivered over one million observations.

## Moored Buoy Network

There are about 55 buoys in the moored buoy network (Fig. 1). NWS receives data from all buoys in support of its warning and forecast service. Of the 55 buoys, some 20 are offshore (greater than 150 km), nearly all of which are funded permanently by NWS. Data from these offshore buoys are vital for detecting the intensity and movement of storms and providing important observations for analysis of pressure and wind fields for numerical weather prediction.

There are about 35 buoys in nearshore areas, including eight permanently NWS-funded buoys in the Great Lakes. These 35 also include U.S. Coast Guard (USCG) Large Navigational Buoys (LNBs) of the Coastal-Marine Automated Network (C-MAN) buoys supporting Minerals Management Service studies and U.S. Army Corps of Engineers directional wave surveys, and several NDBC engineering development buoys. (N.B. Buoys will not be deployed at the stations shown as open circles (Fig. 1) in the foreseeable future, due to funding restrictions. These locations are based on National Weather Service priorities, and they are a "Dream Sheet" of where buoys would be placed if the funds could be identified.)

The 6m-long, boat-shaped Navy Oceanographic and Meteorological Automatic Device (NOMAD) buoy is normally used for deep-ocean applications (Fig. 2). In coastal areas, a 3m-diameter discus buoy (Hamilton, 1988) is ordinarily used (Fig. 3). In very severe environments, such as the Bering Sea, the 12m-diameter discus buoy is deployed. In less severe regions, like the Gulf of Mexico, 10m-diameter discus buoys are deployed. LNBs are similar to the 12m discus buoys. All buoys have redundant wind and pressure sensors. On large discus buoys, the wind sensors are located at 10 m above the water; on NOMAD and 3m buoys, they are at approximately the 5m level.

## Coastal-Marine Automated Network

In response to the need for more coastal observations, the C-MAN program was established in 1981 by NWS. The existing network (Fig. 4) includes USCG offshore platforms, USCG lighthouses, beach areas, and public fishing piers (cf. Fig. 5). One station was established in 1988 on Faraulep Island in the western tropical Pacific, and two more are now being implemented on other islands as part of a network in Micronesia that will consist of approximately 20 stations. In addition, six LNBs and two Exposed Location Buoys form part of the C-MAN program. All stations have redundant wind sensors.

## Observational data

A typical moored buoy electronics payload reports the data in Table 1. The accuracies listed refer to the system and include signal processing as well as sensor errors. The accuracy of sensors can drift with time in a harsh marine environment, and the accuracy statements signify the value to which the measurement can be quality controlled.

An additional parameter that is being implemented on some buoys is continuous measurement of 10-minute averaged winds. This capability was developed for the satellite community to provide ground truth data for satellite-derived surface winds. This has long been an oceanographic requirement for a more complete description of winds used in air-sea interaction studies.

All C-MAN stations measure wind speed and direction, wind gust, barometric pressure, and air temperature. Certain other stations may report one or more of the other parameters listed in Table 1.

## Drifting buoys

Drifting buoys are playing an important role in the Tropical Ocean and Global Atmosphere (TOGA) research program in the Southern Hemisphere, and they are also used in various programs in the Northern Hemisphere (cf. Fig. 6). However, they are almost all deep ocean programs as drifters tend to go aground in coastal areas and lose their usefulness.

## Data Transmission, Processing, and Dissemination

The buoy and C-MAN data flow through an elaborate network (Fig. 7). The National Environmental Satellite, Data, and Information Service (NESDIS) acquires the data, and the NWS Telecommunications Gateway (NWSTG) processes the data. (The lower part of Fig. 7 shows the time sequence for moored buoy and C-MAN data reported hourly through the Geostationary Operational Environmental Satellite (GOES) system.) NWSTG performs real-time, gross-error checks for range and



time-continuity limits and encodes the data into World Meteorological Organization (WMO) message formats. The messages are transmitted over NWS and other communications circuits and to NDBC for further quality control.

Drifting buoy data are reported through the NOAA polar orbiting satellites and, after receipt by NESDIS ground stations, they are acquired by Service Argos, Inc. in Landover, MD. The data are processed, run through range-limit checks, and sent to NWSTG, where the 40 to 50 NDBC-deployed drifters are subjected to other checks, entered on the Global Telecommunications System (GTS) and other circuits, and transmitted to NDBC for further quality control. At the present time, data from other drifters are put directly on the GTS. Plans are for the National Ocean Service (NOS) and the Ocean Products Center (OPC) to quality control the data from other drifters in the future.

### Data Quality

Moored buoy and C-MAN data are received at NDBC in raw form from NESDIS. The data are processed, and compared with the messages transmitted from NWSTG. Drifting buoy data received from NWSTG are also put into the NDBC data base. At NDBC, observations from each station are quality checked each day. More stringent automated quality checks test for range and time-continuity limits. Differences between redundant sensors and differences between the reports and NMC numerical analyses are calculated. Suspicious data are flagged. Color graphics, such as line plots, scatterplots, and contour maps, are produced on demand by data quality analysts in response to the flagged data. Time-series plots and wave-spectra curves help analysts distinguish between true sensor or system failure and legitimate data in near-real-time (Gilhousen, 1988). Through the NDBC computer center, a data base at NWSTG is maintained, and data from the best sensor are selected for transmission. Sensor drift is corrected by scaling parameters in the NWSTG data base to ensure that accurate data are released.

Every month the validated data are forwarded to the National Climatic Data Center (NCDC) and the National Oceanographic Data Center (NODC). Over 90 percent of all possible data that can be collected from NDBC stations are routinely received in real time and archived. NDBC data can be obtained from NCDC or NODC. Spectral wave data can only be ordered from NODC.

Of special interest is the quality of NDBC winds. Several field inter-comparisons have been conducted to investigate the quality (Gilhousen, 1987), and errors of  $1\text{ms}^{-1}$  or less have been found. To account for the different heights of anemometers on buoys and C-MAN stations, winds extrapolated to common heights of 10 and 20 m are given in the real-time reports.

Table 1.

Moored buoy payload data.

## MOORED BUOY PAYLOAD DATA

<u>PARAMETER</u>	<u>REPORTING RANGE</u>	<u>REPORTING RESOLUTION</u>	<u>SAMPLE INTERVAL</u>	<u>SAMPLE PERIOD</u>	<u>TOTAL SYSTEM ACCURACY</u>
WIND SPEED	0 TO 62 M/S	0.1 M/S	1 SEC	8.5 MIN	± 1 M/S OR 10%
WIND DIRECTION	0 TO 360°	1°	1 SEC	8.5 MIN	± 10°
WIND GUST	0 TO 82 M/S	1 M/S	1 SEC	8.5 MIN	± 1 M/S OR 10%
AIR TEMPERATURE	-50° TO 50° C	0.1° C	90 SEC	90 SEC	± 1° C
BAROMETRIC PRESSURE	900 TO 1100 hPa	0.1 hPa	4 SEC	8.5 MIN	± 1 hPa
SURFACE WATER TEMPERATURE	-7° TO 41° C	0.1°C	1 SEC	8.5 MIN	± 1° C
SOLAR RADIATION*	0 TO 2150 WATTS/M <sup>2</sup>	0.5 WATTS/M <sup>2</sup>	1 SEC	8.5 MIN	± 5%
RELATIVE HUMIDITY*	0 TO 100%	0.1%	1 SEC	8.5 MIN	± 6%
SIGNIFICANT WAVE HEIGHT	0 TO 35 M	0.1 M	0.39 SEC	20 MIN	± 0.2 M OR 5%
WAVE PERIOD	3 TO 30 SEC	0.1 SEC	0.39 SEC	20 MIN	± 1 SEC
NONDIRECTIONAL WAVE SPECTRA	0.03 TO 0.40 Hz	0.01 Hz	0.39 SEC	20 MIN	—
DIRECTIONAL WAVES*	0.03 TO 0.35 Hz	0.01 Hz	1.0 SEC	20 MIN	± 5° OF AZIMUTH

\*PARAMETER REPORTED ON SELECTED BUOYS

EAM 6/89



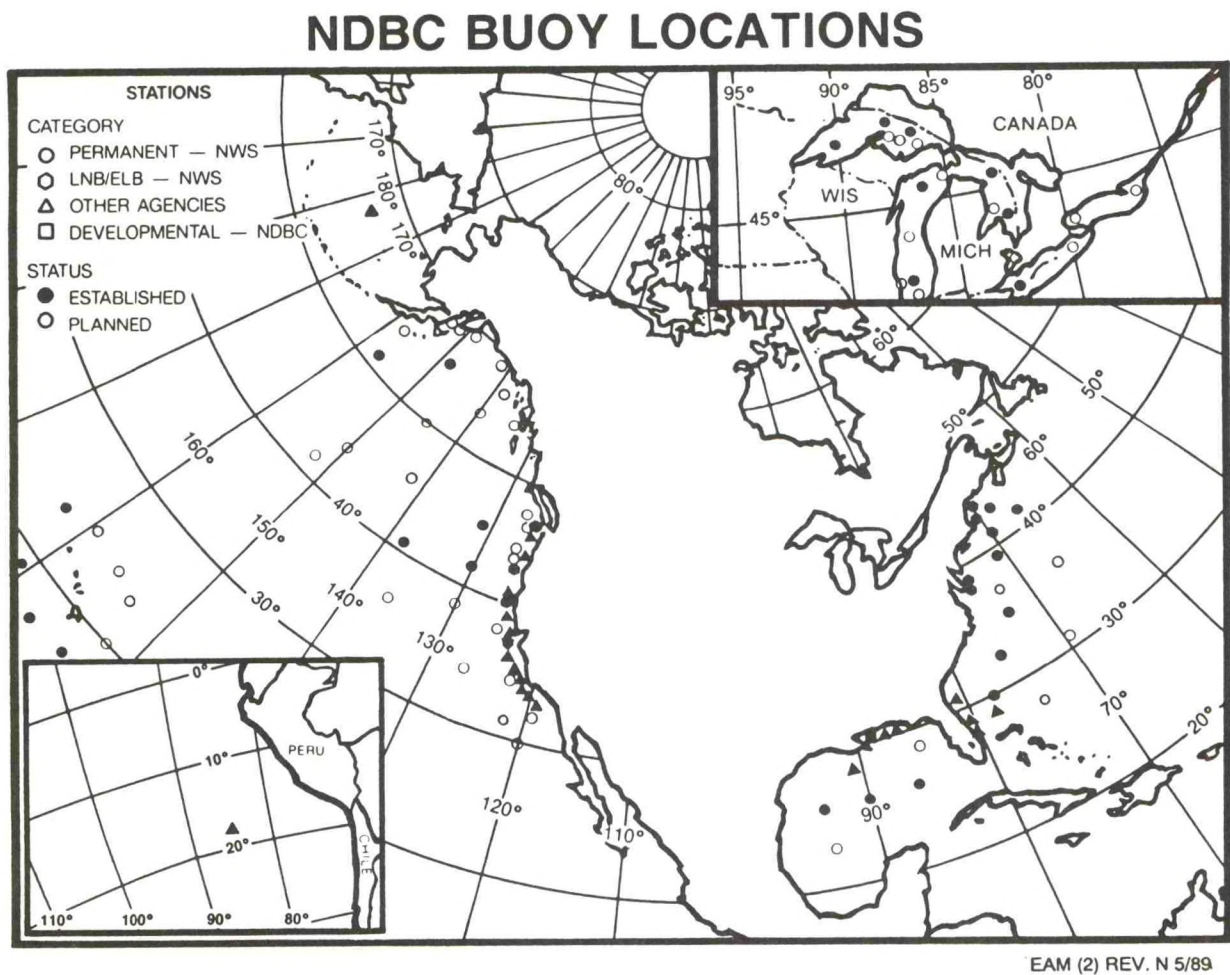


Figure 1. Moored buoy location map.



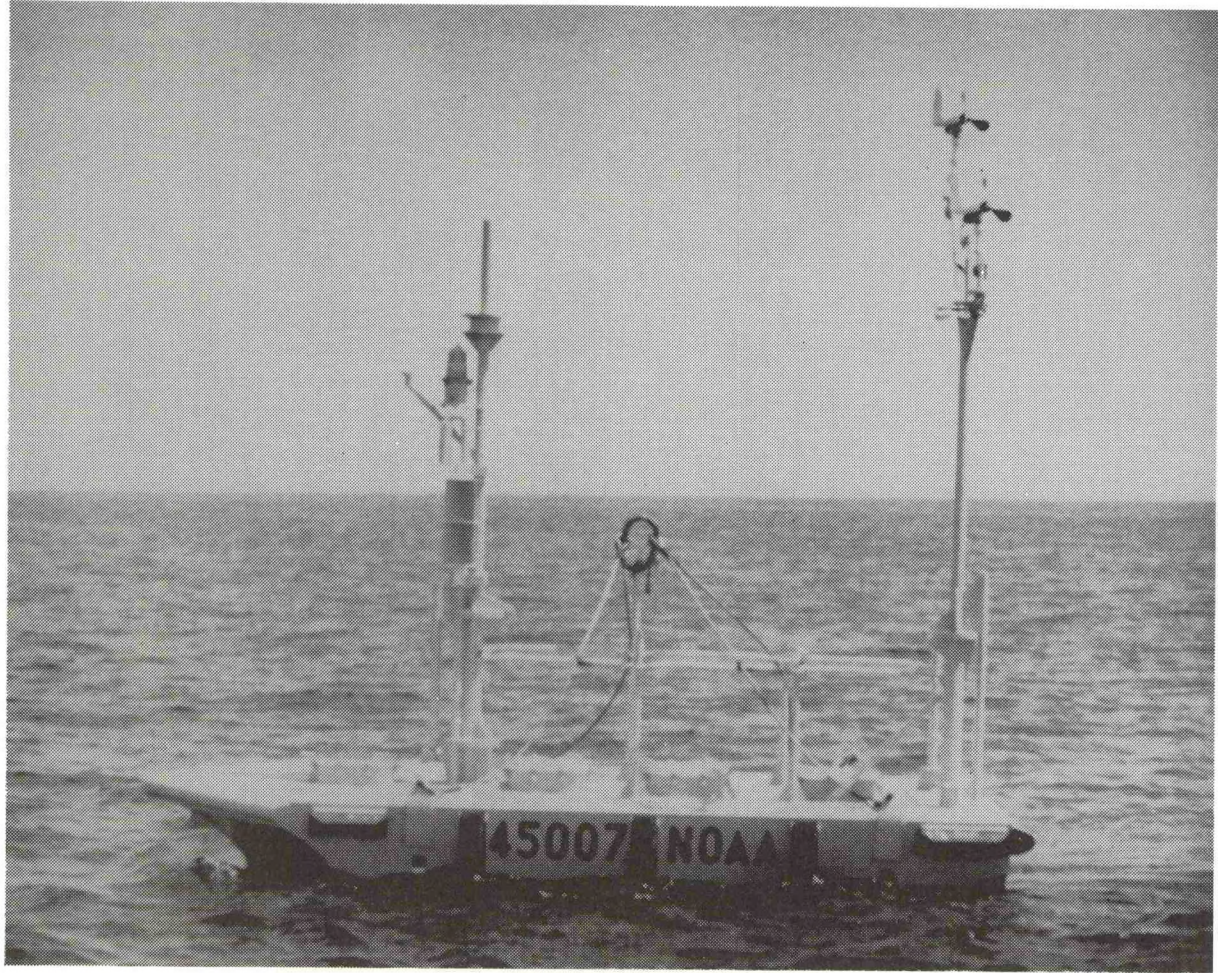


Figure 2. NOMAD buoy.



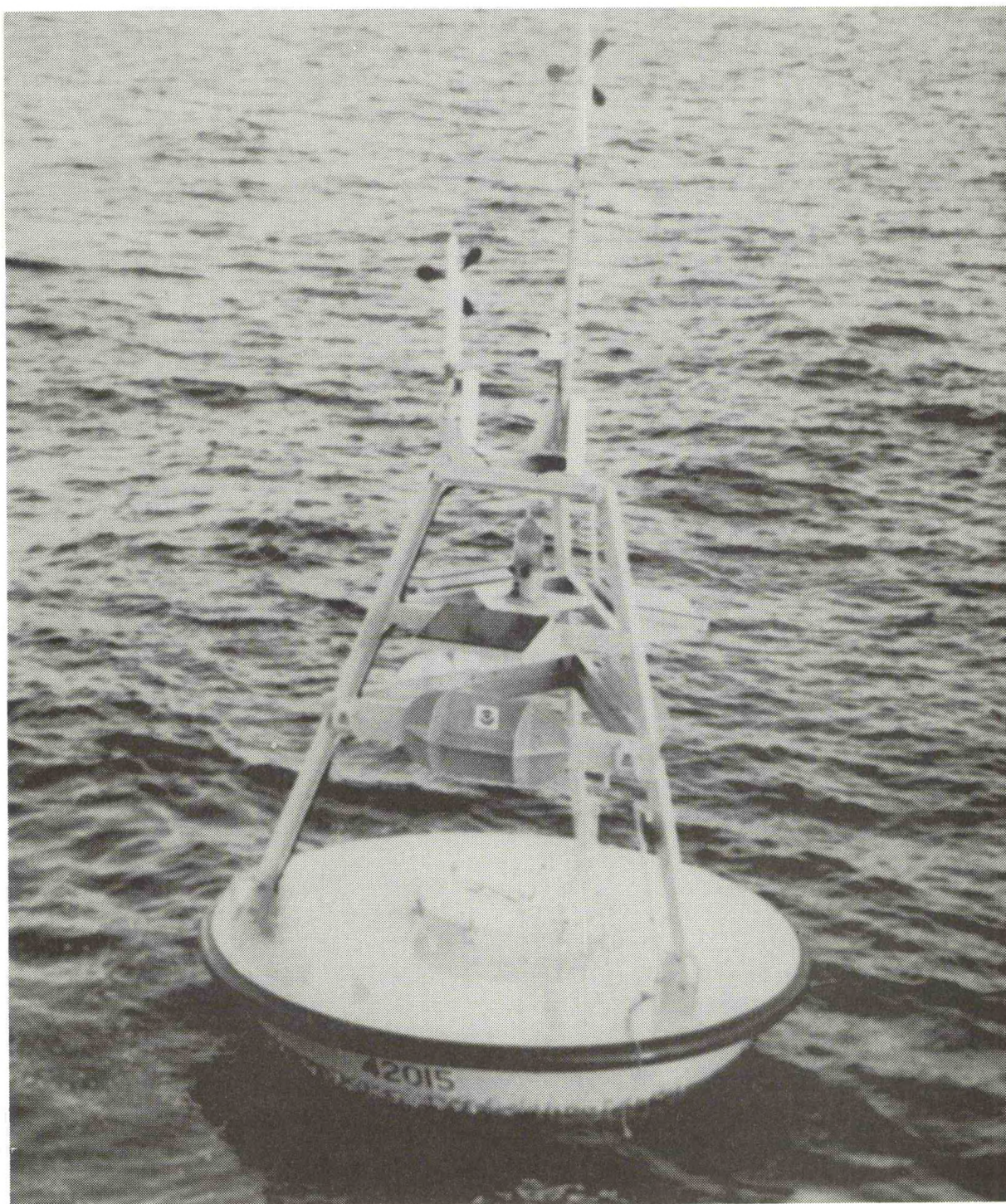


Figure 3. 3-meter buoy.



# C-MAN SITES

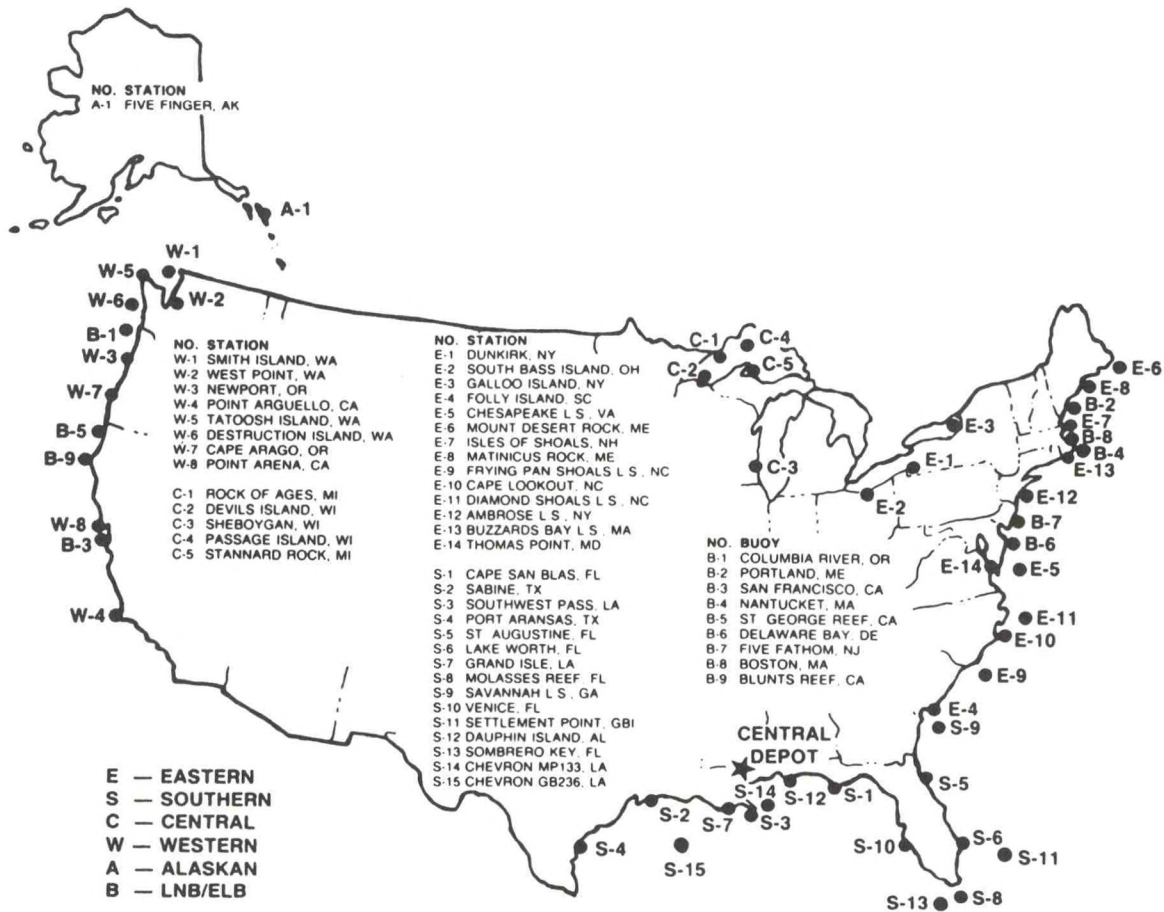


Figure 4. C-MAN site map.



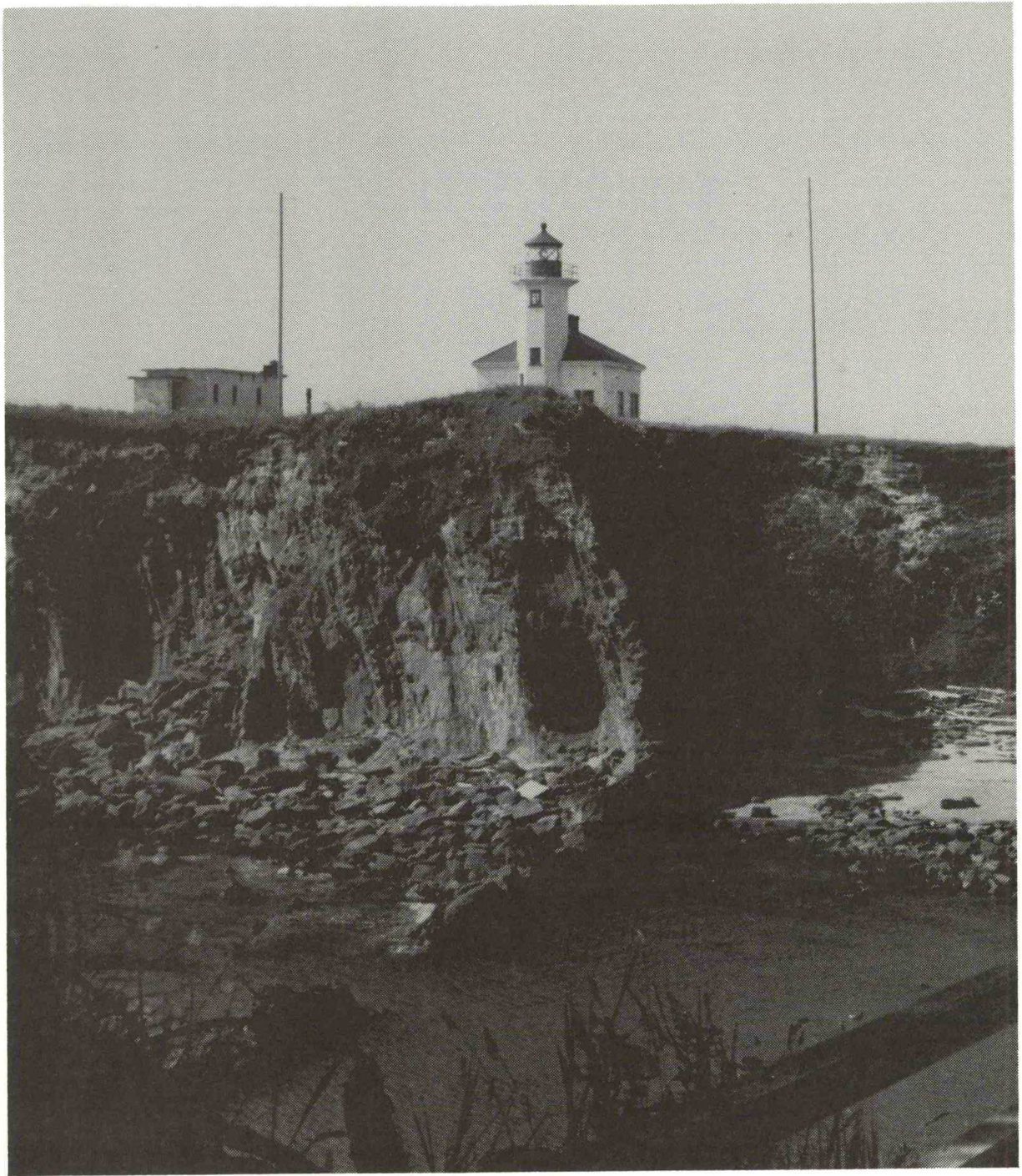


Figure 5. C-MAN station, Cape Arago.



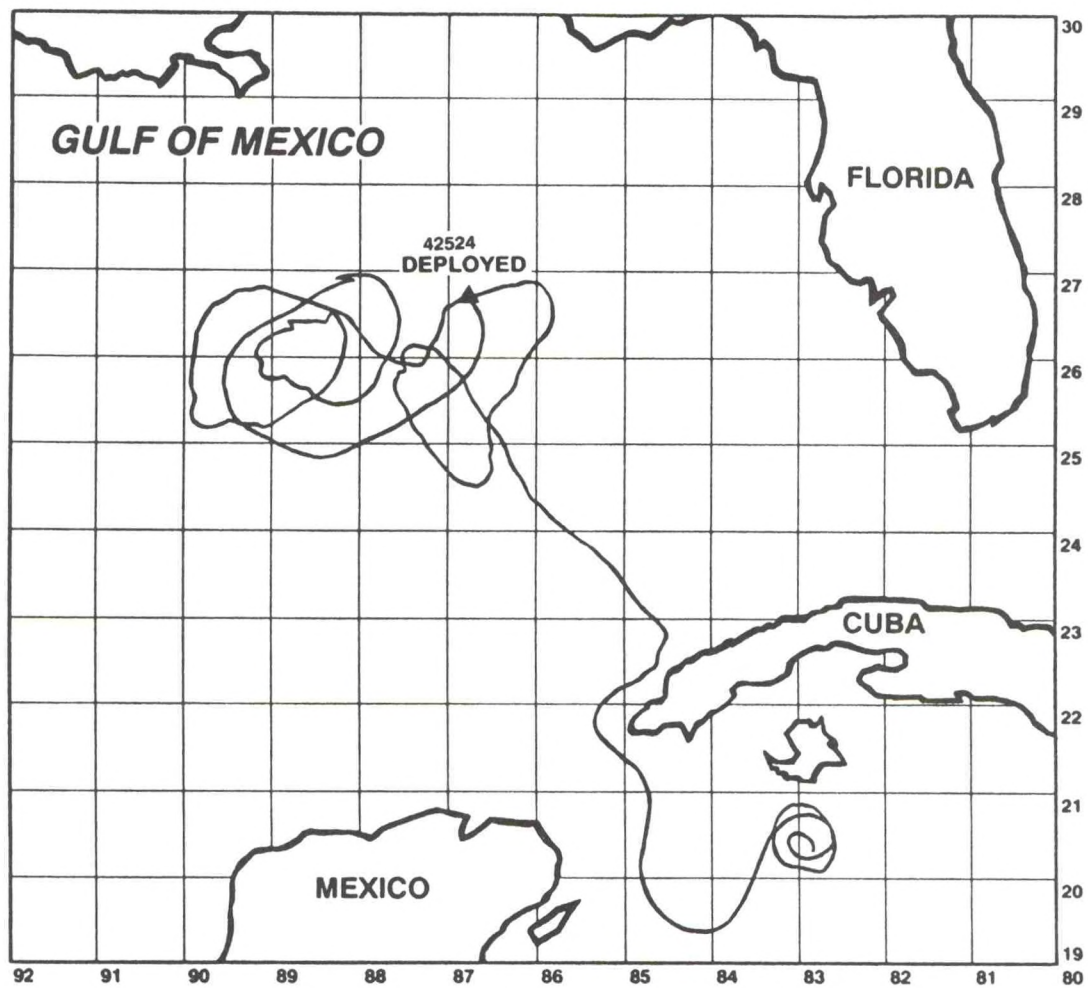


Figure 6. Drifting buoy track in the Gulf of Mexico.



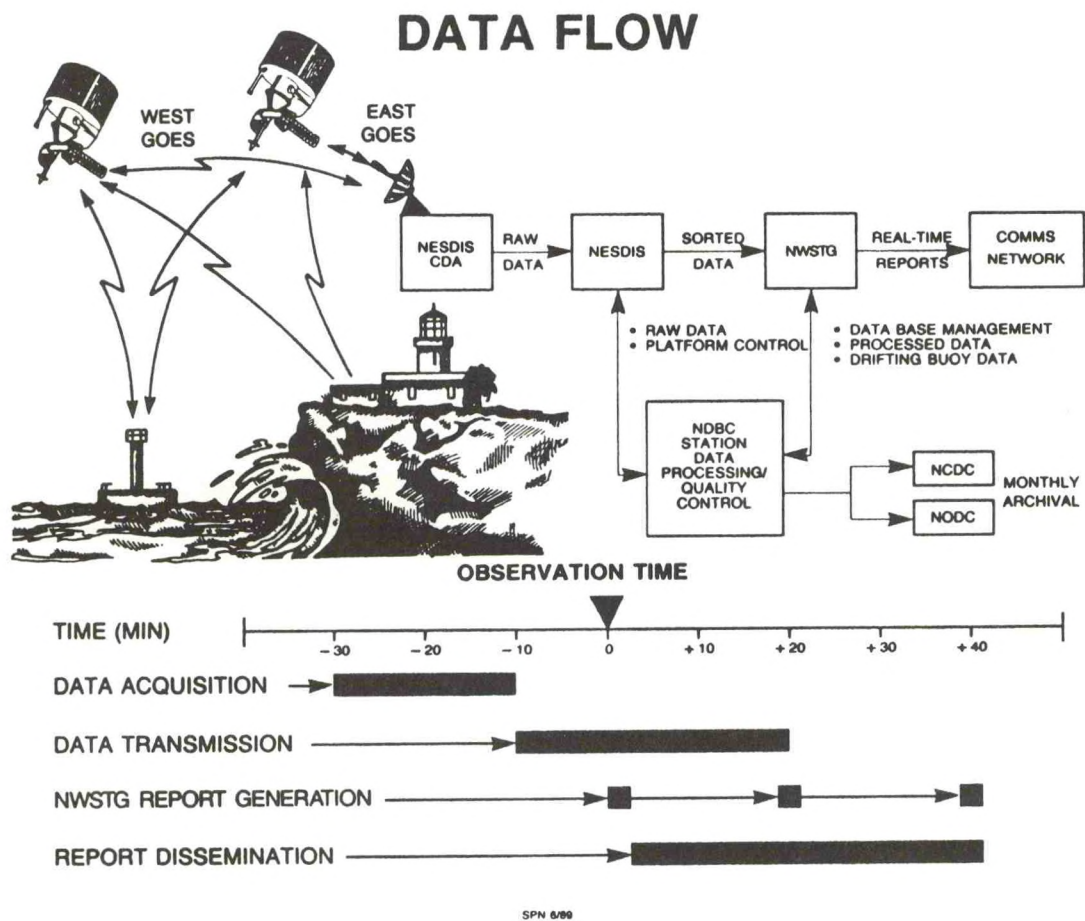


Figure 7. Data flow.

# FIELD WAVE GAGING PROGRAM: A CONSPECTUS

David D. McGehee, PE  
U.S. Army Corps of Engineers  
Coastal Engineering Research Center  
Vicksburg, MS 39180-0631

## Introduction

The need for quality, long-term wave data comparable to data routinely available for other natural phenomena has been recognized by the coastal engineering community and expressed by leaders in the field. A better understanding of coastal wave conditions is needed to cope effectively with increasing competition for coastal resources and to avoid costly mistakes. Past gaging efforts emphasized deepwater measurements or have been too site specific and brief to provide reliable climatological statistics. With the establishment of the Field Wave Gaging Program (FWGP), the U.S. Army Corps of Engineers initiated collection of long-term, nearshore wave data that are necessary for planning, design, construction, operation, and maintenance of coastal projects.

The objective of the FWGP is to collect and analyze wave data from around the U.S. coastline in order to contribute to a national wave climatology. A data base consisting of wave measurements, and numerically-generated wave hindcasts (calibrated and verified by those measurements), will allow reliable predictions of wave conditions for any place on the U.S. coastline.

In 1975, the Corps established the Coastal Field Data Collection Program (CFDCP), with separate elements for (1) numerical wave hindcasts for all U.S. coastlines (Wave Information Study (WIS)); (2) Littoral Environmental Observations (LEO); (3) a data base management system (Coastal Engineering Management Information System (CEMIS)); (4) measurement of conditions during episodic events (Episodic Events Program (EEP)); and (5) the FWGP (Hemsley and Brooks, 1989). That same year, the Scripps Institution of Oceanography (SIO) initiated a regional gaging network for the State of California and the National Sea Grant Program. Through continued support from the State of California and the Corps, it evolved into the Coastal Data Information Program (CDIP), a real-time reporting network of, at present, 20 gages on the West Coast and Hawaii that has been part of the FWGP since 1977 (Seymour et al., 1985).

A similar network now part of the FWGP was begun by the University of Florida (UF) in 1977 under sponsorship of the Nuclear Regulatory Commission to obtain storm surge and wave measurements. Continued support by the State of Florida and the Corps has resulted in the Florida Coastal Data Network, with nine real-time gages along Florida's East and Gulf Coasts (Howell, 1980).

The third regional network incorporated into the FWGP is the Alaska Coastal Data Collection Program (ACDCP), which derives additional support from the State



Department of Transportation and Public Facilities (DOT/PF). Three ACDGP sites use meteor burst transmission from Datawell Waverider buoys to overcome unreliable telephone links and long distances.

Recent development of buoy-mounted directional wave measurement capability by the National Data Buoy Center (NDBC) has spurred inclusion in the FWGP of intermediate-depth sites to supplement the nearshore gages. Full or partial support for ten NDBC buoys is provided by the Corps.

Finally, an "in-house" gaging effort is carried out by the U.S. Army Engineer Waterways Experiment Station's Coastal Engineering Research Center (CERC), the entity charged with management of the FWGP as well as advancing the arts of wave gage technology, wave data analysis, and wave information management. Presently, seven CERC-developed directional gages are deployed on the East and Gulf Coasts and provide real-time data on a regular schedule.

The existence of the regional networks has provided a firm foundation for the continued expansion of the FWGP toward its goals, with over 300 gage-years of data collected and reported to date. Current projections call for operation of 80 gages around the U.S. coastline within 5 years; however, coordination with other federal and local needs could bring the total to well over 100.

## Approach

Validation of wave propagation and transformation models will be emphasized in future expansion of the network. The existing deepwater NDBC buoys will provide pressure and wind fields over the open ocean. Intermediate-depth "index" sites will provide directional energy spectra of the incident waves on a region of coastline defined by geomorphic or bathymetric boundaries. Index gages will be maintained indefinitely to allow direct observation of normal and extreme climatic conditions. Within a region, nearshore gages will be deployed for several years to calibrate and verify local refraction, diffraction, sheltering and shoaling models.

Priority will be given to existing and planned Corps projects in siting nearshore gages. A survey of all of the Corps' coastal Districts and Divisions was conducted to identify and evaluate their data needs. The result was a list of 241 sites where data were needed to provide guidance in planning, design, or operation of proposed and existing projects. Selection of gage sites will be based on Division priorities, utility for model input, and technical/logistical constraints. A Five-Year Gage Deployment Plan will be prepared and updated annually.

Presently, data products are procured from sources such as SIO through contracts. The potential benefit of these products to the general public and the interest from state and local agencies in acquiring them have prompted the Corps to investigate federal/state cooperative agreements as the more appropriate



mechanism. Federal funds, coming through the FWGP, would be combined with state funds to obtain specific data products from regional operators. The operator may be a state agency, a federal agency, or a private company, depending on the particular task and locality.

## Data Collection

Though they share many attributes, the networks at SIO and UF evolved with different features, reflecting different missions and environments. Both use bottom mounted pressure sensors to detect water level. The signal is sent over a submarine cable to a shore station where a phone data-link connects each gage to a central collection computer. Gages are automatically polled at 3-to-6-hour intervals. Spectral analysis of the pressure signal provides wave parameters.

In Florida, the requirement to obtain surge levels during hurricanes and survive encounters with fishing trawlers dictated a low-profile, single pressure gage design with internal power and memory that can be activated in a "storm mode." Directional wave information and mean currents are obtained from an electromagnetic current meter. On the West Coast, the higher and longer waves, relatively smooth bathymetric contours, and the absence of bottom-trawling allowed use of a larger (10 meter), multi-sensor slope-array. Analysis provides a spectrum of the longshore component of the radiation stress, which, with the energy spectrum from any one sensor, provides estimates of directional spectra.

The CERC directional wave gage (DWG-1), presently under development, will combine features from both types. It uses highly accurate quartz pressure transducers in a short baseline (1 meter) slope array. Internal power, memory and data processing permit untended deployments of up to a year, while retaining the option of real-time data access through a cable. Up to five other channels are available to measure currents, temperature, etc., as required. Sampling schemes are remotely programmable, allowing, for example, more frequent polling during storms, or longer samples to detect tsunamis. Tidal elevations would normally be obtained.

## Reporting

Data from the SIO, UF, Alaska and CERC network are published in monthly reports containing spectral energy density, significant wave height and dominant period for each sample. SIO publishes annual reports that calculate monthly and yearly statistical parameters. Climatic summaries are in the planning stage for those areas that have accumulated ten or more years of measurements.

Another work unit in the CFDCP is developing a data base management system that will combine data from all sources in a major region, including FWGP, NDBC, and hindcasts, onto a single compact disc-read only memory (CD-ROM). Users will be able to access standard reports, statistical summaries, and comparison results



or input the data files into the Automated Coastal Engineering System (ACES) for design calculations (U.S. Army Corps of Engineers, 1990).

### **Other Activities**

Operation of a national gaging network requires utilization of the latest advances in instrument design, signal telemetry and processing, and data base management. The FWGP supports research, development or documentation of several efforts in these arenas. The CERC Wave Data Analysis and Reporting Standard is being written to assure quality and uniformity of products from various sources. A workshop was held on Gage Site Selection Criteria to document the process of efficiently and reliably placing nearshore gages. The Prototype Measurement and Analysis System will allow automation of data collection, analysis and reporting, as well as integration of management, logistic and fiscal activities using relational data base software.

### **Conclusions**

The U.S. Army Corps of Engineers has successfully operated a national wave gaging network for over 15 years, building a data base of over 300 gage-years, as well as considerable technical expertise. The Corps has a long-term commitment to expanding this network into nationwide coverage. Developments in data-collection technology and information management are being pursued to permit efficient and rapid dissemination of the data within and outside the Corps.

### **Acknowledgements**

The work described in this paper was conducted as part of the Coastal Field Data Collection Program of the Coastal Engineering Research Center, Waterways Experiment Station, U.S. Army Corps of Engineers. Permission to publish this paper was granted by the Chief of Engineers.

# THE ROLE OF THE MODERNIZED NATIONAL WEATHER SERVICE IN THE DEVELOPMENT OF A COPS

Stephen T. Rich  
NOAA/NWS Southern Region Headquarters  
Fort Worth, Texas 76102

## Introduction

The National Weather Service (NWS) has embarked upon a very ambitious and far-reaching modernization program which will continue through the 1990s. This program will include major restructuring of the NWS field organization in order to take advantage of recent advances in our ability to observe and understand the atmosphere. Tremendous improvements in data processing and communications technologies will also play a key role in making the Modernization and Associated Restructuring (MAR) possible. The new observing systems and other technologies that will be a part of the modernized NWS will play an important role in the development and implementation of any future Coastal Ocean Prediction System (COPS), although their primary purpose is to greatly improve the basic forecast and warning capabilities of the NWS.

The NWS MAR involves several major programs which will result in improved quality and timeliness of atmospheric observations, along with increased resolution and vastly greater volumes of data (including new types of data that have never before been available in the operational environment). The primary new observing systems are: ASOS (Automated Surface Observing System); NEXRAD (Next Generation Weather Radar); GOES I-M (the upgraded Geostationary Operational Environmental Satellite series); and the wind profilers (ground-based atmospheric sounding systems utilizing Doppler radar technology). NEXRAD and ASOS are actually tri-agency programs (Departments of Commerce, Defense and Transportation).

The tremendous amounts of new data would be of very limited practical use without adequate processing and communications capabilities. AWIPS-90 (Advanced Weather Interactive Processing System for the 1990s) is the integrating element of the MAR, and will be linked with the NOAAPORT satellite communication system that will disseminate data collected and processed by AWIPS, and products generated by AWIPS.

This paper briefly summarizes these systems, with emphasis on their potential roles in satisfying the needs of future coastal ocean prediction models. In addition, mention will be made of a few other systems and programs, both current and future, which should be of varying degrees of interest to those desiring to obtain data relevant to the modeling and/or forecasting of coastal ocean circulations.



## Observing Systems

NEXRAD: This is the network of advanced Doppler radars that will provide measurements of atmospheric motions in addition to conventional reflectivity. The NWS will operate approximately 120 systems, while the Federal Aviation Administration (FAA) and Department of Defense (DOD) will operate about 40. The NEXRAD system will generate numerous products which will be of great benefit in detecting and tracking severe and potentially severe storms, but which will have many other uses as well (estimates/measurements of precipitation accumulation, atmospheric turbulence, wind shear, etc.). Of particular interest to the marine community will be the Velocity Azimuth Display (VAD) winds product from the approximately 30 coastal NEXRAD sites. A vertical profile of winds can be produced and displayed each time the radar makes a volume scan. The system then combines measurements of wind speed and direction from several elevations and times, and generates a time versus height cross section of wind vectors. Spatial resolution is dictated by data spacing in range, azimuth, and elevation. Doppler velocity data will be available at range intervals of 0.25 km.

One of the primary anticipated uses of the VAD winds product is the timely determination of the boundary layer wind profile (which could aid in the computation of surface wind stresses over parts of the coastal ocean). The usefulness of the VAD winds in this regard will depend on such factors as the thickness of the marine layer and the presence of enough tracers to produce a measurable return. Coherent clear air return can extend to ranges of 30 to 50 nautical miles, but boundary layer measurements will be severely limited by the elevation angle of the radar beam. For example, with an elevation angle of  $0.5^\circ$  the height of the radar beam above the surface will be around 2,000 ft at a distance of 30 nautical miles from the radar.

ASOS: This system will take advantage of new sensor and computer technology developed over the past decade, making feasible the automation of the nation's surface weather observations. ASOS will allow the NWS and FAA to meet increasing demands for airport weather observations without adding staff. The system will provide quality, nearly continuous information on present weather: pressure, temperature, dew point, visibility, wind speed and direction, cloud coverage and heights, and precipitation types and amounts.

ASOS will observe, archive and transmit observations automatically, operating with or without observers. Over 1,000 systems will be acquired jointly by the NWS (~250), the FAA (~750), and the Navy (~85). ASOS will provide vital and accurate information for forecasters, pilots, air traffic personnel and others, and will provide it at many small airports and other locations where no such data are currently available.

ASOS will provide a significant increase across the country in the number of locations at which surface weather observations are available. A large number of these sites will be on or near the coast, which will increase the amount of



coastal surface weather data (relative to the present) available for use in developing a coastal ocean prediction system.

**GOES I-M:** Meteorological satellites have provided reliable information for many years and are practically indispensable to the science and practice of meteorology. Future satellites will provide significantly improved information. In the early 1990s, the National Oceanic and Atmospheric Administration (NOAA) will launch GOES-I, the first of a new generation of geostationary environmental satellites. After the launch of GOES-I, launches of GOES-J, GOES-K, GOES-L and GOES-M will follow at approximately two-year intervals.

Operational improvements will include an increased total number of images and soundings, more accurate soundings, increased resolution of infrared images and soundings, more frequent data transmissions, more viewing channels and a longer operational lifetime. The new satellites will have separate imaging and sounding instruments, instead of the current situation where a single instrument shares these responsibilities. However, all of these improvements may not be available on the first two satellites in the GOES I-M series.

The imager will be able to view in five channels at the same time. The channels will include one visible, two infrared (IR), one thermal window and one IR water vapor channel. The IR channels and thermal window will improve from the current 8km resolution to 4km (at the sub-satellite point), and the water vapor channel resolution will improve from 14 to 8km. The products derived from the imager will include at least two that will be of interest to ocean modelers -- low level winds and sea-surface temperature composites.

The sounder on GOES I-M will be able to scan at the same time the imager is scanning, and will scan in more channels more quickly than the current sounder. The soundings will have improved accuracy and resolution, and will result in a number of products, including temperature and moisture profiles.

The NWS currently uses observations from Voluntary Observing Ships (VOS) and NDBC buoys to acquire data on winds and seas. The United States is planning to obtain remotely sensed wind, wave and sea-ice measurements from the European and Japanese polar orbiting satellites (ERS-1 and JERS-1) in the early 1990s. These satellites will carry Synthetic Aperture Radars (SAR) which will provide these measurements in all weather conditions. Similar technology is planned by the National Aeronautics and Space Administration (NASA) for the mid to late 1990s through the Earth Orbiting System (EOS) Polar Platform. NWS operations in the 1990s envision the use of these instruments for improving ocean forecast guidance at the National Meteorological Center (NMC) as well as contributing to a better understanding of air-sea interaction on both regional and global scales.

**WIND PROFILERS:** These are multiple-beam Doppler radar systems that detect atmospheric density fluctuations caused by the turbulent mixing of volumes of air with slightly different temperature and moisture content. The fluctuations are



used as tracers of the mean wind in the clear air. However, the profilers can also operate in the presence of clouds and precipitation.

The profiler radars reflect their energy off fluctuations created by turbulent eddies in the radio refractive index. The system then converts these signals to wind vectors. The NWS is currently in the early stages of deploying a 30-station Wind Profiler Demonstration Network (WPDN) across the central U.S. Future deployment of profilers will depend upon results from the WPDN experiment. Unfortunately, none of the WPDN profilers will be located near the coast.

Also, one factor limiting the applicability of future wind profiler data to the modeling or prediction of coastal ocean currents will be the system's inability to measure winds below 500 m (due to internal electronic constraints). It is stressed that profilers will only supplement--not replace--radiosondes, since the wind profiler cannot measure temperature and moisture profiles.

AWIPS-90/NOAAPORT: When the NWS MAR is completed, the AWIPS system at each Weather Forecast Office (WFO) will integrate data from all the new sources and present the data to the forecaster as coherent information on a common display. AWIPS will provide interactive techniques to analyze and present weather information and to prepare forecast products.

The AWIPS/NOAAPORT communications network will support the prompt distribution of data, analyses and forecast products to all NWS and NOAAPORT users.

There are a number of other NWS programs and products which could play an important role in a future COPS. Several of these are considered briefly below.

The Coastal Marine Automated Network (C-MAN) program provides the NWS with reports from about 55 coastal stations which include U.S. Coast Guard (USCG) unmanned offshore platforms and lighthouses, offshore oil platforms, beach areas, and navigational buoys. The data flow through a high-speed collection network to NWS, which disseminates the reports through the automation of field operations and services (AFOS) communications system.

In addition to the C-MAN sites, the NWS has equipped a number of offshore platforms with automated observing devices. Negotiations with the petroleum industry in 1979 led to the organization of the Gulf Offshore Weather Observing Network (GOWON) off the Louisiana and Texas coasts. Data from GOWON are collected by NWS from the oil companies via several computer interfaces, and have greatly helped the NWS monitor weather conditions in the northwest Gulf of Mexico.

The Voluntary Observing Ship (VOS) program mentioned above includes more than 1800 participating ships from 54 countries. The VOS produces over 100,000 surface synoptic observations each month. VOS ships report the standard atmospheric variables, and some also report oceanic variables such as subsurface



temperature, ocean current data, salinity and oxygen content. The ship reports are sent to collection centers for ultimate transmission to the NMC, using a wide spectrum of methods ranging from voice radio transmissions and Morse code to satellite transmissions.

An NDBC system of about 20 Deep Ocean Moored Buoys (DOMB) reports wind, pressure, air temperature, sea-surface temperature and wave spectra in areas seaward of the continental shelf in the Atlantic and Pacific Oceans, the Gulf of Mexico, and the Great Lakes. About 35 buoys within 150 km of the shore provide these measurements for coastal forecasters.

The operational global spectral models which are run at NMC produce numerical guidance used to generate forecasts of certain variables of marine interest. Although the resolution of the operational numerical models is too coarse to handle these variables in the boundary layer over the ocean surface, additional physical and statistical relations are applied to the numerical model forecasts to derive ocean surface forecasts. Some of the current NMC forecast variables of interest to ocean modelers include surface wind stress, sensible and latent heat flux, radiative heat flux and a 10 m wind forecast (which can be compared with wind observations from ships and buoys). The 10 m wind forecasts are derived on a 2.5 X 2.5 latitude/longitude grid.

The NOAA ocean wave model (NOW) runs once a day with forcing provided by boundary layer winds from the operational global spectral model. Spectral estimates are available on a 2.5 X 2.5 latitude/longitude grid from 70°S to 70°N. In 1988, the NOAA regional ocean wave model (NROW) was implemented. This model is applicable to both deep and shallow waters of the Gulf of Mexico. Unlike the global model, the NROW accounts for the effects of bottom topography on the wave field. Daily forecasts are made on a grid mesh of 53 km at 3 hr intervals out to 48 hours.

Future numerical systems will include a global model with more levels in the boundary layer. The horizontal resolution is a guess, but with an additional order of magnitude in computer power, the current 80 wave resolution of the global spectral model should at least double. By 1992, experiments will have begun on coupled ocean/atmosphere prediction based upon research accomplished at the Geophysical Fluid Dynamics Laboratory (GFDL) and elsewhere. Improvements will be made in procedures to define initial heating rates and divergence fields in areas of tropical convection. In addition, plans call for the implementation of the GFDL hurricane model on the next generation NMC computer.

Current limitations in disk storage space prevent NMC from archiving much of the boundary layer output from the models, although some archiving is being done at NMC's Climatic Analysis Center in connection with some ocean modeling efforts there. Also, near-saturation of the NWS AFOS communication system prevents most of the output from being disseminated beyond NMC. In other words, most of this output is currently discarded, but this could change if there were sufficient demand for it, say, on the part of the ocean modeling community.



To handle the new data systems planned for the 1990s--NEXRAD winds, profiler winds, GOES I-M data, an increase in aircraft winds, etc.--NMC will soon need to implement a system for regional assimilation of high-time-resolution data over the U.S.

Examples of other NWS programs or products that could be of use in developing a COPS include the Sea, Lake and Overland Surges from Hurricanes (SLOSH) model, and experiments such as the Gulf of Mexico experiment (GUFMEX), the Genesis of Atlantic Lows Experiment (GALE), and the Experiment on Rapidly Intensifying Cyclones Over the Atlantic (ERICA).

SLOSH is a diagnostic model that computes a wind field and associated surface stresses, given specified input on a hurricane's track, size and intensity. The National Hurricane Center (NHC) has conducted numerous simulation studies for basins along the Atlantic and Gulf coasts in order to estimate maximum possible storm surges for various scenarios of hurricane strength and movement.

GUFMEX was a brief field experiment conducted from February 20 through April 2, 1988. Atmospheric and oceanic data were collected using the NOAA P-3 aircraft, ships and oil rigs, special rawinsonde and Cross-Chain LORAN (Long-Range Aid to Navigation) Atmospheric Sounding System (CLASS) ascents, and airborne expendable bathythermograph (AXBT) measurements. The purpose of the experiment was to provide data for studies of Gulf of Mexico return flow dynamics in the late winter and early spring, when polar air of Pacific or continental origin pushes into the Gulf of Mexico and subsequently returns northward.

In 1986, GALE investigated the atmospheric processes at work during cyclogenesis over the southeastern U.S., paying particular attention to the mesoscale and air-sea interaction processes associated with cyclone development. Sensors used in the experiment included rawinsondes, Doppler and conventional radars, satellites, dropsondes, ships, automated mesonet stations, buoys, instrumented towers, and research aircraft.

The Office of Naval Research (ONR) recently organized ERICA. This experiment focused on improving the understanding and forecasting of intense storms that develop off the U.S. and Canadian coasts in winter. NOAA and NWS gave considerable support to this project, which used equipment similar to that used in GALE.

Projects and experiments similar to these will undoubtedly continue as the NWS modernization program gets into full swing. As a result of the modernization itself, the NWS will have access to tremendously greater amounts of data than have ever before been available. The oceanographic community will also be able to take advantage of much of the new data in developing a coastal ocean prediction system during the next few years. There will be a need for coordination between the NWS and the oceanographic community as these developments take place.



# RESEARCH OBSERVING AND DATA SYSTEMS

Wendell S. Brown  
Ocean Process Analysis Laboratory  
Institute for the Study of Earth, Ocean and Space  
University of New Hampshire  
Durham, NH 03824

## Introduction

The Ocean Descriptive-Predictive System as described by Robinson and Walstad (1987b) (Fig. 1) is the pertinent context for a Coastal Ocean Prediction System (COPS). In such a scheme, a whole suite of ocean observations (Fig. 2) may be used in driving statistical and dynamical models for simulations and predictions. Both ocean and meteorological observations are needed to specify open boundary and initial conditions for model hindcasts, nowcasts and forecasts of ocean fields for the domain of interest. Ocean predictions are derived by optimizing a combination of fields predicted by data-driven dynamical and statistical models. The quality of the predictions are assessed through comparisons with observations.

A coastal ocean observing system suitable for COPS must resolve pertinent space/time scales, spatially integrate the fields where desirable and possible, and be synoptic, real-time, highly reliable, and inexpensive. With these criteria as a framework, we review the existing research observing systems which should be considered for incorporation into COPS. Both coastal and deep ocean observing systems will be reviewed because a COPS system will require information in the shallower water of the shelf as well as at the seaward boundary of any coastal domain of interest.

Long-term measurement systems for COPS are likely to be based on differing configurations of conventional ocean observation instrumentation. Aircraft, satellite, and acoustic observing systems represent powerful new approaches for obtaining remotely sensed data over large domains. Inexpensive expendable instruments will be important for obtaining more synoptic data sets from ships and airplanes. Measurements, which integrate over some of the fine-scale variability in the environment (such as Doppler current and pressure), are particularly well matched to the model-derived oceanic fields. The prediction mission of COPS will require real-time telemetry of all oceanic observations to a central site, where data quality will be assessed before data is assimilated into models.

## Data Telemetry

COPS will require a comprehensive and reliable real-time data acquisition system to function. The National Weather Service (NWS) of the National Oceanic and Atmospheric Administration (NOAA) already has an operational system of National Data Buoy Center (NDBC) ocean buoys (Fig. 3) and island-based Coastal-Marine



Automated Network (C-MAN) stations (Fig. 4) which provide real-time meteorological and limited oceanographic information to interested users. While significant elements of the technology are available, data telemetry had been viewed as a luxury to research physical oceanographers. Hence, the available technology has not been exploited to its fullest potential. The most successful applications of telemetry, to date, have used a satellite to link ocean surface platforms with/to laboratories (Fig. 5). Real-time acoustic data transfer from the interior ocean to a surface receiver/transmitter has been used in only a handful of cases.

The different moored data telemetry schemes employed by research oceanographers to date have depended primarily on the use of hardwire data transfer (Fig. 6) to the surface and either satellite or radio frequency data transfer to the laboratory (Irish et al., 1987; Brooks, 1984). For the coastal ocean, where surface buoy protection of subsurface instrumentation is required, a hardwire link to the surface (Fig. 4) has been shown to be quite cost-effective (Wood and Irish, 1987). An acoustic link is necessary for the telemetry of data from independent subsurface instrumentation to the surface. Perhaps it will not be too long before a "master" surface receiver/transmitter buoy will be able to telemeter ashore the data received acoustically from a whole array of underwater instruments.

It is not always feasible to maintain permanent surface buoys for data telemetry purposes. Perhaps one of the delayed-time telemetry schemes presently being developed will be used to obtain data occasionally. A Telemetering Lagrangian Capsule (TLC), presently being developed by Irish and Pettigrew at the University of New Hampshire (UNH), is a glass sphere encapsulated device into which data are transferred before being released (by timer or upon command). Once the TLC is at the surface, the data are transferred ashore via ARGOS while the TLC becomes an ARGOS-tracked surface drifter. Another possible delayed-time telemetry scheme worth developing involves a subsurface data-acquisition buoy which could be interrogated acoustically by a ship or a modified air-deployed "sonabuoy."

### Eulerian Current Measurement Systems

A variety of current measurement systems will be employed by COPS to measure the current and transport fields. The list in Figure 7 outlines the possible candidate systems. Moored current systems, akin to that used during the Coastal Ocean Dynamics Experiment (CODE) (Fig. 8), will employ conventional current meters which are selected for performance, cost-effectiveness and reliability. One of the more promising new current sensors is the newly available Doppler Acoustic Profiling Current Meter (DAPCM) or, alternately, Acoustic Doppler Current Profiler (ADCP). The time-gated, Doppler-shifted, backscattered signal provides time series of the vertical structure of horizontal current vectors averaged in layers throughout all of the water column except the near surface and near bottom layers. The DAPCM can be deployed in a number of different mooring configurations (Fig. 9) to maximize its ability to measure current structure in the water column. The DAPCM is being (a) evaluated as a vertical velocity sensor and (b) adopted in a downward-looking mode of operation.



The Coastal Radar (CODAR) system has been employed for remotely measuring surface currents over extended coastal regions. CODAR irradiates the coastal ocean within several tens of kilometers off the coast and uses backscattered signals and some assumed properties of the surface waves to infer time series of surface current distribution. The Janopaul and Frisch (1984) application to the northern coast of the Alboran sea is shown in Figure 10. The advantages of CODAR include the land-basing of the radar stations, a gridded coverage of a significant area of the coastal ocean, and the real-time data acquisition possibilities. On the down side, the measurement is restricted to surface currents only and coverage that varies diurnally. While this system shows promise for COPS application, it requires further evaluation.

### Lagrangian Current Measurement Systems

Lagrangian current measurement systems will be an important part of any COPS plan, because they provide both surface and deeper information on water parcel trajectories and speeds. Drifting instruments define frontal convergences in ways moored arrays cannot. The composite of commercially available surface drifting measurement systems (Fig. 11) depict a typical ARGOS-tracked air- or ship-deployed surface drifter system with its real-time capability. The disadvantage of the existing ARGOS system is its cost. The so called "Davis" drifters (Fig. 12), which can also be air- and ship-deployed, are less expensive, allowing more dense "seedings" of drifters required for some coastal research. Such a seeding helps to define a jet offshore of Point Arena during the Coastal Ocean Dynamics Experiment (CODE) (Fig. 13).

### Shipboard Current Measurement Systems

Shipboard systems can provide detailed three-dimensional structure of currents in regions of complex oceanic circulation patterns (e.g., eddies, fronts, etc.). The Doppler Acoustic Log (DAL) has become one of the more effective shipboard survey tools (Fig. 14). (Despite the different acronym, this is just a hull-mounted DAPCM.) The advantage of this system is its ability to map current structure over extensive areas. The disadvantage is that, because of ship motion, absolute DAL current determinations are noisier than moored DAPCM measurements. Presently under development are towed DAL systems, which are, in principle, subject to less noise than hull-mounted systems. Combined conductivity/temperature/depth Profiler (CTD) and DAL current measurements have begun to provide more accurate property transport estimates than were heretofore available. DAL observations are also variable in the interpretation of satellite infrared (IR) observations (Fig. 15). One of the disadvantages of using the DAL system for the deeper offshore currents is its depth limitation of about 250 m.

Deep current profiling systems will be required in the ocean beyond the shelf over the slope. The Pegasus system (Fig. 16; Spain et al., 1981) is a ship-deployed system worth exploring for offshore COPS current profiling. The system employs a



pair of moored bottom transponders, which in "conversation" with the falling Pegasus are used to determine its three-dimensional position versus time. Current profiles can be obtained at the transponder sites many times over the 3+ year lifetime of the bottom transponders. The disadvantages of this system are the cost of the Pegasus instrument and the relatively long time it takes to obtain a single current profile (e.g., 4 hours per 4 km cast). Less time consuming adaptations of this technology are being researched.

Alternatively, Sanford (1986) has developed a suite of current measurement devices based on electromagnetic (EM) properties of the ocean (Fig. 17). Velocity shear profiles are obtained with Expendable Current Profilers (XCP) which measure the electric field structure of the ocean. Absolute surface currents are monitored using a drifting EM buoy, radio telemetry link, and good navigation. A Towed Transport Meter (TTM) combines observations of the three-axis electric field and other ocean variables including pressure, temperature, conductivity and current for estimating transport.

### Water Property Measurement Systems

Water temperature and conductivity measurements are basic physical oceanographic observations used for calculating salinity and density and tracing water masses in both the coastal and the deep ocean. Geostrophic shear can be inferred from the dynamic height maps produced by shipboard surveys. Shipboard CTD profiling is often augmented by expendable bathythermograph (XBT) profiling measurements to provide more spatial resolution to the three-dimensional, quasi-synoptic maps of temperature distribution. Air-deployed expendable bathythermographs (AXBT) provide more synoptic maps, but have somewhat limited use in the coastal zone, where salinity can often have a significant effect on density. The availability of Sea Bird conductivity sensors has made accurate moored temperature and temperature/conductivity measurements possible. Time histories of water properties from moored CTD chains, including dynamic height, at a few "critical" locations in a particular region can now be used to augment CTD surveys. More recently, satellites (and airplanes) have been providing remote IR imagery which, when available, provides very valuable, truly synoptic pictures on the structure of the surface temperature fields.

Moored temperature chain arrays are relatively inexpensive and useful in defining the variability in the thermal structure. In regions where salinity defines a significant portion of the density variability, it is advantageous to deploy arrays of temperature/conductivity (T/C) chains (Fig. 18). T/C chains monitor salinity and density variability. The temperature/salinity (T/S) time series can be used to monitor water mass variability (Fig. 19). The development of a moored oxygen probe (Langdon, 1984) will enhance our ability to monitor water masses in the future.

The Neil Brown CTD system with rosette continues to have the widest use for quasi-synoptic surveys of the coastal ocean. However, that supremacy is now being challenged by a new generation of CTD profilers which are somewhat less expensive and easier to use and maintain (Fig. 20). For example, the Sea Bird CTD profiler



employs conductivity and temperature sensors which are interchangeable at sea. The tradeoff in this case is ease of use and maintenance versus less vertical resolution than is provided by the Neil Brown CTD. Internally recording CTD profilers, now available, permit routine, accurate measurements from ships (or boats) without a conducting wire. The amount of onboard data processing continues to improve as more computer-power is available at sea. Near real-time previewing of contoured sections of different variables is a reality. It is also possible to correct conductivity profile measurements at sea, with use of the accurate onboard salinometers. It is now possible, given the available computing power, to have final data reports in hand upon arriving at the dock after a cruise. The nagging problem with shipboard surveys is their lack of synopticity.

Airplane surveys of sea surface temperature and atmospheric variables (winds, in particular) provide much more synoptic pictures than ship surveys. The airplane survey, shown in Figure 21, covers a larger (25 x 150 km) region over the northern California continental margin and required only a few hours to conduct. (For comparison, it took two to three days to conduct a shipboard CTD survey of the CODE region.) When combined with AXBT measurements (Figs. 22 and 23), airplane surveys can provide 3-D temperature distributions. There is a significant additional advantage to this approach, in that valuable meteorological information pertinent to local forcing is obtained simultaneously. A serious disadvantage of this approach for the coastal ocean is the lack of a useful air-deployed water conductivity profiler (i.e., AXCTD). Development of the latter system should receive the highest priority in COPS.

In the meantime, there is the possibility of mapping surface salinity using airborne, S-band and L-band microwave radiometers (Fig. 24). In the near term, satellite IR imaging will be the most readily available synoptic product in the coastal ocean. Despite the difficulty in using surface temperature, there are many applications where it is very useful in defining the complexity in coastal ocean circulation. Comparison of satellite IR and Davis surface-drifter tracks, (Fig. 25), demonstrates the relevance of the IR imagery in diagnosing the offshore jet in the California transition zone.

### Pressure/Sea Level Measurement Systems

Pressure field observations provide an integrated view of the ocean because it is the pressure gradients which dictate and control ocean flow response. Surface tides are expressed clearly in ocean pressure or sea level observations. Internal tides reveal themselves in temperature and salinity observations. At subtidal frequencies, across-shelf pressure differences can be used to monitor fluctuations in the quasi-geostrophic alongshelf transport. Subtidal water column pressure fluctuations are the sum of contributions from a variable density field, sea level and atmospheric pressure. Oceanic pressure field is determined by combining bottom pressure measurements with pressure differences derived from water column temperature and conductivity measurements (Fig. 18). When full water column density-related pressure is subtracted from bottom pressure, a quantity called oceanic synthetic



subsurface pressure (SSP) is formed. Coastal nearsurface pressures can be measured directly by shallow pressure gages; or local atmospheric pressure can be added to and sea level to form coastal synthetic subsurface pressure SSP (or, alternately, adjusted sea level). Coastal and oceanic SSP fluctuation records can be differenced to infer surface geostrophic transport histories (Fig. 26).

The National Ocean Service (NOS) coastal sea level gages are now being used routinely to monitor this whole range of coastal ocean phenomena including tides, coastal-trapped waves, etc. Moored bottom pressure observations are used to augment the coastal network and permit pressure gradient time history measurements. The water column density-induced pressure differences are inferred from moored temperature and temperature/conductivity chains.

One inherent disadvantage in measuring subtidal pressure fluctuations is that pressure gauges are mechanical devices, which undergo strain distortion (i.e., "drift") due to the applied stress of the water column weight. While several different strain-gage type pressure sensors are adequate for tidal bottom pressure measurements, Paroscientific sensors are the only commercially available sensors for making subtidal bottom pressure fluctuation measurements. Generally, the temporal mean of a bottom pressure difference observation is not known *a priori* because depth measurements are not accurate enough. In principle, bottom pressures in an across-shelf array can be "leveled" relative to each other by independently measuring the average geostrophic current between pairs of sensors. This has been done using current meter observations in a limited number of cases. With shipboard DAL measurements more widely available, pressure array leveling may become less expensive.

In principle, oceanic sea level distributions are measured directly with satellite altimeters (Fig. 27). A complex set of corrections the raw satellite data is required to derive the oceanic signal. Nevertheless, recent work has shown the usefulness of the sea satellite (SEASAT) and geodetic satellite (GEOSAT) altimetry measurements in inferring near-surface geostrophic flow fluctuations in the deep ocean. Because the signal-to-noise ratio is favorable, the approach is particularly successful for monitoring intense western boundary currents such as the Gulf Stream (Fig. 28). This methodology is difficult to use in the coastal margin because of rapid geoid changes associated with the shallowing bathymetry and the transient difficulty of the radar measurements at the land/ocean boundary. Despite these difficulties, this powerful remote-sensing system is potentially a real-time method and should be explored more fully for COPS use.

For continental slope and deeper ocean waters, bottom-mounted Inverted Echo Sounders (IES) can be used to monitor thermocline displacement. When combined with bottom pressure measurements (Watts and Wimbush, 1981), there is the potential to monitor both sea level and main thermocline fluctuations unambiguously (Fig. 29). A combined system of IES/bottom pressure (BP) on the slope, T/C/BP moorings on the shelf, and satellite altimetry could be a relatively inexpensive way to monitor the shelf/slope geostrophic transport field.



## Meteorological Measurement Systems

NWS priorities have lead to the establishment of the only operational real-time ocean meteorology monitoring system: the NDBC Buoy (Fig. 3) and C-MAN (Fig. 4) systems mentioned previously. Most researchers have used these NOAA observations when possible to characterize both the local and remote meteorological forcing of a particular study site. A notable exception was CODE, during which a "denser-than-normal" array of research meteorological buoys using a newly available suite of meteorological sensors (Fig. 30) was deployed. Presumably NOAA will take advantage of this research in upgrading their operational system. The relatively new Next Generation Weather Radar (NEXRAD) Doppler radar system will begin to measure the wind field over extensive regions of the coastal ocean in the early 1990s. It remains to be seen whether the NEXRAD systems can deliver a wind product of sufficient quality and spatial resolution for COPS purposes.

CODE results show that the coastal wind field had significant spatial/temporal structure which was important to the ocean response. The airborne measurement program (Winant et al., 1988; Fig. 21) provides quasi-synoptic pictures of the pertinent meteorological fields in the marine boundary layer. Bane and Osgood (1989) (Fig. 23) have shown that combined airborne measurements of meteorology and oceanography are crucial to defining air-sea mass momentum and heat exchange. Some combination of airborne, moored, and satellite measurements will be devised for a COPS ocean meteorology monitoring system.

## Long-Term Monitoring Systems

Long-term monitoring of the coastal ocean and atmosphere will be an essential component of COPS if useful predictions are to be made. The practitioners must have a comprehensive understanding of the extreme events and typical interannual variability. This type of information results from long-term monitoring such as that which has been conducted off the Oregon coast by Huyer and Smith (1985) (Fig. 31). Such schemes, however, must include the conditional sampling of high frequency variability which can often be associated with periods of the highest fluxes of momentum, mass, heat, pollutants, etc (Irish, et al. 1984). One solution is to augment the existing NDBC buoy system with a more comprehensive set of oceanographic sensors (e.g., current, temperature, conductivity, and pressure) in order to provide these long-term observations over a sparse array covering the coastal zone. Newly available sensors for making biogeochemical measurements should also be considered in defining a long term coastal ocean monitoring system.

## Biogeochemical Parameter Measurement System

The COPS mission requires a system for observing a critical suite of biogeochemical parameters. Recent developments enable scientists for the first time to obtain moored measurements of oxygen, light intensity, water transparency, chlorophyll, photosynthesis and zooplankton biomass. The time-series measurements



are critically important for the interpretation of the quasi-synoptic ship survey measurements of these parameters. Methods for the airborne and satellite measurement of ocean color provide a powerful means to produce synoptic surface pictures of these complex and highly variable fields.

Suspended organic and inorganic particles in the water column play a critical role in the transport of pollutants. Over the past decade several research groups (Butman and Folger, 1979; Cachione and Drake, 1979; Sternberg et al., 1973) have developed sediment monitoring instrumentation. Bottom tripods (Fig. 32) outfitted with a system of cameras, transmissometers, suspended sediment samplers, current meters, and pressure sensors, have been used to monitor variability in both sediment concentration and the pertinent oceanographic variables. Arrays of these tripods have been part of programs designed to measure bottom stress variability and understand effects on sediment transport and disposition.

Recent years have marked a surge in the development and use of moored sensors for the measurement of the temporal variability of biologically important parameters. Brookhaven National Laboratory (BNL) has embarked on an aggressive effort to develop and implement a system of moored biogeochemical measurements. (Falkowski, this volume, reviews this effort.) Moored systems of oxygen sensors, fluorometers, transmissometers and DAPCMs have been deployed for up to six months. The YSI Instruments pulsed-oxygen sensor is the first practical probe for long-term measurement of oceanic oxygen variability. Its performance is presently being evaluated. Light intensity is being measured with quantum sensors for broad-band radiation and spectral irradiance sensors for narrower-band radiation. Water transparency, measured with Sea Tech transmissometers, is found to be highly correlated with phytoplankton concentration and hence is highly correlated with *in vivo* fluorescence. Fluorometer sensors measure *in vivo* fluorescence, which is related to chlorophyll concentration. Fluorescence measurements are the basis for the Biospherical Instrument and the BNL methods for measuring photosynthesis in "real-time." Both measurements are under evaluation.

In another promising development, oceanographers have begun to use shipboard and bottom-mounted DAPCM technology to measure zooplankton distribution variability. The first direct comparisons between profiles of DAPCM backscatter amplitude and net-tow count structure (Fig. 33; Pettigrew and Irish, 1986; Flagg and Smith, 1989) suggest that the acoustic methods are accurate to within  $\pm 20\%$ .

The Coastal Zone Color Scanner (CZCS)-Chl satellite imagery obtained in the mid-1980s (Abbott and Zion, 1985, 1987; Pelaez and McGowan, 1986) have sparked interest in the potential of this technique for providing data which can be merged with circulation models. CZCS stopped operating in 1986 and there is hope that it will be replaced and upgraded with NASA's Hughes Sea-Wide Field Sensor (Sea-WiFS). Aircraft-borne ocean color instrumentation presently under development, including Light Detection and Ranging (LIDARs), represents great potential in this area.

## Conclusions and Recommendations

We have reviewed some of the observational technologies and methodologies which are pertinent for COPS. While many of the technologies for observational components of COPS exist, their implementation will require a comprehensive effort. Substantial resources are required just to build observation systems with existing technology/methodology.

Further, if COPS is to become a reality, the oceanographic community must commit itself to:

- developing a full suite of "inexpensive" expendable sensors for air deployment;
- establishing an airplane fleet for synoptic surveying of the coastal ocean;
- establishing an array of long-term monitoring stations;
- developing acoustic telemetry links;
- developing acoustic methods for sedimentological and biological monitoring; and
- developing moored sensors for monitoring of other critical biogeochemical parameters.

I encourage the participants of this workshop and ensuing ones to debate issues raised by this and other papers in this volume, and thereby move the community toward a scientifically and technically well-founded Coastal Ocean Prediction System.

## Acknowledgements

This paper benefited from the many times unrecognized creativity and effort of the ocean instrumentation development and implementation community. In particular, I am grateful for the many hours of stimulating conversation on these topics with James D. Irish, Neal R. Pettigrew, Clinton D. Winant, William C. Boicourt, Bruce Magnell, and numerous others with a love for making ocean observations. This work was funded, in part, by NSF grant OCE-8818060.





# OBSERVATION INFORMATION for a COASTAL PREDICTION SYSTEM

## PARAMETERS:

Currents  
Temperature  
Salinity  
Density  
Pressure/Sea Level  
Wind Stress  
(& Other Surface Fluxes)  
Bottom Stress  
Sediments  
Chemicals  
Biology

## TYPES:

- Model Boundary
  - Coastal
  - Across Shelf/Slope
  - Seaward
  - Surface
  - Bottom
- Interior
  - Model Initialization
  - Model Update
  - Model Verification

Figure 2. Ocean information for a Coastal Ocean Prediction System (COPS).



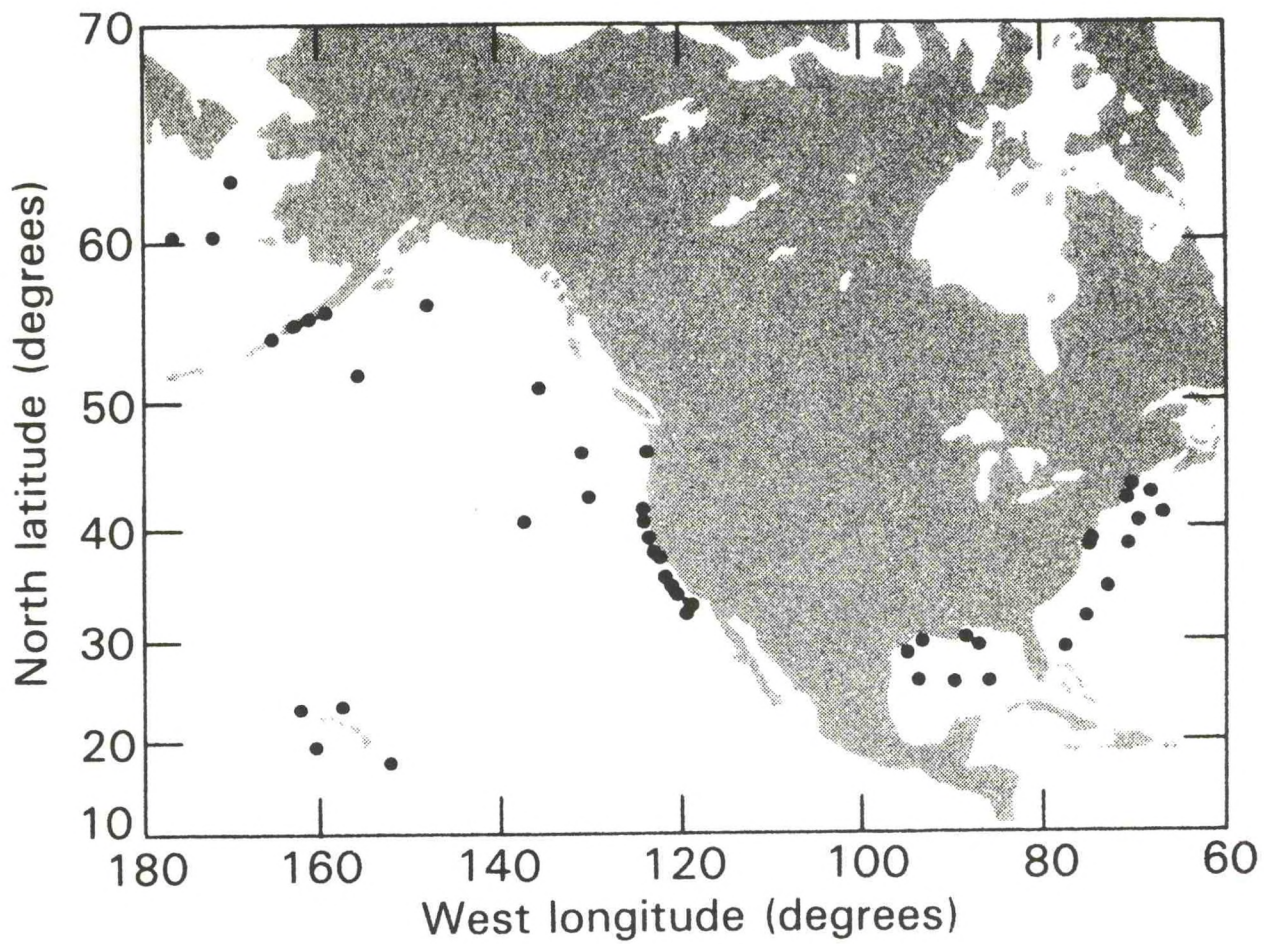
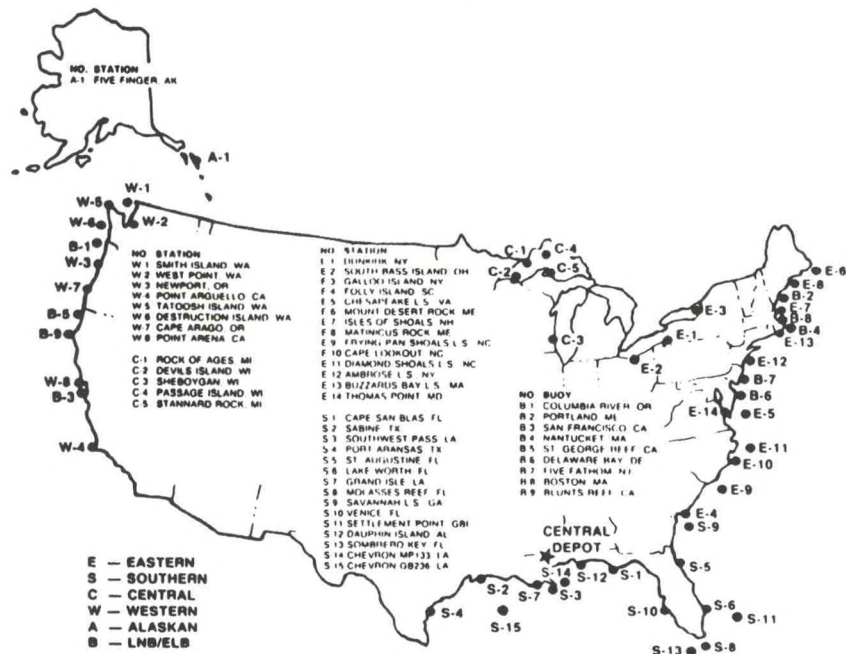


Figure 3. Buoy network of the National Data Buoy Office.

## C-MAN SITES



## DATA FLOW

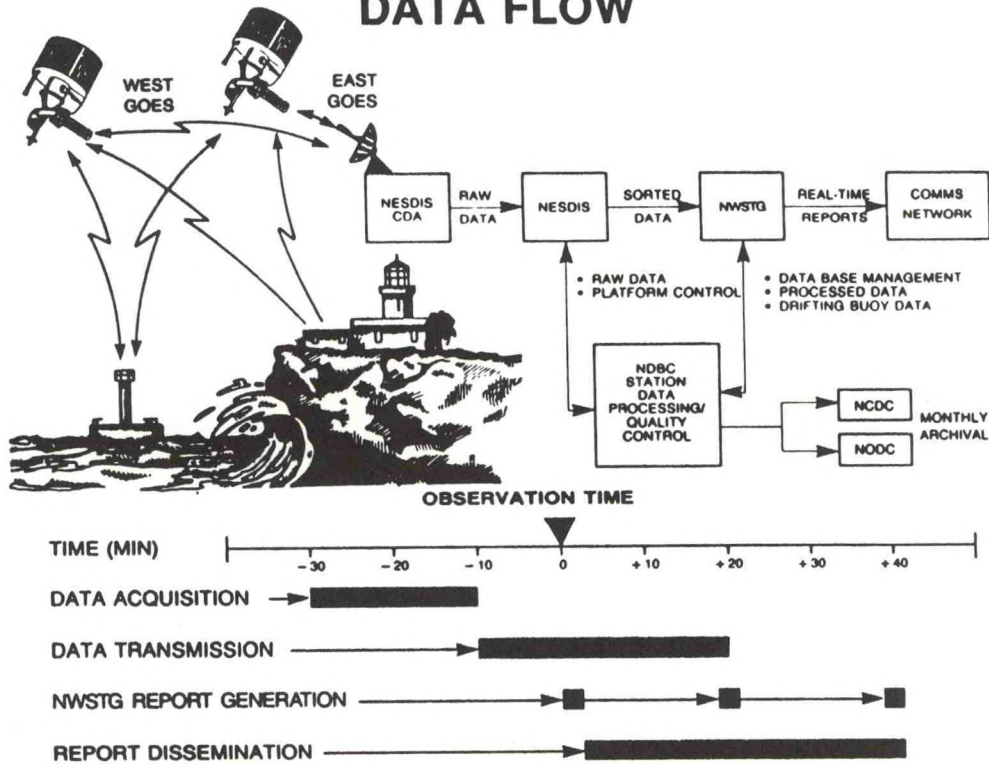


Figure 4. (a) C-Man real-time meteorological observation station distribution. (b) The NDBC real-time data acquisition system (Hamilton, 1990).



# TELEMETRY SYSTEMS

## SURFACE

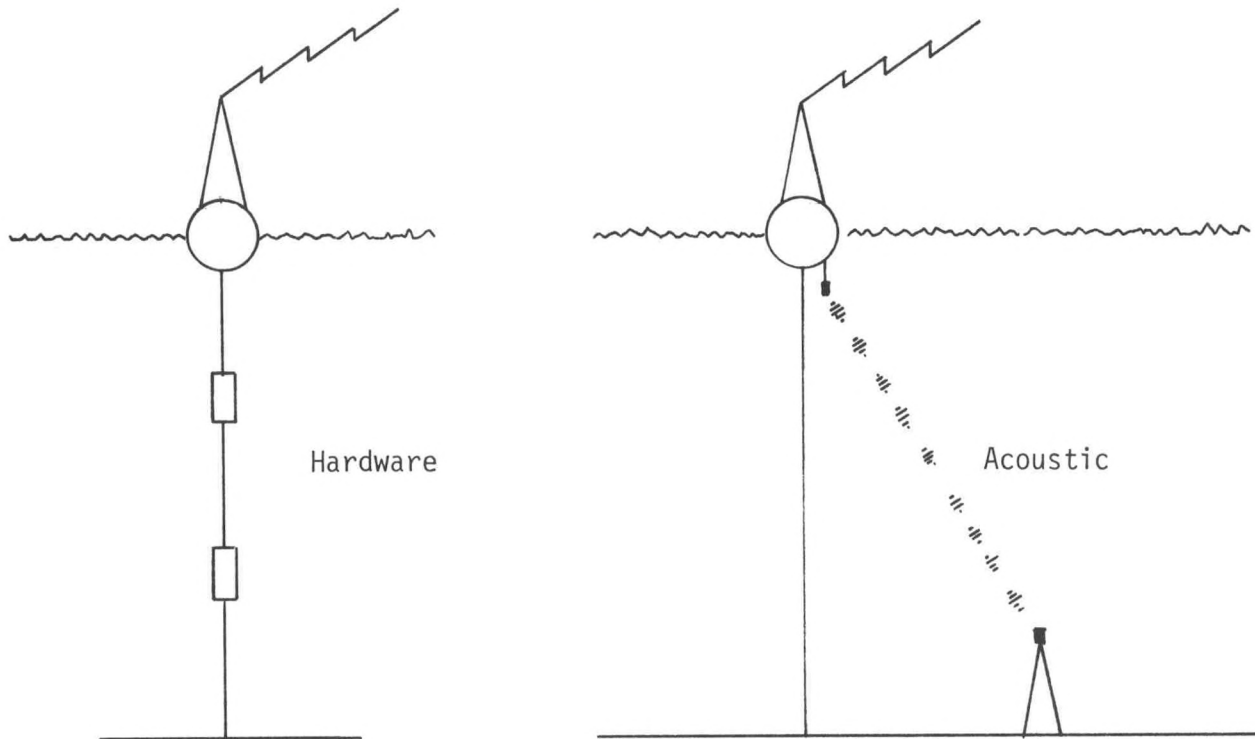
- Satellite
  - ARGOS - (NOAA/TIROS; polar orbiter)
    - Research - platform positioning and data transfer [0.1 bits/s]
    - Operational - Drifting Buoys
  - GOES - (non-polar regions)
    - Research - data transfer [10 bits/s]
    - Operational - NDBC Buoy & C-MAN to NESDIS
- Radio
  - Line-of-sight RF [ ]
  - HF Packet [300 - 1200 bits/s]
- Meteor Burst (?) [50 - 100 bits/s]

## UNDERWATER

- Acoustic
  - Neil Brown "Smart CTD & CM" [5 bits/s over 10km in 100m]
  - PROM (Progress Reporting Ocean Mooring)
- Popup
  - moored spar buoy in ice regime [variable]
  - PROM
  - TLC (Telemetry Lagrangian Capsule)

Figure 5. Observational telemetry schemes. Ocean surface to laboratory and underwater to surface data telemetry links are outlined with estimates of nominal bit rates given.

## REAL-TIME



## DELAYED-TIME

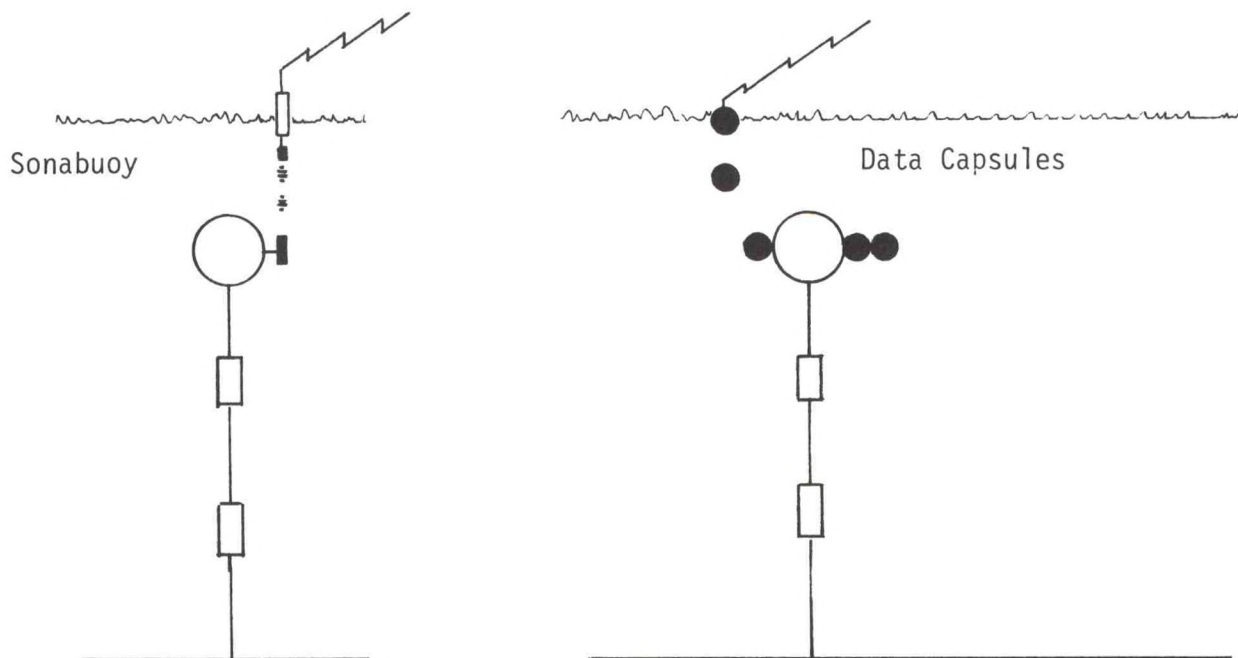


Figure 6. Real-time and delayed-time ocean/atmosphere data telemetry systems. Real-time systems link underwater measurements to surface platforms via hardware and/or acoustic links. The data is then transmitted ashore via satellite or radio links. The delayed-time systems (under development) telemeter bursts of "old" data to a ship, airplane or ashore on occasion.



## CURRENTS

### MOORED SYSTEMS

- Standard Current Meter Arrays
  - mechanical
    - VMCM
    - VACM
    - Endeco
    - Aanderra
  - nonmechanical
    - S4 (electromagnetic)
    - Acoustic CM
- Current Profilers
  - bottom (upward-looking) DAPCM
  - midwater DAPCM
  - surface (downward-looking) DAPCM
  - Cyclesonde
- Surface Current Remote Sensing: CODAR

### LAGRANGIAN

- Drifters
  - Davis
  - Loran
  - TLC

### SYNOPTIC

- Doppler Acoustic Log (DAL)
- GEK
- Expendable Current Profiling (XCP)
  - shipboard
  - aircraft
- Pegasus
- Pogo

### TRANSPORT

- DAPCM
- Pressure/Inverted Echo Sounder
- Electric Field

Figure 7. Ocean Current and Transport Measurement Systems.

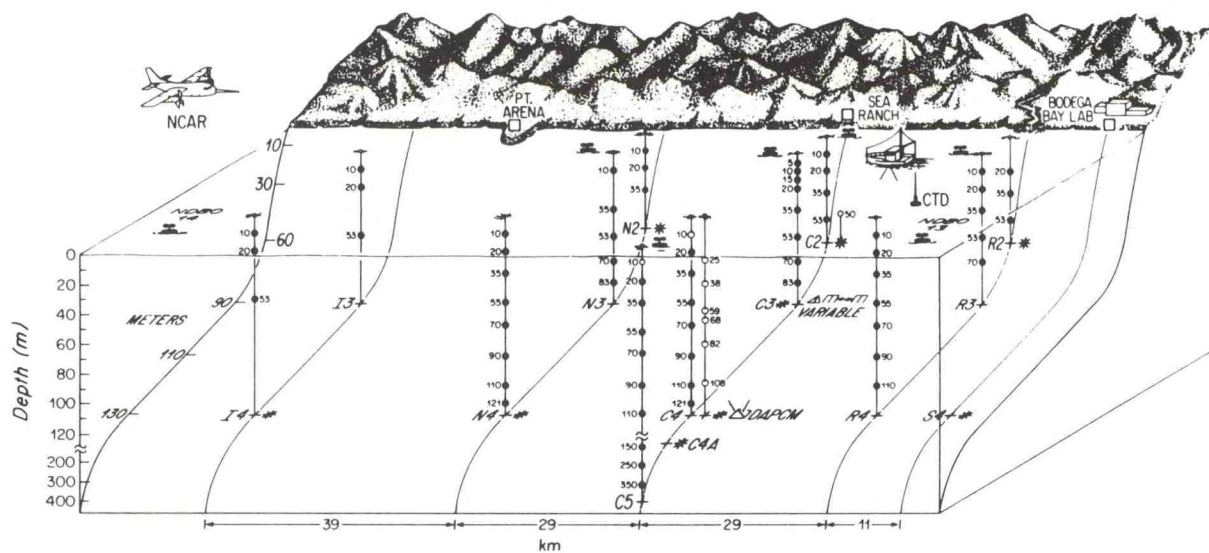
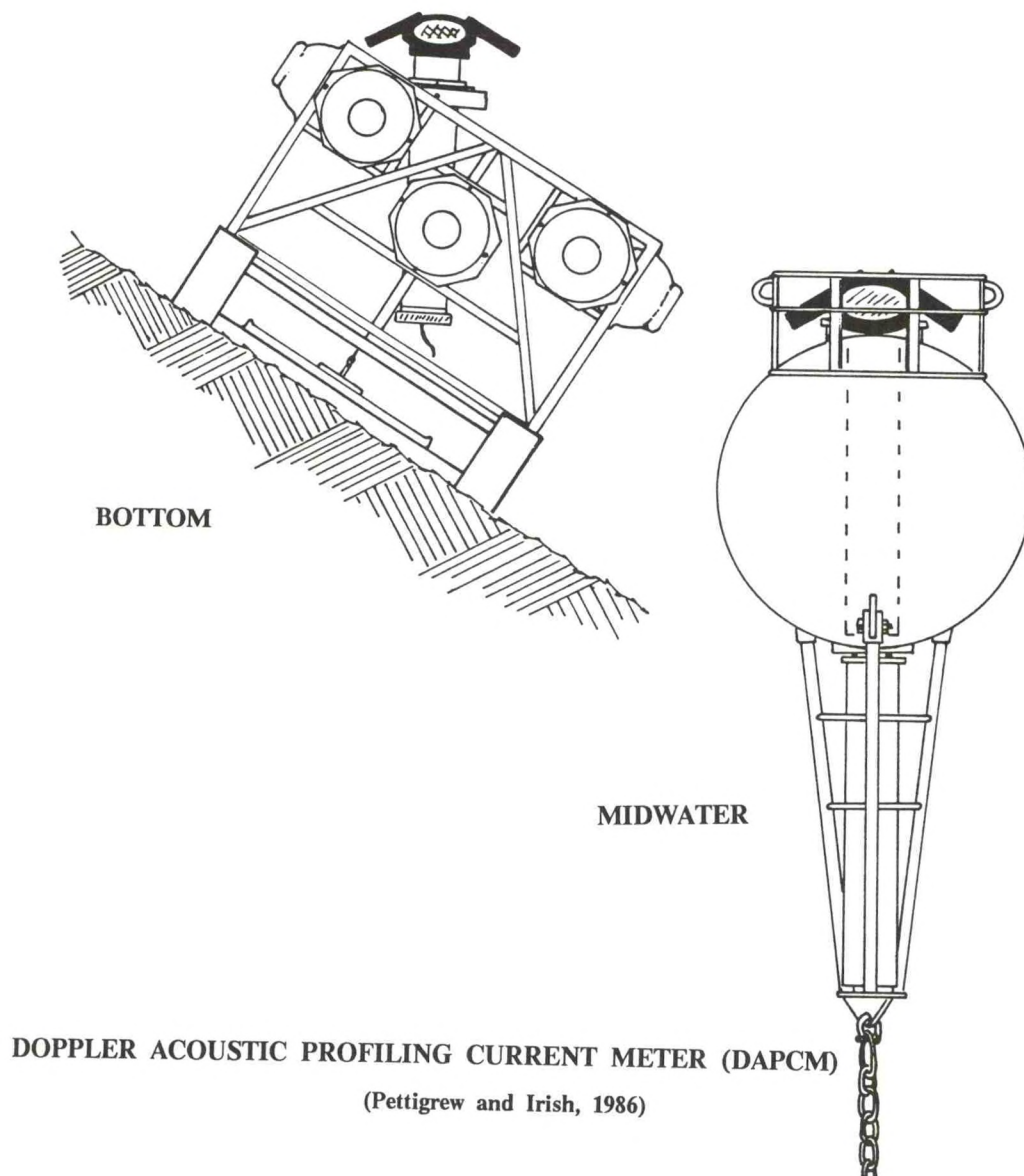


Figure 8. A three-dimensional schematic of the Coastal Ocean Dynamics Experiment (CODE) - 2 array. Current meters (solid dot), temperature/conductivity sensors (open dot), bottom pressure/temperature recorders (asterisk), and coastal meteorological stations (open square) are located, as are meteorological buoys and bottom stress instrumentation.





DOPPLER ACOUSTIC PROFILING CURRENT METER (DAPCM)  
(Pettigrew and Irish, 1986)

Figure 9. Doppler Acoustic Profiling Current Meters (DAPCM or ADCP) in bottom-mounted and midwater mounted configurations. The four acoustic transmitters/receivers (black) receive their own backscattered acoustic signals, whose frequency has been shifted by the moving water at different levels in the water column.

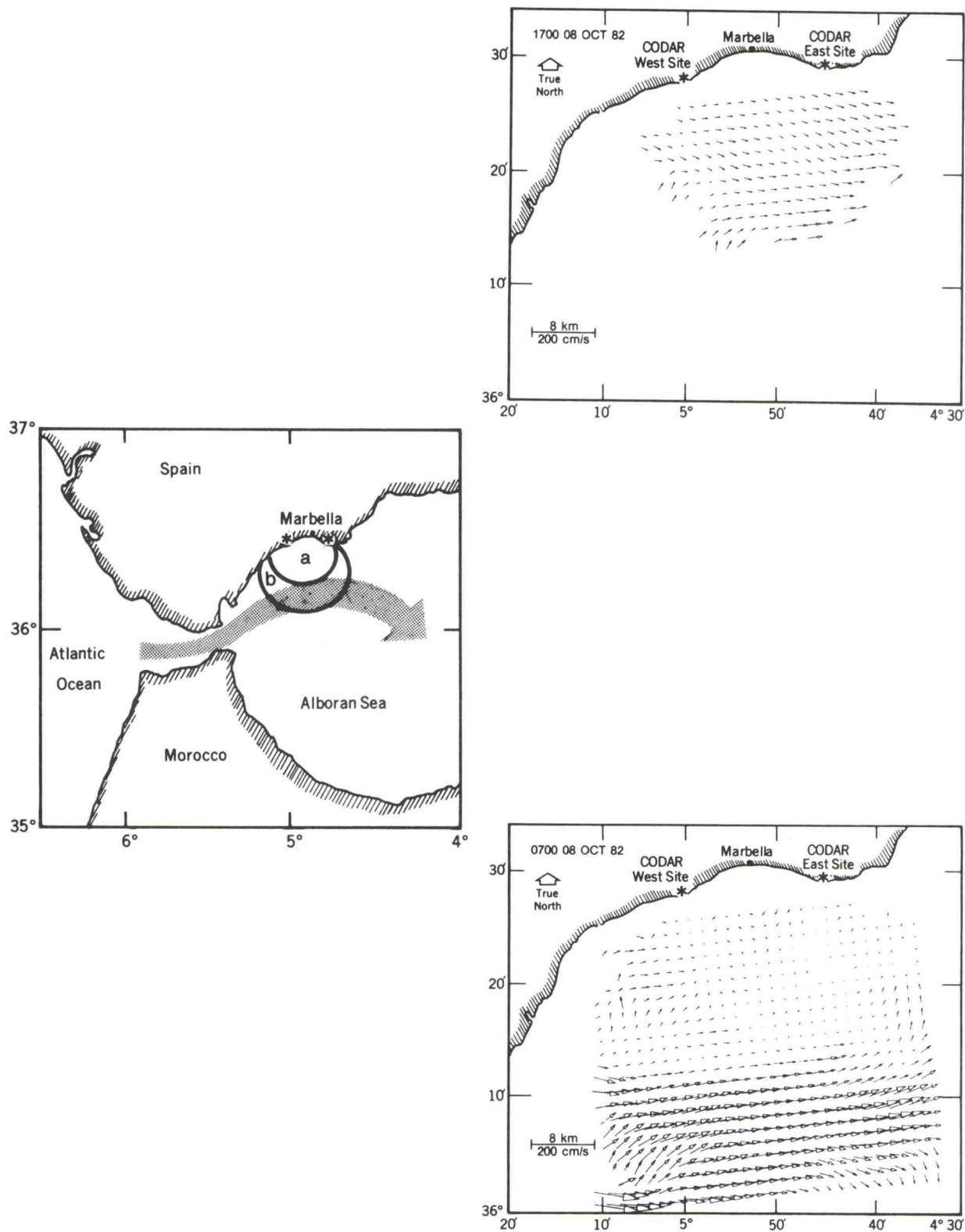


Figure 10. CODAR surface current measurement systems: (a) Alboran Sea sites relative to the inflow of Atlantic surface water; (b) daytime CODAR surface current map, and; (c) nighttime surface current map (Janopaul and Frisch, 1984).



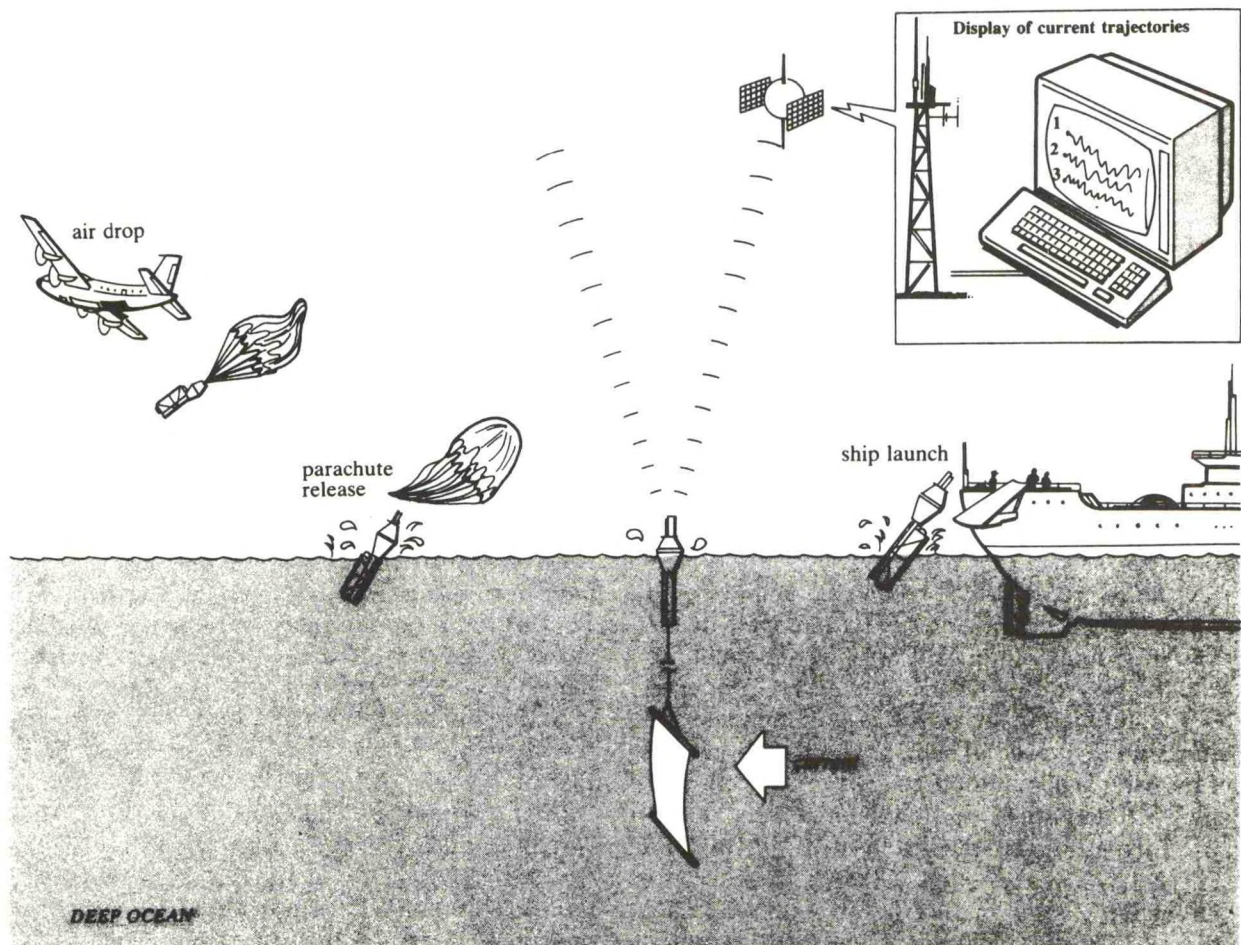


Figure 11. Lagrangian current measurement system(s) (Tolmazin, 1985).

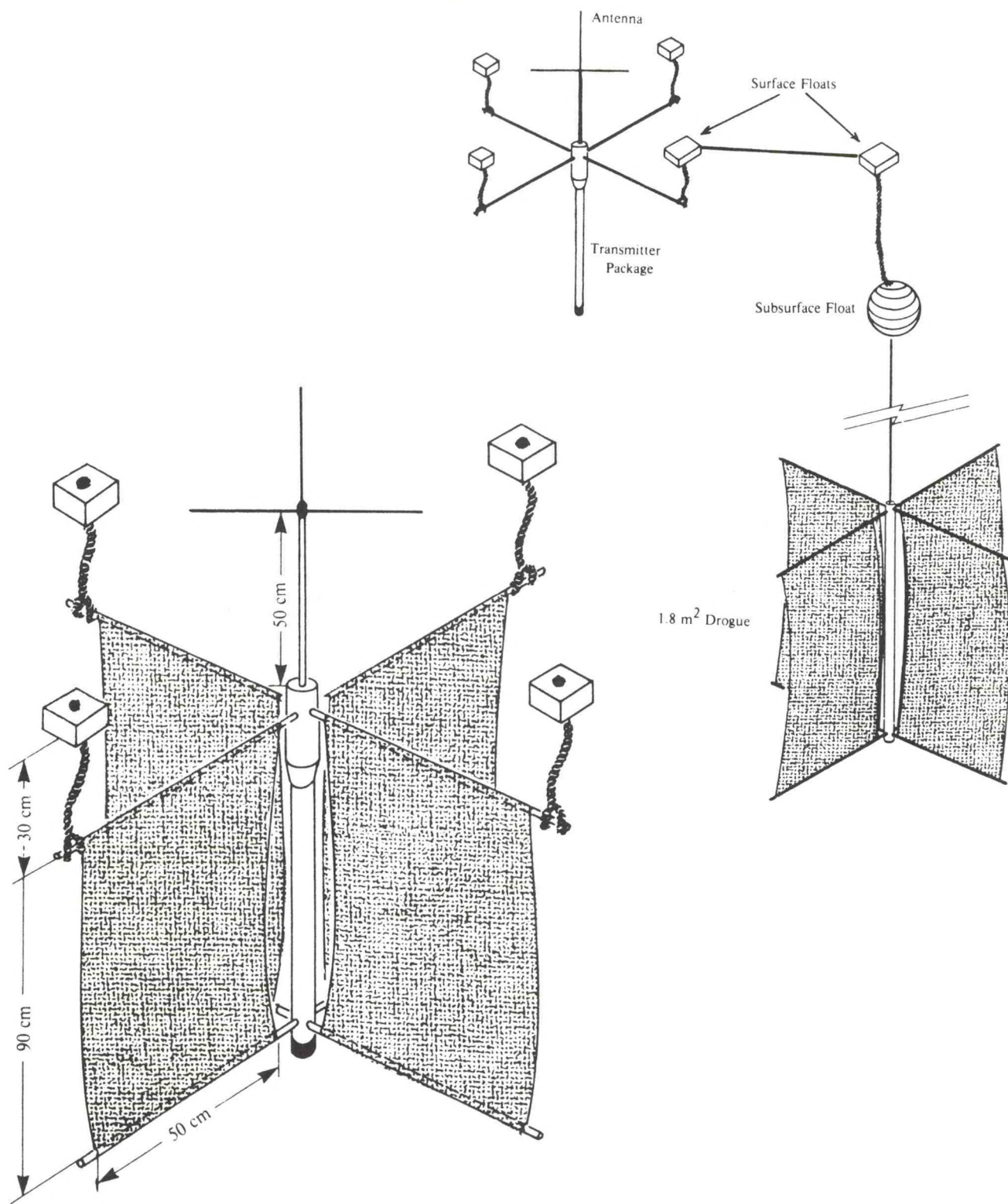


Figure 12. Surface and deeper Davis drifters are VHF-tracked from shore and/or airplane (Davis, 1985).



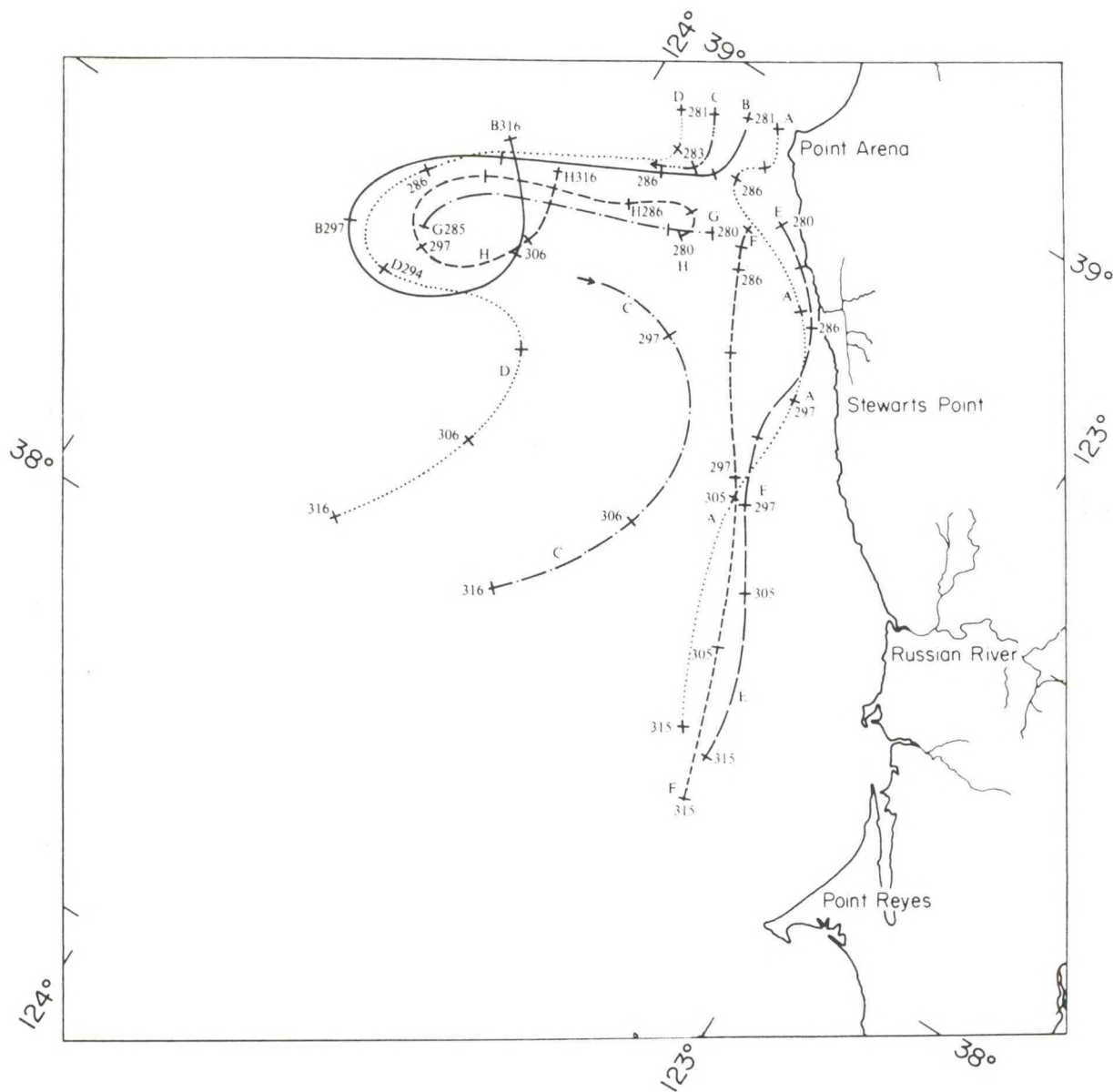


Figure 13. Trajectories of surface drifter deployed 28 May 1981. Buoys A-D were deployed off Pt. Arena and E-H were deployed about 10 miles to the south. Time labels are the decimal day of May times 10. Note how the eddy off Pt. Arena produces a powerful squirt over the shelf as it entrains shelf water (Davis, 1985).

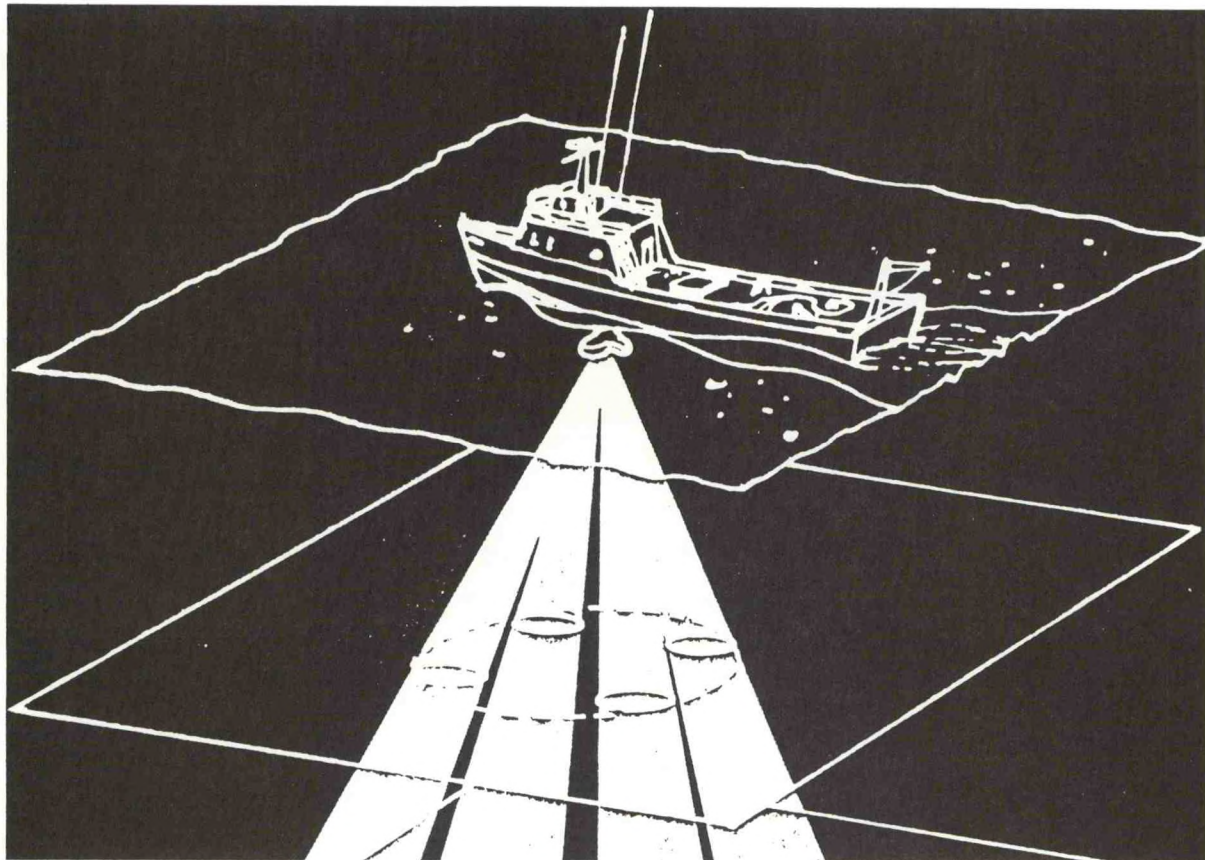


Figure 14. Hull-mounted Doppler Acoustic Log (DAL) current profiling of spatially averaged currents consists of averaging acoustic returns over extended periods while the ship is underway.



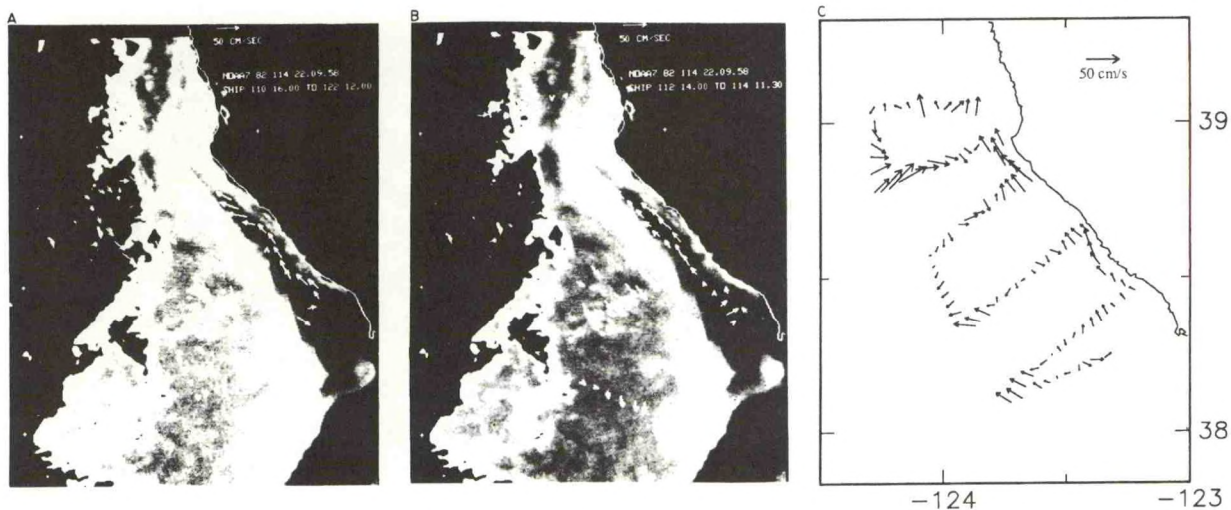


Figure 15. DAL survey results (a) from 1600 UT April 20 through 1200 UT April 22, 1982, with a satellite image from 2210 UT April 24, 1982 (note time delay of the satellite image from the survey and that the labeled time is incorrect); (b) from 1400 UT April 22 through 1130 UT April 24, 1982, with a satellite image from 2210 UT April 24, 1982 (same image as (a) and (c) from 0630 UT May 29 through 0436 UT May 31, 1982 (no satellite image) (Kosro, 1987).

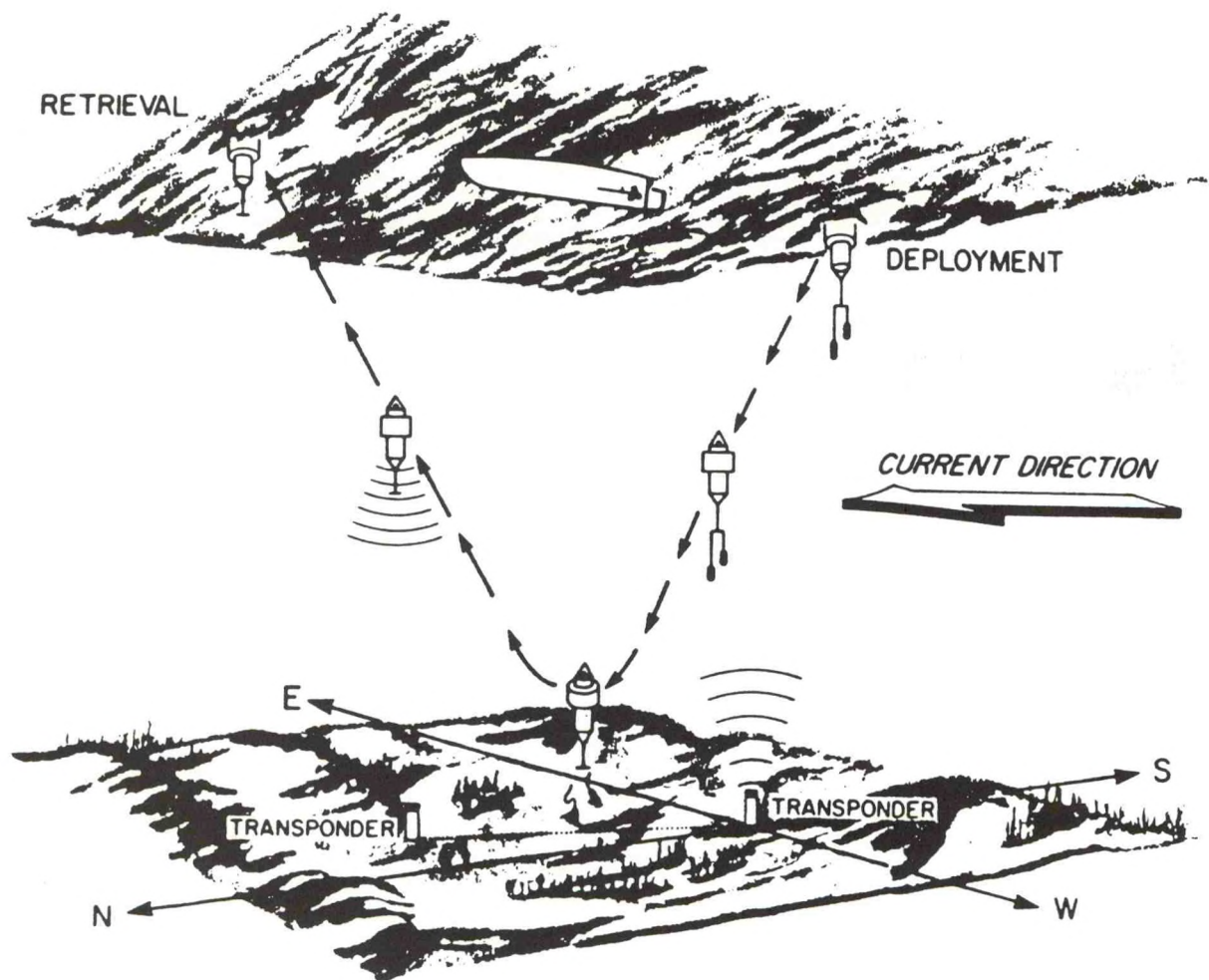


Figure 16. Schematic of the Pegasus current profiler (Wilburn et al., 1987).



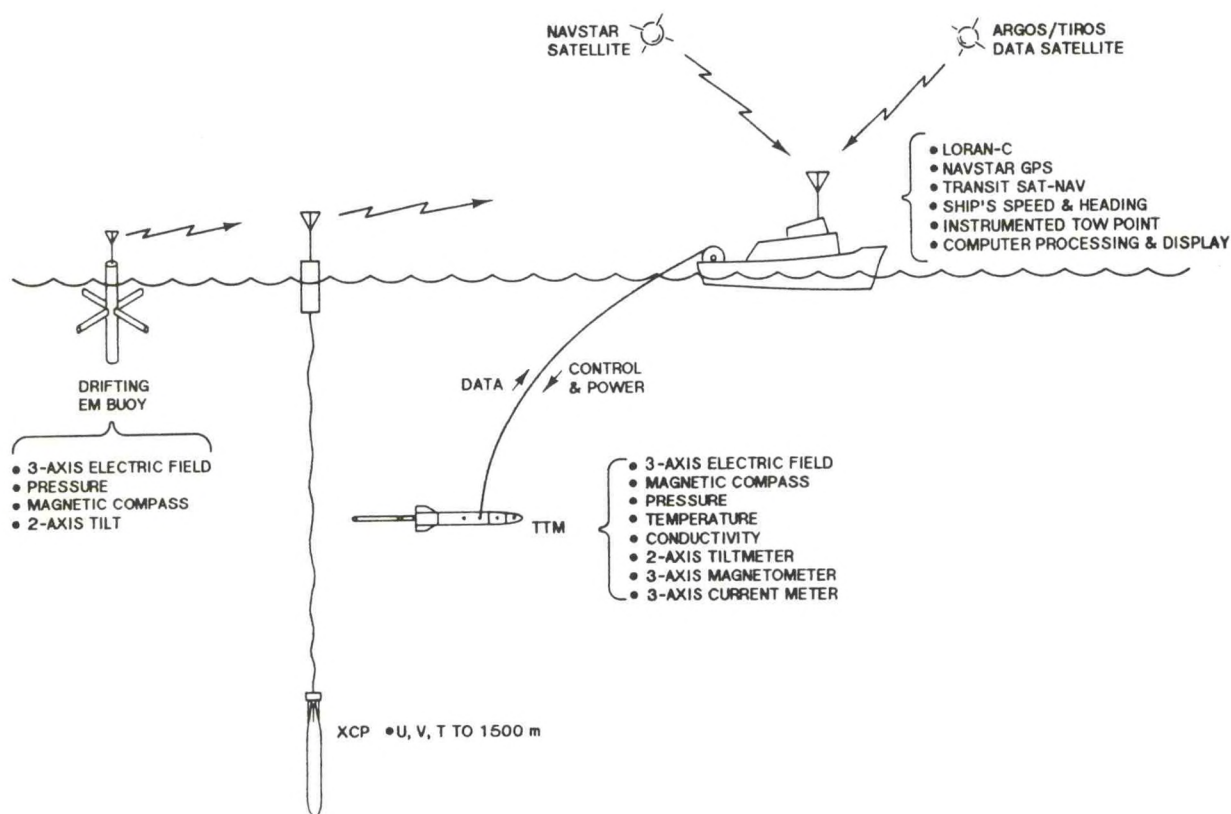
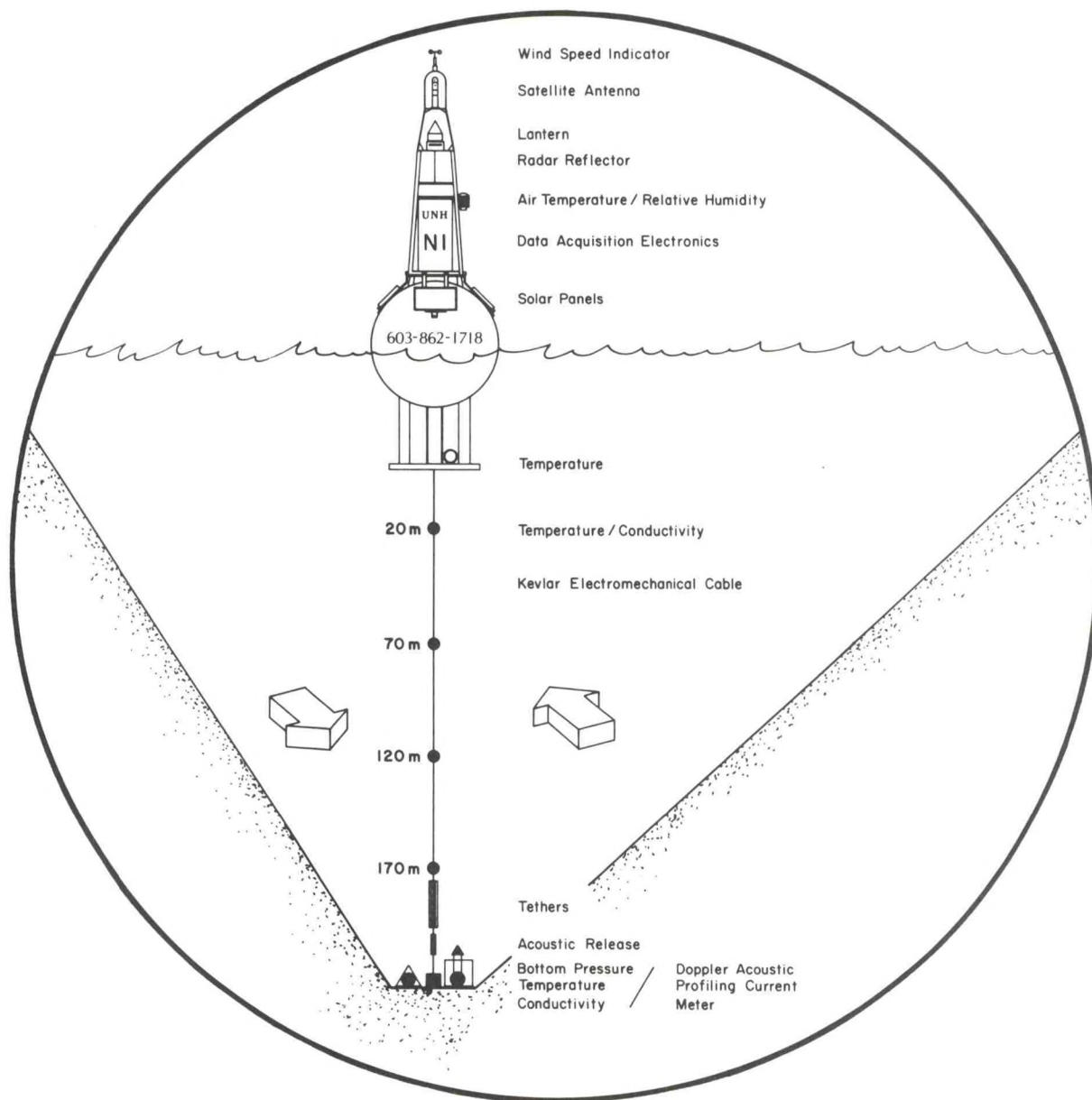


Figure 17. A suite of electromagnetic (EM) current measurement instruments. The towed fish is denoted TTM, for Towed Transport Meter, and is the platform carrying the EM and acoustic systems. The drifting buoy is used near the vessel while the TTM is being towed. A duplex RF link connects the buoy and the vessel, where the control and acquisition functions are located. The XCP is used occasionally to obtain baroclinic velocity profiles (Sanford, 1986).



## Northeast Channel T/C Array

Figure 18. A temperature/conductivity array is hardwire-linked to a synergetic data logger and GOES/ARGOS telemetry link (Brown and Irish, 1990a).



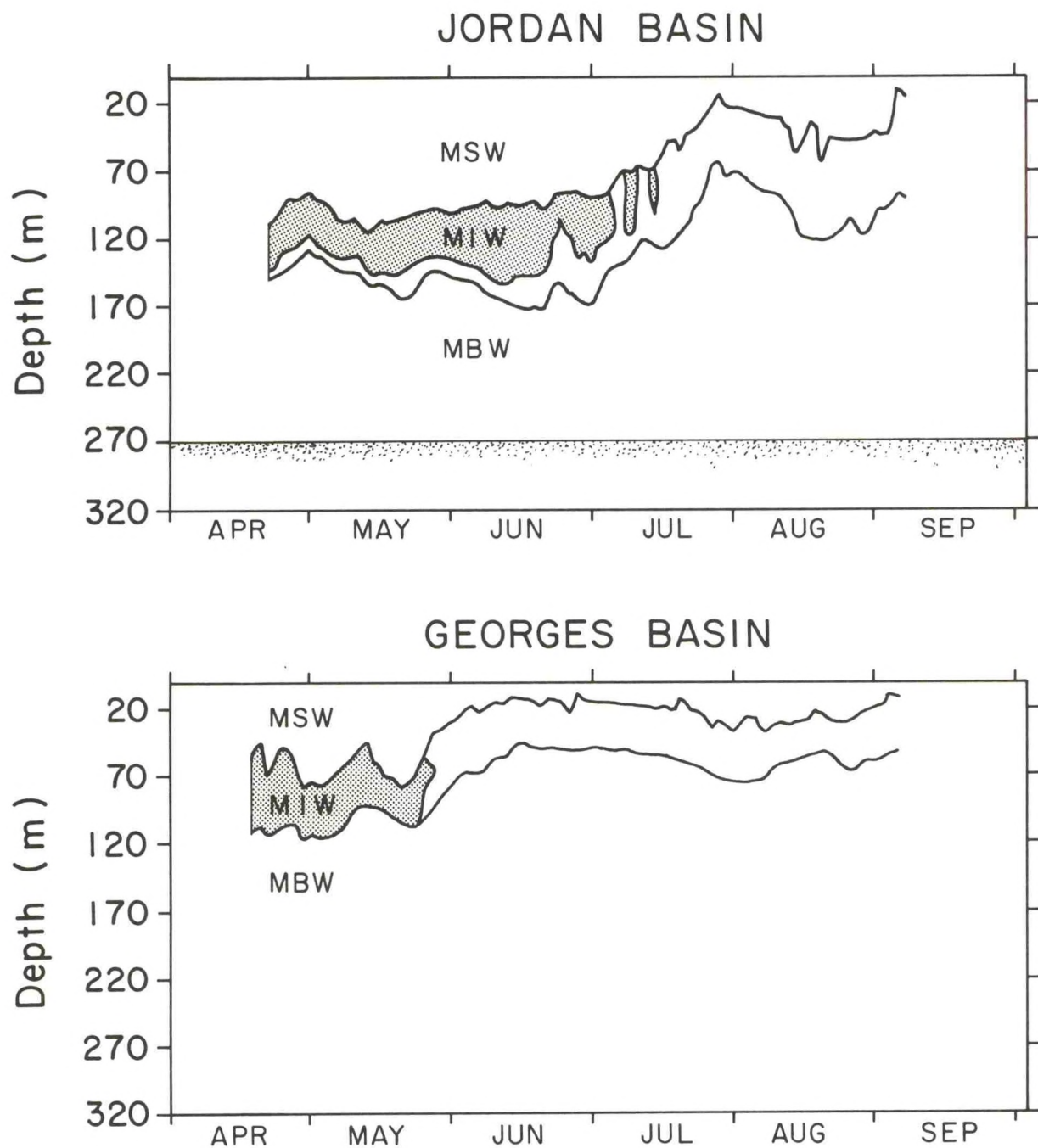


Figure 19. Water mass variability in the Gulf of Maine. The vertical distributions of Maine Surface Water (MSW), Maine Intermediate Water (MIW), and Maine Bottom Water (MBW) at the two mooring sites are monitored (Brown and Irish, 1990a).

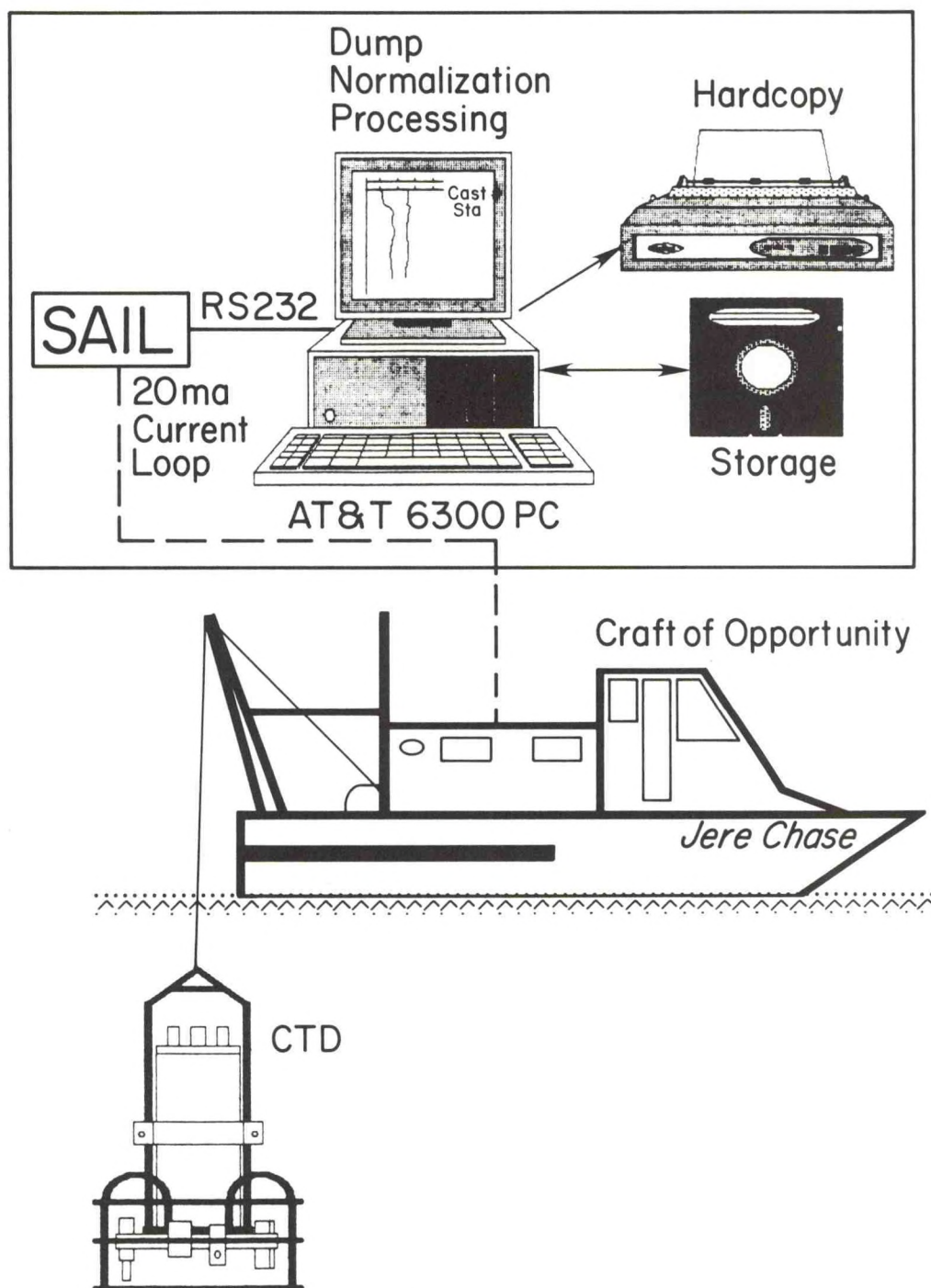


Figure 20. Internally recording CTD system (Irish and Martini, 1989).



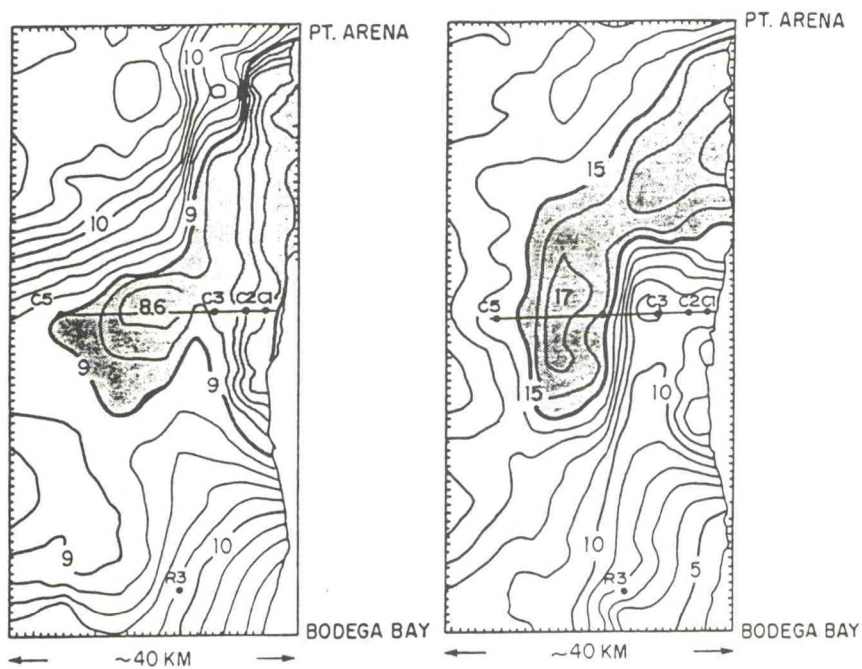
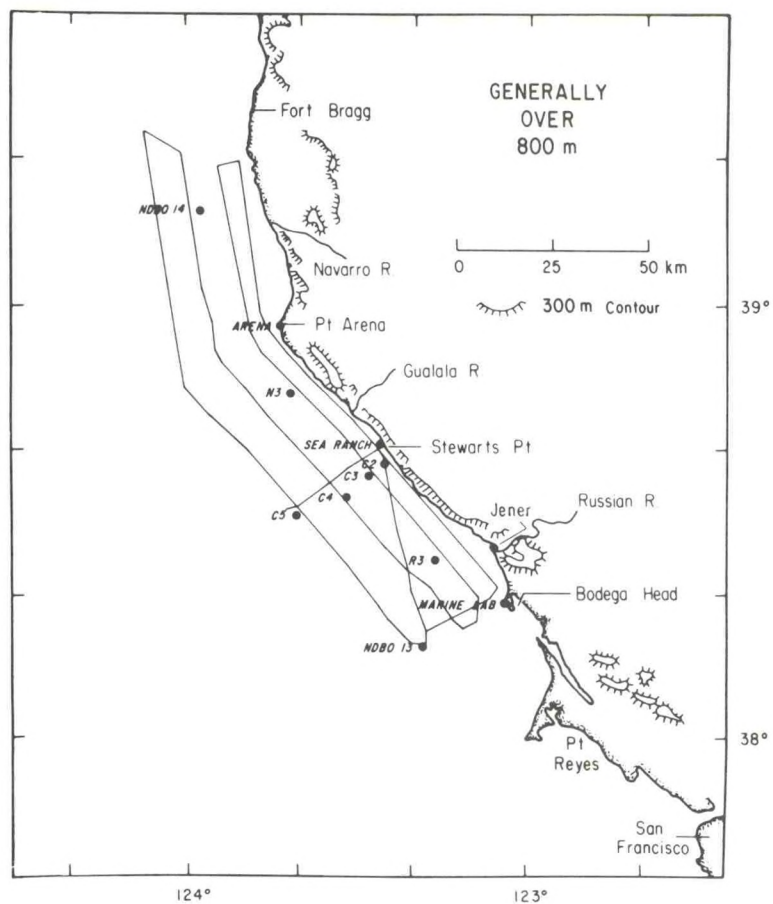


Figure 21. Aircraft measurements of surface temperature and wind speed distributions during CODE (Winant et al., 1988).

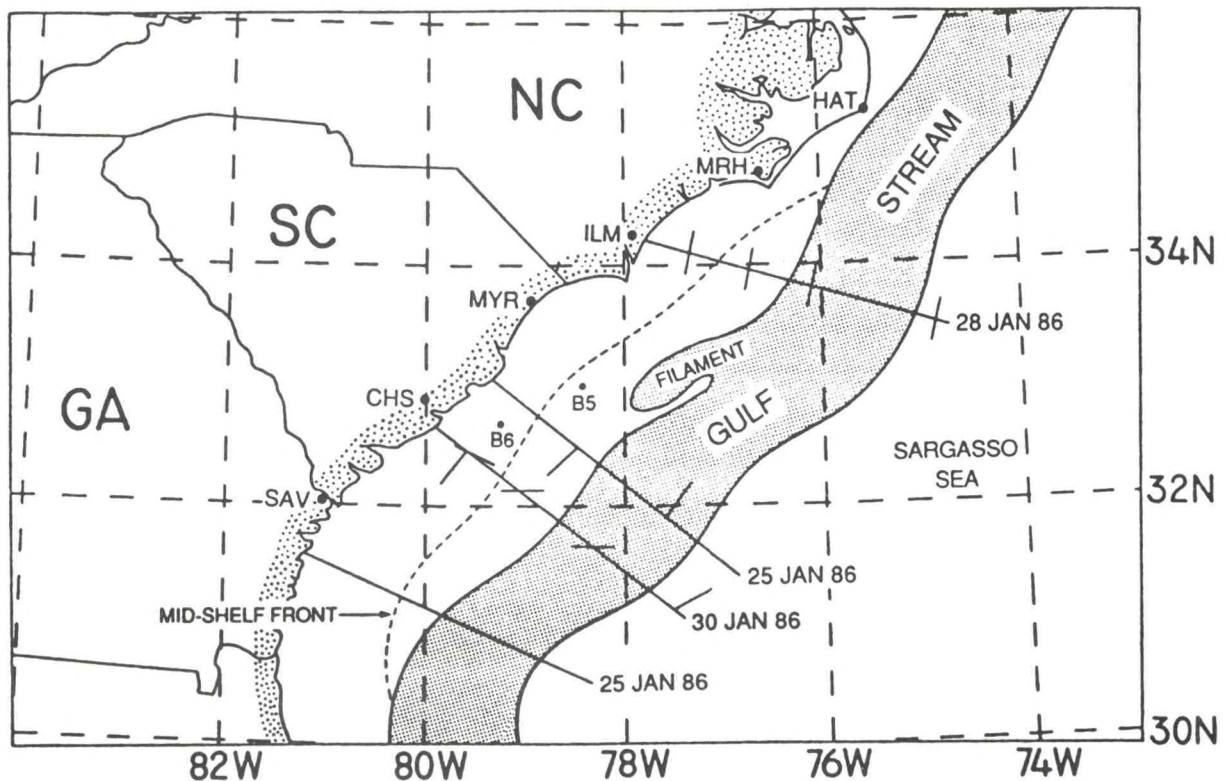
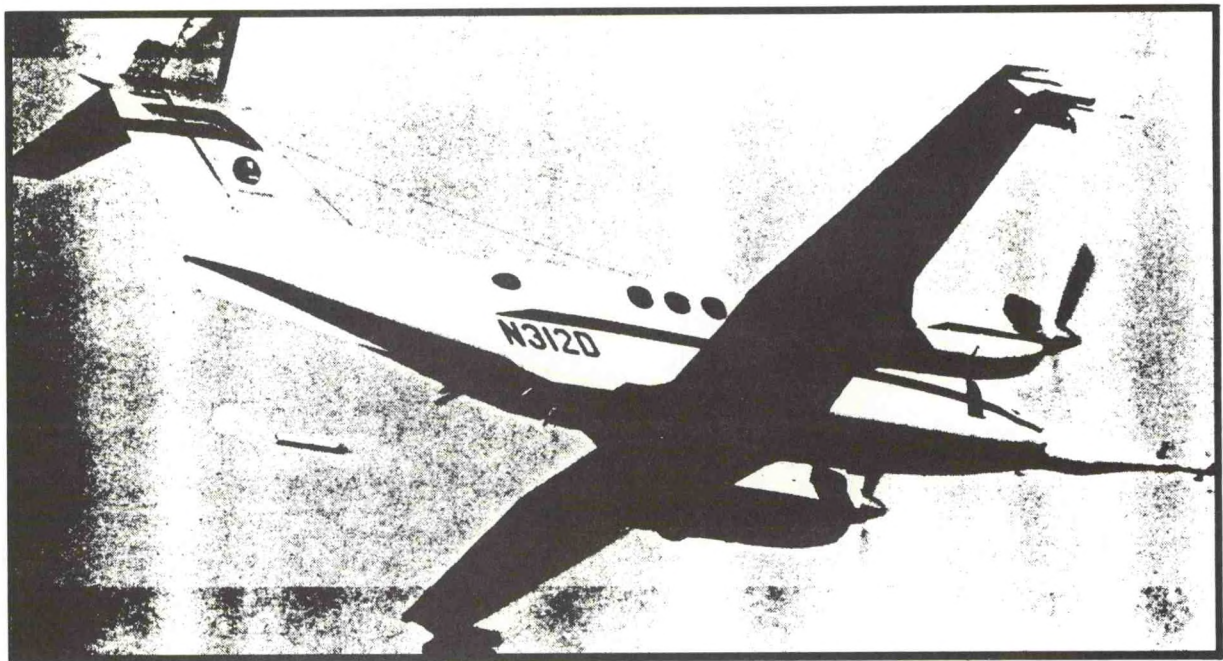


Figure 22. A map of the study area showing the flight tracks flown on January 25, 28, and 30, 1986. The short lines crossing the flight tracks (on all but the southern track of January 25) show the locations of the stacks flown for turbulence measurements. Important oceanographic features of the area are indicated schematically. The Gulf Stream is shown with a warm filament along its shoreward edge, as is a typical mid-shelf front separating cool inner shelf waters from warmer outer shelf waters. The Sargasso Sea is the open ocean region seaward of the Gulf Stream in this part of the North Atlantic (Bane and Osgood, 1989).



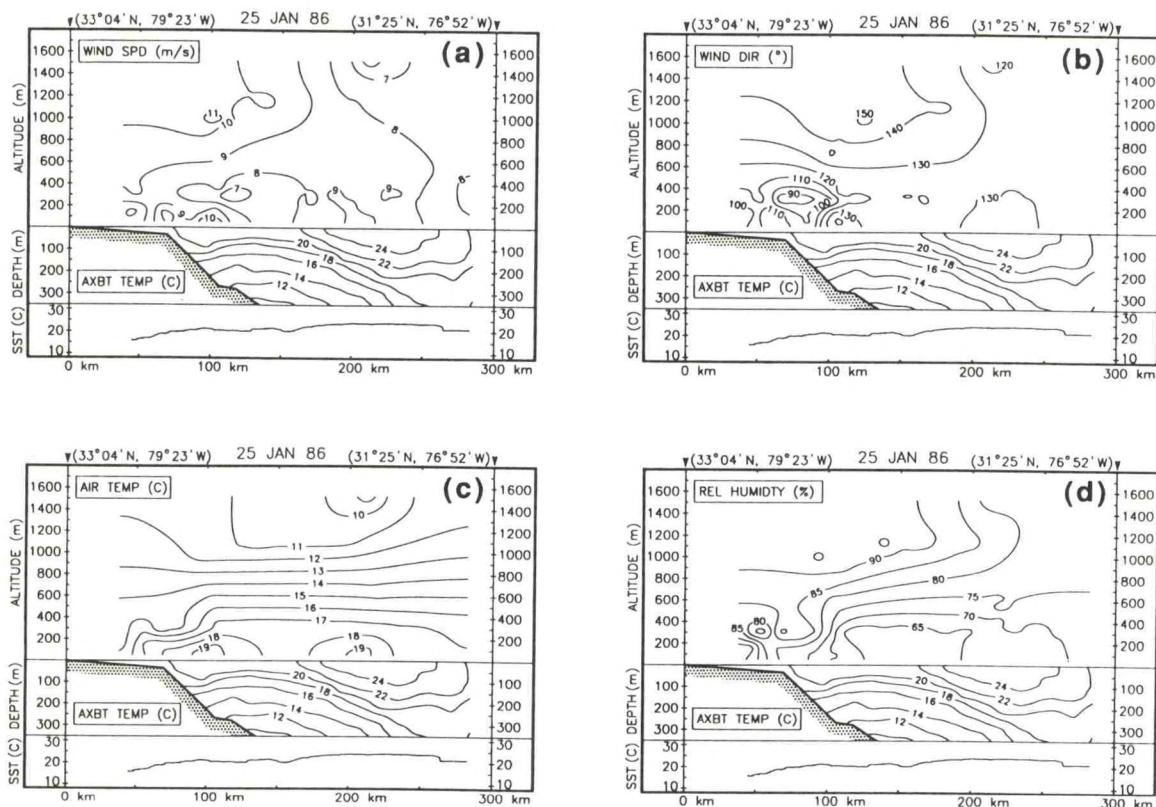


Figure 23. Vertical sections showing atmospheric and oceanic structure along the northern flight line of January 25. Each panel shows the thermal structure in the upper 350 m of the ocean and the atmospheric structure in its lower 1500 m or so. The sea surface temperature profile measured by the aircraft's radiometer is shown at the bottom of each panel. The four panels show (a) wind speed, (b) wind direction, (c) air temperature, and (d) relative humidity. The wind flow was generally from the southeast, although the structure of the coastal front, which may be seen over the shelf portion about 50-100 km from shore, caused variations in wind direction (Bane and Osgood, 1989).

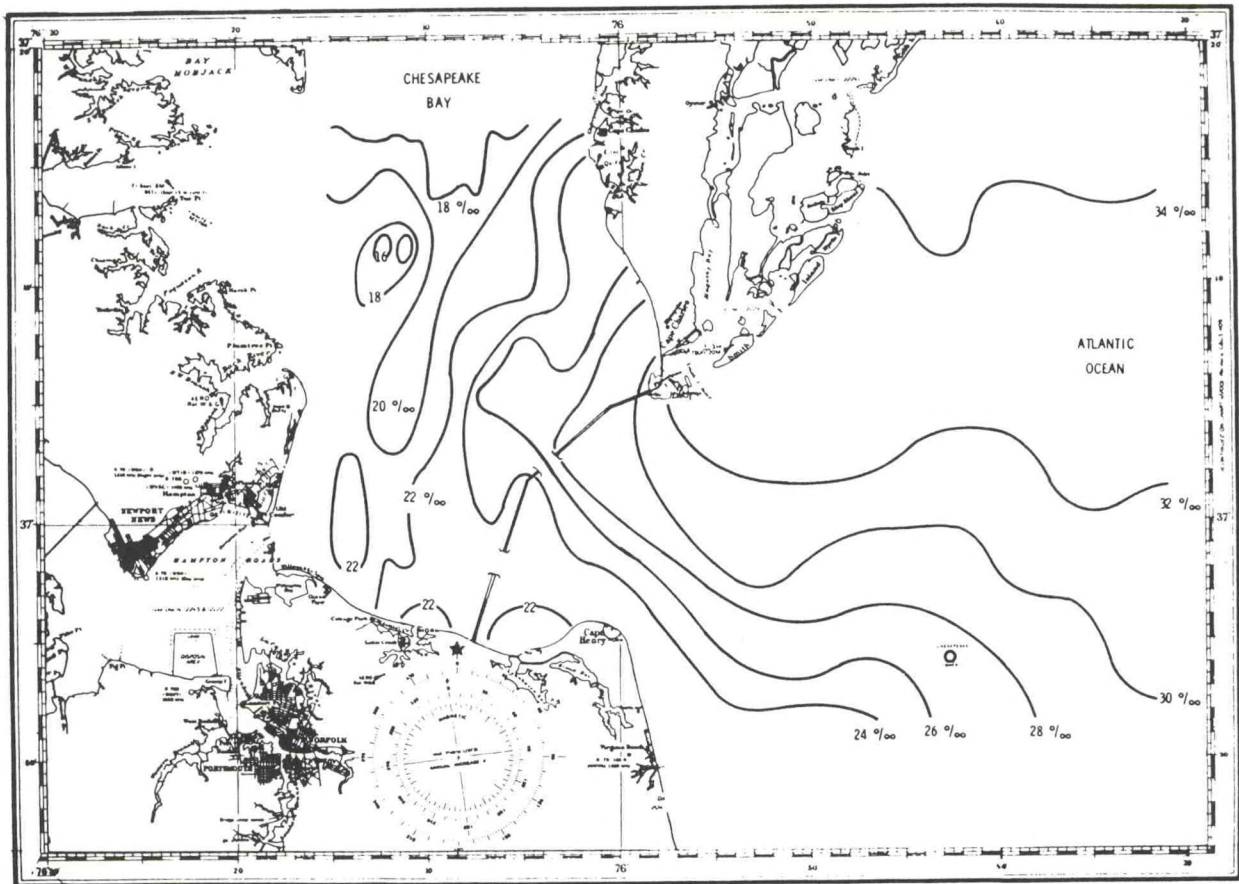


Figure 24. Chesapeake Bay Salinity Study - The Advantage of Airborne Mapping. The figure shows a plot of isohalines (lines of constant salinity) in the lower Chesapeake Bay on August 26, 1976. The increments are in two parts per thousand. The values were derived from airborne S-band and L-band microwave radiometers with nadir views. Mapping was accomplished by flying a total of 12 parallel east-west flight lines over a 25 x 50 mile area in 3-1/2 hours, and included 6,000 independent samples. By contrast, in 1972, in the aftermath of Hurricane Agnes, it took ships and helicopters 3 days to gather 180 point samples for the construction of similar maps. Hurricane Agnes grossly changed the salinity concentration of the Chesapeake Bay, threatening the health of shellfish (Johnson and Melfi, 1989).



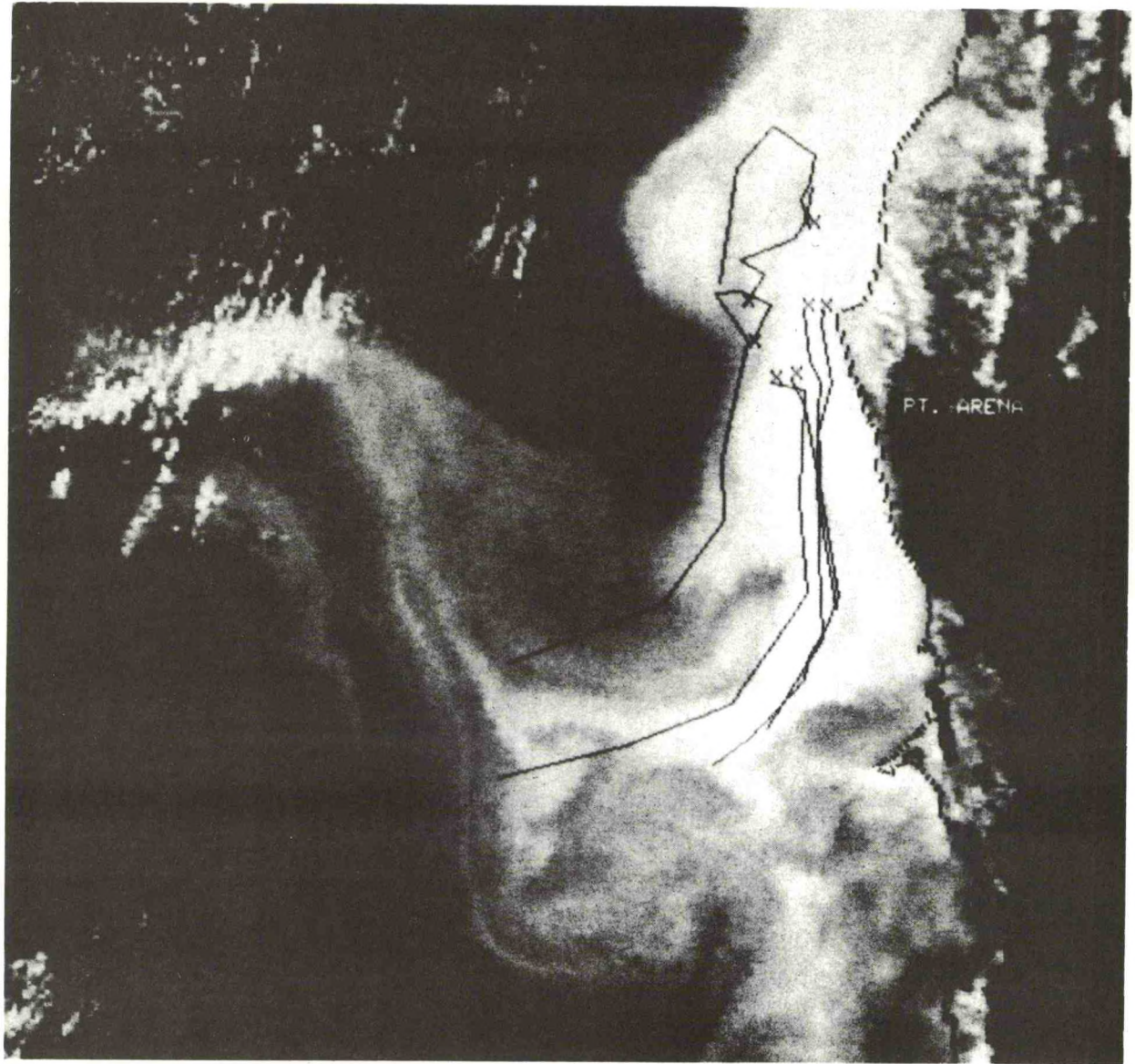


Figure 25. Comparison of surface drifter tracks from July 4-8, 1981 (Davis, 1985), with infrared satellite image for the evening of July 6. Research locations for the drifters are denoted by crosses. Light gray shades correspond to cold water. The cold eddy northwest of Pt. Arena had a southward drift speed of about  $10 \text{ km d}^{-1}$  which places it at the circular drifter track on the release date (Kelly, 1985).

# GOM 1986-87 Seasonal Geostrophic Current

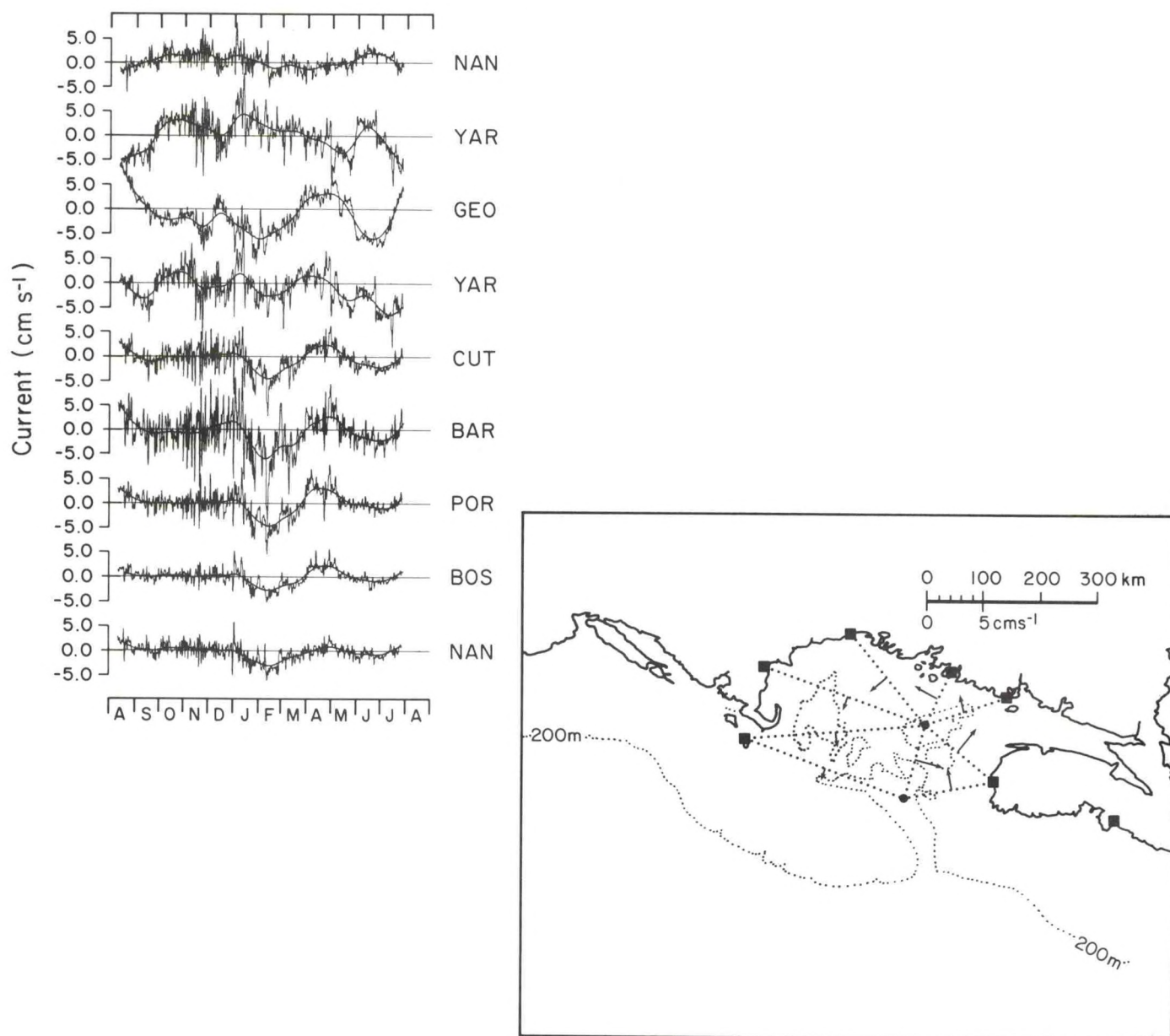


Figure 26. Surface geostrophic currents from pressure differences in the Gulf of Maine. The closed dots locate the Georges Basin (GEO) pressure station (lower) and the Jordan Basin (JOR) pressure station (above). The coastal pressure stations (closed squares) clockwise from lower left are Nantucket (NAN), Boston (BOS), Portland (POR), Bar Harbor (BAR), Cutler (CUT), and Yarmouth (YAR). The direction of the arrows at each of the transects indicates the direction of a positive fluctuation in the transect average geostrophic flow (Brown and Irish, 1990b).



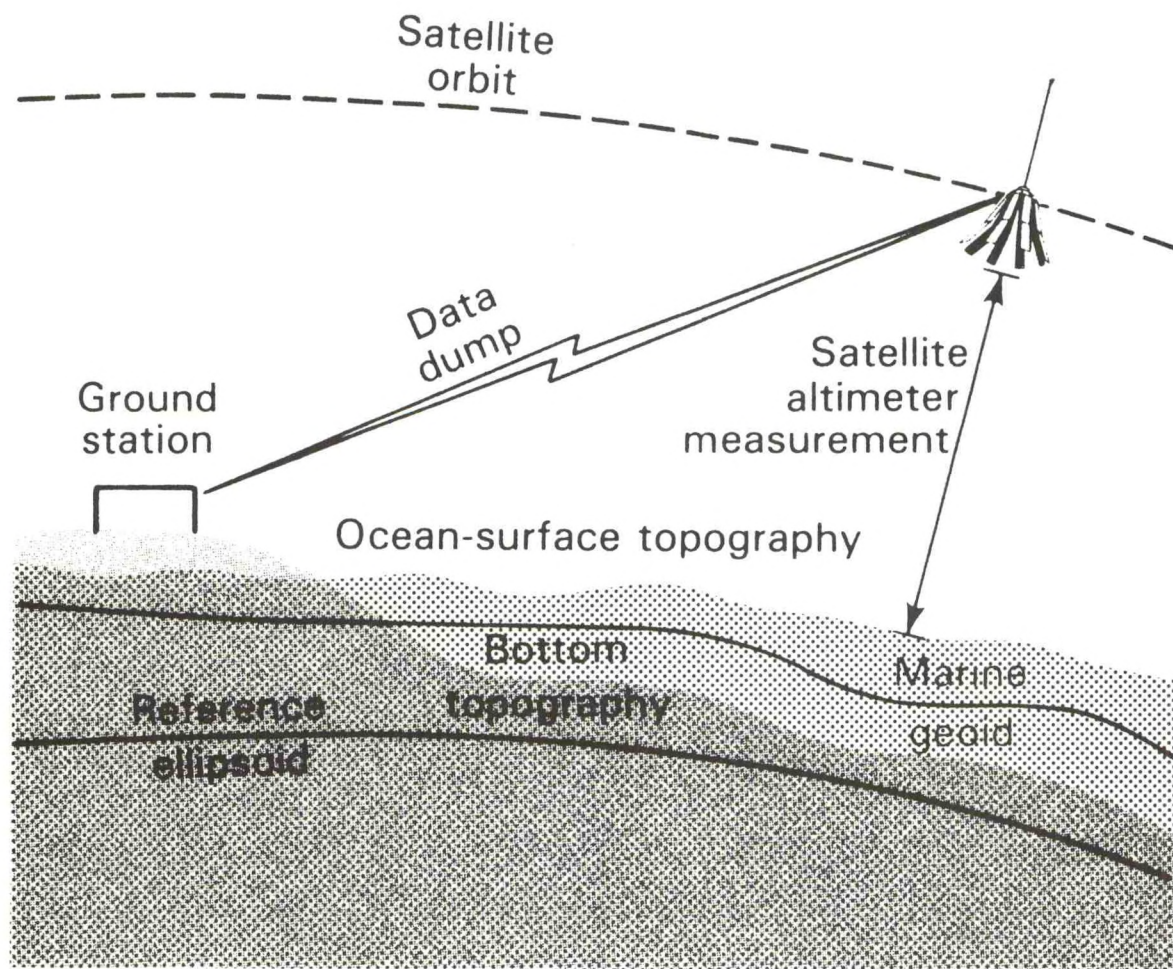


Figure 27. GEOSAT data collection (Jones et al., 1987).

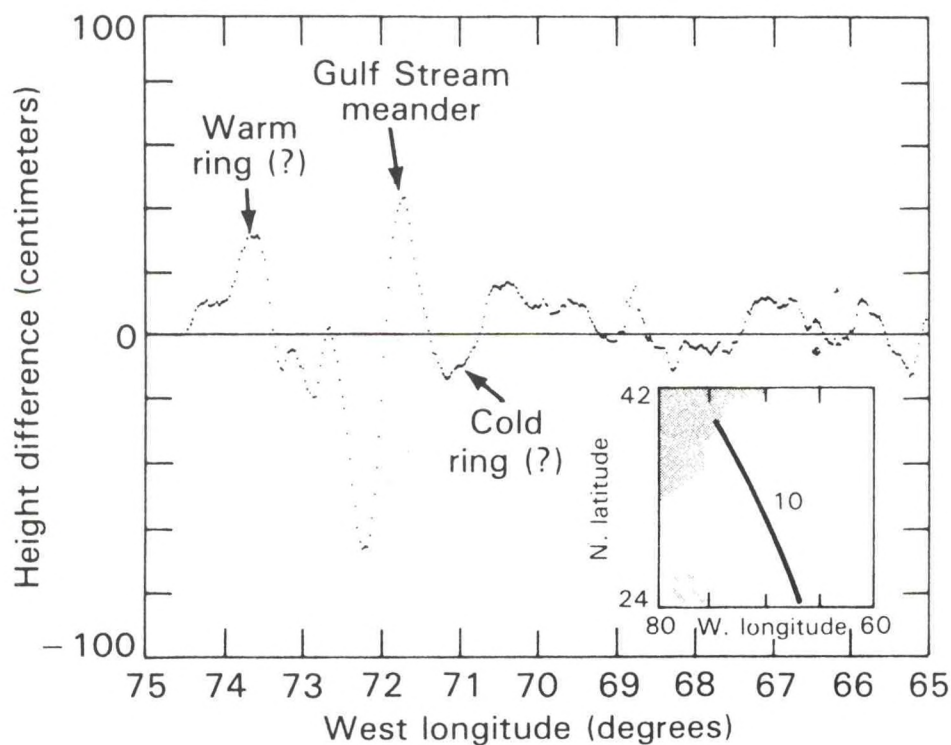
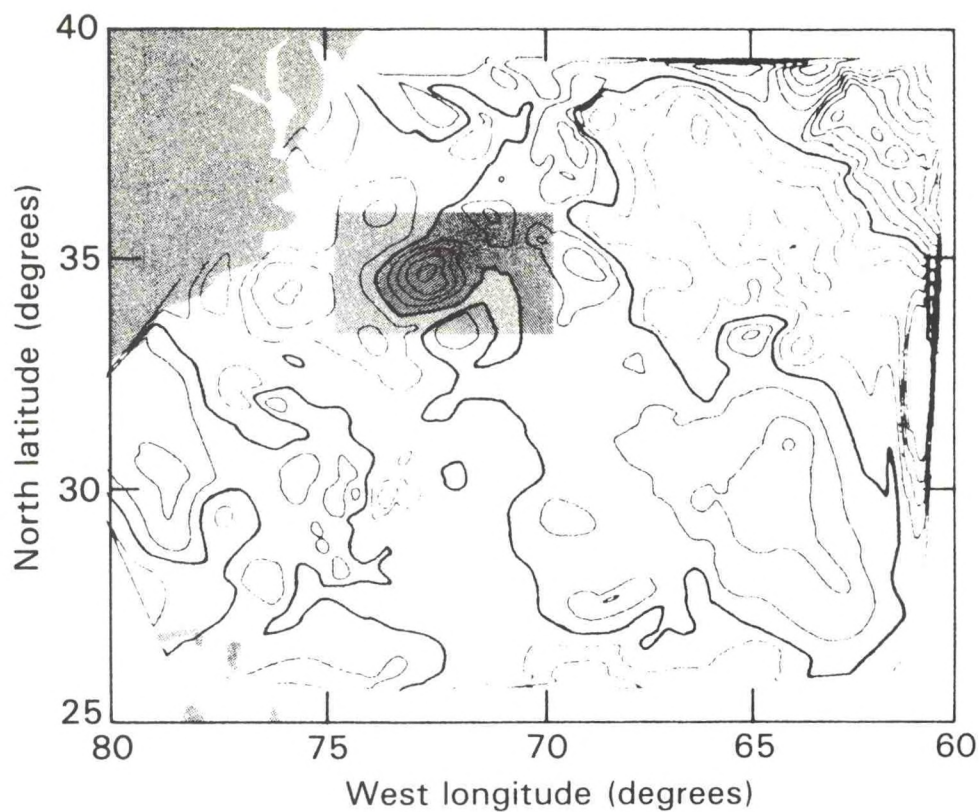
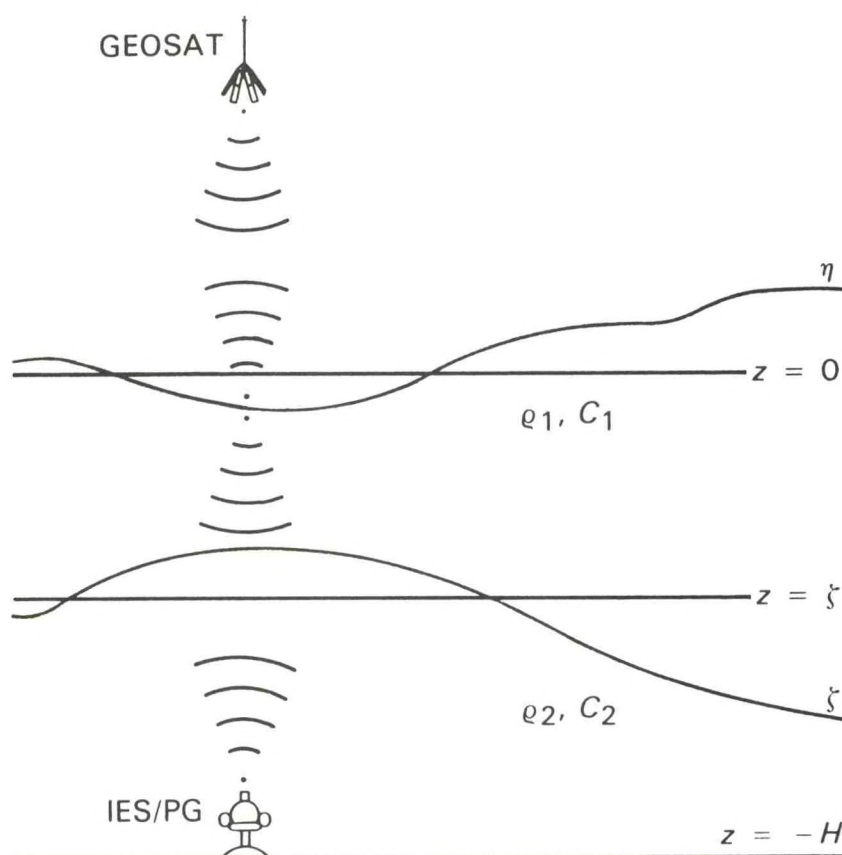


Figure 28. (Above) Time-dependent sea-surface dynamic topography from 30 days of GEOSAT data. (See the examples of a GEOSAT-derived sea surface height difference distribution (Below). Note the highlighted ring-like feature near 33°N, 73°W. (The contour intervals are 20 centimeters apart; negative values are shaded.) (Calman, 1987)





$$\begin{aligned}\zeta' &= A\tau' + B\rho' \\ \eta' &= C\tau' + D\rho'\end{aligned}$$

Figure 29. A schematic diagram of the intercomparison between the overflying GEOSAT altimeter and the bottom-moored IES/BP. Equations express the relationships used to derive fluctuations in the mean thermocline depth ( $\zeta'$ ) and sea-surface topography ( $\eta'$ ) from the measured time series of acoustic round-trip travel time fluctuations ( $\tau'$ ) and pressure fluctuations ( $\rho'$ ). The coefficients A, B, C, and D depend on the regional temperature-salinity characteristics. In the first equation, A is generally much larger than B (i.e., acoustic travel time fluctuations are dominated by thermocline fluctuations). In the second equation, both C and D may be of the same order (i.e., both barotropic and low-order baroclinic modes may be equally important in governing topographic fluctuations) (Watts and Wimbush, 1981).

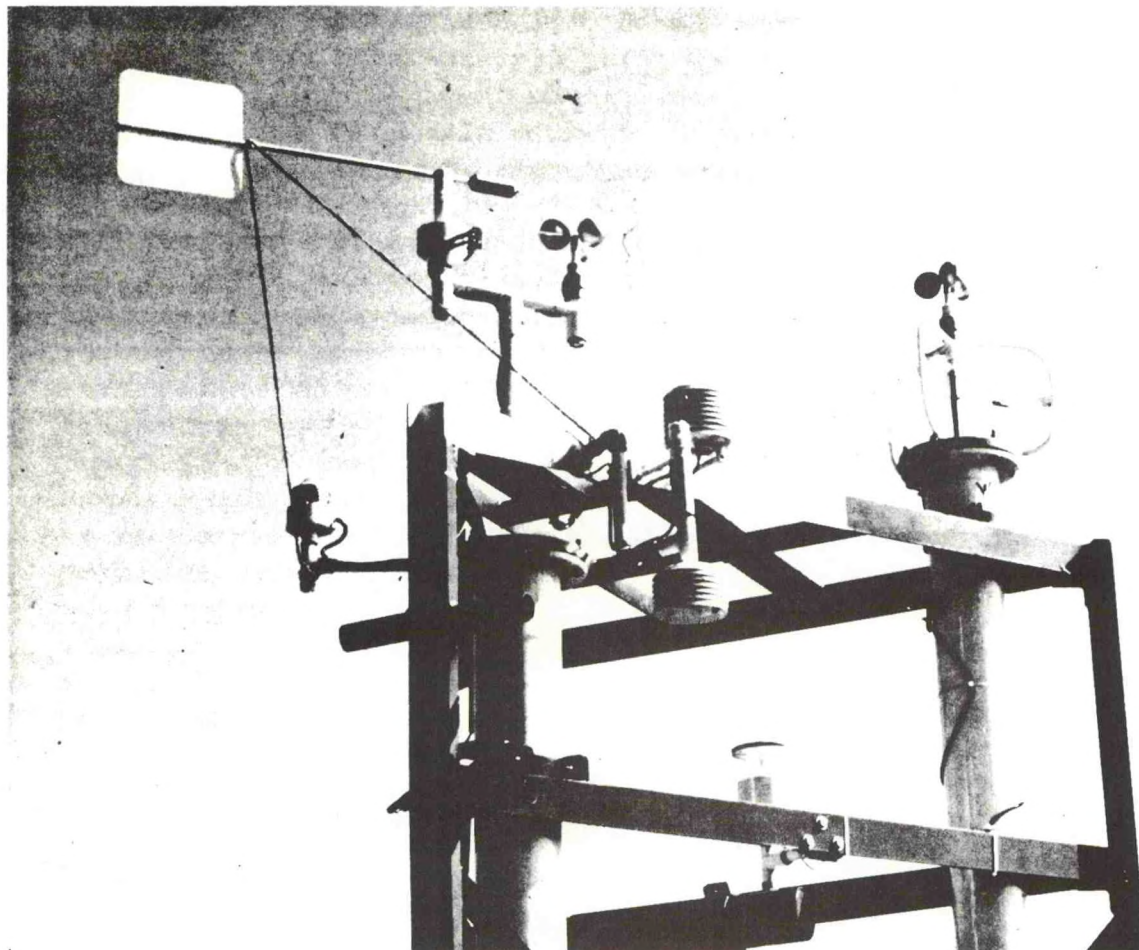


Figure 30. Moored meteorological sensor configuration (Dean and Beardsley, 1988).



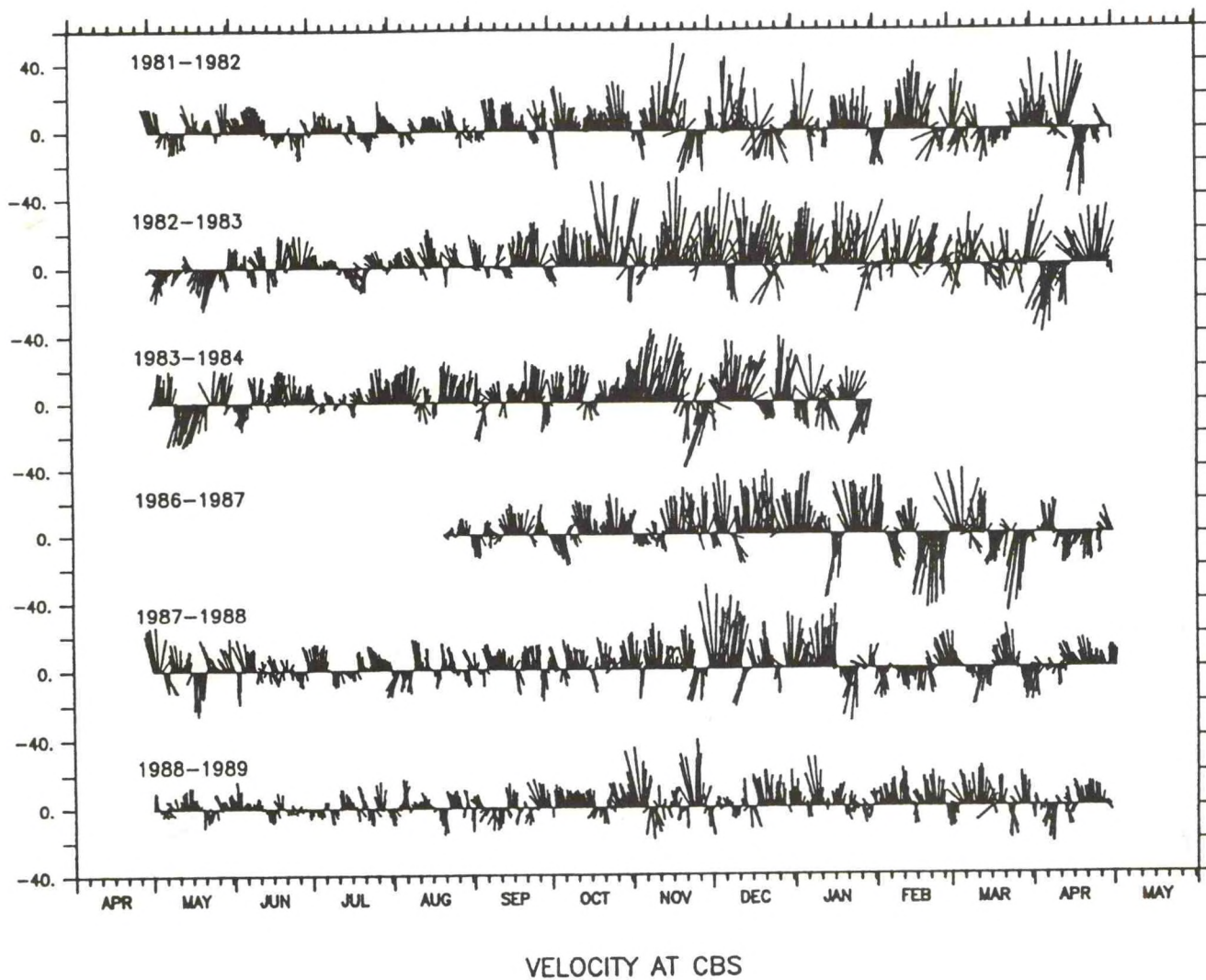


Figure 31. Long-term time series of currents on the Oregon Shelf (after Huyer and Smith, 1985).



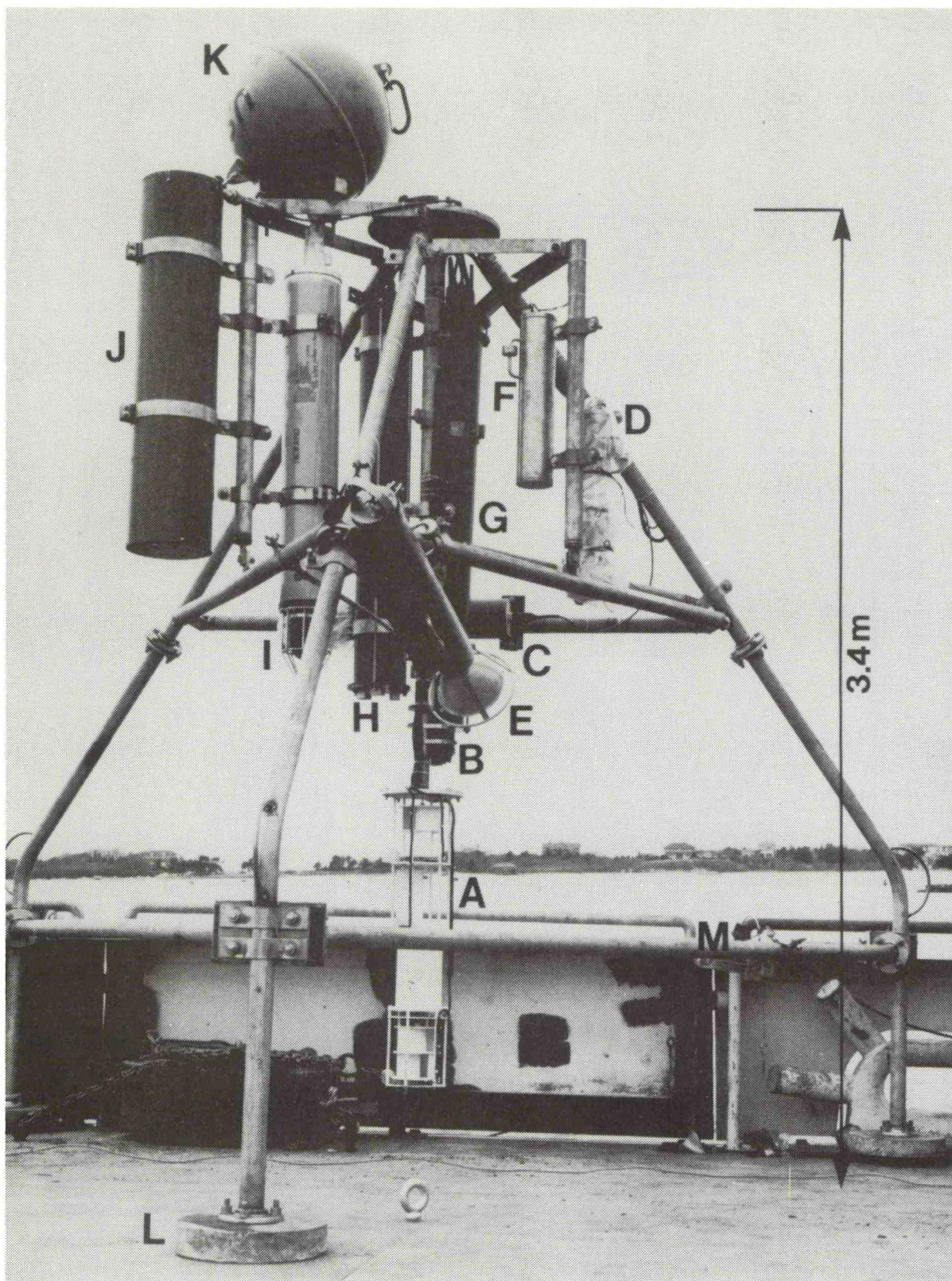


Figure 32. U.S. Geological Survey Tripod System: (A) current sensor (this photograph is of a modified system with two savonius rotors); (B) pressure sensor; (C) transmissometer; (D) camera (wrapped in protective plastic bag to enclose anti-fouling ring); (E) strobe light; (F) camera battery pack; (G) Sea Data electronics; (H) battery pressure housing; (I) acoustic release transponder; (J) rope canister; (K) recovery float; and (L) lead anchor feet. (Butman and Folger, 1979).



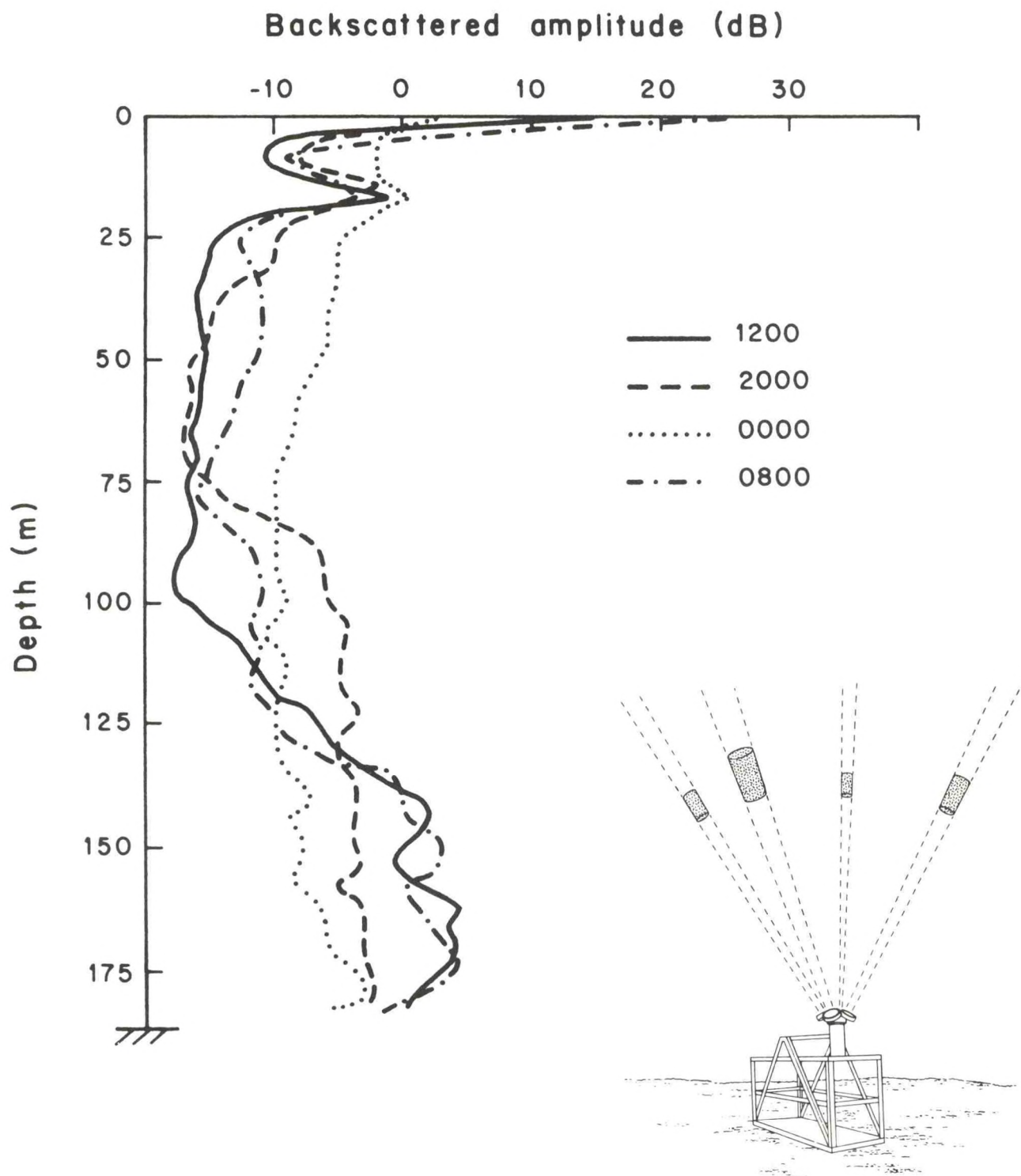


Figure 33. An example of sequential vertical profiles of backscattered amplitude over a 20 hour period during the summer in the Gulf of Maine. Changes in structure reflect the diurnal migration of zooplankton (Pettigrew & Irish, 1986).

# A VIEW (FROM AN OCEAN'S EASTERN BOUNDARY) ON RESEARCH MONITORING (LONG TIME-SERIES) SYSTEMS AND INTERANNUAL VARIABILITY

Robert L. Smith  
College of Oceanography  
Oregon State University  
Corvallis, OR 97331

The two topics "Research Monitoring . . ." and "Interannual Variability" are, of course, intimately connected: without the former one can hardly discuss the latter, and without the latter there would be little reason for the former. In these times, when climate change (and El Nino, El Viejo, greenhouse effect, etc.) is mentioned in virtually every issue of both tabloids and scientific journals, it is important to distinguish between secular trends and interannual variability . . . and to recognize the difficulty of making the distinction without long time-series. The ocean's eastern coastal boundary is particularly sensitive to the El Nino-Southern Oscillation (ENSO) interannual variability because of the equatorial and coastal waveguides (the references would be legion). Its coastal upwelling regions may also be, if Bakun (1989) is correct, sensitive to the global climate change: "greenhouse" warming could intensify the alongshore wind stress.

In the following I will show two examples where we have had longish time-series of currents over the continental shelf, and I will suggest what is the minimal "research monitoring system." Serendipitously, we moored some current meters on the continental shelves of Oregon ( $43^{\circ}$  N) and Peru ( $10^{\circ}$  S) in 1981 and were able to maintain them from before El Nino 1982-3 until after (Huyer and Smith, 1985; Huyer et al., 1987; and Huyer et al., 1989). Thanks to the National Science Foundation (which supported both studies) and the modelers' forecasts of an imminent El Nino, we reinstalled a single mooring off Oregon in the summer of 1986. This mooring has been maintained to date and, hopefully, will be maintained for a few more years. Unfortunately, we were unable to convince the Tropical Ocean and Global Atmosphere (TOGA) program office of the wisdom of maintaining, cooperatively with the Peruvian Navy, the mooring off Peru in 1985. Fortunately, quality tide-gages, which had monitored the ocean for at least a decade prior to our moorings, are maintained in both regions. Sea-level records are extremely valuable, not only because they are perhaps the only truly long-term monitoring of the coastal ocean we have, but also because, when combined with atmospheric and sea surface temperature (SST) records, they can help distinguish local and remote forcing.

The anomalies (from long-term monthly means) for the alongshore wind stress at  $45^{\circ}$  N (Bakun's (1989) upwelling index), the SST measured just inside the jetty at Coos Bay, OR (by the Oregon Department of Fish and Wildlife (ODF&W) and University of Oregon researchers), and the sea level at Newport (Hatfield Marine Science Center) are examined in Figure 1. The El Nino of 1982-3 is the most



prominent feature; note that the warming and the rise in sea level precede the change in wind by a few months. We have argued earlier (Huyer and Smith, 1985) that the coastal oceans off Oregon and Peru began to respond to the ENSO event almost simultaneously (but with greatly different rise-times and magnitudes) due to the rapidity of signal propagation in the waveguides. In other times (e.g., the winter of 1988-9), all three variables show a simultaneous and correlated change, suggesting local (or regional) wind forcing. The current at 25 m above the bottom at mid-shelf near Coos Bay, OR ( $43^{\circ}$  N), is displayed in Figure 2 as low-pass (40 hr half-power) vectors. The mean flow is poleward, more strongly so in winter, and was most strongly poleward during the early phase of El Nino in 1982-3, as was the case off Peru (Smith, 1983). There are now six years for which we can compare a three-month fall to winter (29 October-30 January) mean current. The strongest poleward flow was during 1982-3 ( $13.0 \text{ cm s}^{-1}$ ) and the weakest during 1988-9 ( $5.5 \text{ cm s}^{-1}$ ); among the six years of current observations, these were also extreme for sea level (+49.0 cm and -18.3 cm), and for wind during 1988-9, but not in 1982-3. The rather long time-series from off Peru is also examined (Huyer et al., 1989) (Figs. 3 and 4). Again, the variability of sea level and its rise signaling the advent of El Nino are clear. (See *J. Geophys. Res.*, 93 (C13), 1987, for other papers about ENSO and Peru.)

It is clear to me that sea level monitoring (by means of quality tide-gage measurements) is a *sine qua non* for monitoring the coastal ocean. Winds are, of course, vital, but analysis products such as the Limited-Area Fine Mesh (LFM) and Fleet Numerical Oceanography Center (FNOC) winds are available. We have pitifully few SST monitoring stations along the coasts which are restricted to a few marine biology laboratories. Given the ubiquity of fog and coastal clouds in coastal upwelling regions, satellites have not fully replaced the bucket temperature measurement made off a pier, or its modern equivalent. Direct current measurements, with a satellite data link, would be useful for Synthetic Aperture Radar (SAR) purposes and for providing current velocity monitoring for oil spill response. Funding for monitoring currents for these purposes would probably receive a more favorable response than for research purposes. The practical utility of tide-gage measurements has not affected their research utility; hopefully, there will be other opportunities for similar symbiotic arrangements.

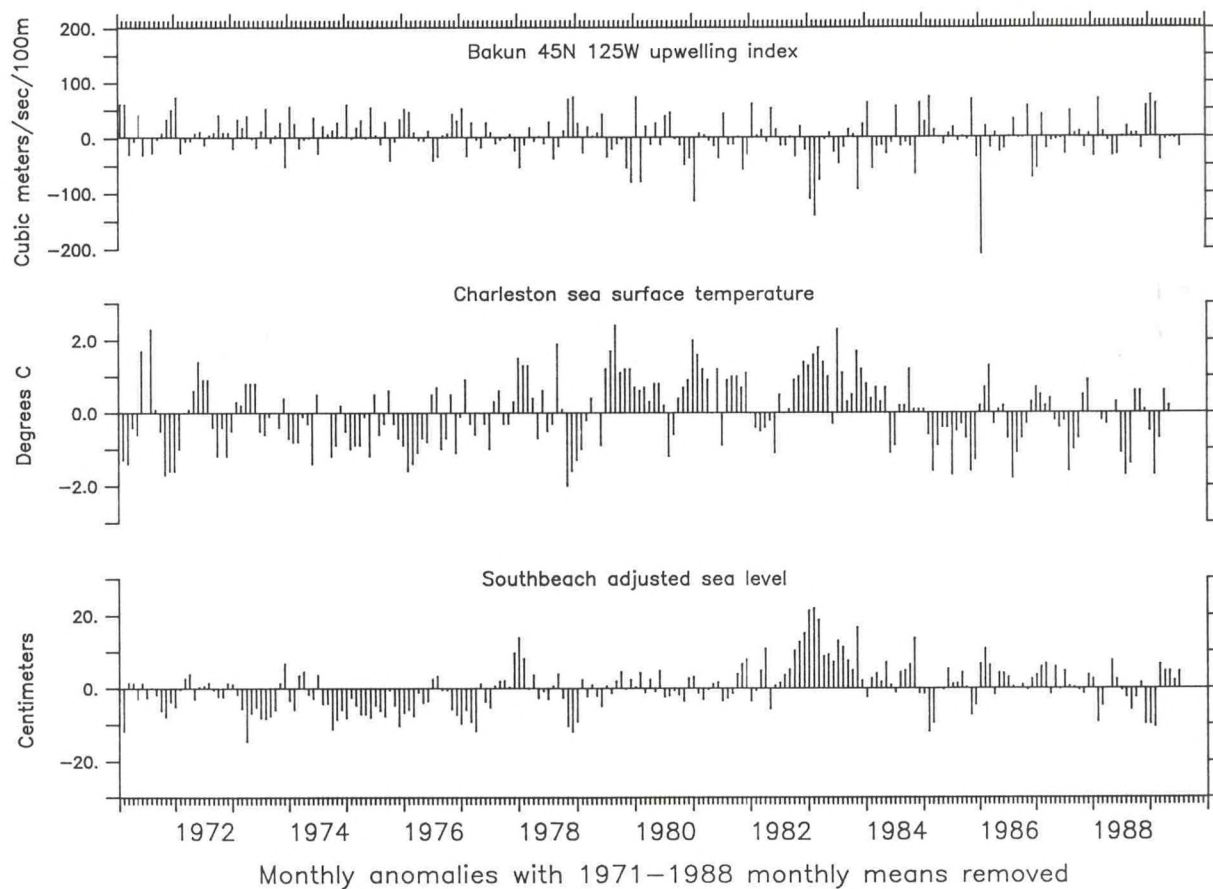


Figure 1. Monthly anomalies off Oregon in upwelling index ( $45^{\circ}$  N), coastal SST ( $43^{\circ}$  N), and sea level ( $45^{\circ}$  N). The means removed for January to December are: -91, -75, -18, 5, 27, 45, 65, 52, 11, -6, -72, -76 for the upwelling index; 9.9, 10.0, 10.4, 10.7, 11.5, 12.2, 12.4, 12.4, 12.4, 11.5, 11.5,  $10.4^{\circ}$  C for SST; 26.4, 24.4, 18.8, 9.3, 4.7, 4.1, 5.2, 6.8, 10.4, 13.2, 22.4, 27.0 cm for adjusted sea level.



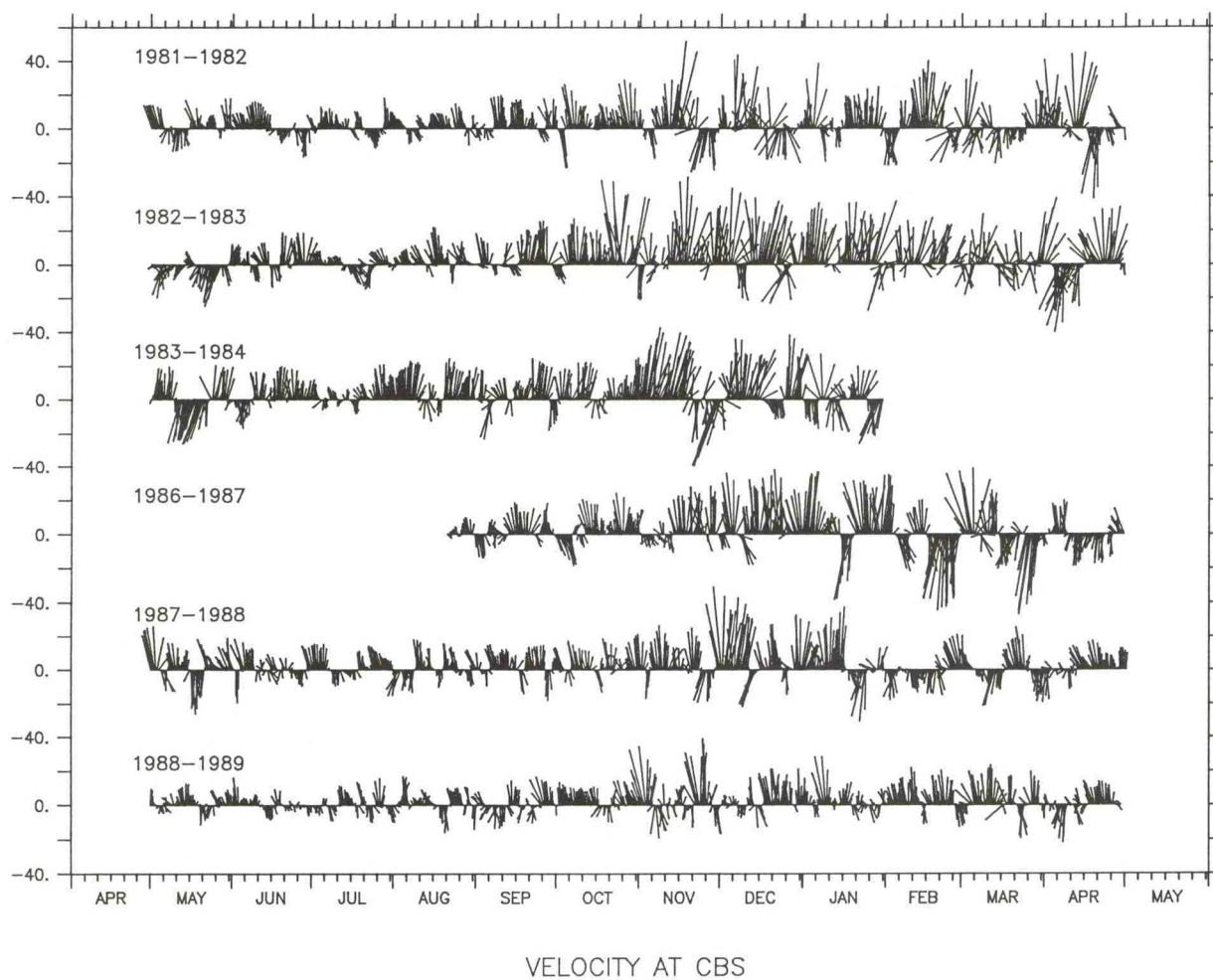


Figure 2. Low-pass filtered (half-power at 40 hr) velocity vectors (north upward) for mooring at mid-shelf (90 m water depth) 25 m above the bottom near 43° N off Oregon.

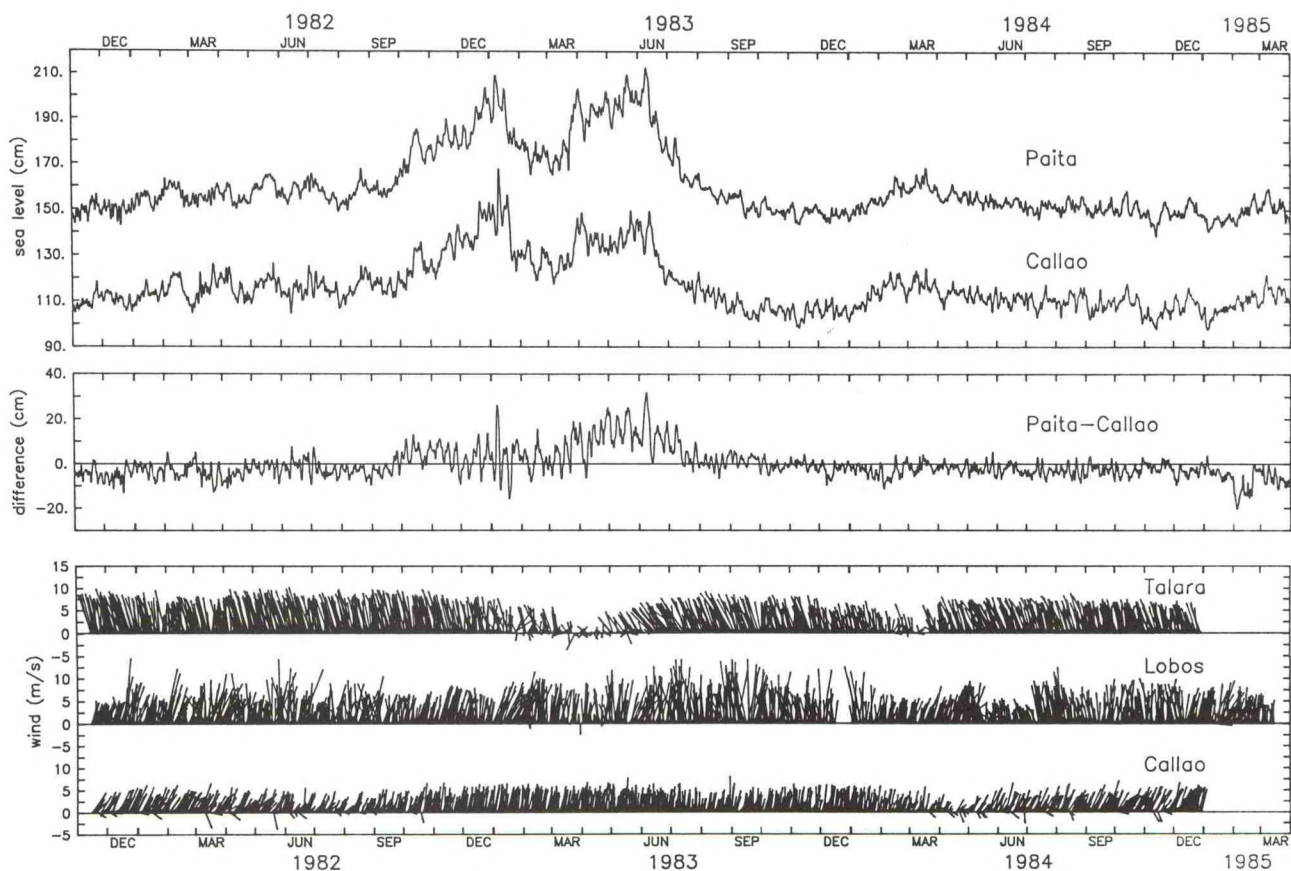


Figure 3. Time-series of coastal sea level (relative to the local datum) at Paita ( $5^{\circ}$  S) and Callao ( $12^{\circ}$  S), the sea level difference between them referred to 500 dbar by least squares fit to steric height (Huyer et al., 1987), and the coastal winds at Talara ( $4.5^{\circ}$  S) and the Lima airport in Callao, and winds from Isla Lobos de Afuera ( $7^{\circ}$  S). From Huyer et al., 1989.



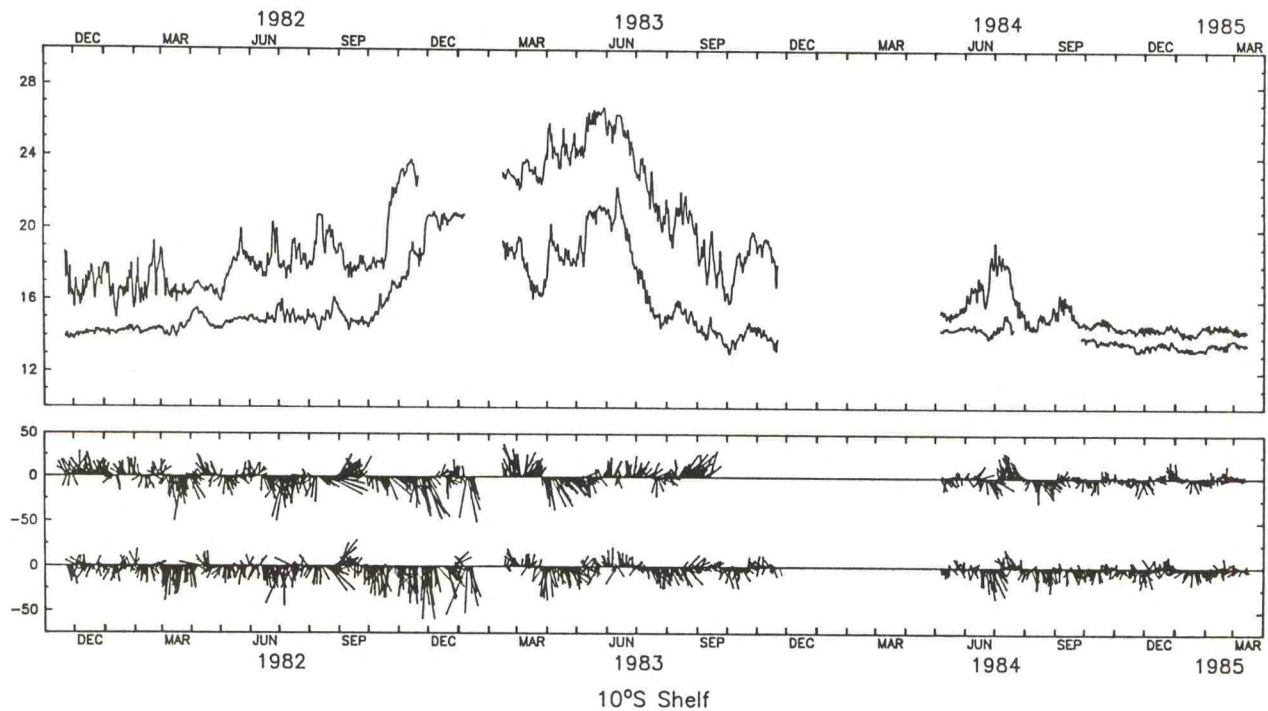


Figure 4. Time-series of low-pass filtered temperature and currents from instruments at nominal depths of 50 and 100 m on mooring at 10° S, bottom depth of 150 m. Vertical axis points toward 315° T, the equatorward along-shore direction. From Huyer et al., 1989.

# COUPLING REMOTE MEASURES OF OCEAN CHLOROPHYLL WITH OBSERVATIONS AND MODELS OF COASTAL CIRCULATION

James A. Yoder  
Graduate School of Oceanography  
University of Rhode Island  
Kingston, RI 02881

## Summary

During the 1980s, studies that merged analyses of Coastal Zone Color Scanner (CZCS) imagery of phytoplankton chlorophyll (CZCS-Chl) with observations and models of coastal circulation often yielded interesting and new results. In most instances, the primary beneficiary was biological oceanography, in that the circulation information explained many of the CZCS-Chl distribution patterns observed in the imagery. In some cases, however, the CZCS imagery provided important clues for understanding coastal circulation. The Sea-Wide Field Sensor (Sea-WiFS) or comparable sensor planned for launch in the mid 1990s will provide much better temporal coverage of coastal waters than did CZCS and will incorporate additional spectral bands to improve on the accuracy of CZCS-Chl estimates in coastal waters. Aircraft-borne ocean color sensors are particularly well-suited for coastal observations, and future applications will be limited only by fiscal constraints and the ability of federal and state agencies to manage chartering arrangements for aircraft.

## Background

In the recent past, studies of upwelling plumes off the West Coast have provided one of the best demonstrations of the potential for merging circulation observations/models with CZCS-Chl imagery. CZCS-Chl imagery showed that plumes of productive upwelled waters extended offshore many hundreds of kilometers at many locations along the western coast of North America (Abbott and Zion, 1985, 1987; Pelaez and McGowan, 1986). Presently, the focus of several research programs is to merge information from the CZCS-Chl time series with *in situ* observations and numerical models to address such questions as: (1) How much carbon is transported offshore within the plumes? (2) How does the California Current interact with the plumes to affect the distribution of productive waters? (3) What are the principal seasons and locations for plumes to form and then dissipate? (Denman and Abbott, 1988; Smith et al., 1988; Michaelsen et al., 1988). Until CZCS-Chl imagery became available, these features were unknown (except in satellite IR imagery). [Editorial Note: As biologically manifested entities; they had been detected earlier as thermal anomalies in Advanced Very High Resolution Radiometer (AVHRR) imagery.] Quantitative assessment of their importance to phytoplankton productivity, and the fate of primary production off the West Coast, cannot be determined without merging circulation observations and models with information derived from the imagery.



Other examples of the utility of CZCS are available from the East Coast where Gulf Stream processes dominate outer shelf and slope waters. CZCS-Chl imagery coupled with hydrographic and current measurements have been the principal observations used to elucidate the complex history of primary production occurring within Gulf Stream rings, which are prevalent in slope waters north of Cape Hatteras (Brown et al., 1985; Evans et al., 1985; Smith et al., 1987). In shelf waters south of Cape Hatteras, Gulf Stream frontal eddies and meanders are the primary features affecting outer shelf productivity. CZCS-Chl imagery has provided observational evidence supporting circulation models of frontal eddies (McClain et al., 1988) and is presently being used to determine effects of frontal eddy upwelling on distributions of outer shelf phytoplankton productivity and biomass, as well as the fate of phytoplankton carbon synthesized during upwelling events (Yoder et al., 1987; Yoder, work in progress; Ishizaka and Hofmann, unpublished).

### Sea-Wide Field Sensor (Sea-WiFS)

The CZCS stopped operating in the summer of 1986. A replacement satellite ocean color sensor has yet to be launched. No other color satellite scanner is available now. During the past four years NASA negotiated first with EOSAT and then with Hughes Aircraft to fly a scientific/commercial sensor, Sea-WiFS, either on Landsat-6 or on a small satellite dedicated to the ocean color mission. The negotiations have yet to be successful, and there now seems to be little hope for a joint venture between a commercial company and NASA for an ocean color mission. Since the commercial option has not proved viable, there is increasing support (born out of increasing frustration!) in the scientific community for NASA to drop its plans for a commercial partner and fly an ocean color sensor in the mid 1990s as part of the NASA's new Earthprobes program. Sea-WiFS (or a comparable NASA sensor flown under the Earthprobes program) will have three very significant improvements over CZCS which should make it particularly attractive to coastal oceanographers.

First, Sea-WiFS has two new spectral bands in the near-IR centered at 765 and 865 nm which should greatly improve the accuracy of the atmospheric correction algorithms over coastal waters compared to CZCS. This increased accuracy of atmospheric correction will greatly improve the accuracy of pigment estimates for coastal waters and will extend the upper range for chlorophyll estimates to 10 or more  $\text{mg m}^{-3}$ .

Secondly, Sea-WiFS will make continuous measurements. In comparison, the CZCS was operated intermittently, making only 10-20% of the possible observations. As a result, Sea-WiFS will have much better temporal coverage with a re-visit interval of about one day for much of the global ocean.

Finally, near-real-time data distribution will be possible. (Access to real-time data downlinked to regional antenna facilities may require payment of a commercial license fee.) Scientific users can expect routine access within about ten days after data acquisition.



## Aircraft Observations

Aircraft remote sensing, both passive and active, is underutilized in coastal oceanography. Underutilization is primarily a financial problem rather than a technical one. Federal agencies are reluctant to pay the high aircraft operating costs from the same pool of money that supports research. In contrast, ship operations are supported by the National Science Foundation (NSF) from a budget distinct from that which supports ocean research. To change the present pattern of agency funding of aircraft remote sensing requires that user groups develop very strong scientific arguments for using aircraft measurements. These arguments must be presented effectively to managers from agencies (e.g., NASA, the National Oceanic and Atmospheric Administration (NOAA), the Office of Naval Research (ONR)) which presently operate research aircraft capable of ocean remote sensing. A second possibility for the future is to request agency funds to charter small planes. Airborne ocean color instrumentation, including lidars, can now be built much smaller than was possible a few years ago. These new, small instruments can be operated from relatively small aircraft which can be chartered for several hundred dollars per hour, as compared to several thousand dollars per hour for a research P-3 airplane. (N.B. Research aircraft are available through NSF's facility at the National Center for Atmospheric Research (NCAR). They have been used successfully in coastal oceanography. The issue is whether they are capable of ocean remote sensing with the new, smaller instruments.)

Aircraft ocean color sensors can be classified within three general categories: (1) scanning spectral radiometers from which 2-D images can be derived with pixel resolution of the order of 10m X 10m, (2) spectral radiometers for collecting a line of data along the flight path of the plane, and (3) lidars for stimulating pigment fluorescence along the flight path of the plane.

Scanning spectral radiometers such as the Airborne Ocean Color Imager (AOCI) (NASA/Ames) and the Airborne Visible and Infrared Imaging Spectrometer (AVIRIS) (Jet Propulsion Laboratory (JPL)) are flown in NASA aircraft at high altitude, generally by a U-2. These radiometers yield 2-D images with ca. 10m X 10m pixel resolution across a swath of the order of 50 km wide. The disadvantages of these instruments is that data processing is a significant chore, and NASA U-2s are difficult to schedule for occasional use and probably impossible to schedule for routine use.

Along-track spectral radiometers such as MARS (Dr. Jim Mueller, San Diego State University) and Ocean Data Acquisition System (ODAS) (Dr. Wayne Esaias, NASA/Goddard Space Flight Center (GSFC)) are presently being operated over coastal waters. They can be flown in single or twin engine aircraft. ODAS is a relatively small and simple instrument that measures upwelling radiance at 460, 490 and 520 nm and incident irradiance from low altitude (<1000 ft) along the flight path of a small aircraft. Radiance data are converted to an estimate of chlorophyll concentration using a spectral curvature algorithm that works well for coastal waters at chlorophyll concentrations ranging from 0.05 to 50 mg m<sup>-3</sup>. The instrument is presently being used extensively in Chesapeake Bay. The instrument package includes



a Long-Range Aid to Navigation (LORAN) receiver, thermal radiometer (PRT-5) (thermal infrared (IR)), aircraft-to-ship data downlink, and real-time display.

MARS is an along-track radiometer built with ONR funding. It has ten downlooking bands in the visible and near-IR spaced between 410 and 725 nm and four uplooking bands at 410, 440, 550 and 725 nm. The data logging system is a laptop personal computer (PC), navigation is provided by the airplane, and the instrument can accommodate a PRT-5.

The Airborne Oceanographic Lidar (AOL) (Dr. Frank Hoge, NASA/Wallops) is a system of instruments built around a lidar that excites the ocean with blue-green laser light. Detectors measure both laser- and sunlight-stimulated spectra at 256 channels in the visible/near IR wavelength bands. Additional instruments include a PRT-5 for near-surface thermal IR and air-deployed expendable bathythermographs (AXBTs), with capability to launch and record the latter. The system presently is flown on the NASA P-3 aircraft. Navigation includes LORAN and Global Positioning System (GPS).

Along-track estimates of laser-induced chlorophyll fluorescence, phycoerythrin fluorescence and surface temperature are produced with a spatial resolution of ca. 10 m. These data are used to study the mesoscale distribution of phytoplankton in relation to near-surface hydrographic features. The AOL was recently operated in support of the 1989 Joint Global Ocean Flux Study spring bloom study in the North Atlantic.

The AOL can also be operated in a scattering mode to determine subsurface profiles of particles, including phytoplankton and sediment. This capability is presently under development with the goal of mapping the depth of the subsurface chlorophyll (or particle) maximum layer in oceanic waters, which occurs at depth near 100 m.

The AOL is a sophisticated sensing system which has been proven under many different operating conditions. The AOL is disadvantaged by the NASA P-3 costs. Using new laser and electronic technology, a much smaller version of the AOL could be built and operated on a smaller aircraft.

# RADAR MAPPING OF OCEAN SURFACE CURRENTS: DESCRIPTION AND USES IN COASTAL OCEANOGRAPHY

Phillip A. McGilivray  
NOAA Center for Ocean Analysis and Prediction Laboratory  
Monterey, CA 93943  
and  
NOAA Wave Propagation Laboratory  
Boulder, CO 80303

## Introduction

### How Surface Current Mapping Radars Work

High-frequency (HF) radar waves (frequencies 3-30 MHz; wavelengths 10-150 m) are strongly reflected from ocean surface waves one-half the radar wavelength. This interaction, Bragg scattering, causes a strongly positive interference with a pronounced spectral peak at one specific frequency (Barrick, 1972; Stewart and Joy, 1974). Ocean surface waves are advected by ocean surface currents, producing a Doppler shift in the frequency of the returning radar Bragg scatter peak. This Doppler shift in frequency is proportional to the current velocity at the ocean surface in a direction radial to the radar receiver. Total horizontal current velocity is obtained by combining radial radar vectors from two radars, usually about 20 km apart.

Radars for ocean surface current measurement were developed in the U.S. by the National Oceanic and Atmospheric Administration (NOAA) Wave Propagation Lab (WPL) in the early 1970s (cf. Barrick et al., 1977). The theory and technology developed at WPL during this period is the basis for all radar ocean surface current measurement devices in use today. The technology for radar surface current measurement, developed as the Coastal Ocean Dynamics and Ranging (CODAR) system (Barrick et al., 1977), was taken through several developmental stages, and its accuracy demonstrated in more than a dozen field experiments by various researchers (Barrick et al., 1977; Collar et al., 1985; Griffiths et al., 1985; Porter et al., 1986; Teague, 1986).

HF radar measurements of surface current speed may be accurately made for speeds  $> 2$  cm/sec, and current direction estimates are accurate for speeds  $> 5$  cm/sec (see references cited above). HF radars typically provide current vectors averaged over  $1 \text{ km}^2$  range cells. Use of two radar sites separated by about 20 km results in an arc-shaped grid of range cells extending from 20-50 km offshore, covering  $O (> 100) \text{ km}^2$  of ocean surface. Surface current maps are typically produced hourly, although they can be made as often as every 15 minutes. Automatic restart software (using a battery-powered clock) is incorporated into these radars to permit resumption of operation following any accidental power interruption. To make operations as autonomous as possible, self-diagnostic software is included to provide error or shut-down messages in case of excessive radar signal drift, electrical interference, or radar component failure.



## Use of Surface Current Mapping Radars in Coastal Oceanography

With the exception of acoustic tomography, most current measurement methods do not provide three-dimensional current field data, but only current vectors at one location and depth (mechanical), or as a vertical profile at one location (acoustic). Moreover, most techniques dramatically fail to estimate currents at the ocean surface, and are not typically available in near-real time. HF radar methods offer much greater temporal and spatial coverage of surface currents than does any other technique for studying currents in coastal areas. As the method is presently land based, the radars can operate automatically and untended at a fraction of the cost of other current monitoring methods: thus, radars are suitable for consideration as part of a coastal ocean monitoring network.

In the 1980s, HF radar surface current mapping technology came under the support of the Canadian and several European governments, with two results. First, radar surface current mapping methods were extensively verified in the field against other current measurement techniques (Canada: Lawrence and Smith, 1986; Dunbar et al., 1989; Germany: Essen et al., 1983 and 1989; Gurgel et al., 1986; England: Collar et al., 1985; Hammond et al., 1987; Griffiths et al., 1985; Prandle and Ryder, 1985). Second, commercial surface current mapping radars, modeled after those initially developed in the U.S. by NOAA, were developed overseas.

Surface current mapping radars are now used in England, Norway, Germany, the Netherlands, France, Australia and Canada to provide data on the location and dynamics of surface current features associated with coastal fronts, eddies, and areas of upwelling divergence. The availability of hourly data makes possible the examination of changes in surface current indications of coastal hydrodynamic features over tidal cycles and through short-term events. Radar methods are also unaffected by weather conditions, and would be useful for monitoring changes through atmospheric frontal passage, etc.. Such routinely available measurements of ocean surface currents would provide essentially real-time searuth data for initial and boundary conditions for coastal ocean models. HF radar surface current technology also provides the ideal means of tracking drifting material, whether ice floes, fish eggs, invertebrate larvae, spilled oil, or humans overboard. When ships, buoys, or drifting gear are equipped with inexpensive (\$1 K) transponders, their multiple locations can likewise be easily tracked over time and space using a HF radar.

In the future, another use of HF radar surface current data may be possible. The capability of combining detided radar-derived ocean surface current maps with fine-scale coastal ocean wind field data (e.g., from networks of buoys, wind profilers or Light Detection and Ranging (LIDAR) devices) would permit estimation of absolute magnitudes of coastal upwelling dynamics, information of great value in coastal ocean studies.

## Role of Surface Current Mapping Radars in COPS

Surface current mapping radars can contribute significantly to the goals of the Coastal Ocean Prediction System (COPS) program. Surface current data are likewise



recognized as fundamental and warranting priority funding as part of national efforts to improve understanding of continental shelf circulation, as stated in the Coastal Physical Oceanography (CoPO) program review documents (Garvine et al., 1989). The most important characteristic of surface current mapping radar is the ability to provide near-real-time (hourly) data for areas of  $O(100 \text{ km}^2)$  from a relatively inexpensive ( $\sim \$200 \text{ K}$ ), shore-based, compact, unmanned remote sensing device which can operate continuously for years in all kinds of weather with very minimal maintenance. If a network of HF radar stations is envisioned, cost per additional site would be only  $\$100 \text{ K}$ . Field data from many sites can be telemetered hourly to one central location for hourly processing and distribution.

Surface current mapping radars would provide data called for by the several elements of the COPS program.

### Coastal Meteorology

Since wind effects and heat flux are both maximal in the ocean surface layer, surface current data would be useful for coastal meteorological studies for several reasons. First, surface current data can be used in studies of wind/seabreeze forcing on coastal ocean circulation. Radar-derived surface current data are particularly useful for recording the 2-D ocean surface structure of mesoscale transient features resulting from wind forcing. Surface current data are also critical for improving parameterization of turbulent boundary fluxes of heat and moisture, important because cooling and evaporation produce buoyancy changes significantly contributing to coastal ocean circulation.

In the future, use of radar-derived surface current data should incorporate wind data from coastal wind profilers or LIDAR, a goal of NOAA's technology development program. Radars which measure current shear across several meter thick strata of the uppermost ocean surface have been developed and used aboard ships (cf. Teague, 1986). Such measures could be used to directly measure wind or seabreeze effects on ocean surface forcing.

### Moored Ocean Measurements

Moored ocean measurements will provide vertical searuth profiles for ocean models, which radar surface current data can be considered to extend by inference over larger areas. Data provided by fixed moorings would have much greater meaning when interpreted with the aid of larger scale surface circulation patterns provided by a radar. A national network of radar devices could easily provide large-scale data to augment information from fixed moorings. Deployment of current mapping radars from moored buoys or ships is possible in the future: a CODAR system has recently been successfully demonstrated from a semi-submerged platform (Lipa et al., 1990). Radar-derived surface current vector maps would permit interpretation of moored Acoustic Doppler Current Profiler (ADCP) vertical current profiles in light of their location relative to larger-scale surface flow fields.



## Synoptic Surveys

Spatial and temporal coverage of airborne synoptic surveys over the coastal ocean would be improved by incorporation of radar-derived surface current data. This information would be useful for abetting interpretation of oceanographic research methods as diverse as Synthetic Aperture Radar (SAR) overflight and satellite imagery feature trajectory analysis.

## Remote Sensing

Remote sensing methods are of great value in monitoring shelf-open ocean boundary exchange processes, including the dynamics of tidal and non-tidal fronts, eddies, etc. However, temporal coverage of these methods is usually spotty, due to sampling constraints of satellites, and weather limitations. Where coastal ocean features are  $< 100$  km from shore, radar surface current maps offer hourly data to extend temporal coverage of remote sensing imagery. The finer temporal sampling of current mapping radars also allows examination of medium time scale forcing events from offshore sources, such as continental shelf edge waves, and shelf-trapped waves indicated in some satellite images. Radar surface current data can likewise be used to increase understanding of satellite data on current interactions with topography, and tidal and other coastal currents, providing data on current separation from the coast and cross-isobath flow. For optimal comparison with remote sensing data, a network of surface current mapping radars would be needed to provide comparable coverage of the ocean surface.

## Lagrangian Drifters

Existing shore-based HF radars can measure frontal currents only where fronts are  $< 50$  km offshore, and hourly maps of  $1 \text{ km}^2$  resolution are adequate. In the near future, commercial HF radar will permit such resolution for fronts  $< 80$  km offshore. The routine availability of such frontal circulation information from HF radars would be a great advance in frontal-land-shelf-edge boundary monitoring.

As HF radar surface current maps may be made hourly and continuously in all weather, they can provide information on flow fields and flow field variability around drifters. Drifters with radar reflectors will show up at these distances, while drifters which incorporate an inexpensive (\$1K) radar transponder can be tracked to 160 km offshore. COPS programs using Lagrangian drifters would benefit directly from radar maps of offshore circulation, which could include locations of the drifter itself to 160 km offshore. Using several transponder frequencies, a number of drifters could be tracked simultaneously.



## **Systems Integration/Data Management**

### **Integration with Existing and Planned COPS Networks**

Radar-derived surface current data would extend data interpretation from the three existing data networks planned as part of the COPS database, most notably wind and weather data from National Data Buoy Center (NDBC) buoys and Coastal-Marine Automated Network (C-MAN) weather stations. The ability of the newer surface current mapping radars to detect storm surge and wave field data could also be developed to extend spatial and temporal coverage of Army Corps of Engineers coastal wave and surge gauges. If additional COPS data stations make use of stations with seafloor-mounted ADCPs or moored current meter string locations, these data can be compared with radar-derived surface current data.

### **Management Concerns for an HF Radar Network**

The federal role in a network of coastal current mapping radars under the COPS program could be that of coordinating efforts to acquire, manage and distribute any such data provided (a role of the National Ocean Service within NOAA), and to advise in the design and operation of such devices (a role of NOAA's Environmental Research Laboratories within NOAA). Data on surface currents will be useful to a broad range of user groups, including physical oceanographers, fisheries researchers, maritime vessels, and hazard monitoring personnel. Both commercial and public vessels would probably welcome the energy savings made possible by using surface current maps to alter ship tracks in order to take advantage of favorable currents.

Data from radar units not part of a national network should also be obtained, archived, and distributed by NOAA in a coordinated manner. This would involve cooperation with state, local, and private as well as government installations. Obtaining these data in near-real-time is not, however, difficult or expensive, requiring only the purchase and upkeep of data telemetering devices. Other radar installations are most likely to be those operated by various states (e.g., for monitoring foreign fishing vessels and offshore ship traffic, or environmentally critical marine habitats) and some local organizations (e.g., harbormasters and research institutes).

The federal role in developing a COPS program for deployment of such radars would be critical in both operational and research aspects. Financial resources would be needed not only for each field radar site (\$100 K), but also for the costs of telemetering data, ensuring short-term analysis quality, conducting long-term record-keeping and analysis, and ensuring distribution to all interested parties in near-real-time as a top priority. Personnel and computer networks are already available in NOAA to handle much of this work, although some additional support would be required. Additional federal support would be required for completion of developments for newer radars, including those providing simultaneous near-coastal wind data in addition to surface current information.



## Short-term Prospects for Surface Current Mapping Radars

A NOAA HF surface current mapping radar now installed in Monterey Bay is intended as a prototype for a possible national network. The radar system will provide surface current coverage for Monterey Bay, telemetering raw data to a central computer for processing. Call-in requests for hourly surface current maps will be filled via telecopier (FAX) service or, alternatively, via transmission over existing computer communications networks serving the oceanographic community and general public. More coverage of the California coast is anticipated from additional radar sites in the future.

New surface current mapping radars available in late 1990 will be considerably superior to existing radars, having: 1) two orders of magnitude lower power requirements; 2) greater reliability due to solid state transmitter construction; 3) coverage to 80 km versus earlier 50 km (25 km for the commercial British Ocean Surface Current Radar (OSCR) system); 4) transponder range extended to 160 km versus earlier 100 km; 5) more compact hardware and antenna; and 6) a personal computer (PC)-based operating system. Also, newer radars will cost only half as much (roughly \$100 K per site) as earlier U.S. and existing commercial foreign HF current mapping radars. The updated surface current mapping radar can also use more than one transmit frequency (e.g., 13 and 26 MHz) to measure ocean currents over two upper depth strata (e.g., 0.5 and 2.0m depths) to permit estimation of vertical shear stress. A new radar prototype has also been demonstrated to provide good data on surface wave field direction (Lipa and Barrick, 1986; Lipa et al., 1990). Although surface current mapping radars are commercially available from foreign companies (e.g., OSCR radar; MAREX Company, England), they are both less sophisticated than and more than double the cost of those available in the U.S.

## Long-term Prospects for Surface Current Mapping Radars

Two new NOAA advanced radars are in the developmental stages: a Spaced Antenna Technique (SAT) radar, and a Delta-K dual Doppler microwave radar (named the Combined Ocean & Atmospheric Sensing Technique (COAST) radar). Both radars have undergone preliminary field tests which have demonstrated their operation. However, further field testing is needed to complete development of operational field systems for these radars.

Development of shipboard surface current mapping radars is now planned by both NOAA and the Navy. Such shipboard radars could map current velocity and direction across oceanic fronts in near-real-time during shipboard operations. Although there are no real obstacles to the development of these devices, they are not likely to be ready for general use for several more years.

Optimal use of coastal current mapping radars would involve analysis using fine-scale wind field data. The present lack of fine-scale coastal wind field data represents a critical deficiency in the present attempt to understand coastal physical dynamics (Brink, 1989). Presently, coastal wind data are available only

from extremely few ocean buoys and land sites which poorly reflect the complex three-dimensional onshore and offshore wind fields which influence fine-scale coastal ocean features. In the future, such data may be available from LIDAR systems which provide wind field data several times per hour to 20 km offshore and 1 km altitude, with data cell resolution of 10 m vertical and 0.1 km horizontal. The next generation of LIDAR devices, made much smaller and less expensive by incorporation of new solid state lasers, should be available within two years, when NOAA contracts to develop "eye-safe" lasers for LIDAR instruments are completed.

### Summary

It seems likely the U.S. will make use of high frequency radar coastal current mapping systems in the future. These systems can be developed as part of the Coastal Ocean Prediction System so as to be part of a coordinated U.S. coastal ocean monitoring system. Otherwise, their installation in the U.S. might be expected to follow European patterns of deployment in a piecemeal fashion to serve local needs for research, offshore monitoring of foreign fishing vessels, or tracking of ship traffic in crowded or ecologically sensitive coastal areas, or possibly at areas of high risk for oil spills. HF radar technology in the U.S. is now ready for deployment at individual sites, or more economically as a network. The cost of U.S. radars is less than half that of foreign versions, and they have much greater range and other advantages. Radar technologies now under development may permit surface current mapping by single station radars, or provide surface current and wind field data simultaneously. Such versions are not expected to be available for at least several more years, however.



# A NATIONAL BUOY NETWORK FOR CONTINUOUS, REAL-TIME MONITORING OF PHYSICAL, CHEMICAL AND BIOLOGICAL PROCESSES IN U.S. COASTAL WATERS

Paul G. Falkowski, Charles N. Flagg,  
Creighton D. Wirick and Zbigniew S. Kolber  
Oceanographic Sciences Division  
Brookhaven National Laboratory  
Upton, NY 11973

## Introduction

The quality of the coastal waters of the U.S. is increasingly threatened by anthropogenic activity. Over 80% of the population of the U.S. lives within 30 miles of a coastline. Urbanization and economic development have led to eutrophication, ocean dumping of toxic noxious wastes, and overfishing. These and other activities threaten the supply and quality of coastal marine and estuarine resources, and the economic future and security of the United States. On longer time scales, global changes in climate and atmospheric chemistry may profoundly affect the morphology of the coastline and, concomitantly, the availability of crucial marine resources. While clearly many of the solutions to these problems require economic and political commitments, in the short term, redirection of economic resources to alleviate an insult to the environment often leads to conflict between economic growth and environmental concerns. To reduce the tensions between these two forces, justification for environmental remediative or preventative actions should be based on robust scientific evidence and understanding. While evidence of human-induced changes in the quality of coastal waters is relatively well documented in many regions, relating those effects quantitatively to the economy and security of the country is tenuous. To achieve such a linkage, there is a critical need to develop predictive models of environmental change which can be used to project the effects of future activities on coastal resources.

The development of scientifically sound models of coastal waters, including physical forcing, chemical loadings and reactions, and biological processes, requires:

- 1) high quality, synoptic data;
- 2) a long-term commitment; and
- 3) a multi-disciplinary approach.

Of these, the acquisition and processing of field data is usually the most expensive and least professionally (?) rewarding activity. Mid-range ships in the research fleet cost on the order of \$10,000 per day to operate, not including gear or salaries for scientists and professional staff. Thus, continuous (realistically, 300 days/year) acquisition of data from ten regional coastal sectors would cost on the order of \$30,000,000/year plus equipment and salaries. (That estimate assumes that continuous sampling by one research vessel would provide adequate synoptic coverage of a



regional domain, which is highly doubtful.) That commitment is about tenfold greater than the support for most process-oriented field studies, which have stronger support from academic scientists. It is no wonder that "monitoring" is disdained by many science administrators as being too costly and giving little "bang for the buck."

We propose that the relevant state and federal agencies consider deploying a national network of instrumented buoys in coastal waters. The technology is presently developed to the extent that such a network could provide real-time information, anywhere in the country, about physical, chemical and biological variables. If, simultaneously, modeling efforts could become more sophisticated and reduce computational overhead, the data acquired in real-time could be used to diagnose and predict short-term changes in the coastal ocean. As data are acquired over extended periods of time, the reliability of predicting anthropogenic and natural processes in the coastal ocean would increase. Such a program is analogous to the development of weather prediction and climate forecasting models, which evolved over the past 50 years.

## The Sensors

Buoys have been used routinely by physical oceanographers for two decades. In the last decade however, biological oceanographers have developed sensors capable of measuring a variety of important variables and processes in real-time, non-destructively. Among these are: (1) chlorophyll, (2) photosynthesis, (3) zooplankton biomass, (4) oxygen, (5) transparency, (6) spectral irradiance, and (7) dissolved hydrocarbons. We will briefly describe how these sensors work and our experiences with them.

### Chlorophyll

Chlorophyll can be measured by *in vivo* fluorescence. At Brookhaven National Laboratory (BNL) we designed and built instruments specifically for moorings (Whitledge and Wirick, 1986), which measure fluorescence and temperature (Fig. 1) and run on 19 D-cell flashlight batteries, which power a xenon flash lamp, driver circuit and a data acquisition system. The instruments have been used since 1983 in a variety of field programs, including the Shelfbreak Exchange Process (SEEP) program in the Mid-Atlantic Bight (Falkowski et al., 1988), the Spring Experiment (SPREX) program in the South Atlantic Bight, the Inter-Shelf Transfer and Recycling (ISHTAR) program in the Bering Sea, the Reef Flux Experiment (REEFLUX) program in the Red Sea, and in a "brown tide" monitoring program in Peconic Bay, Long Island. To prevent fouling, the optical surfaces of the fluorometer are brushed by a mechanical device every 23 hours.

The fluorometer sensors are normally burst sampled. For example, in the summer in the Bering Sea we take six readings in 1 minute, at 34-minute intervals. On long (over winter) deployments, the sensors are sampled three times each 68 minutes. Chlorophyll *a* is calculated from the *in situ* fluorescence using a single fluorescence number (Falkowski and Kiefer, 1985).



## Photosynthesis

There are two methods for measuring photosynthesis in real-time, non-destructively, without incubating a sample; both are based on fluorescence. The first, developed commercially by Biospherical Instruments, calculates the quantum yield of fluorescence induced by natural sunlight. This method is attractive because it is simple, requires little power, and is relatively inexpensive. It is unclear how well the instrument performs in coastal waters (Kiefer et al., 1989).

The second method, developed by Falkowski and Kolber at BNL (Falkowski et al., 1986; Kolber et al., in press), is a pump and probe fluorometer method. It is based on biophysical processes and is basically a modification of a xenon-flash fluorometer. The instrument has been in operation for two years, is used on a conductivity-temperature-depth profiler (CTD), and is compatible with a mooring. It calculates both phytoplankton chlorophyll and instantaneous rates of photosynthesis. The latter requires a simultaneous measure of incident irradiance (see below). The correlation between radiolabeled carbon-based estimates of photosynthesis and those calculated from the pump-and-probe fluorescence data is 0.87 ( $n=59$ ) (Fig. 2). The instrument performs well in coastal waters.

## Zooplankton

The advent of the acoustic Doppler current profiler, the ADCP, and its wide deployment on ships and moorings has changed the way many physical and biological measurements are made. There now are more than 200 ADCP units in the field. The majority of these are in the United States, and virtually all the major University National Oceanographic Laboratory System (UNOLS) vessels now are equipped with ADCPs. Although most of the units have been purchased and are maintained by physical oceanographers for water velocity measurements, their ability to monitor acoustic backscatter, their general accessibility, and their ease of use have made them attractive to biological oceanographers for ecological studies.

Currently available ADCPs operate at acoustic frequencies between 75 kHz and 1.2 MHz, with ranges nominally between 30 and 500 m. For continental shelf work the preferred operating frequency is 300 kHz, which yields a maximum range of about 200 m and which is able to measure currents to better than  $1\text{ cm s}^{-1}$  accuracy with temporal and spatial resolutions of 2 minutes and 4 m, respectively. As for the ADCP's ability to measure zooplankton concentrations, comparisons with net tows to date indicate a precision of 20% for a 10-minute average with a bottom-mounted self-contained instrument (Fig. 3) (Flagg and Smith, 1989). The ADCP data (Fig. 4) allow estimating physical and biological variables over the same spatial and temporal scales, making this instrument unique.

If telemetry of ADCP data is contemplated, then some on-board processing will be necessary to reduce the data volume. Low-powered personal computers (PCs) (drawing less than a watt of power) exist which can process the data to the extent needed to telemeter a subset of the data via satellite as well as write the data to a storage medium. Deploying the ADCPs from surface buoys would take some thought so that



buoy hardware did not interfere with the acoustic beams. An alternative would be to deploy the ADCPs in bottom-mounted configurations and telemeter the data to the surface either through hardwire or acoustic links. Bottom-mounting reduces noise and also simplifies data processing. Hence, it is entirely within the present state of the art to deploy ADCPs on the continental shelf so that they can telemeter data ashore.

### Oxygen

The pulsed oxygen electrode, produced commercially by Yellow Springs Instrument Company, Inc. (YSI), is compatible with long-term deployments. The sensors are stable (Fig. 5), but relatively difficult to calibrate. We have deployed them for up to six months in the Mid-Atlantic Bight in conjunction with fluorometers, transmissometers and ADCPs.

### Transmissometers

We modify fluorometers to support 25cm Sea Tech transmissometers (Bartz et al., 1978). These transmissometers use a red light emitting diode (LED) and a matched photodetector in a 0.25m pathlength. The instrument measures beam attenuation at 660 nm (Fig. 6). In the surface ocean most of the beam attenuation is normally due to phytoplankton, and hence there is a high correlation between beam attenuation and *in vivo* fluorescence. In the bottom boundary layer, however, these two variables are often poorly correlated, reflecting sediment resuspension and or transport.

### Light

A variety of sensors are commercially available to measure light. For broadband, photosynthetically active radiation measurements, we use LI-COR 193SB quantum sensors. The quantum sensors are mounted atop mooring top floats, and their signal cables run to the nearsurface fluorometer. Several different chemical antifoulants are available and can be applied to surfaces near the transmissometer windows and directly onto the quantum sensors. The quantum sensors measure photon flux fluency rate, which has units [ $\mu$  mol quanta  $s^{-1} m^{-2}$ ].

Spectral irradiance can be measured with photodiodes and narrowband interference filters. Biospherical Instruments has deployed a MER-1010 instrument on a mooring at Scripps for a year, powered from a shorebased source. The data is of use for optical models of photosynthesis.

### Hydrocarbons

Hydrocarbons (from spills or natural seeps) fluoresce. The excitation and emission spectra are well characterized and easily distinguished from chlorophyll (Thruston and Knight, 1971). In principle, simply by changing the filter combination on moored fluorometers, one could measure dissolved hydrocarbon concentrations from a moored buoy.



## The Reality of a National Buoy Network

We have briefly described some of the variables which can be measured automatically using either commercially available instruments or instruments we have built at BNL. When these are taken together with physical variables--such as current speed and direction (from the ADCP), vertical profiles of temperature (thermistor chain) and salinity (conductivity chain), and atmospheric variables of interest (sensible heat, wind speed and direction, vapor flux, long- and short-wave radiation, etc.) -- buoys provide an attractive, low-cost alternative to ship-based field measurements. We estimate that a buoy in 50m of water, equipped with an ADCP, a pump-and-probe fluorometer, a light sensor, two oxygen sensors, two xenon flash fluorometers, an ASI sensor package, and data processing and telemetry system, would cost \$500,000. That cost includes hardware and two man-years of labor for construction. Thus, a network of 10 such buoys, operating 365 days/year, would cost about \$5,000,000--one sixth of the cost of a comparable ship-based operation. The costs of the buoys are one-time costs, and the system can be upgraded and expanded according to needs and resources. Moreover, because the buoys can be maintained for extended periods, a long-term (decadal) commitment to monitoring coastal waters can be made by state and federal agencies, with assurance that the overhead will be relatively small. Consequently, subsequent generations of scientists will have access to continuous records of high-quality data, which will provide a basis for quantifying and understanding the long-term effects of human activities in the coastal ocean.

## Acknowledgements

Funding for preparation of this report was prepared by funding provided by the U.S. Department of Energy, Office of Health and Environmental Research under Contract No. DE-AC02-76CH00016.

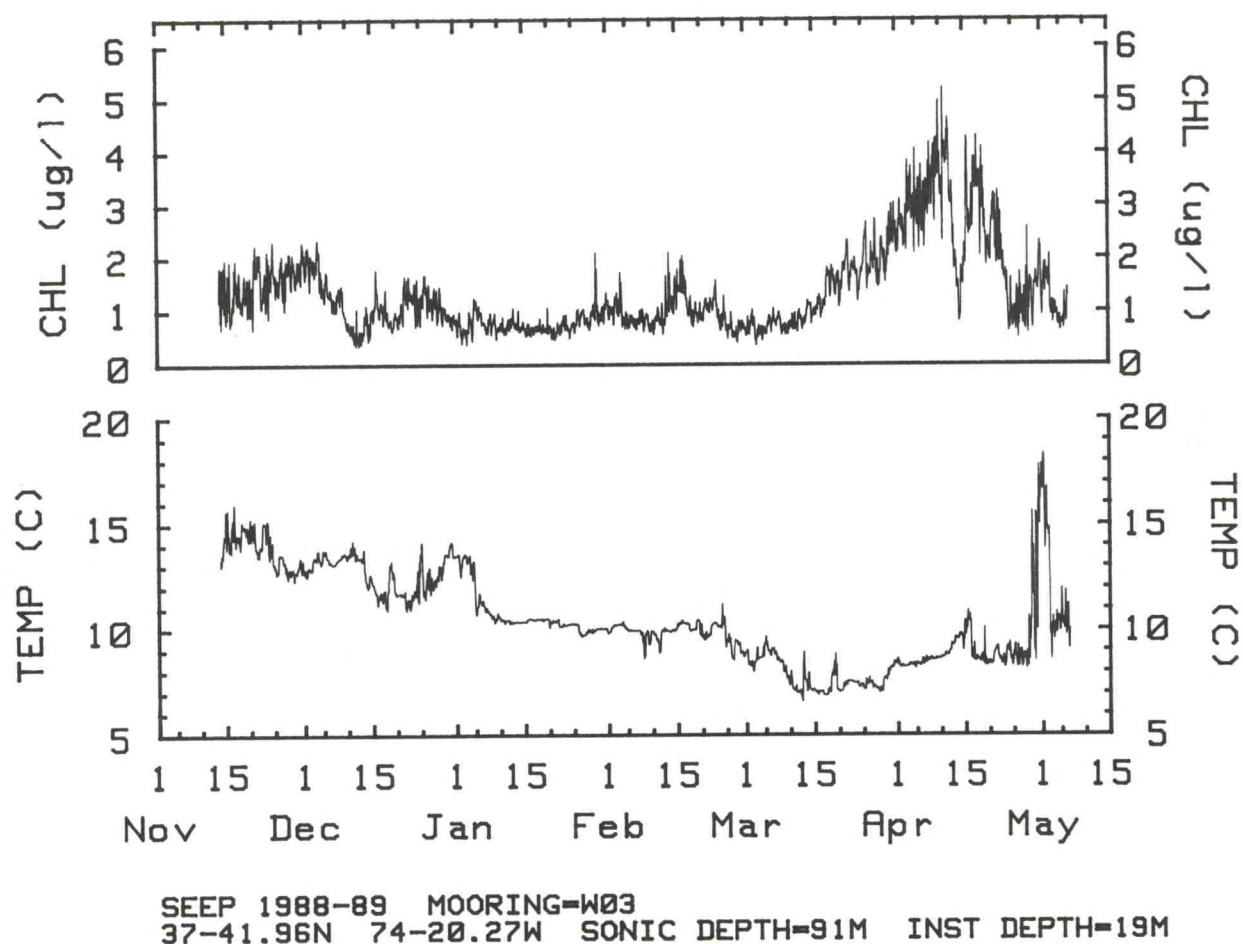


Figure 1. A time series of chlorophyll and temperature obtained from moored fluorometers off the coast of Maryland between November 11, 1988 and May 7, 1989. The data were collected every 34 minutes. The instrument was moored at 19 m below the surface in 91 m of water as part of a larger mooring array.



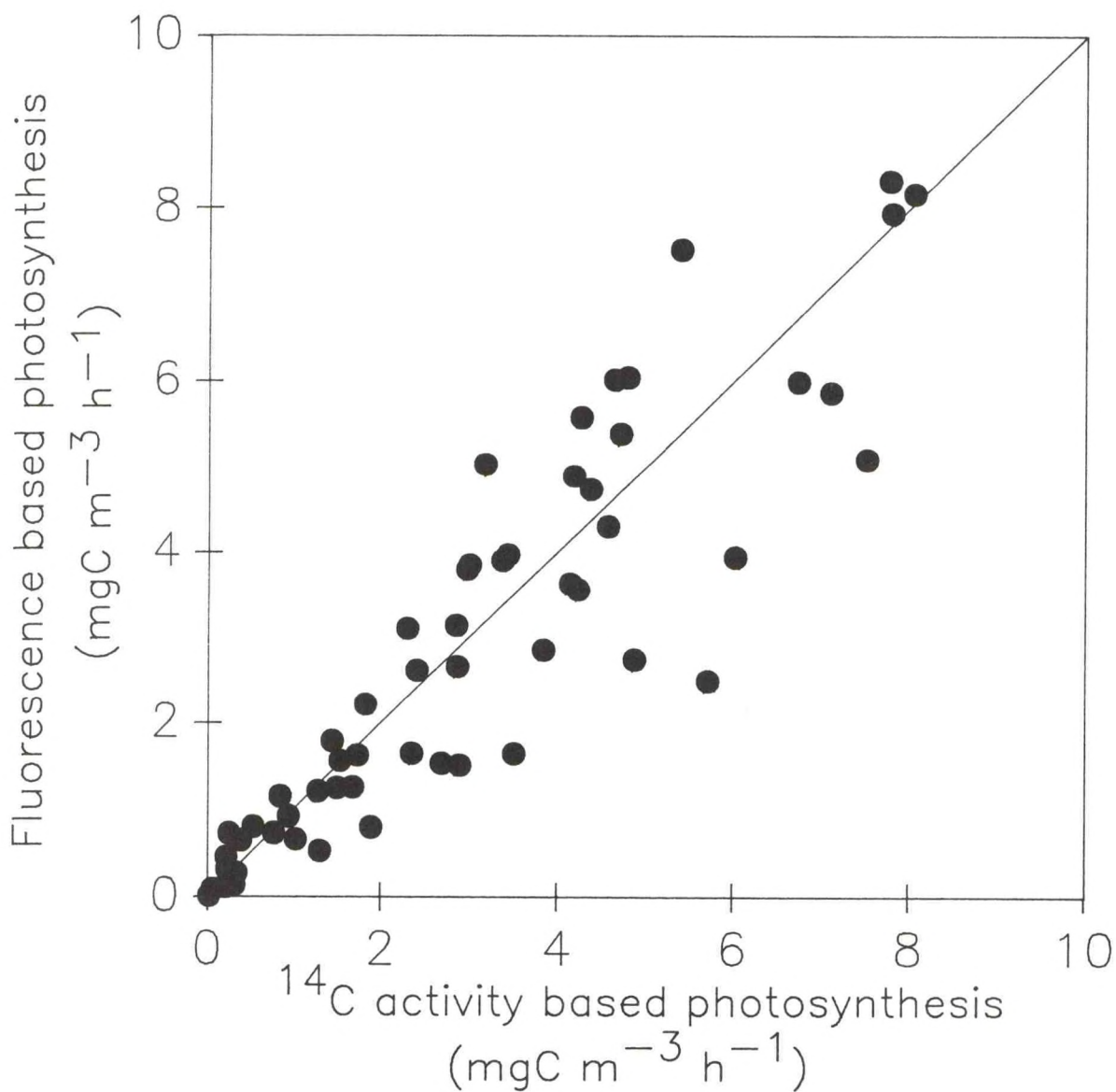
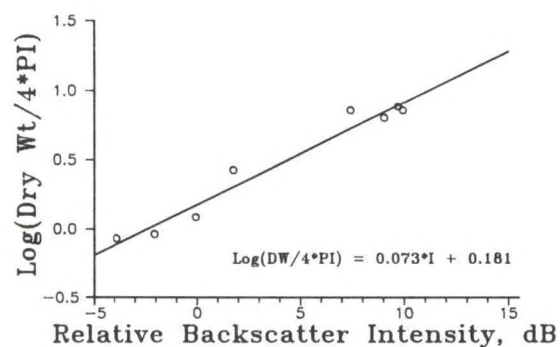
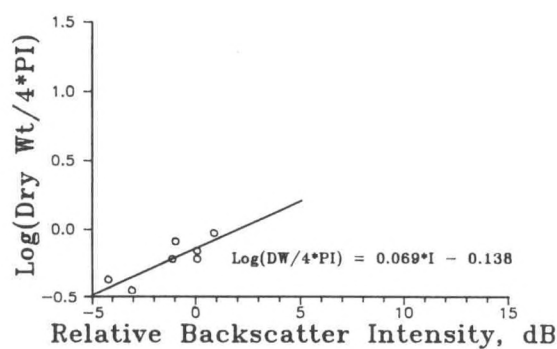


Figure 2. The linear correlation between the pump-and-probe fluorometer estimates of carbon fixation and radiocarbon-measured values. The data were obtained from 59 stations in the northwest Atlantic in 1988 and 1989. The pump-and-probe data were obtained in real-time from a profiling instrument on a CTD.

a) ONR/DOE Zooplankton/ADCP Pilot Study



b) SEEP-II Cruise 1, Tows 1, 2, 3, and 5



c) BIOSYNOP MOCNESS Tows 48 thru 52

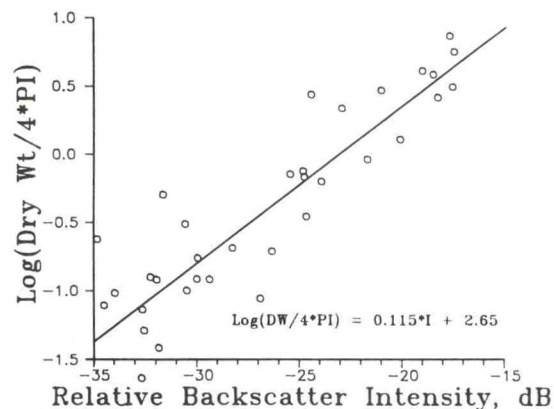


Figure 3. Comparison of acoustic backscatter intensity as measured by ADCPs and zooplankton biomass obtained from net hauls in the vicinity of the ADCPs. Figs 3a and b were obtained using a ship-mounted 150kHz instrument. The correlation coefficients ( $r^2$ ) for the linear regression analyses are 0.96, 0.72 and 0.80, respectively.



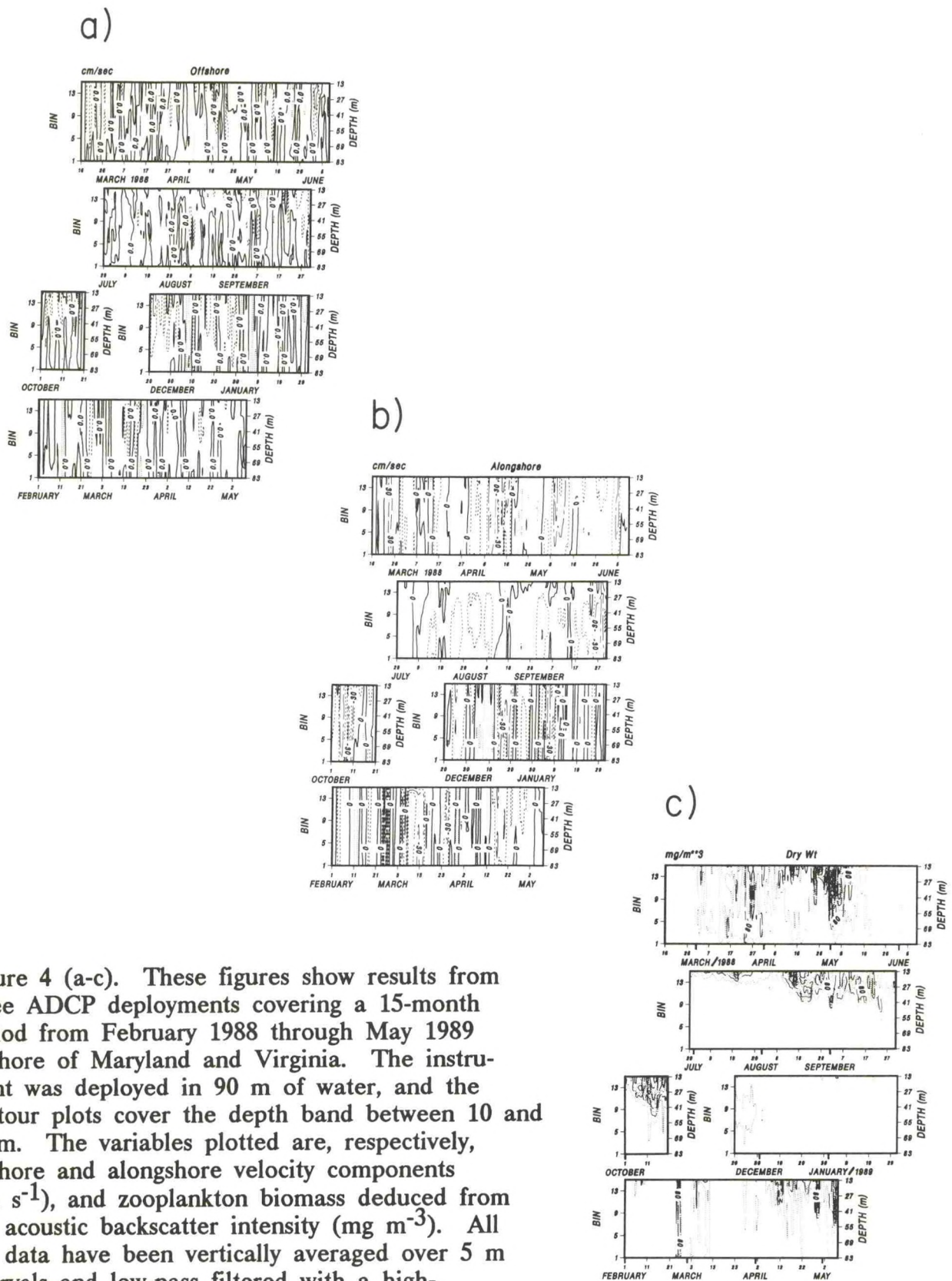
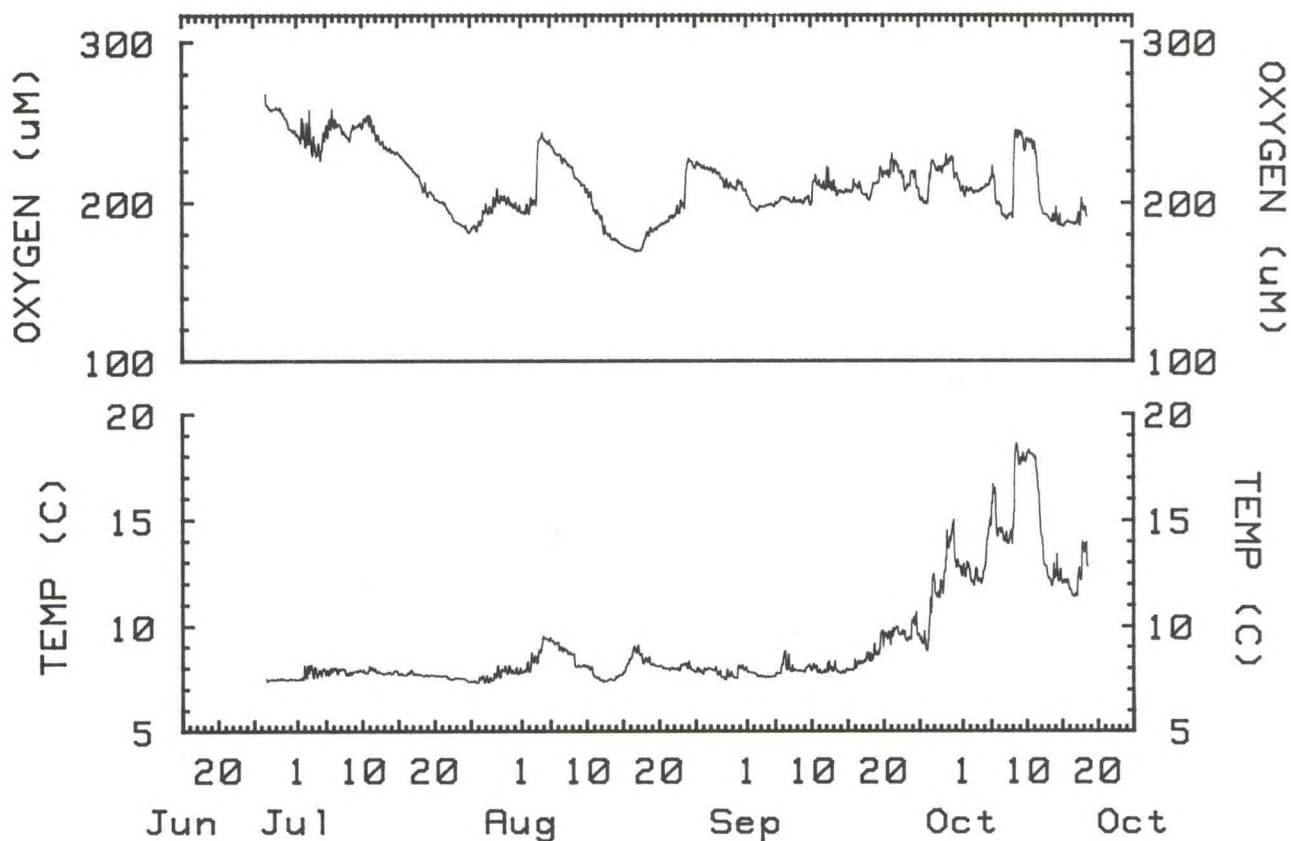


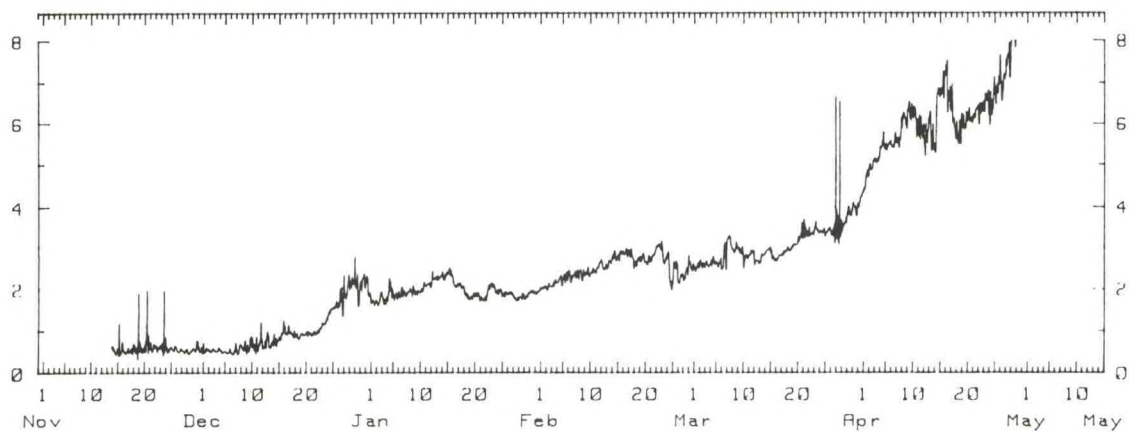
Figure 4 (a-c). These figures show results from three ADCP deployments covering a 15-month period from February 1988 through May 1989 offshore of Maryland and Virginia. The instrument was deployed in 90 m of water, and the contour plots cover the depth band between 10 and 85 m. The variables plotted are, respectively, offshore and alongshore velocity components ( $\text{cm s}^{-1}$ ), and zooplankton biomass deduced from the acoustic backscatter intensity ( $\text{mg m}^{-3}$ ). All the data have been vertically averaged over 5 m intervals and low-pass filtered with a high-frequency cutoff at  $1/33$  h. Contour intervals are  $7.5$  and  $15 \text{ cm s}^{-1}$  for the offshore and alongshore velocities, respectively, and  $40 \text{ mg m}^{-3}$  for zooplankton biomass.



SEEP 1988 MOORING=S01  
 37-52.60N 74-43.90W DEPTH=42M INST=39M

Figure 5. Time series of dissolved oxygen and temperature, measured every 15 minutes at 39 m in a 42 m water column off the coast of Maryland. Note the long-term decline in oxygen, from 260  $\mu$ M to ca. 180  $\mu$ M over the four-month record. The long-term decline is punctuated by increased oxygen events associated with warm water, indicative of an onshore flux of surface slope water onto the continental shelf.





SEEP 1988-89  
 MOORING=W03 37-41.96N 74-20.27W SONIC DEPTH=91M INST DEPTH=88M FILTER=2HLP

Figure 6. Time series of beam transmission from a near-bottom transmissometer. High values of beam attenuation ( $\text{m}^{-1}$ ) at 670 nm are correlated with high particle loads.

# OCEANIC AND ATMOSPHERIC DATA ASSIMILATION

Dale B. Haidvogel  
Chesapeake Bay Institute  
The Johns Hopkins University  
Baltimore, MD 21211

## Preface

This is meant as a brief introduction to the theory and practice of data assimilation, and in particular to those issues which relate in an important way to data assimilation in the coastal ocean. The review is necessarily incomplete--not only because it would simply be impossible to adequately cover such an expanding field in a single lecture, but also (and perhaps more importantly) because the author is only an interested spectator rather than a practicing specialist. This being the case, he is especially grateful to the invited authors for providing the very valuable background materials on which the following overview is based. Particular thanks are therefore due to Don Denbo, Michael Ghil, Paola Rizzoli, Allan Robinson, Leonard Walstad and Warren White.

For those readers who would like a more complete and up-to-date introduction to data assimilation in the atmosphere and ocean, the author recommends two recent topical reviews. The first, by Ghil and Malanotte-Rizzoli (1989), offers a splendid historical survey of data assimilation in meteorology and oceanography. The second, edited by Haidvogel and Robinson (1989), is a collection of recent research papers in the area of oceanic data assimilation. Together, these reviews, and the bibliographies therein, nicely summarize current approaches to data assimilation within the geosciences, including certain techniques (e.g., adjoint methods) which the author has regretfully neglected entirely.

## What is Data Assimilation?

Broadly speaking, data assimilation (DA) is the systematic combination of dynamical and observational information to produce increasingly accurate representations, which can be applied, for example, to descriptions of large- and meso-scale motions in the atmosphere and the ocean.

Since fluid motions on these scales are typically rather energetic, and their behavior intrinsically nonlinear, it is necessary to represent their dynamical evolution through the use of numerical models. Hence, data assimilation procedures usually combine three main elements: first, a numerical model suitable for dynamical simulation of the phenomena of interest; second, observational datasets describing the phenomena; and lastly, data assimilation algorithms expressing the "rules" by which the dynamical and observational estimates are to be combined. Nor are these three elements independent. As discussed more fully below, the construction of "optimal" DA algorithms must reflect in an essential way the specifics of the



datasets (e.g., data type, distribution in space and time, and error properties) and the details of the numerical dynamical model (e.g., the equations and solution procedures, and their respective error characteristics) being used. The resulting DA system is necessarily therefore a highly integrated one.

## DA in Modeling the Atmosphere and Ocean

As described in detail by Ghil and Malanotte-Rizzoli (1989), hereafter 'G&MR,' data assimilation in the atmosphere already has a long history, beginning in the 1950s. As in other areas of dynamical modeling and prediction, oceanic application of DA has lagged its atmospheric counterpart by 20 or 30 years. Nonetheless, the 1980s has seen a growing interest and accomplishment among ocean scientists in predictive studies in general, and the use of DA in particular. The majority of these studies have, however, dealt with phenomena in the deep ocean (e.g., the hindcast and forecast of Gulf Stream meanders and rings), and to a much lesser degree with the coastal ocean. It is likely, therefore, that the 1990s will be the first decade to see rapid progress in the area of coastal ocean data assimilation and prediction, utilizing three-dimensional, time-dependent models for the evolution of coastal current and mass fields.

Fortunately, we as ocean scientists do not have to "start from scratch" in the areas of data assimilation and predictive modeling, but can draw heavily on the perspective and technical expertise within the atmospheric community. This is possible (up to a point) because of the fundamental similarity between the two fluids. As noted by G&MR, for instance: both fluids evolve on relatively short time scales compared with other geo-fluids like the "solid" earth; neither can be observed "completely," that is, in enough detail to allow accurate description and prediction based on observations alone; and finally, the large-scale motions in the two fluids share a common theoretical heritage (Geophysical Fluid Dynamics). Modelers of both fluids, therefore, need to properly balance dynamical and observational information.

In many quite important respects, however, the task of modeling the ocean is different (if not more complicated) than that of modeling the atmosphere. For example, whereas the atmosphere is forced thermally, throughout its volume, the ocean is forced both thermally and mechanically, and primarily at its surface. Also, in contrast to the atmosphere, the geometry of ocean basins is very complex. This has several immediate practical consequences: oceanic mean states are quite complicated (e.g., characterized by boundary currents, etc.); boundary conditions on ocean flows are more difficult to define and to parameterize; and, as a consequence, numerical solution of the basin-scale ocean circulation problem is made substantially more complex.

Perhaps the greatest limitation on ocean modeling and forecasting, however, is that the ocean is more difficult to observe, and data are relatively more sparse than in the atmosphere. G&MR estimate, for example, that the amount of data available to ocean scientists in the decade of the 1990s--including those data expected to be available from satellite sea surface temperature (SST), scatterometer and altimeter



measurements--will still be an order of magnitude fewer than in the atmosphere. Also, the data are not only sparse, but non-uniform (being most plentiful at or near the sea surface and in the Northern Hemisphere, cf. Fig. 1), and indirect (i.e., providing most often measures of the mass field rather than velocity).

For all these reasons, the ocean prediction problem is less tractable from a DA perspective, and will require novel thinking and technical innovation.

## Data Assimilation Methodologies

Mathematically, any linear, unbiased data assimilation scheme can be represented as follows:

$$\begin{aligned}w_f(k) &= \Psi(k-1)w_a(k-1) \\w_a(k) &= w_f(k) + K(k) [w_o(k) - H(k)w_f(k)].\end{aligned}$$

Here:  $w(k)$  is the "state vector" which contains the values of the desired field variables at time  $t(k)$ ,  $\Psi$  is the "system matrix" which prescribes the dynamical "rules" by which previous values of the state vector may be updated;  $H$  is the "observation matrix" which interpolates the state vector onto the grid of available observations at time  $t(k)$ ; and  $K$  is the "weight matrix" which prescribes how to "blend" the dynamically forecast state vector values  $w_f$  with the innovation vector  $[w_o - Hw_f]$  to produce the analysis state vector  $w_a$ . For the purposes of discussion below, we also introduce the "error covariance matrix" for the forecast:

$$P_f(k) = E[w_f(k) - w_t(k)][w_f(k) - w_t(k)]^T.$$

In the previous expressions, the subscripts 'f', 'o', 'a', and 't' denote the "forecast," "observed," "analysis," and "true" values of the state vector  $w(k)$ .

Many alternate methods of continuous data assimilation are in current use. These differ primarily, but not exclusively, in the choice of the weight matrix. For example, a crude form of DA, often used along open boundaries in regional ocean models, is the so-called direct insertion method, in which observations, as they become available, are simply used to replace the forecast values of the state vector. This corresponds to setting

$$K(k) = I$$

where  $I$  is the identity matrix. Alternatively, the new observations can be used to "nudge" the forecast values back towards the observed values on some time-scale  $T$ :

$$K(k) = (1/T)I.$$



Optimal interpolation is now extensively used in atmospheric data assimilation; it results by choosing a weight matrix which is a prescribed function of a sub-optimal error covariance matrix,  $S_f$  i.e.,

$$K(k) = f[S_f(k)].$$

Here,  $S_f$  has been determined by assuming, for example, that the errors are homogeneous, isotropic, time-independent, etc. Lastly, the optimal (Kalman) filter results from using a weight matrix which reflects the (space-and-time-varying!) properties of the full error covariance matrix:

$$K(k) = f[P_f(k)].$$

Although the time evolution of  $P_f$  can be computed, it is computationally quite costly. Hence, sub-optimal procedures, such as optimal interpolation, are often preferred in operational applications (G&MR).

### Some Examples

To illustrate the current status of oceanic data assimilation, we choose two examples of DA in large-scale and regional ocean models. The experiments to be described—including the models, numerical techniques, and DA schemes used—are summarized in Table 1.

#### Assimilation of Simulated GEOSAT Data into an Eddy-Resolving Ocean Circulation Model

In the first, a quasi-geostrophic model of an idealized, wind-driven, mid-latitude gyre is used to investigate the impact of assimilating simulated geodetic satellite (GEOSAT) altimetric data (White et al, 1989). The three-level model is initialized from rest, driven by a two-gyre, steady wind-stress pattern. After many years of integration, a mature, turbulent circulation pattern is reached in which the simulated western boundary current ("gulf stream"), once separated from the coast, undergoes vigorous meandering, eddy-shedding, etc. (Fig. 2). The resulting equilibrium is characterized by strongly non-linear, mesoscale features in the vicinity of the separated boundary current, but by westward-propagating, nearly linear, large-scale motions in the far field (Fig. 3).

To assess the impact of assimilating surface height information into the model, a 200-day segment of the equilibrium fields is chosen to be the "control experiment." Simulated GEOSAT surface height data (surface streamfunction values) are sampled during this 200-day interval along tracks chosen to mimic the GEOSAT sampling pattern. An independent, 200-day numerical experiment (the "hindcast") is then produced in which the surface height data values obtained from the control experiment are inserted via optimal interpolation (Fig. 4) into the hindcast experiment. The resulting correlation between the control experiment and the results of the independent experiment with updating is used as a measure of the efficacy of surface height field assimilation.



An important question raised by this study is what range of scales of motion will be improved in the hindcast experiment by assimilation of the simulated altimetric data. The GEOSAT sampling pattern is, for example, non-uniform, having along-track spacing of data-points of approximately 50 km, and cross-track spacing of 140 km. Also, the data are obtained from, and re-inserted into, only the surface layer of the model ocean. It is not immediately obvious, therefore, at which scale(s) the improvement in the hindcast result will occur. White et al. (1989) show, in fact, that improvement takes place for wavelengths in excess of 300 km, corresponding roughly to the Nyquist sampling wavelength of the cross-track spacing (Fig. 5), rather than at wavelengths corresponding to the estimate of the geometric mean of the along- and cross-track spacing, as might naively be assumed.

### Coastal Transition Zone Data Assimilation Studies

Walstad et al. (1990) have been using the Harvard, limited-area, quasi-geostrophic model to perform hindcast simulations of the circulation patterns observed during the 1987 Coastal Transition Zone (CTZ) field experiment (Fig. 6). The data collected include hydrographic data taken during two surveys approximately two weeks apart. Dynamic height maps were calculated from the corresponding conductivity/temperature/depth (CTD) data (Fig. 7). Acoustic Doppler current profiler (ADCP) estimates of the currents at 35 m depth were also obtained (Fig. 8).

The numerical hindcast strategy used by Walstad et al. (1990) involves first using objective analysis to produce streamfunction maps corresponding to the geostrophic motion field observed during the two cruises. The limited-area model is then initialized with the first of these streamfunction fields. Boundary values of streamfunction are required by the regional quasigeostrophic (QG) model; these are obtained by temporal interpolation on the boundary between the streamfunction values inferred from the two cruises. The resulting boundary values are then provided to the model, which dynamically "predicts" the interior flow field over the course of the two-week period between cruises. The result is an initial-boundary-value problem, with updated boundary conditions--a particular example of the direct insertion scheme mentioned above. At the end of the two-week simulation, the observed streamfunction pattern from the second survey is used to assess the accuracy of the numerical hindcast. (Only the boundary values of the second survey were used in producing the hindcast.)

Before reviewing the hindcast simulation, it is important to point out the sensitivity of the results to the types of data used to produce the initial and boundary conditions. Two sets of objectively analyzed streamfunction maps (Fig. 9) correspond to the first of the two CTZ cruises: one was inferred using the hydrographic data only (assuming a level of no motion at 700 m); the other used the ADCP data to resolve the issue of the level of no motion. The two sets of streamfunction maps thus derived are substantially different, particularly at depth. Walstad et al. (1989) have shown, in fact, that no single choice of level of no motion does an adequate job in accounting for the flow in this region.



Using the best available objectively analyzed maps (i.e., those using both the CTD and ADCP data), a two-week hindcast simulation was carried out as described above. The results are shown in Figure 10, in which the model-derived prediction is compared with the observed streamfunction field. Integrated over the upper 500 m, the correlation between predicted and observed streamfunction is 0.93.

#### Data Assimilation in the Coastal Ocean: Issues

Despite the very rapid progress that has been made in oceanic data assimilation over the last decade, much remains to be done. This is particularly so in the coastal ocean, where, if anything, the situation becomes even more problematic than in the deep ocean. Modelers of the coastal ocean have to contend not only with the complexities mentioned above, but also with a variety of other complicating factors. For instance, coastal regions are associated with some or (more typically) all of the following features:

- a) finite-amplitude and/or steep topography, which dramatically complicates the dynamics, and numerical solution, of coastal currents;
- b) very short length scales of some of the most energetic features;
- c) less geostrophy (intense transient flows, including tidal currents; stronger vertical velocities; narrow intense jets with high Rossby numbers, sharp density fronts arising from multiple mechanisms, etc.);
- d) strong buoyancy-driven, as well as wind-driven, flows;
- e) important local responses due to remote forcing by, for example, coastal trapped waves and adjacent, larger-scale current systems;

and, because of all these,

- f) very complicated error properties for both observations and models.

In one respect, though, the task of the coastal predictive modeler may be made somewhat easier. It is possible that data density will ultimately be better in the coastal oceans than for the global ocean as a whole. Although improvement and innovation will certainly be needed in all three component areas of DA (dynamical models, datasets, and data assimilation algorithms), the eventual success of any coastal ocean predictive system will perhaps most crucially hinge on progress in the area of data acquisition systems.

Table 1. Two Examples of DA in Regional and Large-Scale Models.

Authors	White et al.	Walstad et al.
Model	QG (Holland)	QG (Harvard)
Region	Idealized mid-latitude EGCM	CTZ region
Resolution	20 km x 20 km x 3 levels	9 km x 9 km x 6 levels
BC's	Closed basin	open ( $\zeta, \psi$ )
Dataset(s)	Simulated GEOSAT	CTZ (hydrography, ADCP)
Forcing	Wind-driven (2 gyres)	via open boundaries
DA scheme	Optimal interpolation	IBVP with updated boundary conditions
Strategy	<ul style="list-style-type: none"> <li>• spin-up control experiment</li> <li>• sample for sea surface height</li> <li>• assimilate data into hindcast experiment</li> <li>• measure correlation with control experiment</li> </ul>	<ul style="list-style-type: none"> <li>• objectively analyze to produce <math>\psi</math> maps for 2 cruises</li> <li>• initialize model with first field</li> <li>• <math>\psi</math> on <math>\delta \Omega</math> from linear time interpolation</li> <li>• run hindcast and compare with observations</li> </ul>



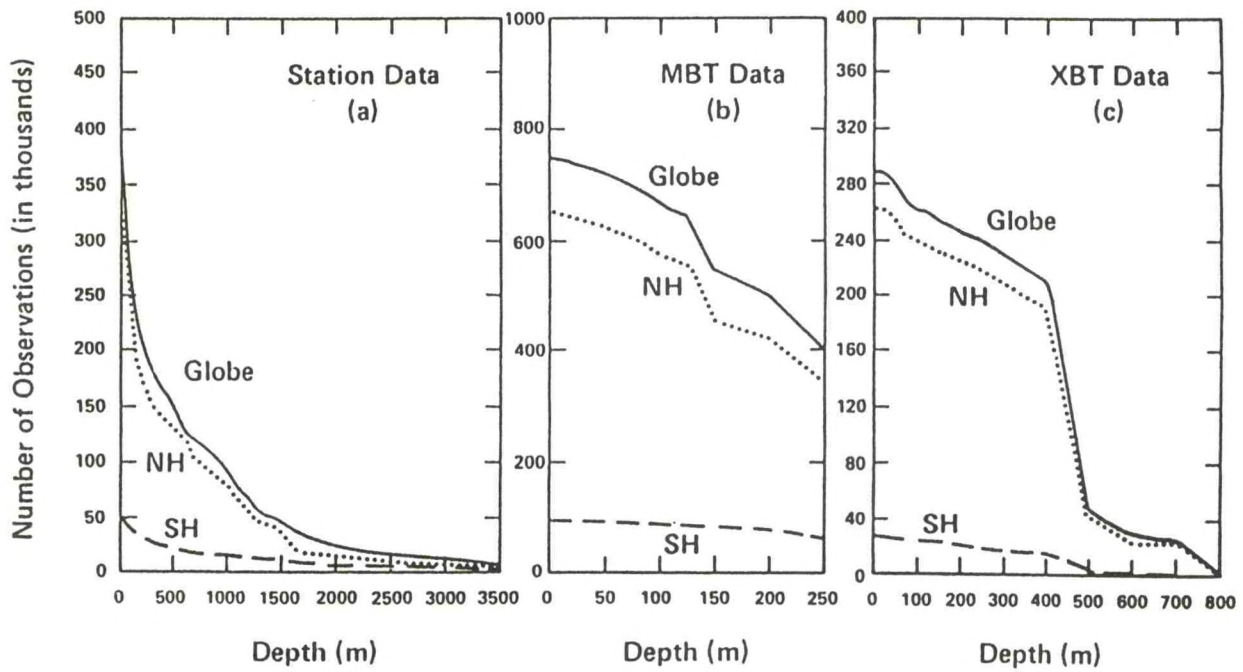


Figure 1. Distribution of temperature observations at standard levels in the NODC archives: (a) station data, (b) MBT's, and (c) XBT's. Each panel shows the distribution with depth over the globe (solid line), Northern Hemisphere (dotted), and Southern Hemisphere (dashed).

SYNOPTIC MODEL  
STREAMFUNCTION ( $\text{m}^2 \text{s}^{-1}$ )

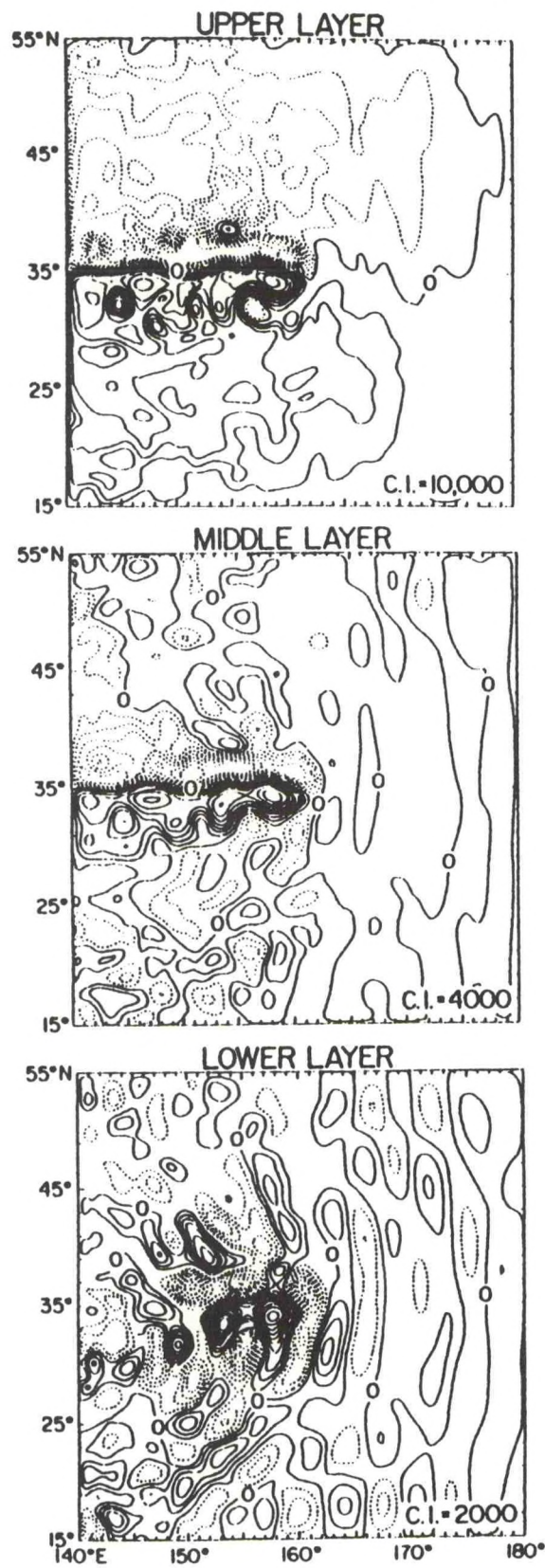


Figure 2. Instantaneous streamfunction maps from the White et al. (1989) control experiment for the upper, middle, and lower layers.



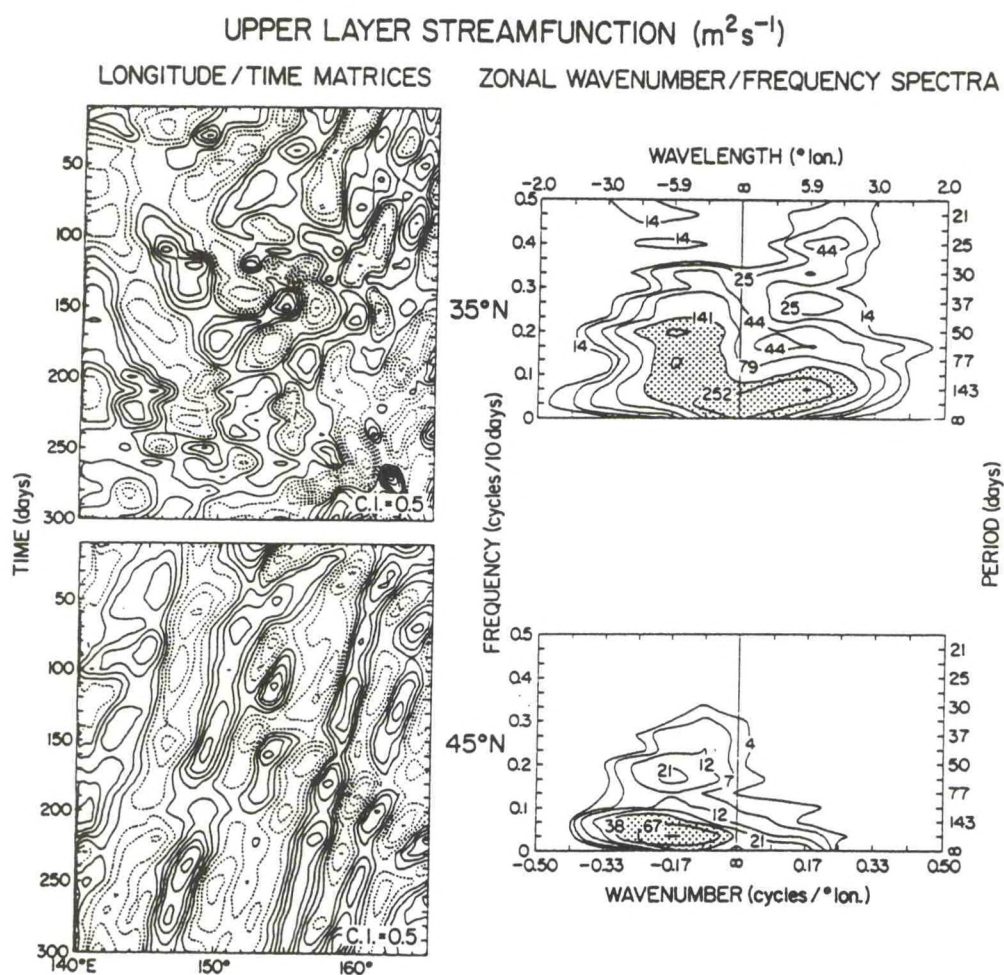


Figure 3. Normalized longitude/time matrices and zonal wavenumber/frequency spectra of the upper layer eddy streamfunction at  $35^\circ\text{N}$  (upper panel) and  $45^\circ\text{N}$  (lower panel).

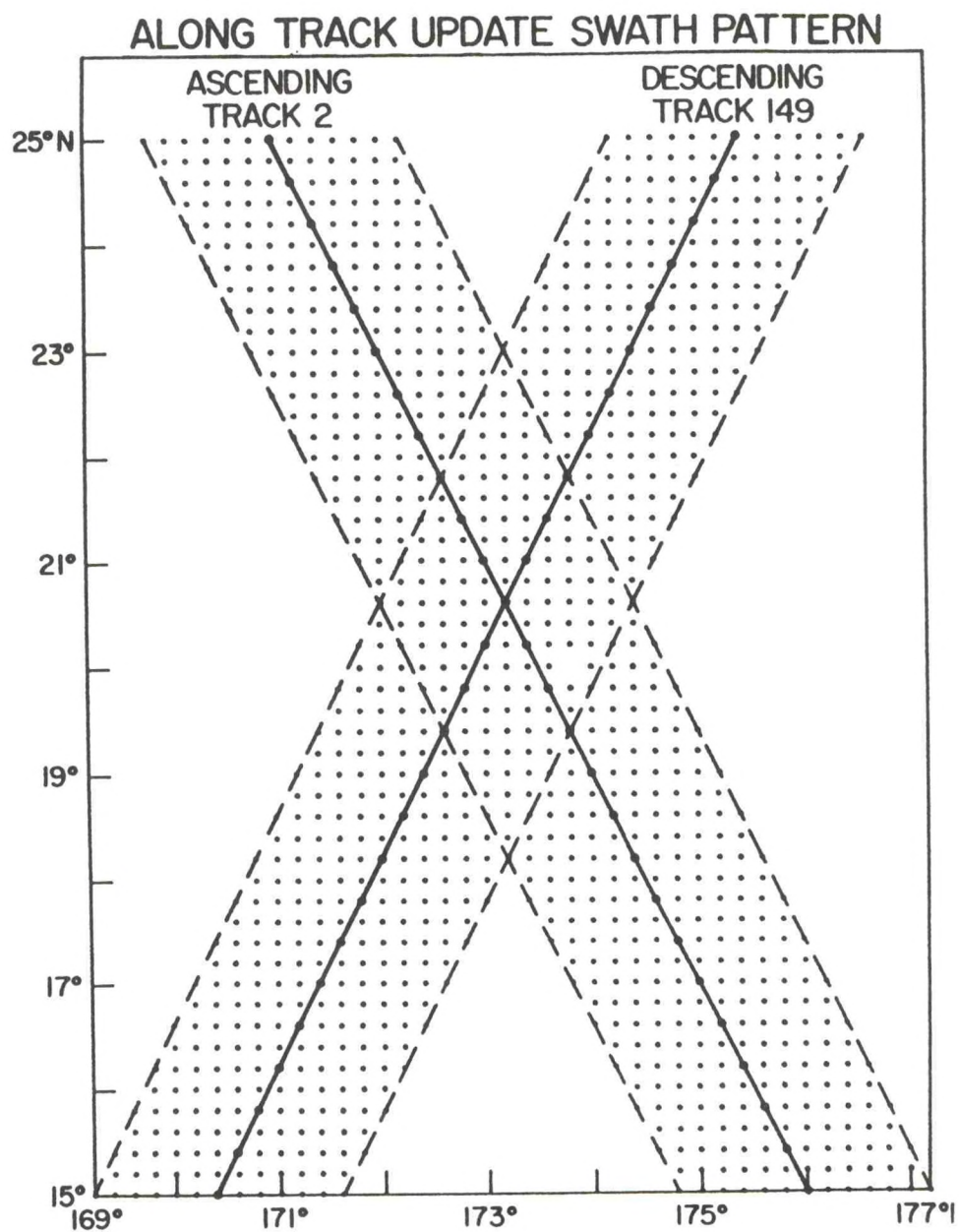


Figure 4. Swath pattern of model grid points updated during the along-track insertion of simulated GEOSAT data in the White et al. (1989) hindcast experiment.



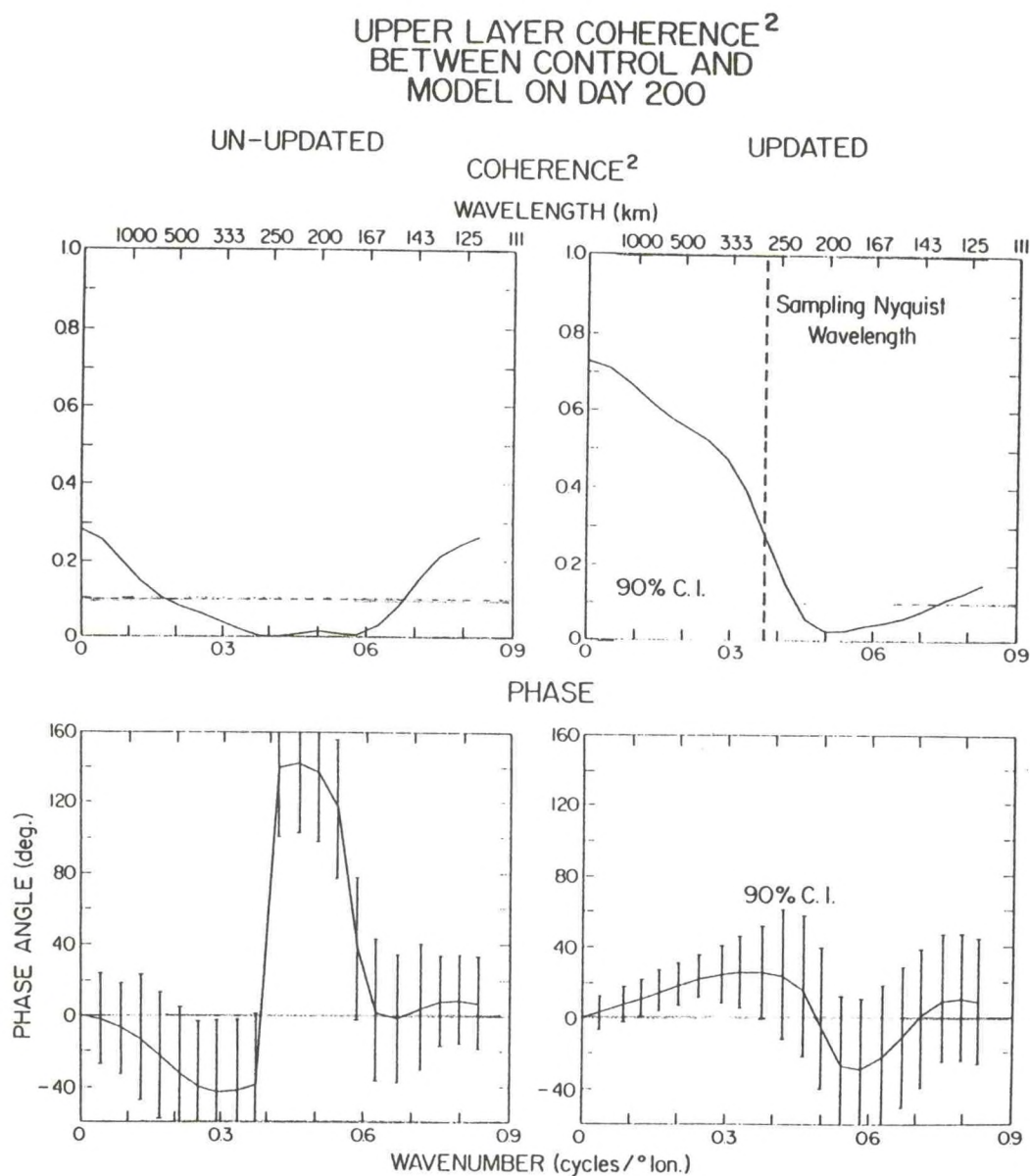


Figure 5. Coherence (squared) and phase between the control model streamfunction and the streamfunction (not updated) at day 200 for the middle layer in the near field of the separated boundary current (30°-40° N, 140°-165° E) (left panel); coherence and phase between the control and hindcast (updated) experiments (right panel).

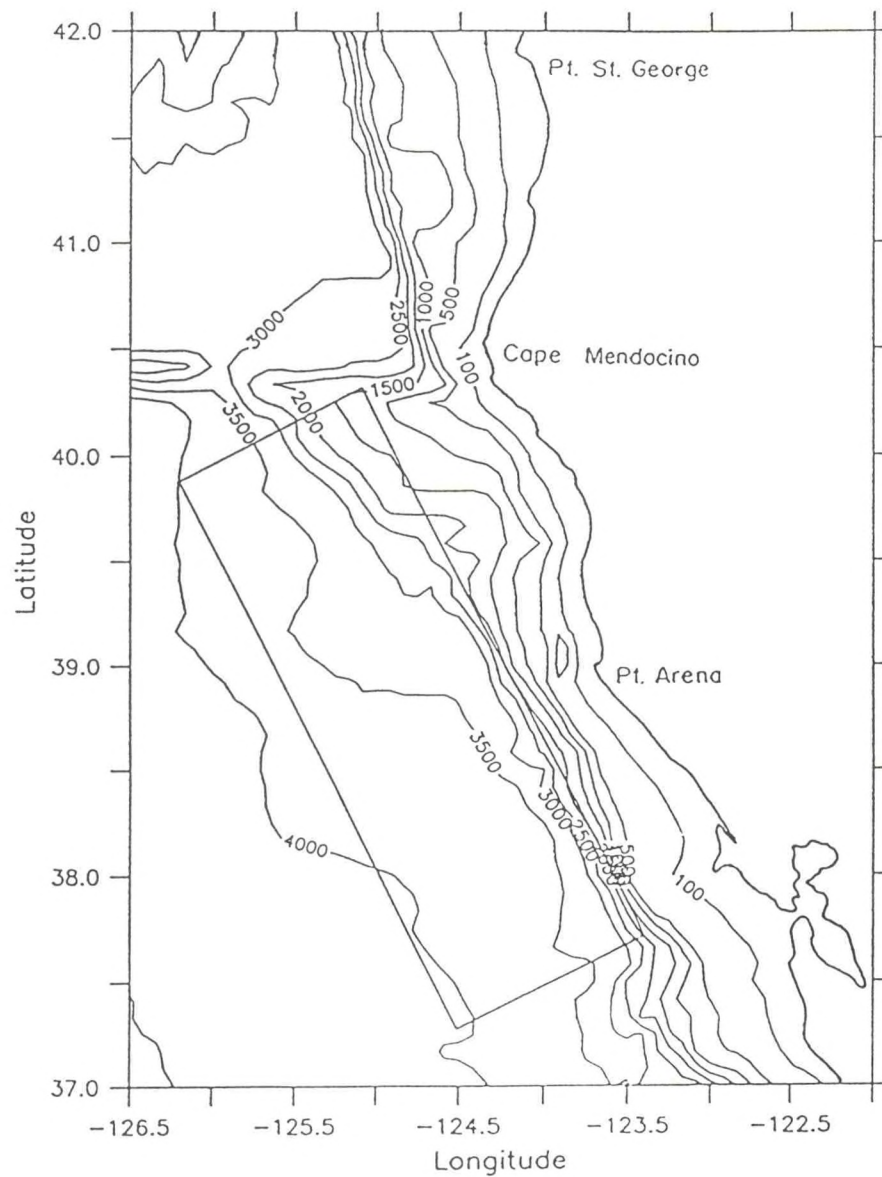


Figure 6. Geometry and topography of the Coastal Transition Zone region. Rectangular box indicates the edges of the Walstad et al. (1990) numerical model domain.



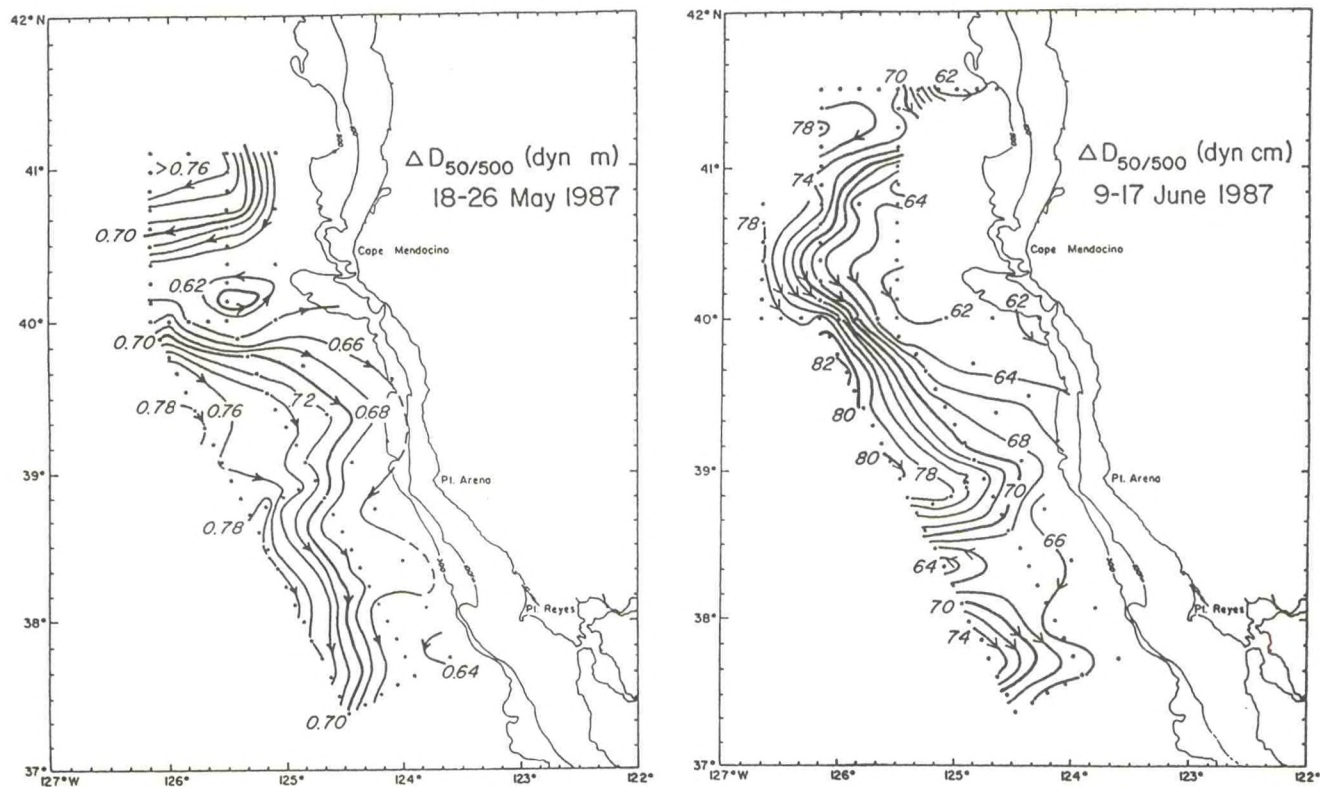


Figure 7. Dynamic height fields observed during the May and June 1987 Coastal Transition Zone experiments from Schramm et al., 1988a, b.

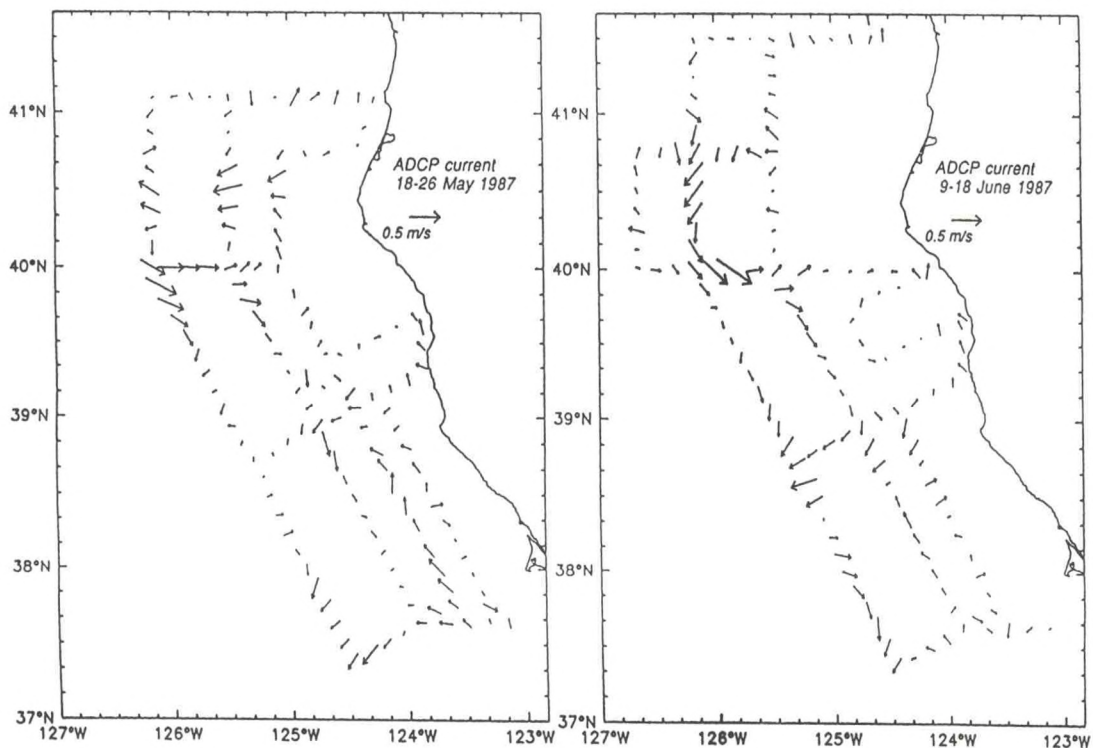


Figure 8. Acoustic Doppler current meter velocities measured during the May and June 1987 Coastal Transition Zone experiments from Kosro et al., 1990: left panel, May cruise; right panel, June cruise.



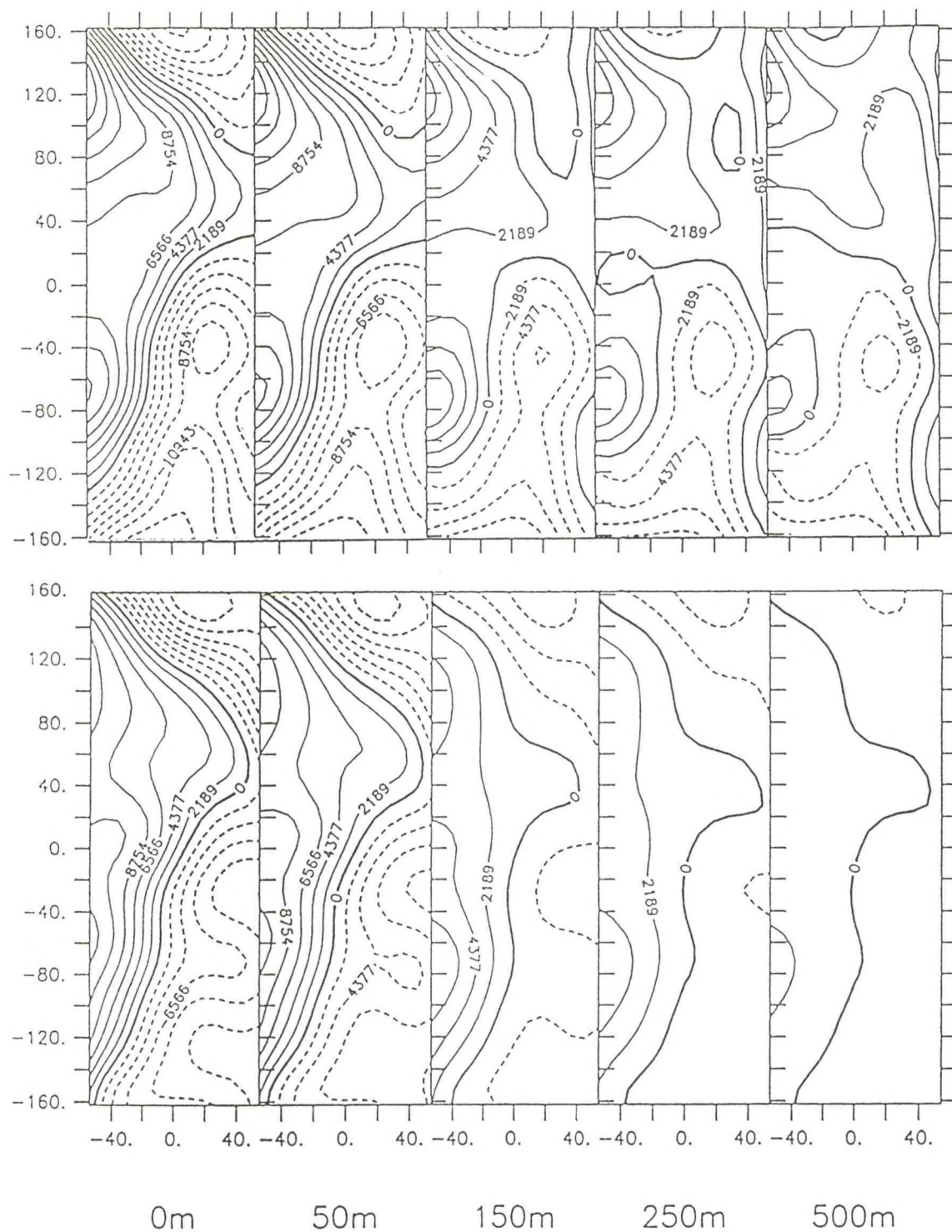


Figure 9. Objectively analyzed streamfunction maps at five depths, as inferred from the May 1987 CTZ survey: upper panels, using ADCP data; lower panels, using CTD data only with an assumed level of no motion at 700 m. The contour interval is equivalent to 2 dynamic cm.

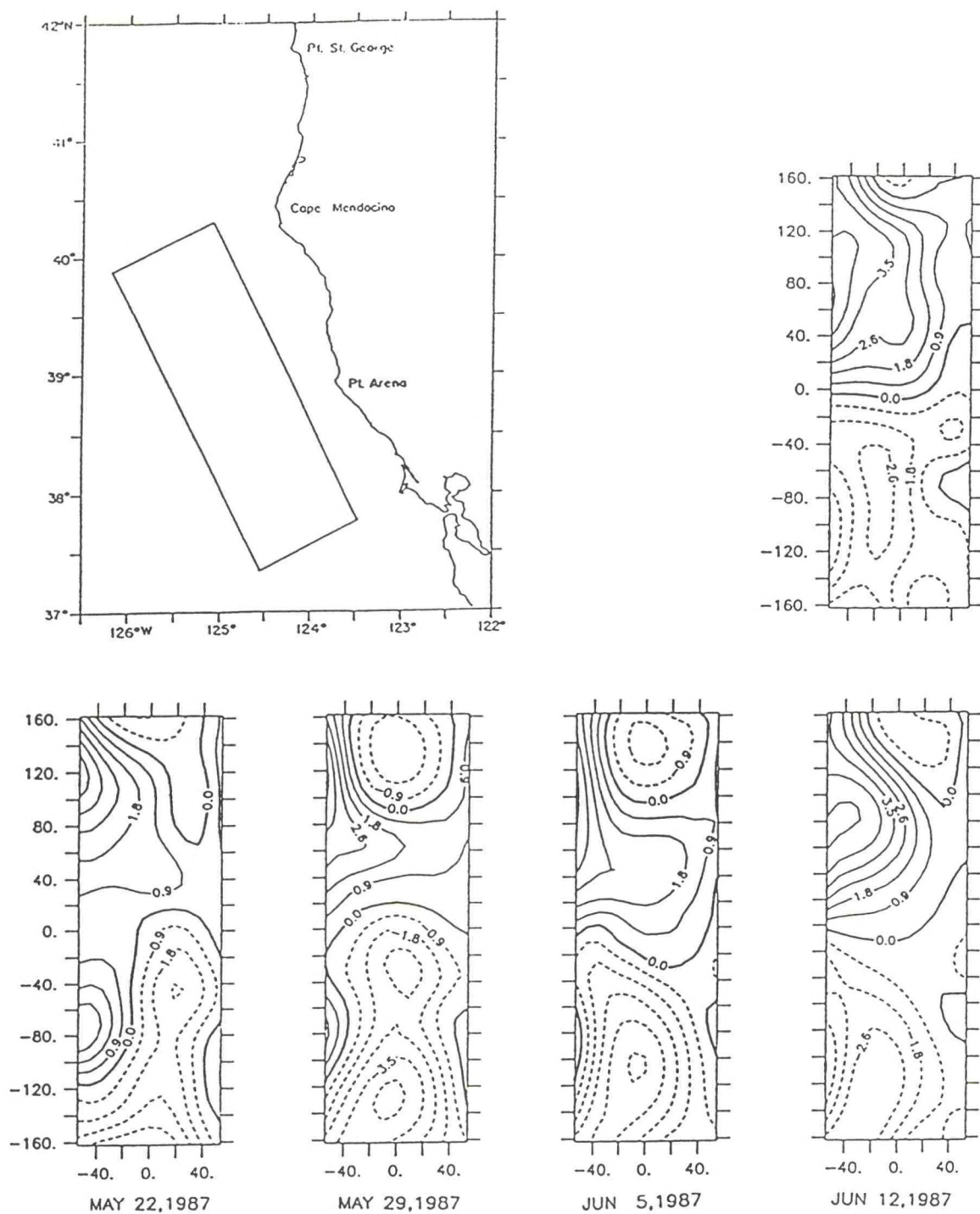


Figure 10. Predicted evolution of the 150 m depth streamfunction fields in the Coastal Transition Zone from May 22 through June 12 (bottom row of maps). The predicted field for June 12 compares very well with the observed field for that date (upper right). The two fields are correlated at .93. The contour interval is equivalent to 2 dynamic cm.



# SUBMARINE CANYONS AND THEIR IMPORTANCE TO MODELS OF COASTAL CIRCULATION

Barbara M. Hickey  
College of Oceanography and Fisheries  
University of Washington  
Seattle, WA 98195

## Introduction

Submarine canyons are a nearly ubiquitous feature of coastal circulation. In some regions, e.g., the Washington coast, canyons indent the continental slope as frequently as every 20-40 km (Hickey, 1989). Two aspects of submarine canyons enter a discussion of predictive modeling of the coastal circulation: 1) prediction of the circulation within the canyon itself and within its immediate vicinity, and 2) parameterization of the "global" effects of canyons (the majority of which are of the order of the grid size of most models) in large-scale models of the coastal circulation.

Measurements in submarine canyons are among the most difficult in the ocean to make. This is because, first, most coastal canyons have extremely steep slopes, making it challenging to safely obtain conductivity-temperature-depth (CTD) profiles and to accurately deploy moored arrays over the slopes. Also, fishing activities often are intense over these same slopes, making it difficult to maintain moored arrays in the water for extended periods. Last, the lateral coherence scales are very small--typically 10 km or less, even along the canyon axis, for both the mean and the subtidal flow, so that arrays must be very heavily instrumented in order to delineate coherent signals. Models of submarine canyon circulation or of the effect of canyons on the prevailing circulation have been few and, for the most part, highly idealized (for example, as in Allen, 1976, requiring that the width of canyons be large relative to the local internal Rossby radius). For these reasons, the understanding of both the circulation within submarine canyons and the effect of canyons on the large-scale coastal circulation is yet relatively immature.

In the sections that follow, the state of our knowledge of the circulation in submarine canyons will first be described. Next, the effects of canyons on regional circulation will be discussed. Where possible, the observed response will be compared with expectations driven by modeling results. The report ends with suggested recommendations for the large-scale models for possible parameterization of canyon effects.

## Circulation in Submarine Canyons

Most direct current measurements in submarine canyons prior to about 1975 were made along the canyon axis and were of very short duration (a few days) (Shepard et al., 1977; Inman et al., 1976). Since then, spatially comprehensive and



long duration measurements have been made in several canyons of differing dimensions, stratification, etc., notably Quinault and Astoria on the West Coast, and Baltimore, Lydonia, Hudson and Oceanographer on the East Coast. Comprehensive hydrographic measurements have been made in the vicinity of several canyons: for example, Quinault, Astoria and Wilmington.

The mean currents along canyon axes do not appear to correspond to any simple spatial pattern: they are sometimes upcanyon and sometimes downcanyon, often within the same canyon. For example, Hunkins (1988) found mean upcanyon flow in Baltimore Canyon at bottom depths less than about 600 m, but downcanyon flow at deeper depths. Hickey (1989) found the exact opposite pattern in Quinault Canyon. Shepard et al. (1977) concluded that of 69 measurements of axial flow, 43 were downcanyon and 26 were upcanyon. They also made the observation that East Coast canyons tend to have more upcanyon mean flow than West Coast canyons. However, presently available data now suggest the opposite: data for Astoria (Hickey, in preparation, hydrographic data), Quinault and Juan de Fuca (Freeland and Denman, 1982, hydrographic data) suggest upwelling at least at the head, whereas Baltimore, Lydonia (Noble and Butman, 1989) and Wilmington (Church et al., 1984, from hydrographic data) all show downwelling at the head. To what extent are the obtained mean flows repeatable from year to year? In the one case for which data exist (Quinault), the spatial pattern of the mean flow direction along the canyon axis was the same during two successive years.

Few current measurements have been made over the canyon slopes: data exist only for Astoria, Lydonia and Baltimore. The most comprehensive data set, that for Astoria, suggests that a cyclonic eddy is trapped over the canyon's slopes (Fig. 1). The eddy decays vertically both above and below the canyon lip, with a scale roughly given by the vertical length scale appropriate for geostrophic flow,  $fL/N$ , where  $f$  is the Coriolis parameter,  $L$  is the canyon width and  $N$  is the Vaisala-Brunt frequency. Note that since the width of Astoria canyon is less than half that of the local internal Rossby radius, the observed flow is unlikely to be geostrophic. In some locations where Astoria data were obtained, the canyon walls were only 3 km apart. Data from the head of Lydonia Canyon provide evidence that the mean flow on the two sides of that canyon is also in opposite directions (Noble and Butman, 1989). In Baltimore Canyon, the only available data are deep, but they too indicate mean flow in opposite directions on the two slopes (Hunkins, 1988) (Fig. 2a). The moorings were similarly spaced in the Baltimore Canyon and Astoria Canyon data sets. Cannon (1972) demonstrates the existence of a cyclonic circulation on the shelf directly adjacent to the Juan de Fuca Canyon. For the cases for which appropriate data are available (Astoria, Quinault and Baltimore), mean flow well above the canyon was not perturbed measurably by the canyon: it was directed straight over the canyon following the curvature of the regional isobaths (Figs. 1, 2b).

Subtidal currents in deep submarine canyons (arbitrarily defined as those for which bottom depths exceed 200 m) have only been examined for three cases: Lydonia, Quinault and Astoria. In each case, the amplitude of the subtidal scale fluctuations is smaller than that of the higher frequency fluctuations. Also, horizontal coherence scales, both along and across the canyon axis are remarkably small (less



than 10-20 km) (Hickey, 1989; Noble and Butman, 1989). Driving mechanisms for the subtidal flow have not been generally explained. Typically, only a small fraction (<25%) of the variance can be explained at all (Hickey, 1989; Noble and Butman, 1989). The across-shelf/slope barotropic pressure gradient is most often invoked in discussions of driving mechanisms, with an onshore increase in pressure being related to downcanyon flow. In particular, Hickey (1989) demonstrates a statistical relationship between alongaxis flow and the cross-shelf/slope barotropic pressure gradient in Quinault Canyon at depths of about 1200 m from the surface (5-50 m above the bottom). Noble and Butman (1989) illustrate a similar result for Lydonia Canyon. They demonstrate that for such dynamics to apply for that canyon, dissipation must be extremely high, which is consistent with results deduced from the large tidal currents that are present. For both the Quinault and Lydonia cases, maximum coherence with the shelf forcing occurs at periods of about 3-5 days. In the shallow heads of some canyons or in shelf valleys such as the Hudson, wind set-up (and thus a cross-shelf pressure gradient force) has been related directly to downcanyon flow (e.g., Nelson et al., 1978; Hsueh, 1980). Coherence scales for such depressions (as opposed to deep canyons), would be expected to be much larger than those for deep ("real") canyons, which lie below the depth of directly wind-driven shelf currents.

The only available model study of flow within a canyon suggests that flows within a canyon should be in opposite directions on the two sides of the canyon (Klinck, 1989) (Fig. 3). This result holds whether the canyon is wide (~100 km) or narrow (~10 km). As mentioned above, the mean flow data, where appropriate data exist, are consistent with this result. For the fluctuating flow, one canyon (Lydonia, on the East Coast) demonstrates flow in the same direction on both sides of the canyon (Noble and Butman, 1989); whereas, another canyon (Astoria, on the West Coast) demonstrates coherent flow in opposite directions on the two sides (Hickey, 1989) (Fig. 4). The different response could be due to the difference in stratification.

Regional model results suggest that upwelling or downwelling should be enhanced in the vicinity of canyons (Peffley and O'Brien, 1976; Cushman-Roisin and O'Brien, 1983). In particular, upwelling is enhanced on the downstream side of a canyon relative to the incident flow. Klinck's (1989) model for the flow within a canyon demonstrates that strong upwelling persists even for extremely narrow canyons for which the actual flow velocities may be very small. A clear example of canyon upwelling was obtained for Astoria Canyon (Fig. 5). Shaffer (1976) demonstrated localized upwelling near the heads of several canyons off the African coast. Time series of temperature data within Quinault Canyon and on the nearby slope illustrate that the canyon upwelling is stronger during each individual upwelling event (Fig. 6). To my knowledge no such explicit examples have been presented for the East Coast canyons.

Models suggest that the internal waves are focused and therefore amplified within canyons (Hotchkiss and Wunsch, 1982; Baines, 1983; Grimshaw et al., 1985). This result has been confirmed in several canyons, notably Hudson (Hotchkiss and Wunsch, 1982) and Quinault (Hickey, 1989) (Fig. 8).



In spite of much conjecture regarding enhanced mixing in the vicinity of canyons, there has been little confirmation of such effects in the field. Mixing, if it occurs, may be relatively subtle and therefore difficult to quantify.

Several models have suggested that submarine canyons are efficient generators of waves, either standing or propagating and at both subtidal and supratidal frequencies as well as the inertial frequency (Klinck, 1989; Wang, 1980). To my knowledge, no experiment has been designed to search for such waves over or within a canyon.

### The Effects of Canyons on Regional Circulation

Canyons may affect the regional circulation in several important ways:

- 1) The mass field may be altered locally via, e.g., preferential upwelling (Peffley and O'Brien, 1976; Cushman-Roisin and O'Brien, 1983). Subsequent mixing may spread the buoyant perturbation into the large scale. The magnitude of the effect is dependent on the number, size and placement of submarine canyons as well as the local and regional stratification.
- 2) Mixing within and especially near the heads of canyons may be enhanced due to the amplification of the internal tide as well as the focusing of the internal wave field (Grimshaw et al., 1985; Hotchkiss and Wunsch, 1982).
- 3) The direction of both the mean and the fluctuating flow field is altered substantially in the immediate vicinity of the canyon. The extent of the alteration is a function of regional current speed, stratification, canyon width and canyon depth.
- 4) The topographic perturbation in the presence of a fluctuating flow field provides a topographic torque that drives a significant mean flow (Holloway, 1987).
- 5) Enhanced local mixing as well as altered flow patterns may cause local perturbations in the structure of the bottom boundary layer. Such perturbations may alter mass balances on regional scales.
- 6) The interaction of the topographic irregularity with the regional circulation results in the generation of waves, both propagating and standing, both upstream and downstream of the canyon, at both subtidal and supratidal frequencies (Allen, 1976; Wang, 1980; Klinck, 1989).

The majority of the effects listed above are derived from the results of model studies. Few field studies have been designed to specifically address such effects. Since the effects are relatively subtle and are embedded in a strong regional circulation with its own set of waves, eddies, etc., observational confirmation of most of the expected effects is weak at best. The most reliable result to date is the directional perturbation of the mean flow.



## Recommendations for Model Parameterization

The preceding summary suggests that it is unlikely that the circulation in any specific canyon will be reasonably predicted by any regional circulation model. The one available model that addresses the subtidal-scale flow field within a deep canyon is severely limited in its representation of reality: for example, the canyon is not closed on its shoreward side, nor is friction included. This model is analytical in nature. Perhaps local numerical models with extremely fine spatial resolution could be developed that would at least partially satisfy predictive needs for the immediate vicinity of the canyon. Additional field studies will be necessary to assess the relative importance of canyon effects so that they may be adequately parameterized in the regional models. Possible methods to embrace canyon effects include the following:

- 1) allow local parameterization of enhanced canyon mixing;
- 2) allow local enhancement of upwelling;
- 3) allow local adjustments to cross-shelf mass transport; and
- 4) embed small-scale canyon models within regional models.

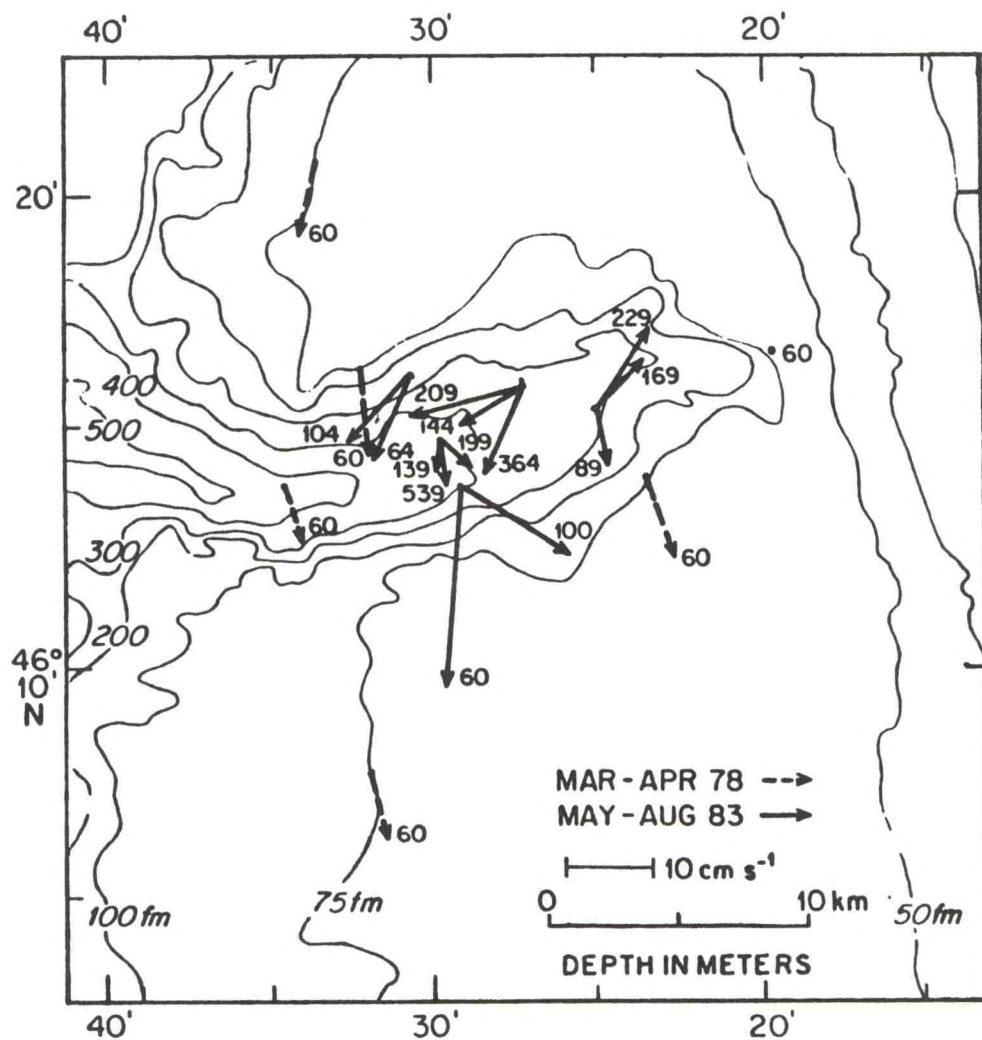


Figure 1. Mean flow in the vicinity of Astoria Canyon (Hickey, 1989).



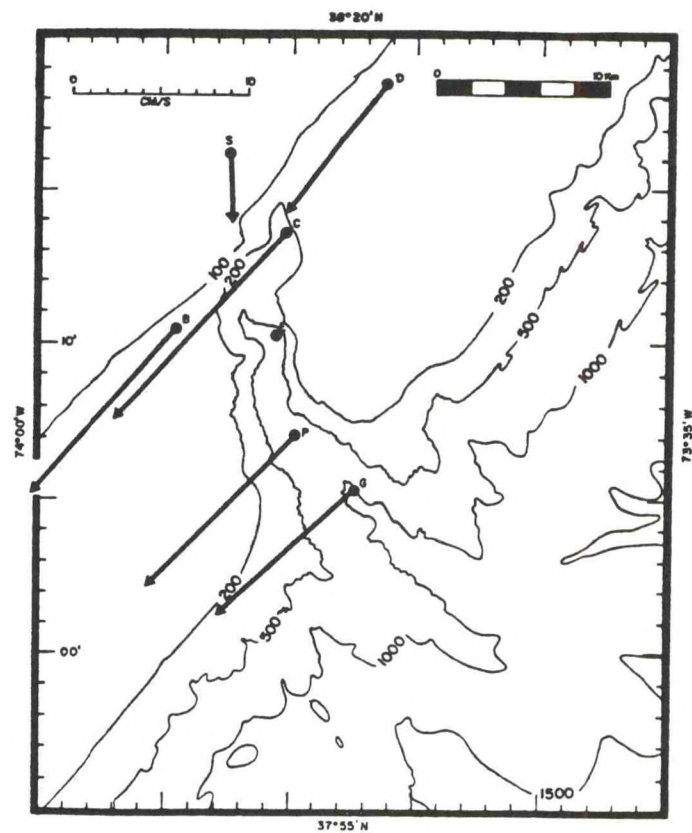
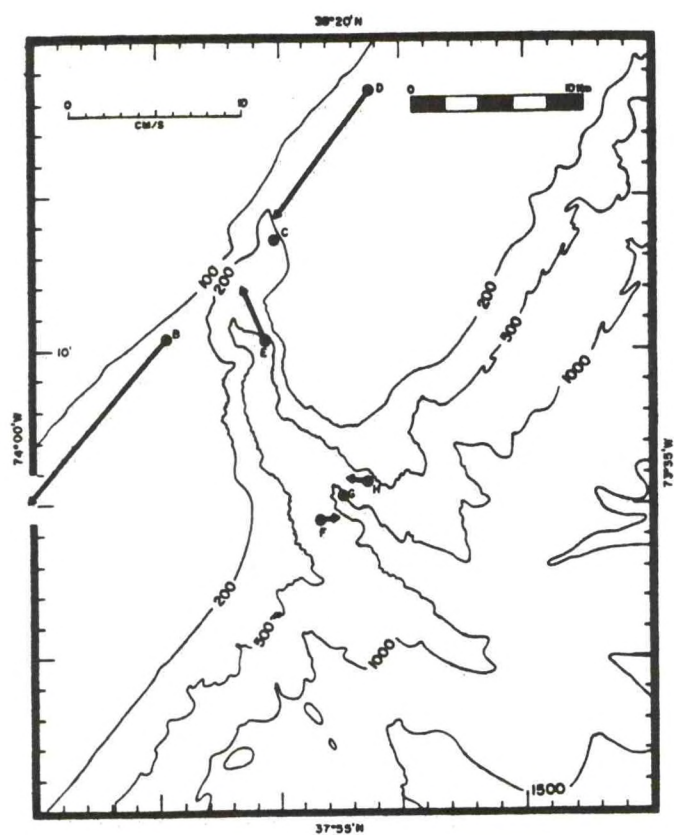


Figure 2. Mean flow in the vicinity of Baltimore Canyon (Hunkins, 1988).

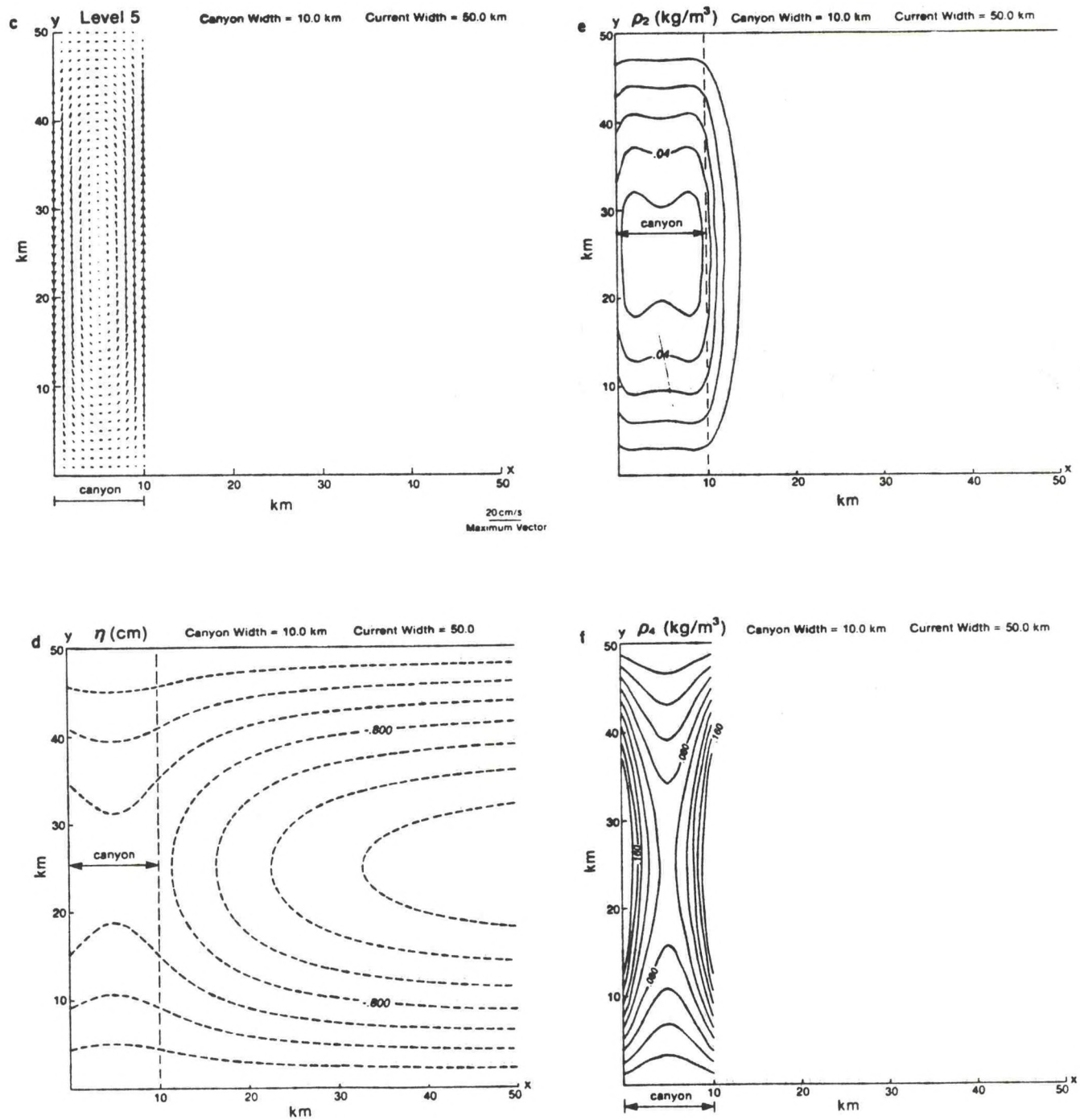


Figure 3. Model results from Klinck (1989). Levels three and deeper are within the canyon.



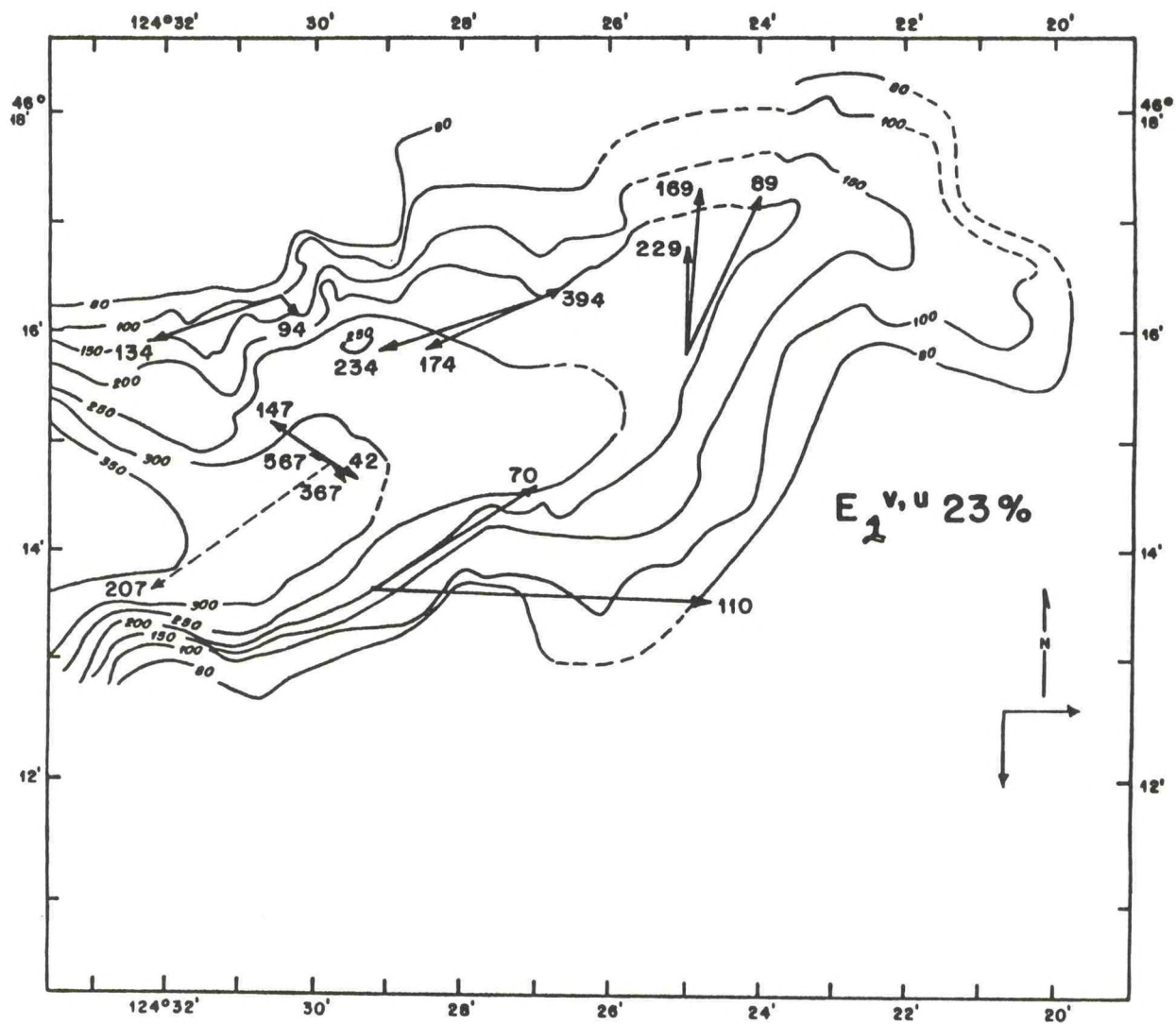


Figure 4. Second EOF for fluctuating velocity field in the vicinity of Astoria Canyon (Hickey, in preparation).

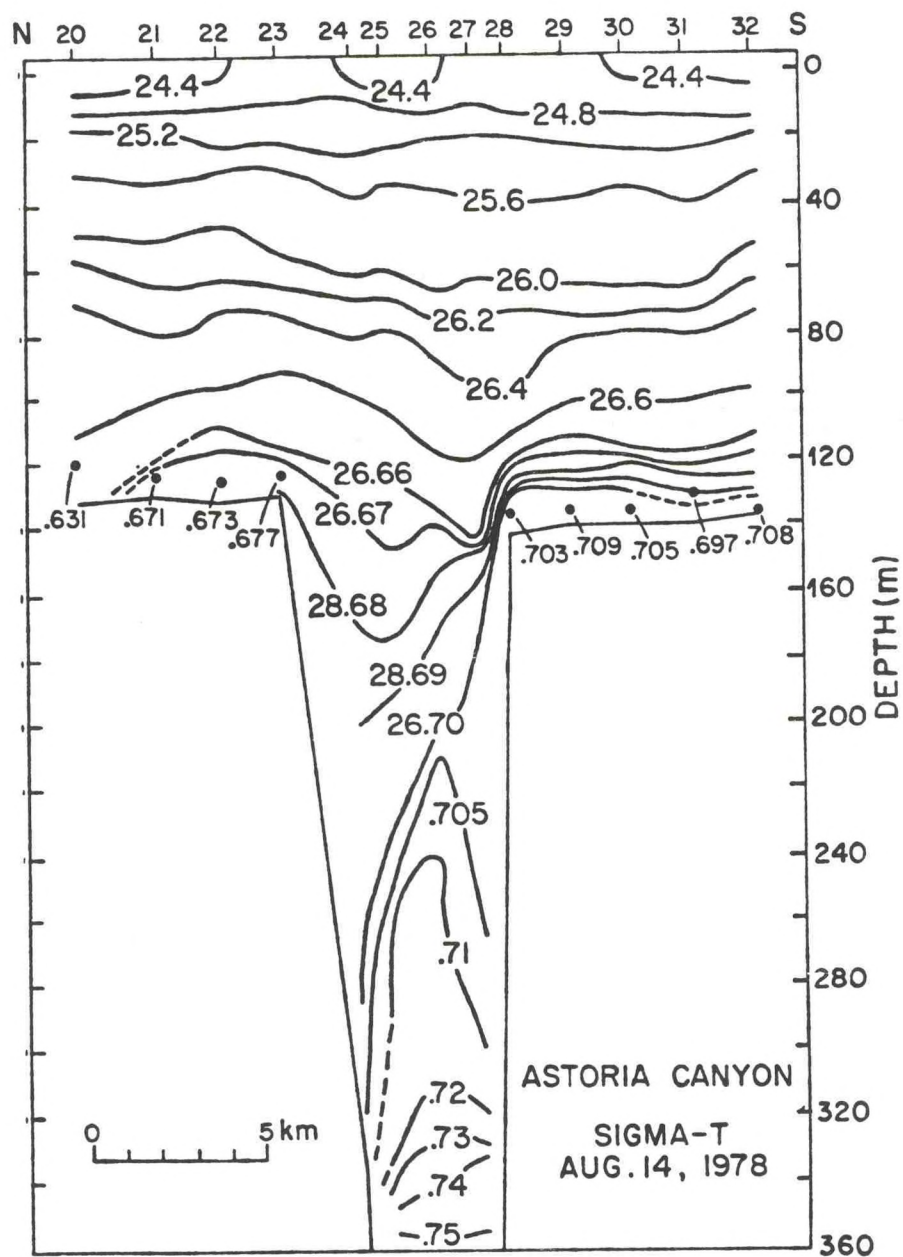


Figure 5. Density on a N-S section across Astoria Canyon (Hickey, 1989).



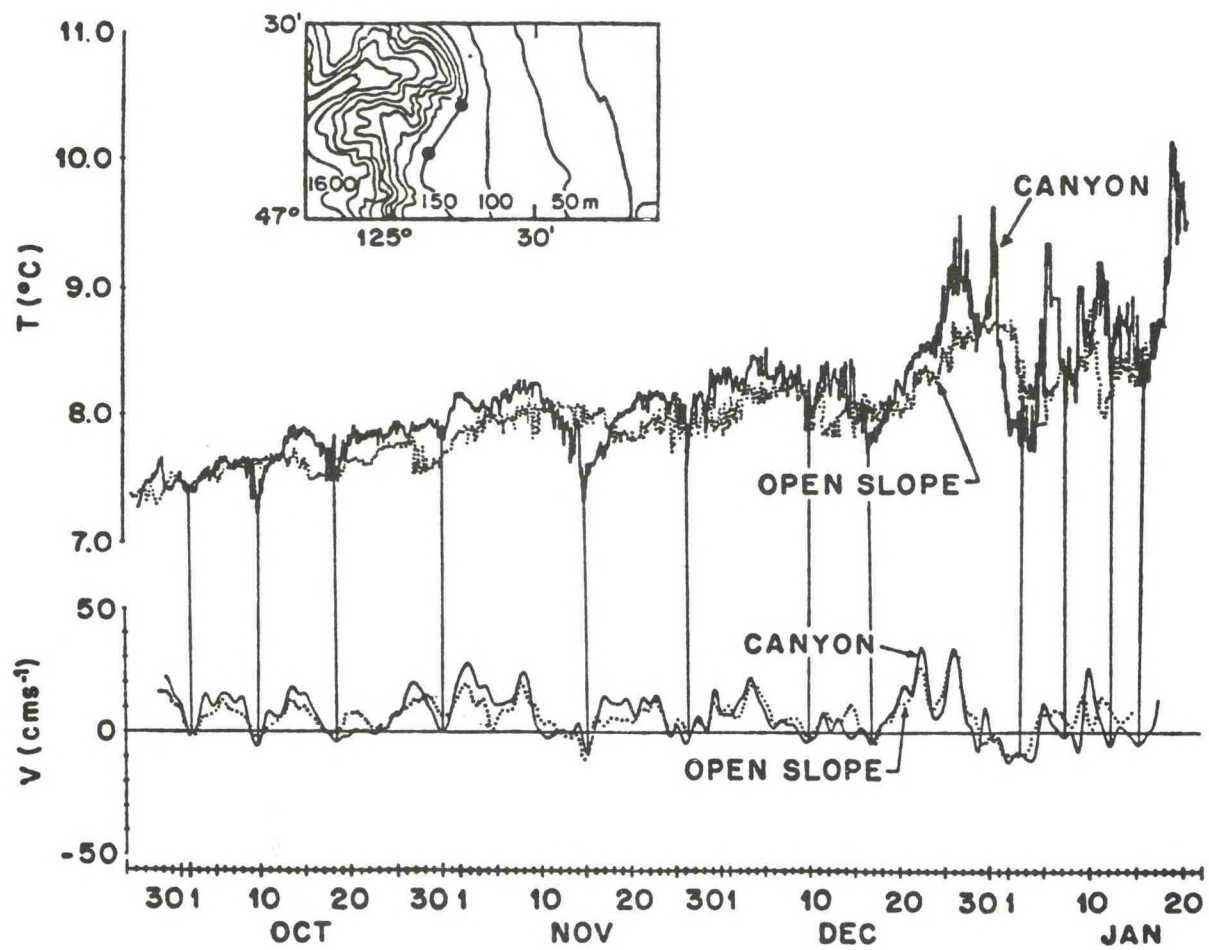


Figure 6. Temperature time series within Quinault Canyon and on the nearby slope (Hickey, 1989).

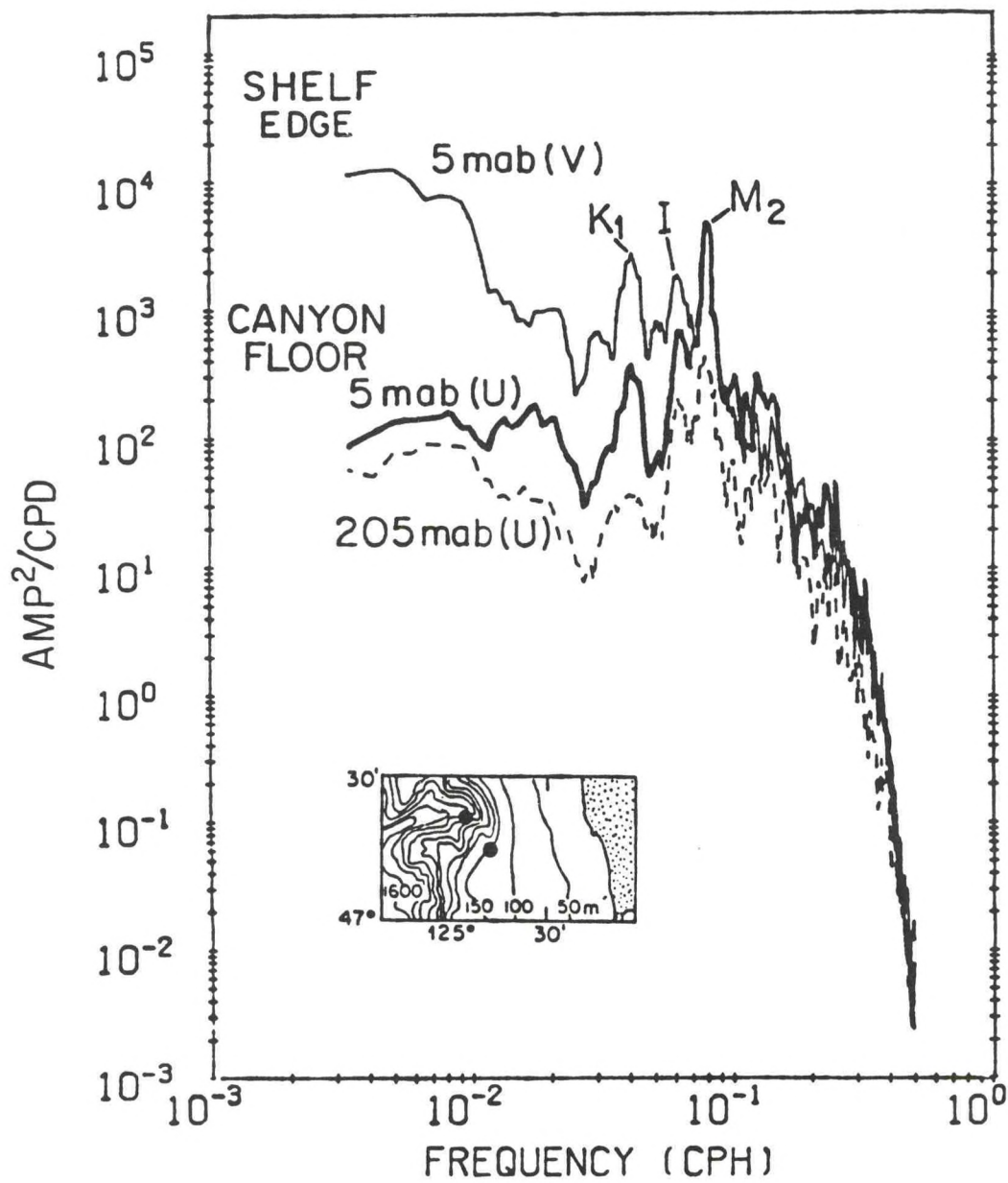


Figure 7. Spectra from Quinault Canyon showing near-bottom enhancement of the internal wave field (Hickey, 1989).



# THE SURFACE BOUNDARY LAYER AND SEA SURFACE FRONTS

Dong-Ping Wang  
Marine Science Research Center  
State University of New York  
Stony Brook, NY

The surface boundary layer in the open ocean is known as the upper mixed layer, that is, a boundary layer of almost uniform temperature distribution. However, the surface boundary layer in the coastal ocean usually is identified with the Ekman layer, that is, a boundary layer which carries the Ekman transport. These two definitions generally are interchangeable; nevertheless, they tend to indicate different aspects of the surface boundary layer dynamics. The mixed-layer concept, on one hand, emphasizes the erosion of the thermocline by cooling and wind-mixing, and is mainly applied to the study of the upper thermal structure. The Ekman-layer concept, on the other hand, emphasizes the wind-induced surface transport, and is mainly applied to the study of coastal motions generated by the divergence of Ekman transport.

In coastal ocean models, the depth of the surface boundary layer is usually assumed to remain constant. This assumption, however, is not supported by observations. The mixed layer on the shelf responds to atmospheric forcing (wind stress and surface heat flux) very much as it does in the open ocean. Variations of mixed-layer depth on the diurnal, event, and seasonal time scales have been clearly documented. From the model viewpoint, there is no difference in upper-ocean thermal evolution as long as the mixed-layer depth is smaller than the total water depth. An interesting situation arises when the upper boundary layer merges with the bottom (tidal) boundary layer. This happens during the fall transition when stratification in the water column breaks down by combined wind, wave, and tidal forcing. The present boundary layer theory is not strictly valid during the breakdown, although the event of complete mixing can be reasonably simulated with a crude approximation of the mixing length (Chen et al., 1988).

In coastal upwelling, the cooling of surface water is associated with the coastal divergence of Ekman transport. Since the Ekman transport is proportional to the local wind stress, the stronger the southward wind, the colder the surface temperature and the more widespread the cold water will be. What happens during the wind relaxation has always been an intriguing question. Since the variation of mixed-layer depth depends on local wind stress, a shallow thermocline will form rapidly during the relaxation if accompanied by surface heating or horizontal heat advection. Based on the temperature evolution during the Coastal Ocean Dynamics Experiment (CODE)-2 (Fig. 1), rapid warming of the upper water column followed each wind relaxation. The situation, however, becomes quite complex when winds vanish progressively. In the CODE area, coastal winds vanished first in the south, causing rapid warming of the surface water in the south, while water in the north was still being cooled by upwelling. The warm water in the south was then advected northward in a narrow filament along the coast when winds in the north also died down



(Send et al., 1987). This process demonstrates the important effect of mixed-layer dynamics on the heat budget. If the mixed-layer depth is not allowed to change with time, the model cannot simulate the strong thermal gradient along the coast.

During active upwelling, the deep cold water is advected offshore in the mixed layer. If the offshore advection is strong, there may be a convergence, and, the cold water may overflow the warmer subsurface water, which leads to convective mixing and deepening of the mixed layer. Consequently, a front is formed between the nearshore cold water and the offshore warm surface water. Based on the combined attributes of temperature, alongshore velocity, streamline, and density cross-sections in the CODE area derived from model prediction (Chen and Wang, 1990) (Fig. 2), a broad upwelling front formed during strong wind (day 130) and a shallow thermocline during wind relaxation (day 178). A double-cell cross-shore circulation is present during active upwelling. The classical one-cell circulation is located seaward of the front, but there is also a strong convergence zone shoreward of the front. The mixed layer is anomalously deep at the front, and the total offshore transport is also smaller at the front than further onshore. Consequently, the streamlines dip down sharply at the front. This process illustrates the coupling between mixing and advection in the upper boundary layer. If the mixed-layer depth is not allowed to change in space, the model cannot simulate the strong coastal recirculation.

We have demonstrated the need to include spatial and temporal variations of the mixed layer in coastal ocean models. We should emphasize that the coupling between advection and mixing is not restricted to coastal upwelling. Convergence along the front should occur whenever the Ekman transport brings cold water over the warm front. Convergence and subduction of tracers along the front are indeed ubiquitous features in the coastal and open ocean. More importantly, the frontal convergence probably also plays a crucial link between the physical model and the biological or environmental (for example, an oil spill) application. On the other hand, the convergence process is Lagrangian in nature; hence, the real significance of subduction cannot be grasped from an Eulerian framework (such as the streamline distribution in Fig. 2). Lagrangian trajectory simulations will be essential to unveiling the true nature of material transport in the upper boundary layer.

The rapid variation of the surface boundary layer offers a special challenge to remote sensing. The sea surface temperature (SST) distribution is the product of surface heating, entrainment cooling, and heat advection. It is customary in SST analysis to completely disregard the effect of mixing. However, even in the active upwelling region off Peru, the similarity between SST and wind distributions was striking (Stuart, 1981), suggesting that the SST distribution partially reflected the spatial variation in mixed-layer depth. The surface wind distribution, the mixed-layer depth distribution, and the SST distribution are three inter-related quantities. As the SST distribution is presently the only easily monitored variable, an interesting question is "How can Coastal Ocean Prediction System(s) (COPS) best utilize (assimilate) SST information in obtaining the prediction of the upper-boundary layer structure?"



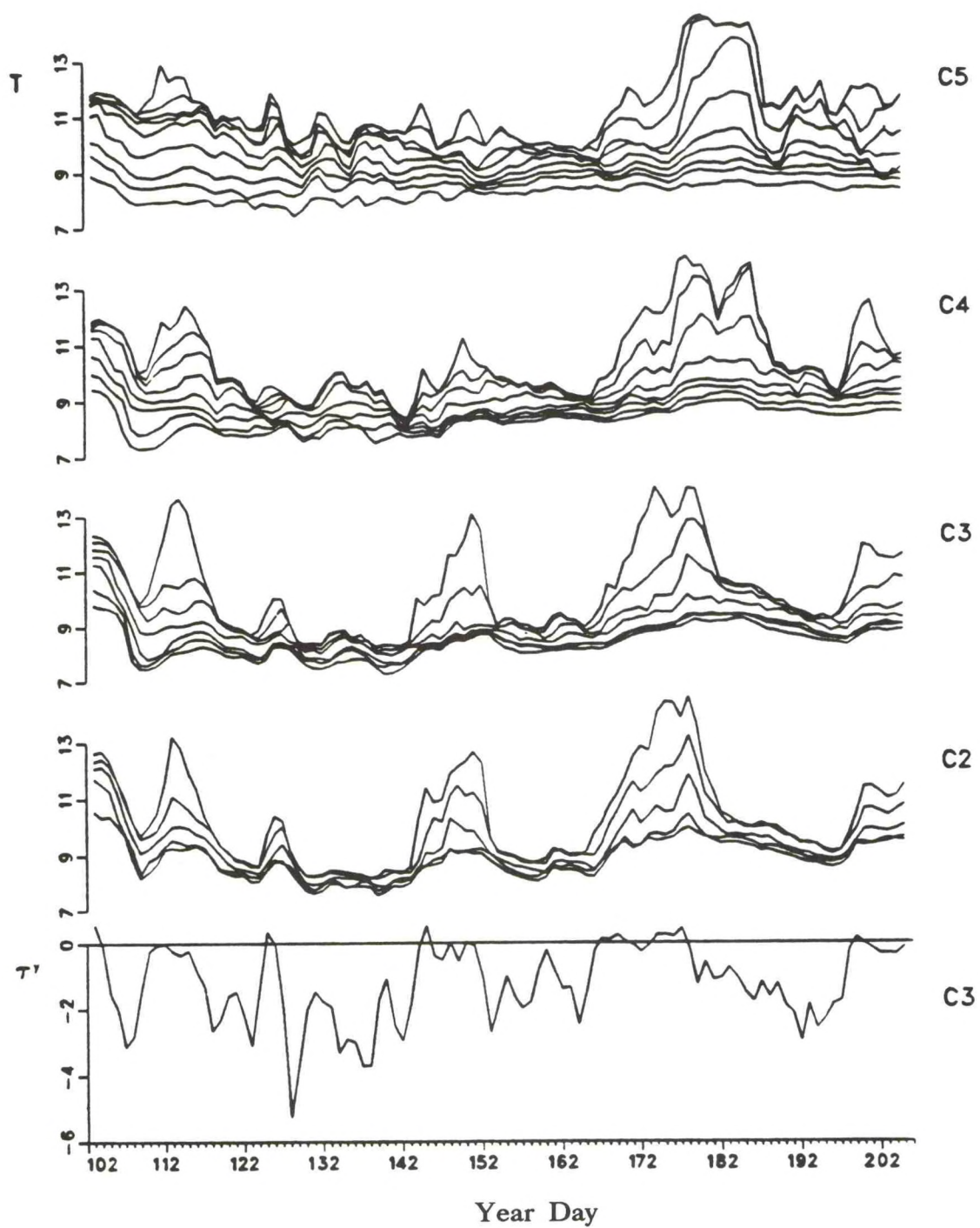


Figure 1. Temperature time series at several mooring locations during CODE-2 experiment.

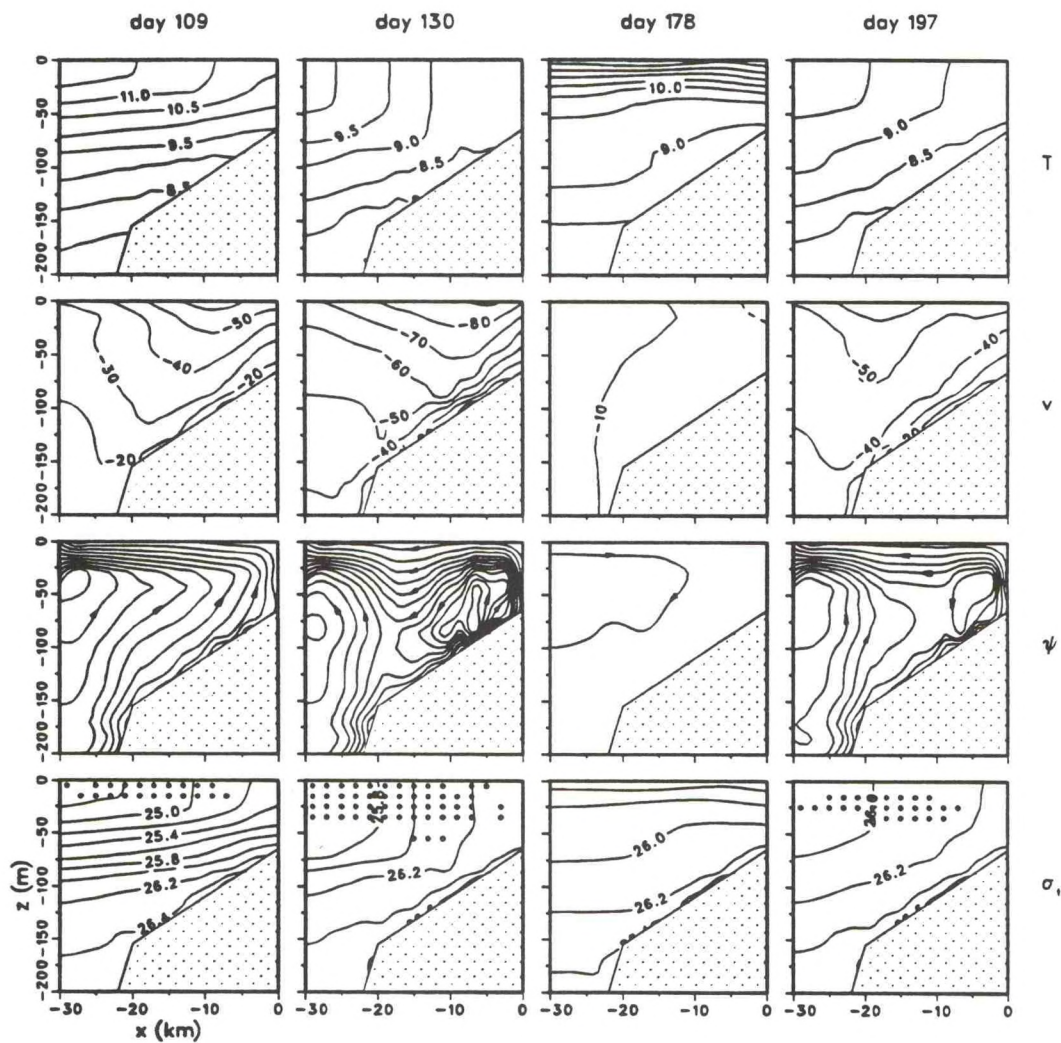


Figure 2. Cross-sectional distributions of temperature ( $T$ ), alongshore velocity ( $v$ ), streamline ( $\psi$ ), and density ( $\sigma_t$ ) from a two-dimensional model simulation.



# ON THE IMPORTANCE OF THE CROSS-SHELF STRUCTURE OF THE WIND STRESS TO SHELF FLOW

Allan J. Clarke  
Department of Oceanography, B-169  
Florida State University  
Tallahassee, FL 32306-3048

Recent work (Lopez and Clarke, 1990) has shown that, at least on the northern California shelf, the cross-shelf structure of the alongshore wind-stress plays a fundamental role in determining the structure of the alongshore flow. Our results, discussed briefly below, suggest that if we are to understand and predict the wind-driven shelf circulation, especially for narrow shelves, it is essential that the wind be measured across the shelf so that its cross-shelf structure is known.

The first empirical orthogonal function (EOF) of the alongshore component of wind-stress for the Coastal Ocean Dynamics Experiment (CODE) region shows (see Fig. 1) that the wind-stress is strongly sheared nearshore. (The measurement at mooring C2 may be in error as the instrument there malfunctioned and the correction factor of two applied (Beardsley et al., 1985) gives an unlikely wind-stress structure (see the dashed line in Fig. 1).) I will ignore the C2 measurement in the discussion to follow. The EOF structure function with the C2 data omitted shows a structure that one might expect: increased friction near the land decreases the wind near the coast, resulting in a strong coastal shear. This shear may exist in other regions and, where the shelf is narrow, it will directly influence a substantial fraction of the shelf.

The cross-shelf change in the wind affects the flow in two ways. First, because the wind-stress approximately balances the bottom-stress near the coast, if the wind-stress changes dramatically nearshore then so must the bottom-stress and, therefore, also the water velocity. Second, across-shelf change in the wind-stress, specifically  $(\tau_0)_{xx}$  [ $\tau_0$  = alongshore wind-stress amplitude,  $x$  = distance from shore] can cause vertical current shear. Physically, non-zero  $(\tau_0)_{xx}$  means that the surface Ekman pumping will vary with  $x$ , tilt isopycnals and produce a vertical shear in the alongshore velocity in accordance with the thermal wind relation.

We found (Lopez and Clarke, 1990) that the above two effects played an important part in determining the structure and amplitude of the CODE alongshore velocity field. Figure 2 shows first mode EOFs of the observed and predicted alongshore velocity fields. The prediction in Figure 2(b) was made using wind-forced coastally-trapped-wave (CTW) theory with four modes as described in Clarke and Van Gorder (1986). The results are essentially the same as those obtained for the CODE region by Chapman (1987). The Clarke and Van Gorder theory does not allow wind-stress to vary across the shelf, and while the observed and CTW-predicted fields are strongly correlated in time, the amplitude and structure of the flows differ markedly (compare Fig. 2(a) and Fig. 2(b)).

The structure and amplitude of the flow in Figure 2(c) is closer to that observed. In this case the prediction was made using a generalized version of the Local Plus Remote (LPR) method of Lopez and Clarke (1989). This method effectively sums all the CTW modes and allows for sloping isopycnals and a wind-stress that can vary across the shelf. Analysis shows that all these effects help to make the predicted alongshore velocity closer to that observed and that the cross-shelf wind-stress change is chiefly responsible for the mid-shelf surface-intensified flow. Note that the LPR theory assumes that the bottom boundary layer is infinitesimally thin; if a finite thickness boundary layer had been taken into account, near bottom amplitudes would be reduced in Figure 2(c), and the 0.25 isolines near the coast would tilt upward more like the observed EOF (compare Fig. 2(a) and Fig. 2(c)).

Thus, physical arguments and hindcast calculations for CODE suggest that, to predict shelf flow, it is important to take into account the cross-shelf variation of the wind-stress. This is especially the case on narrow shelves where the shear in  $\tau_0$  may be strong across a considerable fraction of the shelf.

#### ACKNOWLEDGEMENTS

This work was supported by NSF Grant OCE 87-23157. I thank Paula Tamaddon-Jahromi for ably typing the manuscript.



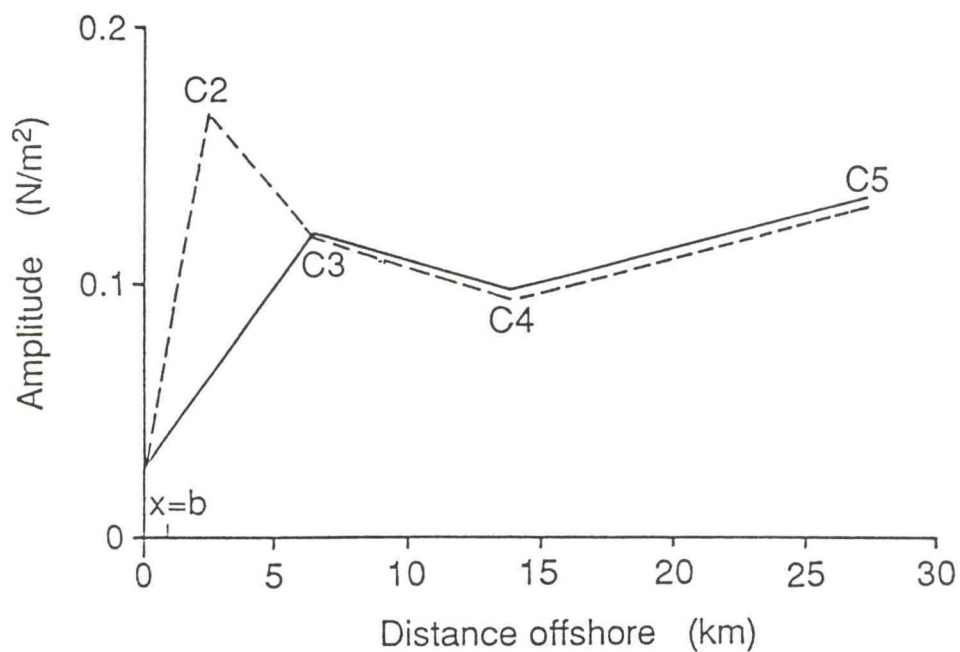


Figure 1. First empirical orthogonal eigenfunction (EOF) of the alongshore components of the wind stress along the CODE 2 central line. Without the data of buoy C2, the first EOF (solid line) explains 95% of the total variance. If all available stations are included, the first (dashed line) EOF explains 89% of the total variance (Lopez and Clarke, 1990).

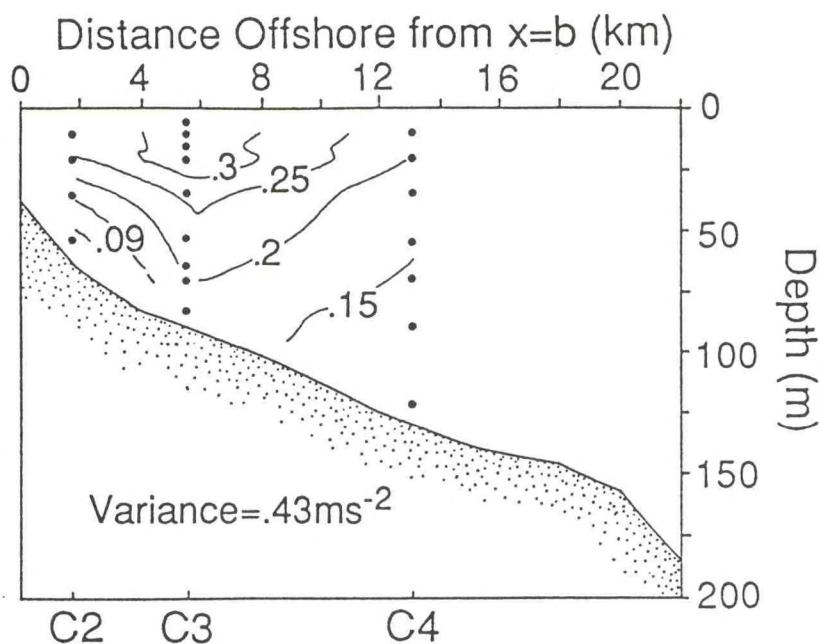


Figure 2(a). Amplitude (dimensionless) of the first empirical orthogonal eigenfunction of the low-frequency alongshelf currents along the C line during CODE 2. The variance associated with this mode is  $0.4344\text{m}^2\text{s}^{-2}$  and constitutes 82% of the total variance. The contour interval is 0.05. The solid dots denote current meter locations (Lopez and Clarke, 1990).

Figure 2(b). As in (a) but for the CTW modeled velocities using four modes. The variance associated with this mode is  $0.1292\text{m}^2\text{s}^{-2}$  and constitutes 100% of the total variance. Only one contour is shown because the offshore shear is slight. Correct to 2 decimal places, the values at the current meter locations (dots) at C3 are all .24 and at C4 either .20 or .21 (Lopez and Clarke, 1990).

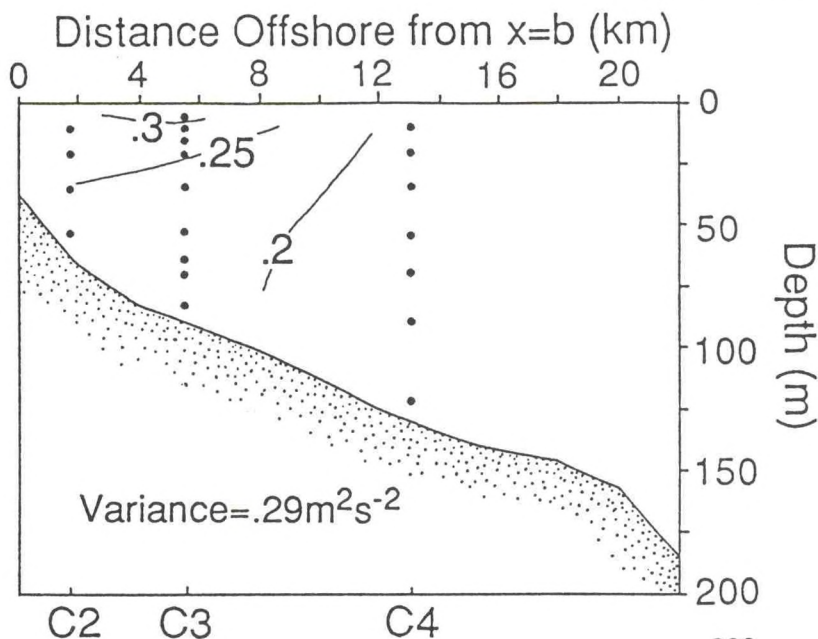
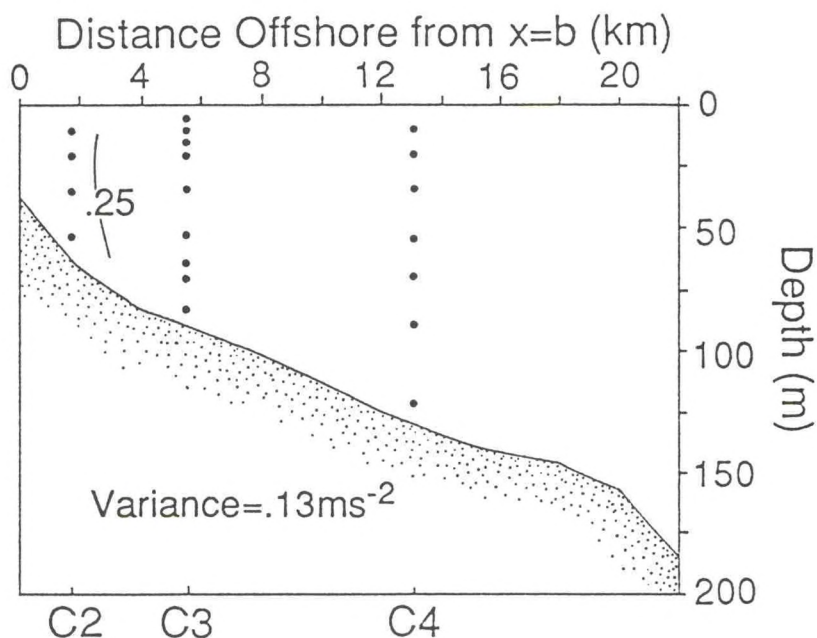


Figure 2(c). As in (b) but for the LPR modeled alongshore currents with near sloping isopycnals and alongshore wind-stress that varies across the shelf. The variance associated with this mode is  $0.2935\text{m}^2\text{s}^{-2}$  and constitutes 96% of the total variance (Lopez and Clarke, 1990).



## TIDAL MODELING

Daniel R. Lynch  
Dartmouth College  
Thayer School of Engineering  
Hanover, NH 03755

### Introduction

#### Tides are important.

The presence of tides is a significant feature of the coastal ocean everywhere, and reflects the detailed interaction of global ocean tides with site-specific shelf and shoreline topography. Tidal ranges of 1 to 15 meters occur routinely in North American coastal oceans, the larger values typically arising from resonance of astronomical forcing with coastal topography. Tidal forcing of this magnitude can account for as much as 80% of the temporal variations in velocity (Moody et al., 1984).

In the Coastal Ocean Prediction System (COPS) context, velocities are the major tidal concern over much of the coastal ocean. Emergency response requires detailed tidal-time predictions of tidal currents, both at surface and at depth, depending on the specifics; and tidal currents can be the principal local generation mechanism for turbulence. At subtidal time scales, tidally induced residual velocities and tidal mixing constitute important advective and dispersive mechanisms in long-term heat, mass, and momentum transport (Wright and Loder, 1985, 1988; Tee, 1985).

In (shallow) nearshore areas the tidal elevation itself is also a matter of significant concern in the COPS context. Tidal ranges which are significant relative to the local depth can dominate estuarine and nearshore processes through nonlinear distortion in tidal time (Aubrey and Speer, 1985) in addition to tidal residual currents, and of course tidal and episodic flooding and dewatering can dominate the long-term physical and ecological processes in coastal systems.

The tuning of resonant tidal systems may be quite sensitive to changes induced by global warming. Smaller-scale estuarine and coastal systems are fundamentally driven by these larger-scale dynamics, with nonlinear tidal interactions influencing their longer-term net exchanges. The coastal/estuarine systems are likely to be the focus of intense scrutiny in the coming decade, as the potential impacts of global sea level rise are likely to be observed there first.

It is therefore imperative that a comprehensive COPS be capable of predicting the tides correctly (both elevation and velocity) as an end in itself and as a prerequisite to dealing with other longer-term coastal ocean processes. Predictive capability is needed for both large-scale regional tides as well as smaller-scale, nearshore tidal processes, and for tidal velocity profiles as well as tidal elevations.



## State of the Art

### Regional elevation may be predicted with confidence.

The basic long-wave physics of horizontal gravity wave propagation is well understood. In the coastal ocean, the primary tidal forcing occurs across the shelf; and the long-wave problem is well-posed as a boundary value problem. In the deeper regions the problem is nearly linear, and conventional numerical methods work well, reinforcing the basic insight gained from analytic solutions in the context of regional topography. Examples of successful elevation predictions abound. 1-D, 2-D, and 3-D solutions have been obtained with finite element, finite difference, and spectral methods, in both the frequency and time domain (Flather, 1976; Greenberg, 1979; Le Provost and Poncet, 1978; Werner and Lynch, 1987; Davies and Furnes, 1980; Walters, 1987; Foreman, 1989). The major nonlinearities arising from interactions on the shelf have also been reproduced, indicating that the nonlinear interactions in these models are working in general (Pingree and Maddock, 1978; Walters and Werner, 1989; Davies, 1986; Le Provost et al., 1981; Le Provost and Fornerino, 1985; Greenberg, 1983). The locations of tidal fronts have also been predicted (Pingree and Griffiths, 1978; Loder and Greenberg, 1986). These and many other studies basically demonstrate that the large-scale, long-wave problem can be solved effectively with numerical methods, provided:

- sufficient resolution of the topography is possible;
- adequate boundary conditions may be posed;
- quality data are available to support the necessary inference of bottom stress and vertical mixing parameters; and
- qualified computational scientists are overseeing the process.

### Velocity predictions remain speculative.

All of the above comments pertain to predictions of tidal elevations. The situation is different for tidal velocities, where the same level of predictive confidence has not yet been reached. In the coastal ocean, tidal velocities are fundamentally 3-D, and depending on the vertical mixing rate the bottom Ekman layer can penetrate the entire water column. Knowledge of the vertical mixing and bottom stress parameters is critical to capturing the vertical velocity profile. The theoretical solution is to simulate the evolution of these parameters by introducing turbulence closure schemes (Mellor and Yamada, 1974, 1982; Johns and Oguz, 1987) and coupling the internal and external modes. Quality modeling systems have been constructed based on this approach (e.g., Blumberg and Mellor, 1987). Our predictive confidence is limited, however, by the data. Velocity profile data, of duration and quality comparable to elevation data, are sparse. Further, inference that velocity is correct from elevation comparisons is weak (Lynch and Werner, 1989b); elevation is relatively insensitive to changes in the vertical structure, and responds to the vertical shear in an average sense only to the extent that bottom stress is significant in the overall force balance. This is basically a foregone conclusion in many tidal studies, wherein reliable harmonic constants are obtained from elevation time-series during which the vertical structure changed. Similar conclusions about



vertical structure inference from velocity data may be reached based on Tee (1982). The point to be reached here is that sound 3-D formulations and modeling approaches are available, but the accumulation of case-specific experience with models and data does not yet support robust conclusions about velocity predictability.

#### A suite of numerical methods.

The basic mathematical structure of the long-wave problem divides into three distinct subdomains: horizontal, vertical, and temporal. The horizontal domain contains the basic gravity wave behavior, and its interaction with topography; these have been successfully modeled using both finite difference (e.g., Praagman et al., 1989) and finite element (e.g., Gray et al., 1987) methods, with comparable success given the same level of topographic precision (Ozer and Jamart, 1988). The vertical is fundamentally a viscous diffusion domain, (Tee, 1979, 1980) and conventional finite difference (e.g., Leendertse, 1989) and finite element (e.g., Lynch and Werner, 1987, 1989a) methods as well as spectral methods (e.g., Gordon and Spaulding, 1987) work well for these physics. Temporal dynamics can be treated by classical harmonic methods with nonlinear perturbations (e.g., Pearson and Winter, 1977; Snyder et al., 1979) or with straightforward time-stepping approaches, both implicit and explicit. Nearly all combinations of these modeling strategies have been examined, and can be expected to work with known sources of error and computational requirements. (See, for example, the so-called Tidal Flow Forum (Werner and Lynch 1988; Ozer and Jamart, 1988), in which most of the 2-D computational options mentioned above were compared with one another in the objective context of a quality field data set (Fig. 1). In an operational context, therefore, one may make nearly independent methodological choices in each of the three mathematical subdomains, based on merit relative to a specific operational goal.

#### Nearshore tidal processes remain a modeling challenge.

Many specific COPS concerns relate ultimately to estuarine and nearshore tidal processes. These occur at length scales much smaller than the basic gravity wavelengths; this and the shallowness of these systems relative to the tidal range dominate the tidal behavior. Gravity wave propagation is no longer the overriding behavior in these systems, but a far-field driving force. Instead, the crucial hydrodynamics are dominated by convective accelerations caused by topographic features, bottom stress and other viscous dissipation, and geometric distortion due to the presence of intertidal areas. These fundamentally nonlinear tidal processes interact in subtle ways to govern the long-term evolution of these systems (Aubrey and Speer, 1985); yet their proper description in an operational context requires high resolution, with far-field coupling to the larger-scale motions in the coastal ocean. The coupling must in general be two-way, as the transport of mass and momentum across the coastal boundary layer can be important and non-intuitive in certain problems (Werner et al., 1988), and the proper parameterization of the boundary layer in terms of boundary conditions for regional-scale models remains problematic (Geyer and Signell, 1989).



In constructing operational models of these nearshore processes, success hangs critically on getting the correct local physics at sufficient resolution, and proper coupling to the coastal ocean. Examples of such coupled systems have been constructed (e.g., Vemulakonda et al., 1988). As in the 3-D velocity structure discussion above, predictive confidence in this arena is limited by data and experience, relative to that available for the regional tidal predictions. Because the nearshore physics is dominated by different processes from the coastal ocean, the computational approach also demands special treatment, enhancing the coupling issues. Finally, some of the physical processes--including flooding/dewatering and convection-dominated flows--are at the frontier of computational fluid mechanics and are likely to continue to mature methodologically for some time.

## Operational Issues in Tidal Prediction

### Operational models are site-specific.

By definition, an operational predictive system must ultimately be tailored to a specific region at a high level of detail. Given that certain aspects of the tides may be confidently modeled, the limiting factor in predictive quality will be the realism which can be obtained in system topography, boundary conditions, and parameterization/calibration. Because some aspects of tidal modeling require continued development, a long-term, flexible computational and software engineering strategy is required.

### Boundary conditions.

The scientific practice of working with individual harmonic constituents and their reproduction in model output has masked an important operational problem: the whole spectrum of motions must be present in a tidal prediction, which means that the whole spectrum must be properly forced at the system boundaries. Some coastal stations require upwards of 100 harmonic constituents for proper reconstruction of the time-domain (Praagman et al., 1989). Particularly for the internally generated constituents, obtaining quality boundary conditions is not simple; and their neglect can lead to serious errors (either apparent or real) in model prediction. For example, in the Tidal Flow Forum, apparent elevation errors of 50 cm were ultimately ascribed to an incomplete harmonic spectrum at both boundary and shoreline points (Werner and Lynch, 1989) (Fig. 2). Wherever possible, one prefers to place open-water boundaries sufficiently far offshore that the pure ocean tide may be used to force the model and the internally generated constituents may be safely ignored as negligible. Most practical systems, however, will require cross-shelf boundaries of significant length, and the problem of boundary condition specification (including the tidal residual) remains problematic on these. (See Garrett and Greenberg (1977) and Chapman (1985) for discussions of the open boundary problem.)



### Topographical resolution.

Pushing the modeled system further offshore alleviates the problem of boundary conditions, at the obvious expense of computational size. At the same time, the estuarine and near-coastal processes demand ever-greater spatial resolution. One strategy in this context is to couple separate models with different length scales (Fig. 4). As a general operational strategy this can pose tricky problems at the model interface. (See for example Molines et al. (1989) in which coupled models were used, and the sequel study (Lynch et al., 1989), in which a single variable-resolution model was used in the same tidal system.) There is a clear operational need, therefore, for effective methods for both generating and using graded meshes.

The finite element method has long been viewed as the answer to this problem. Following the world-wide successes in solid mechanics and diffusion, several early experiments in oceanographic computation established both the promise and the problems with this method (Wang and Connor, 1975; Pearson and Winter, 1977; Gray and Lynch, 1977; Platzman, 1978; Le Provost and Poncet, 1978; Jamart and Winter, 1978). As described in a previous review (Lynch, 1983), important conceptual developments followed which put the method on a firm mathematical footing for tidal simulation (Lynch and Gray, 1979; Platzman, 1981; Foreman, 1983; Walters and Carey, 1984; Kinnmark, 1985). Following this period of analysis and consolidation, effective use of finite elements in field studies has been shown in 2-D (Gray et al, 1987; Walters, 1987; Werner and Lynch, 1987, 1989; Foreman, 1989; Gray, 1989; Walters and Werner, 1989) and 3-D (Lynch and Werner, 1987, 1989, 1990; Foreman, 1989). The finite element method has now advanced to the point where serious consideration should be given to its operational use.

The problem of detailed, site-specific mesh generation requires significant attention in any operational context. Currently there is under development a public-domain finite element mesh generator which keeps the gravity-wave resolution  $(\Delta x)^2/H$  constant, subject to topographic constraints (Henry 1988) (Fig. 5). The union of this application-specific software with the large volume of commercial, generic graphical software will establish a powerful base system within which complex mesh generation and editing can be achieved routinely in an operational setting.

### Parameter inference.

Operational modeling must ultimately resort to calibration in order to a) decide whether a particular discretization is sufficient; and b) to obtain missing or unobtainable data, e.g., boundary conditions or bottom stress parameters. In the calibration process it is crucial that data be handled with a balanced understanding of its limitations. For example, the vast majority of tidal data is in the form of elevation time-series at shore-based stations. These data can contain local anomalies reflecting very local geometric and other effects, which if allowed to dominate a calibration can seriously distort the result unless proper local resolution is available (e.g., Lynch et al., 1989). Additionally, as mentioned above, elevation per se can be insensitive to the vertical mixing processes, and thus

a false sense of confidence can be generated by reliance on elevation data alone. For these and related reasons it is likely that operational tidal modeling will require concurrent, model-focused field efforts.

### Evolution of a computational system.

A collection of coastal ocean prediction systems, each tailored to a specific region, will represent an increasingly significant investment in software and data over time, and this cost will far exceed the cost of the hardware required to run the system. Recognizing that major computational improvements in some aspects of tidal modeling (e.g., estuarine and nearshore processes) are likely to occur during the early lifetime of any effective COPS, a long-term, flexible computational and software engineering strategy is required. The ideal strategy will allow the continuous incorporation of generic computational improvements into an established set of site-specific models with uniform structure. Of major importance is avoiding a situation where new developments require site-specific software engineering for their implementation; or even worse, where the basic computational strategy prohibits the incorporation of significant new advances without scrapping major investments in existing software. Accordingly, an early and continuous emphasis is required in:

- the choice of computational strategy for future flexibility;
- standardizing data structures as well as languages and graphics paradigm; and
- quality, structured software engineering.

A COPS built upon these principles should have a long and useful life, far outlasting the hardware on which it was originally built, and satisfying to the public it serves.



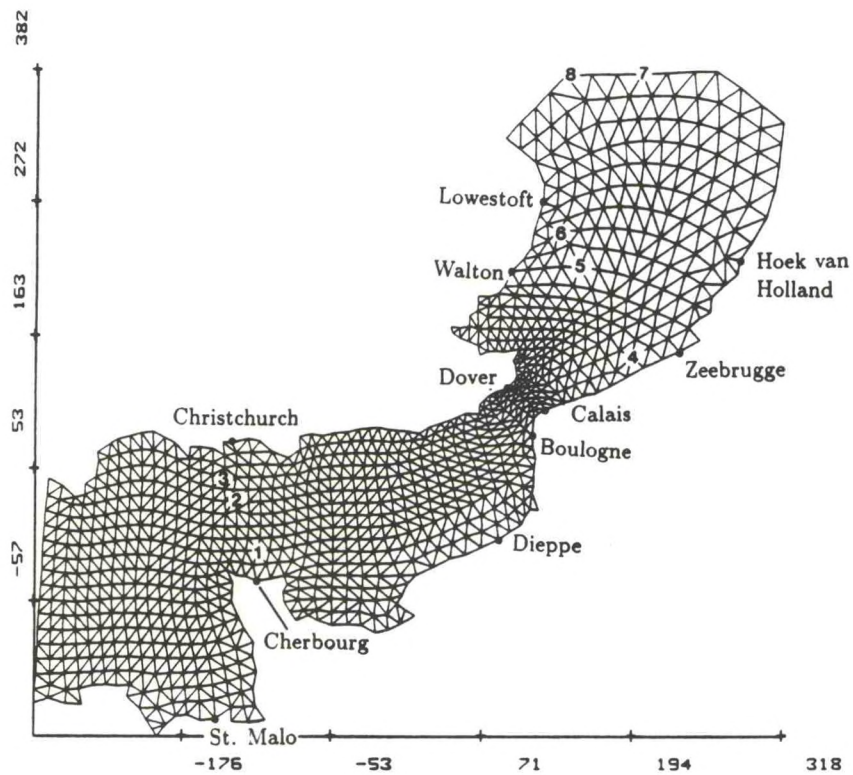
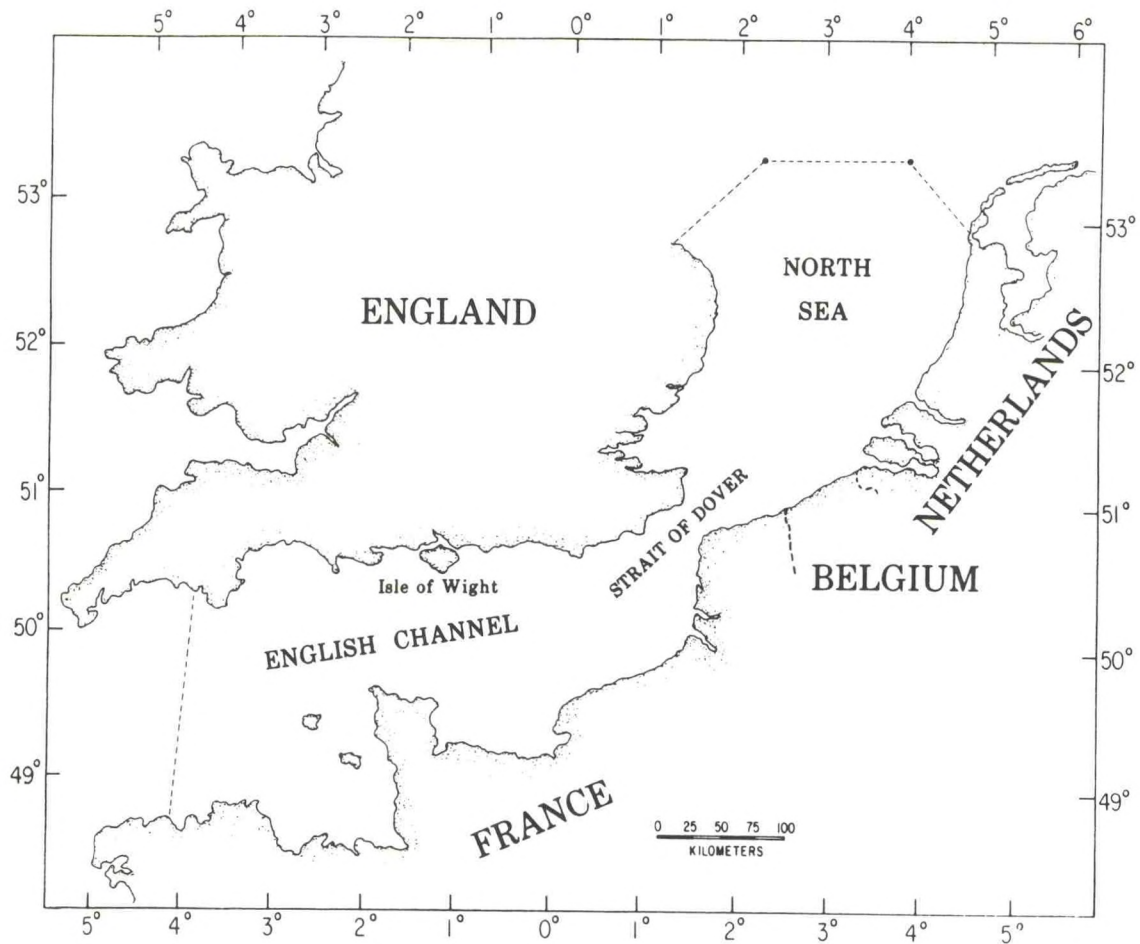


Figure 1. Location and mesh used in the Tidal Flow-Forum. Test-station locations are indicated for sea level by name, and for velocity by number (from Werner & Lynch, 1987).

## Zeebrugge

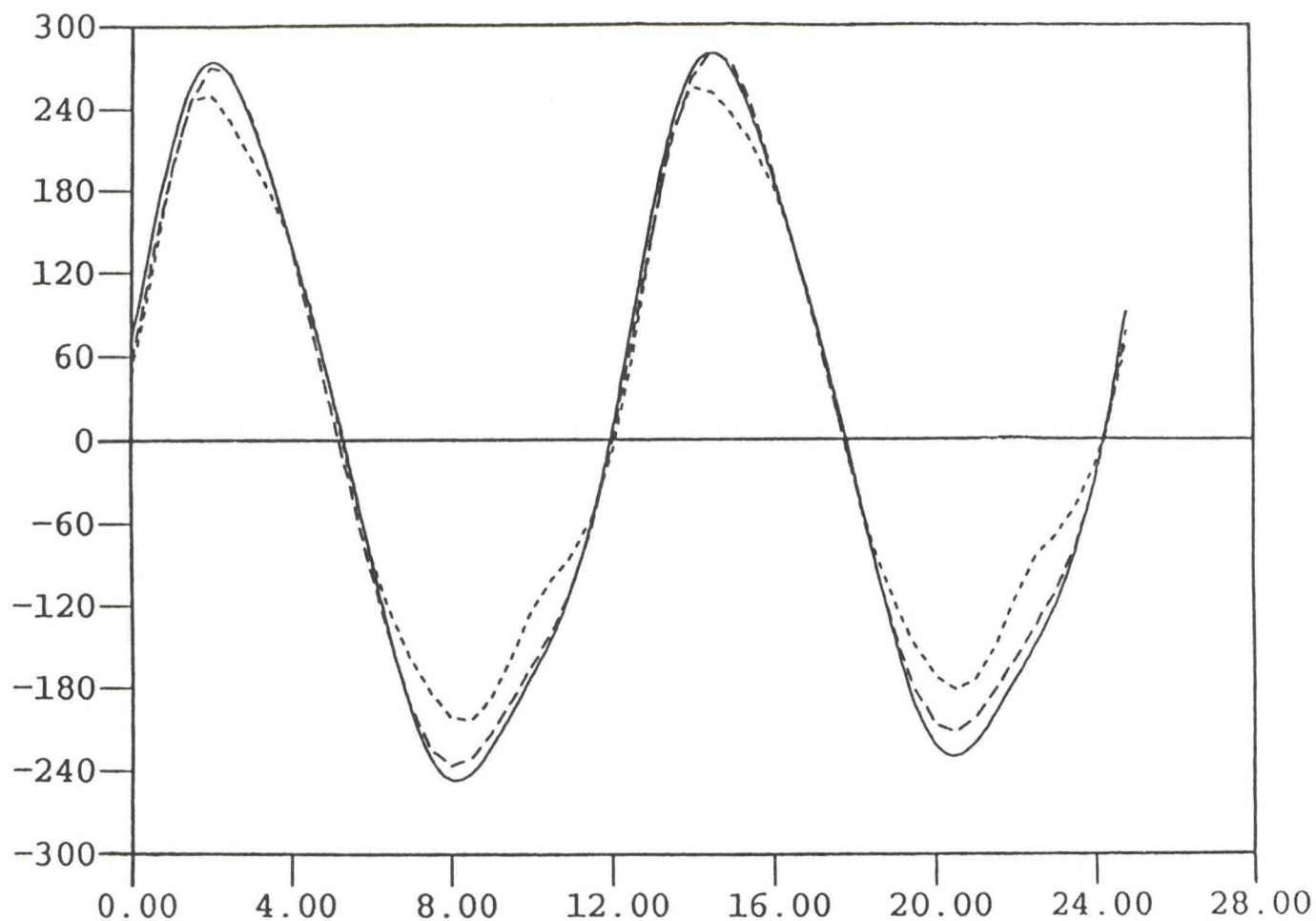


Figure 2. Example illustrating the importance of missing constituents. The solid line is reconstructed from 11 main harmonic constituents; the short-dash line represents time-domain simulation results; the long-dash line is the same result, "filtered" i.e. reconstructed from only the 11 constituents known in the data (from Werner & Lynch, 1989).



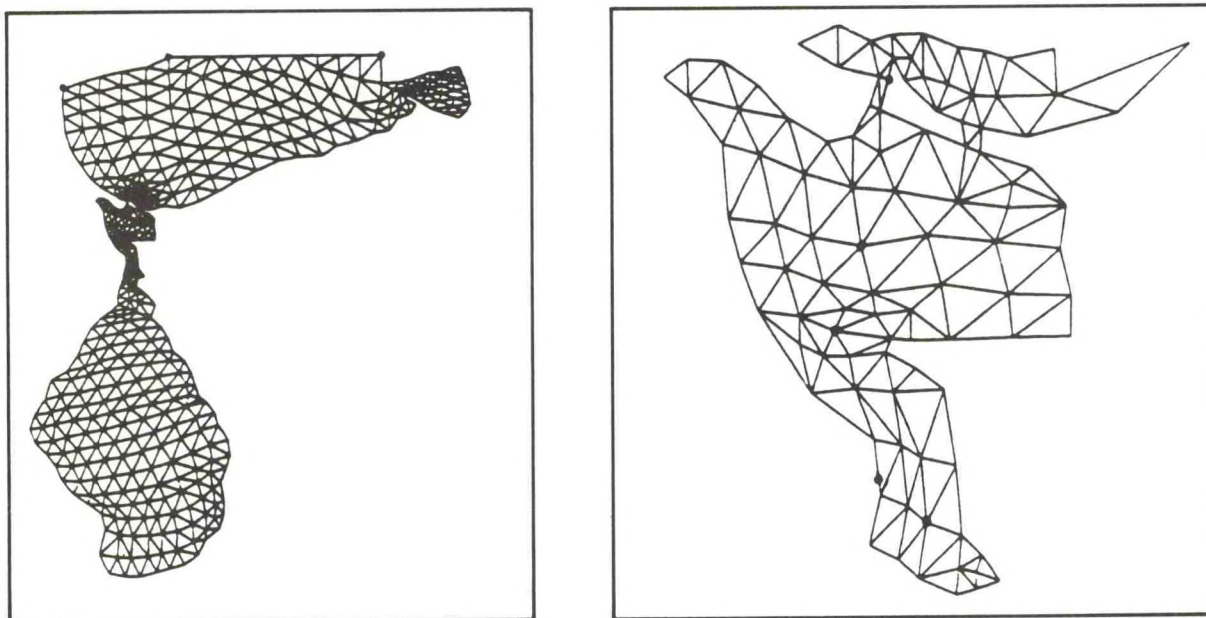
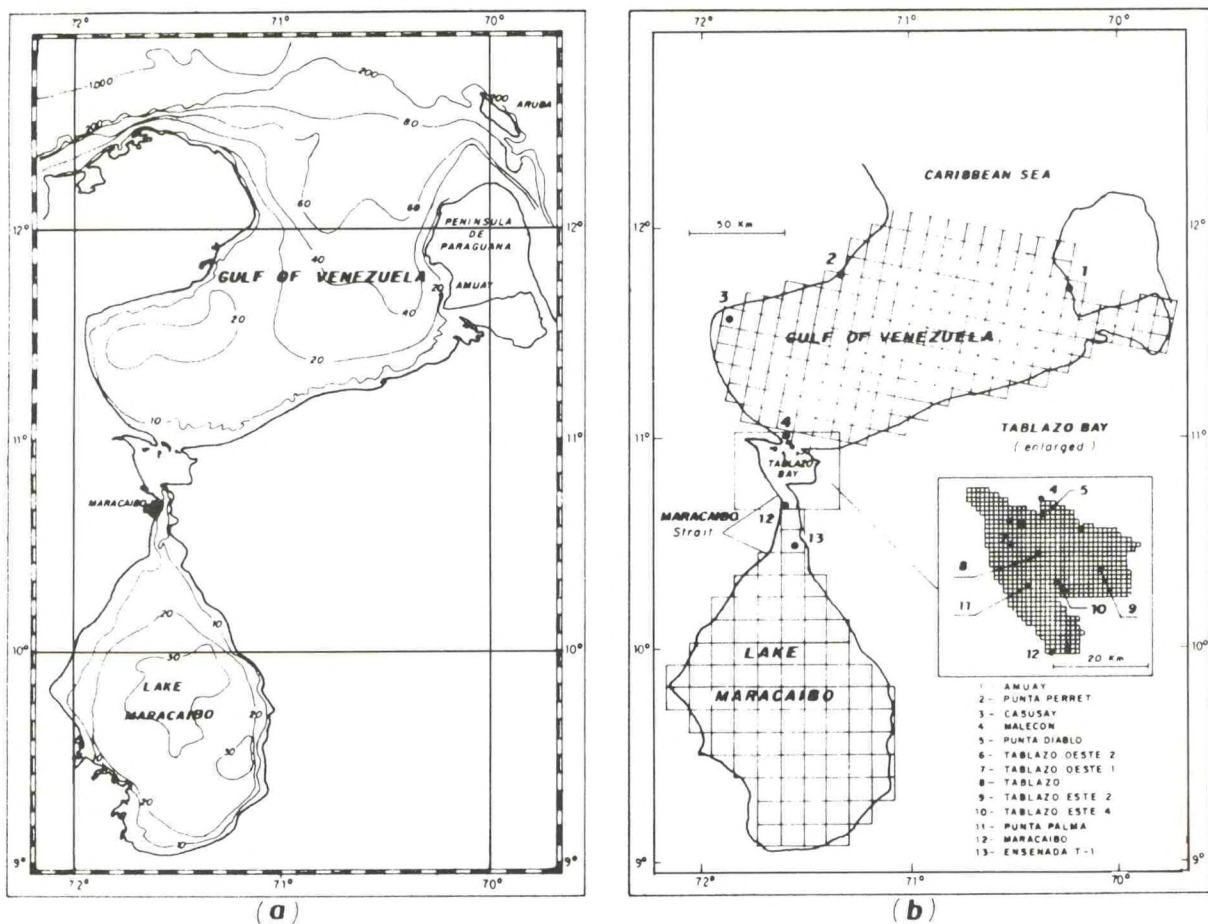


Figure 3. Separate finite difference (top) and graded finite element (bottom) meshes for the Lake Maracaibo System (Molines et al., 1989; Lynch et al., 1989).

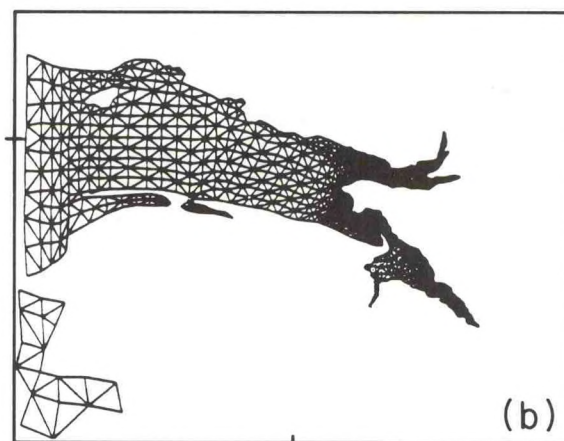
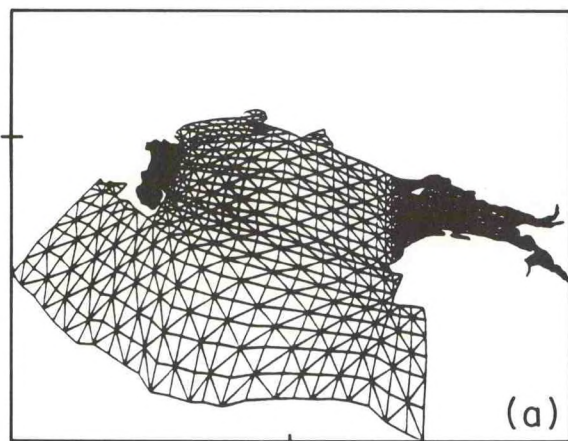
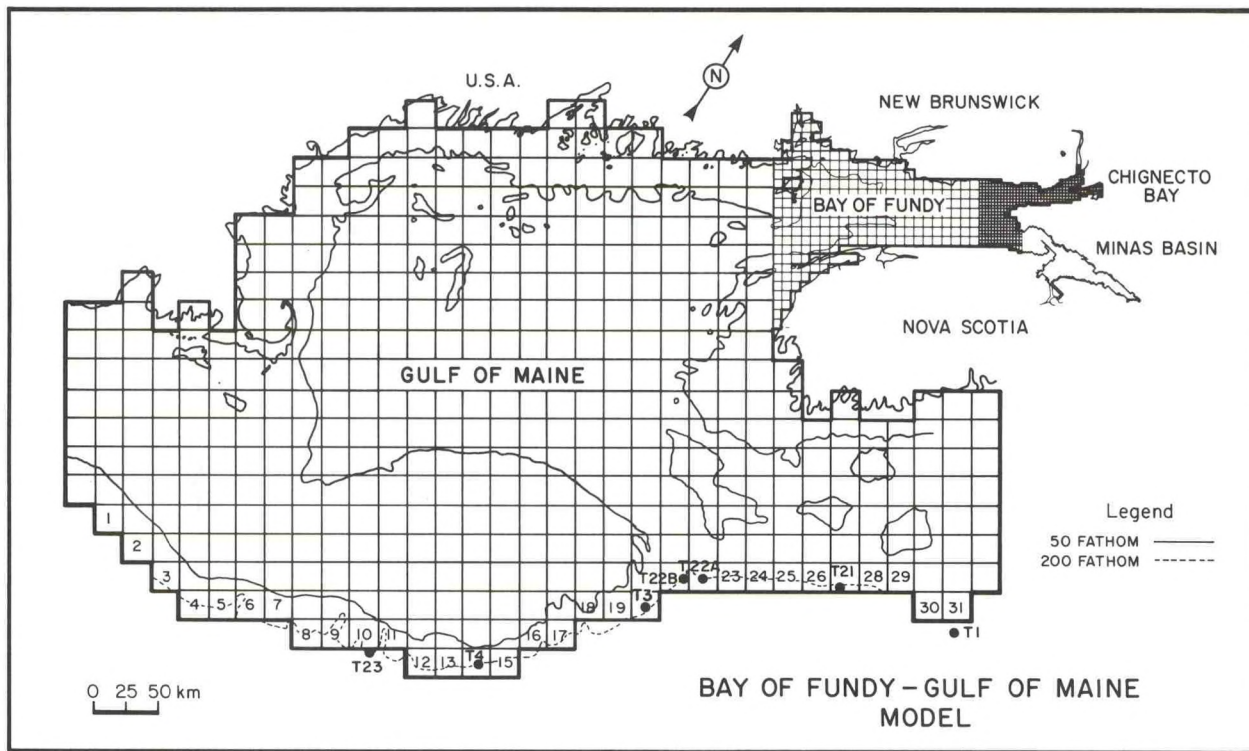


Figure 4. As in figure 3 for the Gulf of Maine system (Greenberg, 1983).



# NORTH SEA / ENGLISH CHANNEL

IOSNGH1.DAT 7 JUNE 1988

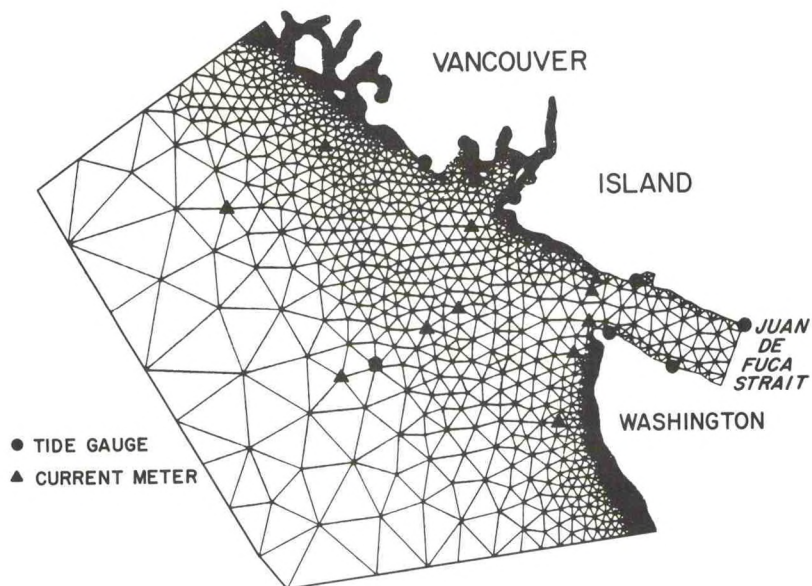
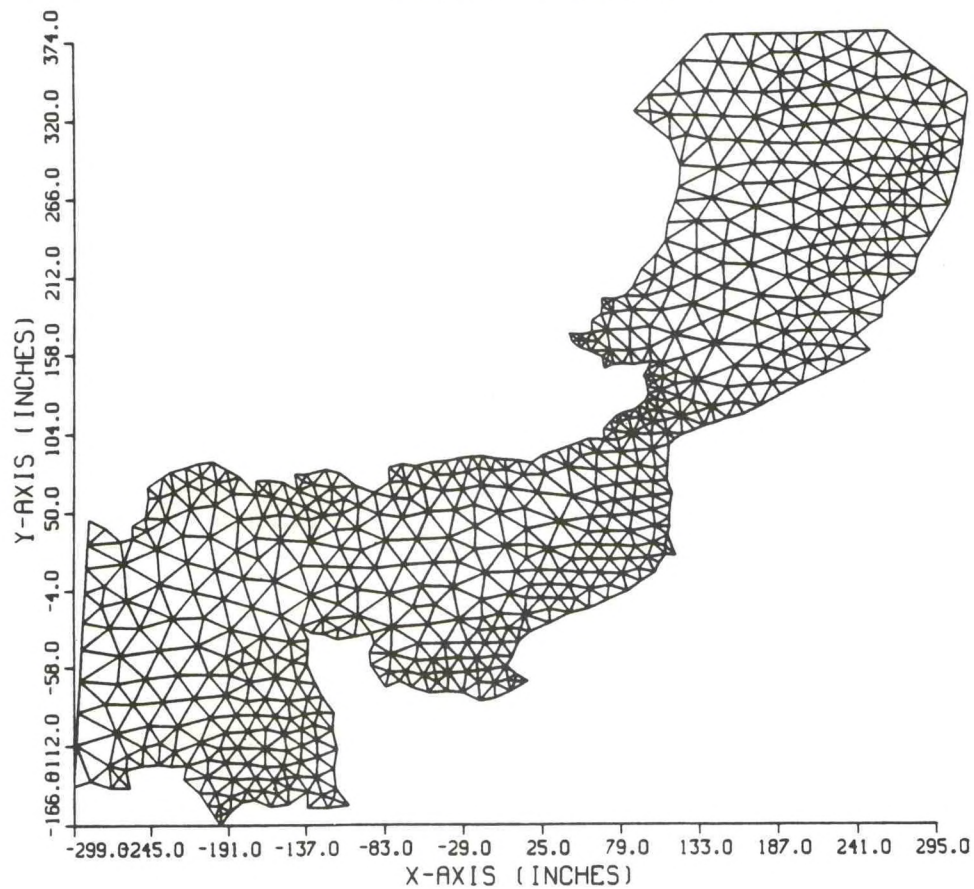


Figure 5. Graded mesh for the Tidal Flow-Forum problem (top) and the southwest coast of Vancouver Island (bottom) based on uniform Courant number (Henry, 1988).

# NEARSHORE PROCESSES

Robert A. Holman  
College of Oceanography  
Oregon State University  
Corvallis, OR 97331-5503

## Introduction

Wind waves and swell, generated offshore, are the primary source of energy to the nearshore region. As they approach the beach, shallowing bathymetry causes a transformation that is slow at first in the shoaling region, then catastrophic within the surf zone. Our research objective is to understand the alteration and fate of this energy, and the impact of incident waves and their descendent motions on the bathymetry through sediment transport.

Some of the most interesting dynamics in the nearshore are just smaller scale analogs of shelf processes. Both act as wave guides with trapped and leaky modes, and both support vorticity waves based on the potential vorticity field. There are also some systematic differences. Understanding the nearshore problem is simplified by neglect of Coriolis and stratification. However, complications arise from the common presence of strong nonlinearities and the fact that the depth goes to zero in the region. Moreover, changes of depth through sediment transport can be a first order effect. The fact that excellent progress has been made has been partially the result of the ease of sampling the nearshore compared with the shelf-scale counterpart; we can usually sample  $O(1000)$  cycles in time, and a number of cycles in space without the need of ship time.

## Structure of the Fluids Problem

Full understanding of the nearshore problem entails detailed knowledge of both the fluid motions and the resulting sediment transport. The latter problem has proved to be quite complicated, so the focus of this note will be on the dynamics of nearshore fluid motions.

The various fluid processes in the nearshore region can be conveniently organized into a conceptual and dynamical framework (Fig. 1). These processes vary with cross-shore location and frequency (vertical and horizontal axes, respectively). Energy from incident waves enters the system at intermediate frequencies, approximately 0.1 Hz. This energy is then redistributed to both higher frequencies (harmonics that are still coherent with the incident band plus turbulence) and lower frequencies through nonlinear shoaling offshore and breaking within the surf zone. While wind can directly drive surface flows with vertical shear offshore, the predominant shallow water mean flows are driven by wave breaking and may be unstable to shear waves at far infragravity frequencies. Swash is included



specifically since it includes that portion of the wave field that reflects from the beach and propagates offshore, a loss of energy from the nearshore energy budget.

With the exception of turbulent dissipation and breaking, excellent progress has been made in understanding these processes. Short descriptions of important results follow.

## Dynamics of Individual Bands

### Incident Band

The nonlinear evolution of a normally incident wave train leads to the generation of waves that are peaky and may be tipped forward (borelike). These tendencies may be parameterized by skewness and asymmetry (skewness of the Hilbert transform) of the time series, respectively. Since sediment transport depends on either the third or fourth power of velocity, proper parameterization of skewness is crucial to understanding sediment transport.

The nonlinear interaction of two waves will transfer energy to motions with frequencies that are the sum and difference of the interacting wave frequencies. Evolution of the shape of incident waves (hence the skewness) results from the sum interactions and the generation of phase-locked harmonics.

In a monochromatic wave field, the first harmonic will occur at twice the incident frequency in a self-self interaction. In a random sea (a spectrum of waves with finite bandwidth) all frequencies can interact, and the computation of the harmonic peak requires a full spectral evolution model based on the Boussinesq equations (Freilich and Guza, 1984; Elgar and Guza, 1986). Based on field data (Fig. 2) of the evolution of a wave field at Torrey Pines, CA, the waves become peaky (high skewness) as they shoal to mid-depths, then bore-like (high asymmetry) in shallower water. Model results, based only on measured initial conditions at 10 m depth, reproduce the evolution with remarkable precision up to the point of wave breaking. Modeling of breaking remains very empirical.

### Mean Flows

Mean flows arise mathematically from the difference interaction of a wave with itself. They are most easily described by the radiation stress of a wave, the flux of momentum associated with the progression of the wave. Horizontal gradients in radiation stress, for instance through shoaling or breaking, yield gradients in this flux of momentum, with the excess being transferred into the mean flow.

The momentum flux associated with waves breaking in the surf zone will force shoreward flows which raise the water level (called 'set-up') until the pressure gradient balances the radiation stress gradient on a depth average. However, wave breaking is often not depth-uniform. Vertical variability in the breaking process



leads to local (vertical) imbalances, hence vertical shears with a mid-depth reversal to an offshore-flowing lower layer called 'undertow.'

If waves approach at an angle to the beach, there is an onshore flux of longshore-directed momentum. Cross-shore gradients due to breaking will force a mean longshore current that is balanced by bottom friction. Since there is no opposing pressure gradient, no current reversals are possible due to vertical structure in wave breaking. Under monochromatic models, all waves begin to break at the same cross-shore location, resulting in a discontinuity of forcing that must be artificially smoothed. However, under a random incident wave field, the location of the initiation of breaking is distributed and smoothing is not required (Thornton and Guza, 1986). Note that monochromatic waves are only observed in the laboratory; all natural wave fields have finite bandwidth.

### Infragravity Waves

Because incident wave spectra have finite bandwidth, many of the possible nonlinear difference interactions will occur at low (not zero) frequency. The resulting motions have the time scale of the ubiquitous incident wave groups ( $O(1 \text{ minute})$ ) and are called 'infragravity waves'. They will have a longshore length scale also determined by that of the incident groups.

Because the phase velocity of shallow water disturbances is a minimum at the shoreline (varies as square root of the local depth), the nearshore can be recognized as being a natural wave guide with potential for resonant modes to be trapped in the wave guide (called edge waves in the nearshore) as well as leaky modes whose energy escapes from the wave guide. Field data confirm this behavior (Fig. 3). Shading indicates concentrations of energy at particular wavenumbers. Solid lines indicate the theoretical dispersion lines for the lowest three edge wave modes, calculated numerically to include the effect of the true bathymetry and the  $90 \text{ cm sec}^{-1}$  longshore current. Clearly, energy is not randomly distributed in wavenumber, but concentrates at edge wave resonances. Leaky modes, at very small wavenumber, have little expression in longshore current (the basis of this spectrum), but are more apparent in the cross-shore velocity.

### Far Infragravity Waves

In addition to edge waves, an anomalous ridge of energy occurs at low frequencies and large positive wavenumbers (Fig. 3). While this energy extends into the traditional infragravity band, the bulk is at lower frequencies ( $O(5 \text{ minutes})$ ), in what has been called the far infragravity band.

These motions have been shown to be shear waves (Oltman-Shay et al., 1990; Bowen and Holman, 1990), arising from an instability of the mean longshore current. The governing physics is the conservation of potential vorticity, in analogy with Rossby waves. However, in the nearshore, the role of Coriolis in determining the background potential vorticity field is played by the shear of the mean longshore



current. Perturbations of this background structure can be unstable and lead to the generation of nearshore vorticity waves.

### Turbulence

Energy is dissipated in a turbulent cascade both in the bottom boundary layer through friction, and in the surface layer through wave breaking. The vertical distribution depends on the nature of the breaking (plunging vs. spilling breakers) and is not well understood. The details of the vertical distribution determine the vertical structure of momentum transfer to the water column. Dissipation in the bottom boundary layer links the water column flows to the transport of sediment.

### **Interactions with Shelf Processes**

The nearshore can act as a significant source or sink of mass and momentum for time-dependent (spin-up/spin-down) shelf flows. Wind or wave-driven vertical shears at the offshore limit of the nearshore may allow diapycnal transport through nearshore mixing. These vertical shears are also very important to the transport of sediment and pollutants onto the shelf. Finally, the nearshore acts as a radiator of energy onto the shelf, particularly in the form of lower-frequency leaky modes which decay little with depth. These may play an important role in the structure of the shelf bottom boundary layer, hence the transport of shelf sediments and the dissipation of shelf flows.

### **The Prognosis for Predictability**

Our understanding of the larger-scale flows has improved enormously in recent years. We can now predict the evolution of an 2-D incident wave field up to breaking and have good empirical knowledge of the breaking-wave energy decay. We can predict the bulk infragravity variance, again based on empirical data interpreted intelligently, and have a good idea of the detailed physics involved. Our capabilities of predicting mean longshore currents are becoming good (especially with the recent inclusion of shear waves as a mixing mechanism), while our understanding of undertow lags behind.

We are only beginning to learn about the details of dissipation through bottom friction and wave breaking. Until our understanding of these processes improves, our knowledge of processes that depend on them, such as nonlinear energy redistribution and sediment transport, will be limited.

# Nearshore Momentum Budget

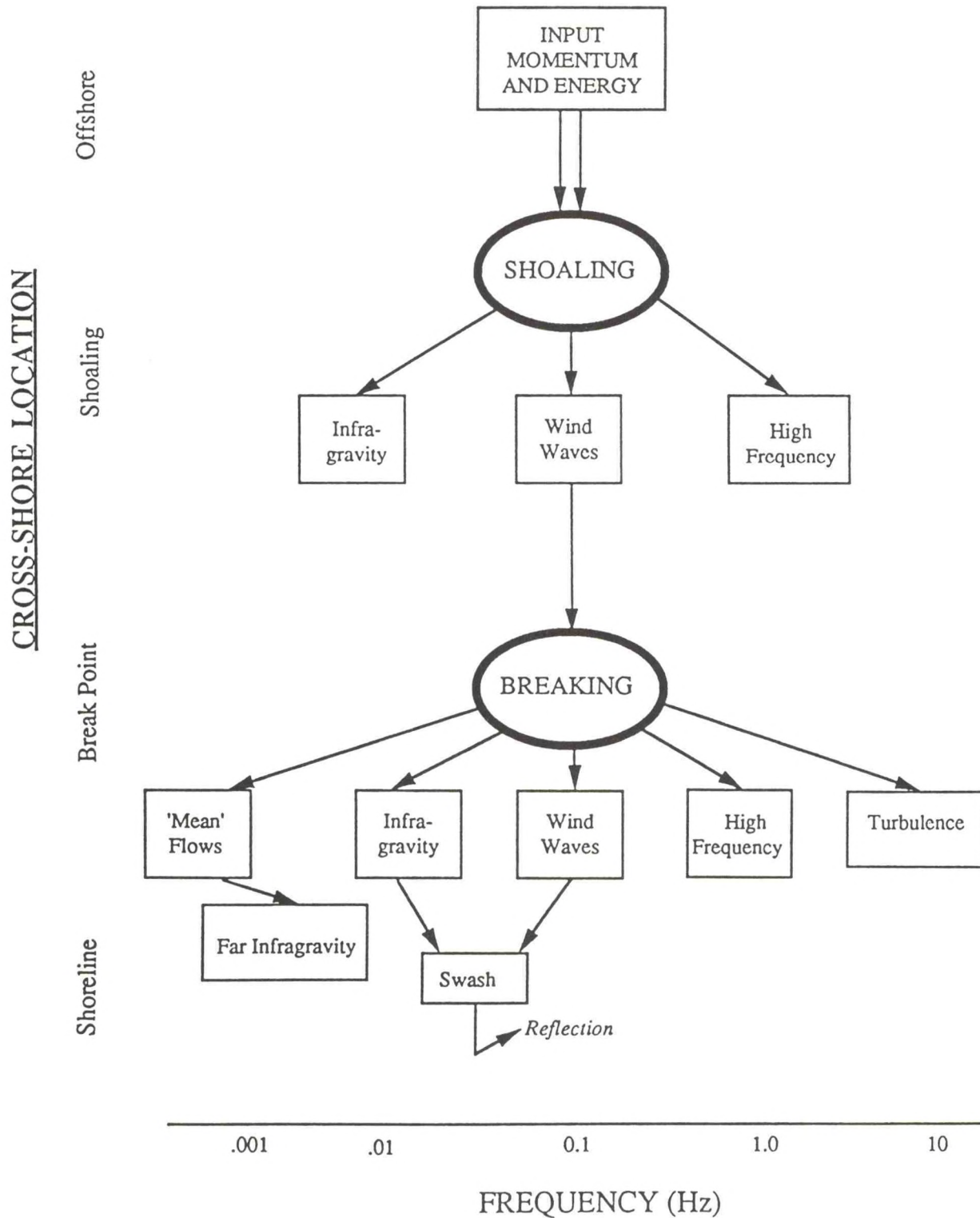
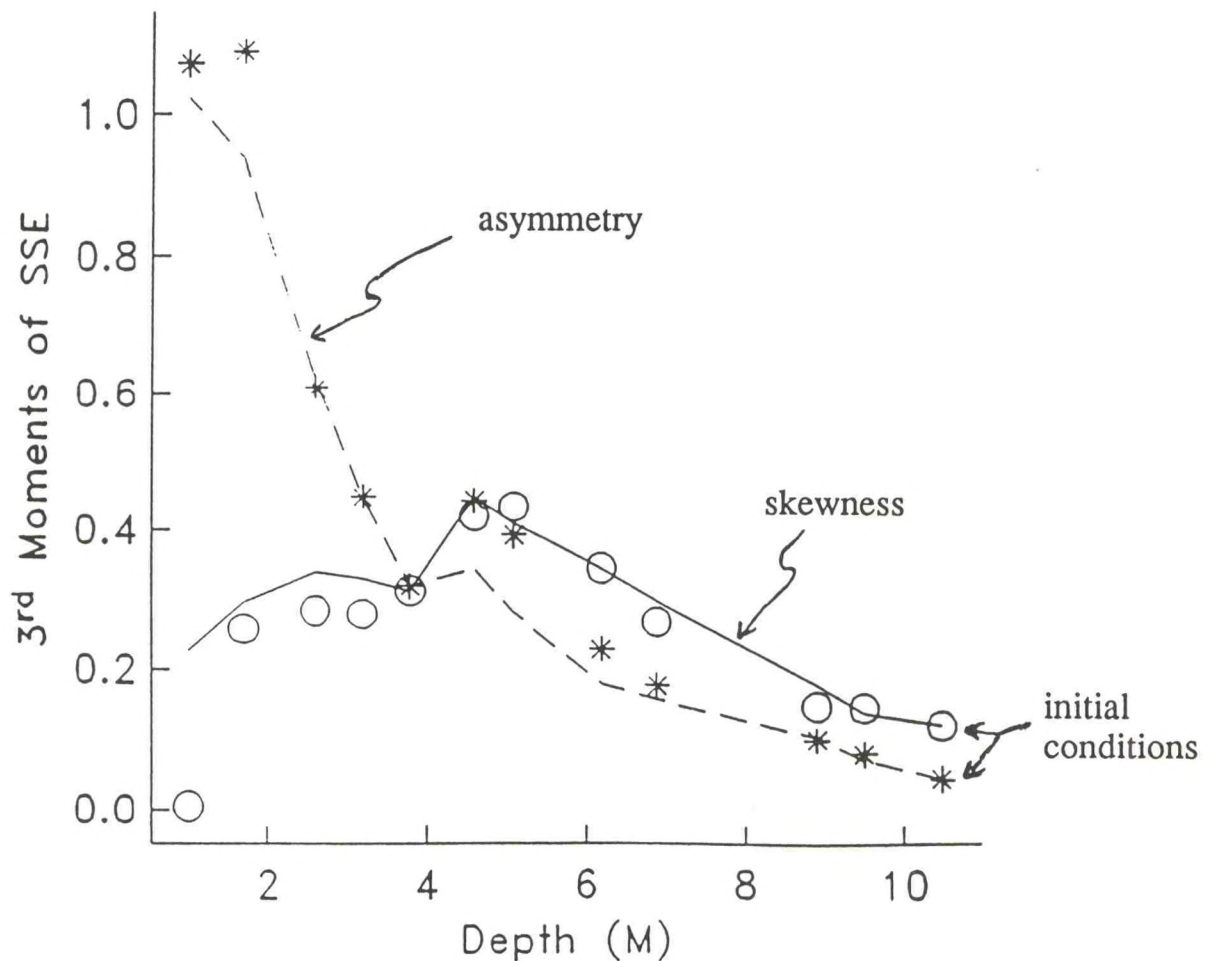


Figure 1. Momentum budget for the nearshore as a function of cross-shore location and frequency. Energy enters the system from offshore at intermediate frequencies, and is redistributed to both higher and lower frequencies by processes of shoaling and breaking.



## 2-D Nonlinear Transformation

data (symbols) vs model (lines)



Elgar, Freilich and Guza

Figure 2. Model/data comparison for the nonlinear evolution of incident wave through the shoaling region. The two components of the third moment of the sea surface elevation time series reflect the nonlinear generation of phase-locked harmonics.

# Edge Waves and Shear Waves

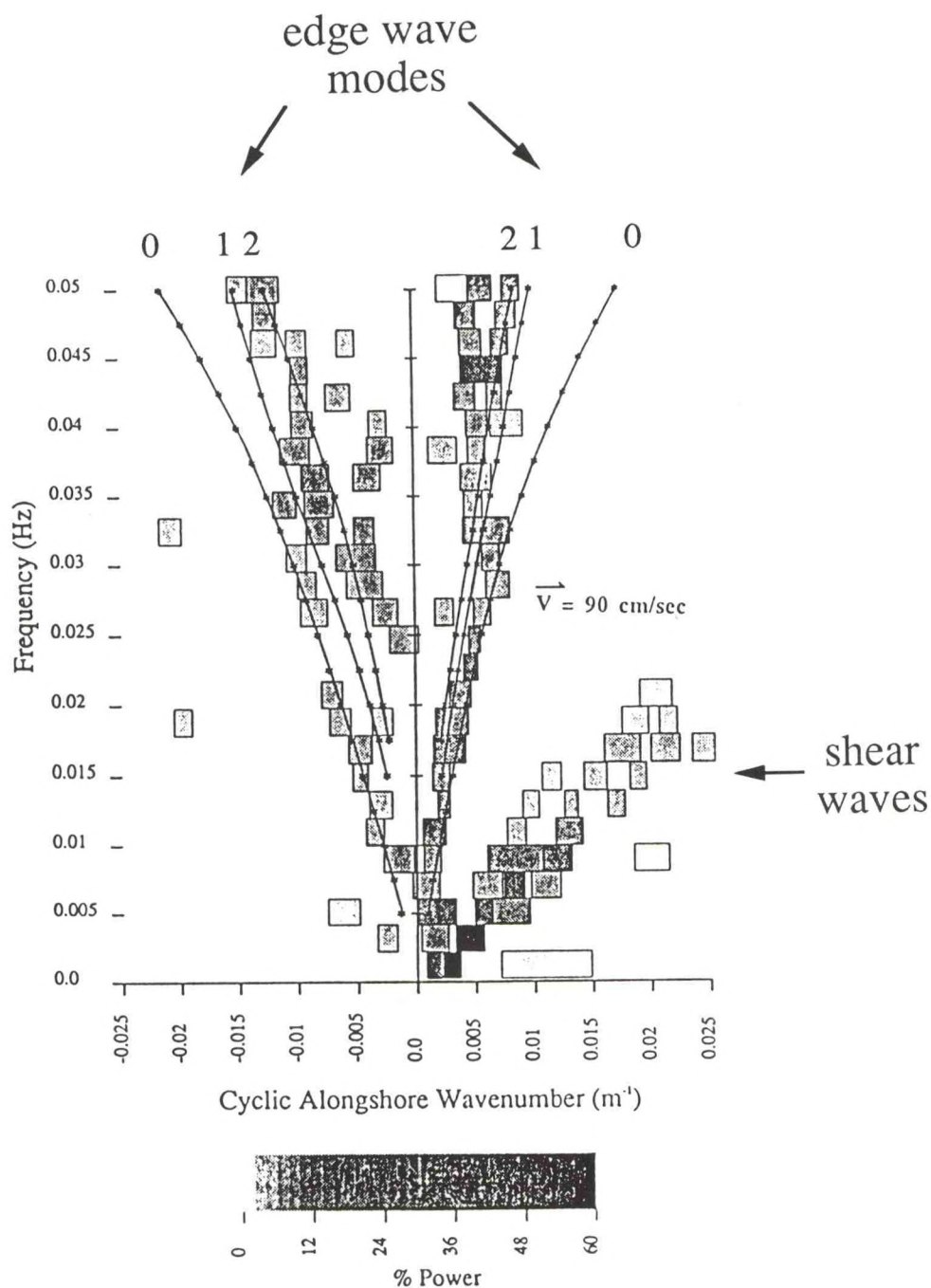


Figure 3. Frequency-wavenumber spectrum of longshore current data from the SUPERDUCK experiment (only sub-incident frequencies are shown). Energy clearly falls along theoretically calculated dispersion lines for low mode edge waves (solid lines). The ridge of energy to the right represents shear waves.



## STRATAGEMS FOR COASTAL SEAS

David A. Brooks  
Texas A & M University  
Department of Oceanography  
College Station, TX 77843

My comments specifically are based on experience over the last decade in the Gulf of Maine - Georges Bank area, but they may apply in general terms to coastal seas in other locations. By 'coastal sea', I mean a semi-enclosed embayment whose water properties and circulation are affected by some combination of "coastal" and "offshore" water types. Other examples are the Georgia Bight and Shelikof Strait in the Gulf of Alaska. In coastal seas, the coastal waters usually are relatively fresh and buoyant, and they contrast with saltier, denser water from offshore near the shelf break. At mid and high latitudes, the coastal water, in spite of its buoyancy, may be much colder than the offshore water, which remains more dense by virtue of much higher salinity than the coastal water. Often such a combination provides a competition of sorts in which the resulting circulation is estuarine-like, but with strong influences imposed by bottom topography and the earth's rotation. In such seas, strong currents in narrow frontal zones are often associated with the contrast between water types, and interactions with the atmosphere through buoyancy modifications or wind stresses are usually intense. In some shelf and coastal seas, tidal resonances produce large tidal currents, which keep the waters vertically well mixed over relatively shallow areas. In short, most of the major physical processes operative in the ocean basins are also found in coastal seas, where they interact in close proximity and usually with great complexity. As a result, the demands on field sampling and numerical modeling are severe (and in fact often not met, or appreciated only *post facto*).

The Gulf of Maine is an extreme example of a coastal sea because it is nearly cut off from the Atlantic by the shoal Georges Bank, which isolates and insulates the waters of the Gulf. The principal access path of offshore water is through the Northeast Channel, which has a sill depth of about 380 m. Tidal currents exceed 1 m/s over the Bank and in the adjacent Bay of Fundy due to a near-perfect M-2 resonance. The frontal contrasts mentioned earlier are sharp, especially around the periphery of the Bank, with strong seasonal modulation due to buoyancy extraction and effective topographic control over basins and sills. Yet the Gulf is large enough that an approximate geostrophic balance often obtains for the non-tidal circulation over the basins, away from the regions of strongest tidal mixing. These statements are based on a historical hydrographic data set extending back to Bigelow's pioneering work early in the century. A greater level of detail, and hence improved understanding, has emerged in the last decade because better and higher-resolution hydrographic data sets have been collected. Moored current meter measurements are still quite sparse in the Gulf and have been mostly confined to the edges of basins or over sills in summer months. A relatively large current and drifter data set was collected from the edges of Georges Bank in the late 70s in association with the trial drilling operations conducted then.



The Gulf Stream affects coastal seas along the eastern U.S., directly and profoundly south of Cape Hatteras, and indirectly by means of meanders and detached rings to the north. In the Gulf of Maine, for example, the offshore water properties depend on the extent to which rings interfere with or penetrate or rupture the so-called shelf-slope front, which tends to separate fresher water with northern, nearshore character from the warmer, saltier water of the Sargasso. When rings carrying Gulf Stream water approach the mouth of the Northeast Channel at times when inflow is favored, the contrast mentioned earlier is enhanced, compared to times when the shelf-slope front is intact and the inflow is cooler and fresher under the influence of Labrador Sea and Laurentian water types. The ring influence may be regarded as an imperfect "switch" that selects between inflowing water types, and similar switching mechanisms may be effective in other coastal seas. The effect is important, because the circulation and frontal characteristics that evolve inside the affected coastal sea may be very different depending on the state of the "switch." It is hypothesized that this mechanism, along with climatic variations, is largely responsible for the interannual differences seen in the interior circulation of the Gulf of Maine; of course, other processes (biological, chemical) that depend on the circulation are similarly affected. Thus, it seems that a prime goal of improved field experiments and numerical modeling aimed at coastal seas should be to better understand how this seasonally modulated interaction works, and how the interior circulation of coastal seas may be controlled by such processes. There may be a very delicate balance involved, where the character of the interior circulation is dramatically different depending on whether or not the "switch" is activated and when. In fact, some of the ideas of limit cycles and chaos theory may be relevant to the modeling philosophy, in the sense that only relatively small changes in the forcing conditions may produce fundamentally different results.

It will be a daunting task indeed to properly model coastal seas, because in addition to the forcing by winds and tides, one must allow for a complex interaction with the offshore ocean. Benign boundary conditions, in which a constant flux or sea level slope are specified, are unsatisfying and probably unrealistic *a priori*. There will have to be some degree of feedback between the coastal sea and the offshore ocean; i.e., it should be possible for the circulation inside the sea to develop in such a way as to augment or inhibit its interaction with the open ocean. In addition, because of the intense water mass contrasts, the resolution of data stations and numerical grid points must be very high in some areas; the internal Rossby radius characterizing the fronts and jet-like currents near Georges Bank, for example, may be only 10 km or even less. In addition, many levels in the vertical must be sampled or modeled to view the circulation realistically in areas of complex bottom topography, particularly those in which the controlling factors are sills, canyons or basins. Furthermore, careful consideration must be given to include buoyancy advection and modification due to interaction with the atmosphere; for example, in the Gulf of Maine, winter cooling typically obliterates contrasts in the upper two-thirds of the water column, whereas springtime and early summer warming reestablishes a thin upper level stratification, leading to a complex three-level circulation pattern that undergoes extreme seasonal variability. These difficulties are probably typical of coastal seas, and they represent some of the greatest observational and modeling challenges in modern ocean sciences. It is a common



misperception to suppose that, because of their relatively small size, coastal seas are uninteresting or well-understood compared to the major ocean basins; this is an erroneous view, as recent data sets have made amply clear.

# COASTAL OCEAN PREDICTION: POSSIBILITIES AND LIMITATIONS

Gabriel T. Csanady  
Old Dominion University  
Norfolk, VA 23529-0276

## Introduction

In the documents outlining the objectives of the present workshop on "Coastal Ocean Prediction Systems," there is more than a glimmer of an idea that these systems would be analogous to the weather forecasting machinery of the government. Within a decade or two one would be able to tune in to the Weather Channel and hear something like the following:

Currents over Georges Bank will be strong due to spring tides. Elsewhere in the Gulf of Maine the flow will be quiescent. There is, however, a 40% chance of internal wave activity.

Of course one never knows; the government spends money on things sillier than this. Yet, hope springs eternal in the human breast, in this instance the hope that the issues of cost and reliability may yet sink the more preposterous ideas. With this in mind, I would like to discuss a few different levels of coastal ocean prediction, estimate our present capacity for making predictions at each level, and give a subjective judgement of their benefit-to-cost ratio.

## Predict Underwater "Weather"

Conditioned by numerical models, many at this workshop probably envisage coastal ocean prediction as calculating current velocity, temperature, salinity, etc., from the hydrodynamic equations, at a large number of grid points covering the entire U.S. coastal ocean, with daily updates of the forecasts, using input from a vast observational network. There are even some who defend such an idea as feasible or useful. Non-fanatics, however, should readily agree with the following propositions:

Our present ability to predict oceanic variables on a daily basis, at a multitude of locations, with any kind of accuracy, is very poor. Neither analytical nor numerical models can yet cope with such problems as strongly sloping isopycnal surfaces, gross topographic irregularity, or the interplay of stratification and turbulence. Shelf-edge boundary conditions remain a puzzle. It is difficult to think of users apart from intelligent dolphins, deriving significant advantages from weather-like forecasts. It is sometimes said that the fishing industry requires information of this kind, but the case has never been convincingly made. In any case, the benefits to the fishing industry, if any, are certainly dwarfed by the costs of establishing and maintaining a "wet weather" bureau.



## Predict Fate of Release

The idea of day-to-day forecasting, whether it is needed or not, may be unappealing, but there are certainly some very important practical problems in which reliable forecasts are (or would be, if we could make them) of great benefit. One class of such problems relates to the fate of some material released into the ocean. Examples are the design of ocean disposal systems, simulation of oil spill trajectories, and the guidance of search and rescue efforts. In all such cases one requires estimates of a released particle's displacement as a function of time, and in many cases also the relative displacement of particles in a group. Forecasts may be required of displacements in a specific event or in an assembly of many events (statistical forecasts).

What is our present capacity to make reliable deterministic forecasts of particle (say, oil spill) displacements in a specific event? Some of the difficulties of solving the hydrodynamic equations have already been mentioned. Even if we had a perfect hydrodynamic model, initial conditions for a given event would have to be specified, requiring the deployment of a vast array of instruments, in a very short time. This being impractical, we are, and probably always will be, reduced to relying on statistical evidence on particle displacements, and making "persistence" forecasts modified in the light of the statistics.

How do we stand on the probabilistic forecasts? The intellectual framework has been there for some time, and is routinely used by air pollution meteorologists as well as engineers designing ocean outfalls. The modeling community in oceanography has not so far made serious efforts to develop statistical models. Many believe (and have argued at this workshop) that by throwing computer power at the problem, hydrodynamic models will be able to generate realistic statistics of displacements, velocities or whatever. Prediction of Lagrangian quantities places unusually stringent accuracy requirements on deterministic models, however: oceanic flow fields being very inhomogeneous, an accurate fix on a particle's position is required, in addition to a good description of the velocity field, a kind of double jeopardy. The analogous problem in the time dimension is that oceanic motions occur at incommensurable frequencies and unrelated phases. As a research tool, a hydrodynamic model is illuminating if it correctly simulates a few scales of motion of interest. To mirror Lagrangian displacements, a model must not only resolve all important scales of motion, but must also correctly portray the interrelationships among them. It is simply utopian to believe that such stringent requirements can be met by hydrodynamic ocean models in the foreseeable future, probably ever.

The alternative is to develop semi-empirical statistical models which predict mean Lagrangian quantities, probability distributions, or even just such crude measures as the size of a diffusing "cloud" (for a single particle, the likely area where it can be found). Such models require considerable empirical input on mean and mean square velocities and bulk exchange parameters (e.g., eddy diffusivities) as a function of a few input data characterizing location, weather, etc. The trouble with this prescription is that while we can import the theoretical framework from



meteorology, the empirical base is lacking. We do not have maps of "eddy energy" for the continental shelves, similar to what Klaus Wyrtki and his collaborators (Wyrtki, et al., 1976) have produced for the deep ocean. Even if we did, they would not be fully useful, because the relationship of the Eulerian mean square velocities to Lagrangian ones is terra incognita. More detailed evidence, even of the Eulerian kind--e.g., current roses (similar to windroses) for inner, mid, and outer shelves, in different geographical regions--is completely nonexistent. About the only thing we are aware of is some kind of "mean circulation" picture on some of the better explored shelves, together with crude estimates of such mixing parameters as an effective horizontal eddy diffusivity, and a shelf edge exchange coefficient. I have recently summarized such evidence for the U.S. east coast shelf, (for Volume 9 of *The Sea*), and a reviewer rightly criticized me for offering quantitative estimates of key mixing parameters on such a flimsy observational basis as exists.

While much remains to be learned about the behavior of the coastal ocean, the accumulation of evidence on Lagrangian properties is probably the most urgent practical need. Much could be done by just processing existing data: e.g., displacements simulated from a current meter record, although clearly not Lagrangian, at least give some idea of the likely directional distribution of particle displacements. On a more difficult level, the Euler-Lagrange relationship in the unique flow environment of the coastal ocean is a problem worthy of serious and exhaustive theoretical study.

To build a satisfactory empirical base for statistical forecasting, it will be necessary to extend research efforts to all U.S. continental shelves, and improve data bases at least to the level that now exists for the East Coast shelf. Intelligent application of the data requires also that we improve our insight into the physics of coastal currents. Some problems badly in need of attention are:

- The physical processes underlying seasonal stratification and destratification (mixed layer formation) on continental shelves.  
We have some solid fundamental ideas on how stratified layers form in the first place and how they may be destroyed, but these have not been satisfactorily related to conditions prevailing in coastal waters. Recent successes in understanding tidal fronts demonstrate how the fundamental ideas can lead to practically useful predictions.
- Interaction with offshore currents.  
One of the most interesting results of research on the East Coast shelf is the coherence of the mean circulation over very long alongshore distances--from Newfoundland to Cape Hatteras, for example. The flow abruptly leaves the shelf at Cape Hatteras, being entrained by the Gulf Stream. We don't know where it crosses onto the shelf from the deep ocean. Yet this "flushing" of the shelf by offshore currents is the most important element in the material balance of the shelf: it is easily shown that some 90% of a conservative substance released into the Hudson



River stays on the shelf until whisked off by the Gulf Stream. Similar large-scale circulation cells exist on other shelves, but have barely been identified on a few, and their precise effects have not been explored.

- Density driving.

Alongshore gradients of density are potent drivers of shelf circulation, and it has so far proved frustratingly difficult to model their effects. River plumes are to some extent understood, although not their long-distance effects. Localized heating or cooling can have dramatic consequences, as winter studies on the Southeast Coast shelf have illustrated. The dynamical problem is flow associated with inclined isopycnal surfaces intersecting an inclined seafloor. This problem must be solved before we can even speculate on the effect of such a constellation on Lagrangian properties of the flow.

A final note in this section on fluid particle displacements is to emphasize again that even when we understand the dynamics of a phenomenon in the Eulerian framework reasonably well, our difficulties are not over. Take the much studied case of wind-induced coastal upwelling, alternating with downwelling along the East Coast on the weather cycle time scale, along the West Coast seasonally. It is well known that upwelling brings nutrients (and pollutants from an ocean outfall) to the surface nearshore. For particle displacements the details are what matter most: precisely from where to where and how much material is brought up. Although some details of frontal motions have been documented, they are certainly not understood or predicted by analytical or numerical models. We can only guess at present how coastal upwelling affects the distribution of effluents discharged from a submarine outfall.

### **Predict Most Damaging Event**

One class of problems in which Eulerian hydrodynamic models have clearly proved useful is the portrayal of extreme events. Examples are the forecasting of storm surge in hurricanes, of maximum wave height to be resisted by an offshore structure, of peak current speed in a "100-year storm." The success of the models is mainly due to simplification of the dynamics, permissible because the forcing dominates. Storm surge prediction has been fairly reliable for some time, and the latest generation of hurricane models (e.g., those recently described by Cooper and Thompson, 1989a,b) also simulates hurricane currents well enough to be useful in the design of offshore structures. While there is room for improvement, e.g., in the prediction of non-extreme currents likely to affect a deepwater port to be constructed, our ability for coastal ocean prediction in this category is fair-to-good, and the benefit-to-cost ratio of further improvement is indisputably high.

## Conclusions

Eulerian hydrodynamic models of the coastal ocean are, (a) excellent research tools, (b) indispensable aids in decision-making relating to the design and licensing of offshore structures, flood plain zoning and similar problems. They require further development, the costs of which are trivial in comparison with the likely benefits from more reliable prediction. Model development has to go hand-in-hand with improved understanding of the underlying physical phenomena, physical insight and model improvement mutually reinforcing each other.

The preceding paragraph notwithstanding, the greatest present needs are for systematic observations of Lagrangian flow properties in the coastal ocean and for intellectual development of models portraying dispersal processes. Work in this area should proceed independently of the development of hydrodynamic models. In particular, simulation of Lagrangian properties of the flow by Eulerian hydrodynamic models should not be substituted for work on the Lagrangian problem. There is not a shred of evidence supporting the notion that such simulations would yield practically useful results, and there is every reason to doubt it. Experience with air pollution models suggests that the modeling of dispersal has to be completely decoupled from the modeling of the dynamics of the flow.

Finally, let me reiterate my principal thesis: coastal ocean prediction systems have to be tailored to financially justifiable needs. The tone of this workshop has generally been: here we have some wonderful solutions (hydrodynamic ocean models), so let us find problems to which they can be applied. A bit like wanting to play with your railroad in the basement. There is nothing really wrong with this, science is like playing with pebbles on the seashore, as Isaac Newton remarked in one of his writings. It is quite another thing trying to sell the proposition to the public that a wet weather bureau-like organization is an important national need. If we ask for public support for the application of our science, as distinct from its development, then we have to demonstrate a favorable benefit-to-cost ratio of the application. What we absolutely must not do is to make phony claims of benefits, based on unrealistic estimates of model accuracy.



## MASTER REFERENCE LIST

- Aagaard, K., A. Roach, and J. D. Schumacher, On the wind-driven variability of the flow through Bering Strait, *J. Geophys. Res.*, 90(C4), 7213-7221, 1985.
- Abbott, M. R., and P. M. Zion, Satellite observations of phytoplankton variability during an upwelling event, *Cont. Shelf Res.*, 4, 661-680, 1985.
- Allen, J. S., Continental shelf waves and alongshore variations in bottom topography and coastline, *J. Phys. Oceanogr.*, 6, 864-878, 1976.
- Amstutz, D. E., and W. B. Samuels, Offshore oil spills: Analysis of risks, *Mar. Environ. Res.*, 13, 303-319, 1984.
- Arakawa, A., and M. J. Suarez, Vertical differencing of the primitive equations in sigma coordinates, *Mon. Weather Rev.*, 111, 34-45, 1983.
- ASA Consulting, Ltd., Halifax study inlet water quality, Phase 2, Report to Metropolitan Area Planning Commission, Halifax, N.S., Canada, 1986.
- Aubrey, D. G., and P. E. Speer, A study of nonlinear tidal propagation in shallow inlet/estuarine systems, Part I: Observations, *Estuarine Coastal Shelf Sci.*, 21, 185-205, 1985.
- Baines, P. G., Tidal motion in submarine canyons--a laboratory experiment, *J. Phys. Oceanogr.*, 13, 310-328, 1983.
- Bakun, A., Coastal upwelling indices, west coast of North America, 1946-71, *Tech. Rep. NMFS SSRF-671*, 103 pp., Natl. Ocean. and Atmos. Admin., Seattle, Wash., 1973.
- Bakun, A., Global climate change and intensification of coastal upwelling systems, submitted to *Science*, 1989.
- Bane, J. M., and K. E. Osgood, Wintertime air-sea interaction processes across the Gulf Stream, *J. Atmos. Res.*, 94(C8), 10,755-10,772, 1989.
- Barrick, D. E., First-order theory and analysis of MF/HF/VHR scatter from the sea, *IEEE Trans. Antennas Propag.*, AP-20, 2-10, 1972.
- Barrick, D. E., The role of the gravity-wave dispersion relation when interpreting HF radar measurements, *IEEE J. Oceanic Eng.*, OE-11, 286-292, 1986.
- Barrick, D. E., M. W. Evans, and B. L. Weber, Ocean surface currents mapped by radar, *Science*, 198, 138-144, 1977.

Barrick, D. E., B. J. Lipa, and R. D. Crissman, Mapping surface currents with CODAR, *Sea Technol.*, 26, 43-48, 1985.

Bartz, R., R. Zaneveld, and H. Pak, A transmissometer for profiling and moored observations in water, *SPIE, 160 Ocean Optics V*, 102-108, 1978.

Batteen, M. L., R. L. Haney, T. A. Tielking, and P. G. Renaud, A numerical study of wind forcing of eddies and jets in the California Current system, *J. Mar. Res.*, 47, 493-523, 1989.

Beardsley, R. C., C. A. Alessi, and R. Limeburner, Coastal and moored meteorological observations in CODE-2: Moored array and large-scale data report, *WHOI Tech. Rpt. No. 85-35*, edited by R. Limeburner, pp. 23-72, Woods Hole Oceanographic Institution, Woods Hole, Massachusetts, 1985.

Blumberg, A. F., and H. J. Herring, Circulation modeling using curvilinear coordinates, *Dynalysis of Princeton Rpt. No. 81*, 62 pp., 1984.

Blumberg, A. F., and L. H. Kantha, A numerical model of the shelf circulation in the Middle Atlantic Bight driven by tides, transient storms and the offshore, large-scale circulation: Formulation of proper open boundary conditions, *Dynalysis of Princeton Rpt. No. 73*, 186 pp., 1982.

Blumberg, A. F., and G. L. Mellor, A whole basin model of the Gulf of Mexico, *Proceedings of the 6th Annual Conference on OTEC*, Department of Energy, Washington, D.C., 1979.

Blumberg, A. F., and G. L. Mellor, A coastal ocean numerical model, in *Math. Model. Estuar. Phys., Proceedings of an International Symposium*, Hamburg, August 24-26, 1978, edited by J. Sundermann and K. P. Holz, Springer-Verlag, Berlin, 1980.

Blumberg, A. F., and G. L. Mellor, A simulation of the circulation in the Gulf of Mexico, *Israel J. Earth Sci.*, 34, 122-144, 1985.

Blumberg, A. F., and G. L. Mellor, A description of a three-dimensional coastal ocean circulation model, in *Three-Dimensional Coastal Ocean Models, Coastal and Estuarine Sciences 4*, edited by N. S. Heaps, pp. 1-16, American Geophysical Union, Washington, D.C., 1987.

Blumberg, A. F., L. H. Kantha, H. J. Herring, and G. L. Mellor, California shelf physical oceanography circulation model--final report, *Dynalysis of Princeton Rpt. No. 88*, 368 pp., 1984.

Bowen, A. J., and R. A. Holman, Shear instabilities of the mean longshore current, 1: Theory, *J. Geophys. Res.*, in press, 1990.



Brink, K., Coastal Physical Oceanography, Towards a National Plan, Report of a Meeting of the Coastal Physical Oceanography Community, Jan. 23-26, Gulf Park, Mississippi, 118 pp., 1989.

Brink, K. H., D. C. Chapman, and G. R. Halliwell, Jr., A stochastic model for wind-driven currents over the continental shelf, *J. Geophys. Res.*, 92, 1783-1797, 1987.

Brooks, D. A., Transhorizon VHF telemetry from ocean moorings, *J. Atmos. Oceanic Technol.*, 1(2), 176-189, 1984.

Brown, O. B., R. H. Evans, J. W. Brown, H. R. Gordon, R. C. Smith, and K. S. Baker, Phytoplankton blooming off the U.S. east coast: A satellite description, *Science*, 229, 163-67, 1985.

Brown, W. S., and J. D. Irish, The annual evolution of water masses in the Gulf of Maine: 1986-87, unpublished manuscript, 1990a.

Brown, W. S., and J. D. Irish, The annual evolution of geostrophic flows in the Gulf of Maine: 1986-87, unpublished manuscript, 1990b.

Browne, D. R., and G. Dingle, New York Harbor circulation survey: 1980-1981, *NOS Oceanographic Circulation Survey Rpt. No. 5*, U.S. Department of Commerce, NOAA/NOS, 92 pp., 1983.

Butman, B., and D. W. Folger, An instrument system for long term sediment studies on the continental shelf, *J. Geophys. Res.*, 84, 1215-1220, 1979.

Cacchione, D. A., and D. E. Drake, A new instrumentation system to investigate the sediment dynamics on continental shelves, *Mar. Geol.*, 30, 299-312, 1979.

Calman, J., Introduction to sea-surface topography from satellite altimetry, *The Johns Hopkins APL Technical Digest*, 8, 206-211, 1987.

Cannon, G. A., Wind effects on currents observed in Juan de Fuca submarine canyon, *J. Phys. Oceanogr.*, 2, 281-285, 1972.

Cannon, G. A. and G. Lagerloef, Topographic influence on coastal circulation: A review, in *Coastal Oceanography*, edited by H. Gade, A. Edwards, and H. Svendsen, pp. 235-252, Plenum, New York, 1983.

Carter, E. F., and A. R. Robinson, Analysis models for the estimation of oceanic fields, *J. Atmos. Oceanic Technol.*, 4(1), 49-74, 1987.

Chapman, D. C., Numerical treatment of cross-shelf open boundaries in a barotropic coastal ocean model, *J. Phys. Oceanogr.*, 5, 1060-1075, 1985.

- Chapman, D. C., A simple model of the formation and maintenance of the shelf/slope front in the Middle Atlantic Bight, *J. Phys. Oceanogr.*, 16, 1273-1279, 1986.
- Chapman, D. C., Application of wind-forced, long, coastal-trapped wave theory along the California coast, *J. Geophys. Res.*, 92, 1798-1816, 1987.
- Chelton, D. B., Large-scale response of the California Current to forcing by wind stress curl, in *CalCOFI Rep.* 23, pp. 130-148, Calif. Coop. Oceanic Fish. Invest., Univ. of Calif., San Diego, La Jolla, 1982.
- Chelton, D. B., P. A. Bernal, and J. A. McGowan, Large-scale interannual physical and biological interaction in the California Current, *J. Mar. Res.*, 40, 1095-1125, 1982.
- Chen D., and D-P. Wang, Three-dimensional simulation of wind relaxation during CODE-2, in preparation.
- Chen, D., and D-P. Wang, Simulating the time-variable coastal upwelling during CODE-2, *J. Mar. Res.*, accepted for publication, 1990.
- Chen, D., S. A. Horrigan, and D-P. Wang, Vertical nutrient mixing in late summer in Long Island Sound, *J. Mar. Res.*, 46, 753-770, 1988.
- Christodoulou, G. C., and J. J. Connor, Dispersion in two-layer stratified water bodies, *J. Hydraul. Eng. Div. Am. Soc. Civ. Eng.*, 106(HY4), 557-573, 1980.
- Church, T. M., C. N. K. Mooers, and A. D. Voorhis, Exchange processes over a Middle Atlantic Bight shelfbreak canyon, *Estuarine Coastal Shelf Sci.*, 19, 393-411, 1984.
- Clarke, A. J., and A. Van Gorder, A method for estimating wind-driven, frictional, time-dependent, stratified shelf and slope water flow, *J. Phys. Oceanogr.*, 16, 1013-1028, 1986.
- Collar, P. G., D. Eccles, M. J. Howarth, and N. W. Millard, An intercomparison of HF radar observations of surface currents with moored current meter data and displacement rates of acoustically tracked drogued floats, in *Proceedings of Ocean Data Conference*, Soc. for Underwater Technology, London, 1985.
- Cooper, C. and J. D. Thompson, Hurricane-Generated Currents on the Outer Continental Shelf, 1: Model Formulation and Verification, *J. Geophys. Res.*, 94(9), 12,513-12,539, 1989a.
- Cooper, C. and J. D. Thompson, Hurricane-Generated Currents on the Outer Continental Shelf, 1: Model Sensitivity Studies, *J. Geophys. Res.*, 94(9), 12,540-12,554, 1989b.



- Cox, M. D., An eddy-resolving numerical model of the ventilated thermocline, *J. Phys. Oceanogr.*, 15, 1312-1324, 1985.
- Csanady, G. T., "Pycnobathic" currents over the upper continental slope, *J. Phys. Oceanogr.*, 15, 306-315, 1985.
- Csanady, G. T., Ocean currents over the continental slope, *Adv. Geophys.*, 30, 95-203, 1988.
- CTZ Group, The coastal transition zone program, *EOS Trans. AGU*, 69, 698-699, 704, 707, 1988.
- Cushman-Roisin, B., and J. J. O'Brien, The influence of bottom topography on baroclinic transports, *J. Phys. Oceanogr.*, 13, 1600-1611, 1983.
- Davies, A. M., A three-dimensional model of the northwest European continental shelf with application to the M<sub>4</sub> tide, *J. Phys. Oceanogr.*, 16, 797-813, 1986.
- Davies, A. M., and G. K. Furnes, Observed and computed M<sub>2</sub> tidal currents in the North Sea, *J. Phys. Oceanogr.*, 10, 237-257, 1980.
- Davis, R. E., Drifter observations of coastal surface currents during CODE: The method and descriptive view, *J. Geophys. Res.*, 90(C3), 4741-4755, 1985.
- Dean, J. P., and R. C. Beardsley, A vector-averaging wind recorder (VAWR) system for surface meteorological measurements in CODE (Coastal Ocean Dynamics Experiment), *Woods Hole Oceanographic Institution Tech. Rept. No. WHOI-88-20, CODE Tech. Rept. No. 44*, 74 pp., 1988.
- DeMargerie, S., and D. DeWolfe, Development of hydrodynamic model for Cumberland Basin for tidal power applications, Report prepared for Department of Energy, Mines and Resources, Ottawa, Canada, 1987.
- Denbo, D. W., and J. S. Allen, Large-scale response to atmospheric forcing of shelf currents and coastal sea level off the west coast of North America: May-July 1981 and 1982, *J. Geophys. Res.*, 92, 1757-1782, 1987.
- Denman, K. L., and M. R. Abbott, Time evolution of surface chlorophyll patterns from cross-spectrum analysis of satellite color, *J. Geophys. Res.*, 93, 6789-6798, 1988.
- Dorman, C. E., Evidence of Kelvin waves in California's marine layer and related eddy generation, *Mon. Weather Rev.*, 113, 827-839, 1985.
- Dorman, C. E., Possible role of gravity currents in northern California's coastal summer wind reversals, *J. Geophys. Res.*, 92, 1497-1506, 1987.

Dunbar, D. S., J. S. Hardy, and D. O. Hodgins, Remote sensing of surface currents off the west coast of Vancouver Island using CODAR, in *IGARSS '89 Conference Rec.*, Vancouver, 1989.

Eide, L. I., Evidence of a topographically trapped vortex on the Norwegian continental shelf, *Deep-Sea Res.*, 26, 601-621, 1979.

Elgar, S., and R. T. Guza, Nonlinear model predictions of bispectra of shoaling surface gravity waves, *J. Fluid Mech.*, 167, 1-18, 1986.

EnviroSphere Company, Summary Report, Workshop on Coastal Circulation Along Washington and Oregon, February 8-9, 1988, Seattle, Washington, MMS Contract No. 14-12-0001-30389, 164 pp., 1988.

Essen, H.-H., K.-W. Gurgel, and F. Schirmer, Tidal and wind-driven parts of the surface currents as measured by radar, *Dtsch. Hydrogr. Z.*, 36, 81-96, 1983.

Essen, H.-H., K.-W. Gurgel, and F. Schirmer, Surface currents in the Norwegian Channel measured by radar in March 1985, *Tellus*, 41A, 162-174, 1989.

Evans, R. E., K. S. Baker, R. C. Smith, and O. B. Brown, Chronology and event classification of Gulf Stream Warm-Core Ring 82B, *J. Geophys. Res.*, 90, 8803-11, 1985.

Falkowski, P., and D. A. Kiefer, Chlorophyll-a fluorescence in phytoplankton: Relationship to photosynthesis and biomass, *J. Plankton Res.*, 7, 715-731, 1985.

Falkowski, P. G., K. Wyman, A. C. Ley, and D. Mauzerall, Relationship of steady-state photosynthesis to fluorescence in eucaryotic algae, *Biochim. Biophys. Acta*, 849, 183-192, 1986.

Falkowski, P. G., C. N. Flagg, G. T. Rowe, S. L. Smith, T. E. Whitledge, and C. D. Wirick, The fate of a spring phytoplankton bloom: Export or oxidation?, *Cont. Shelf Res.*, 8, 457-484, 1988.

Feng, S., M. Reed, and D. P. French, The chemical database for the natural resource damage assessment model system, *Oil and Chemical Pollution*, 5(237), 165-194, 1989.

Flagg, C. N., and S. L. Smith, On the use of the acoustic Doppler current profiler to measure zooplankton abundance, *Deep-Sea Res.*, 36, 455-474, 1989.

Flather, R. A., A tidal model of the northwest European continental shelf, *Mem. Soc. R. Sci. Liege*, 9, 141-164, 1976.

Flemming, B. W., Factors controlling shelf sediment dispersal along the southeast African continental margin, *Mar. Geol.*, 42, 259-277, 1981.



Foreman, M. G. G., An analysis of the "Wave Equation" model for finite element tidal computations, *J. Comput. Phys.*, 52, 290-312, 1983.

Foreman, M. G. G., Two finite element tidal models for the southwest coast of Vancouver Island, submitted to *Tidal Hydrodynamics*, B. Parker, editor, 1989.

Freeland, H. J., and K. L. Denman, A topographically controlled upwelling centre off southern Vancouver Island, *J. Mar. Res.*, 40(4), 1069-1092, 1982.

Freilich, M. H., and R. T. Guza, Nonlinear effects on shoaling surface gravity waves, *Philos. Trans. R. Soc. London, Ser. A311*, 1-41, 1984.

French, D. P., and F. W. French, III, The biological effects component of the natural resource damage assessment model system, *Oil and Chemical Pollution*, 5(273), 125-164, 1989.

Fukushima, Y., G. Parker, and H. M. Pantin, Prediction of ignitive turbidity currents in Scripps submarine canyon, *Mar. Geol.*, 67, 55-81, 1985.

Galperin, B., and G. L. Mellor, A time-dependent, three-dimensional model of the Delaware Bay and River system, Part I: Description of the model and tidal analysis, *Estuarine Coastal Shelf Sci.*, accepted for publication, 1990a.

Galperin, B., and G. L. Mellor, A time-dependent, three-dimensional model of the Delaware Bay and River system, Part II: Three-dimensional flow fields and residual circulation, *Estuarine Coastal Shelf Sci.*, accepted for publication, 1990b.

Garrett, C., and D. Greenberg, Predicting changes in tidal regime: The open boundary problem, *J. Phys. Oceanogr.*, 7, 171-181, 1977.

Garvine, R. (Chairperson), Buoyancy-driven exchange in the coastal ocean: A CoPO working group report, 21 pp., 1989.

Geyer, W. R., and R. Signell, Measurements and modeling of the spatial structure of nonlinear tidal flow around a headland, submitted to *Tidal Hydrodynamics*, B. Parker, editor, 1989.

Ghil, M., and P. Malanotte-Rizzoli, Data assimilation in meteorology and oceanography, submitted for publication, 1989.

Gilhousen, D. B., A field evaluation of NDBC moored buoy winds, *J. Atmos. Oceanic Technol.*, 4, 94-104, 1987.

Gilhousen, D. B., Quality control of meteorological data from automated marine stations, preprint, *Fourth International Conference on Interactive Information and Processing Systems for Meteorology, Oceanography and Hydrology*, Jan. 31-Feb. 5, 1988, Anaheim, Calif., American Meteorological Society, Boston, Mass., 1988.

Gordon, R. B., A numerical model of wind driven circulation in Narragansett Bay, Ph.D. dissertation, Dept. of Ocean Engineering, Univ. of Rhode Island, Kingston, 161 pp., 1982.

Gordon, R. B., and M. L. Spaulding, Numerical simulations of the tidal- and wind-driven circulation in Narragansett Bay, *Estuarine Coastal Shelf Sci.*, 15, 611-636, 1987.

Gordon, R. L., Internal modes in a submarine canyon, *J. Geophys. Res.*, 87, 582-584, 1982.

Gray, W. G., A finite element study of tidal flow data for the North Sea and English Channel, *Adv. Water Resour.*, in press, 1989.

Gray, W. G., and D. R. Lynch, Alternative time stepping schemes for finite element tidal computations, *Adv. Water Resour.* 1(2), 83ff, 1977.

Gray, W. G., J. Drolet, and I. P. E. Kinnmark, A simulation of tidal flow in the southern part of the North Sea and the English Channel, *Adv. Water Resour.*, 10, 131-137, 1987.

Greenberg, D., A numerical model investigation of tidal phenomena in the Bay of Fundy and in the Gulf of Maine, *Mar. Geod.*, 2, 161-187, 1979.

Greenberg, D., Modeling the mean barotropic circulation in the Bay of Fundy and Gulf of Maine, *J. Phys. Oceanogr.*, 13, 886-904, 1983.

Griffin, D. A., and J. H. Middleton, Coastal trapped waves behind a large continental shelf island, southern Great Barrier Reef, *J. Phys. Oceanogr.*, 16, 1651-1664, 1986.

Griffiths, C. R., D. A. Booth, D. Eccles, and F. D. G. Bennett, Comparison of near-surface currents measured by acoustic and electromagnetic current meters with HF radar measurements, Proc. Intl. Council Explor. Seas, London, 1985.

Grigalunas, T., J. J. Opaluch, and T. J. Tyrrell, The economic damages component of the natural resource damage assessment model system, *Oil and Chemical Pollution*, 5(273), 195-216, 1989a.

Grigalunas, T., J. J. Opaluch, D. P. French, and M. Reed, Perspective on validating the natural resource damage assessment model system, *Oil and Chemical Pollution*, 5(273), 217-238, 1989b.

Grimshaw, R. H. J., P. G. Baines, and R. C. Bell, The reflection and diffraction of internal waves from the junction of a slit and a half-space, with application to submarine canyons, in *Dynam. Atmos. Oceans*, 9, 85-120, 1985.



Gurgel, K.-W., H.-H. Essen, and F. Schrimmer, CODAR in Germany--a status report, *IEEE J. Oceanic Eng.*, OE-11, 251-257, 1986.

Haidvogel, D. B., and K. H. Brink, Mean currents driven by topographic drag over the continental shelf and slope, *J. Phys. Oceanogr.*, 16, 2159-2171, 1986.

Haidvogel, D. B., and A. R. Robinson, editors, *Dynam. of Atmos. Oceans*, 13, Special issue on data assimilation, 1989.

Haidvogel, D. B., J. Wilkin, and R. Young, A semi-spectral primitive equation ocean circulation model using vertical sigma and horizontal orthogonal curvilinear coordinates, submitted to *J. Comp. Phys.*, accepted for publication, 1990.

Halliwell, G. R., and J. S. Allen, The large-scale coastal wind field along the west coast of North America, *J. Geophys. Res.*, 92, 1861-1884, 1987.

Hamilton, G. D., Small coastal data buoys, Preprint, *Fourth International Conference on Interactive Information and Processing Systems for Meteorology, Oceanography and Hydrology*, Jan. 31-Feb. 5, 1988, Anaheim, Calif., American Meteorological Society, Boston, Mass., 1988.

Hamilton, G. D., National Data Buoy Center real-time environmental data, this publication, 1990.

Hammond, T. M., C. B. Pattiaratchi, D. Eccles, M. J. Osborne, L. A. Nash, and M.B. Collins, Ocean Surface Current Radar (OSCR) vector measurements on the inner continental shelf, *Cont. Shelf Res.*, 7, 411-431, 1987.

Haney, R. L., Mid-latitude sea surface temperature anomalies: A numerical hindcast, *J. Phys. Oceanogr.*, 15, 787-799, 1985.

Haney, R. L., On the pressure gradient force over steep topography in sigma coordinate ocean models, *J. Phys. Oceanogr.*, accepted for publication, 1990.

Hardy, J. S., D. S. Dunbar, and D. O. Hodgins, An evaluation of methods for extracting surface currents from CODAR data, IGARSS '89 Conf. Rec., Vancouver, 1989.

Hedstrom, K. S., User's manual for a semi-spectral primitive equation regional ocean circulation model, INO Technical Note, available in draft form, 1989.

Hemsley, J. M., and R. M. Brooks, Waves for coastal design in the United States, *Jour. Coastal Res.*, 5(4), 639-663, Fall, 1989.

Hendricks, T. J., Currents in the Los Angeles area, in Southern California Coastal Water Research Project Biennial Report, pp. 243-256, 1980.

Hendricks, T. J., and H. H. Stubbs, Currents in the San Gabriel Canyon, in Southern California Coastal Water Research Project Biennial Report, pp. 143-153, 1984.

Henry, R. F., Interactive design of irregular triangular grids, in *Computational Methods in Water Resources, vol. II: Numerical Methods for Transport and Hydrologic Processes*, Proceedings of the VIIth International Conference, edited by M. A. Celia, L. A. Ferrand, C. A. Brebbia, W. G. Gray, and G. F. Pinder, pp. 445-450, MIT, Boston, Mass., June 1988.

Heteren, J. van, D. M. A. Schaap, and H. C. Peters, Rijkswaterstaats interest in HF radar, *IEEE J. Oceanic Eng., OE-11*, 235-240, 1986.

Hickey, B. M., Patterns and processes of circulation over the Washington continental shelf and slope, in *Coastal Oceanography of Washington and Oregon*, edited by M. Landry and B. Hickey, pp. 41-115, Elsevier, Amsterdam, 1989.

Hickey, B. M., A fluctuating vortex over Astoria Submarine Canyon, in preparation.

Hickey, B. M., E. Baker, and N. Kachel, Suspended particle movement in and around Quinalt Submarine Canyon, *Mar. Geol.*, 71, 35-83, 1986.

Holloway, G., Systematic forcing of large-scale geophysical flows by eddy-topography interaction, *J. Fluid. Mech.*, 184, 463-476, 1987.

Holloway, G., and B. J. West (editors), *Predictability of Fluid Motions*, American Institute of Physics, Proceedings No. 106, New York, 612 pp., 1984.

Hotchkiss, F. S., and C. Wunsch, Internal waves in Hudson Canyon with possible geological implications, *Deep-Sea Res.*, 29, 415-422, 1982.

Howell, G. L., Florida coastal data network, Conference on Coastal Engineering, Sydney, Australia, 1980.

Hsueh, Y., On the theory of deep flow in the Hudson Shelf Valley, *J. Geophys. Res.*, 85, 4913-4918, 1980.

Hunkins, K., Mean and tidal currents in Baltimore Canyon, *J. Geophys. Res.*, 93, 6917-6929, 1988.

Hussaini, M. J., and T. A. Zang, Spectral methods, *Ann. Rev. Fluid Mech.*, 19, 339-367, 1987.

Huthnance, J. M., Slope currents and "JEBAR," *J. Phys. Oceanogr.*, 14, 795-810, 1984.



Huyer, A., and R. L. Smith, The signature of El Nino off Oregon, 1982-1983, *J. Geophys. Res.*, 90, 7133-7142, 1985.

Huyer, A., R. L. Smith, and T. Paluszkievicz, Coastal upwelling off Peru during normal and El Nino times, 1981-1984, *J. Geophys. Res.*, 92, 14297-14307, 1987.

Huyer, A., M. Knoll, T. Paluszkievicz, and R. L. Smith, The Peru Undercurrent: A study in variability, submitted to *Deep-Sea Res.*, 1989.

Inman, D. L., C. E. Nordstrom, and R. E. Flick, Currents in submarine canyons: An air-sea-land interaction, in *Ann. Rev. Fluid Mech.*, 8, 275-310, 1976.

Institute for Naval Oceanography, Archived Ocean Data Bases Workshop Report, 16-17 April, INO, NSTL, Mississippi, 1987.

Irish, J. D., and M. A. Martini, Removing ship's motion effects from CTD data, in *Proc. Oceans '89*, pp. 1615-1620, 1989.

Irish, J. D., W. S. Brown, and T. L. Howell, The use of microprocessor technology for the conditional sampling of intermittent ocean processes, *J. Atmos. Oceanic Tech.*, 1, 58-68, 1984.

Irish, J. D., J. M. Joy, R. M. Gelinis, and D. D. Ball, Quasi-real-time measurements of density in the Gulf of Maine, in *Proc. Oceans '87*, pp. 110-116, 1987.

Isaji, T., and M. L. Spaulding, A model of the tidally induced residual circulation in the Gulf of Maine and Georges Bank, *J. Phys. Oceanogr.*, 14, 1119-1128, 1984.

Isaji, T., and M. L. Spaulding, A numerical model of the M2 and K1 tide in the northwestern Gulf of Alaska, *J. Phys. Oceanogr.*, 17, 698-704, 1987.

Isaji, T., M. L. Spaulding, and J. C. Swanson, A three-dimensional hydrodynamic model of wind and tidally induced flows on Georges Bank, Appendix A in *Interpretation of the Physical Oceanography of Georges Bank*, EG&G Environmental Consultants Contract #AA851-CT1-39, 1982.

Isaji, T., M. L. Spaulding, and M. Reed, A numerical modeling characterization of the annual three-dimensional circulation in the Georges Bank-Gulf of Maine region, Applied Science Associates, Inc., Narragansett, Rhode Island, 1984.

Jamart, B. M., and D. F. Winter, A new approach to the computation of tidal motions in estuaries, in *Proc. 9th Int. Liege Colloquium on Ocean Hydrodynamics*, edited by J. C. J. Nihoul, pp. 261-281, Elsevier, Amsterdam, 1978.

Janopaul, M. M., and A. S. Frisch, CODAR measurements of surface currents in the northwest Alboran Sea during the Donde Va experiment, *Ann. Geophys.*, 2(4), 443-448, 1984.

Johns, B., and T. Oguz, Tubulence energy closure schemes, in *Three-Dimensional Coastal Ocean Models, Coastal and Estuarine Sciences*, 4, edited by N. S. Heaps, pp. 17-39, American Geophysical Union, Washington, D.C., 1987.

Johnson, C. D., Numerical ocean prediction in the California coastal region using a high-resolution primitive equation model, Naval Postgraduate School (NPS) Master's Thesis in Meteorology and Oceanography, *NPS Tech. Rpt. 68-88-007*, June 1988.

Johnson, W., and H. Melfi, Ocean science: Scientific challenges and airborne observational needs, in *Airborne Geoscience: The Next Decade*, pp. 43-47, 1989.

Jones, S. C., B. E. Tossman, and L. M. Dubois, The GEOSAT ground station, *The Johns Hopkins APL Technical Digest*, 8, 190-196, 1987.

Kantha, L. H., On open boundary conditions in a numerical model, *Dynalysis of Princeton Rpt. No. 89*, 96 pp., 1985.

Karl, H. A., and P. R. Carlson, Surface current patterns suggested by suspended sediment distribution over the outer continental margin, Bering Sea, *Mar. Geol.*, 74, 301-308, 1986.

Kelly, K. A., The influence of winds and topography on the sea surface temperature patterns over the northern California Slope, *J. Geophys. Res.*, 90(C6), 11,783-11,841, 1985.

Kiefer, D. A., W. S. Chamberlin, and C. R. Booth, Natural fluorescence of chlorophyll-a: Relationship to photosynthesis and chlorophyll concentration in the western South Pacific Gyre, *Limnol. Oceanogr.*, 34, 868-881, 1989.

Kinnmark, I. P. E., The shallow water equations: Formulation, analysis and application, *Lecture Notes in Engineering*, 15, edited by C. A. Brebbia and S. A. Orszag, 187 pp., Springer-Verlag, 1985.

Klein, P., A simulation of the effects of air-sea transfer variability on the structure of marine upper layers, *J. Phys. Oceanogr.*, 10, 824-841, 1980.

Klinck, J. M., Geostrophic adjustment over submarine canyons, *J. Geophys. Res.*, 94, 6133-6144, 1989.

Kolber, Z., K. Wyman, and P. G. Falkowski, Natural variability in photosynthetic energy conversion efficiency: A field study in the Gulf of Maine, *Limnol. Oceanogr.*, in press, 1990.



Kosro, P. M., Structure of the coastal current field off northern California during the Coastal Ocean Dynamics Experiment, *J. Geophys. Res.*, 92(C2), 1637-1654, 1987.

Kosro, P. M., and A. Huyer, Results of ADCP/CTD surveys in the California Current in May and June of 1987, in preparation; (see *CTZ Newsletter*, 2(4), 1987).

Kosro, P. M., A. Huyer, T. Cowles, S. Ramp, L. Small, R. T. Barber, F. A. Chavez, M. R. Abbott, and P. T. Strub, The structure of the transition zone between coastal waters and the open ocean off northern California, spring 1987, in preparation, 1990.

Kourafalou, V., J. D. Wang, and T. N. Lee, Circulation on the southeast U.S. continental shelf, Part 3: Modeling the winter wind-driven flow, *J. Phys. Oceanogr.*, 14(6), 1022-1031, 1984.

Langdon, C., Dissolved oxygen monitoring system using a pulsed electrode: Design, performance, and evaluation, *Deep-Sea Res.*, 31(11), 1357-1367, 1984.

Lawrence, D. J., and P. C. Smith, Evaluation of HF ground-wave radar on the east coast of Canada, *IEEE J. Oceanic Eng.*, OE-11, 246-250, 1986.

Leendertse, J. J., A new approach to three-dimensional free-surface flow modeling, *Rand Corp. Rpt. R-3712-NETH/RC*, March 1989.

Le Provost, C., and M. Fornerino, Tidal spectroscopy of the English Channel with a numerical model, *J. Phys. Oceanogr.*, 15, 1009-1031, 1985.

Le Provost, C., and A. Poncet, Finite element method for spectral modeling of tides, *Int. J. Numer. Meth. Eng.*, 12, 853-871, 1978.

Le Provost, C., G. Rougier, and A. Poncet, Numerical modeling of the harmonic constituents of the tides, with application to the English Channel, *J. Phys. Oceanogr.*, 11, 1123-1138, 1981.

Liese, J. A., The analysis and digital signal processing of NOAA's surface current mapping system, *IEEE J. Oceanic Eng.*, OE-9, 106-113, 1977.

Lipa, B. J., and D. E. Barrick, Tidal and storm surge measurements with single-site CODAR, *IEEE J. Oceanic Eng.*, OE-11, 241-245, 1986a.

Lipa, B. J., and D. E. Barrick, Extraction of sea state from HF radar echoes: Mathematical theory and modeling, *Radio Sci.*, 21, 81-100, 1986b.

Lipa, B. J., R. Crissman, and D. Barrick, HF Radar observations of Arctic ice pack breakup, *IEEE J. Oceanic Eng.*, OE-11, 270-275, 1986.

- Lipa, B. J., D. E. Barrick, J. Isaacson, and P. M. Lilleboe, CODAR wave measurements from a North Sea semi-submersible, *IEEE J. Oceanic Eng.*, OE-15(1), 1990.
- Loder, J. W., and D. A. Greenberg, Predicted positions of tidal fronts in the Gulf of Maine region, *Cont. Shelf Res.*, 6, 397-414, 1986.
- Lopez, M., and A. J. Clarke, The wind-driven shelf and slope water flow in terms of a local and a remote response, *J. Phys. Oceanogr.*, 19, 1091-1101, 1989.
- Lopez, M., and A. J. Clarke, Modeled low-frequency, wind-driven flow over the northern California continental shelf during CODE 1 and CODE 2, submitted to *J. Phys. Oceanogr.*, 1990.
- Lorenzzetti, J. A., and J. D. Wang, On the use of wave-absorbing layers in the treatment of open boundaries in numerical coastal circulation models, *Appl. Math. Mod.*, 10, 339-345, 1986.
- Lorenzzetti, J. A., J. D. Wang, and T. N. Lee, Two-layer model of summer circulation on the southeast U.S. continental shelf, *J. Phys. Oceanogr.*, 18(4), 591-608, 1988.
- Lynch, D. R., Progress in hydrodynamic modeling, Review of U.S. contributions, 1979-1982, in *Rev. Geophys. Space Phys.*, 21, 741-754, 1983.
- Lynch, D. R., and W. R. Gray, A wave equation model for finite element computations, *Comp. and Flu.*, 7, 207-228, 1979.
- Lynch, D. R., and F. E. Werner, Three-dimensional hydrodynamics on finite elements, Part I: Linearized harmonic model, *Int. J. Numer. Meth. FL*, 7, 871-909, 1987.
- Lynch, D. R., and F. E. Werner, Wave equation hydrodynamics on simple 3-D elements, in *Proceedings of the VIIth International Conference on Finite Elements and Flow Problems*, April 1989, edited by T. J. Chung and G. R. Karr, pp. 1373-1382, The University of Alabama in Huntsville Press, 1989a.
- Lynch, D. R., and F. E. Werner, Three-dimensional velocities from a finite element model of English Channel/Southern Bight tides, submitted to *Tidal Hydrodynamics*, B. Parker, editor, 1989b.
- Lynch, D. R., and F. E. Werner, Three-dimensional hydrodynamics on finite elements, Part II: Nonlinear time-stepping model, submitted to *Int. J. Numer. Meth. FL*, 1990.
- Lynch, D. R., F. E. Werner, J. M. Molines, and M. Fornerino, Tidal hydrodynamics in a coupled ocean/lake system, submitted to *Estuarine Coastal Shelf Sci.*, 1989.



Mathisen, J. P., O. O. Jenssen, M. L. Spaulding, and J. C. Swanson, A three-dimensional numerical model for ocean current in which the horizontal grid spacing is varied using boundary fitted coordinates, in *Proceedings of SUT Conference on Modelling of the Offshore Environment*, pp. 295-309, London, 1987.

Mathisen, J. P., O. O. Jenssen, T. Utne, J. C. Swanson, and M. L. Spaulding, A three-dimensional boundary fitted coordinate hydrodynamic model, Part II: Testing and application of the model, *Dtsch. Hydrogr. Z.*, in press.

May, P. T., B. L. Weber, R. G. Strauch, R. J. Laititis, K. P. Moran, and D. A. Merritt, Single station ocean current vector measurement: Application of the spaced antenna technique, *Geophys. Res. Lett.*, 16(9), 999-1002, 1989.

McClain, C. R., J. A. Yoder, L. P. Atkinson, J. O. Blanton, T. N. Lee, J. J. Singer, and F. Muller-Karger, Variability of surface pigment concentrations in the South Atlantic Bight, *J. Geophys. Res.* 93, 10675-10697, 1988.

McWilliams, J. C., N. J. Norton, P. R. Gent, and D. B. Haidvogel, A linear balance model of the wind-driven, mid-latitude ocean circulation, *J. Phys. Oceanogr.*, accepted for publication, 1990.

Mellor, G. L., Analytic prediction of the properties of stratified planetary surface layers, *J. Atmos. Sci.*, 30, 1061-1069, 1973.

Mellor, G. L., and P. A. Durbin, The structure and dynamics of the ocean surface mixed layer, *J. Phys. Oceanogr.*, 5, 718-728, 1975.

Mellor, G. L., and T. Yamada, A hierarchy of turbulence closure models for planetary boundary layers, *J. Atmos. Sci.*, 31, 1791-1806, 1974.

Mellor, G. L., and T. Yamada, A turbulence model applied to geophysical fluid problems, *Proceedings of Symposium on Turbulent Shear Flows*, Pennsylvania State University, pp. 6.1-6.14, 1977.

Mellor, G. L., and T. Yamada, Development of a turbulence closure model for geophysical fluid problems, *Rev. Geophys. Space Phys.*, 20, 851-875, 1982.

Mendelsohn, D., M. Spaulding, E. Anderson, T. Isaji, M. Reed, and A. Odulo, Simulation of selected test cases for the Metocean Modeling Project (MOMOP), Report to MOMOP Committee, Veritas Offshore Technology and Services A/S, Oslo, Norway, 1989.

Mendenhall, B. R., M. M. Holl, and M. J. Cuming, Development of a marine history of analyzed sea-level pressure fields and diagnosed wind fields, *FNOC Tech. Rep. M-227*, 28 pp., Fleet Numer. Oceanogr. Cent., Monterey, Calif., 1977.

Michaelsen, J., X. Zhang, and R. C. Smith, Variability of pigment biomass in the California current system as determined by satellite imagery, 2: Temporal variability, *J. Geophys. Res.*, 93, 10883-10896, 1988.

Mihok, W. F., and J. E. Kaitala, U.S. Navy Fleet Numerical Center operational five-level global fourth-order primitive equation model, *Mon. Weather Rev.*, 12, 1227-1550, 1976.

Milliff, R.F., Quasigeostrophic Ocean Flow in Coastal Domains, *Harvard Open Ocean Model Reports 34*, Reports in Meteorology and Oceanography, Cambridge, MA (Ph.D. Thesis, carried out at Harvard University for the University of California, Santa Barbara), April 1989.

Milliff, R.F., A modified capacitance matrix method to implement coastal boundaries in the Harvard Open Ocean Model, *Mathematics and Computers in Simulation*, 31, (6), 541-564, 1990.

Milliff, R.F., and A.R. Robinson, Structure and dynamics of the Rhodes gyre system, and dynamical interpolation for estimates of the mesoscale variability, submitted for publication, 1990.

Miyakoda, L., and J. Sirutis, Comparative integrations of global models with various parameterized processes of subgridscale vertical transports: Description of the parameterizations, *Beitr. sur Phy. Atmos.*, 50, 445-487, 1977.

Molines, J. M., M. Fornerino, and C. Le Provost, Tidal spectroscopy of a coastal area: Observed and simulated tides of the Lake Maracaibo system, *Cont. Shelf Res.*, 9(4), 301-323, 1989.

Moody, J. A., B. Butman, R. C. Beardsley, W. S. Brown, P. Daifuku, J. D. Irish, D. A. Mayer, H. O. Mofjeld, B. Petrie, S. Ramp, P. Smith, and W. R. Wright, Atlas of tidal elevation and current observations on the northeast American continental shelf and slope, *U.S. Geological Survey Bulletin 1611*, 122 pp., 1984.

Mooers, C. N. K., R. W. Garvine, and W. J. Martin, Summertime synoptic variability of the middle Atlantic shelf water/slope water front, *J. Geophys. Res.*, 84, 4837-4854, 1979.

National Research Council, *Opportunities to Improve Marine Forecasting*, National Academy Press, Washington, D.C., 1989.

Nelson, C. S., Wind stress and wind stress curl over the California Current, *NMFS Rpt. SSRF-714*, 87 pp., Natl. Ocean. and Atmos. Admin., Monterey, Calif., 1977.

Nelson, T. A., P. E. Gadd, and T. L. Clarke, Wind-induced current flow in the upper Hudson Shelf valley, *J. Geophys. Res.*, 83, 6073-6082, 1978.



Niiler, P. P., P.-M. Poulain, and L. R. Haury, Synoptic three-dimensional circulation in an onshore-flowing filament of the California Current, *Deep-Sea Res.*, 36, 385-405, 1989.

NOAA, Fisheries applications of a portable surface current mapping radar system, Southwest Fisheries Center Technical Memo, 24 pp., NMFS, NOAA, 1977.

NOAA, *U.S. Ocean Data Management Master Plan--An End-to-End Strategy*, U.S. Dept. of Commerce, 115 pp., 1989.

Noble, M., and Butman, B., The structure of subtidal currents within and around Lydonia Canyon: Evidence for enhanced cross-shelf fluctuations over the mouth of the canyon, *J. Geophys. Res.*, 94, 8091-8110, 1989.

Oey, L.-Y., G. L. Mellor, and R. I. Hires, A three-dimensional simulation of the Hudson-Raritan Estuary, Part I: Description of the model and model simulations, *J. Phys. Oceanogr.*, 15(12), 1676-1692, 1985.

Oltman-Shay, J. M., P. A. Howd, and W. A. Birkemeier, Shear instabilities of the mean longshore current, 2. Field observations, *J. Geophys. Res.*, in press, 1990.

Ozer, J., and B. M. Jamart, Tidal motion in the English Channel and southern North Sea: Comparison of various observational and model results, in *Computational Methods in Water Resources, vol. I: Modeling Surface and Sub-Surface Flows*, edited by M. A. Celia, L. A. Ferrand, C. A. Brebbia, W. G. Gray, and G. F. Pinder, pp. 267-273, Proceedings of the VIIth International Conference, MIT, Boston, Mass., June 1988, Computational Mechanics Publications, Elsevier, Amsterdam, 1988.

Pares-Sierra, A., and J. J. O'Brien, The seasonal and interannual variability of the California Current System: A numerical model, *J. Geophys. Res.*, 94, 3159-3180, 1989.

Pearson, C. E., and D. F. Winter, On the calculation of tidal currents in homogeneous estuaries, *J. Phys. Oceanogr.*, 7, 20-531, 1977.

Peffley, M. B., and J. J. O'Brien, A three-dimensional simulation of coastal upwelling off Oregon, *J. Phys. Oceanogr.*, 6, 164-180, 1976.

Pelaez, J., and J. A. McGowan, Phytoplankton pigment patterns in the California Current as determined by satellite, *Limnol. Oceanogr.*, 31, 927-50, 1986.

Pettigrew, N. R., and J. D. Irish, Acoustic Doppler profiling from the sea floor, in *Current Practices and New Technology in Ocean Engineering*, edited by T. McGuinness and H. H. Shih, pp. 15-21, American Society of Mechanical Engineers, New York, 1986.

Pinardi, N., Report of the POEM Mapping Group: August/September 1987 General Circulation Survey Data Set Preparation, *Technical Report No. 1-88*, 1988.

Pinardi, N., and R.F. Milliff, A note on consistent quasigeostrophic boundary conditions in partially open, simply and multiply connected domains, *Dynam. Atmos. Oceans*, 14(1-2), 65-77, 1989.

Pingree, R. D., Spring tides and quadratic friction, *Deep-Sea Res.*, 30, 929-944, 1983.

Pingree, R. D., and D. K. Griffiths, Tidal fronts on the shelf seas around the British Isles, *J. Geophys. Res.*, 83, 4615-4622, 1978.

Pingree, R. D., and D. K. Griffiths,  $S_2$  tidal simulations on the northwest European shelf, *J. Mar. Biol. Assoc. U.K.*, 61, 609-616, 1981a.

Pingree, R. D., and D. K. Griffiths, The  $N_2$  tide and semidiurnal amphidromes around the British Isles, *J. Mar. Biol. Assoc. U.K.*, 61, 617-625, 1981b.

Pingree, R. D., and L. Maddock, The  $M_4$  tide in the English Channel derived from a nonlinear numerical model of the  $M_2$  tide, *Deep-Sea Res.*, 25, 53-63, 1978.

Pingree, R. D., D. K. Griffiths, and L. Maddock, Quarter diurnal shelf resonance and tidal bed stress in the English Channel, *Cont. Shelf Res.*, 3, 267-289, 1984.

Platzman, G. W., Normal modes of the world ocean. Part I. Design of a finite element barotropic model, *J. Phys. Oceanogr.*, 8, 323-343, 1978.

Platzman, G. W., Some response characteristics of finite element tidal models, *J. Comp. Phys.*, 40, 36-63, 1981.

Porter, D. L., R. G. Williams, and C. R. Swassing, CODAR intercomparison: Delaware Bay, 1984, *Proceedings of the Third Working Conference on Current Measurements*, IEEE, 1986.

Praagman, N., J. Dijkzeul, R. van Dijk, and R. Pleiger, A finite difference simulation model for tidal flow in the English Channel and southern North Sea, *Adv. Water Resources*, in press, 1989.

Prandle, D., and D. K. Ryder, Measurements of surface currents in Liverpool Bay by high-frequency radar, *Nature*, 315, 128-131, 1985.

Price, J. F., R. A. Weller, and R. Pinkel, Diurnal cycling: Observations and models of the upper ocean response to diurnal heating, cooling, and wind mixing, *J. Geophys. Res.*, 91, 8411-8427, 1986.

Reed, M., The physical fates component of the natural resource damage assessment model system, *Oil and Chemical Pollution*, 5(273), 99-124, 1989.



Reed, M., D. French, T. Grigalunas, and J. Opaluch, Overview of a natural resource damage assessment model system of coastal and marine environments, *Oil and Chemical Pollution*, 5(273), 85-98, 1989.

Rienecker, M. M., and L. L. Ehret, Wind stress curl variability over the North Pacific from the Comprehensive Ocean-Atmosphere Data Set, *J. Geophys. Res.*, 93, 5069-5077, 1988.

Rienecker, M. M., and C. N. K. Mooers, Mesoscale eddies, jets and fronts off Point Arena, California, July 1986, *J. Geophys. Res.*, 94, 12555-12570, 1989.

Rienecker, M. M., C. N. K. Mooers, D. E. Hagan, and A. R. Robinson, A cool anomaly off northern California: An investigation using IR imagery and *in situ* data, *J. Geophys. Res.*, 90, 4807-4818, 1985.

Rienecker, M. M., C. N. K. Mooers, and A. R. Robinson, Dynamical interpolation and forecast of the evolution of mesoscale features off northern California, *J. Phys. Oceanogr.*, 17, 1189-1213, 1987.

Robinson, A. R., and L. J. Walstad, The Harvard Open Ocean Model: Calibration applications to dynamical process, forecasting and data assimilation studies, *J. Appl. Numer. Meth.*, 3, 89-131, 1987a.

Robinson, A. R., and L. J. Walstad, Altimetric data assimilation for ocean dynamics and forecasting, *The Johns Hopkins APL Technical Digest*, 8, 267-271, 1987b.

Robinson, A. R., M. Golnaraghi, W. G. Leslie, and the POEM Group, The eastern Mediterranean general circulation: Features, structure and variability, *Dynam. Atmos. Oceans*, submitted for publication, 1990.

Ross, B. M., and I. Orlanski, The evolution of an observed cold front. Part I: Numerical simulation, *J. Atmos. Sci.*, 39, 296-327, 1982.

Sanford, T. B., Recent improvement in ocean current measurement from motional electric fields and currents, *Proceedings of the IEEE Third Working Conference on Current Measurement*, pp. 65-76, Airlie, Virginia, January 22-24, 1986.

Schramm, R. E., J. Fleischbein, R. Marsh, A. Huyer, P. M. Kosro, T. Cowles, and N. Dudek, CTD observations in the coastal transition zone off northern California, 18-27 May 1987, *Data Rpt. 141, Ref. 88-3*, College of Oceanography, Oregon State University, Corvallis, Oregon, 1988a.

Schramm, R. E., J. Fleischbein, A. Huyer, P. M. Kosro, T. Cowles, and N. Dudek, CTD observations in the coastal transition zone off northern California, 9-18 June 1987, *Data Rpt. 142, Ref. 88-4*, College of Oceanography, Oregon State University, Corvallis, Oregon, 1988b.

- Schwiderski, E. W., On charting global ocean tides, *Rev. Geophys. Space Phys.*, 18, 243-268, 1980.
- Send, U., R. C. Beardsley, and C. D. Winant, Relaxation from upwelling in the Coastal Ocean Dynamics Experiment, *J. Geophys. Res.*, 92, 1683-1689, 1987.
- Seymour, R. J., M. H. Sessions, and D. Castel, Automated remote recording and analysis of coastal data, *J. Waterw. Port Coastal Ocean Eng. Div. Am. Soc. Civ. Eng.*, 3(2), March, 1985.
- Shaffer, G., A mesoscale study of coastal upwelling variability off NW-Africa, *Meteor. Forsch.-Ergebn. A.*, 17, 21-72, 1976.
- Shepard, F. P., Progress of internal waves along submarine canyons, *Mar. Geol.*, 19, 131-138, 1975.
- Shepard, F. P., and N. F. Marshall, Dives into outer Coronado Canyon system, *Mar. Geol.*, 18, 313-323, 1975.
- Shepard, F. P., P. A. McLoughlin, N. F. Marshall, and G. G. Sullivan, Current-meter recordings of low-speed turbidity currents, *Geology*, 5, 297-301, 1977.
- Shepard, F. P., N. F. Marshall, P. A. McLoughlin, and G. G. Sullivan, *Currents in Submarine Canyons and Other Seavalleys*, 173 pp., Am. Assoc. Petrol. Geol., 1979.
- Simpson, J. J., and T. D. Dickey, The relationship between downward irradiance and upper ocean structure, *J. Phys. Oceanogr.*, 11, 309-332, 1981a.
- Simpson, J. J., and T. D. Dickey, Alternative parameterizations of downward irradiance and their dynamical significance, *J. Phys. Oceanogr.*, 11, 876-882, 1981b.
- Smith, R. C., O. B. Brown, F. E. Hoge, K. S. Baker, R. H. Evans, R. N. Swift, and W. E. Esaias, Multiplatform sampling (ship, aircraft, and satellite) of a Gulf Stream warm core ring, *Appl. Opt.*, 26, 2068-2081, 1987.
- Smith, R. C., X. Zhang, and J. Michaelson, Variability of pigment biomass in the California Current system as determined by satellite imagery, 1: Spatial variability, *J. Geophys. Res.*, 93, 10863-10882, 1988.
- Smith, R. L., Peru coastal currents during El Nino: 1976 and 1982, *Science*, 221, 397-1399, 1983.
- Snyder, R. L., M. Sidjabat, and J. H. Filloux, A study of tides, setup and bottom friction in a shallow semi-enclosed basin, Part II: Tidal model and comparison with data, *J. Phys. Oceanogr.*, 9, 170-188, 1979.



Spain, P. F., D. L. Dorson, and H. T. Rossby, Pegasus: A simple acoustically tracked acoustic profiler, *Deep-Sea Res.*, 28A, 1553-1567, 1981.

Spaulding, M. L., W. Huang, and D. Mendelsohn, Application of a boundary fitted coordinate hydrodynamic model, Proceedings of Estuarine and Coastal Modeling Conference, Am. Soc. Civ. Eng., Newport, Rhode Island, in press.

Spaulding, M. L., and T. Isaji, *Three-dimensional hydrodynamic model of the Norwegian Coastal Current: Results of preliminary simulations*, Continental Shelf Institute, Trondheim, Norway, 1984.

Spaulding, M. L., and T. Isaji, Design flow conditions near the sea floor--coupling of a continental shelf hydrodynamics model to a bottom boundary layer model, Report prepared for American Gas Association, 1985.

Spaulding, M. L., and T. Isaji, Three-dimensional continental shelf hydrodynamics model including wave current interaction, in *Three-Dimensional Models of Marine and Estuarine Dynamics*, edited by J. C. J. Nichol and B. M. Jamart, pp. 405-426, Elsevier Oceanography Series, 45, Elsevier, Amsterdam, 1987.

Spaulding, M. L., and J. C. Swanson, A three-dimensional hydrodynamic model using boundary fitted coordinates, in *Applications of Real Time Oceanographic Circulation Modeling, Symposium Proceedings*, edited by B. R. Parker, pp. 227-244, Johns Hopkins University, Applied Physics Laboratory, Laurel, Maryland, 1985.

Spaulding, M., T. Isaji, D. Mendelsohn, and A. C. Turner, Numerical simulation of wind-driven flow through the Bering Strait, *J. Phys. Oceanogr.*, 17(10), 1987.

Spaulding, M. L., T. Isaji, K. Jayko, E. Anderson, C. Turner, and D. Mendelsohn, An oil spill model system for arctic waters, in *Proceedings of 1989 Oil Spill Conference*, pp. 517-524, San Antonio, Texas, 1989.

Sternberg, R. W., D. R. Morrison, and J. A. Trimble, An instrumentation system to measure near bottom conditions on the continental shelf, *Mar. Geol.*, 3, 181-189, 1973.

Stewart, R. H., and J. W. Joy, HF radio measurements of surface currents, *Deep-Sea Res.*, 21, 1039-1049, 1974.

Strub, P. T., C. James, A. C. Thomas, and M. R. Abbott, Seasonal and non-seasonal variability of satellite-derived surface pigment concentration in the California Current, *J. Geophys. Res.*, in press, 1990.

Stuart, D. W., Sea surface temperatures and winds during JOINT II, Part II: Temporal fluctuations, in *Coastal Upwelling*, edited by F. R. Richards, pp. 32-38, American Geophysical Union, Washington, D.C., 1981.

Swanson, J. C., A three-dimensional numerical model system of coastal circulation and water quality, Ph.D. dissertation, Dept. of Ocean Engineering, Univ. of Rhode Island, Kingston, 1986.

Swanson, J. C., Model of the mean winter circulation in the Gulf of Maine and adjacent areas, in preparation.

Swanson, J. C., and M. L. Spaulding, The ASA/IKU three-dimensional boundary fitted coordinate hydrodynamic model, *ANODA Rpt. No. 12*, Continental Shelf Institute, Trondheim, Norway, 1985.

Swanson, J. C., M. L. Spaulding, J. P. Mathisen, and O. O. Jenssen, A three-dimensional boundary fitted coordinate hydrodynamic model, Part I: Development and testing, *Dtsch. Hydrogr. Z.*, in press.

Teague, C., Multifrequency HF radar observations of currents and current shears, *IEEE J. Oceanic Eng.*, *OE-11*, 258-269, 1986.

Tee, K. T., The structure of three-dimensional tide-generated currents, Part I: Oscillating Currents, *J. Phys. Oceanogr.*, *9*, 930-944, 1979.

Tee, K. T., The structure of three-dimensional tide-induced currents, Part II: Residual Currents, *J. Phys. Oceanogr.*, *10*, 2035-2057, 1980.

Tee, K. T., The structure of three-dimensional tide-generated currents. Experimental verification of a theoretical model, *Estuarine Coastal Shelf Sci.*, *14*, 27-48, 1982.

Tee, K. T., Depth dependent studies of tidally induced residual circulation on the sides of Georges Bank, *J. Phys. Oceanogr.*, *15*, 1818-1846, 1985.

Tee, K. T., P. C. Smith, and D. Lefaivre, Estimation and verification of tidally induced residual currents, *J. Phys. Oceanogr.*, *181*, 1415-1434, 1988.

Thornton, E. B., and R. T. Guza, Surf zone longshore currents and random waves: Field data and models, *J. Phys. Oceanogr.*, *16*(7), 1165-1178, 1986.

Thruston, A. D., Jr., and R. W. Knight, Characterization of crude and residual-type oils by fluorescence spectroscopy, *Environ. Sci. Technol.*, *5*, 64-9, 1971.

Tolmazin, D., *Elements of Dynamic Oceanography*, Allen and Unwin, Inc., Winchester, MA, 181 pp., 1985.

U.S. Army Corps of Engineers, Automated Coastal Engineering System (ACES), Coastal Engineering Research Center, CETN-VI-20, Vicksburg, Mississippi, March, 1990.



Vemulakonda, S. R., J. R. Houston, and A. Swain, Development and application of coastal and inlet processes modeling system, in *Hydrodynamics and Sediment Dynamics of Tidal Inlets*, edited by D. G. Aubrey and L. Weishar, pp. 54-70, Springer-Verlag, 1988.

Walstad, L., J. S. Allen, P. M. Kosro, and A. Huyer, Coastal Transition Zone data assimilation studies: 1987, unpublished materials, 1989.

Walstad, L.J., J.S. Allen, P.M. Kosro, and A. Huyer, Dynamical processes in the Coastal Transition Zone through data assimilation studies, in preparation, 1990.

Walters, R. A., A model for tides and currents in the English Channel and southern North Sea, *Adv. Water Resour.*, 10, 138-148, 1987.

Walters, R. A., and G. F. Carey, Numerical noise in ocean and estuarine models, *Adv. Water Resour.*, 7, 15-20, 1984.

Walters, R. A., and F. E. Werner, A comparison of two finite element models using the North Sea data set, *Adv. Water Resour.*, in press, 1989.

Wang, D-P., Diffraction of continental shelf waves by the irregular alongshore geometry, *J. Phys. Oceanogr.*, 10(8), 1188-1199, 1980.

Wang, D-P., Development of a three-dimensional limited-area (island) shelf circulation model, *J. Phys. Oceanogr.*, 12, 605-617, 1982.

Wang, D-P., Mutual intrusion and density front, *J. Phys. Oceanogr.*, 14, 1191-1199, 1984.

Wang, D-P., Numerical study of gravity currents in a channel, *J. Phys. Oceanogr.*, 15, 299-305, 1985.

Wang, D-P., Strait surface outflow, *J. Geophys. Res.*, 92, 10,807-10,825, 1987.

Wang, D-P., Transport model for water exchange between coastal inlet and the open ocean, *American Fisheries Society Symposium* 3, 9-15, 1988.

Wang, D-P., Model of mean and tidal flows in the Strait of Gibraltar, *Deep-Sea Res.*, 36, 1535-1548, 1989.

Wang, D-P., D. Chen, and T. J. Sherwin, Coupling between mixing and advection in shallow sea fronts, *Cont. Shelf Res.*, 1989.

Wang, J. D., Real-time flow in unstratified shallow water, *J. Waterw. Port Coastal Ocean Eng. Div. Am. Soc. Civ. Eng.*, 104(WW1), 1978.

Wang, J. D., Hurricane effects on surface Gulf Stream currents, *Ocean Eng.*, 14(3), 165-180, 1987.

Wang, J. D., and J. J. Connor, Mathematical modeling of near coastal circulation, *Tech. Rep. No. 200*, Ralph M. Parsons Laboratory, MIT, Cambridge, MA, 1975.

Wang, J. D., V. Kourafalou, and T. N. Lee, Circulation on the southeast U.S. continental shelf, Part 2: Model development and application to tidal flow, *J. Phys. Oceanogr.*, 14(6), 1013-1021, 1984.

Wang, J. D., S. V. Cofer-Shabica, and J. Chin Fatt, Finite element characteristic advection model, *J. Hydraul. Eng. Div. Am. Soc. Civ. Eng.*, 114(9), 1098-1114, 1988.

Watts, D. R., and M. Wimbush, Sea surface height and thermocline variations measured from the sea floor, unpublished manuscript, 1981.

Weatherly, G., and P. J. Martin, On the structure and dynamics of the ocean bottom boundary layer, *J. Phys. Oceanogr.*, 8, 447-470, 1978.

Werner, F. E., and D. R. Lynch, Field verification of wave equation tidal dynamics in the English Channel and southern North Sea, *Adv. Water Resour.*, 10, 115-130, 1987.

Werner, F. E., and D. R. Lynch, Meeting report: 2nd Tidal Flow Forum, *EOS Trans. AGU*, 69(44), 1027-1028, 1988.

Werner, F. E., and D. R. Lynch, Tides in the southern North Sea/English Channel: Data files and procedure for reference computations, Dartmouth College Numerical Lab. Report, February 1988 distribution, 1988b.

Werner, F. E., and D. R. Lynch, Harmonic structure of English Channel/Southern Bight tides from a wave equation simulation, *Adv. Water Resour.*, in press, 1989.

Werner, F. E., A. Cantos-Figuerola, and G. Parrilla, A sensitivity study of reduced-gravity open-channel flows with application to the Alboran Sea, *J. Phys. Oceanogr.*, 18, 373-383, 1988.

White, W., C.-K. Tai, and W. Holland, Continuous assimilation of simulated altimetric sea level into an GEOSAT eddy resolving numerical ocean model, Part I: Sea level differences, submitted for publication, 1989.

Whitledge, T. E., and C. D. Wirick, Development of a moored in situ fluorometer for phytoplankton studies, in *Tidal Mixing and Plankton Dynamics*, edited by M. J. Bowman, C. M. Yentsch, and W. J. Peterson, vol. 17, Lecture Notes on Coastal and Estuarine Studies, pp. 449-462, Springer-Verlag, New York, 1986.

Wilburn, A. M., E. Johns, and M. Bushnell, Current velocity and hydrographic observations in the Straits of Florida, the Caribbean Sea, and the Antillean Archipelago: Subtropical Atlantic Climate Studies (STACS), *NOAA Data Report ERL AOML-10*, Nov. 1987.



- Wilkin, J. L., A computer program for calculating frequencies and modal structures of free coastal-trapped waves, *WHOI Tech. Rpt. WHOI-87-53*, 50 pp., 1987.
- Wilkin, J. L., and D. C. Chapman, Scattering of continental shelf waves at a discontinuity in shelf width, *J. Phys. Oceanogr.*, *17*, 713-724, 1987.
- Wilkin, J. L., and D. C. Chapman, Scattering of coastal-trapped waves by irregularities in coastline and topography, *J. Phys. Oceanogr.*, *20*, 396-416, 1990.
- Williams, R., The need for radar measurements of current, National Ocean Service Technical Memo., 10 pp., NOAA, 1989.
- Winant, C. D., C. E. Dorman, C. A. Friehe, and R. C. Beardsley, The marine layer off northern California: An example of supercritical channel flow, *J. Atmos. Sci.*, *45*, 3588-3605, 1988.
- Wood, J. D., and J. D. Irish, A compliant surface mooring system for real-time data acquisition, *Proc. Oceans '87*, 652-657, 1987.
- World Meteorological Organization (WMO), Commission for Basic Systems Working Group on Codes, Seventh Session, Final Report, Geneva, 20-31 October, 156 pp., 1986.
- Wright, D. G., and J. Loder, A depth-dependent study of the topographic rectification of tidal currents, *Geophys. Astrophys. Fluid Dyn.*, *31*, 169-220, 1985.
- Wright, D. G., and J. Loder, On the influences of nonlinear bottom friction on the topographic rectification of tidal currents, *Geophys. Astrophys. Fluid Dyn.*, *42*, 227-245, 1988.
- Wyrтки, K., L. Magard, and J. Hager, Eddy Energy in the Oceans, *J. Geophys. Res.*, *81*(15), 2641-2646, 1976.
- Yerkes, R. F., D. S. Gorsline, and G. A. Rusnak, Origin of Redondo Submarine Canyon, southern California, *Geo. Surv. Res.*, C97-C105, 1967.
- Yoder, J. A., C. R. McClain, J. O. Blanton, and L. Y. Oey, Spatial structure in CZCS-chlorophyll imagery of the southeastern U.S. continental shelf, *Limnol. Oceanogr.*, *32*, 929-941, 1987.

## GLOSSARY OF ACRONYMS

ABCN - Adams-Bashforth-Crank-Nicolson  
ABL - Atmospheric Boundary Layer  
ACDCP - Alaska Coastal Data Collection Program  
ACES - Automated Coastal Engineering System  
ADCP - Acoustic Doppler Current Profiler (a.k.a. DAPCM)  
AFOS - Automation of Field Operations and Services  
ANODA - Analysis of Oceanographic Data  
AO - Announcement of Opportunity  
AOCI - Airborne Ocean Color Imager  
AOL - Airborne Oceanographic LIDAR  
AOML - Atlantic Oceanographic and Meteorological Laboratory  
APL - Applied Physics Laboratory  
ARI - Advance Research Initiative  
ASA - Applied Science Associates, Inc.  
ASCE - American Society of Civil Engineers  
ASI - Air-Sea Interaction  
ASOS - Automatic Surface Observing System  
AVHRR - Advanced Very High Resolution Radiometer  
AVIRIS - Airborne Visible and Infrared Imaging Spectrometer  
AWIPS - Advanced Weather Interactive Processing System  
AWIPS-90 - Advanced Weather Interactive Processing System for the 1990s  
AXBT - Air-deployed Expendable Bathythermograph  
AXCP - Air-deployed Expendable Current Profiler  
AXCTD - Air-deployed Water Conductivity-Temperature Profiler  
AXPOGO - Air-deployed Expendable POGO  
BCs - Boundary Conditions  
B.I.O. - Bedford Institute of Oceanography  
BNL - Brookhaven National Laboratory  
BP - Bottom Pressure  
BSR LMER - Biotic Systems and Resources Land-Margin Ecosystem Research  
BSR LTER - Biotic Systems and Resources Long-Term Ecosystem Research  
BT - Bottom Temperature; Bathythermograph  
CABS - California Basins Study



CaBS - California Bight Study  
 CAC - Climate Analysis Center  
 CAFE - Circulation Analysis with Finite Elements  
 CAFE-1 - One-layer model CAFE  
 CAFE-2 - Two-layer model CAFE  
 CAFE-3D - Three-layer model CAFE  
 CalCOFI - California Cooperative Fisheries Investigation  
 CBI - Chesapeake Bay Institute  
 CBS - Coos Bay Shallow Mooring  
 CC - California Current  
 CDIP - Coastal Data Information Program  
 CD-ROM - Compact Disc-Read Only Memory  
 CEMIS - Coastal Engineering Management Information System  
 CERC - U.S. Army Corps of Engineers/Coastal Engineering Research Center  
 CERCLA - Comprehensive Environmental Response, Compensation, and Liability  
                   Act of 1980  
 CES - Committee on Earth Sciences  
 CFDCP - Coastal Field Data Collection Program  
 CI - Contour Interval  
 CIRES - Cooperative Institute for Research in Environmental Science  
                   (NOAA/University of Colorado)  
 CLASS - Cross-Chain LORAN Atmospheric Sounding System  
 C-MAN - Coastal-Marine Automated Network  
 CNSF - Cornell National Supercomputer Facility  
 COADS - Comprehensive Ocean-Atmosphere Data Set  
 COAP - Center for Ocean Analysis and Prediction  
 COAST - Combined Ocean and Atmospheric Sensing Technique  
 CODAR - Coastal Ocean Dynamics and Ranging  
 CODE - Coastal Ocean Dynamics Experiment  
 CODE 1 - First CODE Experiment  
 CODE 2 - Second CODE Experiment  
 COE - United States Army Corps of Engineers (also, 'USACE')  
 CoOP - Coastal Ocean Processes  
 CoPO - Coastal Physical Oceanography  
 COPS - Coastal Ocean Prediction Systems  
 CROSS - Center for Research on Ocean and Space Science (UNO)

C-SCAT - C-labelled Scatterometer (C denotes model number)  
CTD - Conductivity-Temperature-Depth Profiler  
CTD/STD - Conductivity-Temperature-Depth/Salinity-Temperature-Depth  
CTW - Coastal-Trapped Wave  
CTZ - Coastal Transition Zone  
CUEA - Coastal Upwelling Ecosystem Analysis program  
CZCS - Coastal Zone Color Scanner  
CZCS-Chl - Coastal Zone Color Scanner of phytoplankton chlorophyll  
DA - Data Assimilation  
DAL - Doppler Acoustic Log  
DAPCM - Doppler Acoustic Profiling Current Meter (a.k.a. ADCP)  
DAS - Data Acquisition System  
DCP - Data Collection Platform  
DCS - Data Communication System  
DISPER - Dispersion Analysis  
DOD - Department of Defense  
DOE - Department of Energy  
DOMB - Deep Ocean Moored Buoy  
DOT/PF - State Department of Transportation and Public Facilities  
DPAS - Data Processing and Analysis Subsystem  
DWG-1 - Directional Wave Gage  
EEP - Episodic Events Program  
EEZ - Exclusive Economic Zone  
EIS - Environmental Impact Statement  
EM - Electromagnetic  
EMAP - Environmental Monitoring and Assessment Program  
ENSO - El Nino-Southern Oscillation  
EOF - Empirical Orthogonal Function  
EOS - Earth Orbiting/Observing System; Institute for the Study of Earth, Oceans  
and Space  
EOSAT - Earth Observation Satellite Company  
EPA - Environmental Protection Agency  
EPOC - Eastern Pacific Oceanic Conference  
ERICA - Experiment on Rapidly Intensifying Cyclones over the Atlantic  
ERL - Environmental Research Laboratory  
ERS-1 - European Remote Sensing satellite





IIP - International Ice Patrol  
 IKU - Continental Shelf Institute, Trondheim, Norway  
 INO - Institute for Naval Oceanography  
 IOS - Institute of Ocean Sciences  
 IPG - Interim (Scientific) Planning Group  
 IR - Infrared  
 ISG - Interim Steering Group  
 ISHTAR - Inter-Shelf Transfer and Recycling  
 JAYCOR - Company name  
 JEBAR - Joint Effect of Barclinity and Bottom Relief  
 JERS-1 - Japanese Remote Sensing Satellite  
 JIMAR - Joint Institute of Marine and Atmospheric Research (U. of Hawaii)  
 JOI - Joint Oceanographic Institutions  
 JOIDES - Joint Oceanographic Institutions Deep Earth Sampling project  
 JPL - Jet Propulsion Laboratory  
 LAC - Local Area Coverage  
 LATEX - Louisiana/East Texas Shelf program  
 LED - Light-Emitting Diode  
 LEO - Littoral Environmental Observations  
 LFM - Limited-Area Fine Mesh  
 LIDAR - Light Detection and Ranging  
 LMER - Land-Margin Ecosystem Research  
 LNB - Large Navigational Buoy  
 LORAN - Long-Range Aid to Navigation  
 LPR - Local Plus Remote  
 LSU - Louisiana State University  
 LUMCON - Louisiana University Marine Consortium  
 MABPOM - Middle Atlantic Bight Physical Oceanography and Meteorology  
 MAR - Modernization and Associated Restructuring  
 MAREX - Company which makes the OSCAR radar  
 MARS - Marine Airborne Radiometer System  
 MBT - Mechanical Bathythermograph  
 MBW - Maine Bottom Water  
 MIS - Management Information Systems  
 MIT - Massachusetts Institute of Technology  
 MIW - Maine Intermediate Water





NSTL - National Space and Technology Laboratories  
NUSCAT - NU-labelled Scatterometer (NU denotes model number)  
NWLON - National Water Level Observation Network  
NWS - National Weather Service  
NWSTRG - National Weather Service Telecommunications Gateway  
OAG - Ocean Applications Group  
OCI - Ocean Color Imager  
OCS - Outer Continental Shelf  
ODAS - Ocean Data Acquisition System  
ODF&W - Oregon Department of Fish and Wildlife  
ODU - Old Dominion University  
OMB - Office of Management and the Budget  
ONR - Office of Naval Research  
OPAL - Ocean Process Analysis Laboratory  
OPC - Ocean Products Center  
OPTOMA - Ocean Prediction Through Observation, Modeling, and Analysis  
OSCR - Ocean Surface Current Radar  
OSRA - Oil Spill Risk Assessment  
OSU - Oregon State University  
OTEC - Ocean Thermal Energy Conversion  
P-3 - Aircraft model number  
PC - Personal Computer  
PE - Primitive Equation  
PMEL - Pacific Marine Environmental Laboratory  
POGO - Nickname for an instrument to measure mass transport in the ocean  
PORTS - Physical Oceanographic Real-Time Systems  
PROBES - Process and Resource of the Bering Sea  
PRT-5 - Model number for a thermal radiometer  
PSTN - Public Switched Telephone Network  
QC - Quality Control  
QG - Quasigeostrophic  
R&D - Research and Development  
REEFLUX - Reef Flux experiment  
RMS - Root Mean Square (also, 'rms')  
ROWS - Radar Ocean Wave Spectrometer  
RSMAS - Rosenstiel School of Marine and Atmospheric Sciences (U. of Miami)



R/V - Research Vessel  
 S - Salinity; South  
 SAB - South Atlantic Bight  
 SAIC - Science Applications Incorporated  
 SAR - Synthetic Aperture Radar  
 SAT - Spaced Antenna Technique  
 SCR - Surface Contour Radar  
 SCTD - Salinity Conductivity Temperature Depth  
 SEAS - Shipboard Environmental Data Acquisition System  
 SEASAT - Sea Satellite  
 Sea-WiFS - Sea-Wide Field Sensor  
 SEEP - Shelfbreak Exchange Processes  
 SERB - Science and Engineering Research Building  
 SFE - Simulated Forecast Experiments  
 SG - Steering Group  
 SIO - Scripps Institution of Oceanography  
 SLOSH - Sea, Lake and Overland Surges from Hurricanes  
 SMMR - Scanning Multichannel Microwave Radiometer  
 SPEM - Semi-spectral Primitive Regional Ocean Circulation Model  
 SPIE - Society of Photo-optical Instrumentation Engineers  
 SPREX - Spring Experiment  
 SSP - Synthetic Subsurface Pressure  
 SST - Sea Surface Temperature  
 SUPERDUCK - Nickname of an experiment conducted by the U.S. Army Corps of  
                     Engineers in Duck, NC  
 SUT - Society for Underwater Technology  
 SWADE - Surface Wave Dynamics Experiment  
 SYNAPS - Synthetic Bathymetric Profiling System  
 T - Temperature  
 TAMU - Texas A&M University  
 T/C - Temperature/Conductivity  
 TLC - Telemetering Lagrangian Capsule  
 TOGA - Tropical Ocean and Global Atmosphere program  
 T/S - Temperature/Salinity  
 TTM - Towed Transport Meter  
 U-2 - Aircraft model number

UF - University of Florida  
UM - University of Miami  
UNESCO - United Nations Educational, Scientific, and Cultural Organization  
UNH - University of New Hampshire  
UNO - University of New Orleans  
UNOLS - University National Oceanographic Laboratory System  
URI - University of Rhode Island  
USACE - United States Army Corps of Engineers (also, 'COE')  
USCG - United States Coast Guard  
USGS - United States Geological Survey  
USN - United States Navy  
V - Velocity  
VACM - Vector Averaging Current Meter  
VAD - Velocity Azimuth Display  
VAWR - Vector-Averaging Wind Recorder  
VOS - Voluntary Observing Ships  
VSTOL - Vertical Short Take Off and Landing  
WDC-A - World Data Center-A  
WES - Waterways Experiment Station  
WFO - Weather Forecast Service  
WG - Working Group  
WHOI - Woods Hole Oceanographic Institution  
WIS - Wave Information Study  
WMO - World Meteorological Organization  
WOCE - World Ocean Circulation Experiment  
WPDN - Wind Profiler Demonstration Network  
WPL - Wave Propagation Laboratory  
XBT - Expendable Bathythermograph  
XCP - Expendable Current Profiler  
XCTD - Expendable Conductivity-Temperature-Depth Profiler  
YSI - Yellow Springs Instrument Company, Inc.



## ACKNOWLEDGEMENTS

The financial and programmatic support of the co-sponsoring agencies is gratefully acknowledged. While each agency made unique and important contributions, a few individuals made exceptional efforts. In particular, Ms. Theresa Paluszkiewicz, MMS, Drs. Melvin Peterson, Joseph Huang, Glenn Flittner, and Joseph Bishop, NOAA, and Dr. George Saunders, DOE were early and consistent supporters of the Workshop. Dr. Thomas Spence, NSF, stepped forward at a crucial time to serve as a focal point for interagency transfers of funds. The Office of Naval Research, via the Institute for Naval Oceanography (INO), provided salary support for the convenor in the planning and preparation phases. Staff of INO contributed to some of the early planning tasks.

The University of New Orleans (UNO) hosted the Workshop by providing courtesy use of its meeting rooms. Mrs. Doris Rucker, UNO, served as the Workshop Coordinator during the planning, preparatory, and execution phases. Chancellor Gregory O'Brien, Prof. George Ioup, and Dr. James Rucker, all of UNO, were helpful throughout the course of preparations for the Workshop.

Ms. Kim Bremermann, New Orleans, provided gratuitous typing assistance, and Mrs. Elizabeth E. Mooers organized the banquet at Patous' Restaurant and created the table decorations.

Mariellen Carpenter Lee, University of New Hampshire, coordinated preparation of the report. She was assisted by Ms. Elaine Drapeau and Ms. Rebecca Camenzind with word processing, Ms. Luanne Garbe with word processing and communications, and Mr. Frank O. Smith, Jr. with editing.

Drs. James Baker and Frank Eden, JOI, arranged for overall project management. Ms. Andrea Johnson and Ms. Grace Torres, JOI, were responsible for final production of the report.

Ultimately, the quality of the Workshop, and of the Report, depended upon the competent and enthusiastic participation of its attendees, other contributors, and the Organizing Committee. The invited speakers and the working group chairs and rapporteurs, deserve special recognition for their scientific leadership and arduous efforts.

**Front Cover**  
(clockwise)

Biological Productivity in Gulf of Mexico (from Nimbus-7) - Courtesy of NASA  
Fish Harvest - Courtesy of NOAA  
Deploying Data Buoy - Courtesy of MMS  
Offshore Oil Platform - Courtesy of MMS

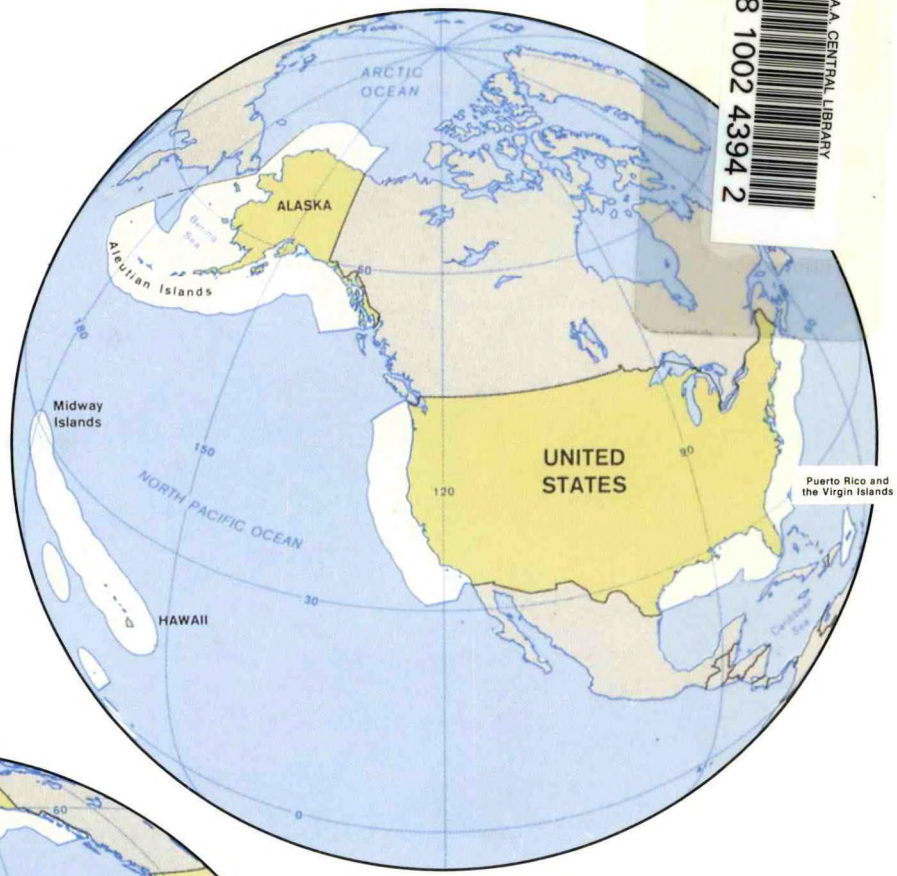
**Back Cover**

U.S. Exclusive Economic Zone (illustration) - Courtesy of DOS



3 8398 1002 4394 2

NOAA CENTRAL LIBRARY



Puerto Rico and the Virgin Islands

